Det Kongelige Danske Videnskabernes Selskab

Matematisk-fysiske Meddelelser, bind **27**, nr. 1

Dan. Mat. Fys. Medd. **27**, no. 1 (1951)

STRUCTURE AND PROPERTIES OF ICE

I. POSITION OF THE HYDROGEN ATOMS AND THE ZERO-POINT ENTROPY

II. CHANGE IN CONFIGURATION AND MOLECULAR TURNS

III. IONISATION OF ICE AND MOLECULAR TURNS PRODUCED BY THE IONS. THE PROTON JUMP CONDUCTIVITY OF ICE (AND WATER)

BY

NIELS BJERRUM

København

i kommission hos Ejnar Munksgaard

1951

FOTOGRAFISK OPTRYK
S. L. MØLLERS BOGTRYKKERI, KØBENHAVN

I

THE POSITION OF THE HYDROGEN ATOMS AND THE ZERO-POINT ENTROPY OF ICE

1. Historical introduction.

In the middle of the thirties, a certain finality appeared to have been reached with regard to the opinion on the structure of ice. BARNES[1]) had shown that the oxygen nuclei lay in puckered hexagonal layers, in which oxygen atoms were raised and lowered alternately (see fig. 1). Adjacent layers were mirror-images and

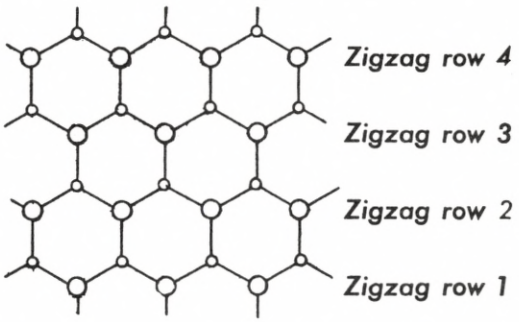

Fig. 1. Projection of a layer of oxygen atoms in an ice crystal. The small circles are oxygen atoms below the level of the paper, and the large circles, oxygen atoms above the level of the paper.

the parameters were adjusted so that each oxygen nucleus was surrounded by 4 oxygen nuclei in a regular tetrahedral arrangement at a distance of 2.76 Å. BERNAL and FOWLER[2]) had shown that it is probable that the *protons* lie on the linkages between the oxygen nuclei, ca. 1 Å. from one and 1.76 Å. from the other. One and only one proton lies on each linkage, and the arrangement is such that each oxygen nucleus has two and only two protons at a distance of ca. 1 Å. from it. In this way the ice is built up of molecules closely approaching the form and size, which MECKE[3]) has calculated for the molecule of water vapour from the infra-red spectrum (isosceles triangle with the oxygen nucleus at the apex, apical angle ca. 106° and sides 0.97 Å.). An

extremely large number of such proton arrangements are possible. BERNAL and FOWLER tended to assume that the arrangement in ice was irregular, in any case in the region of the melting point. They write: "In that case ice would be crystalline only in the position of its molecules, but glass-like in their orientation."

Finally, in 1935 PAULING[4]) pointed out that DEBYE's investigations on the dielectric properties of ice showed that the configuration of ice must alternate between the many alternatives given by BERNAL and FOWLER. PAULING calculates the number of possible configurations of an ice crystal to $(^3/_2)^N$, where N is the number of molecules in the crystal, and by assuming that all these configurations, even at low temperature, are equally probable, he arrives at the result that ice must have a zero-point entropy of $k\,ln(^3/_2)^N = R\,ln(^3/_2) = 0.806$ kcal/gmol/degree. This value agrees extremely well with the value of 0.82 ± 0.15 kcal/gmol/degree found experimentally by GIAUQUE[5]). On account of this excellent agreement, the problem of the structure of ice had since generally been considered as solved.

The way in which PAULING develops his formula for the number of configurations only gives the formula as an approximation. PAULING considers the proton-condition for a first, randomly chosen, oxygen atom in the lattice, while an exact development requires that also, and especially, the conditions for the other atoms should be considered. For these the proton-position in the direction of the previously considered adjacent atoms is already defined.

An exact development of the formula can be obtained in the following way: We have an ice crystal, in which the position of all the oxygen atoms is known, and we will now determine the number of possible proton configurations. Let us imagine that we have decided on the proton configurations around all the oxygen atoms in and beneath one of the puckered hexagonal layers. Let us furthermore assume that we have decided on the situation around the oxygen atoms in a zig-zag row above this layer, and are now going to investigate the number of configurations during the construction of an adjacent zig-zag row. It can easily be seen that, if the crystal is large, it is only the conditions during this construction that must be investigated in order to solve the problem. We will now choose to place the new zig-zag

row at that side of the first, where the low-lying molecules are present. In fig. 1, this means that the new zig-zag lines must be placed in the order 1, 2, 3, 4. When we do this, the new oxygen atoms, for which the proton configuration must be decided, will always have two adjacent atoms already in position, for which the configuration is decided. If these two adjacent atoms both have protons in the direction towards the atom considered, or if they both have no protons in this direction, then the proton placing around the atom considered is unambiguously decided. On the other hand, if the proton situation is different towards the two adjacent atoms, the proton placing can be performed in two ways.

Let us call the number of configurations in the system so far constructed, $A + B$, where A is the number of configurations, in which the two adjacent atoms show the same proton situation, and B, the number of configurations in which they show different proton situations towards the new oxygen atom. Hence the number of possible configurations rises from $A + B$ to $A + 2B$, when this atom is included in the system. Around each oxygen atom, and hence also around the oxygen atom last added, two protons can be placed in six different ways. In the group of configurations, the number of which we have calculated above to be $A + 2B$, the 6 ways occur in the following numbers: $A/2$, $A/2$, $B/2$, $B/2$, $B/2$ and $B/2$. Since, for reasons of symmetry, these numbers must be equally large, A must be equal to B. As a result, the number of possible configurations for each oxygen atom in the ice crystal rises in the ratio $(A + 2B)/(A + B) = {}^3/_2$ and the total number of configurations becomes $({}^3/_2)^N$.*

2. Mirror symmetric and centric symmetric atom pairs in ice.

In PAULING's calculation of the zero-point entropy of ice it is assumed that all the possible configurations are so similar in energy that, even at the temperature at which they are fixed by freezing, they can be considered as equally probable. PAULING

* The demonstration given above is the result of a correspondance with PAULING. For the valuable help, which I have thus received, I wish to offer professor PAULING my best thanks.

expressed this (in "Nature of Chemical Bond" 2nd ed. 1945 p. 302) in the following words: "and that under ordinary conditions the interaction of non-adjacent molecules is such as not to stabilize appreciably any one of the many configurations satisfying these conditions with reference to the others." The excellent agreement found by PAULING between the calculated and the found zero-point entropy of ice made such a great impression that this assumption was accepted without any serious examination. It is, however, possible that too great emphasis has been laid on this agreement. GIAUQUE's value for the zero-point entropy occurs as a small difference between two large values: GORDON's[6]) spectroscopic value for the entropy of water vapour at 25° C and 1 atmos. (45.1 ± 0.1) and GIAUQUE's[5]) thermically determined value for the difference between the entropy of water vapour at 25° C and 1 atmos. and of ice at 0° K (44.28 ± 0.05). It is perhaps possible that these values are not so accurately determined as the authors themselves think. In addition to the random errors, which are given in the above expressions, there may be systematic errors. We will therefore now try to investigate whether the assumption of PAULING has been justified.

As an introduction to the investigation of the energy content of the different configurations, we will attempt to find an explanation for the reason why ice crystallizes differently from diamond, although the arrangement of the 4 adjacent atoms around an atom is the same in both cases, when we consider only the carbon and oxygen atoms and disregard the protons. The difference between the two arrangements can first be seen, when the six adjacent atoms around an atom pair are considered. The same circumstances, which cause the oxygen atoms in ice to be arranged in another way than the carbon atoms in diamond, can also be expected to make the configurations in ice energetically different.

In diamond, the arrangement around an atom pair is always *centre symmetric* (see fig. 2). If the 6 adjacent atoms are projected onto a plane at right angles to the linkage between the two atoms, the 6 atoms form a regular hexagon.

In an ice crystal, the arrangement around oxygen atom pairs, which lie in the same puckered hexagonal layer, is centre symmetric, as in diamond; but around atom pairs, whose atoms lie

in different layers, the arrangement is *mirror symmetric* (see fig. 2). If the 6 adjacent atoms are projected onto a plane perpendicular to the linkage between the two atoms, the adjacent atoms coincide in pairs. In ice $^1/_4$ of the atom pairs are in mirror symmetric and $^3/_4$ in centric symmetric positions. It is probably not possible

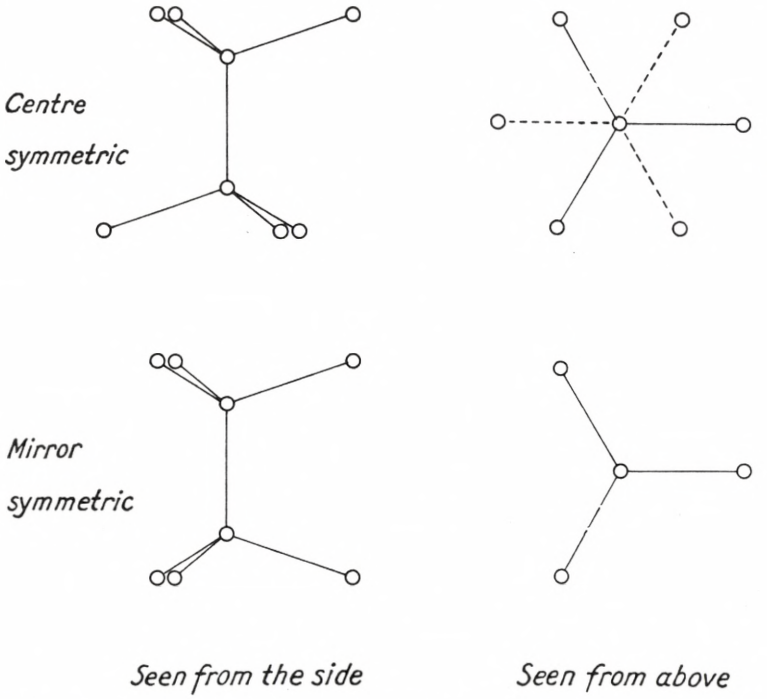

Fig. 2. Centre symmetric and mirror symmetric positions of oxygen atoms in ice.

to construct a crystal in which more than $^1/_4$ of the atom pairs are in mirror symmetric positions, if the arrangement around all the atoms is to be regularly tetrahedral. In an ice crystal, there are presumably as many mirror symmetric atom pairs as possible present.

The centric symmetric arrangement in diamond can be explained as a result of the repulsion between the electrons around the 6 adjacent atoms. But why does the mirror symmetric arrangement occur in ice and even in as high a proportion as possible? This suggests that the mirror symmetric position for water molecules is more stable and poorer in energy, than the centric sym-

metric. If this is actually the case, then the distance between the atoms in mirror symmetric atom pairs ought to be less than the distance between atoms in centric symmetric atom pairs.

Accurate measurements on ice crystals have been carried out by HELEN D. MEGAW[7]). She made her measurements in order to investigate whether there was a difference between ice from heavy and from light water, but she found no difference. From her measurements it is possible to calculate the ratio c/a between the hexagonal main axis and the secondary axes perpendicular to the main axis to 1.6283, varying between 1.6276 and 1.6287 for both heavy and light ice. In the ideal structure, with equally large distances and equally large angles everywhere, the ratio is $c/a = \sqrt{\frac{8}{3}} = 1.6330$. The deviation from this figure is small, but must be considered as indubitably significant. If the deviation is to be explained by differences in atomic distances, the distances in mirror symmetric atom pairs must be 0.55 % shorter than the distance in centre symmetric atom pairs. $\left(\left(\frac{2}{3}+2x\right) : \sqrt{\frac{8}{3}} = 1.6283\right.$ gives $x = 0.9945$). A little of the deviation may perhaps be explained by inequality in the angles between the linkages of the atoms; but this inequality can scarcely be considerable, since no reasonable cause for this can be seen. The mirror symmetric linkages must therefore be several $^1/_{10}$ % shorter than the centre symmetric. In consideration of the slight compressibility of ice ($1.2 \cdot 10^5$ per bar) this is not an inconsiderable difference.

If the mirror symmetric linkage between the H_2O molecules is shorter than the centric symmetric, this linkage must also be more stable and poorer in energy than the centric symmetric. This gives us a cause for the fact that ice crystallizes hexagonally and not regularly.

3. An electrical model of the H_2O molecule.

One may well ask, why the mirror symmetric linkage is firmer than the centric symmetric. In order to attempt to find an explanation for this, we will consider the forces which hold the molecules together in ice crystals. A H_2O molecule is an electrical dipole. Assuming that electrostatic forces hold the molecules

together in ice just as electrostatic forces are responsible for holding the ions together in sodium chloride, we will attempt to calculate, from plausible assumptions, the electrostatic internal energy.

Our assumption is not a contradiction of the general practice of designating the bonds between molecules in ice as hydrogen bonds. The so-called hydrogen-bonds must principally be considered to be of electrostatic nature.

In order to calculate the effect of the electrostatic forces between molecules of ice, we must construct an electrical model of a water molecule. We know that the *positive* charges on the nuclei form an isosceles triangle with the oxygen nucleus at the apex and the two protons on the base line. In the water vapour molecule, according to MECKE[3]) the sides are 0.97 Å., but in the molecules of ice, according to CROSS, BURNHAM and LEIGHTON[8]) and PAULING[4]) they are slightly larger, ca. 0.99 Å. The apical angle in the water vapour molecule, according to MECKE, is ca. 106°, hence nearly equal to the tetrahedral angle 109.5°. Even if it is not certain that the protons in an ice crystal lie exactly on the linkages between the oxygen atoms, they must lie very close to them, and in our model, we will assume that they lie on the linkages (fig. 3a). The three nuclei are encircled by 10 *electrons*. Two of the orbits are quite close to the oxygen nucleus at the apex, and the 8 remaining electrons circle in pairs in 4 eccentric orbits, which radiate tetrahedrally from the oxygen nucleus (comp. BARNES[1]), MULLIKEN[9]) and BERNAL and FOWLER[2])) (fig. 3b). The two protons lie within two of these eccentric orbits. The electron orbits completely screen the positive charge of the oxygen nucleus. They also screen a considerable part of the charge of the protons, but give an excess of negative charge in the two eccentric orbits which do not contain protons. We will therefore consider an ice molecule from the electrostatic viewpoint as a regular tetrahedron of radius 0.99 Å. with positive charges in two corners and negative charges in the other two (figs. 3c and 3d). As we shall see later, it is of little importance for our calculations whether the tetrahedron-model should in fact have deviated somewhat from regularity.

It is known from measurements of the dielectric constant of

water vapour that the dipole moment of the water molecule is 1.87 Debye. If the tetrahedral model is to have this dipole moment, the electrical charges in the corners must be $\pm$ 0.171 e (e = the electronic charge). Hence the electrons screen most of the electrical charge of the protons, and only give small negative charges in the remaining corners. In ice these tetrahedra are placed

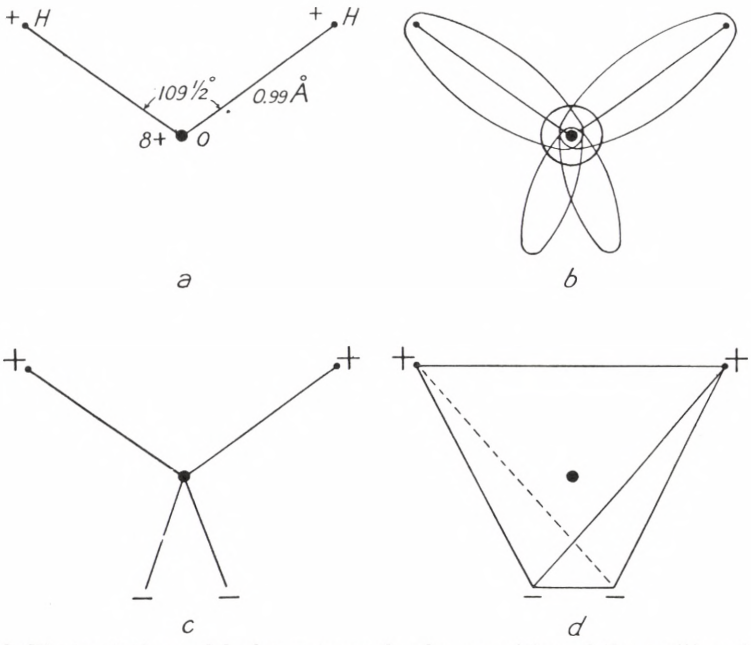

Fig. 3. Electrostatic model of a water molecule: *a* position of the positive charges in a molecule, *b* the electron orbits, *c* and *d* two different representations of the regular tetrahedron model used.

at a mutual distance of 2.76 Å., calculated from their centres. We will therefore imagine an ice molecule as a sphere of radius 1.38 Å., inside which 4 electrical charges are placed in a regular tetrahedral arrangement, as described above.

This molecular model of course only represents a rough approximation to the actual molecule with the negative electricity of the electrons distributed over large volumes. The simplicity of the model, however, permits many calculations to be performed with it, and if these give results, which agree with experience, it is probable that the model gives us a good representation of the electrical structure of the H_2O molecule.

4. The electrostatic energy between adjacent molecules in ice.

Two adjacent molecules in ice can have 6 different positions relative to each other. These are presented in figure 4. Position no. 1 can suitably be designated as *inverse* mirror symmetric (ms_1) because the electrical charges at symmetrical places have

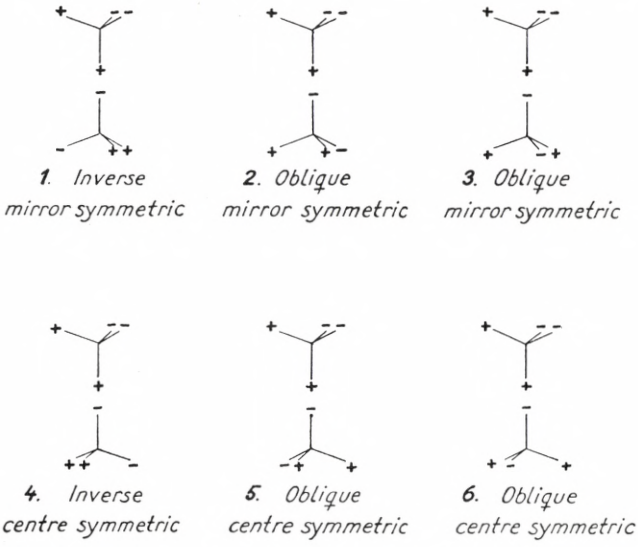

Fig. 4. The 6 positions relative to each other of two adjacent molecules in ice.

opposite signs. No. 2 and no. 3 are energetically alike and can be designated as *oblique* mirror symmetric (ms_2 and ms_3).

Similarly, two molecules in centric symmetric positions can have three different relative positions (see fig. 4). No. 4 will be designated as *inverse* centric symmetric (cs_1) because the electrical charges at symmetrical places have opposite signs. The two remaining (no. 5 and no. 6) are energetically alike and can be designated as *oblique* centric symmetric (cs_2 and cs_3).

The electrostatic energy, to be overcome on separating two electrical molecular models (A and B) is $E_{AB} = (0.171\ e)^2 \Sigma\, 1/r$, where r is the distance between two charges, and the summation must include all 16 combinations of two charges, one from each molecule.

These energies are given in table 1, column 2, headed tetrahedron, $r = 0.99$ Å. It can be seen that the energy is rather different for the 4 possible positions. These E_{AB} values given in italic type are those with which we shall deal in the following section.

TABLE 1.

Electrostatic energies E_{AB} between adjacent molecules in ice, given in 10^{-12} erg.

	Tetrahedron					triangle
	$r =$ 0.99 Å	$r =$ 0.69 Å	$r =$ 0.46 Å	$r =$ 0.276 Å	infinit. small	$r =$ 0.99 Å
Mirror sym. inverse (ms_1) . .	*0.5067*	0.312	0.261	0.240	0.220	0.387
— — obliq. (ms_2, ms_3)	*0.4319*	0.217	0.144	0.105	0.055	0.309
Centric sym. inverse (cs_1). . .	*0.4117*	0.191	0.111	0.058	0.000	0.290
— — obliq. (cs_2, cs_3).	*0.4792*	0.279	0.233	0.195	0.165	0.355

In order to obtain some idea of the significance of taking the radius to be 0.99 Å., the other columns in table 1 give the energies for smaller tetrahedra ($r = 0.69$, 0.46 and 0.276 Å. respectively) and for an infinitely small dipole. In all cases, it was of course assumed that the electrical charges had such a size as to give the dipole moment 1.87 Debye. It will be seen that the energy falls, when the model is made smaller. The fall is initially rapid, but later becomes slow. On the other hand, the differences between the energies of the different positions increase, but this increase is rather slow. The figures show the importance of not being satisfied with assuming an infinitely small dipole, but using a more developed picture of the distribution of the charges.

The last column in table 1 shows the energy values obtained by using as model a triangle with apical angle 109.5° and sides 0.99 Å., and with two equally large charges (0.342 e) placed on the base, and a negative charge, twice as large (—0.684 e) at the apex. It can be seen that this triangular model gives slightly less energy than a tetrahedron of radius 0.99 Å., but the differences between the energies are about the same. Triangular models, placed in the tetrahedral orientation, which is, however, not very

probable for them, thus give similar energies as tetrahedron models. Hence it may be concluded that the results, drawn from the following discussion, would not have been altered appreciably, if another tetrahedral model had been used, in which the two negative charges had been moved slightly nearer to the centre and the tetrahedron had thus not been regular. It would have been reasonable to use such a model, if it had not made the calculations more difficult.

BERNAL and FOWLER[2]), who first tried to calculate the electrostatic energies of ice crystals, used, for their calculations, a triangular model with positive charges (0.49 e) on the base and a negative charge, twice as large, placed on the bisector of the apical angle, slightly below the apex. This model does not fit our views on the electrons in the water molecule, and can not explain the tetrahedral layering of the molecules in ice. It is not easy to see why BERNAL and FOWLER have used this triangular model. They themselves point out the tetrahedral placing of the 8 external electrons of the molecule and the possibility of using this to explain the tetrahedral grouping of the molecules in ice.

5. The electrostatic lattice energy of ice crystals.

The differences between the energies of inverse and oblique positions are, according to table 1, considerable:

$$E_{AB}ms_1 - E_{AB}ms_2 = 0.0748\ 10^{-12}\ \text{erg.}$$
$$E_{AB}cs_2 - E_{AB}cs_1 = 0.0675\ 10^{-12}\ \text{erg.}$$

Since, at 273° K, kT is equal to 0.0374×10^{-12} erg., it must be expected that at the melting point ms_1-positions will be present in greater amount than ms_2 and ms_3 and that cs_2- and cs_3-positions will be present in greater amount than cs_1-positions, and the preferences must be expected to be even more pronounced at lower temperatures. The size of this temperature dependence will be considered later. We will here just assume that at low temperature the inverse position (ms_1) will be predominant among the centric symmetric, while at high temperature the inverse and the two oblique positions will approach equal probability.

This result is not in opposition to the observations made by

WOLLAN, DAVIDSEN and SHULL[10]) on the diffraction of neutron beams. These authors have shown that in ice "on the average two hydrogen atoms will be found close to a given oxygen atom", and that the arrangement on the whole is irregular. This does not contradict the view given above, as according to that view there should be no periodic regularities in the placing of the protons in the crystal lattice of ice.

At low temperature the mean electrostatic lattice energy between adjacent molecules in an ordinary *hexagonal* ice crystal will be in mean $^1/_4\, E_{AB} ms_1 + {}^3/_4\, E_{AB} cs_2$ and at high temperature (which, however, is far from being reached at the melting point of ice) it will be: $^1/_{12}\, E_{AB} ms_1 + {}^1/_6\, E_{AB} ms_2 + {}^1/_4\, E_{AB} cs_1 + {}^1/_2\, E_{AB} cs_2$. In a hypothetical ice crystal with diamond structure, in which all positions are centric symmetric, the electrostatic energy between adjacent molecules would be in mean: at low temperature $E_{AB} cs_2$ and at high temperature $^1/_3\, E_{AB} cs_1 + {}^2/_3\, E_{AB} cs_2$. The total lattice energy between all adjacent molecules is obtained by multiplying these mean values by $2N$, where N is the number of molecules. In table 2 are presented the lattice energies thus calculated, given in kcal/gmol.

TABLE 2.

The electrostatic lattice energy of ice crystals, calculated from the energies between adjacent molecules.

	Ordinary hexagonal ice crystal	Hypothetic ice crystal with diamond structure
At low temperature	14.04 kcal/gmol.	13.88 kcal/gmol.
At high temperature	13.21 —	13.23 —

The electrostatic lattice energy must be assumed to constitute the main part of the heat of sublimation of ice. The values for hexagonal ice in table 2 are somewhat higher than the experimentally determined heat of sublimation of ice: 12.14 kcal/gmol at 0° C. In order to obtain from the electrostatic lattice energy an accurate value for the heat of fusion of ice, it is, however, necessary to subtract the potential of the repulsive forces, which hold the molecules in place at a distance of 2.76 Å. and to add the potential of the VAN DER WAAL's forces, hence a better agree-

ment could scarcely be expected. BERNAL and FOWLER[2]) have shown that it is possible to obtain a heat of sublimation of the right order of magnitude by electrostatic calculation from their triangular molecular model. Using their estimated corrections for the repulsive forces (— 6.8), for the VAN DER WAAL's attraction (+ 4.1) and for the attraction of next neighbours (+ 1.1), the latter however with opposite sign, we calculate for the heat of sublimation of ice:

at low temperature ..... 14.0 — 6.8 + 4.1 + 1.1 = 12.4
at high temperature ..... 13.2 — 6.8 + 4.1 + 1.1 = 11.6

The electrostatic lattice energies in table 2 give us a possibility of obtaining a better understanding of the reason why ice crystallizes hexagonally and not as diamond cubically. Admittedly the energies at high temperature are practically speaking the same for the hexagonal and for the cubic lattice, but at low temperature the lattice energy is 0.16 kcal/gmol higher for the hexagonal than for the cubic lattice, and as we shall see later, the melting point of ice must, in this connection, be considered as a low temperature. A difference in the lattice energies of 0.16 kcal/gmol is perhaps rather small to explain why the hexagonal lattice is to be preferred; however, it will later be shown that the difference increases to 0.42 kcal/gmol, when the electrostatic energies between molecules, which are separated by a single molecule, (next neighbours) are taken into consideration (table 4). For polymorphous compounds having a temperature of transformation in the region of ordinary temperatures, the heat of transformation is often no greater. Thus the heats of transformation between the different known modifications of ice lie within values of from 0.016 to 0.304 kcal/gmol, and the heats of transformation for the solid modifications: of HCl is 0.248, of HBr 0.165 and 0.113, of HJ 0.126 and of H_2S 0.108 and 0.361. For NH_4Cl the two heats of transformation have been found to be: 0.200 and 0.427, for NH_4NO_3 0.402 and for $CaCO_3$ 0.30, all figures in kcal/gmol and according to Landolt-Börnstein, 3rd suppl. The heat of transformation for transformation of rhombic sulphur to monoclinic sulphur is 0.84. The molecule of sulphur is, however, also rather large, S_8.

6. The electrostatic energies between molecules of ice, which are separated by one or more molecules.

The electrostatic energies between molecules which are not adjacent have been ignored in the considerations so far described. However, the orientation of the other molecules around an adjacent molecular pair may be dependent on whether this pair is in centric symmetric or mirror symmetric position and whether this position is inverse or oblique. It is therefore possible that the electrostatic energies of the surrounding molecules could neutralize the differences in energy found for the 4 different positions of a molecular pair. If this was the case, the inverse and the two oblique positions would be equally probable and the proportion between them would be independent of temperature. We will therefore examine the electrostatic energies between molecules which are not adjacent, more closely.

The electrostatic energies (E_{AC}) between two molecules, (A and C), which are separated by a single molecule (B), are far lower than the energies E_{AB} between adjacent molecules, and the electrostatic energies (E_{AD}) between two molecules (A and D), which are separated by two molecules (B and C), are even lower still. These molecules lie farther from each other and they are in addition more randomly orientated. A completely random orientation would reduce their contribution to zero.

Table 3 gives the result of a calculation of the electrostatic energies (E_{AC}) between molecules, which are separated by one molecule.

The three molecules A, B and C can have a total of 72 different positions relative to each other. The energy for all these positions can be read off in the table.

A and C present either a positive or negative corner to B. Since the energy of the system can not be changed, when we invert all charges, however, we only need to examine the two possibilities: that A and C present differently charged corners to B and that they present similarly charged corners to B. In the first case, when the energy is positive, we will designate the position as an a-position, and in the other case, when the energy is negative, as a b-position. In ice, A and C must either both be in centric symmetric (cs) position to B, or one must be in centric symmetric

TABLE 3.

Electrostatic energies E_{AC} between two molecules (A and C) in ice, separated by one molecule (B), given in 10^{-12} erg.

A and C's position to B	a	b	A and C's position to B	a	b
cs_1 cs_1	0.0267	−0.0450	cs_1 ms_1	0.0439	−0.0151
cs_1 cs_2	0.0611	−0.0300	cs_1 ms_2	0.0194	−0.0451
cs_1 cs_3	0.0300	−0.0300	cs_1 ms_3	0.0516	−0.0451
cs_2 cs_1	0.0611	−0.0300	cs_2 ms_1	0.0194	−0.0516
cs_3 cs_1	0.0300	−0.0300	cs_3 ms_1	0.0451	−0.0516
cs_2 cs_2	0.0267	−0.0267	cs_2 ms_2	0.0439	−0.0439
cs_2 cs_3	0.0300	−0.0611	cs_2 ms_3	0.0516	−0.0194
cs_3 cs_2	0.0300	−0.0611	cs_3 ms_2	0.0451	−0.0194
cs_3 cs_3	0.0450	−0.0267	cs_3 ms_3	0.0151	−0.0439

and the other in mirror symmetric (*ms*) position to *B*. Of the 6 *AC* pairs around a *B* molecule, 3 are *cs-cs* and 3 *cs-ms*. Finally, both for *cs-* and *ms*-positions there are 3 possibilities: an inverse position (cs_1 and ms_1) and two oblique positions (cs_2 and cs_3, ms_2 and ms_3). The symbol $b\,cs_1\,ms_2$ denotes a position, in which *A* and *C* present similarly charged corners to *B*, and *A* is in inverse centric symmetric position to *B*, while *C* is in oblique mirror symmetric position to *B*. Since the two oblique positions in the asymmetric *ABC*-system are no longer necessarily energetically alike, we must now differentiate between them.

This is done in the following way. When a molecule (*A*), as seen from an other molecule (*B*), must be turned through 120° *clockwise* in order to obtain an inverse position to it, we will denote the position as a 2-position (cs_2, ms_2). When the same effect is obtained by turning it 120° *counterclockwise*, we will call the position a 3-position (cs_3, ms_3). For *a*-positions it is furthermore necessary to clear that the charges of the *B* molecule must be placed so that by turning the *B* molecule 120° clockwise, seen from *A* (or *C*) around an axis through the *A* (or *C*) molecule, the corner towards *C* (or *A*) is brought over to a corner with the same sign. Let us denote the other possibility as an *a'*-position. On mirroring and subsequent inversion of an *A B C*-system, 2-positions are changed to 3-positions, 3-positions to 2-positions and *a*-positions to *a'*-positions. Since mirroring and inversion do not change the energy, we need not consider *a'*-positions especially. A *b*-position on inversion becomes a *b*-position again.

A control of the correctness of the calculations is obtained in

the following way. It can be shown that the following rule is valid: the E_{AC}-value for an a-position is numerically equal to the E_{AC}-value for a b-position, if the indices are calculated for the a-positions according to the following rule: $1 \rightarrow 2$, $2 \rightarrow 3$, $3 \rightarrow 1$.

7. The electrostatic lattice energy of ice crystals calculated with consideration of the energies between non-adjacent molecules.

Six molecules are connected with a pair AB of adjacent molecules. We consider the E_{AC}-values of these 6 C-molecules correctly if we add half of their 6 E_{AC}-values to the E_{AB}-value in question. When calculating the lattice energy of the whole crystal from E_{AB}-values, each E_{AC}-value will be accounted for by two adjacent molecular pairs (AB and BC). The calculation of such corrected E_{AB}-values is made difficult by the fact that the ratio between inverse and oblique positions depends on the temperature. In the following section, the calculation is performed for the two limiting cases, corresponding to high temperature and to low temperature. By high temperature we understand here a temperature at which the inverse and oblique positions, in spite of their different energies, are equally probable, not only within whole ice crystals, but also within the different types of positions (a and b, cs and ms). (This state, however, is far from being reached at the melting point of ice). By low temperature we understand a state in which inverse positions are quite predominant among ms-positions, and oblique positions are quite predominant among cs-positions (comp. table 6).

Around a mirror symmetric molecular pair in an ordinary hexagonal ice crystal, all AC-positions will be of the type cs-ms, and $^2/_3$ of them will be a-positions, and $^1/_3$, b-positions. Around a centric symmetric molecular pair 4 positions will be of cs-cs type and two of cs-ms type. Of the 6 positions, $^2/_3$ will be of the a-type, and $^1/_3$ of the b-type, and we will assume that this is also true within the cs-cs group and the cs-ms group.

If this assumption should not be justified, it will only serve to increase the inaccuracy of the assumption that all $(^3/_2)^N$ configurations of an ice crystal are equally probable.

By using the E_{AC}-values in table 3 and the E_{AB}-values in table 1, the corrected E_{AB}-values (E_{AB} cor.) presented in table 4 are obtained.

If these corrected E_{AB}-values are used in place of those previously used, the electrostatic energies between molecules, which are separated by a single molecule, are taken into consideration in the correct way.

TABLE 4.

Electrostatic energies between two adjacent molecules in ice, corrected for the E_{AC}-values of the adjacent 6 molecules. The values are given in 10^{-12} erg.

A. Ordinary *hexagonal* ice crystal.

	E_{AB}	$6/2\, E_{AC}$	E_{AB} cor.
1. At *low temperature.*			
AB mirror sym. inverse (ms_1)	0.5067	0.0129	0.5196
AB — — oblique (ms_2, ms_3)	0.4319	0.0462	0.4781
AB centric sym. inverse (cs_1)	0.4117	0.0415	0.4532
AB — — oblique (cs_2, cs_3)	0.4792	0.0351	0.5143
2. At *high temperature.*			
AB mirror sym. inverse (ms_1)	0.5067	0.0328	0.5395
AB — — oblique (ms_2, ms_3)	0.4319	0.0394	0.4713
AB centric sym. inverse (cs_1)	0.4117	0.0430	0.4547
AB — — oblique (cs_2, cs_3)	0.4792	0.0351	0.5143

B. Hypothetical ice crystal with diamond structure.

	E_{AB}	$6/2\, E_{AC}$	E_{AB} cor.
1. At *low temperature.*			
AB centric sym. inverse (cs_1)	0.4117	0.0611	0.4728
AB — — oblique (cs_2, cs_3)	0.4792	0.0220	0.5012
2. At *high temperature.*			
AB centric sym. inverse (cs_1)	0.4117	0.0435	0.4552
AB — — oblique (cs_2, cs_3)	0.4792	0.0351	0.5143

The results of similar calculations for a hypothetical ice crystal with diamond structure are also given in table 4. At low temperature it is assumed that the majority of positions is oblique

(cs_2 and cs_3) and at high temperature that the positions cs_1, cs_2 and cs_3 are equally frequent.

Calculations on the energies between molecules, which are separated from each other by two or more molecules, would be almost impossible to perform. The energies E_{AD} between molecules A and D, which are separated by the two molecules B and C, will, however, only contribute a very small effect, and the effect will tend to make the differences between the 4 "corrected" E_{AB} slightly larger. This can be estimated by considering systems of 4 consecutive molecules A, B, C, D, the outermost molecules of which are simplified to real dipoles by coalescence of the three outermost charges in the tetrahedral models to a single charge at the centre of the triangle formed by the corners at which they are placed. It is permissible to make this approximation when it may be assumed that the three ways in which the three charges can be placed are equally probable. Molecules, separated from each other by more than three molecules, will be so randomly orientated with respect to each other that their mutual internal energy can be considered as being, on the average, insignificant.

With the corrected E_{AB} from table 4, the following differences between the energies for inverse and oblique positions are obtained, (the figures expressed in 10^{-12} erg):

	With corrected E_{AB}-values		Previous calculation with uncorrected E_{AB}-values
	Low temp.	High temp.	
$E_{AB}ms_1$—$E_{AB}ms_2$	0.0415	0.0682	0.0748
$E_{AB}cs_2$—$E_{AB}cs_1$	0.0611	0.0594	0.0675

It will be seen that consideration of the E_{AC}-values has made the differences less. It is, however, only the difference between the two types of *ms*-bonds, which has become appreciably less, and only at low temperature. The differences are still larger than kT at 0° C (0.0374×10^{-12} erg). Our previous considerations on the predominance of inverse positions among *ms*-positions and oblique positions among *cs*-positions, are therefore still valid.

If the electrostatic lattice energy is calculated (by the method given on p. 14) from the corrected E_{AB}, the figures given in table 5 are obtained.

TABLE 5.

The electrostatic lattice energy of ice crystals, calculated from the corrected E_{AB}-values given in table 4.

	Ordinary hexagonal ice crystal	Hypothetical ice crystal with diamond structure
At low temperature	14.93 kcal/gmol	14.51 kcal/gmol
At high temperature	14.32 —	14.32 —

These electrostatic lattice energies are about 1 kcal higher than those calculated in table 2. At high temperature the difference between the lattice energies for hexagonal and for cubic ice is, as in the previous calculations, extremely small, but at low temperature the lattice energy for hexagonal ice is 0.42 kcal higher than for cubic ice. According to the previous calculation it was only 0.16 kcal higher. The new higher value makes it easier to understand the reason why ice crystallizes hexagonally and not cubically. Even at the melting point of ice, as we shall see later, ms_1- and cs_2- and cs_3-positions are so predominant that the lattice energy must be assumed to lie nearer to that calculated for low temperature than to that calculated for high temperature.

8. Quantitative calculation of the percentage of inverse and oblique positions.

Difficulties are encountered in exact calculation of the amount of inverse and oblique positions in ice. As an approximation, we will try to express the probability of the different positions by a BOLTZMANN e-function:

$$W = e^{-E/kT}$$

where E is the energy of the position. If no correlation existed between positions of pairs close to one another, it can be shown that this formula is correct. There is, however, a considerable correlation; this appears from the fact that, without correlation, the number of configurations of an ice crystal should be 3^{2N}, while it is actually only $(^3/_2)^N$. We may hope that, nothwithstanding this, the formula will be a useful approx-

imation. Using the corrected E_{AB}-values* from table 4, we have calculated the percentages of the 4 different positions at four different temperatures. The results are given in table 6.

TABLE 6.

Calculated percentages of inverse and oblique positions in ice.

	273° K	136.5° K	90° K	68.25° K
Inverse *ms*-positions	68.4 %	90.4 %	97.7 %	99.44 %
Oblique *ms*-positions	31.6 -	9.6 -	2.3 -	0.56 -
Inverse *cs*-positions	9.1 -	2.0 -	0.38 -	0.08 -
Oblique *cs*-positions	90.9 -	98.0 -	99.62 -	99.92 -

The figures in table 6 show that, even at the highest possible temperature, the melting point, the ratio between inverse and oblique positions is still far from being the statistical ratio 1:2. At the boiling point of liquid air (90° K) only about 1 per cent of the oblique mirror symmetric and inverse central symmetric positions remain.

When the figures in table 6 are used, it must not be forgotten that they are rather uncertain; partly because they rest on the assumption of a rough molecular model, and partly because the forces between molecules, which are not adjacent molecules, are only considered incompletely, and finally because the use of BOLTZMANN's equation is only an approximation. On the whole, however, the figures are to be considered as a useful approximation.

9. The effect of temperature on the rate at which the equilibrium between inverse and oblique positions is reached.

The equilibrium between the energetically different inverse and oblique positions must be reached very rapidly at the melting point of ice. This can be concluded from the fact that the heat of fusion of ice has a very well defined size (1.4357 $\pm$ 0.0009

* It is preferred to use the mean of the values corresponding to high temperature and to low temperature. The corrections for the E_{AD} values have such a sign that it seems reasonable to use mean values in place of values nearer to the low temperature values.

kcal/gmol. Cf. also the use of the ice calorimeter). If only 0.1 per cent of the positions are changed from inverse to oblique, this would change the heat of fusion by 0.0012 kcal/gmol, hence more than the indicated uncertainty of the determination.

If the temperature is lowered, a temperature range will finally be reached, at which the equilibrium between the positions of the molecules freezes in. MURPHY[11]) has given some observations on how cooling of an electrically polarized ice crystal to the temperature of liquid air (90° *K*) freezes a permanent dipole moment into it. This shows that at this temperature the molecules in ice have ceased to change their orientation. GIAUQUE and STOUT[5]), who have carried out very accurate measurements on the heat capacity of ice down to very low temperatures, write: "At temperatures between 85 and 100° *K* the attainment of thermal equilibrium in the solid was very much less rapid than at other temperatures. For this reason the heat capacity measurements in this region are somewhat less accurate than the others." This slow attainment of equilibrium is, according to them, presumably due to the initial stages of excitation of some new degrees of freedom. They suspect that these new degrees of freedom are associated with the dipole orientation mechanism. It is tempting to explain slow attainment of equilibrium as due to fixation by freezing of the equilibrium between inverse and oblique positions. According to table 6, in this temperature range the energetically preferred positions are already so predominant (they constitute about 99 %) that it might seem reasonable to suppose that differences in the fixation of the configuration by cooling have had a perceptible, but only slight influence. In order to investigate this, a theoretical calculation of the specific heat of ice is given and is compared with experimental data in the following chapter.

10. The heat capacity of ice.

In ice the H_2O molecules can be considered as rigid systems, vibrating and oscillating without undergoing changes themselves (the slowest atomic oscillation in a H_2O molecule (1590 cm^{-1}) contributes, even at the melting point, only 0.03 to the heat capacity

(C_v in cal/mol/degree) according to EINSTEIN's function). Thus the ice molecules only contain heat energy in the form of "hindered translations" and "hindered rotations", we will call these movements *vibrations* and *oscillations*, respectively.

From the RAMAN spectrum of ice [8]) we know that the wave number of the vibrations is 210 ± 2 cm^{-1} and that of the oscillations 700—900 cm^{-1}. The observed frequency 210 ± 2 must be due to vibrations, as it changes in the ratio $\sqrt{18/20}$ from light to heavy ice, and the frequency 700—900, to oscillations as it changes in the ratio $\sqrt{1/2}$ from light to heavy ice. The spectroscopic vibration frequency is in good agreement with the frequencies calculated from the volume compressibility of ice. For the most rapid vibration in the direction of the main axis we have calculated 223 cm^{-1}, for vibrations perpendicular to the main axis and to the line between two adjacent molecules, 218 cm^{-1}, and for the vibrations perpendicular to the two former, 203 cm^{-1}. The calculations are carried out on the assumption that the forces between the molecules are pure central forces, not influenced by valency angle forces, and that the compressibility is the same in all directions.

A heat capacity of ice (C_v(Debye)) is calculated from the spectroscopic frequencies as the sum of three DEBYE functions [13]) corresponding to 210 cm^{-1} (C_v(210)) and three others corresponding to 800 cm^{1-} (C_v(800)). Table 7 contains the results.

TABLE 7.

Heat capacity of ice, determined spectroscopically.

$T°K$	C_v (210)	C_v (800)	C_v (Debye)
10.0	0.017	0	0.017
15.05	0.058	0.001	0.059
20.1	0.137	0.002	0.139
30.1	0.452	0.008	0.460
37.6	0.823	0.016	0.839
50.2	1.582	0.039	1.621
60.2	2.197	0.067	2.264
75.2	2.996	0.131	3.127
100.3	3.947	0.309	4.256
150.5	4.918	0.933	5.851
200.7	5.337	1.741	7.078
273	5.609	2.822	8.431

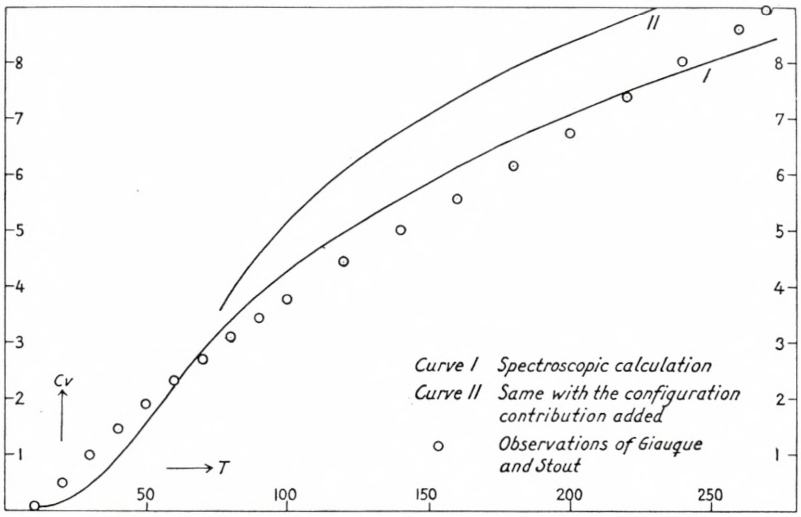

Fig. 5. Heat capacity of ice (C_v). Curve I: spectroscopic calculation. Curve II: Same with the configuration contribution added. ○: Determinations of GIAUQUE and STOUT.

In fig. 5 curve I represents the spectroscopically calculated values (C_v(Debye), and GIAUQUE and STOUT's[5]) experimental values for C_p (which do not deviate appreciably from C_v) are introduced as small circles. It can be seen that the general trend is not badly reproduced.

We will now calculate the contribution to C_v of the change in configuration in ice. Let α_{ms} be the fraction of mirror symmetric positions, which are oblique, Q_{ms} the difference in energy between inverse and oblique mirror symmetric positions and $C_v(ms)$ the contribution to C_v of the change of mirror symmetric positions from inverse to oblique. Using BOLTZMANN's e function as an approximation we obtain:

$$\frac{\alpha_{ms}}{1-\alpha_{ms}} = \frac{e^{-Q_{ms}/RT}}{2}, \qquad \frac{d\alpha_{ms}}{dT} = \frac{Q_{ms}}{RT^2} \cdot \frac{2\, e^{Q_{ms}/RT}}{(e^{Q_{ms}/RT}+2)^2},$$

$$C_v(ms) = \left(\frac{Q}{RT}\right)^2 \frac{Re^{Q_{ms}/RT}}{(e^{Q_{ms}/RT}+2)^2},$$

and similarly for centre symmetric positions (α_{cs} fraction of inverse positions):

$$\frac{\alpha_{cs}}{1-\alpha_{cs}} = 2\, e^{-Q_{cs}/RT}, \qquad \frac{d\alpha_{cs}}{dT} = \frac{Q_{cs}}{RT^2} \cdot \frac{2\, e^{Q_{cs}/RT}}{(2\, e^{Q_{cs}/RT}+1)^2},$$

$$C_v(cs) = \left(\frac{Q_{cs}}{RT}\right)^2 \frac{3\, Re^{Q_{cs}/RT}}{(2\, e^{Q_{cs}/RT}+1)^2}.$$

By introducing 0.793 and 0.871 kcal/gmol as values for Q_{ms} and Q_{cs} respectively, (mean of values for high and low temperatures) these equations lead to the contributions to the heat capacity given in table 8.

TABLE 8.

Contributions ($C_v(ms)$ and $C_v(cs)$) to the heat capacity of ice from the change of configuration with temperature. $Q_{ms} = 0.793$ and $Q_{cs} = 0.871$ kcal/gmol.

T	90° K	136.5° K	273° K
$C_v(ms)$	0.442	0.743	0.470
$C_v(cs)$	0.269	0.596	0.636
$C_v(ms) + C_v(cs)$	0.711	1.339	1.106

These contributions, when added to the spectroscopic C_v values, give a curve for the heat capacity (curve II in fig. 5) which deviates more from the experimental values than does the spectroscopical curve itself. This is not a serious objection against our calculated Q-values, as the spectroscopic calculation of the heat capacity of solids by means of DEBYE functions for substances with polyatomic molecules generally is only a poor approximation. A more serious objection is the high value (0.711) of the contribution to the heat capacity at the temperature (90° K), at which GIAUQUE and STOUT observed their small thermal irregularities. The contribution in this temperature range should have been considerably less than 0.1 in order to be in agreement with GIAUQUE and STOUT's observations. Small changes in Q cannot remove this disagreement. The contribution $(C_v(ms) + C_v(cs))$ has a maximum in the neighbourhood of $T = Q/2R$ and with our Q-values the maximum lies at about 200° K. If the Q-values had been twice as high the maximum would have been removed to about 400° K and the contribution would have been:

at 90° K 0.030, at 136.5° K 0.276, at 273° K 1.339

Also with lower Q-values acceptable values for the contribution can be obtained, but the lowering must be very great. If the Q-values had been 10 times as small, the contributions would have been:

at 90° K 0.172, at 136.5° K 0.067, at 273° K 0.021,

and first with Q-values twenty times lower acceptable values would have been reached:

at 90° K 0.047, at 136.5° K 0.021, at 273° K 0.005.

We must conclude that acceptable values for the contribution to the heat capacity of ice from changes in the configuration equilibrium cannot be obtained with our formulas and with Q-values in reasonable agreement with our calculations based on the tetrahedron model.

It is most probable that the use of the BOLTZMANN function has been an unsatisfactory approximation, and that the α-values are much smaller than those in table 6 (~ 0.1 % instead of 1 % at 90° K). When the number of configurations is lowered from 3^{2N} to 1.5^N on account of correlations (see p. 21) it does not seems improbable that the energy differences between the configurations have a strongly increased effect on the configuration equilibrium.

11. The zero-point entropy of ice.

The views on the structure of ice, presented here, are presumably correct in the main lines, even if the calculated figures must be treated with some caution. If, however, they are correct in the main lines, then PAULING's explanation of the zero-point entropy of ice can not be used. It requires that the energetic difference between the possible orientations of the molecules in ice must be so small that they are all almost equally probable, even at the low temperature at which they are fixed by freezing, and this seems to be very far from the case.

As a possible explanation for the zero-point entropy of ice, GIAUQUE and ASHLEY[5]) have proposed the existence of ortho-

and para-states in the H_2O molecule. Against this view, however, is the fact that a similar zero-point entropy (0.77 kcal/gmol, LANG and KEMP[12])) has been found for heavy water. According to GIAUQUE and STOUT[5], the ortho-para-hypothesis should give a considerably smaller zero-point entropy for heavy water than for light.

The question of the cause for the zero-point entropy of ice, therefore, for the present, remains open.

Summary.

1. A crystal in which every atom has 4 neighbours in regular tetrahedral arrangement is either cubic or hexagonal. In a cubic crystal the arrangement around two neighbours is always centre symmetric (see fig. 2), but in a hexagonal crystal the arrangement around two neighbour atoms is in some cases (maximally in a fourth of the cases) mirror symmetric and only in the rest centre symmetric. The fact that ice crystallises hexagonally and that in ice a fourth of the bonds are mirror symmetric suggests that the bond energy between two H_2O molecules in mirror symmetric position is greater than that between H_2O molecules in centre symmetric position. Earlier measurements by H. D. MEGAW show, in agreement with this suggestion, that the mirror symmetric bond in ice is actually $^1/_2\ ^0/_0$ shorter than the centre symmetric.

2. Using a tetrahedron with positive charges on two corners and negative charges on the other two as a model of a H_2O molecule (fig. 3), the suggestion given above can be supported. For the ordinary hexagonal ice crystal the electrostatic lattice-energy is calculated to 14.91 kcal/gmol and for a hypothetical cubic ice crystal to 14.51 kcal/gmol. These values are valid for low temperatures. For reasons given in the following, the values increase with temperature and approach each other somewhat.

3. An ice crystal can posses a large number of different configurations (1.5^N, where N is the number of molecules). The reason is that both centre symmetric and mirror symmetric positions can be either inverse or oblique (see fig. 4). It has been assumed that all these configurations have nearly the same lattice energy (PAULING). Using the tetrahedral model described above it is found, however, that the electrostatic bond energy is con-

siderably greater for the *inverse* mirror symmetric and for the *oblique* centre symmetric than for the two other positions (see table 4).

4. In an ice crystal the number of the two bond types with the highest bond energy must increase with decreasing temperature at the cost of the two other types. By means of BOLTZMANN's *e*-function, approximate values are calculated for the ratio between inverse and oblique positions at several temperatures (table 6). Even at the melting point the ratio is far from the statistical one, corresponding to equal bond energy.

5. At the melting point the configuration of ice changes very rapidly, but at the temperature of liquid air (90° *K*) the configuration freezes in. At this temperature, according to BOLTZMANN's *e*-function, about 99 % of the positions are the most stable inverse mirror and oblique centre symmetric positions (see table 6). Consequently it could seem reasonable that the irregularities in the thermal behaviour of ice in this temperature range, found by GIAUQUE and STOUT, were rather insignificant.

A calculation, however, revealed that even the small proportion of about 1 % oblique mirror and inverse centre symmetric positions should create irregularities much greater than those observed by GIAUQUE and STOUT. It is suggested that the application of BOLTZMANN's *e*-function here represents a poor approximation, and that at 90° *K* the most stable positions predominate to a proportion of perhaps 99.9 %.

6. If the 1.5^N configurations of an ice crystal are not all equally probable at the temperature when the configuration freezes in, then the zero-point entropy of ice must be smaller than PAULING's value $R \ln 1.5 = 0.806$ kcal/gmol/degree. The values in table 6 suggest that the value of the zero point entropy should be only about a hundredth of this value. It is not yet possible to give another explanation for the experimentally found value 0.82 ± 0.15.

References.

1) W. H. Barnes, Proc. Roy. Soc. A **125** (1929) 670. See also D. M. Dennison, Phys. Rev. **17** (1921) 20 and W. H. Bragg jun. Proc. Roy. Soc. **34** (1922) 103.
2) J. D. Bernal and R. H. Fowler, J. Chem. Phys. **1** (1933) 515.
3) R. Mecke and coworkers, Z. f. Physik **81** (1932) 313, 445, 465.
4) L. Pauling, Journ. Am. Ch. Soc. **57** (1935) 2680. The Nature of the Chemical Bond, 2. Ed. (1945) 301.
5) W. F. Giauque and M. Ashley, Phys. Rev. **43** (1933) 81 and W. F. Giauque and J. W. Stout, Journ. Am. Ch. Soc. **58** (1936) 1144.
6) A. L. Gordon, J. Chem. Phys. **2** (1934) 65.
7) Helen D. Megaw, Nature **134** (1934) 900.
8) P. C. Cross, J. Burnham and P. A. Leighton, Journ. Am. Ch. Soc. **59** (1937) 1134.
9) R. S. Mulliken, Phys. Rev. **41** (1932) 756.
10) E. A. Wollan, W. L. Davidson and C. G. Shull, Phys. Rev. **75** (1949) 1348.
11) E. J. Murphy, Trans. Am. Electroch. Soc. **65** (1931) 133.
12) A. E. Long and J. D. Kemp, Journ. Am. Ch. Soc. **58** (1936) 1829.
13) Landolt-Börnstein's tables, 1 Erg.bd. (1927) 702.

II.

CHANGE IN CONFIGURATION AND MOLECULAR TURNS

1. Information, gained from the dielectric properties of ice.

It is mentioned in part I of this series that ice changes configuration very frequently at the melting point, and that its configuration is first frozen in near the temperature of liquid air (ca. 90° *K*).

Investigations on the dielectric properties of ice have yielded more accurate information about the power of ice to change configuration. P. DEBYE[1]) has shown that it is possible to explain the dielectric properties of ice by assuming that its dipole molecules, under the influence of thermal movements, frequently turn. In the absence of external electrical forces, the molecules are orientated so that their dipole moments are mutually neutralized, but under the influence of an external electrical force the molecules become arranged so that the ice has a dipole moment in the direction of the force. DEBYE writes that under the influence of a field strength of 1 volt/cm it is only necessary for one molecule in 5 million to turn in order to produce the dipole moment which the ice obtains under the effect of this field strength. The rate at which the orientation of the molecules takes place can be investigated by subjecting ice to an alternating current field. At low frequencies the molecules have time to adjust themselves to the field, and a dielectric constant equal to the static is found; but if the frequency is increased, a frequency range can be reached, at which the molecules of ice do not have time to adjust themselves, and at sufficiently high frequencies ice possesses a dielectric constant, corresponding only to the electron- and atom-polarization of the molecules.

SMYTH and HITCHCOCK[2]) have performed measurements of this type. From their measurements DORSEY[3]) has calculated, by means of DEBYE's equations, values for τ, the relaxation time for the molecular turns in ice. Table 1 gives these values for a few temperatures. Values for $n = 1/\tau$, the rate of turns performed by a molecule, are also given in the table.

TABLE 1.

Relaxation time (τ) and rate ($n = 1/\tau$) of molecular turns, determined dielectrically.

$t°$ C	0°	—30°	—70°
$\tau \times 10^6$ sec	1.205	25.3	1467
$n \times 10^{-6}$ sec^{-1}	0.831	0.0395	0.00068

No great accuracy must be ascribed to these calculations of τ and n. DEBYE's equation does not reproduce SMYTH and HITCHCOCK's measurements quite exactly, especially not at temperatures of below —30°. According to W. KAUZMANN's[4]) opinion, the LORENTZ correction used for the internal field is probably too large. This correction makes the n values ca. 16 times higher. It is not improbable that all the n values are e. g. 5 times too high.

From the decrease of n in the interval 0° to —30°, an energy of activation E for the dipole turns of 13.4 kcal/gmol is calculated by means of the expression $E = R d\ln n / d(1/\tau)$. Since DORSEY has smoothed the figures of SMYTH and HITCHCOCK rather strongly, I have carried out a new calculation of n and E from SMYTH and HITCHCOCK's unsmoothed figures. This led to almost the same E value (13.5 kcal/gmol). From the same experimental material KAUZMANN has calculated 12.2 kcal/gmol. He has presumably arrived at the lower value by also considering the more uncertain measurements at temperatures below —30°. From the measurements of WINTSCH[5]) and E. J. MURPHY[6]), KAUZMANN calculates 9.3 and 14.6 respectively (here and in the future the energies of activation are always stated in kcal/gmol). Finally HØJENDAHL[7]) by calculations from the size of the dielectric loss in SMYTH and HITCHCOCK's measurements, obtained the value of 10.8. The equation presented by HØJENDAHL for the loss angle,

however, only fits after the introduction of an empirical coefficient in place of the theoretical. Everything considered, a value for the energy of activation of ca. 13 seems to be most probable.

2. Energies of activation for turns of ice molecules, calculated from molecular models.

It is not possible by turning a single molecule to transform an ideal ice crystal of the type described in part I into a new stable configuration. A consequence of this is that even at the melting point changes in configurations can be rare: The thermal movements of the molecules will cause the disappearance of the forces which are responsible for the crystal structure, before the molecules can turn into a new configuration to any great extent.

If a new stable configuration is to be obtained, a ring of molecules must turn simultaneously. Such a ring contains at least 6 molecules. The ring must fulfill the condition that the order of positive and negative corners is the same throughout the whole ring. This condition is only fulfilled by a small fraction of all existing rings. Turns of molecular rings, which fulfill this condition, will certainly change the configuration of the crystal, but not its dipole moment, and hence the large dielectric constant of ice can not be caused by such turns. Turns of molecular rings must be rare, because a coordinated turning of many molecules simultaneously is statistically not very probable and also and especially because a ring during its turning must pass a high energy threshold. If, as molecules, we use the tetrahedral model described in the previous paper, and only consider the electrostatic forces, we obtain for the critical energy threshold (the energy of activation) a value of at least 21.6 kcal/gmol (for a six membered ring).

Details of the calculation. In a ring of the type described above, it is possible, by simultaneously turning all molecules through 120° round one of their tetrahedral axes, to reach a new stable configuration. The axis of rotation must be one of the two tetrahedral axes which do not lie in the ring itself. During the turning a critical energy threshold is passed when the molecules have turned through 60°. In order to reach this threshold position, work must be performed against the electrostatic attraction between the molecules of the ring and the surrounding molecules and also between the molecules of the

ring themselves. If we only pay attention to the forces between adjacent molecules and disregard the small forces, which are active between two adjacent molecules, when the one molecule rotates around their common axis, we shall, for each of the molecules in the ring, only consider the forces from a single molecule outside the ring. Hence the problem is to bring two molecules (A and B) into the positions shown in fig. 1 a. Since, however, the calculations can only be made approximately and are easier to carry

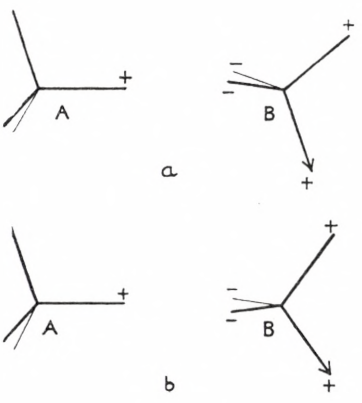

Fig. 1.

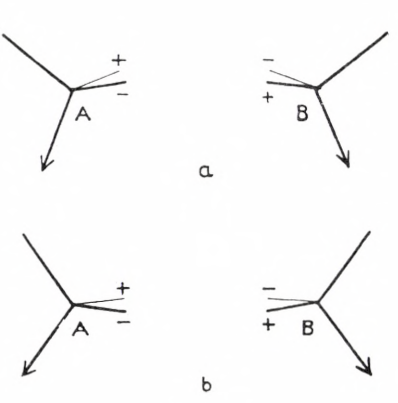

Fig. 2.

Fig. 1. Threshold position between a ring molecule and a molecule outside the ring. *a* correct. *b* modified. Rotation axes marked with an arrow.

Fig. 2. Threshold position between two ring molecules. *a* correct. *b* modified. Rotation axes marked with an arrow.

through for the modified position shown in fig. 1 b, the calculations, are performed for the latter. The modification consists of a rotation of the B molecule ca. $12^3/_4{}^\circ$ around an axis perpendicular to the plane of the drawing. This modification will only change the energy of activation slightly and will generally make it a little lower. The energy necessary for bringing the molecules to the threshold position is somewhat dependent on the position of the negative and positive charges on those corners of the A molecule, which are furthest away from the B molecule, and on whether the initial position has been centric symmetric or mirror symmetric (the modified threshold position is the same in both cases). The calculation shows that 2.3 to 3.6, mean ca. 3 kcal/gmol, is necessary. If there are 6 molecules in the ring the consideration of the surrounding molecules alone thus causes an energy of activation of *at least* $6 \times 2.3 = 13.8$.

The energy necessary in order to bring two adjacent molecules in a ring into the critical threshold position depends on the mutual positions of the molecules (mirror symmetric or centric symmetric, inverse or oblique) and of the position of the axes of rotation in the molecules. The lowest transfer of energy is required, when the molecules are in

mirror symmetric position and the axes of rotation lie in the same plane (fig. 2a). The modified position 2b, in which the mutual position of the molecules is more symmetric, is used in the calculations and can be expected to give a slightly lower energy of activation. The amount of energy necessary depends somewhat on the position of the charges on the corners of the molecules which in 2b are furthest apart. A mean value of at least 1.3 kcal/gmol must be considered. Since there are at least six molecules in the ring, the contribution to the energy of activation from the electrostatic forces between the molecules in the ring must be at least $6 \times 1.3 = 7.8$. Hence the total energy of activation will be at least $13.8 + 7.8 = 21.6$.

While turns of molecular rings do not change the dipole moment of an ice crystal, turns of a molecular row between two surface points will change the dipole moment. If the ice crystal, however, is not ultramiscropically small such turns of molecular rows can not be of much importance. Impurities in the ice will produce internal surfaces in it, but it is not probable that turns of molecular rows, beginning and ending in impurities in the crystal, will be decisive for the rate of dipole turns responsible for the dielectric properties of ice. In contrast to the many molecules in the interior, the few molecules which lie in the surfaces, both external and internal, of the crystal will be able to turn and thus alter the dipole moment of the ice crystal, but it is not probable that such turns of surface molecules can play any important role. Even in an ideal, pure ice crystal, however, lattice faults occur and at these fault sites single molecules will be able to turn and their dipole axes to change direction. We must here turn our attention to the lattice faults which are caused by the thermal movements of the molecules and which occur at a concentration determined by the temperature. There are two types of such fault sites: some, which are due to the incorrect mutual *orientation* of two neighbour molecules, there being either two protons or no protons between them, and others, which are due to *ionization*, the presence of H_3O^+ and HO^- ions in the lattice. We will in this paper examine the orientation fault sites.

3. Orientation fault sites as cause of molecular turns in ice.

If an ice molecule, on account of especially strong thermal movements, has turned around such a large angle that two protons

have come between its oxygen atom and the oxygen atom of an adjacent molecule and no proton between its oxygen atom and the oxygen atom of another neighbouring molecule (fig. 3b) the chance that it will turn back is very great; but it may happen that one of the neighbours has turned before it can turn back. In such a case the two sites with two or no protons respectively have been separated (fig. 3c). Continued molecular turns can

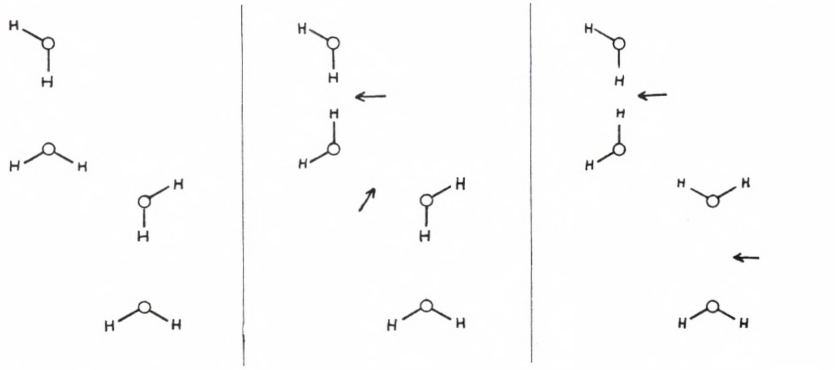

Fig. 3. Formation of orientation fault sites.

separate the two sites completely and cause the appearance of two independent fault sites of opposite types: sites with two protons and sites with no protons between the oxygen atoms. These fault sites will migrate through the crystal until they meet a fault site of the opposite type with which they will recombine. Under the influence of formation and recombination of such fault sites, an equilibrium will be reached in the ice crystal with equally high concentration of these two types of orientation fault sites.

Two molecules, between which there is an orientation fault site, can easily turn, and every time a molecule turns the fault site will move over to an adjacent site and the dipole moment of the molecule will be turned through 90°. The fault sites will thus act as a kind of catalyst for the promotion of dipole turns.

If the tetrahedral model, previously described in part I, is used, the formation of such fault sites is estimated to require a accumulation of energy E of between 10.2 and 13.6 kcal/gmol, and the critical energy threshold for turns of the molecules

between which the fault site lies, can be estimated to be 2.5 kcal/gmol. Consequently the concentration (c) of the fault sites will change with temperature according to the expression $dln\ c/dT = E/RT^2$, where E is a figure between 10.2 and 13.6, and the rate of turns (n') per fault site will change according to the equation $dln\ n'/dT = 2.5/RT^2$. The rate of turns per H_2O molecule ($n = c \times n'$) will therefore change according to the equation $dln\ n/dT = (E + 2.5)/RT^2$. The apparent energy of activation for the number of turns must therefore lie between 12.7 and 16.1. The energy of activation for dipole moments estimated from the dielectric properties of ice was 13. The calculation shows that it is permissible to assume that the dipole turns which are required by DEBYE's theory are the turns made by the molecules at the orientation fault sites. On the basis of this assumption and assuming a threshold value of 2.5, the energy content of the orientation fault sites can be estimated to be 10.5.

The accumulation of energy necessary for the formation of an orientation fault site is calculated in the following way. In a gram molecule of ice, the electrostatic lattice energy originates chiefly as the result of the attraction between the $2N$ adjacent molecular pairs. The total lattice energy, according to table 2 in the first part of this paper, is about 13.6 kcal/gmol and the bond energy between a single molecular pair is consequently $13.6/2N$. At an orientation fault site the two adjacent molecules possess a bond energy numerically equal to the normal energy, but with the opposite sign. Hence every such fault site will diminish the lattice energy by $13.6/N$ and the formation of a gram molecule of fault sites will require 13.6 kcal. This value must be considered as a maximum value. For in the calculations it is assumed that the two similarly charged tetrahedral corners are in the normal position to one another, and that both lie on the connecting line between the centres of the tetrahedra. When the corners are differently charged the existence of this position is due to electrostatic attractions between the charges in the corners. The repulsion between two similarly charged corners must cause the corners to be forced away from the connecting line between the centres in opposite directions. If they are removed in this way 0.3 Å from the connecting line (the radius of the tetrahedron is 0.99 Å), the distance between the corners increases ca. 30 %, and if the distances between the differently charged tetrahedral corners at the other places of the lattice are assumed not to be altered appreciably from the normal value 0.78 Å, the total lattice energy will not be decreased by $13.6/N$ on account of a fault site, but only by $10.2/N$. We will assume that the formation of a gram molecule of fault sites must require between 10.2 and 13.6 kcal.

The critical threshold energy for molecular turns at a fault site can be calculated in the following way. Fig. 4 shows the initial, the threshold and the final positions during turning of a molecule (A). Before turning the fault site lies between molecules A and B and after turning between A and C. In the initial position the contribution made by the molecular pairs AB, AC and AD to the lattice energy amounts to $2 \times 6.8/N - 6.8/N = 6.8/N$, and

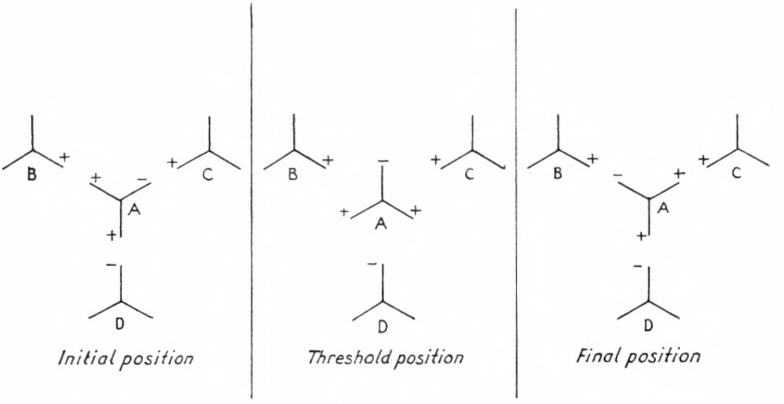

Fig. 4. Positions during moving of an orientation fault site.

the same contribution is given by the three pairs in the final position. In the threshold position the contributions of AB and AC are both zero. The contribution of AD (using the same approximations as on p. 34) can be calculated to $3.8/N$. In order to reach the threshold value an energy accumulation of $(6.8 - 3.8)/N$ is consequently required, corresponding to 3.0 kcal/gmol. This accumulation of energy will also be decreased on account of the deformation of the lattice at the fault site. In the following we will assume this value to be 2.5.

The rate of turns (n) per H_2O molecule is the product of the number (c) of fault sites per molecule and the rate of turns (n') per fault site ($n = c \times n'$). It is not possible to carry out the separation of n into these two factors with certainty; but in order to obtain a plausible value of c we have tried to carry out a reasonable separation, paying attention to the energy content of the fault sites (10.5) and to the critical energy threshold for turns at a fault site (2.5). From the RAMAN spectrum of ice it is known that the frequency (ν) of the hindered rotation of the ice mole-

cules is ca. 2.4×10^{13}. Since turning of a molecule to a new equilibrium position requires that an energy threshold of 2.5 must be passed, we will assume that the rate of such turns per fault site is $n' = \nu \times 2 \times e^{-2.5/RT}$ (the factor of 2 is due to the fact that at each fault site there are two molecules that can turn). From this expression the value of n' at 0° C is calculated to 4.8×10^{11}. The rate of dipole turns (n) per molecule is according to table 1 0.83×10^{6} at 0°. If the dipole turns are due to fault sites, the number of these fault sites per molecule must be $c = n/n' = 1.7 \times 10^{-6}$ at 0° and hence about 10^{-6} of each of the two types. This number is rather too large for a state with an energy content of 10.5 kcal/gmol. According to BOLTZMANN's e-function the number should lie somewhere near $e^{-10.5/RT} = 0.36 \times 10^{-8}$. It must be remembered, however, that BOLTZMANN's function here represents only an approximation. If the uncertain LORENTZ correction for the internal field is omitted in the calculation of n from the dielectric properties of ice, the number of fault sites per molecule decreases to 1.1×10^{-7}. Even with this modification the number of orientation fault sites, necessary to explain the dielectric properties of ice, is 30 times higher than expected from the BOLTZMANN calculation. This is, however, no sufficient reason to discard this explanation.

Summary.

1. DEBYE has explained the dielectric properties of ice by the existence in ice of dipoles which can turn. From the dielectric properties of ice the rate of dipole turns is calculated to ca. 0.83×10^{6} per second per molecule at 0° and the energy of activation to ca. 13 kcal/gmol. If the LORENTZ correction used for the internal field is too large or even may be perhaps completely omitted, the rate of dipole turns may be up to ca. 16 times less.

2. The configuration of an ideal ice crystal can not change by turning of a single molecule, but only by the simultaneous turning of a closed ring of molecules. Such turns of molecular rings do not alter the dipole moment of the crystal and therefore can not represent the dipole turns required by DEBYE's theory. If the tetrahedral model with electric charges on the corners,

described in part I of this series, is used as a model of a water molecule, the energy of activation for a turning of a ring of six molecules is calculated to at least 21.6 kcal/gmol.

3. In an ice crystal fault sites are present where two or no protons are found between two oxygen atoms instead of the one normally present. These two types of fault sites occur in equal amounts. Molecules, between which such orientation fault sites are present, can easily turn and thereby rotate their dipole moments 90°. The apparent energy of activation for such turns is calculated from the above mentioned molecular model to between 12.7 and 16.1 kcal/gmol. The energy of activation thus has a size similar to that required for dipole turns in DEBYE's theory (ca. 13 kcal/gmol). It may therefore be assumed that the molecular turns at orientation fault sites represent the dipole turns required by DEBYE's theory.

4. The rate of molecular turns at an orientation fault site is estimated to be ca. 4.8×10^{11} per second at 0°, and the concentration of each of the two types of fault sites to be ca. 1 in each 10^6 ice molecules. If the rate of dipole turns in ice should be less than 0.83×10^6 sec^{-1} per molecule the concentration of fault sites will be correspondingly higher.

References.

1) P. DEBYE, Polare Molekeln, Leipzig (1929) 118.
2) SMYTH and HITCHCOCK, Journ. Amer. Chem. Soc. **54** (1932) 4631.
3) N. E. DORSEY, Properties of ordinary water-substance, New York (1940).
4) W. KAUZMANN, Rev. Mod. Physics, **14** (1942) 32.
5) H. WINTSCH, Helv. Phys. Acta, **5** (1932) 126.
6) E. J. MURPHY, Trans. Amer. Electroch. Soc. **65** (1934) 133.
7) K. HØJENDAHL, 6. nordiska kemist møtet i Lund 1947. Berättelse och föredrag (1948) 248.

III.

IONISATION OF ICE AND MOLECULAR TURNS PRODUCED BY THE IONS. THE PROTON JUMP CONDUCTIVITY OF ICE (AND WATER)

1. Ions as producers of molecular turns.

In addition to orientation fault sites, there exist in ice fault sites, which are due to the presence of ions. If a proton jumps from an H_2O molecule to a neighbouring molecule, an H_3O^+ and an HO^- ion are formed. The chance that the proton will jump back again is great; but before there is time for this to happen, a proton may have jumped over from the H_3O^+ ion to a third H_2O molecule (or from another H_2O molecule to the HO^- ion). Hereby two spacially separated ions have appeared (see fig. 1). By new proton jumps of the types $H_3O^+ + H_2O \rightarrow H_2O + H_3O^+$ and $H_2O + HO^- \rightarrow HO^- + H_2O$ the ions may be separated further from each other and migrate freely in the crystal lattice and cause the ice to become electrically conducting. As is well known, it is usual to explain the exceptionally high conductivity of the H_3O^+ ion in water in a similar way by assuming that this ion can move its charge, not only in the same way as normal ions, by moving as a unit through the medium of the solution, but also by the jumping of one of its protons over to an adjacent H_2O molecule, and similarly, the abnormally high conductivity of the HO^- ion is explained by the jumping of a proton from an adjacent H_2O molecule over to the HO^- ion[1]). In ice, the H_3O^+ and HO^- ions formed will continue to migrate until an H_3O^+ and an HO^- ion meet and thus have the possibility of recombination. Formation and recombination of the ions will lead to a state of equilibrium with definite ion concentrations.

The ion concentrations in ice must be of a similar order of magnitude to those in water, since the conductivities of ice and water do not differ considerably. J. H. L. JOHNSTONE[2]) gives the following values for the static conductivity of ice ($\varkappa$):

Temp.	$-1°$	$-4°$	$-10°$	$-19°$
$\varkappa \times 10^8$	2.8	0.23	0.11	0.026

His determination at $-1°$ appears improbably high. According to the other determinations, a rise in temperature of ca. 5° causes

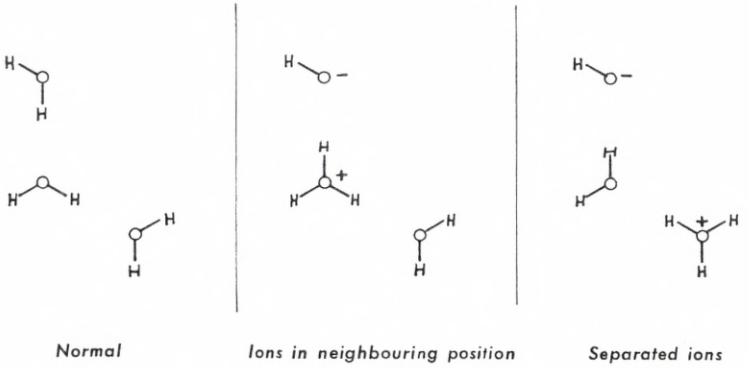

Fig. 1. Formation of ions by proton jumps.

a doubling of the conductivity, hence it is not natural that a rise from $-4°$ to $-1°$ should make the conductivity 12 times higher. A value of 0.35×10^{-8} at $-1°$ (and 0.4×10^{-8} at 0°) would be more reasonable. Perhaps the high value at $-1°$ is due to the presence of impurities in the ice, which have contributed to the conductivity, because they were still present in the form of aqueous solution between the ice crystals.

The conductivity of water at 0° is calculated from the ionisation constant of water (0.119×10^{-14}) and the molecular conductivity of the ions (345) to $\varkappa = 1.2 \times 10^{-8}$. This value is 2.3 times lower than the conductivity given by JOHNSTONE for ice at $-1°$, and 3 times higher than the value obtained for ice at 0° by extrapolation from the determinations by JOHNSTONE at lower temperatures.

A calculation of the ion concentration in ice can be performed as follows. We will assume that the conductivity of ice is due

exclusively to its content of H_3O^+ and HO^- ions, and that these ions move exclusively by means of proton jumps. It is improbable that these ions as a unit can migrate through the crystal lattice of the ice at rates which are of significance in this connection or that other ions can do it.

In passing, it should be mentioned that, on account of these considerations, impurities do not have the same large effect on the conductivity of ice as they have on that of water. It is therefore easier to determine experimentally the conductivity of pure ice than that of pure water.

Only a fraction of the conductivity of pure water (1.2×10^{-8} at 0° C) is due to proton jumps. Of the molecular conductivity of H_3O^+ ions at 0°, $\mu = 240$, only 200 is due to proton jumps, and of the molecular conductivity of HO^- ions at 0°, $\mu = 105$, only 64 is due to proton jumps (see section 6 for further details). Hence the proton jump conductivity of pure water at 0° is $1.2 \times 10^{-8} \times 264/345 = 0.92 \times 10^{-8}$. We will now make the assumption that proton jumps between ions and H_2O molecules in ice are just as frequent as they are in water at the same temperature between ions and H_2O molecules in the right positions (hydrogen bond positions) to each other. According to conceptions developed later, the rate of proton jumps in water is reduced, on account of the more random orientation of the H_2O molecules to the ions, at 0° in the ratio 0.93 for H_3O^+ ions and 0.77 for HO^- ions. When this reduction is taken into consideration, the molecular conductivities of the ions in ice amounts to: for H_3O^+ ions, $200/0.93 = 215$ and for HO^- ions, $64/0.77 = 83$, total 298. If the specific conductivity of ice is taken to be 0.4×10^{-8} at 0°, the molecular concentrations of the H_3O^+ and the HO^- ions are calculated to 1.34×10^{-8}, corresponding to the transformation of 0.27×10^{-9} parts of the H_2O molecules to H_3O^+ ions and of the same amount of H_2O molecules to HO^- ions.

2. Rates of proton jumps in ice.

From the specific conductivity of ice it is possible to calculate how frequently proton jumps of the types $H_3O^+ + H_2O \rightarrow H_2O + H_3O^+$ and $H_2O + HO^- \rightarrow HO^- + H_2O$ take place. The cal-

culation can be performed by the use of EINSTEIN's theory for BROWNIAN movements.

EINSTEIN[3]) has developed the following equation:

$$D = \overline{\Delta^2}/(6\tau)$$

where D is the coefficient of diffusion of a particle and $\overline{\Delta^2}$ the mean value of the square of the displacement of the particle in space in the time τ. The coefficient of diffusion for a monovalent ion can be calculated from its molecular conductivity by means of the following equation:

$$D = \mu \times RT/F^2 \times 10^7 = \mu \times 0.244 \times 10^{-6} \text{ at } 0^\circ \text{ C.}$$

If the molecular conductivity of an ion is known, it is possible, from EINSTEIN's equation, to calculate an expression for the time τ taken by the ion to be displaced a certain distance. To give an exact result, EINSTEIN's equation requires that the displacements of the particle are changed by collisions many times within the time τ. We will, however, use the equation for the approximate determination of the mean time (τ_0), in which the ion is displaced 2.76 Å, corresponding to a proton jump. The rate of proton jump displacements of an ion will then be

$$n' = \frac{1}{\tau_0} = \frac{6\,D}{(2.76 \times 10^{-8})^2} = \mu \times 0.193 \times 10^{10}\ \text{sec}^{-1}.$$

If the values of μ for H_3O^+ (215) and for HO^- (83) are substituted in this equation, we obtain for the rate of proton jumps at an H_3O^+ ion, 41.5×10^{10} and at an HO^- ion, 16.0×10^{10}, all per second. For the rate of proton jumps per H_2O molecule we finally obtain (c is the molar ion concentration and 50.9 the number of gram moles in 1000 cm³ of ice):

$$n = n' \times c/50.9 = c \times \mu \times 3.79 \times 10^7 = \varkappa \times 3.79 \times 10^{10}.$$

If the specific conductivity of ice at 0° is taken as 0.4×10^{-8}, the rate of proton jumps per H_2O molecule in ice is calculated by means of this equation to 152 per second. Even at the melting point, where the proton jumps must be most frequent, an H_2O molecule only turns ca. 150 times in a second owing to the presence of the H_3O^+ and HO^- ions in the ice.

3. Ionisation and proton jumps at the ions cannot explain the dielectric properties of ice.

The idea that proton jumps and ionisation may be of significance for the occurrence of the frequent dipole turns, required by DEBYE's theory for the dielectric properties of ice, has been advanced from several quarters.

M. L. HUGGINS[4]), who was perhaps the first to put forward this view, was doubtful of the idea as it leads to the existence of H_3O^+ and HO^- ions in ice. He therefore considered proton displacements in rings of H_2O molecules as the explanation for the high dielectric constants of ice and water. He does not appear to have noticed that proton displacements in rings do not change the dipole moment.

W. M. LATIMER[5]) has put forward the idea that the configuration changes in ice are connected with the processes during which the ions H_3O^+ and HO^{--} appear and disappear in ice. Since the rate at which these processes occur may be high, even if the concentration of the ions is low, LATIMER thinks that there is a possibility of explaining the rapid configuration changes in ice in this way. Quantitatively viewed, this is, however, not possible. Formation and recombination of the ions must be a far more infrequent process than molecular turns during migration of the ions.

W. KAUZMANN[6]) has expanded HUGGINS' idea in an interesting way. He has put forward the proposition that the changes in the configuration of ice could be due to the proton jumps, which accompany migration of the ions in ice. An H_2O molecule which, during migration of the ions, has momentarily been an ion, is left in a new position, if the proton does not jump back to the same H_2O molecule from which it came. I myself have worked with this proposition, without knowing KAUZMANN's work. There is no doubt that migrations of the ions must produce molecular turns, during which the dipole moments of the ions are turned through 90°. These turns, however, are far from sufficiently frequent to explain the dielectric properties of ice (ca. 150 per sec. per ice molecule, whereas ca. 10^6 are required). An even more important objection is the following. The dipole moment produced by these molecular turns is in the opposite direction

to that which is required. This can be shown in the following way. The dipole moment produced by migration of the ions in an isolated ice block is the vector sum of a series of proton jumps, each of 0.78 Å. The dipole moment produced can also be considered as the sum of the dipole changes, caused by displacements of the ions, and the dipole changes, caused by turns of the H_2O molecules. The change of the dipole moment, due to displacements of the ions, is 2.76/0.78 times larger than the dipole moment corresponding to the proton jumps (the displacement of the ion is 2.76 Å, when the proton jumps 0.78 Å). Consequently the dipole moment due to turns of molecules must be in the opposite direction and numerically 1.98/0.78 times larger than the dipole moment corresponding to the proton jumps (1.98/2.76 parts of the dipole moment produced by displacements of the ions).

Hence it is not possible to use the molecular turns connected with the migration of the ions as an explanation for the dielectric properties of ice. Only the molecular turns produced at orientation fault sites, which are described in part II of this paper, can be used.

4. The proton jump conductivity of ice (and water).

In the previous section an account is given of how the ions H_3O^+ and HO^- move in ice by means of proton jumps and how these movements are connected with molecular turns, which produce dipole moments in the direction opposite to the movements and amounting to 1.98/2.76 parts of the dipole moment produced by the ion displacements. If an electric current is passed through a block of ice, avoiding polarization (electric charges) at the two ends, where the current is lead in and out, the ion movements in themselves will not give the block a dipole moment. On the contrary, it might be expected that the turns of the molecules would produce a gradually increasing dipole moment in the opposite direction to that of the electric force. The molecules are, however, also able to turn at orientation fault sites, and since the turns at orientation fault sites are ca. 10^4 times as frequent as the turns at the ions, they are not only able to prevent the appearance of this dipole moment, but in addition

to produce the dipole moment required by DEBYE's theory in the direction of the force.

For the hypothesis of the proton jump conductivity of ice it is thus of vital importance that the molecular turns produced at orientation fault sites are far more frequent than the molecular turns produced at ions.

In water the molecular turns at orientation fault sites are even more frequent than in ice (according to the dielectric properties ca. 10^5 to 10^6 times more frequent). There is therefore very good reason to consider the abnormally high conducivity of the H_3O^+ and HO^- ions in water as a result of the ability of these ions to move, not only as a unit, but also by means of proton jumps.

5. Ion concentration and proton jumps in ice at lower temperatures. Energies of activation.

The specific conductivity of ice ($\varkappa$) decreases on cooling. From JOHNSTONE's determination at $-4°$ and $-19°$ (see p. 42) an apparent energy of activation $E = 19.6$ kcal/gmol is calculated by means of the expression $E = -R\, d\ln\varkappa/d\,(1/T)$. Let us try to calculate theoretically a value for this energy of activation.

Assuming that the total conductivity is due to proton jumps, the conductivity must decrease in the same ratio as the rate of proton jumps. The rate of proton jumps decreases partly because of the decrease in the ion concentration and partly because proton jumps require a certain energy of activation. *The decrease in the ionisation* depends on the heat production during the process of "neutralization" $H_3O^+ + HO^- \rightarrow 2\,H_2O$. In water this process is accompanied by an evolution of heat of 13.7 kcal/gmol. This heat production (disregarding the difference between production of heat and of energy) can be separated into two parts: the energy, liberated during the actual proton jump, and the energy, liberated on account of the electrostatic attraction between the ions when they approach each other. The latter part can be calculated from the expression $e^2/\varepsilon a$ to 1.4 kcal/gmol, when the dielectric constant (ε) in water at $0°$ is taken as 88, and the distance (a) between the ions when they touch as 2.76 Å. The energy which is released during the proton jump itself from

H_3O^+ to HO^- is therefore $13.7 - 1.4 = 12.3$ and hence forms the greater part. In ice we will assume that the production of energy during the proton jump itself is the same as it is in water and since the static dielectric constant in ice is of a similar size to that in water, we will for the present assume that also that part of the energy production, which is due to the electrostatic attraction between the ions, has the same size in both ice and water. Hence the formation of the ions in ice requires the same amount of energy as in water (13.7) and the ion concentration in ice should therefore decrease with temperature according to the expression:

$$-R\, d\, ln\, c/d\,(1/T) = 13.7/2 = 6.85. \qquad (1)$$

The energy of activation (E_p) *for proton jumps* between the ions and the H_2O molecules can be calculated from the temperature coefficient for that part of the conductivity of the ions in water, which is due to proton jumps. As will be shown later, the following energies of activation are thus obtained:

For H_3O^+ $E_p = 2.5$ and for HO^- $E_p = 4.7$.

The fact that the energy of activation is lower for H_3O^+ than for HO^- is of course in agreement with the higher proton jump conductivity of H_3O^+.

Let the number of proton jumps per H_2O molecule be n, per H_3O^+ ion n' and per HO^- ion n'', and let c be the molecular concentration of the ions H_3O^+ and HO^- (these concentrations must be equal, assuming that the ice lattice contains no other ions), then:

$$n = c\,(n' + n'')/50.9$$

(50.9 is the number of H_2O molecules in 1000 cm^3 of ice).

For the change of c with temperature (1) is valid and for changes of n' and n'':

$$-\mathrm{R}\; d\; ln\; n'/d\,(1/T) = 2.5 \quad \text{and} \quad -R\, d\, ln\, n''/d\,(1/T) = 4.7.$$

For the variation of n with temperature we obtain:

$$-R\, d\, ln\, n/d\,(1/T) = 6.85 + E,$$

where $E = 2.5 \times n'/(n' + n'') + 4.7 \times n''/(n' + n'')$.

At 0° C according to the statement on p. 43 the proton jump conductivity in ice of H_3O^+ is 215 and of HO^- 83. n' and n'' are proportional to these figures. Hence we obtain $E = 3.1$ at 0° C. At lower temperatures the ratio n'/n'' will increase and E will decrease gradually towards 2.5.

The apparent energy of activation, corresponding to the temperature coefficient of the conductivity of ice, should hence be $6.85 + 3.1 = 9.95$ near the melting point. This is only half of the value calculated from JOHNSTONE's determinations of the conductivity of ice. The reason may be that JOHNSTONE's determinations are not sufficiently accurate to be used for determination of temperature coefficient. It is, however, more probable that in the calculation of the energy required for separation of the ions it has not been permissible to use the high static dielectric constant of water (88). If we had used a value 15 times lower (5.9, this is the size of the dielectric constant of ice in an alternating field, which changes ca. 40,000 times in a second) a release of 21.0 and not 1.4 kcal/gmol would have been found when the ions approached contact. The evolution of heat by the process of "neutralization" would have in this case been calculated to $12.3 + 21.0 = 33.3$ and the apparent energy of activation to $33.3/2 + 3.1 = 19.75$ and thus have been in agreement with JOHNSTONE's conductivity determinations.

On the other hand, it must not be forgotten that the ion concentrations in water and ice are of about the same size, and that this is an indication that the heat of "neutralization" in ice and water should also be expected to be approximately the same.

The use of the *static* dielectric constant has been shown to be permissible in calculations of the forces between the ions in water. This is apparent e. g. from DEBYE and HÜCKEL's work on the coefficients of ion activity[7]) and from BJERRUM's calculations on the relation between the dissociation constants of poly-acidic acids[8]).

The molecules in ice, however, turn ca. 10^6 times less frequently than they do in water. Therefore it appears reasonable that in ice, not the static dielectric constant, but a dielectric constant corresponding to an alternating field of high frequency, has to be used.

6. Calculation of the energies of activation for the reactions $H_3O^+ + H_2O \rightarrow H_2O + H_3O^+$ and $H_2O + HO^- \rightarrow HO^- + H_2O$ from temperature coefficients of proton jump conductivities of the ions H_3O^+ and HO^- in water.

In table 2 the electrical conductivities at infinite dilution (μ_∞) are given for the ions H_3O^+, K^+, HO^- and Cl^- at temperatures from 0° to 100° according to J. JOHNSTONE[9]).

If it is assumed that the H_3O^+ ion, in the absence of proton jumps, would have the same conductivity as the potassium ion, and the HO^- ion the same conductivity as the chloride ion, the figures given in table 3 are obtained for that part of the conductivity (μ_p) which is due to proton jumps. From these proton jump conductivities energies of activation are calculated by means of the usual equation:

$$E = -R\, d\, ln\, \mu / d\,(1/T).$$

These energies of activation are presented in table 4. (In the calculation, in place of differentials, differences have been used).

TABLE 2.

Molar conductivities at infinite dilution (μ_∞) in water.

t	0°	25°	50°	75°	100°
H_3O^+	240	350	465	565	644
K^+	40.4	74.5	115	159	206
HO^-	105	192	279*	360	439
Cl^-	41.1	75.5	116	160	207

* JOHNSTONE gives 284. An interpolation between the value at the four other temperatures makes 279 more probable.

TABLE 3.

Molar conductivities due to proton jumps (μ_p).

t	0°	25°	50°	75°	100°
H_3O^+	199.6	275.5	350	406	438
HO^-	63.9	116.5	163	200	232

TABLE 4.

Energies of activation (E) expressed in kcal/gmol, calculated from the proton jump conductivities of the ions in water.

$t°$ C	0–25	25–50	50–75	75–100
H_3O^+	2.07	1.83	1.33	0.78
HO^-	3.85	2.58	1.83	1.53

In the range 0° to 25° the energies of activation for H_3O^+ are ca. 2 and for HO^- ca. 4. These values ought not, however, to be considered, without reservations, as the energies of activation E_p for the proton transitions $H_3O^+ + H_2O \rightarrow H_2O + H_3O^+$ and $HO^- + H_2O \rightarrow H_2O + HO^-$. The energies of activation in the table decrease steeply with rising temperature. This fall can be explained in the following way: In order that the proton jump can take place, an H_2O molecule must be orientated towards the ion in a so-called hydrogen bond position, i. e. so that a positive proton-containing corner in the H_3O^+ ion is turned towards a negative proton-free corner in an H_2O molecule, and a negative proton-free corner in the HO^- ion turned towards a positive proton-containing corner in an H_2O molecule. This condition is always fulfilled for the ions in ice, but on the contrary not always in water. With rising temperature the number of favourable positions in water will decrease. This will reduce the rise in μ_p with temperature and thus make the calculated E values, given in table 4, lower than the true energies of activation E_p for proton jumps in a hydrogen bond position.

This effect can be corrected for as follows: Let α be the fraction of the protons in the H_3O^+ ions, which are associated with an H_2O molecule in hydrogen bond position. The following equation can be used for the variation of α with temperature:

$$ln \frac{\alpha}{1-\alpha} = \frac{Q}{RT} - A = \frac{Q}{R\theta}\left(\frac{\theta}{T} - 1\right) \qquad (2)$$

Q is here the evolution of heat on association of an H_2O molecule with the ion in hydrogen bond position, and A is a constant, which can be calculated when the value of α is known at one temperature, e. g. if we know the temperature θ at which

α is equal to 0.5. This temperature θ is substituted for A in equation (2). Equation (2) is correct if the value of Q is the same whether other H_2O molecules are already associated with the ion or not, and if the tendency of the ion to associate with an H_2O molecule is also independent of this.

The rate h of proton jumps $H_3O^+ + H_2O \rightarrow H_2O + H_3O^+$ per H_3O^+ ion may be equated to $3\alpha\beta$, where α is the fraction of associated protons defined above and β is the rate of proton jumps per hydrogen bond $H_3O^+ - H_2O$. Hence we obtain:

$$E = -R\frac{d\ln h}{d(1/T)} = -R\frac{d\ln\alpha}{d(1/T)} - R\frac{d\ln\beta}{d(1/T)} = -R\frac{d\ln\alpha}{d(1/T)} + E_p \quad (3)$$

From (2) it can be deduced that $R\,d\ln\alpha/d(1/T) = Q(1-\alpha)$. If we use this equation we obtain from (3):

$$E_p = E + Q(1-\alpha). \quad (4)$$

By means of (2) and (4) E_p for H_3O^+ is calculated for a series of different pairs of values for Q and θ. Table 5 gives the

TABLE 5.

E_p values for H_3O^+, calculated from E values for a series of sets of values of Q and θ.

Q	θ	0°–25°	25°–50°	50°–75°	75°–100°	mean of E_p (H_3O^+)
3	200	4.84	4.64	4.20	3.68	..
3	273	3.75	3.81	3.54	3.16	..
3	320	3.16	3.23	2.99	2.67	..
3	400	2.66	2.69	2.30	1.97	..
4	273	4.39	4.47	4.52	4.21	..
4	300	3.74	4.06	4.01	3.76	..
4	320	3.34	3.64	3.62	3.47	..
4	400	2.54	2.63	2.43	2.24	..
4.5	273	4.71	5.13	5.13	4.76	..
4.5	320	3.41	3.84	3.95	3.88	..
4.5	360	2.79	3.04	3.07	3.17	..
4.5	400	2.49	2.55	2.46	2.36	2.46
5	273	5.06	5.59	5.56	5.30	..
5	320	3.47	4.04	4.28	4.32	..
5	400	2.44	2.53	2.47	2.46	..

results of these calculations. Similar calculations are performed for HO^- and the results are presented in table 6.

TABLE 6.

E_p values for HO^-, calculated from E values for a series of sets of values of Q and θ.

Q	θ	0°–25°	25°–50°	50°–75°	75°–100°	mean of E_p (HO^-)
3	200	6.62	5.39	4.70	4.43	..
3	273	5.53	4.56	4.04	3.91	..
3	320	4.94	3.98	3.49	3.42	..
3	400	4.44	3.44	2.80	2.72	..
4	273	6.17	5.22	5.02	4.96	..
4	300	5.52	4.81	4.51	4.51	..
4	320	5.12	4.39	4.12	4.22	..
4	400	4.32	3.38	2.93	2.99	..
4.5	273	6.49	5.88	5.63	5.51	..
4.5	320	5.19	4.59	4.45	4.63	..
4.5	360	4.57	3.79	3.57	3.92	..
4.5	400	4.27	3.30	2.96	3.11	..
5	273	6.84	6.34	6.06	6.05	..
5	320	5.25	4.79	4.78	5.07	4.97
5	400	4.22	3.28	2.97	3.21	..

It is not possible, solely by the use of the figures in table 5, to find the set of Q and θ which make the calculated E_p values for H_3O^+ independent of the temperature, or to solve the corresponding problem for HO^-. The conductivities, on which these calculations are based, are too inaccurate for this purpose and this is especially true for HO^-. We know, however, that the energy of the hydrogen bond $H_2O - H_2O$ in water generally is considered to be ca. 4.5 [10]), and we will therefore use Q values near this figure. Considering this and also that the E_p values of course should be as uniform as possible in all temperature ranges, it appears reasonable to choose

for H_3O^+ $Q = 4.5$ and $\theta = 400°$ K
for HO^- $Q = 5$ and $\theta = 320°$ K.

This choice leads to the following E_p values:

for H_3O^+ $E_p = 2.5$; for HO^- $E_p = 4.7$.

For H_3O^+ in water, α (the fraction of the protons of the ion which have an H_2O molecule in hydrogen bond position) is 0.95 at 0° C and 0.61 at 100° C. For HO^-, α (the fraction of the proton-free corners of the ion which have an H_2O molecule in hydrogen bond position) is 0.77 at 0° C and 0.44 at 100° C. For comparison it should be stated that BERNAL and FOWLER[11]) have roughly estimated, from the heat of fusion of ice and from the heat capacity of water, that in water at 0° 0.88 of the hydrogen bonds between the H_2O molecules are intact and at 100°, 0.75.

Summary.

1. Ice contains in its lattice H_3O^+ and HO^- ions in equal concentrations. They are formed, without displacements of oxygen atoms, by proton jumps between two adjacent H_2O molecules: $H_2O + H_2O \rightarrow H_3O^+ + HO^-$, and they are separated similarly, without displacements of oxygen atoms, by proton jumps between the ions and H_2O molecules: $H_3O^+ + H_2O \rightarrow H_2O + H_3O^+$ and $H_2O + HO^- \rightarrow HO^- + H_2O$. The ions migrate in the ice by means of proton jumps, until oppositely charged ions meet again and have the possibility of recombining.

2. The conductivity of ice may be assumed to be due exclusively to migration of H_3O^+ and HO^- ions by means of proton jumps. The molecular conductivity of these ions in ice can be calculated from the proton jump conductivity of the ions in water to be: 215 for H_3O^+ and 83 for HO^- at 0° C. The molecular concentration of the ions in ice is calculated from the specific conductivity of ice to 1.34×10^{-8}, corresponding to the transformation of 0.27×10^{-9} parts of the molecules to H_3O^+ ions, and of an equal fraction of the molecules to HO^- ions.

3. The rate of proton jumps in ice can be calculated, by means of EINSTEIN's equation for BROWNIAN movements, to be:

per H_2O molecule 152
per H_3O^+ ion (type $H_3O^+ + H_2O \rightarrow H_2O + H_3O^+$) . 4.15×10^{11}
per HO^- ion (type $H_2O + HO^- \rightarrow HO^- + H_2O$) . . . . . 1.6×10^{11}

all per second at 0° C.

4. The energies of activation for the proton jumps at the ions are calculated, from the temperature coefficient for the proton jump conductivity of the ions in water to be:

for H_3O^+ 2.5 kcal/gmol, for HO^- 4.7 kcal/gmol.

Using these values it is possible to calculate the temperature coefficient for the rate of proton jumps at the ions. The temperature coefficient for the molecular conductivity of the ions is the same as for the rate of proton jumps.

The fall in the ion concentration with temperature is dependent on the evolution of heat by the process of neutralization $H_3O^+ + HO^- \rightarrow 2\ H_2O$. This must be of a similar size in ice and in water (13.7), if it is permissible to use the static dielectric constant for the electrostatic forces between the ions in ice. A heat of neutralization of this order seems probable, as the ionization in ice is not very different from that in water. If, on account of the lower mobility of the dipoles in ice, a lower dielectric constant has to be used, the heat of neutralization in ice will be higher than that in water. If, e. g., a dielectric constant of 5.9 is assumed (corresponding to an alternating field frequency of 40 kc) the value is calculated to 33.3 kcal/gmol.

From JOHNSTONE's not very reliable determinations of the conductivity of ice, an apparent energy of activation of 19.6 kcal/gmol is calculated. The same energy of activation is calculated from the energies of activation for the proton jumps and from the heat of neutralization to only 9.95, when the heat of neutralization is taken as 13.7. On the other hand, a heat of neutralization of 33.3 gives an energy of activation of 19.75, which is in agreement with JOHNSTONE's figure.

5. The migration of the ions in ice is connected with turns of the H_2O molecules. If the ions migrate under the influence of an electric force, these turns will produce a dipole moment in the opposite direction to that of the force. The molecular turns produced by migration of the ions can not therefore be those required by DEBYE's theory for the dielectric properties of ice. They are also too infrequent to account for these properties.

6. For the justification of assuming the conductivity of ice to be the result of proton jumps in ice, it is of decisive importance that the molecular turns at orientation fault sites are between

10^3 and 10^4 times as frequent as molecular turns at the ions. This means that they are able to neutralize the dipole moment produced by the migration of the ions in an electrical field.

7. For the justification of assuming the abnormally high conductivity of the H_3O^+ and HO^- ions in water to be the result of proton jumps between the ions and the water molecules, it is of decisive importance that the molecular turns, connected with these proton jumps, only amount to a very small fraction of all the molecular turns in water.

References.

1) See e. g. H. Danneel, Zeitsch. f. Elektroch. **11** (1905) 249, A. Hantzsch and Kenneth S. Caldwell, Zeitschr. f. physik. Ch. **58** (1907) 575, L. Lorenz, l. c. **63** (1910) 252, E. Hückel, Zeitschr. f. Elektroch. **34** (1928) 546, Bernal and Fowler, Jour. Chem. Physics **I** (1933) 541, H. Ulich, Handbuch u. Jahrbuch d. chem. Physik **6** II (1933) 177.
2) J. H. L. Johnstone, Proc. Trans. Nova Scotian Inst. **13** (1912) 126.
3) A. Einstein, Ann. of Phys. (4) **17** (1905) 549, **19** (1906) 371.
4) M. L. Huggins, Journ. Phys. Chem. **40** (1936) 723.
5) W. M. Latimer, Chem. Rev. **44** (1949) 59.
6) W. Kauzmann, Rev. Mod. Physics, **14** (1942) 40.
7) Debye and Hückel, Physik. Zeitschr. **24** (1923) 185, 305.
8) Niels Bjerrum, Zeitschr. physik. Ch. **106** (1923) 219 and Ergebnisse der exakten Naturwissenschaften **5** (1926) 125.
9) J. Johnstone, Journ. Amer. Chem. Soc. **31** (1909) 1015.
10) L. Pauling, Nature of the chemical bond, New York (1945) 333.
11) Bernal and Fowler, Journ. Chem. Physics **I** (1933) 531.

Indleveret til selskabet den 19. oktober 1951.
Færdig fra trykkeriet den 31. december 1951.

Det Kongelige Danske Videnskabernes Selskab
Matematisk-fysiske Meddelelser, bind **27**, nr. 2

Dan. Mat. Fys. Medd. **27**, no. 2 (1952)

ON THE CHARGE OF THE RECOIL ATOM IN THE β-DECAY OF HE^6

BY

AAGE WINTHER

København
i kommission hos Ejnar Munksgaard
1952

Printed in Denmark
Bianco Lunos Bogtrykkeri

1. Introduction.

The β-decay of a nucleus will often be accompanied by excitation or ionization processes in the atomic core. Partly, the β-particle may collide with an atomic electron during its passage through the atom, partly the sudden change of the nuclear charge from Z to $Z \pm 1$ will cause a rearrangement of the electrons as a consequence of which the atom may be excited or ionized. The importance of this latter effect is evident in case of positon emission, but also in β^--decay there is an appreciable probability for secondary ionization processes.

The charge of the recoil atom may thus exceed one unit and the effect is therefore of importance for many types of measurements of the energy and momentum spectrum of the recoil atoms. Considerable interest attaches to these measurements which may yield detailed information regarding the mechanism of β-decay (KOFOED-HANSEN 1951).

The ionization accompanying β-decay has been investigated theoretically by FEINBERG (1941) and MIGDAL (1941). FEINBERG has shown that the dominating effect is due to the "shaking" of the atomic core due to the change of nuclear charge. This result follows also from a simple qualitative consideration: The time taken for a relativistic β-particle to leave a shell of electrons bound by a charge Ze is $t \approx \hbar^2/Zme^2c$. If now this time is short compared with the period of revolution for these electrons $1/\nu \approx \hbar^3 Z^2/me^4$, that is, if $\nu t \approx Z\alpha$ is small compared with unity, the change in the potential for the atomic electrons takes place so rapidly that the wave function after the β-process is almost equal to the original wave function (ψ). The relative change $\Delta\psi/\psi$ in the wave function during the emission of the β-electron will just be of the order νt. The calculation of the resulting excitation and ionization processes thus amounts to the expansion of the ground state

wave function of the original atom on the stationary state wave functions of the new atom.

In the case of H transforming into He, this expansion can readily be performed, and one finds an ionization probability of 2.5 %. For heavier atoms the calculation becomes rather complicated due to the complex character of the wave functions. Estimates based on approximate wave functions were obtained by MIGDAL, but they only apply to the ionization probability of the K, L and M electrons in heavy atoms.

We have attempted a more detailed calculation in the case of He transforming into Li. The β-decay of He^6 is of particular interest for the β-recoil studies (ALLEN 1949).

The ground state of He has angular momentum 0 and positive parity. The only states of Li II of this character, which lie below the ionization limit, are the states usually designated as $1s\ ns\ {}^1S_0$. The notation refers to the approximation in which the wave equation separates in the coordinates of the two electrons. All other 0 + states, such as $2s\ ns$ ($n \geq 2$) or $2p\ np$ etc., which would be bound states if the interaction between the electrons could be replaced by a central potential, lie in the continuum. They are therefore virtual states which, on account of the interaction, decay by auto-ionization (Auger effect).

The ionization probability may thus be calculated by subtracting from unity the probabilities for transition to the bound states ($1s\ ns$). Since this difference is relatively small it is necessary to use rather accurate wave functions for the bound states. Still, this method is advantageous because it is difficult to obtain adequate wave functions for the continuous spectrum and since calculations with continuum wave functions are very laborious.

Accurate wave functions for the ground state of He and Li II have been given by HYLLERÅS. In section 2, we derive wave functions for the $1s\ ns$ ($n \geq 2$) states of Li II for which sufficiently accurate expressions have not previously been given. The expansion coefficients are evaluated in section 3, and the results obtained are compared in section 4 with approximate direct estimates of the transition to free states, including the virtual states. In section 5 we shall consider various minor effects neglected in previous sections. A few remarks will also be made concerning the ionization by β-decay in heavier atoms.

2. Wave functions for bound states.

In order to calculate the probabilities for transitions to bound states of Li we need wave functions for the ground state of He (ψ_{He}) and for the $1s\,ns\,{}^1S_0$ states of Li II ($\psi_{1s\,ns}$).

Ground state of He.

For ψ_{He} we have used the very exact wave function

$$\psi^{(1)}_{\mathrm{He}} = 1.388\, e^{-1.818\,s}(1 + .3534\,u + .1282\,t^2 - .1007\,s + .0331\,s^2 - .0317\,u^2).$$

In calculations where such great accuracy is not necessary we have used the wave functions

$$\psi^{(2)}_{\mathrm{He}} = 1.34\; e^{-1.82\,s}\,(1 + .290\,u + .132\,t^2) \quad \text{and}$$
$$\psi^{(3)}_{\mathrm{He}} = 1.68^3/\pi\; e^{-1.68\,s}.$$

Here as in the following we have used atomic units (Bethe 1933).

The variables u, s, and t are defined as follows

$$s = \left|\vec{r}_1\right| + \left|\vec{r}_2\right|$$
$$t = \left|\vec{r}_1\right| - \left|\vec{r}_2\right|$$
$$u = \left|\vec{r}_1 - \vec{r}_2\right|,$$

where $\vec{r}_1$ and $\vec{r}_2$ are the radii vectors for the two electrons. The wave functions $\psi^{(1)}_{\mathrm{He}}$ and $\psi^{(2)}_{\mathrm{He}}$ have, with the exception of the normalizing factor, been calculated by Hylleraas (1929), and are cited by Bethe in Handbuch der Physik (p. 358). In our quotation, they are normalized for the whole configuration space of the two electrons according to the formula

$$2\,\pi^2 \int_0^\infty ds \int_0^s du \int_0^u (\psi)^2\; u\,(s^2 - t^2)\; dt = 1.$$

Ground state of Li II.

For $\psi_{1s\,1s}$ we have used the very exact wave function given by Hylleraas (1930a)

$$\psi_{1s\,1s} = 6.219\, e^{-3s}(1 + .11475\,s + .37594\,u + .18468\,t^2 + 0.1412\,s^2 - .17939\,u^2 + .05666\,us - .05506\,t^2 u + .02918\,u^3)$$

which is normalized according to the above formula. BETHE's quotation in Handbuch der Physik (p. 362) seems to lack a factor $^1/_2$ on the coordinate dependent terms in the paranthesis.

$1s\,2s\ {}^1S_0$ state of Li II.

A sufficiently good approximation for the wave function of this state appears not to have been given previously. We have carried out a calculation according to the scheme used by HYLLERÅS (1930 b) for the calculation of the $1s\,2s$ state wave function of He. Since the interaction between the electrons is relatively less important for Li II than for He, we can expect to get a rather good approximation to the wave function by means of the variational function

$$\psi = e^{-ks}\ [(a_1 + a_2\, s)\ \cosh\ \beta t + a_3\, t\ \sinh\ \beta t],$$

where k, β, a_1, a_2 and a_3 are varied.

Rather long and tedious calculations, quite analogous to those performed by HYLLERÅS, lead to the normalized wave function

$$\psi_{1s\,2s} = e^{-2.04\,s}\,[(1.334\,s - 2.172)\cosh\ 1.000\,t + 1.114\sinh\ 1.000\,t].$$

The ionization energy corresponding to this wave function is

$$\mathrm{I_{theor}} = 117900\ \mathrm{cm^{-1}}$$

while the energy found experimentally is

$$\mathrm{I_{exp}} = 118700\ \mathrm{cm^{-1}}$$

(extrapolated value given by WERNER 1927; cf. also MOORE 1949). The difference amounts to .7 %.

$1s\,3s\ {}^1S_0$ state of Li II.

For this state we have used the following Hartree approximation. The motion of the inner electron is considered to be unperturbed, and the resultant potential for the second electron is found. Then, using the experimentally known term value, we get the following differential equation for the radial wave function (ψ_1) of the outer s-electron,

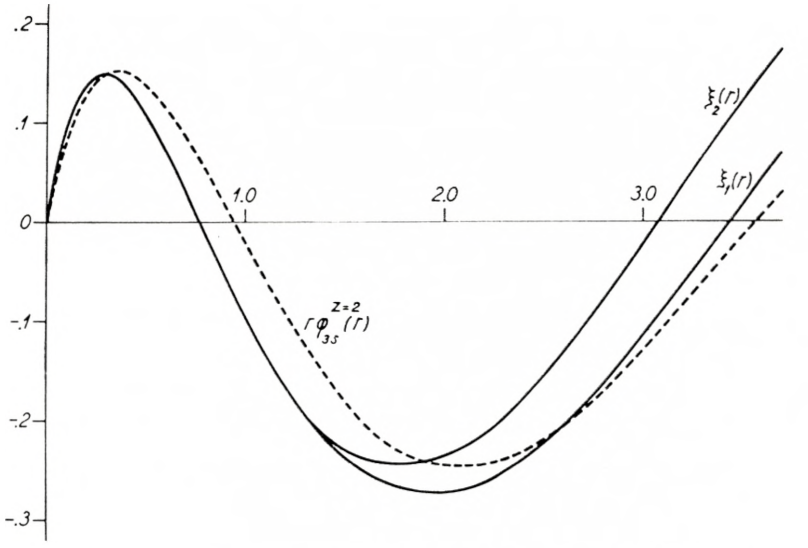

Fig 1. Radial wave functions for the outer electron in the $1s\,3s$ state (ξ_1) and the $1s\,4s$ state (ξ_2) compared with the Coulomb wave function ($r\varphi_{3s}^{Z=2}(r)$) for the $3s$ state corresponding to complete screening ($Z = 2$).

$$d^2\,\xi_1/dr^2 + [4/r + 2\,e^{-6r}(1/r + 3) - .46]\;\xi_1 = 0,$$

where $\xi_1 = r\psi_1$.

This differential equation is solved numerically for $r < 1.2$. For greater values of r, where the second term in the paranthesis is negligible, the solution which tends to 0 as $r \to \infty$ is a confluent hypergeometric function with the asymptotic expansion

$$\xi_1(r) = -e^{-y_1} y_1^{2.95}(1 - 2.874/y_1 + 1.257/y_1^2 + .0101/y_1^3 - .0007/y_1^4),$$

where $y_1 = .678r$. This solution turns out to fit rather well with the numerical solution at $r = 1.2$, as shown in fig. 1. The difference between logarithmic derivatives is about 10 per cent.

As a total normalized wave function for the $1s\,3s$ state we have used

$$\psi_{1s\,3s} = .659\,(e^{-3r_2}\,\xi_1(r_1)/r_1 + e^{-3r_1}\,\xi_1(r_2)/r_2).$$

In order to obtain an estimate of the accuracy of this wave function we have calculated the scalar product to the two functions $\psi_{1s\,2s}$ and $\psi_{1s\,3s}$ which were derived by quite different methods. One finds

$$\iint \psi_{1s\,2s}\,\psi_{1s\,3s}\,d\tau_1\,d\tau_2 = -.054.$$

$1s\,4s\ {}^1S_0$ state of Li II.

For this state we use a similar treatment. The wave function for the outer electron is supposed to be a solution of the equation

$$d^2\xi_2/dr^2 + [4/r + 2e^{-6r}(1/r + 3) - .26]\xi_2 = 0,$$

where $\xi_2 = r\psi_2$.

For $r < 1.5$ the solution is almost identical to ξ_1 (cf. BETHE, loc. cit., p. 288). For $r > 1.5$ we use the asymptotic expansion

$$\xi_2(r) = -.83\,e^{-y_2}\,y_2^{3.93}(1 - 5.74/y_2 + 8.09/y_2^2 - 2.41/y_2^3 - .021/y_2^4),$$

where $y_2 = .509r$. The factor .83 is chosen such as to make $\xi_2(r)$ coincide with $\xi_1(r)$ for r small (fig. 1).

The normalized wave function for the $1s\ 4s$ state is then

$$\psi_{1s\,4s} = .421\,(e^{-3r_2}\,\xi_2(r_1)/r_1 + e^{-3r_1}\,\xi_2(r_2)/r_2).$$

The wave functions for the higher s states will, in nearly the whole region where $\psi_{\mathrm{He}} \neq 0$, be similar to $\psi_{1s\,4s}$. The normalizing factor will be approximately proportional to $n_{\mathrm{eff}}^{-3/2}$, where n_{eff} is the effective quantum number for the outer electron.

3. Expansion coefficients for transitions to bound states.

We denote the probability for transition to the rs ns state by

$$P(\mathrm{r.n}) = |\mathrm{a}(\mathrm{r.n})|^2 = \left|\iint \psi_{\mathrm{He}}\ \psi_{\mathrm{rs\,ns}}\ d\tau_1\ d\tau_2\right|^2$$

and from the wave functions given in the previous section we obtain the following results:

$$\begin{aligned}
a(1.1) &= \iint \psi^{(1)}_{\mathrm{He}}\,\psi_{1s\,1s}\,d\tau_1\,d\tau_2 = .8184\\
P(1.1) &= .670\\
a(1.2) &= \iint \psi^{(1)}_{\mathrm{He}}\,\psi_{1s\,2s}\,d\tau_1\,d\tau_2 = .408\\
P(1.2) &= .166\\
a(1.3) &= \iint \psi^{(2)}_{\mathrm{He}}\,\psi_{1s\,3s}\,d\tau_1\,d\tau_2 = .163\\
P(1.3) &= .027\\
a(1.4) &= \iint \psi^{(2)}_{\mathrm{He}}\,\psi_{1s\,4s}\,d\tau_1\,d\tau_2 = .088\\
P(1.4) &= .008.
\end{aligned}$$

In view of the inaccuracy of $\psi_{1s\,3s}$ and $\psi_{1s\,4s}$ we have, in the last two cases, used the less accurate wave function $\psi^{(2)}_{\mathrm{He}}$. Probably the most uncertain of the values quoted above are $a\,(1.2)$ and $a\,(1.3)$. To illustrate the strong dependence of these quantities on the wave functions, we quote two results for the expansion coefficients, obtained by means of less accurate helium wave functions

$$a^*\,(1.2) = \iint \psi^{(2)}_{\mathrm{He}}\,\psi_{1s\,2s}\,d\tau_1\,d\tau_2 = .399$$
$$P^*\,(1.2) = .159$$
$$a^*\,(1.3) = \iint \psi^{(3)}_{\mathrm{He}}\,\psi_{1s\,3s}\,d\tau_1\,d\tau_2 = .142$$
$$P^*\,(1.3) = .020.$$

It is to be emphasized that the difference between these results and the values given above provides no direct indication of the accuracy of the values since the essential sources of error probably are the lithium wave functions. The results exhibit a tendency of $P(1.\mathrm{n})$ $(\mathrm{n} \geq 2)$ to increase with increasing accuracy of the wave functions, a tendency which was found to be very characteristic of the whole calculation. It thus appears probable that the use of more accurate wave functions would lead to still higher values for $P(1.\mathrm{n})$.

According to section 2, we may assume the expansion coefficients of ψ_{He} on the higher s states to be proportional to $n_{\mathrm{eff}}^{-3/2}$, that is

$$P\,(1.5) + P\,(1.6) + \ldots\ldots =$$
$$(4 - .075)^3\;P\,(1.4)\;[1/(5 - .075)^3 + 1/(6 - .075)^3 + \ldots] = .012$$

since n_{eff} equals $\mathrm{n} - .075$.

The total probability for transitions to bound states is found to be

$$P_{\mathrm{bound}} = \sum_{n=1}^{\infty} P\,(1.\mathrm{n}) = .883.$$

The uncertainty of P_{bound} has roughly been estimated on the basis of the scalar product of $\psi_{1s\,2s}$ and $\psi_{1s\,3s}$ (p. 7) to be of the order of one to two per cent.

According to the result for P_{bound} the probability for transitions to free states should be .117. However, in view of the indication that the use of more accurate wave functions would lead to a slightly larger value of P_{bound}, an indication which is supported by the estimates in the next section, we give as final estimate of the ionization probability

$$P_{\text{ion}} = (10.5 \pm 1.5) \text{ per cent.}$$

This rather large value for P_{ion} may be of significance in recoil experiments. The corrections to be made to the results obtained by ALLEN (1949) in such experiments may easily be evaluated. They are found to be almost of the same order of magnitude as the difference between the curves for the different coupling cases. Still, with the present experimental uncertainties, the corrections hardly alter the conclusions which may be drawn from the measurements.

An experimental test of the value for P_{ion} may be possible by measurements of the motion of recoil atoms in combined electric and magnetic fields (KOFOED-HANSEN 1951). Measurements of the photons emitted from excited states of Li II might also give a valuable test of the theoretical calculations.

4. Transitions to free states.

In a discussion of free states we may use two different approaches.

I) The interaction between the electrons is represented by a screening of the nuclear potential; we thus write $1/r_{12} = V_1(r_1) + V_2(r_2) + W$ and neglect the potential W. In this approximation the states with energy greater than the ionization potential are of three different types: 1) States, where both electrons are free ($E_1\, E_2$), 2) states, where one electron is bound the other free ($1s E, 2s E \ldots$), 3) states, where both electrons are "bound" ($2s\ 2s, 2s\ 3s, \ldots$). States of the last type are virtual; they decay by Auger effect (auto-ionization) into states of the second type.

The Auger transition is caused by the neglected potential W, and the decay time may be calculated by considering this potential as a perturbation (WENTZEL 1927).

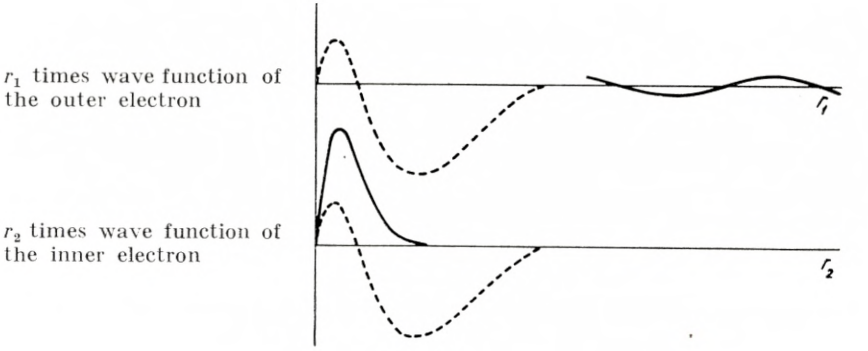

Fig. 2.

II) In a more rigorous treatment only states of the first two types in I) exist. For nearly all values of E we may in good approximation separate the wave equation in the two electrons as in I). For energy values close to the energy of the virtual states this approximation however breaks down and a sort of resonance phenomenon occurs. As illustrated in fig. 2, the wave function for the stationary states may be looked upon as a combination of a $1sE$ state with a $2s\,2s$ state. This figure should be understood in the sense that for great distances of the outer electron the total wave function is the symmetrized product of the two full-drawn curves, that is of a Coulomb wave function for the continuous spectrum and a Coulomb wave function for the $1s$ state approximately. For smaller distances the amplitude of the total wave function grows up rapidly, and its dependence on both electron-coordinates is quite changed. For small values of r_1 and r_2 the wave function may be approximated by the $2s\,2s$ wave function (dotted curves).

From the wave function described in this way, the decay time of the $2s\,2s$ state may be calculated as the outgoing probability current.

An accurate computation of the expansion coefficients on the free states of Li II would be highly complicated. We shall attempt an approximate calculation in order to estimate the order of magnitude of the ionization probability and its distribution on the various types of free states.

For energies different from those of the virtual states the wave function for the free states may be approximated by the

product of $1s, 2s \ldots$ Coulomb wave functions (with $Z = 3$) and Coulomb wave functions (with $Z = 2$) for the continuous spectrum. The total transition probability to these states is given by

$$P_{\text{cont}} = \int_0^\infty \{ |a(1.E)|^2 + |a(2.E)|^2 + \ldots \} dE + \int_0^\infty \int_0^\infty |a(E_1.E_2)|^2 dE_1 dE_2.$$

Since the widths of the virtual states are small ($< 100\ \text{cm}^{-1}$) the contribution to P_{cont} from the energy regions of the virtual states is negligible.

In the neighbourhood of the energies of the virtual states, the amplitude of the wave functions for small r is much larger than the amplitude of simple Coulomb wave functions used above. An approximate estimate of the transition probability for this energy region may be obtained by using the normalized wave functions for the virtual states. If we write

$$P_{\text{virt}} = P(2.2) + P(2.3) + P(2.3) + \ldots + P(3.3) + \ldots$$

the sum

$$P_{\text{free}} = P_{\text{cont}} + P_{\text{virt}}$$

will give the total transition probability to free states.

The value of P_{cont} may be calculated by noting that

$$\left| \int \varphi_{1s}^{z=2}(1) \int \psi_{\text{He}} \varphi_{ns}^{z=3}(2)\, d\tau_1 d\tau_2 \right|^2 + \left| \int \varphi_{2s}^{z=2}(1) \int \psi_{\text{He}} \varphi_{ns}^{z=3}(2)\, d\tau_2 d\tau_1 \right|^2 + \ldots$$

$$+ \frac{1}{2} \int_0^\infty |a(n_1 E)|^2\, dE = \left| \iint \varphi_{ns}^{z=3}(2)\, \psi_{\text{He}}\, d\tau_1\, d\tau_2 \right|^2.$$

$\varphi_{ns}^{z=m}(1)$ represents the normalized Coulomb wave function for electron 1 in the ns state with $Z = m$. The factor $^1/_2$ comes from the symmetrization.

In view of the approximate character of the free state wave functions used, we have calculated the transition probability by using $\psi_{\text{He}} = \psi_{\text{He}}^{(3)}$ and found

$$P_{\text{cont}} = .015.$$

The contribution to this result from the $E_1 E_2$ states is negligible ($< .001$).

The evaluation of P_{virt} can only be made with rather great uncertainty. Several authors have derived approximate wave functions for virtual states of He I (WU 1934, WILSON 1935). For Li II apparently no calculations exist. Since, however, it has not been possible with the wave functions so far constructed to account adequately for the properties of virtual states in light atoms (WU 1944, 1950), we shall here only attempt order of magnitude estimates based on simple Coulomb wave functions.

If we assume for the wave function of the $2s\,2s$ state

$$\psi_{2s\,2s} = \varphi^z_{2s}(1)\,\varphi^z_{2s}(2)$$

the most appropriate value of Z is expected to lie in the interval $2.7 < Z < 3$. The corresponding limit for $P(2.2)$ is $.011 < P(2.2) < .03$. In the same approximation we get a maximum value for $P(2.3)$ of .007 and for $P(3.3)$ of .0002.

Altogether we find

$$P_{\text{virt}} \lesssim .04 \qquad \text{and} \qquad P_{\text{free}} \lesssim .06.$$

There is a considerable discrepancy between this estimate and the result $P_{\text{bound}} = .883$ obtained in section 3, since the sum of P_{bound} and P_{free} should equal unity. This discrepancy may partly be due to the uncertainty in P_{bound}, but for the larger part must be ascribed to the very uncertain determination of P_{free}.

The estimates made in this section serve primarily to indicate the distribution on the free state transitions and to show the importance of transitions to virtual states. From the very small probability for double ionization ($E_1 E_2$ states) we may further conclude that the average charge on the lithium recoil is

$$\underline{\langle z \rangle = 1.105 \pm .015,}$$

provided we use the value for P_{ion} quoted on p. 10.

5. Discussion.

In the above treatment a number of minor effects have been neglected. Although, as we shall see, they are all negligible in case of He, some may become significant for heavier atoms.

I) As mentioned in section 1, the β-electron will have a chance, by direct interaction with the atomic electrons, to knock one of these out of the atom. The probability for this process (P_{dc}) as compared with the probability for ejection of this electron due to the effect of "shaking" (P_s), has been estimated by FEINBERG (1941).

For a relativistic β-particle he finds

$$P_{dc}/P_s \approx I/mc^2 \approx (Z\alpha)^2,$$

where I is the ionization energy of the electron and Z is the effective nuclear charge.

In the case of the He^6 decay the contribution of direct collision thus amounts to

$$P_{dc} \approx .0001,$$

which obviously can be neglected. In heavier atoms P_{dc} and P_s may become of the same order of magnitude only for electrons in the inner shells. As P_s is small for these electrons (MIGDAL 1941) the contribution of P_{dc} to the total ionization probability will always be negligible. Since, however, the removal of one of the inner electrons will give rise to a cascade of Auger electrons (cf. section III) the direct collision may become important for that small fraction of the recoil atoms which are highly ionized.

II) Our results have to be corrected for the recoil motion of the nucleus, since the expansion of ψ_{He} on lithium wave functions must be carried out using wave functions referring to a lithium atom in motion.

The velocity (v) of the lithium recoil, corresponding to the maximum recoil energy $\approx$ 1500 eV, is of the order of $v_0/20$, where $v_0 = Z\,\alpha\,c$ (the velocity of the atomic electrons). In this case we would expect the correction for the transition probabilities to be of the order $(v/v_0)^2 \approx .003$.

We have also carried out a more exact calculation using lithium

wave functions corresponding to a moving atom and obtained substantially the same result.

The result shows that in general we may neglect the effect of the recoil motion when we have to do with free atoms. For atoms bound in molecules this effect will be of great importance, since the molecule may be disrupted.

III) In the calculations we have made the assumption that the lifetime of the virtual states against Auger effect (τ_{aug}) is small compared with the radiation lifetime (τ_{rad}). According to WENTZEL (1927), the ratio of the two lifetimes is of the order $\tau_{aug}/\tau_{rad} \approx 10^{-6} Z^4$ and thus very small for lithium. All states in which both electrons are excited therefore practically always lead to ionization.

According to the estimates in section 4 the Auger effect is actually responsible for the main part of the ionization. For heavier atoms we would expect the Auger effect to play a similar role. In earlier papers on the ionization of atoms by β-decay, the Auger effect has not been taken into account (FEINBERG 1941, MIGDAL 1941). MIGDAL thus calculates the ionization probability due to the "shaking" effect by expanding the wave functions for the original atom only on the wave functions for the continuous spectrum of the resulting atom.

If we take into account the Auger effect, the emission of an electron, from the K-shell say, would, as long as the condition $\tau_{aug}/\tau_{rad} < 1$ is fulfilled, give rise to a shower of Auger electrons, which would leave the atom several times ionized. (This would also be the case if the K-electron were only excited into some allowed bound state). As Z increases the Auger effect will be less probable, but only for the inner shells, where the screening is small.

For the most loosely bound electrons the situation is very similar to the case of He $\rightarrow$ Li, and one has to take into account that only a small part of the ionization is due to direct transition to the continuous spectrum.

We have made some rough estimates on the average charge of heavier recoil atoms, using the results of MIGDAL and correcting them for the effects mentioned above. It appears that the average extra charge of the recoil from a β-process will increase with the

nuclear charge Z, so that for heavy atoms it may be quite considerable (of the order 0.5—1).

I wish to express my sincere thanks to Mr. AAGE BOHR for suggesting this problem and for many helpful discussions. My thanks are further due Professor NIELS BOHR for his continuous interest in my work.

Institute for Theoretical Physics,
University of Copenhagen,
Denmark.

References.

ALLEN, J. S., H. R. PANETH, and A. H. MORRISH, 1949: Phys. Rev. **75**, 570.
BETHE, H., 1933: Handbuch der Physik XXIV/1.
FEINBERG, E. L., 1941: Journ. of Phys. USSR. **4**, 423.
HYLLERÅS, E., 1929: Zs. f. Phys. **54**, 347.
— 1930a: Zs. f. Phys. **65**, 209.
— and B. UNDHEIM 1930b: Zs. f. Phys. **65**, 759.
KOFOED-HANSEN, O., 1951: Dan. Mat. Fys. Medd. **26**, no. 8.
MIGDAL, A., 1941: Journal of Phys. USSR. **4**, 449.
MOORE, CHARLOTTE, 1949: Atomic Energy Levels Vol. 1. NBS Circular 467.
WENTZEL, G., 1927: Zs. f. Phys. **43**, 524.
WERNER, S., 1927: Studier over spektroskopiske Lyskilder.
WILSON, WM. S., 1935: Phys. Rev. **48**, 536.
WU, TA-YOU, 1934: Phys. Rev. **46**, 239.
— 1944: Phys. Rev. **66**, 291.
— and OUROM 1950: Canad. Journ. of Res. A **28**, 542.

Indleveret til selskabet den 19. oktober 1951.
Færdig fra trykkeriet den 22. marts 1952.

Det Kongelige Danske Videnskabernes Selskab
Matematisk-fysiske Meddelelser, bind **27**, nr. 3

Dan. Mat. Fys. Medd. **27**, no. 3 (1952)

ON THE ORIGINAL ORBIT OF COMET 1899 I

BY

HANS Q. RASMUSEN

København
i kommission hos Ejnar Munksgaard
1952

Printed in Denmark.
Bianco Lunos Bogtrykkeri.

Comet 1899 I belongs to the group of comets for which a definitive calculation gives a hyperbolic orbit and therefore is fit to be used as basis of an investigation of the original orbit before the comet entered the region of the Sun and the major planets. The following elements have been computed by Merfield from 580 observations from March 4 to August 10, 1899 (159 days), all perturbations being taken into account (*Astronomische Nachrichten* 3748).

Osculation 1899, March 12

$$
\begin{aligned}
T &= \text{1899, April } 12.978010 \text{ G.M.T.} \\
\omega &= 8^\circ 41' 46''.48 \\
\Omega &= 24\ 59\ 59.93 \quad 1900.0 \\
i &= 146\ 15\ 30.29 \\
q &= 0.32657237 \pm 0.00000162 \\
e &= 1.00035029 \pm 0.00000404
\end{aligned}
$$

Probable errors.

From the values of q and e we compute the reciprocal value of the semi-major axis and its mean error:—

$$\frac{1}{a} = -0.0010726 \pm 0.0000184.$$

The orbit does not quite fulfil Elis Strömgren's requirement, not having a period of observations of at least 6 months. As the number of observations, however, is large and as moreover another computation by Wedemeyer has given practically the same elements, I have all the same carried out a computation of the perturbed orbit in the years before the time of perihelion.

As the distance of perihelion is small, we have to start the computation by Encke's method. If we take all perturbations into account we get the following rectangular, ecliptical perturbations in units of the 8th decimal referred to the equinox of 1900.0:—

G. M. T.			ξ	η	ζ
1899	Mar.	30....	+ 32	0	+ 18
		20....	7	0	4
		10....	1	0	1
	Feb.	28....	15	— 5	15
		18....	54	31	58
		8....	123	87	135
	Jan.	29....	228	182	246
		19....	367	322	389
		9....	537	518	563
1898	Dec.	30....	730	778	769
		20....	941	1111	1012
	Nov.	30....	1377	2022	1613
		10....	1848	3299	2400
	Oct.	21....	2413	4971	3414
		1....	3112	7061	4707
	Sep.	11....	3968	9596	6340
	Aug.	22....	4983	12616	8388
		2....	6142	16181	10940
	July	13....	7431	20374	14106
	June	23....	+ 8832	— 25296	+ 18018

On July 13, 1898, the comet had a distance from the Sun sufficient for the direct integration of the co-ordinates. From the elements we compute the unperturbed co-ordinates and velocities:—

$$x_0 = -3.9804483 \qquad 20\frac{dx_0}{dt} = +0.22685216$$

$$y_0 = +0.7341700 \qquad 20\frac{dy_0}{dt} = +0.01624977$$

$$z_0 = -1.5681124 \qquad 20\frac{dz_0}{dt} = +0.05420179$$

From the scheme of perturbations we get:—

$$\xi = +0.0000743 \qquad 20\frac{d\xi}{dt} = -0.00001342$$

$$\eta = -0.0002037 \qquad 20\frac{d\eta}{dt} = +0.00004540$$

$$\zeta = +0.0001411 \qquad 20\frac{d\zeta}{dt} = -0.00003515$$

The additions give the perturbed co-ordinates and velocities:—

$$x = -3.9803740 \qquad 20\frac{dx}{dt} = +0.22683874$$

$$y = +0.7339663 \qquad 20\frac{dy}{dt} = +0.01629517$$

$$z = -1.5679713 \qquad 20\frac{dz}{dt} = +0.05416664$$

These values lead to the following perturbed co-ordinates:—

G. M. T.	x	y	z
1898 July 13....	— 3.9803740	+ 0.7339663	— 1.5679713
June 23....	4.2044239	0.7171655	1.6210429
3....	4.4232304	0.6994595	1.6720819
May 14....	4.6372405	0.6809836	1.7212956
Apr. 24....	4.8468382	0.6618484	1.7688573
4....	5.0523545	0.6421448	1.8149146
Mar. 15....	5.2540889	0.6219487	1.8595938
Feb. 23....	5.4522899	0.6013243	1.9030045
3....	5.6471875	0.5803266	1.9452424
Jan. 14....	5.8389844	0.5590028	1.9863921
1897 Dec. 25....	6.0278616	0.5373940	2.0265296
5....	6.2139831	0.5155363	2.0657228
Oct. 26....	6.5785402	0.4711939	2.1415169
Sep. 16....	6.9336942	0.4261793	2.2142024
Aug. 7....	7.2803209	0.3806469	2.2841321
June 28....	7.6191655	0.3347153	2.3515993
May 19....	7.9508669	0.2884762	2.4168488
Apr. 9....	8.2759793	0.2420035	2.4800880
Feb. 28....	8.5949862	0.1953550	2.5414930
Jan. 19....	8.9083123	0.1485781	2.6012166
1896 Dec. 10....	— 9.2163332	+ 0.1017119	— 2.6593910

G. M. T.	x	y	z
1896 Oct. 31....	— 9.5193835	+ 0.0547878	— 2.7161315
Sep. 21....	9.8177625	+ 0.0078325	2.7715408
Aug. 12....	10.1117395	— 0.0391322	2.8257091
July 3....	10.4015580	0.0860880	2.8787173
May 24....	10.6874388	0.1330196	2.9306380
Apr. 14....	10.9695831	0.1799144	2.9815361
Mar. 5....	11.2481749	0.2267614	3.0314711
1895 Dec. 16....	11.7953637	0.3202778	3.1286603
Sep. 27....	12.3302033	0.4135133	3.2225805
July 9....	12.8537214	0.5064280	3.3135462
Apr. 20....	13.3668048	0.5989955	3.4018256
Jan. 30....	13.8702286	0.6911966	3.4876483
1894 Nov. 11....	14.3646750	0.7830189	3.5712130
Aug. 23....	14.8507477	0.8744537	3.6526935
June 4....	15.3289852	0.9654958	3.7322420
Mar. 16....	15,7998699	1.0561418	3.8099939
1893 Dec. 26....	16.2638365	1.1463891	3.8860687
Oct. 7....	16.7212784	1.2362363	3.9605741
July 19....	17.1725529	1.3256820	4.0336066
Apr. 30....	17.6179854	1.4148261	4.1052531
1892 Nov. 21....	18.492489	1.591596	4.244696
June 14....	19.346884	1.766834	4.379456
Jan. 6....	20.182939	1.940422	4.509993
1891 July 30....	21.002159	2.112340	4.636698
Feb. 20....	21.805827	2.282577	4.759908
1890 Sep. 13....	22.595045	2.451126	4.879910
Apr. 6....	23,370768	2.617996	4.996957
1889 Oct. 28....	24.133827	2.783206	5.111272
May 21....	24.884957	2.946793	5.223048
1888 Dec. 12....	25.624805	3.108802	5.332460
July 5....	26.353957	3.269292	5.439662
Jan. 27....	27.072941	3.428330	5.544792
1887 Aug. 20....	27.782241	3.585990	5.647975
Mar. 13....	28.482303	3.742348	5.749324
1886 Oct. 4....	— 29.173540	— 3.897486	— 5.848941

G. M. T.	x	y	z
1886 Apr. 27....	— 29.856341	— 4.051488	— 5.946919
1885 Nov. 18....	30.531069	4.204437	6.043342
June 11....	31.198073	4.356416	6.138289
Jan. 2....	31.857683	4.507503	6.231829
1884 July 26....	32.510216	4.657781	6.324029
Feb. 17....	33.155984	4.807318	6.414948
1883 Sep. 10....	33.795284	4.956179	6.504643
Apr. 3....	34.428409	5.104419	6.593163
1882 Oct. 25....	35.055646	5.252079	6.680556
May 18....	35.677272	5.399183	6.766867
1881 Dec. 9....	36.293551	5.545740	6.852136
July 2....	36.904735	5.691738	6.936401
Jan. 23....	37.511055	5.837145	7.019699
1880 Aug. 16....	38.112718	5.981919	7.102065
Mar. 9....	38.709904	6.126002	7.183530
1879 Oct. 1....	39.302761	6.269335	7.264126
Apr. 24....	39.891415	6.411861	7.343884
1878 Nov. 15....	40.475960	6.553532	7.422832
June 8....	41.056474	6.694311	7.500997
1877 Dec. 30....	41.633020	6.834176	7.578406
July 23....	42.205647	6.973122	7.655083
Feb. 13....	42.774405	7.111148	7.731053
1876 Sep. 6....	43.339337	7.248303	7.806338
Mar. 30....	43.900489	7.384592	7.880959
1875 Oct. 22....	44.457911	7.520064	7.954936
May 15....	45.011650	7.654769	8.028288
1874 Dec. 6....	45.561767	7.788758	8.101034
June 29....	46.108323	7.922090	8.173190
Jan. 20....	46.651385	8.054823	8.244773
1873 Aug. 13....	47.191028	8.187019	8.315796
Mar. 6....	47.727332	8.318737	8.386275
1872 Sep. 27....	48.260387	8.450037	8.456223
Apr. 20....	48.790289	8.580972	8.525653
1871 Nov. 12....	49.317141	8.711593	8.594575
June 5....	— 49.841056	— 8.841938	— 8.663002

On November 12, 1871, when the comet had a distance of 50.8 units from the Sun, it was so remote from the planets that the perturbations had only insignificant influence on the movement of the comet.

Now we compute the following velocity components $\frac{dx}{dt}$, $\frac{dy}{dt}$, $\frac{dz}{dt}$ and reductions to the centre of gravity of the Sun and the 8 major planets $\xi_\odot$, $\eta_\odot$, $\zeta_\odot$, $\frac{d\xi_\odot}{dt}$, $\frac{d\eta_\odot}{dt}$, $\frac{d\zeta_\odot}{dt}$. The addition gives the resulting centre co-ordinates and velocities $\bar{x}$, $\bar{y}$, $\bar{z}$, $\frac{d\bar{x}}{dt}$, $\frac{d\bar{y}}{dt}$, $\frac{d\bar{z}}{dt}$.

$x = -49.31714$	$y = -8.71159$	$z = -8.59458$
$\xi_\odot = +\ 14$	$\eta_\odot = -\ 320$	$\zeta_\odot = -\ 1$
$\bar{x} = -49.31700$	$\bar{y} = -8.71479$	$\bar{z} = -8.59459$

$\frac{dx}{dt} = +0.00328353$	$\frac{dy}{dt} = +0.00081548$	$\frac{dz}{dt} = +0.00042916$
$\frac{d\xi_\odot}{dt} = +\ 566$	$\frac{d\eta_\odot}{dt} = +\ 173$	$\frac{d\zeta_\odot}{dt} = -\ 10$
$\frac{d\bar{x}}{dt} = +0.00328919$	$\frac{d\bar{y}}{dt} = +0.00081721$	$\frac{d\bar{z}}{dt} = +0.00042906$

From these we find:—

$$\bar{r} = \sqrt{\bar{x}^2 + \bar{y}^2 + \bar{z}^2} = 50.81320$$

$$V^2 = \left(\frac{d\bar{x}}{dt}\right)^2 + \left(\frac{d\bar{y}}{dt}\right)^2 + \left(\frac{d\bar{z}}{dt}\right)^2 = 0.00001167070\,.$$

If these values are substituted in the equation of conservation of energy:—

$$\frac{V^2}{k^2(1+m)} = \frac{2}{\bar{r}} - \frac{1}{\bar{a}}\,,$$

in which:—

$$k^2(1+m) = 0.0002963093\,,$$

we find:—

$$\frac{1}{\bar{a}} = -0.0000270 \pm 0.0000184\,.$$

Thus the computation has given the result that the original orbit was hyperbolic, though only in a slight degree.

The result of the investigations up to now is that in 22 out of 23 cases the orbits have changed in a hyperbolic direction during the time when the comets moved from far off to the region of perihelion. Only in 3 cases the computations have shown an original hyperbolic orbit, but two of the results must be considered inconclusive as all perturbations had not been taken into account. The third case is comet 1899 I, where the original $\frac{1}{a}$ is negative, and numerically larger than the mean error.

In fact we have here the first example of a comet for which all perturbations have been taken into account and which all the same shows an originally hyperbolic orbit. However, since a change in $\frac{1}{a}$ equal to 1.5 times the computed mean error would make the orbit elliptical, it cannot be said that an originally hyperbolic orbit has been established.

Indleveret til selskabet den 21. september 1951.
Færdig fra trykkeriet den 10. marts 1952.

Det Kongelige Danske Videnskabernes Selskab
Matematisk-fysiske Meddelelser, bind **27**, nr. 4

Dan. Mat. Fys. Medd. **27**, no. 4 (1952)

ON THE SUMMABILITY FUNCTION AND THE ORDER FUNCTION OF DIRICHLET SERIES

BY

HARALD BOHR †

København
i kommission hos Ejnar Munksgaard
1952

Printed in Denmark
Bianco Lunos Bogtrykkeri

§ 1. Introduction.[1]

The aim of the present paper is to give a contribution to the study of the connection between the so-called summability function $\psi(\sigma)$ and the order function $\mu(\sigma)$ of an ordinary Dirichlet series $f(s) = \sum_{n=1}^{\infty} a_n n^{-s}$. Before stating the results of the paper we shall recall the definitions of these functions and some known theorems.

Let $f(s) = \sum a_n n^{-s}$ be an ordinary Dirichlet series which is neither everywhere divergent nor everywhere convergent. Let for every integer $r \geq 0$ the number λ_r denote the abscissa of summability of the r^{th} order, in particular λ_0 the abscissa of convergence. Then, as shown by the author ([2], and [3], pp. 99—104),

(1) $0 \leq \lambda_r - \lambda_{r+1} \leq 1$ and $\lambda_r - \lambda_{r+1} \geq \lambda_{r+1} - \lambda_{r+2}$ $(r = 0, 1, 2, \cdots)$.

When we follow M. Riesz and consider summability of *arbitrary* order $r \geq 0$, the abscissa λ_r exists as a function of r in the interval $0 \leq r < \infty$. In generalization of the above inequalities the function $\sigma = \lambda_r$ is a non-increasing continuous convex function with numerical slope ≤ 1 (see [6], pp. 57 and 60, and [8], p. 118). We introduce the number $\Omega\,(\geq -\infty)$ as the limit $\Omega = \lim_{r \to \infty} \lambda_r$. It follows from the results just mentioned that when r increases from 0 to ∞, then λ_r will be either a strictly decreasing function which tends to Ω for $r \to \infty$, or λ_r will from a certain step r_0, i. e. for $r \geq r_0$, be constant $= \Omega$.

We define now for every number σ in the interval $\Omega < \sigma < \infty$ the number $r = \psi(\sigma)$ as the greatest lower bound of those values $r' \geq 0$ for which $\lambda_{r'} \leq \sigma$. The function $r = \psi(\sigma)$ is called the *summability function* of the Dirichlet series. It is equal to 0 for $\sigma \geq \lambda_0$ and in the interval $\Omega < \sigma \leq \lambda_0$ (when we suppose that $\Omega < \lambda_0$) it is simply

[1] This paper is based on notes left by Professor Harald Bohr. The manuscript has been prepared by Dr. Erling Følner.

the inverse function of $\sigma = \lambda_r$. Hence it follows from the above results that $r = \psi(\sigma)$ is a continuous convex function which in the interval $\Omega < \sigma \leqq \lambda_0$ is strictly decreasing with numerical slope $\geqq 1$, i.e. with a left derivative $\psi'(\lambda_0 - 0) \leqq -1$ at the point $\sigma = \lambda_0$. Further, if λ_r is constant $= \Omega$ from a certain step r_0, then $\psi(\sigma) \to r_0$ for $\sigma \to \Omega$; otherwise $\psi(\sigma) \to \infty$ for $\sigma \to \Omega$.

Contrary to the abscissa of convergence λ_0, the abscissa Ω has a simple function theoretical meaning (H. Bohr [2], and [3], p. 124; M. Riesz [7]). Indeed, for every $\sigma_0 > \Omega$, the function $f(s)$ represented by the series is of finite order with respect to t in the half plane $\sigma > \sigma_0$, i.e. there exists a number $l \geqq 0$ such that

$$f(\sigma + it) = O(|t|^l) \tag{2}$$

when $|t| \to \infty$, uniformly for all $\sigma > \sigma_0$, whereas $f(s)$ is not regular and of finite order in any half plane $\sigma > \sigma_0$ where $\sigma_0 < \Omega$. For every $\sigma > \Omega$ we define the number $\mu(\sigma)$ as the greatest lower bound of those values $l \geqq 0$ for which (2) holds for this value of σ. This function $\mu(\sigma)$ is called the *order function*, or the Lindelöf μ-function, of $f(s)$. It is equal to 0 for $\sigma > \lambda_0 + 1$ because the Dirichlet series is absolutely convergent for $\sigma > \lambda_0 + 1$. It follows from the Phragmén-Lindelöf theorem that the function $\mu(\sigma)$ is a continuous convex function. Thus, denoting by ω_μ ($\leqq \lambda_0 + 1$) the smallest number with the property that $\mu(\sigma) = 0$ for $\sigma \geqq \omega_\mu$, the function $\mu(\sigma)$ is (when $\Omega < \omega_\mu$) strictly decreasing in the interval $\Omega < \sigma \leqq \omega_\mu$. We mention that $\mu(\sigma_0)$ ($\Omega < \sigma_0 < \infty$) is also the order of $f(s)$ in the half plane $\sigma > \sigma_0$, i.e. the greatest lower bound of those values $l \geqq 0$ for which (2) holds uniformly for all $\sigma > \sigma_0$.

As to the connection between $\psi(\sigma)$ and $\mu(\sigma)$ it is known (see [6], pp. 49 and 53) that

$$\psi(\sigma) \leqq \mu(\sigma) \leqq \psi(\sigma) + 1.$$

The present paper deals with the problem whether the above results concerning the functions $\psi(\sigma)$ and $\mu(\sigma)$ and the connection between them are the best possible, i. e. whether conversely for two functions $\psi(\sigma)$ and $\mu(\sigma)$ which have all the properties mentioned above there exists an ordinary Dirichlet series $f(s) = \sum a_n n^{-s}$ with $\psi(\sigma)$ as summability function and $\mu(\sigma)$ as order function. No complete answer is obtained, but it is shown that if we impose on the function $\mu(\sigma)$ the additional condition

that it, too, has a numerical slope ≥ 1 in the interval in which it is strictly decreasing, i. e. that (when $\Omega < \omega_\mu$) we have $\mu'(\omega_\mu - 0) \leq -1$, then the answer is in the affirmative. In other words, we shall prove the following

Main Theorem. *Let $\psi(\sigma)$ be a continuous convex function defined in an interval $\sigma > \Omega\ (\geq -\infty)$ and equal to 0 to the right of a certain finite abscissa $\omega_\psi \geq \Omega$ and (if $\omega_\psi > \Omega$) such that $\psi'(\omega_\psi - 0) \leq -1$. Further, let $\mu(\sigma)$ be a continuous convex function defined in the same interval $\sigma > \Omega$ and equal to 0 to the right of a certain finite abscissa $\omega_\mu \geq \Omega$ and (if $\omega_\mu > \Omega$) such that $\mu'(\omega_\mu - 0) \leq -1$. Finally, let*

$$\psi(\sigma) \leq \mu(\sigma) \leq \psi(\sigma) + 1$$

for all $\sigma > \Omega$.

Then there exists a Dirichlet series $f(s) = \sum a_n n^{-s}$ which has the given functions $\psi(\sigma)$ and $\mu(\sigma)$ as summability function and order function, respectively.

We remark that as a consequence of the assumptions of the theorem we have $\omega_\psi \leq \omega_\mu \leq \omega_\psi + 1$. The condition $\omega_\mu \leq \omega_\psi + 1$, which according to the above results is necessary whether $\mu'(\omega_\mu - 0) \leq -1$ or not, therefore has not been included in the theorem.

We do not know whether there exist ordinary Dirichlet series $f(s) = \sum a_n n^{-s}$ for which the order function $\mu(\sigma)$ is not identically zero and does not satisfy the condition $\mu'(\omega_\mu - 0) \leq -1$. For the zeta-series with alternating signs

$$\zeta(s)(1 - 2^{1-s}) = \sum_{n=1}^{\infty} (-1)^{n+1} n^{-s}$$

it is known that $\mu(\sigma) = 0$ for $\sigma \geq 1$ and $\mu(\sigma) = \frac{1}{2} - \sigma$ for $\sigma \leq 0$. The question as to whether $\mu'(\omega_\mu - 0) \leq -1$ therefore amounts to whether $\mu\left(\frac{1}{2}\right) = 0$ $\left(\text{and hence } \mu(\sigma) = 0 \text{ for } \sigma \geq \frac{1}{2} \text{ and } \mu(\sigma) = \frac{1}{2} - \sigma \text{ for } \sigma \leq \frac{1}{2}\right)$, i. e. to the Lindelöf hypothesis $\zeta\left(\frac{1}{2} + it\right) = O(|t|^\varepsilon)$ for every $\varepsilon > 0$.

If we restrict our attention to the summability function $\psi(\sigma)$,

we immediately see from the Main Theorem, that the known results are the best possible, i.e. any continuous convex function $\psi(\sigma)$ defined in an interval $\sigma > \Omega (\geq -\infty)$ and equal to 0 to the right of a certain finite abscissa $\omega_\psi \geq \Omega$ and (if $\omega_\psi > \Omega$) such that $\psi'(\omega_\psi - 0) \leq -1$, is the summability function of an ordinary Dirichlet series. Indeed, we have only to apply the Main Theorem, choosing $\mu(\sigma) = \psi(\sigma)$. This result generalizes a result of the author ([3], pp. 104—110) concerning the abscissae of summability of integral order, according to which the inequalities (1) are the best possible.

In the proof of the Main Theorem certain basic examples play a decisive role. In these examples $\Omega = -\infty$ (so that we are dealing with entire functions) and the ψ-curve as well as the μ-curve are half lines as soon as they have left the real axis, i.e. in the intervals $-\infty < \sigma < \omega_\psi$ and $-\infty < \sigma < \omega_\mu$, respectively. It appears immediately from the above inequalities that these half lines must be parallel and that the μ-line must lie above or coincide with the ψ-line. Further, their distance measured on a vertical line must be ≤ 1. Our basic examples correspond to those extreme cases where the two half lines coincide or have the vertical distance 1. In the special case where the numerical slope α of the half lines has its minimum value $\alpha = 1$ examples have already been constructed by the author ([4], pp. 10—14, and [5], pp. 713—720). Generalizing these examples we construct in § 2 and § 3 examples for an arbitrary $\alpha \geq 1$. (The reader need not know the examples for $\alpha = 1$.)

In § 4 we construct from the extreme cases in § 2 and § 3 all intermediate cases where still both the ψ-curve and the μ-curve are half lines to the left of ω_ψ and ω_μ, respectively. The Dirichlet series obtained in § 4 are to serve as our "bricks" in the final construction in § 6 in which a Dirichlet series is formed by linear combination of denumerably many such series. § 5 is inserted for the purpose of giving two lemmas concerning the summability function and the order function of a Dirichlet series obtained by linear combination of denumerably many Dirichlet series.

§ 2. Construction, for an arbitrary $\alpha \geqq 1$, of a Dirichlet series with $\psi(\sigma) = \mu(\sigma) = \begin{cases} 0 & \text{for } \sigma \geqq 0 \\ -\alpha\sigma & \text{for } \sigma \leqq 0. \end{cases}$

Let $p_1, p_2, p_3, \cdots$ be a sequence of positive integers which satisfy the condition

$$p_{m+1} \geqq (m+1)\, p_m \tag{1}$$

for all m and let

$$d_m = [p_m^{1-\theta}],$$

where for brevity's sake we have put $\frac{1}{\alpha} = \theta$ $(0 < \theta \leqq 1)$. We consider the Dirichlet series

$$\sum_{n=1}^{\infty} a_n n^{-s} = p_1^{-s} - (p_1 + d_1)^{-s} + p_2^{-s} - 2(p_2 + d_2)^{-s} + (p_2 + 2d_2)^{-s} + \cdots$$

$$+ p_m^{-s} - \binom{m}{1}(p_m + d_m)^{-s} + \binom{m}{2}(p_m + 2d_m)^{-s} - \cdots + (-1)^m \binom{m}{m}(p_m + md_m)^{-s}$$

$$+ \cdots = \sum_{m=1}^{\infty} \Delta_{d_m}^m (p_m^{-s}).$$

Here we have used the notation $\Delta_d^m u_p$ for the m^{th} difference with span d, i. e.

$$\Delta_d^m u_p = u_p - \binom{m}{1} u_{p+d} + \binom{m}{2} u_{p+2d} - \cdots + (-1)^m \binom{m}{m} u_{p+md}.$$

For such differences we shall use the known inequality (see for instance H. Bohr [4], p. 15)

$$|\Delta_d^m (p^{-s})| \leqq 2^{m-h} |s| |s+1| \cdots |s+h-1|\, d^h p^{-\sigma-h}, \tag{2}$$

which is valid for $d > 0$, $p > 0$, $\sigma + h > 0$, and $h = 0, 1, 2, \cdots, m$.

The above series has previously been considered by the author ([3], pp. 94—99), and it was shown that its abscissae of summability λ_h of integral order h are determined by

$$\lambda_h = -h\theta \quad (h = 0, 1, 2, \cdots).$$

Thus $\Omega = -\infty$, and $\psi(-h\theta) = h$ for $h = 0, 1, 2, \cdots$. Since $\psi(\sigma)$ is convex, this implies that $\psi(\sigma) = -\alpha\sigma$ for $\sigma \leqq 0$, and hence

$\psi(\sigma) = 0$ for $\sigma \geq 0$. Thus it only remains to prove that $\mu(\sigma) = -\alpha\sigma$ for $\sigma \leq 0$, which implies that $\mu(\sigma) = 0$ for $\sigma \geq 0$.

Since $\mu(\sigma) \geq \psi(\sigma)$ it is enough to show that $\mu(\sigma) \leq -\alpha\sigma$ for $\sigma \leq 0$. Further, in order to prove this latter relation it suffices to prove that

$$f(s) = O(|t|^h) \quad \text{for} \quad \sigma = -h\theta + \varepsilon, \tag{3}$$

where h runs through the numbers $0, 1, 2, \cdots$ and $\varepsilon > 0$ is arbitrary. Indeed, the inequality $\mu(-h\theta + \varepsilon) \leq h$ together with the continuity of $\mu(\sigma)$ implies that $\mu(-h\theta) \leq h$, and this latter inequality for $h = 0, 1, 2, \cdots$ together with the convexity of $\mu(\sigma)$ implies that $\mu(\sigma) \leq -\alpha\sigma$ for all $\sigma \leq 0$.

In the proof of (3) we shall use the fact that $\sum 2^m p_m^{-\varepsilon}$ is convergent for every $\varepsilon > 0$. This fact, however, follows at once from (1) in view of which

$$\frac{2^{m+1} p_{m+1}^{-\varepsilon}}{2^m p_m^{-\varepsilon}} \to 0 \quad \text{for} \quad m \to \infty.$$

We write

$$f(s) = \sum_{m=1}^{h} \Delta_{d_m}^m (p_m^{-s}) + \sum_{m=h+1}^{\infty} \Delta_{d_m}^m (p_m^{-s}),$$

where the sum $f_1(s) = \sum_{m=1}^{h} \Delta_{d_m}^m (p_m^{-s})$ consists only of a finite number of terms $a_n n^{-s}$ and therefore is bounded on every line $\sigma = \sigma_0$. In the series $\sum_{m=h+1}^{\infty} \Delta_{d_m}^m (p_m^{-s})$ we shall apply the above inequality (2) to each of the terms $\Delta_{d_m}^m (p_m^{-s})$, $m = h+1, h+2, \cdots$. We obtain for $m > h$ and s on the line $\sigma = -h\theta + \varepsilon$ (where $\sigma + h > 0$)

$$|\Delta_{d_m}^m (p_m^{-s})| \leq 2^{m-h} |s| |s+1| \cdots |s+h-1| d_m^h p_m^{-\sigma-h} \leq$$

$$2^{-h} |s| |s+1| \cdots |s+h-1| 2^m p_m^{h(1-\theta)+h\theta-\varepsilon-h} =$$

$$2^{-h} |s| |s+1| \cdots |s+h-1| 2^m p_m^{-\varepsilon}.$$

Since $\sum 2^m p_m^{-\varepsilon}$ is convergent we see that $\sum_{m=h+1}^{\infty} \Delta_{d_m}^m (p_m^{-s})$ converges absolutely for $\sigma = -h\theta + \varepsilon$ and that its sum $f_2(s)$ satisfies the relation $f_2(s) = O(|t|^h)$. Finally, since $f(s) = f_1(s) + f_2(s)$, we see that $f(s) = O(|t|^h)$ for $\sigma = -h\theta + \varepsilon$, as we had to prove.

§ 3. Construction, for an arbitrary $\alpha \geqq 1$, of a Dirichlet series with

$$\psi(\sigma) = \begin{cases} 0 & \text{for } \sigma \geqq 0 \\ -\alpha\sigma & \text{for } \sigma \leqq 0 \end{cases} \quad \text{and} \quad \mu(\sigma) = \begin{cases} 0 & \text{for } \sigma \geqq \frac{1}{\alpha} \\ 1-\alpha\sigma & \text{for } \sigma \leqq \frac{1}{\alpha}. \end{cases}$$

In view of the general properties of the summability function and the order function it suffices to show that the constructed series has the right order function and the abscissa of convergence $\lambda_0 = 0$. Thus our task is to construct a Dirichlet series with $\lambda_0 = 0$ and $\Omega = -\infty$ and with the given function $\mu(\sigma)$ as order function.

We start again with a sequence of positive integers $p_1 < p_2 < p_3 < \cdots$ which increase rapidly. We assume here that they increase so rapidly that $\sum 2^m p_m^{-\varepsilon}$ converges for every $\varepsilon > 0$ and so that

$$\sum_{m=M+1}^{\infty} 2^m p_m^{-\varepsilon} = o(p_M^{-\varepsilon}) \quad \text{and} \quad 2^{M-1} p_{M-1}^{L} = o(p_M^{\varepsilon})$$

for $M \to \infty$ and every $\varepsilon > 0$ and $L > 0$. Next, we choose integers l_m and d_m of the orders of magnitude p_m^{α} and $p_m^{\alpha-1}$, respectively. It will be convenient to choose

$$l_m = [p_m^{\alpha}] + 1 \quad \text{and} \quad d_m = [p_m^{\alpha-1}].$$

Further, we put

$$t_m = \pi p_m$$

and choose the numbers q_m of a slightly smaller order of magnitude than the p_m. We set

$$q_m = \left[\frac{p_m}{(m+1)^3}\right].$$

We remark that the p_m from the beginning must be chosen so that certain inequalities which on account of the above demands are fulfilled for large m will be fulfilled for all m. The inequalities to which we refer (we shall not write them out explicitly) are those which express that the term groups given by the braces $\{\cdots\}_m$ in the series immediately below do not overlap.

Our Dirichlet series $f(s) = \sum a_n n^{-s}$ is now constructed from term groups $\{\cdots\}_m (m = 1, 2, \cdots)$, the m^{th} term group of which

consists of altogether $(q_m+1)(m+1)$ terms $a_n n^{-s}$. These terms are distributed in q_m+1 smaller term groups $[\cdots]_{m,\nu}$ $(\nu = 0, 1, 2, \cdots, q_m)$ each of which apart from a complex sign is simply an m^{th} difference (with span d_m) and thus contains $m+1$ terms $a_n n^{-s}$. More specifically, our series is defined in the following way:

$$f(s) = \sum_{n=1}^{\infty} a_n n^{-s} = \sum_{m=1}^{\infty} \{\cdots\}_m = \sum_{m=1}^{\infty} \sum_{\nu=0}^{q_m} [\cdots]_{m,\nu}$$

where for $m \geq 1$, $0 \leq \nu \leq q_m$ the square bracket $[\cdots]_{m,\nu}$ has the meaning

$$[\cdots]_{m,\nu} = \left(l_m + \nu(m+1)\, d_m\right)^{it_m} \Delta_{d_m}^m \left(l_m + \nu(m+1)\, d_m\right)^{-s} =$$

$$\left(l_m + \nu(m+1)\, d_m\right)^{it_m} \Big(\left(l_m + \nu(m+1)\, d_m\right)^{-s} - \binom{m}{1} \left(l_m + \nu(m+1)\, d_m + d_m\right)^{-s}$$

$$+ \cdots + (-1)^m \binom{m}{m} \left(l_m + \nu(m+1)\, d_m + m d_m\right)^{-s} \Big).$$

We shall now prove that this series $\sum a_n n^{-s}$ possesses all the desired properties. We divide the proof into three steps.

1°. We prove first that our series has the abscissa of convergence $\lambda_0 = 0$. Since $|a_n| = |l_m^{it_m}| = 1$ for $n = l_m (m = 1, 2, \cdots)$ we see that the series is divergent at the point $s = 0$ and it is consequently plain that $\lambda_0 \geq 0$. In order to show that $\lambda_0 \leq 0$, i. e. that the series is convergent for $\sigma > 0$, we first show that our series is absolutely convergent for $\sigma > 0$ when we preserve the square brackets (but not the braces). On account of a later application we shall even show that under preservation of the square brackets the series is absolutely convergent in the whole plane. We do this by showing the absolute convergence in the half plane $\sigma > \sigma_h = \dfrac{-h+1}{a}$ for $h = 0, 1, 2, \cdots$. We write

$$f(s) = \sum_{m=1}^{\infty} \{\cdots\}_m = \sum_{m=1}^{h} \{\cdots\}_m + \sum_{m=h+1}^{\infty} \{\cdots\}_m,$$

where the first sum $\sum_{m=1}^{h} \{\cdots\}_m$ only contains a finite number of square brackets $[\cdots]_{m,\nu}$. In order to prove that the second sum $\sum_{m=h+1}^{\infty} \{\cdots\}_m$ is absolutely convergent when we keep the square

brackets (but not the braces) we estimate each of the q_m+1 brackets $[\cdots]_{m,\nu}$ in the term $\{\cdots\}_m$ with index $m>h$ by the inequality (2), § 2. For $m>h$ and s in the half plane $\sigma>\sigma_h$ (where a fortiori $\sigma+h>0$) we get

$$|[\cdots]_{m,\nu}| = |\Delta^m_{d_m}(l_m+\nu(m+1)d_m)^{-s}|$$
$$\leqq 2^{m-h}|s||s+1|\cdots|s+h-1|d_m^h l_m^{-\sigma-h}.$$

Hence the sum of the absolute values of the q_m+1 brackets $[\cdots]_{m,\nu}$ in $\{\cdots\}_m$ is estimated by

$$\sum_{\nu=0}^{q_m}|[\cdots]_{m,\nu}| \leqq (q_m+1)2^{m-h}|s||s+1|\cdots|s+h-1|d_m^h l_m^{-\sigma-h}$$

and consequently, since $q_m<p_m$, $d_m\leqq p_m^{\alpha-1}$, and $l_m>p_m^\alpha$ by

$$(1)\quad \sum_{\nu=0}^{q_m}|[\cdots]_{m,\nu}| \leqq 2^{-h}|s||s+1|\cdots|s+h-1|2^m p_m^{-\alpha\sigma-h+1},$$

where $\sigma>\sigma_h$ and $m>h$. From this inequality we immediately infer the stated absolute convergence in the half plane $\sigma>\sigma_h=\frac{-h+1}{\alpha}$; in fact, the series $\sum 2^m p_m^{-\alpha\sigma-h+1}$ is convergent since the exponent $-\alpha\sigma-h+1$ is smaller than $-\alpha\sigma_h-h+1=0$. Thus, in order to show that the series $\sum a_n n^{-s}$ itself (i. e. the series without any brackets whatsoever) is convergent for $\sigma>0$, we only have to show that the partial sums of $[\cdots]_{m,\nu}$ for $\sigma>0$ tend to 0 for $m\to\infty$. That this is the case is, however, obvious since the sum of the absolute values of all the terms $a_n n^{-s}$ in $[\cdots]_{m,\nu}$ for $\sigma>0$ is

$$\leqq \sum_{j=0}^{m}\binom{m}{j}l_m^{-\sigma} = 2^m l_m^{-\sigma} < 2^m p_m^{-\alpha\sigma},$$

which tends to 0 for $m\to\infty$.

2°. Next, we shall show that $\Omega=-\infty$ and $\mu(\sigma)\leqq 1-\alpha\sigma$ for $\sigma\leqq\frac{1}{\alpha}$. We first remark that it will suffice to show that $f(s)$ is regular for $\sigma>\sigma_h=\frac{-h+1}{\alpha}$, where h runs through the numbers $0,1,2,\cdots$, and that

$$f(s)=O(|t|^h) \quad \text{for} \quad \sigma>\sigma_h+\varepsilon.$$

In fact, this will immediately imply that $\Omega = -\infty$ and

$$\mu(\sigma_h) \leqq h = 1 - a\sigma_h \quad \text{for} \quad h = 0, 1, 2, \cdots,$$

and next, by help of the convexity of $\mu(\sigma)$ we get

$$\mu(\sigma) \leqq 1 - a\sigma \quad \text{for all} \quad \sigma \leqq \frac{1}{a}.$$

For $\sigma > \sigma_h$ we write again

$$f(s) = \sum_{m=1}^{h} \{\cdots\}_m + \sum_{m=h+1}^{\infty} \{\cdots\}_m.$$

The first sum $\sum_{m=1}^{h} \{\cdots\}_m$ contains only a finite number of terms $a_n n^{-s}$ and is therefore an entire function $f_1(s)$ bounded in every half plane $\sigma > \sigma_0$. In the second sum $\sum_{m=h+1}^{\infty} \{\cdots\}_m$ we estimate each of the terms $\{\cdots\}_m (m = h+1, h+2, \cdots)$ by the above inequality (1). For $m > h$ and s in the half plane $\sigma > \sigma_h + \varepsilon$ we get

$$|\{\cdots\}_m| \leqq \sum_{\nu=0}^{q_m} |[\cdots]_{m,\nu}| \leqq 2^{-h} |s| |s+1| \cdots |s+h-1| 2^m p_m^{-a\sigma-h+1} \leqq$$

$$2^{-h} |s| |s+1| \cdots |s+h-1| 2^m p_m^{-a\varepsilon}.$$

Since $\sum 2^m p_m^{-a\varepsilon}$ is convergent we infer that the infinite series $\sum_{m=h+1}^{\infty} \{\cdots\}_m$ is uniformly convergent in every bounded part of the half plane $\sigma > \sigma_h + \varepsilon$. Consequently, since $\varepsilon > 0$ is arbitrary, the function $f_2(s)$ represented by this series is regular in the half plane $\sigma > \sigma_h$; furthermore, it satisfies for $\sigma_h + \varepsilon < \sigma <$ (say) 2 (and hence of course also in the whole half plane $\sigma > \sigma_h + \varepsilon$) the inequality

$$f_2(s) = O(|t|^h).$$

Since $f(s)$ is obtained as the sum of $f_1(s)$ and $f_2(s)$, we see that $f(s)$ is regular for $\sigma > \sigma_h$ and equal to $O(|t|^h)$ for $\sigma > \sigma_h + \varepsilon$ as we had to prove.

3°. We come now to the salient point, namely the proof that $\mu(\sigma) \geqq 1 - a\sigma$ for $\sigma < \frac{1}{a}$. Let σ_0 be an arbitrary abscissa $< \frac{1}{a}$;

we consider the behaviour of $f(s)$ at the points $s_M = \sigma_0 + it_M$ on the line $\sigma = \sigma_0$, where t_M are the previously introduced ordinates $t_M = \pi p_M$, and we shall (even) prove that for sufficiently large M

$$|f(s_M)| > t_M^{1-\alpha\sigma_0}. \tag{2}$$

For this purpose we first determine a positive integer h so that $\sigma_h = \frac{-h+1}{\alpha} < \sigma_0 < \frac{1}{\alpha}$. For $M > h$ we write

$$f(s_M) = \sum_{m=1}^{M-1} \{\cdots\}_m + \{\cdots\}_M + \sum_{m=M+1}^{\infty} \{\cdots\}_m = B_M(s_M) + T_M(s_M) + R_M(s_M),$$

and we shall prove that both the "beginning" $B_M(s_M)$ and the "remainder" $R_M(s_M)$ for $M \to \infty$ are equal to $o(t_M^{1-\alpha\sigma_0})$ while the M^{th} term $T_M(s_M)$ for sufficiently large M is numerically larger than $2t_M^{1-\alpha\sigma_0}$. In this way the inequality (2) will be proved.

(1) For the "beginning" $B_M(s_M)$ we use a rough estimate. The numerical value of each of its coefficients $a_n \neq 0$ is a binomial coefficient $\binom{m}{l}$ with $m \leqq M-1$ and hence it is $\leqq 2^{M-1}$. Thus

$$|B_M(s_M)| \leqq 2^{M-1} \sum_{n=1}^{l'_{M-1}} n^{-\sigma_0},$$

where

$$l'_{M-1} = l_{M-1} + q_{M-1} M d_{M-1} + (M-1)\, d_{M-1} \leqq 2\, l_{M-1}$$

for M sufficiently large. Hence, since $\sigma_0 < 1$,

$$|B_M(s_M)| \leqq 2^{M-1} \sum_{n=1}^{2\,l_{M-1}} n^{-\sigma_0} = O(2^{M-1}\, l_{M-1}^{1-\sigma_0}) = O(2^{M-1}\, p_{M-1}^{\alpha(1-\sigma_0)})$$

and consequently, since $1 - \alpha\sigma_0 > 0$,

$$B_M(s_M) = o(p_M^{1-\alpha\sigma_0}) = o(t_M^{1-\alpha\sigma_0}).$$

(2) For the "remainder" $R_M(s_M)$ we can apply the inequality (1) since all occurring m are $> M > h$ and $\sigma_0 > \sigma_h$. We get, since $-\alpha\sigma_0 - h + 1 < 0$,

$$|R_M(s_M)| \leqq 2^{-h} |s_M| |s_M + 1| \cdots |s_M + h - 1| \sum_{m=M+1}^{\infty} 2^m p_m^{-\alpha\sigma_0 - h + 1} =$$

$$O(t_M^h)\, o(p_M^{-\alpha\sigma_0 - h + 1}) = O(t_M^h)\, o(t_M^{-\alpha\sigma_0 - h + 1}) = o(t_M^{1-\alpha\sigma_0}).$$

(3) We shall finally prove that the M^{th} term $T_M(s_M)$ satisfies the inequality

$$|T_M(s_M)| > 2\, t_M^{1-a\sigma_0}$$

for all sufficiently large M. The reason for the validity of this inequality is that all the terms $a_n n^{-s}$ occurring in $T_M(s_M)$ (and there are rather many of them on account of the choice of the q_m), namely the $(q_M+1)\,(M+1)$ terms distributed in the q_M+1 brackets $[\cdots]_{M,\nu}$ with $M+1$ terms in each bracket, for sufficiently large M "almost point in the same direction"; more precisely: these terms all lie in the angle $-\frac{\pi}{3} < v < \frac{\pi}{3}$. We postpone the verification of this fact for a moment and shall first show that when once this property is established we can immediately complete the proof. In fact, we may argue as follows. The sum of the binomial coefficients occurring in each of the q_M+1 square brackets is equal to 2^M, and every n occurring in the sum belongs to the interval $l_M \leqq n \leqq l'_M$ and a fortiori to the interval $l_M \leqq n \leqq 2\,l_M$ when M is large. Thus, for sufficiently large M we have

$$|T_M(s_M)| \geqq \Re\, T_M(s_M) \geqq \cos\frac{\pi}{3}\,(q_M+1)\,2^M \operatorname*{Min}_{l_M \leqq n \leqq 2l_M} n^{-\sigma_0} \geqq$$

$$\frac{1}{2}\,(q_M+1)\,2^M\,\frac{1}{2}\,l_M^{-\sigma_0} > \frac{1}{2}\,2^M\,\frac{p_M}{(M+1)^3}\,\frac{1}{2}\,\frac{1}{2}\,p_M^{-a\sigma_0} =$$

$$\frac{1}{8}\,\frac{2^M}{(M+1)^3}\,p_M^{1-a\sigma_0} = \frac{1}{8}\,\frac{2^M}{(M+1)^3}\left(\frac{l_M}{\pi}\right)^{1-a\sigma_0},$$

and this last quantity is larger than $2\,t_M^{1-a\sigma_0}$ for large M.

It remains to prove the decisive fact that all terms $a_n n^{-s}$ in $T_M(s_M)$ lie in the angle $-\frac{\pi}{3} < v < \frac{\pi}{3}$ for M sufficiently large. That this is the case is of course due to our choice of the complex signs of the occurring coefficients $a_n \neq 0$. We consider an arbitrary one of the q_M+1 brackets $[\cdots]_{M,\nu}$

$$\left(l_M + \nu\,(M+1)\,d_M\right)^{it_M} \Delta_{d_M}^M \left(l_M + \nu\,(M+1)\,d_M\right)^{-s_M} \quad (\nu = 0, 1, 2, \cdots, q_M).$$

Denoting the number $l_M + \nu\,(M+1)\,d_M$ by $r = r(M, \nu)$ we get

$$[\cdots]_{M,\nu} = r^{it_M}\left(r^{-s_M} - \binom{M}{1}(r+d_M)^{-s_M} + \cdots + (-1)^M\binom{M}{M}(r+Md_M)^{-s_M}\right).$$

The amplitudes of the single terms

$$r^{it_M}(-1)^\lambda\binom{M}{\lambda}(r+\lambda d_M)^{-(\sigma_0+it_M)} \quad (\lambda = 0, 1, 2, \cdots, M)$$

are given by

$$-t_M\log(r+\lambda d_M) + t_M\log r + \lambda\pi = -t_M\log\left(1+\frac{\lambda d_M}{r}\right) + \lambda\pi =$$

$$-\lambda\frac{t_M d_M}{r}\frac{\log\left(1+\dfrac{\lambda d_M}{r}\right)}{\dfrac{\lambda d_M}{r}} + \lambda\pi.$$

When we take account of the fact that $0 \leqq \lambda \leqq M$ and $0 \leqq \nu \leqq q_M$ and insert the known expressions for t_M, d_M, r, q_M, we see at once that

$$\frac{t_M d_M}{r} \to \pi \quad \text{and} \quad \frac{\lambda d_M}{r} \to 0 \quad \text{for} \quad M \to \infty$$

independently of ν and λ. In view of this, the above formula for the amplitudes together with the relation

$$\lim_{x\to 0} x^{-1}\log(1+x) = 1$$

yields the result that the amplitudes of the single terms in $T_M(s_M)$ tend to 0 for $M \to \infty$. In particular, these amplitudes lie in the angle $-\frac{\pi}{3} < v < \frac{\pi}{3}$ for M sufficiently large.

Thus, all our statements concerning $f(s) = \sum a_n n^{-s}$ are proved.

§ 4. Our "bricks".

We shall now, for an arbitrary $\alpha \geqq 1$, construct a class of Dirichlet series for which again the ψ-curve and μ-curve when they have left the real axis are half lines with numerical slope α, but where the vertical distance from the ψ-half-line to the μ-half-line no longer assumes just one of its extreme values 0 or 1, but has an arbitrary value between these two limits. At the same time we shall perform a trivial translation in the direction of the real axis. For the sake of convenience, we characterize a function of σ which is 0 for $\omega \leqq \sigma < \infty$ and equal to $-\alpha(\sigma-\omega)$

for $-\infty < \sigma \leqq \omega$ by the symbol $\{\omega; \alpha\}$. We shall prove the following

Theorem. *For arbitrary ω, α, and d such that $\alpha \geqq 1$ and $0 \leqq d \leqq \frac{1}{\alpha}$ there exists a Dirichlet series $f(s) = \sum a_n n^{-s}$ with the summability function $\{\omega; \alpha\}$ and the order function $\{\omega + d; \alpha\}$.*

In the proof we may evidently assume that $\omega = 0$. Also, we may assume that $0 < d < \frac{1}{\alpha}$. We know that there exist two Dirichlet series $f_1(s) = \sum a'_n n^{-s}$ and $f_2(s) = \sum a''_n n^{-s}$, where the ψ- and μ-functions of the first series are given by

$$\psi_1 = \mu_1 = \{0; \alpha\}$$

while the ψ- and μ-functions of the second series are given by

$$\psi_2 = \{0; \alpha\} \quad \text{and} \quad \mu_2 = \left\{\frac{1}{\alpha}; \alpha\right\}.$$

We now replace s by $s + \frac{1}{\alpha} - d$ in $f_2(s)$, i.e. we consider instead of $f_2(s)$ the function $f_3(s) = f_2\left(s + \frac{1}{\alpha} - d\right) = \sum a'''_n n^{-s}$. The ψ- and μ-functions of $f_3(s)$ are given by

$$\psi_3 = \left\{d - \frac{1}{\alpha}; \alpha\right\} \quad \text{and} \quad \mu_3 = \{d; \alpha\}.$$

We shall now show that the series

$$f(s) = f_1(s) + f_3(s) = \sum (a'_n + a'''_n) n^{-s} = \sum a_n n^{-s}$$

will satisfy our demands.

First, $\Omega = -\infty$. Secondly, the summability function $\psi(\sigma)$ is equal to 0 for $\sigma \geqq 0$ since both $\sum a'_n n^{-s}$ and $\sum a'''_n n^{-s}$ are convergent for $\sigma > 0$, and $\psi(\sigma) = \psi_1(\sigma)$ for every negative σ since $\psi_1(\sigma) > \psi_3(\sigma)$. (We have used here the fact that the sum of two series of constant terms both of which are summable of the r^{th} order is again a series summable of the r^{th} order, while the sum of two series of which the one series is summable of the r^{th} order and the other is not, is a series which is not summable of the r^{th} order.) Thirdly, the order function $\mu(\sigma)$ is equal to 0 for $\sigma \geqq d$ since both $\mu_1(\sigma)$ and $\mu_3(\sigma)$ are equal to 0 here, and

$\mu(\sigma) = \mu_3(\sigma)$ for $\sigma < d$ since $\mu_3(\sigma) > \mu_1(\sigma)$. (We have used here the fact that the sum of two functions of t which are both $O(|t|^h)$ is again $O(|t|^h)$ while the sum is not $O(|t|^h)$ if one of the functions is $O(|t|^h)$ and the other is not.)

§ 5. Two lemmas.

In this section we shall prove two lemmas concerning summability and order of magnitude of Dirichlet series which are formed by linear combination of infinitely many Dirichlet series.

Before passing to these theorems we start with the following

Remark. *Let*

$$f_0(s) = \sum a_n^{(0)} n^{-s}, \quad f_1(s) = \sum a_n^{(1)} n^{-s}, \cdots$$

be a sequence of Dirichlet series which we assume to be all absolutely convergent (at least) for $\sigma \geq \sigma_0$. We assert that it is possible to determine a sequence of positive numbers $E_0, E_1, \cdots$ so that the infinite series

$$(1) \qquad \sum_{N=0}^{\infty} \varepsilon_N a_1^{(N)}, \quad \sum_{N=0}^{\infty} \varepsilon_N a_2^{(N)}, \cdots$$

are convergent for every sequence $\varepsilon_0, \varepsilon_1, \cdots$ with

$$0 < \varepsilon_0 < E_0, \quad 0 < \varepsilon_1 < E_1, \cdots$$

and that further, when the sums of these infinite series are denoted by $A_1, A_2, \cdots$, the series

$$(2) \qquad \varepsilon_0 f_0(s) + \varepsilon_1 f_1(s) + \cdots$$

and the Dirichlet series (obtained by formal calculation from (2))

$$(3) \qquad \sum_{n=1}^{\infty} A_n n^{-s}$$

will be absolutely convergent for $\sigma \geq \sigma_0$ and have the same sum.

Proof. We put

$$\sum_{n=1}^{\infty} |a_n^{(0)}| n^{-\sigma_0} = K_0, \quad \sum_{n=1}^{\infty} |a_n^{(1)}| n^{-\sigma_0} = K_1, \cdots$$

and choose the positive numbers $E_0, E_1, \cdots$ so that the series $\sum E_n K_n$ is convergent. Then

$$\sum_{N,n} \varepsilon_N |a_n^{(N)}| n^{-\sigma} < \infty \quad \text{for} \quad \sigma \geqq \sigma_0$$

so that

$$\sum_{N=0}^{\infty} \varepsilon_N f_N(s) = \sum_{N=0}^{\infty} \varepsilon_N \sum_{n=1}^{\infty} a_n^{(N)} n^{-s} = \sum_{n=1}^{\infty} n^{-s} \sum_{N=0}^{\infty} \varepsilon_N a_n^{(N)} = \sum_{n=1}^{\infty} A_n n^{-s},$$

where all occurring series are absolutely convergent ($\sigma \geqq \sigma_0$). It is plain that the conclusion still holds (with the same E's) when we omit the assumption $0 < \varepsilon_N < E_N$ for finitely many indices N.

Lemma 1. *Let*

$$g_0(s) = \sum b_n^{(0)} n^{-s}, \quad g_1(s) = \sum b_n^{(1)} n^{-s}, \quad g_2(s) = \sum b_n^{(2)} n^{-s}, \cdots$$

be a sequence of Dirichlet series (each of which possesses a half plane of convergence). Denoting by $\Lambda_r^{(N)}$ the r^{th} abscissa of summability of the function $g_N(s)$ $(N = 0, 1, 2, \cdots)$ we assume that there exists a number $r\,(\geqq 0)$ such that

$$\Lambda_r^{(N)} < \Lambda_r^{(0)} = \Lambda \quad (N = 1, 2, \cdots).$$

It follows immediately that the ψ-curve of all the Dirichlet series for $\sigma > \Lambda$ must lie under or on the curve $\{\Lambda + r; 1\}$ so that all the Dirichlet series must be absolutely convergent for $\sigma > \Lambda + r + 1$, in particular for $\sigma \geqq \Lambda + r + 2$.

Then there exists a sequence of positive numbers $e_1 < E_1, e_2 < E_2, \cdots$ [where E_N $(N = 0, 1, 2, \cdots)$ are obtained from the above remark applied to the functions $g_N(s)$ $(N = 0, 1, 2, \cdots)$ and $\Lambda + r + 2$ instead of σ_0] such that the Dirichlet series

$$(4) \qquad G(s) = g_0(s) + \varepsilon_1 g_1(s) + \varepsilon_2 g_2(s) + \cdots = \sum B_n n^{-s},$$

where

$$(5) \qquad B_n = b_n^{(0)} + \varepsilon_1 b_n^{(1)} + \varepsilon_2 b_n^{(2)} + \cdots$$

for every sequence $\varepsilon_1, \varepsilon_2, \cdots$ such that

(6) $$0 < \varepsilon_1 < e_1,\ 0 < \varepsilon_2 < e_2, \cdots$$

will have its r^{th} *abscissa of summability equal to the number* Λ. (The series (5) converge and the two series in (4) are absolutely convergent for $\sigma \geqq \Lambda + r + 2$ with the same sum $G(s)$. This follows immediately from the above remark since $e_N < E_N$ for $N = 1, 2, \cdots$.)

Proof. We have to prove that we can choose the positive numbers $e_N < E_N$ so that the series $G(s) = \sum B_n n^{-s}$ under the assumption (6) is summable of the r^{th} order for $\sigma > \Lambda$, but not summable of the r^{th} order for any $\sigma < \Lambda$. We divide the proof into two parts.

1°. In this part we choose the positive numbers $e_N < E_N$ so that the series $G(s) = \sum B_n n^{-s}$ under the assumption (6) is summable of the r^{th} order for $\sigma > \Lambda$. In order to obtain this result, it is obviously enough to secure that the series

$$G^*(s) = \varepsilon_1 g_1(s) + \varepsilon_2 g_2(s) + \cdots = \sum B_n^* n^{-s}$$

becomes summable of the r^{th} order at the point $s = \Lambda$; for when both of the series $g_0(s) = \sum b_n^{(0)} n^{-s}$ and $G^*(s) = \sum B_n^* n^{-s}$ are summable of the r^{th} order for $\sigma > \Lambda$, then their sum $G(s) = \sum B_n n^{-s}$ will have the same property. In the proof we shall suppose that $\Lambda = 0$. This is of course no real limitation since when $\Lambda \neq 0$ we may replace s by $s + \Lambda$. Since the abscissae of summability $\Lambda_r^{(1)}, \Lambda_r^{(2)}, \cdots$ are all smaller than Λ, the series $\sum b_n^{(1)}, \sum b_n^{(2)}, \cdots$ are all summable of the r^{th} order. We have

(7) $$B_n^* = \sum_{N=1}^{\infty} \varepsilon_N b_n^{(N)} \text{ (convergent for } \varepsilon_N < E_N).$$

In our proof we make use of the fact (see [6], pp. 21—22) that a series $\sum_{n=1}^{\infty} a_n$ is summable of a given order r if and only if a certain linear expression $S_n = \sum_{\nu=1}^{n} k_\nu a_\nu$ in the first n terms of the series (with coefficients k_ν which depend not only on ν but also on n and r) tends to a limit, the summability value of the series, for $n \to \infty$. We denote the expression S_n for the series $\sum b_n^{(1)}$,

$\sum b_n^{(2)}, \cdots$ by $T_n^{(1)}, T_n^{(2)}, \cdots$, respectively, and the expression S_n for the series $\sum B_n^*$ by T_n^*. Then from (7) it follows that

$$T_n^* = \varepsilon_1 T_n^{(1)} + \varepsilon_2 T_n^{(2)} + \cdots. \tag{8}$$

Here, the quantity $T_n^{(N)}$ will for each $N = 1, 2, \cdots$ tend to a limit $U^{(N)}$, the summability value of the series $\sum_n b_n^{(N)}$, when $n \to \infty$. Hence there exist constants K_N such that

$$|T_n^{(N)}| \leqq K_N \quad (n = 1, 2, \cdots).$$

We now choose the positive numbers $e_N < E_N$ so that

$$\sum_{N=1}^{\infty} e_N K_N$$

converges; then for every choice of the numbers ε_N in the intervals $0 < \varepsilon_N < e_N$ the series (8) will be uniformly convergent in n since it is majorized by $\sum e_N K_N$. Since each of the terms $\varepsilon_N T_n^{(N)}$ tends to a limit for $n \to \infty$ (namely $\varepsilon_N U^{(N)}$) it follows that the sum T_n^* of the series will also tend to a limit for $n \to \infty$ (namely $U^* = \varepsilon_1 U^{(1)} + \varepsilon_2 U^{(2)} + \cdots$), as we had to prove.

2°. In this part we choose the positive numbers $e_N < E_N$ so that the series $G(s) = \sum B_n n^{-s}$ under the assumption (6) is not summable of the r^{th} order for any $\sigma < A$, i.e. so that the r^{th} abscissa of summability is $\geqq A$. If the series $g_0(s) = \sum b_n^{(0)} n^{-s}$ (with the r^{th} abscissa of summability A) is not summable of the r^{th} order at the point $s = A$ we can use the numbers e_N found under 1°. In fact, we saw that $G^*(s) = \sum B_n^* n^{-s}$ under the assumption (6) is summable of the r^{th} order at the point $s = A$ so that the series $\sum B_n n^{-s}$, which arises by termwise addition of $\sum b_n^{(0)} n^{-s}$ and $\sum B_n^* n^{-s}$, cannot be summable of the r^{th} order at the point $s = A$ and therefore must have its r^{th} abscissa of summability $\geqq A$. However, we have not made this special assumption concerning the series $\sum b_n^{(0)} n^{-s}$ and as a matter of fact we could not make it in view of the applications. Hence we must proceed differently, and we shall use the known expression for the r^{th} abscissa of summability λ_r of a Dirichlet series $\sum a_n n^{-s}$ by means of the coefficients of the series. In the proof we shall assume that

the number A is > 0, say $= 1$ (since the expression just mentioned is only valid when $\lambda_r > 0$). This is of course no real limitation since when $A \neq 1$ we may replace s by $s - \lambda$, where $\lambda + A = 1$. As to this expression of λ_r by the coefficients of the series we shall only use the following fact (see [6], p. 45 and [3], p. 86 and [1], pp. 70—71). There exists a linear expression $S_n = \sum_{\nu=1}^{n} k_\nu a_\nu$ in the first n coefficients of the series (with coefficients k_ν, which depend not only on ν but also on n and r) such that the necessary and sufficient condition in order that the series $\sum a_n n^{-s}$ have its r^{th} abscissa of summability $\lambda_r \geq 1$ is that

S_n is not equal to $O(n^{-\delta})$ for any $\delta > 0$, or equivalently
S_n is not equal to $o(n^{-\delta})$ for any $\delta > 0$.

(The expression S_n here is not, of course, the same as the expression S_n under 1°.)

We shall denote the expressions S_n corresponding to the series $\sum b_n^{(0)} n^{-s}, \sum b_n^{(1)} n^{-s}, \cdots$ by $T_n^{(0)}, T_n^{(1)}, \cdots$, respectively, and the expression S_n for the series $\sum B_n n^{-s}$ by T_n. Since by assumption the series $\sum b_n^{(0)} n^{-s}$ has its r^{th} abscissa of summability $= A = 1$ we know that to any given $\delta > 0$ there exist infinitely many values of n for which

$$|T_n^{(0)}| > n^{-\delta}.$$

Since each of the series $\sum_n b_n^{(N)} n^{-s}$ $(N = 1, 2, \cdots)$ has its r^{th} abscissa of summability $A_r^{(N)} < A = 1$ there exists for every $N = 1, 2, \cdots$ a number $\Delta_N > 0$ such that

$$T_n^{(N)} = o(n^{-\Delta_N}).$$

It suffices to show that T_n for a suitable choice of the positive constants $e_N < E_N$ under the assumption (6) for every $\delta > 0$ satisfies the inequality

$$|T_n| > \frac{1}{3} n^{-\delta}$$

for infinitely many values of n. This is equivalent to saying that for some sequence $\delta_1, \delta_2, \cdots$ of positive numbers which tends

to 0 there must exist a corresponding sequence of positive integers $n_1 < n_2 < \cdots$ such that the inequality

$$|T_{n_m}| > \frac{1}{3} n_m^{-\delta_m}$$

is satisfied for all $m = 1, 2, \cdots$. As δ-sequence we shall here use an arbitrary sequence of positive numbers which tends to 0 and satisfies the conditions

$$\delta_2 \leq \Delta_1, \quad \delta_3 \leq \min(\Delta_1, \Delta_2), \cdots.$$

We shall now indicate positive numbers $e_N < E_N$ with the desired properties. We proceed in steps.

First step. We choose a positive integer n_1 so that

$$|T_{n_1}^{(0)}| > n_1^{-\delta_1}.$$

For this $n = n_1$ the expressions $T_n^{(1)}, T_n^{(2)}, \cdots$ assume certain values, say $k_{11}, k_{12}, \cdots$. We choose the positive numbers $e_{11} < E_1$, $e_{12} < E_2, \cdots$ so that

$$\sum_{N=1}^{\infty} e_{1N} |k_{1N}|$$

is convergent with sum $< \frac{1}{2} n_1^{-\delta_1}$. On the analogy of (8) we have

$$(9) \qquad T_n = T_n^{(0)} + \varepsilon_1 T_n^{(1)} + \varepsilon_2 T_n^{(2)} + \cdots \quad (\text{for } 0 < \varepsilon_N < E_N).$$

Hence, for every choice of $\varepsilon_1, \varepsilon_2, \cdots$ in the intervals $0 < \varepsilon_1 < e_{11}$, $0 < \varepsilon_2 < e_{12}, \cdots$ we have

$$|T_{n_1}| \geq |T_{n_1}^{(0)}| - \sum_{N=1}^{\infty} \varepsilon_N |T_{n_1}^{(N)}| > n_1^{-\delta_1} - \sum_{N=1}^{\infty} e_{1N} |k_{1N}| > \frac{1}{2} n_1^{-\delta_1}.$$

Second step. We choose an integer $n_2 > n_1$ so that

$$|T_{n_2}^{(0)}| > n_2^{-\delta_2} \quad \text{and also} \quad E_1 |T_{n_2}^{(1)}| < \frac{1}{3} n_2^{-\delta_2}.$$

The latter inequality may be obtained since $\delta_2 \leq \Delta_1$. For this $n = n_2$ the expressions $T_n^{(2)}, T_n^{(3)}, \cdots$ assume certain values, say $k_{22}, k_{23}, \cdots$. We choose the positive numbers $e_{22} < E_2, e_{23} < E_3, \cdots$ so that

$$\sum_{N=2}^{\infty} e_{2N} |k_{2N}|$$

is convergent with sum $< \frac{1}{3} n_2^{-\delta_2}$. Then for every choice of $\varepsilon_1, \varepsilon_2, \cdots$ in the intervals $0 < \varepsilon_1 < E_1$, $0 < \varepsilon_N < e_{2N}$ $(N = 2, 3, \cdots)$ we have, on account of (9),

$$|T_{n_2}| \geqq |T_{n_2}^{(0)}| - E_1 |T_{n_2}^{(1)}| - \sum_{N=2}^{\infty} e_{2N} |k_{2N}| >$$

$$n_2^{-\delta_2} - \frac{1}{3} n_2^{-\delta_2} - \frac{1}{3} n_2^{-\delta_2} = \frac{1}{3} n_2^{-\delta_2}.$$

...

m^{th} *step*. We choose an integer $n_m > n_{m-1}$ so that

$$|T_{n_m}^{(0)}| > n_m^{-\delta_m}$$

and also

$$E_1 |T_{n_m}^{(1)}| + E_2 |T_{n_m}^{(2)}| + \cdots + E_{m-1} |T_{n_m}^{(m-1)}| < \frac{1}{3} n_m^{-\delta_m}.$$

The latter inequality may be obtained since $\delta_m \leqq \min(\Delta_1, \cdots, \Delta_{m-1})$. For this $n = n_m$ the expressions $T_n^{(m)}, T_n^{(m+1)}, \cdots$ assume certain values, say $k_{mm}, k_{m,m+1}, \cdots$. We choose the positive numbers $e_{mm} < E_m, e_{m,m+1} < E_{m+1}, \cdots$ so that

$$\sum_{N=m}^{\infty} e_{mN} |k_{mN}|$$

is convergent with sum $< \frac{1}{3} n_m^{-\delta_m}$. Then for every choice of $\varepsilon_1, \varepsilon_2, \cdots$ in the intervals $0 < \varepsilon_1 < E_1, \cdots, 0 < \varepsilon_{m-1} < E_{m-1}$, $0 < \varepsilon_N < e_{mN}$ $(N = m, m+1, \cdots)$ we have, on account of (9),

$$|T_{n_m}| \geqq |T_{n_m}^{(0)}| - \left(E_1 |T_{n_m}^{(1)}| + \cdots + E_{m-1} |T_{n_m}^{(m-1)}|\right) - \sum_{N=m}^{\infty} e_{mN} |k_{mN}| >$$

$$n_m^{-\delta_m} - \frac{1}{3} n_m^{-\delta_m} - \frac{1}{3} n_m^{-\delta_m} = \frac{1}{3} n_m^{-\delta_m}.$$

...

It appears from the above that the numbers

$$e_N = \min\{e_{1N}, \cdots, e_{NN}\} \quad (N = 1, 2, \cdots)$$

may be used to satisfy our demands under 2°.

Finally, for each N we choose the smaller one of the two numbers e_N found under 1° and 2° as our final e_N. These e_N satisfy the demands in Lemma 1. This completes the proof of Lemma 1.

Lemma 2. *Let*

$$h_0(s) = \sum c_n^{(0)} n^{-s}, \quad h_1(s) = \sum c_n^{(1)} n^{-s}, \quad h_2(s) = \sum c_n^{(2)} n^{-s}, \cdots$$

be a sequence of Dirichlet series (each of which possesses a half plane of convergence). We assume that all the functions $h_N(s)$ are regular and of finite order in a certain half plane $\sigma > \sigma_0$; further, denoting their orders of magnitude in this half plane by μ_N, we assume that

$$\mu_N < \mu_0 = \mu \quad \text{for} \quad N = 1, 2, \cdots.$$

It follows immediately that the ψ-curves of the Dirichlet series for $\sigma > \sigma_0$ must lie under or on the curve $\{\sigma_0 + \mu; 1\}$ so that all the Dirichlet series must be absolutely convergent for $\sigma > \sigma_0 + \mu + 1$, in particular for $\sigma \geq \sigma_0 + \mu + 2$.

Then there exists a sequence of positive numbers $e_1 < E_1, e_2 < E_2, \cdots$ [where E_N $(N = 0, 1, 2, \cdots)$ are obtained from the previous remark applied to the functions $h_N(s)$ $(N = 0, 1, 2, \cdots)$ and $\sigma_0 + \mu + 2$ instead of σ_0] such that the function

$$(10) \qquad H(s) = h_0(s) + \varepsilon_1 h_1(s) + \varepsilon_2 h_2(s) + \cdots = \sum C_n n^{-s},$$

where

$$(11) \qquad C_n = c_n^{(0)} + \varepsilon_1 c_n^{(1)} + \varepsilon_2 c_n^{(2)} + \cdots$$

for every sequence $\varepsilon_1, \varepsilon_2, \cdots$ such that

$$(12) \qquad 0 < \varepsilon_1 < e_1, \quad 0 < \varepsilon_2 < e_2, \cdots$$

will be regular in the half plane $\sigma > \sigma_0$ and in this half plane have the order of magnitude μ. (The series (11) converges and the two series in (10) are absolutely convergent for $\sigma \geq \sigma_0 + \mu + 2$ with the same sum $H(s)$. This follows immediately from the previous remark since $e_N < E_N$ for $N = 1, 2, \cdots$.)

Proof. We have to prove that we can choose the positive numbers $e_N < E_N$ so that the function

$$H(s) = h_0(s) + \varepsilon_1 h_1(s) + \varepsilon_2 h_2(s) + \cdots$$

under the assumption (12) will be regular in the half plane $\sigma > \sigma_0$ and in this half plane satisfy the relation

$$H(s) = O(|t|^{\mu+\delta})$$

for every $\delta > 0$ but not for any $\delta < 0$. We divide the proof into two parts.

1°. In this part we choose the positive numbers $e_N < E_N$ so that the function $H(s)$ under the assumption (12) will be regular in the half plane $\sigma > \sigma_0$ and in this half plane equal to $O(|t|^{\mu+\delta})$ for every $\delta > 0$.

In the proof we shall use only that $\mu_N \leq \mu$ for $N = 0, 1, 2, \cdots$ and not that $\mu_N < \mu$ for $N = 1, 2, \cdots$. Let $\delta_1, \delta_2, \cdots$ be a sequence of positive numbers which tends to 0. On account of the assumptions there exist positive constants K_{mN} $(m = 1, 2, \cdots; N = 0, 1, 2, \cdots)$ such that

$$|h_N(s)| \leq K_{mN}(|t|+1)^{\mu+\delta_m} \quad \text{for} \quad \sigma > \sigma_0.$$

We choose the constants $e_N < E_N$ so that

$$\sum_{N=m}^{\infty} e_N K_{mN}$$

is convergent for every $m = 1, 2, \cdots$. This may be done by subjecting the e_N to the following demands (only in a finite number for each e_N)

$$e_1 K_{11} < \frac{1}{2}, \quad e_2 K_{12} < \frac{1}{4}, \quad e_3 K_{13} < \frac{1}{8}, \cdots$$

$$e_2 K_{22} < \frac{1}{4}, \quad e_3 K_{23} < \frac{1}{8}, \cdots$$

$$e_3 K_{33} < \frac{1}{8}, \cdots$$

$$\cdots\cdots\cdots$$

Then we have under assumption (12)

$$|H(s)| \leq (|h_0(s)| + \varepsilon_1 |h_1(s)| + \cdots + \varepsilon_{m-1} |h_{m-1}(s)|) + (\varepsilon_m |h_m(s)| + \cdots) \leq$$

$$A_1(|t|+1)^{\mu+\delta_m} + \left(\sum_{N=m}^{\infty} e_N K_{mN}\right)(|t|+1)^{\mu+\delta_m} \leq$$

$$A_2(|t|+1)^{\mu+\delta_m} \quad \text{for} \quad \sigma > \sigma_0,$$

where A_1 and A_2 are constants.

From this follows our above statement concerning the order of magnitude of $H(s)$. In order to see that $H(s)$ is regular for $\sigma > \sigma_0$ we remark that the series

$$h_0(s) + \varepsilon_1 h_1(s) + \varepsilon_2 h_2(s) + \cdots$$

in the half strip $\sigma > \sigma_0$, $|t| < T$, where T is any fixed positive number, will be majorized by the series

$$\left(K_{10} + \sum_{N=1}^{\infty} e_N K_{1N}\right)(T+1)^{\mu+\delta_1}$$

so that it is uniformly convergent in this half strip.

2°. In this part we choose the positive numbers $e_N < E_N$ so that $H(s)$ under the assumption (12) is not equal to $O(|t|^{\mu-\delta})$ in the half plane $\sigma > \sigma_0$ for any $\delta > 0$, or, in other words, that $H(s)$ is not equal to $o(|t|^{\mu-\delta})$ in the half plane $\sigma > \sigma_0$ for any $\delta > 0$. Thus it suffices to show that to every $\delta > 0$ there exist points $s = \sigma + it$ with $\sigma > \sigma_0$ and $|t|$ arbitrarily large such that

$$|H(s)| > \frac{1}{3}|t|^{\mu-\delta}.$$

We do this by showing that for a certain sequence of positive numbers $\delta_1, \delta_2, \cdots$ which tends to 0 there exists a corresponding sequence $s_1 = \sigma_1 + it_1, s_2 = \sigma_2 + it_2, \cdots$ with $\sigma_m > \sigma_0$ and $|t_m| \to \infty$ so that

$$|H(s_m)| > \frac{1}{3}|t_m|^{\mu-\delta_m} \quad \text{for} \quad \sigma > \sigma_0.$$

On account of the assumptions we know that to every $h_N(s)$, $N = 1, 2, \cdots$ there exists a positive number Δ_N such that

$$|h_N(s)| = o\left(|t|^{\mu-\Delta_N}\right) \quad \text{for} \quad \sigma > \sigma_0.$$

We now choose an arbitrary sequence of positive numbers $\delta_1, \delta_2, \cdots$ which tends to 0 and satisfies the conditions

$$\delta_2 \leqq \Delta_1, \quad \delta_3 \leqq \min(\Delta_1, \Delta_2), \cdots.$$

Our task is to choose the positive numbers $e_N < E_N$ in such a way that it is possible under the assumption (12) to find complex numbers s_m corresponding to the numbers δ_m with the above-mentioned properties. We shall do this in a sequence of steps.

First step. We choose a complex number $s_1 = \sigma_1 + it_1$ with $\sigma_1 > \sigma_0, |t_1| > 1$ so that

$$|h_0(s_1)| > |t_1|^{\mu-\delta_1}.$$

At the point $s = s_1$ the functions $h_1(s), h_2(s), \cdots$ assume certain values $k_{11}, k_{12}, \cdots$. We choose the positive constants $e_{11} < E_1$, $e_{12} < E_2, \cdots$ so that

$$\sum_{N=1}^{\infty} e_{1N} |k_{1N}|$$

is convergent with sum $< \frac{1}{2} |t_1|^{\mu_1-\delta_1}$. Then for $0 < \varepsilon_N < e_{1N}$ $(N = 1, 2, \cdots)$ we have

$$|H(s_1)| \geqq |h_0(s_1)| - \sum_{N=1}^{\infty} e_{1N} |k_{1N}| > \frac{1}{2} |t_1|^{\mu-\delta_1}.$$

Second step. We choose $s_2 = \sigma_2 + it_2$ with $\sigma_2 > \sigma_0, |t_2| > 2$ so that

$$|h_0(s_2)| > |t_2|^{\mu-\delta_2}$$

and at the same time

$$E_1 |h_1(s_2)| < \frac{1}{3} |t_2|^{\mu-\delta_2}.$$

The latter inequality may be obtained since $\delta_2 \leqq \Delta_1$. At the point $s = s_2$ the functions $h_2(s), h_3(s), \cdots$ assume certain values $k_{22}, k_{23}, \cdots$. We choose the positive numbers $e_{22} < E_2, e_{23} < E_3, \cdots$ so that

$$\sum_{N=2}^{\infty} e_{2N} |k_{2N}|$$

is convergent with sum $< \frac{1}{3} |t_2|^{\mu-\delta_2}$. Then for $0 < \varepsilon_1 < E_1$, $0 < \varepsilon_N < e_{2N}$ $(N = 2, 3, \cdots)$ we have

$$|H(s_2)| \geqq |h_0(s_2)| - E_1 |h_1(s_2)| - \sum_{N=2}^{\infty} e_{2N} |k_{2N}| >$$

$$|t_2|^{\mu-\delta_2} - \frac{1}{3} |t_2|^{\mu-\delta_2} - \frac{1}{3} |t_2|^{\mu-\delta_2} = \frac{1}{3} |t_2|^{\mu-\delta_2}.$$

...

m^{th} *step.* We choose $s_m = \sigma_m + it_m$ with $\sigma_m > \sigma_0$ and $|t_m| > m$ so that

$$|h_0(s_m)| > |t_m|^{\mu-\delta_m}$$

and at the same time

$$E_1 | h_1(s_m) | + E_2 | h_2(s_m) | + \cdots + E_{m-1} | h_{m-1}(s_m) | < \frac{1}{3} | t_m |^{\mu - \delta_m}.$$

The latter inequality may be obtained since $\delta_m \leqq \min(\Delta_1, \cdots, \Delta_{m-1})$. At the point s_m the functions $h_m(s), h_{m+1}(s), \cdots$ assume certain values $k_{mm}, k_{m,m+1}, \cdots$. We choose positive constants $e_{mm} < E_m$, $e_{m,m+1} < E_{m+1}, \cdots$ so that

$$\sum_{N=m}^{\infty} e_{mN} | k_{mN} |$$

is convergent with sum $< \frac{1}{3} | t_m |^{\mu - \delta_m}$. Then for $0 < \varepsilon_1 < E_1, \cdots$, $0 < \varepsilon_{m-1} < E_{m-1}$, $0 < \varepsilon_N < e_{mN}$ $(N = m, m+1, \cdots)$ we have

$$| H(s_m) | > | h_0(s_m) | - (E_1 | h_1(s_m) | + \cdots + E_{m-1} | h_{m-1}(s_m) |) - \sum_{N=m}^{\infty} e_{mN} | k_{mN} | > | t_m |^{\mu - \delta_m} - \frac{1}{3} | t_m |^{\mu - \delta_m} - \frac{1}{3} | t_m |^{\mu - \delta_m} = \frac{1}{3} | t_m |^{\mu - \delta_m}.$$

$\cdots$

It appears from the above that the numbers

$$e_N = \min \{ e_{1N}, \cdots, e_{NN} \} \quad (N = 1, 2, \cdots)$$

may be used in order to satisfy our demands under 2°.

Finally, for each N we choose the smaller one of the two numbers e_N found under 1° and 2° as our final e_N. These e_N satisfy the demands in Lemma 2. This completes the proof of Lemma 2.

§ 6. Proof of the Main Theorem.

We are now in a position to prove the Main Theorem stated in § 1. Since the function $f(s) = 0$ has $\omega_\mu = \omega_\psi = \Omega = -\infty$ we need only consider the following three cases: (α) $\omega_\mu = \omega_\psi = \Omega > -\infty$, ($\beta$) $\omega_\mu > \omega_\psi = \Omega > -\infty$, and the "general" case (γ) $\omega_\mu \geqq \omega_\psi > \Omega \geqq -\infty$.

As an example of the special case (α) we can obviously use the series

$$\zeta(s - \Omega + 1) = \sum n^{\Omega - 1} n^{-s}.$$

In fact, the series is absolutely convergent for $\sigma > \Omega$, and the function has a pole at $s = \Omega$.

The "intermediate" case (β) will be treated at the end of this section by specializing, and slightly modifying, the construction used in the "general" case (γ).

Let us therefore assume for the present that $\omega_\mu \geqq \omega_\psi > \Omega \geqq -\infty$. In the main, our Dirichlet series $\sum A_n n^{-s}$ is constructed by linear combination of infinitely many of the "bricks" from § 4, i. e. by linear combination of Dirichlet series whose summability function and order function have the form $\{\omega_1; a\}$ and $\{\omega_2; a\}$ with common $a \geqq 1$ and $0 \leqq \omega_2 - \omega_1 \leqq \frac{1}{a}$ (viz. with the vertical distance from the ψ-half-line to the μ-half-line ≥ 0 and ≤ 1). This construction, however, requires some caution because we have to build up at the same time two convex curves and because each of these curves may contain infinitely many vertices, i. e. points with different tangents from the right and the left.

We call a pair (T^ψ, T^μ) of parallel (perhaps coinciding) straight lines T^ψ and T^μ *a pair of supporting lines* (in a generalized sense) of our ψ-curve and our μ-curve when one of the lines T^ψ and T^μ is a proper supporting line of the corresponding curve at a point outside the real axis while the other line is defined by the upper position of all lines with the given slope which lie under the other curve. If the latter line contains at least one point of the curve in question, this line is of course a proper supporting line. In any case it is easily seen from the convexity of the two curves $\psi(\sigma)$ and $\mu(\sigma)$ and the relations $\psi(\sigma) \leqq \mu(\sigma) \leqq \psi(\sigma) + 1$ that the vertical distance from the line T^ψ to the line T^μ is ≥ 0 and ≤ 1. Furthermore, since $\psi'(\omega_\psi - 0) \leqq -1$ and $\mu'(\omega_\mu - 0) \leqq -1$ the slope $-a$ of the two lines is $\leqq -1$, i. e. $a \geq 1$.

We start by choosing a denumerable set of abscissae $\sigma_1, \sigma_2, \cdots$ which lie everywhere dense in the interval $\Omega < \sigma < \omega_\mu$. These abscissae are chosen arbitrarily with the exception that we do not use any abscissa σ at which any of the functions $\psi(\sigma)$ and $\mu(\sigma)$ has different derivatives from the left and the right (i. e. which corresponds to a vertex on any of the two curves). For each of the above chosen abscissae σ_i which lie in the sub-interval $\Omega < \sigma < \omega_\psi$ of $\Omega < \sigma < \omega_\mu$ we consider both the supporting line S_i^ψ of the ψ-curve at the point $(\sigma_i, \psi(\sigma_i))$ and the supporting line S_i^μ of the μ-curve at the point $(\sigma_i, \mu(\sigma_i))$. For each of the abscissae

σ_i of the above chosen sequence which (if $\omega_\psi < \omega_\mu$) lie in the complementary sub-interval $\omega_\psi < \sigma < \omega_\mu$ of $\Omega < \sigma < \omega_\mu$ we consider only the supporting line S_i^μ of the μ-curve at the point σ_i. The supporting lines S_i^μ and (in the first case) S_i^ψ are uniquely determined since none of the two curves has a vertex at a point σ_i. For each of the abscissae σ_i which lie in the interval $\Omega < \sigma < \omega_\psi$ we now determine two pairs of supporting lines (T^ψ, T^μ) (which may coincide), one pair being determined by $T^\psi = S_i^\psi$, the other pair by $T^\mu = S_i^\mu$. For the first pair we mark the point $(\sigma_i, \psi(\sigma_i))$ on the line $T^\psi = S_i^\psi$; for the second pair we mark the point $(\sigma_i, \mu(\sigma_i))$ on the line $T^\mu = S_i^\mu$. For each of the abscissae σ_i which (if $\omega_\psi < \omega_\mu$) lie in the interval $\omega_\psi < \sigma < \omega_\mu$ we determine one pair of supporting lines (T^ψ, T^μ), namely the pair defined by $T^\mu = S_i^\mu$, and for this pair we mark the point $(\sigma_i, \mu(\sigma_i))$ on the line $T^\mu = S_i^\mu$. We arrange the pairs of supporting lines (T^ψ, T^μ) thus obtained (for each of our abscissae either one or two pairs) in a sequence

$$(T_1^\psi, T_1^\mu), \quad (T_2^\psi, T_2^\mu), \cdots.$$

As mentioned above, we have marked for each of these pairs a point on one of its lines, T^ψ or T^μ. If we do not take notice of the marked points, it is evident that some of our pairs of supporting lines may coincide. (If for instance both the ψ-curve and the μ-curve are of the type $\{\omega; \alpha\}$ with the same α, then all our pairs of supporting lines will be identical.) If such a coincidence between pairs occurs we shall only keep one of the coinciding pairs, but at the same time we shall change the point marking of the pairs according to the following specification. Let us assume that the pairs of supporting lines

$$(T_{m_1}^\psi, T_{m_1}^\mu), (T_{m_2}^\psi, T_{m_2}^\mu), \cdots$$

coincide.—For orientation we note that this sequence can either contain just two pairs of supporting lines, one with point-marking on the line T^ψ, the other with point-marking on the line T^μ, or the sequence will contain infinitely many pairs of supporting lines. This latter case will only occur when at least one of the curves $\psi(\sigma)$ or $\mu(\sigma)$ contains a straight segment outside the axis of abscissa.—As mentioned above, we keep only one of these

pairs, but we now mark more points on the pair, namely all points on its T^{ψ}-line which are marked on one of the lines $T^{\psi}_{m_1}, T^{\psi}_{m_2}, \cdots$ as well as all points on its T^{μ}-line which are marked on one of the lines $T^{\mu}_{m_1}, T^{\mu}_{m_2}, \cdots$. If more than one point is marked on the line T^{ψ} we arrange these points in a sequence; analogously, if more than one point is marked on the line T^{μ} we arrange these points in a sequence.

The set of pairs of supporting lines (with their arranged marked points) obtained by the above procedure is now arranged in a (finite or infinite) sequence

$$\left(T^{\psi}_{\mathrm{I}}, T^{\mu}_{\mathrm{I}}\right), \left(T^{\psi}_{\mathrm{II}}, T^{\mu}_{\mathrm{II}}\right), \cdots, \left(T^{\psi}_{N}, T^{\mu}_{N}\right), \cdots.$$

It is plain that each of our abscissae σ_i which lie in the interval $\Omega < \sigma < \omega_{\psi}$ will occur as abscissa of a marked point on one of our lines T^{ψ} as well as on one of our lines T^{μ}, while each of the abscissae σ_i which (if $\omega_{\psi} < \omega_{\mu}$) lie in the interval $\omega_{\psi} < \sigma < \omega_{\mu}$ will occur as abscissa of a marked point on one of our lines T^{μ}.

For these pairs of supporting lines we introduce "bricks" in accordance with § 4, i. e. Dirichlet series

$$f_1(s) = \sum a_n^{(1)} n^{-s}, \; f_2(s) = \sum a_n^{(2)} n^{-s}, \cdots, \; f_N(s) = \sum a_n^{(N)} n^{-s}, \cdots$$

such that those parts of the ψ-function and the μ-function of the series $f_N(s)$ where these functions are positive are determined by the half lines over the real axis which lie on T^{ψ}_N and T^{μ}_N, respectively. This is possible since the slope $-a_N$ of the two lines is $\leqq -1$ and the vertical distance from T^{ψ}_N to T^{μ}_N is $\geqq 0$ and $\leqq 1$.

The series we are going to construct is formed by linear combination of these series $f_1(s), f_2(s), \cdots$; in fact, it has the form

$$F(s) = \varepsilon_1 f_1(s) + \varepsilon_2 f_2(s) + \cdots + \varepsilon_N f_N(s) + \cdots = \sum A_n n^{-s},$$

where $A_n = \sum_{N=1}^{\infty} \varepsilon_N a_n^{(N)}$. We shall show that we can choose the positive numbers $\varepsilon_1, \varepsilon_2, \cdots$ so that $\varepsilon_1 f_1(s) + \varepsilon_2 f_2(s) + \cdots$ is represented by a Dirichlet series $\sum A_n n^{-s}$ which for $\sigma > \Omega$ has its summability function $\Psi(\sigma)$ equal to the given function $\psi(\sigma)$ and its order function $M(\sigma)$ equal to the given function $\mu(\sigma)$. However, when $\Omega > -\infty$ we cannot always be sure that our construc-

tion yields a function $F(s)$ which does not have a limit abscissa of summability Ω_F smaller than the given number Ω.

In order to obtain the said properties of $F(s)$ it is enough to prove, *first, that the summability function $\Psi(\sigma)$ of $F(s)$ satisfies the equation $\Psi(\sigma_i) = \psi(\sigma_i)$ for those of our σ_i which lie in the interval $\Omega < \sigma < \omega_\psi$* (this includes that Ω_F must be $\leq \Omega$) *and, secondly, that the order function $M(\sigma)$ of $F(s)$ satisfies the equation $M(\sigma_i) = \mu(\sigma_i)$ for all our σ_i*. In fact, the abscissae σ_i lie everywhere dense in the interval $\Omega < \sigma < \omega_\mu$; so for reasons of continuity we may conclude that the equations

$$\Psi(\sigma) = \psi(\sigma) \quad \text{and} \quad M(\sigma) = \mu(\sigma)$$

hold in the intervals $\Omega < \sigma \leq \omega_\psi$ and $\Omega < \sigma \leq \omega_\mu$, respectively; furthermore, since $\Psi(\omega_\psi) = \psi(\omega_\psi) = 0$ and $M(\omega_\mu) = \mu(\omega_\mu) = 0$, we get $\Psi(\sigma) = 0 = \psi(\sigma)$ for $\sigma > \omega_\psi$ and $M(\sigma) = 0 = \mu(\sigma)$ for $\sigma > \omega_\mu$ so that the above equations will hold in the whole interval $\Omega < \sigma < \infty$.

We remarked above that the constructed function $F(s)$ when $\Omega > -\infty$ might have $\Omega_F < \Omega$ and not $\Omega_F = \Omega$ as desired.

There are some cases with $\Omega > -\infty$ when automatically $\Omega_F = \Omega$, namely when $\psi'(\sigma - 0) \to -\infty$ or $\mu'(\sigma - 0) \to -\infty$ for $\sigma \to \Omega$. In fact, it is impossible in these cases to prolong the given ψ- and μ-curve to the left under preservation of their convexity, so that we can be sure that the constructed function $F(s)$ will have $\Omega_F = \Omega$ as desired.

In the other cases with $\Omega > -\infty$ we can prolong the ψ- and the μ-curve to the whole interval $-\infty < \sigma < \infty$ under preservation of all the properties demanded in the theorem, for instance by two parallel half lines with a common slope $\leq \min\left(\lim_{\sigma \to \Omega} \psi'(\sigma - 0), \lim_{\sigma \to \Omega} \mu'(\sigma - 0)\right)$. This we do before passing to the construction of $F(s)$, i. e. before choosing our σ_i.

The function $F(s)$ obtained will then be an entire function with these prolonged functions $\psi(\sigma)$ and $\mu(\sigma)$ as its summability function and order function, respectively. In order to obtain a function $F^*(s)$ from $F(s)$ which has the right Ω and without changing the Ψ-curve and the M-curve for $\sigma > \Omega$ we may for instance add the function

$$\zeta(s-\Omega+1) = \sum n^{\Omega-1} n^{-s}.$$

In this way we obtain a function $F^*(s)$ with all the desired properties.

We now pass to the actual construction of $F(s)$ referred to above. We determine the positive numbers $\varepsilon_1 = \varepsilon_1^*, \varepsilon_2 = \varepsilon_2^*, \cdots$ successively by the following procedure.

First step. We choose $\varepsilon_1 = \varepsilon_1^*$ as an arbitrary positive number. We consider the pair of supporting lines (T_I^{ψ}, T_I^{μ}) belonging to $f_1(s)$ with its marked points and distinguish between the following three cases.

1°. There exist marked points on the line T_I^{ψ}, but not on the line T_I^{μ}. If only one marked point is lying on T_I^{ψ} we denote its abscissa by σ_0 (where $\Omega < \sigma_0 < \omega_{\psi}$). If infinitely many marked points lie on T_I^{ψ} we denote by σ_0 (where $\Omega < \sigma_0 < \omega_{\psi}$) the abscissa of that point on T_I^{ψ} which comes first in the given ordering of the marked points on T_I^{ψ}. In the present case we are only interested in the Ψ-function at the point σ_0, and not in the M-function at this point.

We put the demand on the sequence $\varepsilon_2, \varepsilon_3, \cdots$ that

$$(1) \qquad F(s) = \varepsilon_1^* f_1(s) + \varepsilon_2 f_2(s) + \varepsilon_3 f_3(s) + \cdots = \sum A_n n^{-s}$$

is to have $\Psi(\sigma_0) = \psi(\sigma_0)$. In other words, we demand that the r_0^{th} abscissa of summability Λ_{r_0} of $F(s)$ where r_0 denotes the positive number $\psi(\sigma_0)$ is exactly equal to σ_0. We apply Lemma 1 of § 5 to the functions

$$g_0(s) = \varepsilon_1^* f_1(s), \quad g_1(s) = f_2(s), \quad g_2(s) = f_3(s), \cdots$$

and the numbers $A = \sigma_0$ and $r = r_0$ just determined. The supporting lines $T_{II}^{\psi}, T_{III}^{\psi}, \cdots$ of the ψ-curve cut the line $\sigma = \sigma_0$ below the point $(\sigma_0, \psi(\sigma_0))$ (because the point $(\sigma_0, \psi(\sigma_0))$ is no vertex on the ψ-curve). Hence the r_0^{th} abscissa of summability of the series $g_1(s), g_2(s), \cdots$ all lie to the left of σ_0 while the r_0^{th} abscissa of summability of $g_0(s)$ is equal to σ_0. It follows from Lemma 1 that there exist positive constants $e_{22}, e_{23}, \cdots$ with the property that the function (1) for $0 < \varepsilon_2 < e_{22}$, $0 < \varepsilon_3 < e_{23}, \cdots$ has its r_0^{th} abscissa of summability equal to σ_0, as desired.

2°. There exist marked points on the line T_{I}^{μ} but no marked points on the line T_{I}^{Ψ}. If only one marked point is lying on T_{I}^{μ} we denote its abscissa by σ_0 (where $\Omega < \sigma_0 < \omega_\mu$). If infinitely many marked point lie on T_{I}^{μ} we denote by σ_0 (where $\Omega < \sigma_0 < \omega_\mu$) the abscissa of that point on T_{I}^{μ} which comes first in the given ordering of the marked points on T_{I}^{μ}. In the present case we are only interested in the M-function at the point σ_0, and not in the Ψ-function at this point.

We put the demand on the sequence $\varepsilon_2, \varepsilon_3, \cdots$ that the function (1) must be regular for $\sigma > \sigma_0$ and have $M(\sigma_0) = \mu(\sigma_0)$. In other words, we demand that the function (1) is to be regular in the half plane $\sigma > \sigma_0$ and in this half plane have (exactly) the order of magnitude μ_0, where $\mu_0 = \mu(\sigma_0) > 0$. We apply Lemma 2 of § 5 to the functions

$$h_0(s) = \varepsilon_1^* f_1(s), \quad h_1(s) = f_2(s), \quad h_2(s) = f_3(s), \cdots$$

and the numbers σ_0 and μ_0 just determined. The supporting lines $T_{\mathrm{II}}^{\mu}, T_{\mathrm{III}}^{\mu}, \cdots$ cut the line $\sigma = \sigma_0$ below the point $(\sigma_0, \mu(\sigma_0))$ (because the point $(\sigma_0, \mu(\sigma_0))$ is no vertex on the μ-curve). Hence the orders of magnitude of the functions $h_1(s), h_2(s), \cdots$ in the half plane $\sigma > \sigma_0$ are all $< \mu_0$, while the order of magnitude of the function $h_0(s)$ in the half plane $\sigma > \sigma_0$ is equal to μ_0. It follows from Lemma 2 that there exist positive constants $e_{22}, e_{23}, \cdots$ with the property that the function (1) for $0 < \varepsilon_2 < e_{22}, 0 < \varepsilon_3 < e_{23}, \cdots$ is regular in the half plane $\sigma > \sigma_0$ and has the order of magnitude μ_0 in this half plane, as desired.

3°. There exist marked points on the line T_{I}^{Ψ} as well as on the line T_{I}^{μ}. We consider two abscissae σ_0' and σ_0'' (they may coincide) where σ_0' denotes the abscissa of *the* marked point or the first of the marked points on the line T_{I}^{Ψ} while σ_0'' denotes the abscissa of *the* marked point or the first of the marked points on the line T_{I}^{μ}. By exactly the same considerations as under 1° and 2°, using the first time Lemma 1 and the second time Lemma 2, we find two sequences of positive numbers $e_{22}', e_{23}', \cdots$ and $e_{22}'', e_{23}'', \cdots$ such that the function (1) for $0 < \varepsilon_2 < e_{22}, 0 < \varepsilon_3 < e_{23}, \cdots$, where $e_{2j} = \min(e_{2j}', e_{2j}'')$ has $\Psi(\sigma_0') = \psi(\sigma_0')$, is regular for $\sigma > \sigma_0''$, and has $M(\sigma_0'') = \mu(\sigma_0'')$.

Summarizing, we have by this first step found a positive

constant ε_1^* and positive constants $e_{22}, e_{23}, \cdots$ such that the function (1) for $0 < \varepsilon_2 < e_{22}, 0 < \varepsilon_3 < e_{23}, \cdots$ has the property that its Ψ-curve will pass through *the* marked point or the first of the marked points on T_{I}^{ψ} (if such points exist) and the M-curve will pass through *the* marked point or the first of the marked points on T_{I}^{μ} (if such points exist).

...

N^{th} *step.* ($N \geq 2$). We assume that by the $1^{\text{st}}, 2^{\text{nd}}, \cdots, (N-1)^{\text{th}}$ step we have determined positive constants $\varepsilon_1^*, \varepsilon_2^*, \cdots, \varepsilon_{N-1}^*$ and (by the $(N-1)^{\text{th}}$ step) positive constants $e_{N,j}$ ($j = N, N+1, \cdots$) such that the function

$$F(s) = \varepsilon_1^* f_1(s) + \cdots + \varepsilon_{N-1}^* f_{N-1}(s) + \varepsilon_N f_N(s) + \\ + \varepsilon_{N+1} f_{N+1}(s) + \cdots = \sum A_n n^{-s} \tag{2}$$

for $0 < \varepsilon_N < e_{NN}, 0 < \varepsilon_{N+1} < e_{N,N+1}, \cdots$ has the property that its Ψ-curve passes through the first $N-1$ of the marked points on T_{I}^{ψ}, through the first $N-2$ of the marked points on $T_{\mathrm{II}}^{\psi}, \cdots$, through the first of the marked points on T_{N-1}^{ψ}, and that its M-curve passes through the first $N-1$ of the marked points on T_{I}^{μ}, through the first $N-2$ of the marked points on $T_{\mathrm{II}}^{\mu}, \cdots$, through the first of the marked points on T_{N-1}^{μ}. It is plain how this is to be understood when one of the supporting lines T^{ψ} or T^{μ} only has one marked point or none at all.

We choose an arbitrary constant ε_N^* in the interval $0 < \varepsilon_N < e_{NN}$ and shall show that we can find positive constants $e_{N+1,N+1} \leq e_{N,N+1}, e_{N+1,N+2} \leq e_{N,N+2}, \cdots$ such that the function

$$F(s) = \varepsilon_1^* f_1(s) + \cdots + \varepsilon_N^* f_N(s) + \varepsilon_{N+1} f_{N+1}(s) + \\ + \varepsilon_{N+2} f_{N+2}(s) + \cdots = \sum A_n n^{-s} \tag{3}$$

for $0 < \varepsilon_{N+1} < e_{N+1,N+1}, 0 < \varepsilon_{N+2} < e_{N+1,N+2}, \cdots$ has the property that its Ψ-curve passes through the first N of the marked points on T_{I}^{ψ}, through the first $N-1$ of the marked points on $T_{\mathrm{II}}^{\psi}, \cdots$, through the first of the marked points on T_N^{ψ}, and that its M-curve passes through the first N of the marked points on T_{I}^{μ}, through the first $N-1$ of the marked points on $T_{\mathrm{II}}^{\mu}, \cdots$, through the first of the marked points on T_N^{μ}.

It is evident that the conclusion from the $(N-1)^{\text{th}}$ step still holds good under the new conditions since

$$0 < \varepsilon_N^* < e_{NN} \quad \text{and} \quad 0 < \varepsilon_j < e_{N+1,j} \leq e_{N,j} \, (j = N+1, N+2, \cdots).$$

Thus we have only to make sure that the Ψ-curve (M-curve) passes through the N^{th} marked point on T_{I}^{ψ} $\left(T_{\text{I}}^{\mu}\right)$, through the $(N-1)^{\text{th}}$ marked point on T_{II}^{ψ} $\left(T_{\text{II}}^{\mu}\right), \cdots$, through the first marked point on T_N^{ψ} $\left(T_N^{\mu}\right)$.

We consider the J^{th} pair of supporting lines $\left(T_J^{\psi}, T_J^{\mu}\right)$ $(J = \text{I}, \text{II}, \cdots, N)$. Let σ_0' (where $\Omega < \sigma_0' < \omega_{\psi}$) and σ_0'' (where $\Omega < \sigma_0'' < \omega_{\mu}$) denote the abscissae of the $(N+1-J)^{\text{th}}$ marked point on the lines T_J^{ψ} and T_J^{μ}, respectively (if they exist).

First, we put the demand on the sequence $\varepsilon_{N+1}, \varepsilon_{N+2}, \cdots$ that the function (3) (if σ_0' exists) has $\Psi(\sigma_0') = \psi(\sigma_0')$. In other words, we demand that the r_0^{th} abscissa of summability Λ_{r_0} of $F(s)$, where r_0 denotes the positive number $\psi(\sigma_0')$, is exactly equal to σ_0'. We apply Lemma 1 of § 5 to the functions

$$g_0(s) = \varepsilon_1^* f_1(s) + \cdots + \varepsilon_J^* f_J(s) + \cdots + \varepsilon_N^* f_N(s),$$

$$g_1(s) = f_{N+1}(s), \; g_2(s) = f_{N+2}(s), \cdots$$

and the numbers $\Lambda = \sigma_0'$ and $r = r_0$ just determined. The supporting lines T_P^{ψ} $(P \neq J)$ of the ψ-curve cut the line $\sigma = \sigma_0'$ below the point $(\sigma_0', \psi(\sigma_0'))$ (because the point $(\sigma_0', \psi(\sigma_0'))$ is no vertex on the ψ-curve). Hence the r_0^{th} abscissae of summability of the series $f_P(s)$, $P \neq J$, all lie to the left of σ_0', while the r_0^{th} abscissa of summability of $f_J(s)$ is equal to σ_0'. It follows immediately that the r_0^{th} abscissa of summability of $g_0(s)$ is equal to σ_0', while the r_0^{th} abscissae of summability of $g_1(s), g_2(s), \cdots$ are smaller than σ_0'. It follows from Lemma 1 that there exist positive constants ${}^{J}e'_{N+1,N+1}, {}^{J}e'_{N+1,N+2}, \cdots$ with the property that the function (3) for $0 < \varepsilon_{N+1} < {}^{J}e'_{N+1,N+1}, 0 < \varepsilon_{N+2} < {}^{J}e'_{N+1,N+2}, \cdots$ has its r_0^{th} abscissa of summability Λ_{r_0} equal to σ_0'.

Next, we put the demand on the sequence $\varepsilon_{N+1}, \varepsilon_{N+2}, \cdots$ that the function (3) (if σ_0'' exists) must be regular for $\sigma > \sigma_0''$ and have $M(\sigma_0'') = \mu(\sigma_0'')$. In other words, we demand that the function (3) is to be regular in the half plane $\sigma > \sigma_0''$ and in this half plane have (exactly) the order of magnitude μ_0 where $\mu_0 = \mu(\sigma_0'') > 0$. We apply Lemma 2 of § 5 to the functions

$$h_0(s) = \varepsilon_1^* f_1(s) + \cdots + \varepsilon_J^* f_J(s) + \cdots + \varepsilon_N^* f_N(s),$$

$$h_1(s) = f_{N+1}(s),\ h_2(s) = f_{N+2}(s), \cdots$$

and the numbers σ_0'' and μ_0 just determined. The supporting lines T_P^{μ}, $P \neq J$, cut the line $\sigma = \sigma_0''$ below the point $(\sigma_0'', \mu(\sigma_0''))$ (because the point $(\sigma_0'', \mu(\sigma_0''))$ is no vertex on the μ-curve). Hence the orders of magnitude of the functions $f_P(s)$ in the half plane $\sigma > \sigma_0''$ for $P \neq J$ are smaller than μ_0, while the function $f_J(s)$ in the half plane $\sigma > \sigma_0''$ has the order of magnitude μ_0. It follows immediately that the order of magnitude of the function $h_0(s)$ in the half plane $\sigma > \sigma_0''$ is equal to μ_0, while the orders of magnitude of the functions $h_1(s), h_2(s), \cdots$ in the half plane $\sigma > \sigma_0''$ are smaller than μ_0. It follows from Lemma 2 that there exist positive constants ${}^{J}e''_{N+1,N+1}, {}^{J}e''_{N+1,N+2}, \cdots$ with the property that the function (3) for $0 < \varepsilon_{N+1} < {}^{J}e''_{N+1,N+1}$, $0 < \varepsilon_{N+2} < {}^{J}e''_{N+1,N+2}, \cdots$ is regular for $\sigma > \sigma_0''$ and has $M(\sigma_0'') = \mu(\sigma_0'')$.

It follows from the above that the numbers

$$e_{N+1,j} = \min\left\{e_{N,j};\ {}^{1}e'_{N+1,j}, \cdots, {}^{N}e'_{N+1,j};\ {}^{1}e''_{N+1,j}, \cdots, {}^{N}e''_{N+1,j}\right\}$$
$$(j = N+1, N+2, \cdots)$$

have the desired properties (under step N).

...

The conclusion is still missing, namely that the sequence $\varepsilon_1^*, \varepsilon_2^*, \cdots$ found above is such that the function

$$F(s) = \varepsilon_1^* f_1(s) + \varepsilon_2^* f_2(s) + \cdots = \sum A_n n^{-s} \tag{4}$$

has the desired properties. This, however, follows at once from the remark that

$$0 < \varepsilon_{N+1}^* < e_{N+1,N+1} \leqq e_{N,N+1}$$
$$0 < \varepsilon_{N+2}^* < e_{N+2,N+2} \leqq e_{N+1,N+2} \leqq e_{N,N+2}$$
$$\cdots\cdots\cdots\cdots\cdots\cdots\cdots\cdots\cdots\cdots$$

so that (4) gets the properties of (3) from the arbitrary step N ($N = 1, 2, \cdots$), q. e. d.

This completes the proof of the Main Theorem in the "general" case (γ) $\omega_{\mu} \geqq \omega_{\psi} > \Omega \geqq -\infty$.

The remaining case $(\beta)\ \omega_\mu > \omega_\psi = \Omega > -\infty$ can be treated in a similar way as the general case. However, a small modification is necessary, due to the fact that the ψ-curve does not leave the real axis, but consists of the interval $\Omega < \sigma < \infty$ on the real axis. If we are in a case where the pair of functions $\psi(\sigma)$ and $\mu(\sigma)$ can be prolonged no modification is of course necessary since the prolonged curves fall under case (γ). In any case, the "bricks" $f_1(s), f_2(s) \cdots$ are obtained in the same way as before, but if we proceed as before (in the case where $\psi(\sigma)$ and $\mu(\sigma)$ could not be prolonged) by the determination of the numbers $\varepsilon_1^*, \varepsilon_2^*, \cdots$ it is plain, since no marked points occur on the lines T^ψ of our pairs of supporting lines $\left(T_N^\psi, T_N^\mu\right)$, that we have taken care only of the M-function, but not of the Ψ-function. However, from the determination of the pairs $\left(T_N^\psi, T_N^\mu\right)$ it follows that all the Dirichlet series $f_N(s)$ are convergent for $\sigma > \Omega$, for all the lines T_N^ψ pass through the end-point Ω of the ψ-curve.

In order to obtain that (4) also becomes convergent for $\sigma > \Omega$, and hence $\Psi(\sigma) = 0$ for $\sigma > \Omega$ as desired, we choose a sequence $\sigma_1^* > \sigma_2^* > \cdots \to \Omega$. By our first step we add the demand to the previous demands that (1) is also to be convergent for $s = \sigma_1^*$, and in order to obtain this situation we use a result obtained in the first part of the proof of Lemma 1 in the case $r = 0$, namely the result that if the Dirichlet series $g_1(s), g_2(s), \cdots$ are summable of the r^{th} order at the point $s = A$, then the positive numbers $e_1, e_2, \cdots$ can be chosen so that the Dirichlet series $G^*(s) = \varepsilon_1 g_1(s) + \varepsilon_2 g_2(s) + \cdots = \sum B_n^* n^{-s}$ becomes summable of the r^{th} order at the point $s = A$ when only $0 < \varepsilon_1 < e_1,\ 0 < \varepsilon_2 < e_2, \cdots$. In our N^{th} step we add the demand to the previous demands that (3) is also to be convergent for $s = \sigma_N^*$. Except for this slight modification our previous method remains unchanged.

Thus the proof of our Main Theorem is completed.

References.

[1] A. F. Andersen. Studier over Cesàro's Summabilitetsmetode. Doctoral Dissertation, Copenhagen 1921.

[2] H. Bohr. Ueber die Summabilität Dirichletscher Reihen. Nachr. Ges. Wiss. Göttingen. Math. Phys. Kl. 1909, 247-262.

[3] H. Bohr. Bidrag til de Dirichlet'ske Rækkers Theori. Doctoral Dissertation, Copenhagen 1910.

[4] H. Bohr. On the Convergence Problem for Dirichlet Series. Dan. Mat. Fys. Medd. **25**, no. 6 (1949).

[5] H. Bohr. Zur Theorie der Dirichletschen Reihen. Math. Z. 52 (1950), 709-722.

[6] G. H. Hardy and M. Riesz. The General Theory of Dirichlet Series. Cambridge Tracts, no. 18, Cambridge 1915.

[7] M. Riesz. Sur les séries de Dirichlet. C. R. Acad. Sci. Paris 148 (1909), 1658-1660.

[8] M. Riesz. Sur un théorème de la moyenne et ses applications. Acta Sci. Math. Szeged 1 (1923), 114-126.

Indleveret til selskabet den 28. januar 1952.
Færdig fra trykkeriet den 26. maj 1952.

Det Kongelige Danske Videnskabernes Selskab
Matematisk-fysiske Meddelelser, bind **27**, nr. 5

Dan. Mat. Fys. Medd. **27**, no. 5 (1952)

ON THE INTERNAL CONSTITUTION OF RELATIVISTICALLY DEGENERATE STARS

BY

MOGENS RUDKJØBING

København
i kommission hos Ejnar Munksgaard
1952

Printed in Denmark
Bianco Lunos Bogtrykkeri

It is well known that in a first approximation white dwarf stars are such equilibrium configurations, which masses of matter with completely degenerate electrons take up under the influence of their own internal gravitational fields. The gravitational forces act on the electrons mainly through a small radial displacement of the heavy particles relative to the electrons. CHANDRASEKHAR [1] has in his theory of white dwarf stars taken account of the relativistic relation between energy and momentum of a particle in finding the equation of state of a relativistically degenerate electron gas.

We shall here investigate the influence of another relativistic effect, namely the "spin-orbit interaction", which is well known from the theory of the fine structure of the hydrogen spectrum. The star will be considered as a kind of THOMAS-FERMI atom, and we are thus using an approximation, which is well suited for the problem in question, even if it is not very good in the case of ordinary atoms. In the stellar interior we may namely deal with volume elements having linear dimensions that are small by a factor of about 10^9 in comparison with the dimensions of the star as a whole and still large by a similar factor in comparison with electronic wave lengths.

We place the origin of our co-ordinate system at the center of the spherically symmetric star and are then going to use DIRAC's equations for electrons in a central field.

The angle-dependent part of the solution is well known and is, independent of the form of the potential as a function of the distance from the center, leading to the following two simultaneous differential equations for two radial functions R_1 and R_2: (*cf.* A. SOMMERFELD: Wellenmechanik, Ch. IV, § 7. [2])

$$\left.\begin{aligned}\left(\frac{d}{dr}+\frac{1-k}{r}\right)R_1 &= \frac{1}{\hbar c}(E-V+E_0)\,R_2\\ \left(\frac{d}{dr}+\frac{1+k}{r}\right)R_2 &= \frac{1}{\hbar c}(-E+V+E_0)R_1.\end{aligned}\right\} \tag{1}$$

The notations used here and in the following have their usual meaning. The quantum number k is restricted to positive and negative integers.

Introducing the functions $P_1 = rR_1$ and $P_2 = rR_2$ we get

$$\left.\begin{aligned}\left(\frac{d}{dr}-\frac{k}{r}\right)P_1 &= \frac{1}{\hbar c}(E-V+E_0)\,P_2\\ \left(\frac{d}{dr}+\frac{k}{r}\right)P_2 &= \frac{1}{\hbar c}(-E+V+E_0)\,P_1.\end{aligned}\right\} \tag{2}$$

In order to deduce a wave equation that enables us to apply the principles of quantum statistics we proceed as follows: We differentiate the first of equations (2) and substitute for $\frac{dP_2}{dr}$ the expression from the second equation and get

$$\left.\begin{aligned}&\frac{d^2P_1}{dr^2}-\frac{k}{r}\frac{dP_1}{dr}+\frac{k}{r^2}P_1 =\\ &\frac{1}{\hbar c}(E-V+E_0)\left[\frac{1}{\hbar c}(-E+V+E_0)\,P_1-\frac{k}{r}P_2\right]-\frac{1}{\hbar c}\frac{dV}{dr}P_2.\end{aligned}\right\} \tag{3}$$

Then P_2 is eliminated from the bracket by the aid of the first of equations (2), so that we get

$$\frac{d^2P_1}{dr^2}+\left[\frac{(E-V)^2-E_0^2}{\hbar^2c^2}-\frac{k^2-k}{r^2}\right]P_1 = -\frac{1}{\hbar c}\frac{dV}{dr}P_2. \tag{4}$$

By an exactly similar procedure we find

$$\frac{d^2P_2}{dr^2}+\left[\frac{(E-V)^2-E_0^2}{\hbar^2c^2}-\frac{k^2+k}{r^2}\right]P_2 = +\frac{1}{\hbar c}\frac{dV}{dr}P_1. \tag{5}$$

In the case of a vanishing potential gradient these two differential equations are two wave equations. They have identical

eigenfunctions and eigenvalues for values of k that differ by one, and they are changed into each other by the interchange of $+k$ and $-k$.

In order to treat the general case of a non-vanishing potential gradient, when equations (4) and (5) describe coupled oscillations, we introduce a linear combination

$$Q = a_1 P_1 + a_2 P_2 , \tag{6}$$

where a_1 and a_2 are as yet undetermined constants. Multiplying (4) and (5) by a_1 and a_2 respectively and adding, we get

$$\left.\begin{aligned} &\frac{d^2Q}{dr^2} + \left[\frac{(E-V)^2 - E_0^2}{\hbar^2 c^2} - \frac{k^2}{r^2}\right] Q + \\ &\frac{k}{r^2} a_1 P_1 + \frac{1}{\hbar c}\frac{dV}{dr} a_1 P_2 - \frac{k}{r^2} a_2 P_2 - \frac{1}{\hbar c}\frac{dV}{dr} a_2 P_1 = 0 . \end{aligned}\right\} \tag{7}$$

We can now determine the ratio of the a's and a new constant, g, and arrive at a wave equation for Q of the following form:

$$\frac{d^2Q}{dr^2} + \left[\frac{(E-V)^2 - E_0^2}{\hbar^2 c^2} - \frac{k^2+g}{r^2}\right] Q = 0, \tag{8}$$

provided $r^2 \dfrac{dV}{dr}$ can be treated as a constant in that region, characterized by a small interval of r, which we will consider. Equating the coefficients of P_1 and P_2 in (7) and (8) we get the following two equations

$$\left.\begin{aligned} \frac{k}{r^2} a_1 - \frac{1}{\hbar c}\frac{dV}{dr} a_2 &= -\frac{g}{r^2} a_1 \\ \frac{1}{\hbar c}\frac{dV}{dr} a_1 - \frac{k}{r^2} a_2 &= -\frac{g}{r^2} a_2 . \end{aligned}\right\} \tag{9}$$

Writing k_0 for the constant $\dfrac{r^2}{\hbar c}\dfrac{dV}{dr}$ we have

$$\left.\begin{aligned} k a_1 - k_0 a_2 + g a_1 &= 0 \\ k_0 a_1 - k a_2 + g a_2 &= 0 . \end{aligned}\right\} \tag{10}$$

In order that the above equations have finite solutions for the a's, the determinant

$$\begin{vmatrix} k+g & -k_0 \\ k_0 & -k+g \end{vmatrix}$$

must vanish.

This leads to the (secular) equation

$$g^2 = k^2 - k_0^2. \tag{11}$$

The constant g may then take one of the two values

$$g = \pm \sqrt{k^2 - k_0^2}. \tag{12}$$

If we choose the upper sign we have the differential equation

$$\frac{d^2Q_{\mathrm{I}}}{dr^2} + \left[\frac{(E-V)^2 - E_0^2}{\hbar^2 c^2} - \frac{k^2 + \sqrt{k^2 - k_0^2}}{r^2}\right] Q_{\mathrm{I}} = 0, \tag{13}$$

and with the lower sign

$$\frac{d^2Q_{\mathrm{II}}}{dr^2} + \left[\frac{(E-V)^2 - E_0^2}{\hbar^2 c^2} - \frac{k^2 - \sqrt{k^2 - k_0^2}}{r^2}\right] Q_{\mathrm{II}} = 0. \tag{14}$$

The functions Q_{I} and Q_{II} then are two different linear combinations of P_1 and P_2. The request that P_1 and P_2 both fulfill the boundary conditions leads to a similar request for the Q's.

The equations (13) and (14) may both, independent of the sign of g, be written as

$$\frac{d^2Q}{dr^2} + \left[\frac{(E-V)^2 - E_0^2 - \left(r\frac{dV}{dr}\right)^2}{\hbar^2 c^2} - \frac{g(g+1)}{r^2}\right] Q = 0. \tag{15}$$

The above equation is in the case of a hydrogen atom identical with the iterated DIRAC equation given by TEMPLE [3]. Our Q is equal to his Ψ multiplied by r. In that special case the terms V^2 and $-\left(r\frac{dV}{dr}\right)^2$ cancel each other, and k_0 is equal to the fine-structure constant.

For every energy value determined by this equation there is a $2\,|k|$-fold degeneracy due to the angular parts of the functions. The quantum number j is namely equal to $|k|-\frac{1}{2}$ (*cf.* SOMMERFELD, loc. cit. Ch. IV, § 8). For the hydrogen atom *e.g.* the ${}^2S_{\frac{1}{2}}$- and ${}^2P_{\frac{1}{2}}$-states both correspond to $k^2 = 1$ and are both double. Similarly the ${}^2P_{\frac{3}{2}}$- and ${}^2D_{\frac{3}{2}}$-states, which correspond to $k = \pm 2$, are both quadruple etc.

For each sign and numerical value of g the number of states with energy constants lower than a maximal value E_m, characteristic of the star, in a volume element in the form of a shell concentric with the star, is equal to $2\,|k|$ times the number of half oscillations of the radial function Q for the maximum energy value, because each state has one node less than that lying immediately above it.

The minimum value of k^2 is k_0^2, because a smaller value would cause E to be complex. (For the hydrogen atom this is no problem, since the fine-structure constant is much smaller than one, the lowest allowed value of k).

The minimum radial wave length $\lambda_{\min}$ is determined as a function of E_m and g by

$$\left(\frac{2\pi}{\lambda_{\min}}\right)^2 = \frac{(E_m - V)^2 - E_0^2 - \left(r\frac{dV}{dr}\right)^2}{\hbar^2 c^2} - \frac{g(g+1)}{r^2}. \tag{16}$$

For a thickness of the shell of one cm the total number of states with a certain numerical value of g then is equal to

$$2 \cdot \frac{2}{\lambda_{\min}} \cdot 2|k| = \frac{4|k|}{\pi r}\left[r^2 \frac{(E_m - V)^2 - E_0^2 - \left(r\frac{dV}{dr}\right)^2}{\hbar^2 c^2} - g^2\right]^{\frac{1}{2}}, \tag{17}$$

because we need not here distinguish between g and $g+1$. The first factor two to the left is due to the double sign of g.

We find the total number of states by integrating over $|k|$ from $g^2 = 0$ to its maximal value, which value makes the integrand vanish. We use the relation

$$2\,|k|\,d\,|k| = d(g^2). \tag{18}$$

The total number N of states with energy less than E_m is then determined by

$$N = \frac{2}{\pi r} \int_{g=0}^{g\,\max} \left[r^2 \frac{(E_m - V)^2 - E_0^2 - \left(r \frac{dV}{dr}\right)^2}{\hbar^2 c^2} - g^2 \right]^{\frac{1}{2}} d(g^2), \qquad (19)$$

and we find

$$N = \frac{4}{3\pi r} \left[r^2 \frac{(E_m - V)^2 - E_0^2 - \left(r \frac{dV}{dr}\right)^2}{\hbar^2 c^2} \right]^{\frac{3}{2}}. \qquad (20)$$

The number of states per cubic cm is found by dividing N by $4\pi r^2$. When all states with energy constants less than E_m are occupied by electrons, the material density ϱ is found by multiplying the density of states by $\mu_e m_H$, the mass per electron, where the mass of a hydrogen atom is denoted by m_H. For pure hydrogen the molecular weight μ_e is equal to one. We get

$$\varrho = \frac{\mu_e m_H}{3\pi^2 \hbar^3 c^3} \left[(E_m - V)^2 - E_0^2 - \left(r \frac{dV}{dr}\right)^2 \right]^{\frac{3}{2}}. \qquad (21)$$

If the gravitational potential per unit mass is called U, we have Poisson's equation:

$$\frac{d^2 U}{dr^2} + \frac{2}{r} \frac{dU}{dr} = 4\pi G \varrho. \qquad (22)$$

The potential function V is equal to $\mu_e m_H U$, so that we arrive at the following differential equation for V (writing h for $2\pi\hbar$):

$$\frac{d^2 V}{dr^2} + \frac{2}{r} \frac{dV}{dr} = \frac{32\pi^2 \mu_e^2 m_H^2 G}{3 h^3 c^3} \left[(E_m - V)^2 - E_0^2 - \left(r \frac{dV}{dr}\right)^2 \right]^{\frac{3}{2}}. \qquad (23)$$

In deriving (21) and (23) we have neglected such non-uniformity in the distribution of the heavy particles as has been taken into account by Schatzman [4].

Introducing as a new variable

$$y = \frac{E_m - V}{E_0} \qquad (24)$$

we get

$$\frac{d^2y}{dr^2}+\frac{2}{r}\frac{dy}{dr}=-\frac{32\,\pi^2\mu_e^2 m_H^2 m_0^2 G c}{3\,h^3}\left[y^2-\left(r\frac{dy}{dr}\right)^2-1\right]^{\frac{3}{2}}, \tag{25}$$

where we have made use of the relation

$$E_0 = m_0 c^2. \tag{26}$$

If the term $-\left(r\frac{dy}{dr}\right)^2$ in the bracket in equation (25) is neglected, we find CHANDRASEKHAR's equation [5]. Our aim is, however, to find the effect of this term on the mass-radius relation for white dwarf stars. If we introduce CHANDRASEKHAR's variables

$$\left.\begin{aligned} r &= \alpha\eta,\quad y = y_0\varphi,\\ \alpha &= \frac{1}{4\,\pi\mu_e m_H m_0 y_0}\left(\frac{3\,h^3}{2\,Gc}\right)^{\frac{1}{2}} = l_1 y_0^{-1} = \frac{7{,}71\cdot 10^8\ \mathrm{cm}}{\mu_e y_0}, \end{aligned}\right\} \tag{27}$$

we can write the differential equation as

$$\frac{1}{\eta^2}\frac{d}{d\eta}\left(\eta^2\frac{d\varphi}{d\eta}\right)=-\left(\varphi^2-\left(\eta\frac{d\varphi}{d\eta}\right)^2-\frac{1}{y_0^2}\right)^{\frac{3}{2}}, \tag{28}$$

where φ has to take the value one at the center. The boundary condition is $\frac{d\varphi}{d\eta}=0$ at the center. The surface is found where the density vanishes (at $\eta=\eta_1$).

In the limiting case when $\frac{1}{y_0^2}$ is very near one, the limiting solution is, just as is that of CHANDRASEKHAR's equation, that of an EMDEN equation of index $\frac{3}{2}$. (Then all relativistic effects are negligible).

Following CHANDRASEKHAR we deduce the following expression for the mass of the whole configuration:

$$M=-\frac{\sqrt{3}}{4\sqrt{2}\,\pi\mu_e^2 m_H^2}\left(\frac{hc}{G}\right)^{\frac{3}{2}}\left(\eta^2\frac{d\varphi}{d\eta}\right)_{\eta=\eta_1}, \tag{29}$$

where the numerical factor is 2,85 μ_e^{-2} solar masses. (For comparison with CHANDRASEKHAR's results we have used his adopted values of the natural constants throughout this paper).

The differential equation (28) has been integrated numerically for three values of the parameter $\frac{1}{y_0^2}$. The results for the radii and masses of the corresponding stellar configurations are given below. For comparison, CHANDRASEKHAR's values are also given. Our central densities are the same as in his models for the same parameter values.

TABLE I.

$\frac{1}{y_0^2}$	$\frac{R}{l_1}$	$-\left(\eta^2 \frac{d\varphi}{d\eta}\right)_{\eta=\eta_1}$	Chandrasekhar's values	
			$\frac{R}{l_1}$	$-\left(\eta^2 \frac{d\varphi}{d\eta}\right)_{\eta=\eta_1}$
0,5	2,58	0,597	2,50	0,707
0,2	1,84	0,926	1,67	1,243
0,1	1,55	1,091	1,29	1,519

The density distributions are given in *Table II*. The unit of density is

$$B = \frac{8\pi \mu_e m_H m_0^3 c^3}{3h^3} = 9{,}82 \cdot 10^5 \mu_e \, \mathrm{g\,cm^{-3}}.$$

The unit of radius is l_1.

A comparison of the results with those of CHANDRASEKHAR shows that the radii are larger and the masses smaller than his for the same values of $\frac{1}{y_0^2}$. For the same value of the mass the radius is smaller than CHANDRASEKHAR's.

The limiting case of vanishing $\frac{1}{y_0^2}$ has also been treated by numerical integration. *Table III* gives the variable φ together with $-\eta^2\varphi'$ and $\frac{\varrho}{\varrho_c}$ as functions of η. In this case there is no definite radius measured in units of $l_1 y_0^{-1}$. For any value of the parameter we have namely the following limiting form of φ as a function of η:

$$\varphi \sim c_1 + \frac{c_2}{\eta}. \qquad (30)$$

TABLE II.

$\frac{r}{l_1}$ \ $\frac{1}{y_0^2}$ =	0,5	0,2	0,1
0,0	1,00	8,00	27,00
0,1	0,99	7,81	25,71
0,2	0,97	7,29	22,01
0,3	0,94	6,44	16,59
0,4	0,89	5,37	11,03
0,5	0,83	4,21	6,68
0,6	0,76	3,13	3,86
0,7	0,69	2,22	2,20
0,8	0,61	1,53	1,26
0,9	0,53	1,03	0,73
1,0	0,45	0,68	0,42
1,1	0,38	0,45	0,24
1,2	0,32	0,29	0,13
1,3	0,26	0,19	0,07
1,4	0,20	0,12	0,03
1,5	0,16	0,07	0,01
1,6	0,13	0,04	..
1,7	0,10	0,02	..
1,8	0,07	0,00	..
1,9	0,05	..	..
2,0	0,04	..	..
2,1	0,03	..	..
2,2	0,02	..	..
2,3	0,01	..	..
2,4	0,00	..	..
2,5	0,00	..	..

In the case of $\frac{1}{y_0^2} = 0$, however, the constant c_1 vanishes, because we have here

$$|\varphi| \to \left| \eta \frac{d\varphi}{d\eta} \right| \tag{31}$$

as we approach the surface. The radius might therefore be finite in units of l_1.

The limiting mass can be estimated from the data in the table to be some 85 per cent of CHANDRASEKHAR's limiting mass. This, which is that of an EMDEN polytrope of index 3, corresponds to a value of $-\eta^2 \frac{d\varphi}{d\eta}$ equal to 2,018 at the surface.

A more detailed investigation of the model considered would not be of very much interest, because we have here still neglected the influence of exchange effects. EDDINGTON's criticisms of the

"current" theory of white dwarf stars have therefore not yet been properly answered, also because we have still preserved dividing walls (here spherical) inside the star for determining energy states instead of determining them for the star as a whole. The present method of approach to the problem might serve as a starting point for investigations as to the effect due to the introduction of such refinements into the theory.

TABLE III.

η	φ	$-\eta^2\varphi'$	ϱ/ϱ_c	η	φ	$-\eta^2\varphi'$	ϱ/ϱ_c
0,0.....	1,0000	0,0000	1,000	3,9	0,3747	1,2453	0,008
0,1.....	0,9984	0,0003	0,995	4,0	0,3667	1,2563	0,007
0,2.....	0,9934	0,0026	0,980	4,1	0,3590	1,2669	0,006
0,3.....	0,9853	0,0088	0,955	4,2	0,3516	1,2768	0,006
0,4.....	0,9740	0,0203	0,920	4,3	0,3445	1,2862	0,005
0,5.....	0,9600	0,0386	0,876	4,4	0,3377	1,2949	0,005
0,6.....	0,9433	0,0643	0,823	4,5	0,3311	1,3038	0,004
0,7.....	0,9244	0,0978	0,763	4,6	0,3248	1,3120	0,004
0,8.....	0,9035	0,1389	0,697	4,7	0,3187	1,3194	0,003
0,9.....	0,8811	0,1868	0,628	4,8	0,3129	1,3270	0,003
1,0.....	0,8576	0,2402	0,558	4,9	0,3072	1,3338	0,003
1,1.....	0,8332	0,2978	0,489	5,0	0,3017	1,3407	0,003
1,2.....	0,8084	0,3580	0,424				
1,3.....	0,7836	0,4195	0,364	5,5	0,2771	1,371	0,0018
1,4.....	0,7589	0,4806	0,310	6,0	0,2561	1,395	0,0012
1,5.....	0,7346	0,5406	0,262	6,5	0,2381	1,416	0,0009
1,6.....	0,7109	0,5984	0,221	7,0	0,2225	1,433	0,0007
1,7.....	0,6879	0,6536	0,186	7,5	0,2087	1,448	0,0005
1,8.....	0,6657	0,7058	0,156	8,0	0,1966	1,461	0,0004
1,9.....	0,6443	0,7544	0,131	8,5	0,1858	1,473	0,0003
2,0.....	0,6239	0,8000	0,110	9,0	0,1762	1,484	0,0002
2,1.....	0,6043	0,8424	0,092	9,5	0,1675	1,493	0,0002
2,2.....	0,5857	0,8815	0,078	10,0	0,1596	1,501	0,0002
2,3.....	0,5679	0,9179	0,066				
2,4.....	0,5510	0,9515	0,056	15	0,1087	1,56	0,000034
2,5.....	0,5349	0,9826	0,048	20	0,0825	1,59	0,000012
2,6.....	0,5195	1,0112	0,041	25	0,0665	1,61	0,000005
2,7.....	0,5049	1,0377	0,035	30	0,0558	1,62	0,000003
2,8.....	0,4910	1,0624	0,030	35	0,0481	1,63	0,000002
2,9.....	0,4778	1,0855	0,026	40	0,0422	1,64	0,000001
3,0.....	0,4652	1,1067	0,023	45	0,0376	1,65	0,000001
3,1.....	0,4532	1,1266	0,020	50	0,0340	1,65	..
3,2.....	0,4418	1,1448	0,017	55	0,0310	1,66	..
3,3.....	0,4308	1,1620	0,015	60	0,0284	1,66	..
3,4.....	0,4204	1,1781	0,014	65	0,0263	1,67	..
3,5.....	0,4104	1,1933	0,012	70	0,0245	1,67	..
3,6.....	0,4009	1,2075	0,011	75	0,0229	1,68	..
3,7.....	0,3918	1,2210	0,009	80	0,0215	1,68	..
3,8.....	0,3831	1,2333	0,008	85	0,0202	1,68	..
				90	0,0191	1,69	..

References.

[1] S. Chandrasekhar, Stellar Structure, X—XI, Chicago 1939.
[2] A. Sommerfeld, Atombau und Spektrallinien, Braunschweig 1939.
[3] G. Temple, Proc. Roy. Soc. **A, 145,** 344, eq. (3, 6) 1934.
[4] E. Schatzman, Dan. Mat. Fys. Medd. **25,** no. 7 (1950), Kbhvns Obs. Publ. Nr. 149.
[5] S. Chandrasekhar, loc. cit. 416, eq. (25).

Indleveret til selskabet den 21. november 1951.
Færdig fra trykkeriet den 6. maj 1952.

Det Kongelige Danske Videnskabernes Selskab
Matematisk-fysiske Meddelelser, bind **27**, nr. 6

Dan. Mat. Fys. Medd. **27**, no.6 (1952)

SOME PROBLEMS IN RADIOCARBON DATING

BY

ERNEST C. ANDERSON AND HILDE LEVI

København
i kommission hos Ejnar Munksgaard
1952

CONTENTS

Printed in Denmark.
Bianco Lunos Bogtrykkeri.

Introduction.

Since the discovery of natural radiocarbon[1), 2)] and its application to dating problems[3)] by LIBBY and coworkers, a number of papers have appeared describing the technique[4), 5), 6)] and the results obtained at Chicago[7), 8)] and elsewhere[9)]. In addition, the concordance of the results with geological and archaeological expectation has been discussed[10), 11), 12), 13)]. However, no extensive treatment of the limitations and errors of the method has been given although several isolated examples have been discussed[11), 14), 15), 16)]. It is the purpose of the present paper to present some general conclusions regarding the range of the method, its accuracy, possible sources of error other than that of provenience, and the rationale of the instrumentation. The problems are considered from the theoretical viewpoint and no new experimental data are given. Since the fundamentals of the method are well summarized in the literature and in LIBBY's book[17)], it is assumed that the reader is familiar with them.

Instrumentation.

Description of Screen Wall Counter.

For the measurement of natural radiocarbon, the screen wall counter[4)] was selected. The design of this instrument is based on two considerations, namely, the desire to obtain the maximum net count from a sample in a detector of a given size, and the necessity of establishing accurately a net count which may be small compared with the background of the counter. The carbon powder to be measured is mixed with water to form a thick paste and is spread evenly over the inside surface of a cylinder

which is placed concentrically to the axis of the counter. In this way, all absorption losses other than self-absorption are eliminated, a geometry of essentially 50 per cent is obtained, and the sample fills the maximum solid angle around the counter. The cathode of the counter consists of an open grid or screen of wires. The screen does not define the radial extent of the sensitive volume of the counter which, in fact, extends to the surface of the sample. The purpose of the screen is simply to improve the electrical characteristics of the system. Through the use of

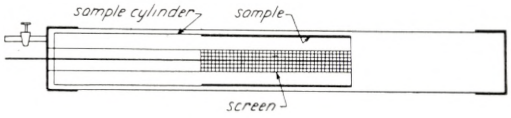

Fig. 1. Screen wall counter.

a double sample cylinder, one half holding the sample, the other a blank, frequent alternation between the two is possible without affecting the counter filling. Thus, the effects of temporal changes in background are minimized.

Comparison with Gas Sample Counter.

The fundamental problem in the selection of the proper detector unit is to obtain the maximum counting rate from a detector of minimum physical size. The physical size is an important parameter, since the background rate of the instrument is proportional to the size, and the effect to be determined is of the same order as or smaller than the background even under the most favourable circumstances.

For a gas sample counter, practically all the disintegrations occurring in the sample will be detected and, therefore, the efficiency defined as the fraction of the disintegrations detected is essentially unity. For the screen wall counter, using a thick sample of elemental carbon, the efficiency is only 5.46 $^0/_0$[4), 5)]*.

* When this value for the efficiency is used in equation 1, the range ϱ must be taken as 20 mg/cm². If the more recent value for the range of 28 mg/cm² is used, the efficiency E_1 is 3.8 $^0/_0$. The quantity which has been determined experimentally is the product $E \cdot \varrho = 1.10$ mg/cm². Physically, this is the thickness of the layer which—in the absence of self-absorption—would give the same counting rate as the thick sample.

However, a screen wall counter of conventional size will contain some 20 times the amount of carbon that can be used in a gas sample counter having the same background. The two methods thus happen by chance to be similar with respect to this parameter and a more detailed comparison is in order.

This can be made as follows. The counting rate S_1 to be expected from a screen wall counter is

$$S_1 = E_1 \varrho A S, \tag{1}$$

where E_1 is the efficiency as defined above, ϱ is the range in mg/cm² of the C-14 β-particle, A is the sample area which is equal to $\pi d_1 l_1$, d_1 being the inside diameter and l_1 the length of the sample cylinder, S is the specific activity of the sample in disintegrations per minute and milligram.

For a spherical gas counter, assuming an efficiency of unity, we have

$$S_2 = M \frac{\pi}{6} d_2^3 S, \tag{2}$$

where M = mg of carbon per cm³. If the filling gas contains one atom of carbon per molecule and has a pressure of one atmosphere, M = 0.54 mg/cm³.

In order to consider counters having the same background we will assume the background to be proportional to the horizontal cross-sectional area, which is for a cylindrical screen wall $l_1 d_1$ and for a spherical gas counter $\frac{\pi}{4} d_2^2$. Therefore,

$$l_1 d_1 = \frac{\pi}{4} d_2^2 \tag{3}$$

is the condition for identical background rates. Since the sample area of a screen wall A is π times its background area, the screen wall sample area can also be expressed as π times the background area of the corresponding spherical gas counter, viz. $\frac{\pi^2}{4} d_2^2$. Combining equations (1) and (2), using the numerical values $E_1 \cdot \varrho = 1.10$ and M = 0.54, and setting $A_1 = \frac{\pi^2}{4} d_2^2$, we find

$$\frac{S_1}{S_2} = \frac{1.10 \frac{\pi^2}{4} d_2^2}{0.54 \frac{\pi}{6} d_2^3} = \frac{9.60}{d_2}. \tag{4}$$

This equation is plotted in Fig. 2, using the volume of the spherical counter as the independent variable.

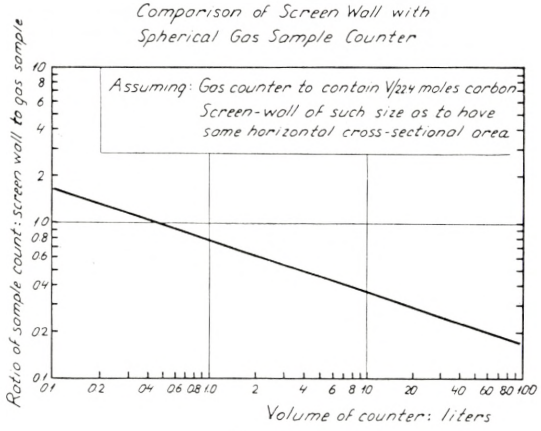

Fig. 2.

This figure offers a comparison of the sample count ratio of a screen wall counter to that of a gas counter as a function of the sample size.

It is clear that the screen wall counter is superior to the gas counter in the case of small detectors, while the gas counter is to be preferred when the detectors are large. Although it is always desirable for reasons of counting statistics to use as large a sample as possible, other considerations (such as difficulty of operation of large counters and the mass of the shield required) usually limit one to a volume of a few liters. It is seen from Fig. 2 that, in this region, the ratio of counting rates is not much different from unity and is slightly in favour of a gas sample counter. Because of the geometrical requirements of the anti-coincidence shielding method, however, the sphere is not the optimum shape. That is to say, a bundle of anti-coincidence counters of conventional design makes a cylindrical cavity for the sample counter. Therefore, from the viewpoint of the mass

of shielding required as well as the electrical and the construction characteristics, the comparison should be made between a screen wall counter and a *cylindrical* gas sample counter of the same dimensions.

Such a comparison is given in Fig. 3, where the additional parameter α of the ratio of counter length to diameter has been introduced. The principles of good counter design will in general

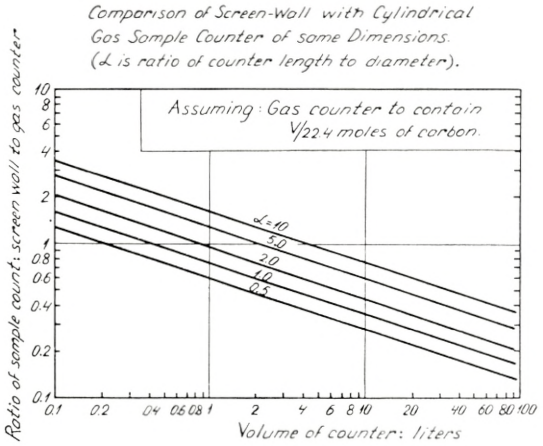

Fig. 3.

dictate that α be greater than 1. Although this shifts the curves in favour of the screen wall counter, it is apparent that the count ratio is still so close to unity that the choice will probably be made on the basis of considerations other than sample: background ratio. One such consideration is the amount of sample available. From this point of view the gas counter is to be preferred. But this advantage will in general be of considerably less importance than the ease of operation (stability, reliability). The gas counter assumed in the previous analysis requires operation in the proportional region with a filling pressure of 1 atm. This necessitates an operating voltage of the order of 5 kV and the detection of pulses of the order of millivolts. Such a system is inherently more difficult to operate than a Geiger counter at 1 kV, giving pulses of several volts.

Statistical Considerations.

Effect of Background Rate.

To maximize the statistical precision obtainable in a given counting time it is desirable to maximize the ratio S^2/B, where S is the net sample count and B the background counting rate[18].

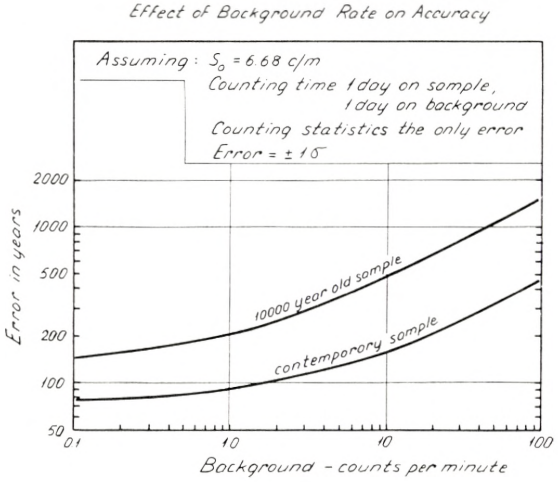

Fig. 4.

For a screen wall counter, where both the background and the sample counting rate are linear functions of counter size, the larger of two counters is always better from this point of view. As pointed out in the preceding section, the maximum possible size of the counter is determined by practical considerations and therefore the only possibility to improve the accuracy obtainable in a given counting time is to reduce the background count. The extent to which this is necessary and profitable is indicated in Fig. 4, in which the error in years calculated merely on the basis of statistical considerations is plotted as a function of the background rate for a contemporary sample and for a 10,000 year old sample. The counting rate from a contemporary sample is assumed to be 6.68 counts/min.[4] and the counting time 24 hours on sample and on background. In practice, the background of the counter shielded with lead is found to be about 100 counts/min.,

and when shielded with anti-coincidence it becomes 4 to 6 counts a minute. It is clear from the curves that, while it is essential to make use of the gain from the anti-coincidence shielding, further reduction of the background gives no spectacular gain in accuracy except for very old samples. The assumption of equal times spent on sample and background is not optimum when the background rate becomes small compared

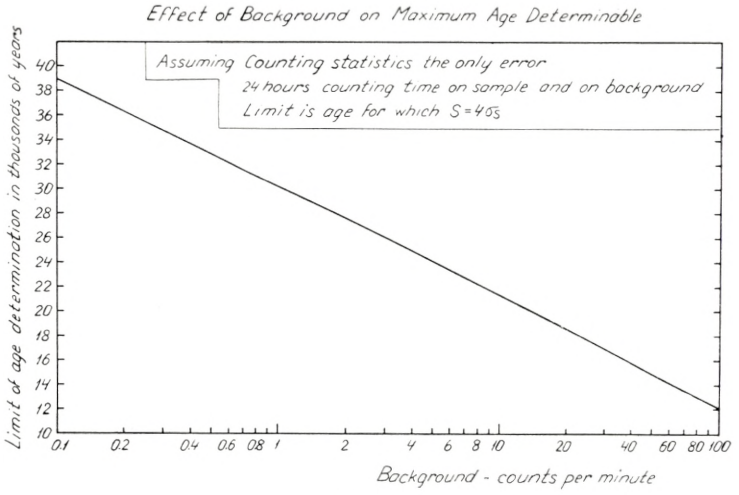

Fig. 5.

to sample rate[18]. This effect will be noticeable in Fig. 4 only for fairly recent samples. It will make the curve somewhat steeper over the middle cycle of the abscissae and will make the asymptote a factor of $\sqrt{2}$ lower.

The principal gain from background reduction is the extension of the method to older samples. This effect is shown in Fig. 5 which represents the maximum age determinable (with 2 days' counting) as a function of background rate.

The limiting age is here arbitrarily defined as the age for which the net sample count is equal to four times its statistical standard deviation. It is necessary to be rather conservative in the choice of this limit since, as the difference between background and sample becomes very small, one is less certain that the statistical error is the limiting one. It is apparent from the curve that every time the background is reduced by a factor of two, 2500 years are added to the range of the method.

The extension of the method to older samples through the reduction of background is clearly a difficult process because of the logarithmic relationship between these quantities. Moreover, other sources of error which are not considered in this calculation, such as low level chance contamination, may become the limiting factors preventing the attainment of the limit given by the curve.

In the measurement of the contemporary assay and of the samples of known age, the limiting factor in the accuracy appears to be counting statistics.

Effect of Counting Time.

In Figs. 4 and 5 the counting time has been assumed to be 48 hours. This time has proved in practice to be a good compromise between the gain in accuracy with prolongation of counting

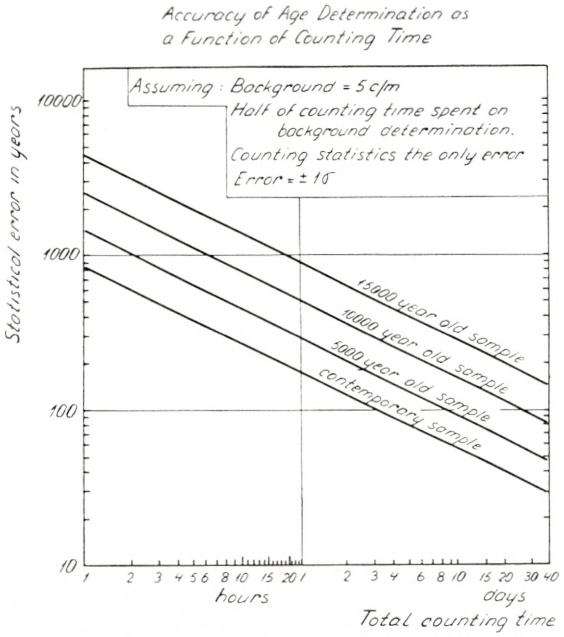

Fig. 6.

times and the desire to measure more samples. The two days counting time is a convenient one in that this period fits in well with the time required to prepare a sample. The effect on the

accuracy of changing the total counting time is presented in Fig. 6, where the statistical error is plotted against total counting time on a double logarithmic scale. It is obvious from this figure that the accuracy increases rapidly during the first day of counting and much more slowly thereafter. For example, after two hours of counting on a 5000 year old sample, the age is determined

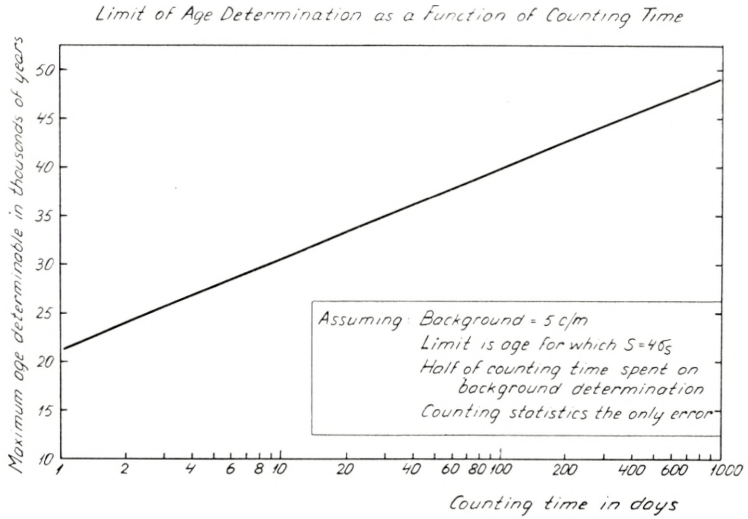

Fig. 7.

to ± 1000 years. After one day of counting the accuracy is ± 300 years, and after two days of counting it is ± 200 years. To reduce the error to 100 years would require counting for eight days.

Because of the possibility of other sources of error, such as contamination of the sample during processing, it is to be preferred that greater statistical accuracy be obtained through the measurement of independently prepared samples rather than through the extended counting of a single sample.

The extreme difficulty encountered in an attempt to extend the method to very old samples by the extension of the counting time is illustrated by Fig. 7. Even in the *reductio ad absurdum* of counting 100 days with a background of 5 counts per minute, the limit of the method is seen to be 40.000 years. The maximum age so far reported by radiocarbon dating is 28.000 years[19].

Effect of Isotopic Enrichment.

The discovery of natural radiocarbon was made on samples which were isotopically enriched by methane thermal diffusion columns[1), 2)], and a similar apparatus was constructed at the University of Chicago for possible use with very old samples. There are several practical difficulties associated with the use of this technique, such as the large amounts of sample necessary,

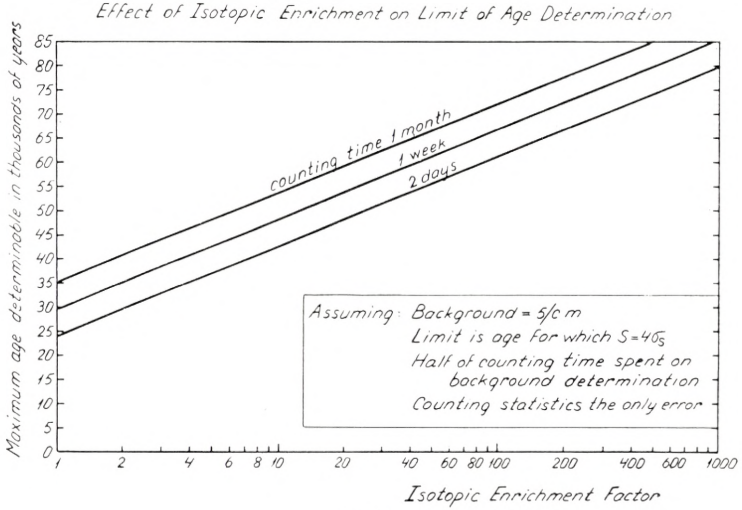

Fig. 8.

the length of time required, the cost of the process, and the difficulty in establishing the exact value of the enrichment factor. This will of necessity limit the application of isotopic enrichment to a few samples of extreme importance. The results which can be accomplished by this technique are indicated in Fig. 8, in which the maximum age as previously defined is plotted against the isotopic enrichment factor for three different counting times. It seems unlikely that enrichment factors more than a few hundred can be obtained in practice, and it must be remembered that the sample size requirement will increase by a factor at least as large as the enrichment factor. Again, the gain in maximum age determinable is a function of the logarithm of the independent variable so that appreciable extension of the method is accomplished only with great difficulty.

It is clear from a consideration of all the factors as represented on Figs. 5, 7, and 8 that, while the method can easily reach back to periods of a few tens of thousands of years, further extension can result only from a very considerable expenditure of effort.

This fundamental limitation of the method derives directly from the exponential decay law, and it can be said in general that any dating method based on radioactive decay will have a range of applicability of approximately $k \cdot t_{1/2}$, where k is of the order of 10.

Sources of Error.

Contamination by other Radionuclides.

Contamination errors can result from the intrusion into the sample of carbon of a different specific activity or of other radioactive species. One of the main purposes of the chemical treatment of the sample before counting is to separate radiocarbon from all chemically different activities. The widespread occurrence of radium and its decay products as well as the high specific activity of these nuclides make them the principal source of such contamination. Most rocks contain of the order of 10^{-12} parts of radium, and soil contains 10^{-13} parts of radium[20]. Therefore, samples consisting of many small pieces of material of large surface area can carry along with them comparatively large quantities of such activities. Fortunately, chemical separation is particularly easy. When the sample is burnt to CO_2, radium and its solid decay products are left behind. However, the gaseous member of the decay chain (radon) is collected with the CO_2 and, if not eliminated, will give rise to active deposit on the carbon sample. If the CO_2 is precipitated as $CaCO_3$, and the CO_2 regenerated by acid treatment, contamination from this source can be eliminated.

Obviously, it is of prime importance that the reagents used during the preparation of elemental carbon from the sample be of extreme purity with respect to other radio-elements. The only criterion of adequate purity of all reagents used prior to mounting the sample is the attainment of a truly zero count from a dead sample such as coal or petroleum.

Because of the extremely high adsorptive properties of the elemental carbon samples prepared by magnesium reduction (surface areas of the order of 200 m^2/g) great care must be exercised to prevent recontamination. The principal danger is again radon, this time the radon which is present in the atmosphere to the extent of 10^{-16} curies/cc[20]. Exposure of the sample to the air, especially when the sample is dried, should be kept to an absolute minimum. It has been observed, for example, that a sample which had been carefully mounted and had given a count equal to background, may show an activity above background if simply removed from the sample cylinder in the dry state and remounted.

It seems possible that contamination from aerial radon together with low level contamination of reagents may be the limiting factors preventing the extension of the method to the ultimate ages which seem possible from a consideration of errors due to counting statistics, only. As the activity of the sample decreases, it will probably be found that the errors indicated by analyses of duplicate samples prove to exceed the errors calculated on the basis of counting statistics.

For this reason, one should be cautious in accepting as practicable the limits of age which have been calculated as being accessible to the method on a statistical basis.

Contamination by Carbon of Different Specific Activity.

Contamination by carbon of different specific activity (i. e. different age) is a more difficult problem, since chemical methods may be of little or no use in rectifying the situation. Processes of contamination may be separated in two groups, viz. mechanical inclusion and exchange or chemical reactions. In all cases, the contamination may be by carbon older or younger than the sample.

Under mechanical inclusion may be grouped such events as penetration of a sample by rootlets of plants, crystallization of carbonates or deposition of organic compounds (e. g. humic acids) from solution onto or within a porous sample, and stirring and mixing of strata of different ages by the action of natural forces or by human or animal activity.

Direct exchange of carbon atoms between chemical species, without a net chemical reaction, occurs, for example, in the following equilibrium

$$CO_3^{=(aq)} + C^*O_2^{(g)} \rightleftarrows C^*O_3^{=(aq)} + CO_2^{(g)}.$$

This type of reaction is improbable with organic compounds. The ease of exchange of $BaC^{14}O_3$ with atmospheric CO_2 is well known[22], but, on the other hand, UREY[23] found shell carbonate capable of resisting oxygen exchange with dissolved carbonate over geologic periods. The results of KULP[9] indicate that finely divided carbonate in ocean sediments can maintain itself at a specific activity different from that of its environment for a period of at least 14,000 years (sample no. 107 B). Therefore, the situation looks encouraging for the use of shell carbonate as a dating material; however, the possibility of exchange under certain

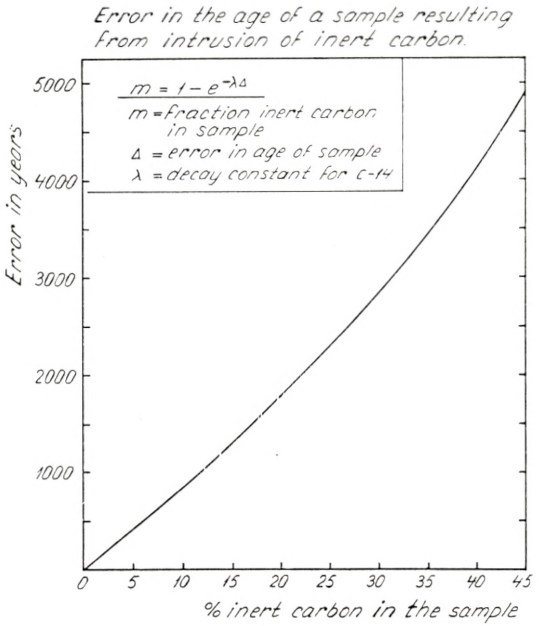

Fig. 9.

conditions remains, and research is planned to investigate this point by comparison of the specific activity of shell and wood from the same provenience and under different conditions of

exposure. (The problem of the initially different specific activities of shell due to isotopic fractionation is discussed below.)

While the strongly bound carbon in organic molecules is not subject to direct exchange, such molecules can serve as a substrate for micro-organisms. For example, micro-organisms can break down cellulose and resynthesize other compounds. During

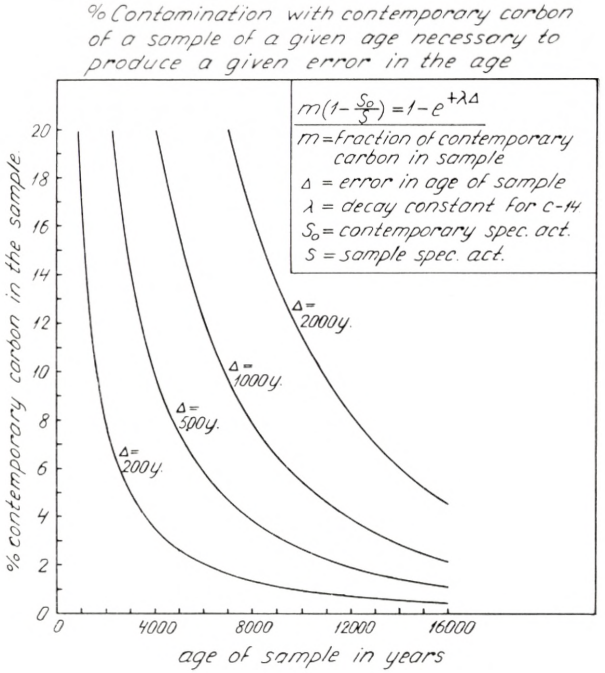

Fig. 10.

this process, carbon of different specific activity, if present in the surrounding medium, can be incorporated into the new compounds and invalidate measurements made indiscriminately on the whole mass. For this reason, it may be necessary in some cases to isolate the unaffected cellulose or lignin for dating purposes.

Another example of indirect exchange must be envisaged when aquatic plants grow in a hard water lake and have their specific activity displaced since the carbon they photosynthesize is derived partly from redissolved limestone[15].

The effect on the measured age caused by intrusion of inert carbon into a sample is shown in Fig. 9. It is clear that an error

from this source of more than 1000 years can arise only if gross replacement (intrusion) of the carbon, i. e. amounting to more than 10 per cent, has occurred.

Fig. 10 shows the effect of contamination by contemporary carbon. In this case, the error is a function of the age of the sample. Each of the family of curves gives the degree of contamination by contemporary carbon necessary to produce a given error as a function of the age of the sample. Errors of 200, 500, 1000, and 2000 years are given. For example, to produce an error of 1000 years in the age of a 6000 year old sample, a contamination by 12 per cent with contemporary carbon is required. These curves may permit a decision as to the probability of a suspected error being due to this type of contamination.

Other Sources of Error.

Since the age of a sample is determined by the ratio of its activity to the activity of contemporary samples of the same material, it is unnecessary to make absolute specific activity determinations for age measurements. All that is required is the measurement of the counting rates of the unknown and of the reference sample under identical conditions. This is clear from the exponential decay law $S = S_0 e^{-\lambda T}$ which, when solved explicitely for sample age T, gives

$$T = 18{,}500 \log S_0/S,$$

S_0 and S being the activities of materials of age zero and T, respectively.

Obviously, the efficiency factor for the counter, which would appear in this equation if conversion were made to absolute disintegration rates, would appear in both numerator and denominator and, hence, cancel out. However, great care must be taken in the choice of the proper value of the contemporary activity, S_0.

Extensive measurements on contemporary samples[4), 9)] have shown, for example, that shell carbonate gives a counting rate 11 per cent higher than wood, so that S_0 for carbonate samples

is 1.11 times S_0 for wood samples. A neglect of this difference would result in a dating error of some 900 years.

The analogous fractionation of carbon 13 has been known for some time[24]. The ratio C-12/C-13 is 91.8 for wood and 89.2 for limestone, corresponding to a fractionation factor of 1.03 for C-13. While no further C-14 data are available, the C-13 measurements indicate the possible existence of a group of material with still a different isotopic composition. This group is rather poorly characterized due to the few data, (single measurements on each of seven samples) but seems to consist of such diverse materials as weeds, algae, spores, peat, linseed oil, chinawood oil, and rubber, which show a C-12/C-13 ratio of about 92.8.

C-14 measurements on contemporary samples from similar sources are highly desirable from the point of view of our understanding of the detailed chemistry of the exchange reservoir, and they are equally essential for the dating of such materials.

Any error in the half life of radio-carbon will appear as the corresponding percentage error in the measured age of the sample. Since the estimated uncertainty of the best value for the half life of C-14 is less than one per cent[4], this error is small compared with other uncertainties of the method and need be considered only in those cases where the sample is measured to an unusually high accuracy.

Improvements in Instrumentation.

Double Screen Wall Counter.

Since the long counting time required for obtaining sufficient precision is at present a limiting factor, it is desirable to introduce improvements which would reduce the required counting time. This has been accomplished in Copenhagen through the use of the double screen wall counter*. In this instrument (Fig. 11), two independent detector units in a common envelope are used together with a triple sample cylinder. The sample is mounted

* The assistance of R. L. Schuch of the Los Alamos Scientific Laboratory in the design and construction of the double screen wall counter is gratefully acknowledged.

on the middle cylinder, while the two end cylinders provide backgrounds. As in the conventional screen wall, the cylinder unit can be alternated between two positions. In one position, the sample is exposed to detector A (cf. Fig. 11) and a background to detector B, in the other position, the sample is exposed to B and a background to A. Two advantages are obtained by the use of this system. First, the counting time necessary to obtain

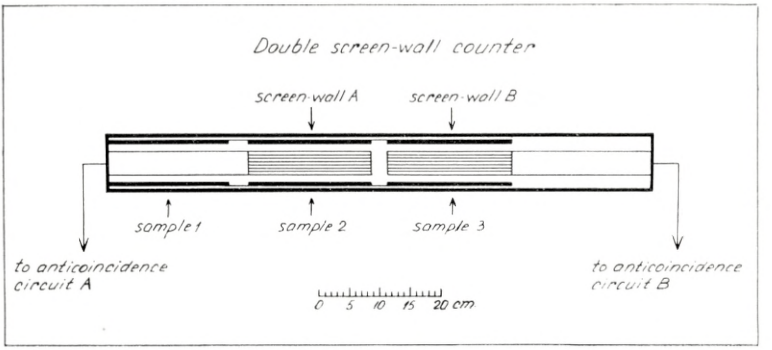

Fig. 11.

a given statistical accuracy is reduced by $\frac{1}{2}$, and second, simultaneous background and sample counts are obtained, whereby the effect of any temporal changes in the background is eliminated. Considerably less than twice the conventional equipment is required for the double screen wall system. Duplication of the mixing and the recording stages of the anti-coincidence circuit is necessary, but only one set of anti-coincidence counters is needed. The shield dimensions need be increased only slightly, since the counter length increases by only $\frac{1}{3}$. Moreover, the necessity for frequent alternation between the two positions is considerably reduced in the case of the double screen wall counter so that the complexity of an automatic sample changer is avoided.

Solution Scintillation Counter.

An alternative system of measurement suggested by J. Arnold in 1948 is based on the scintillation counter method. It is proposed to convert the carbon of the sample into the chemical form of a suitable solvent in which some material can be dissolved to form

a system with high efficiency for the detection of the C-14 β-particles. Some work has been done in this direction, but many technical difficulties must be solved before the method is proved to be practical. It is, however, worth considering the possibilities of this method in some detail, since it is difficult to imagine a system capable of giving a higher sample count combined with as low a background. The peculiar advantage of this system, which makes it so outstanding, is that it is able—theoretically at least—to use a sample in a condensed phase as a detector of nearly 100 per cent efficiency. Suppose, for example, that the carbon from the sample to be measured be converted to carbon disulfide or a similar organic liquid of a density about unity and containing of the order of 10 % carbon. A small amount of a scintillator, e. g. terphenyl, is dissolved in this liquid sample and coincidence counts recorded from a pair of photomultiplier tubes triggered by scintillations from this system. On the assumption of 100 per cent counting efficiency, 80 cc of carbon disulfide would give a counting rate of 120 counts/min. In the form of a cube, this volume will have a cross-sectional area of about 18 cm^2 and, therefore, might be expected to have a background of 0.03 counts/min. if background could be reduced as efficiently as in the case of the screen wall counter.

With such an idealized instrument the maximum age determinable as defined above becomes 58,000 years.

The principal advantages of the system are its extreme compactness, thus eliminating the need for a massive shield, and the great economy of counting time obtained for samples of reasonable age. On the other hand, the gain in the maximum age determinable while significant is not spectacular.

The authors wish to express their gratitude to Professor P. Brandt Rehberg, head of the Zoophysiological Laboratory, where the dating apparatus is installed, for his hospitality and kind interest in the work.

The Copenhagen "dating project" was initiated jointly by members of the Danish National Museum, the Danish Geological Survey (D.G.U.), and the Zoophysiological Laboratory. It is supported financially by the Carlsberg Foundation whose sponsorship is gratefully acknowledged.

One of us (E. C. ANDERSON) wishes to thank the Rask Ørsted Foundation for a fellowship and travel grant and the Wenner-Gren Foundation for Anthropological Research for a grant in aid. The Los Alamos Scientific Laboratory generously granted a leave of absence for participation in the project.

Summary.

A detailed comparison of the screen wall counter with a gas sample counter with respect to the problems of radio-carbon dating is given. Curves are presented showing the accuracy and range of the method as functions of the background rate and the counting time. The errors due to intrusion of extraneous carbon are presented and discussed and certain improvements in the method are described.

Zoophysiological Laboratory, University of Copenhagen.

References.

1) E. C. Anderson, W. F. Libby, S. Weinhouse, A. F. Reid, A. D. Kirshenbaum, and A. V. Grosse, Phys. Rev. 72, 931, 1947.
2) E. C. Anderson, W. F. Libby, S. Weinhouse, A. F. Reid, A. D. Kirshenbaum, and A. V. Grosse, Science 105, 576, 1947.
3) W. F. Libby, E. C. Anderson, and J. R. Arnold, Science 109, 227, 1949.
4) E. C. Anderson and W. F. Libby, Phys. Rev. 81, 64, 1951.
5) E. C. Anderson, J. R. Arnold, and W. F. Libby, Rev. Scient. Instr. 22, 225, 1951.
6) H. R. Crane, Nucleonics 9, no. 6, 1951.
7) J. R. Arnold and W. F. Libby, Science 113, 111, 1951.
8) W. F. Libby, Science 114, 291, 1951.
9) J. L. Kulp, H. W. Feely, and L. E. Tryon, Science 114, 565, 1951.
10) R. F. Flint and E. S. Deevey jr., Amer. J. Sci. 249, 257, 1951.
11) R. F. Flint, Nature 167, 833, 1951.
12) F. Johnson et al. "Radiocarbon Dating", Society for American Archaeology, Memoir no. 8, 1951.
13) H. Godwin, Amer. J. Sci. 249, 301, 1951.
14) F. E. Zeuner, Nature 166, 756, 1950.
15) H. H. Bartlett, Science 114, 55, 1951.
16) V. G. Childe, Nature 166, 1068, 1950.
17) W. F. Libby, "Radiocarbon Dating", University of Chicago Press, Chicago 1952.
18) R. Loevinger and M. Berman, Nucleonics 9, no. 7, 1951.
19) W. F. Libby, unpublished data.
20) G. Hevesy and F. Paneth "Radioactivity" 1938, p. 274.
21) Baronow and Tseitlin, Doklady Akad. Nauk, U.S.S.R. **30,** 328, 1941.
22) W. D. Armstrong and J. Schubert, Science 106, 403, 1947.
23) H. C. Urey, Science 108, 489, 1948.
24) K. Rankana, J. Geol. 56, 199, 1948.

Indleveret til selskabet den 24. april 1952.
Færdig fra trykkeriet den 18. august 1952.

Det Kongelige Danske Videnskabernes Selskab
Matematisk-fysiske Meddelelser, bind **27**, nr. 7

Dan. Mat. Fys. Medd. **27**, no. 7 (1952)

ON A CONVERGENT MESON THEORY. I

BY

P. KRISTENSEN AND C. MØLLER

København
i kommission hos Ejnar Munksgaard
1952

CONTENTS

Printed in Denmark.
Bianco Lunos Bogtrykkeri.

Introduction.

In recent years, important progress in the field of quantum electrodynamics has been obtained by introducing the idea of charge and mass renormalization[1]. According to this method, the usual field equations in quantum electrodynamics, which are obtained from the classical equations by a correspondence argument and which contain the well known divergencies, are transformed by a canonical transformation into a set of equations in which only the observable renormalized mass and charge of the particles occur. Since the whole procedure is relativistically invariant one can expect the transformed equations to give a correct description of electromagnetic phenomena, and this expectation has been decisively confirmed by the remarkable accuracy with which this theory allows to calculate the Lamb shift as well as by the predictions of new effects like the anomalous magnetic moment on the basis of the theory.

The application of the renormalization method to the case of nucleons in interaction with mesons seems, however, in some cases to meet with serious difficulties[2]. Further, it should be kept in mind that the method itself, in spite of its practical success, is not entirely satisfactory from a theoretical point of view, since the transformation leading to the renormalized equations is not a mathematically well defined unitary transformation, as is obvious from the fact that its purpose is to remove infinities. It would therefore be more attractive, at least in the case of nucleons in interaction with meson fields, to replace the usual field equations by slightly modified equations which, from the beginning, are free of divergencies.

Since the early times of quantum electrodynamics, it has been clear that an essential part of the divergencies inherent in

the usual field theories are due to the use of the point particle picture of the elementary particles. Instead of taking the wave functions of the interacting fields at the same space-time point in the interaction Lagrangian, it has, therefore, repeatedly been suggested to introduce a form factor describing a kind of non-localized interaction of the fields[4, 5, 6, 8]. It does not seem possible, however, inside the frame of usual quantum mechanics, to introduce such a form factor in a relativistically invariant way, and for many years all such attempts were regarded as impossible.

In the meantime, the *S*-matrix theory was developed by HEISENBERG[3]. His starting point was the idea that the frame-work of ordinary quantum mechanics might be too narrow to comprise a consistent field theory and that the difficulties could be removed only by giving up to some extent the more detailed description of the elementary processes, which is claimed to be possible in the usual quantum mechanics. The directly observable quantities like the cross-sections for the various elementary processes are fully described by the *S*-matrix and one might take the extreme point of view that a field theory should be considered complete if it only allows of a unique determination fo the *S*-matrix.

In the present paper, it is shown that the introduction of a form factor in the interaction between particles of spin one half (nucleons) and pseudoscalar mesons leads to a consistent *S*-matrix theory with correspondence to the usual field theory. Section 1 contains the general formalism including the field equations as well as the expressions for the total energy and momentum of the system. These quantities are in general not constants of the motion but, since they are conserved over infinite time intervals, they may be regarded as constants of collision in the sense of the *S*-matrix theory. In this section is also given a brief discussion of the general properties of the form factor following from the requirements of relativity, reality, and correspondence. A detailed discussion of the consequences of these requirements is postponed to Section 4.

In the following section, the *S*-matrix is derived to the second order in the coupling constants by means of the extension of the method of YANG and FELDMAN[10] given by BLOCH[7]. In

Section 3, the expressions for the self-energies of mesons and nucleons are derived from the one-particle part of the S-matrix. The necessary mathematical tools are found in the Appendixes.

The values of the self-energies will, of course, depend on the choice of the form factor and, in Section 4, it is shown that the form factor can be chosen in accordance with the general conditions stated above in such a way that the self-energies are finite and small.

The correspondence requirement implies that the present formalism must be identical with the conventional field theory when the fields are slowly varying. The definition of a slowly varying field involves the introduction of a constant λ of the dimension of a length which also enters into the expression for the form factor in such a way that we get all the results of the usual theory for processes which take place in regions of an extension large compared with λ. This means that, for instance, the second order cross-sections for nucleon-nucleon or nucleon-meson scattering are the same as in the usual meson theory as long as the transferred momentum is smaller than h/λ in the centre of mass system. For high energy processes, however, the form factor causes deviations from the usual theory and, in principle, the results of high energy scattering experiments could be used for an empirical determination of the form factor. At the moment, we have no theory which would allow of a closer determination of the form factor and we do not even know if the constant λ is a universal constant[3 a)]. A theory of the present type should perhaps rather be regarded as an approximation to a more general theory applicable to processes in which only particles of the kind considered play an essential role. Hence, the introduction of a form factor may be looked upon as a crude way of taking into account the influence of the external world on the system and it must be expected that the form of the form factor will depend on the particular system considered. Thus, a theory of the form factor itself will require the development of a unified theory of all elementary particles. It is an open question whether this general theory can be developed inside the frame of ordinary quantum mechanics.

In Section 5, some of the most striking differences between the present formalism and ordinary quantum mechanics are

discussed, in particular as regards their physical interpretation and the transformation theory. In the present theory, a wider class of transformations—the quasi-canonical transformations—take over the role of the canonical transformations which retain their importance only in the limit of slowly varying fields. It is shown that the theory can be made gauge invariant in the sense that a gauge transformation is equivalent to a quasi-canonical transformation, which means that a gauge transformation has no effect on the physical predictions derived from the theory.

Finally, in Section 6, it is shown that the introduction of the form factor also makes the vacuum polarization finite to the approximation considered. In the present paper, we have discussed the consequences of the theory for scattering processes only. In a subsequent paper, we hope to deal with the properties of composed systems of elementary particles on the basis of this theory. Since the introduction of the form factor effectively means a cut-off, it may be expected that we can avoid the difficulties which, in the usual theory of nuclear forces, arise from the strong singularities of the potentials.

1. General formalism.

In this paragraph, we shall consider the general case of spin one-half particles (nucleons) in interaction with an arbitrary meson field of integer spin. Let $\psi(x)$ be the field variable of the nucleon field, and let the meson field be described by one or several real field variables $u_\alpha(x)$. We assume that the field equations can be derived from a variational principle

$$\delta\left[\int\{L_N(x)+L_M(x)\}\,dx+\int L_{\text{int}}(x',x'',x''')\,dx'\,dx''\,dx'''\right]=0, \quad (1)$$

where dx is the volume element in Minkowski space, $dx = dx_1 dx_2 dx_3 dx_0$, $x_0 = -i\,x_4$. L_N and L_M refer to the free nucleon and meson fields, respectively, and L_{int} describes the non-localized interaction between the fields. Thus, using units $\hbar = 1$, $c = 1$,

$$\left.\begin{aligned} L_N &= -\left\{\frac{1}{2}(\overline{\psi}\gamma_\mu\partial_\mu\psi-\partial_\mu\overline{\psi}\cdot\gamma_\mu\psi)+M\overline{\psi}\psi\right\} \\ L_M &= -\frac{1}{2}\left\{\partial_\mu u\cdot\partial_\mu u+m^2u^2\right\} \end{aligned}\right\} \quad (2)$$

$$L_{\text{int}} = -\sum_{\zeta'\zeta''\alpha}\overline{\psi}_{\zeta'}(x')\,\Phi^\alpha_{\zeta'\zeta''}(x',x'',x''')\,u_\alpha(x'')\,\psi_{\zeta''}(x'''), \quad (3)$$

where $\Phi^\alpha_{\zeta'\zeta''}(x', x'', x''')$ in general is a combination of the Dirac matrices depending on three different space-time points. In the following, we shall take Φ as a product of a one-particle matrix operator and a scalar form factor F depending on the coordinates of the three space-time points, i. e.

$$\Phi^\alpha_{\zeta'\zeta''} = \Lambda^\alpha_{\zeta'\zeta''}\cdot F(x',x'',x'''). \quad (4)$$

For simplicity, we write

$$L_{\text{int}} = -\overline{\psi}(x')\,\Phi(x',x'',x''')\,u(x'')\,\psi(x'''), \tag{5}$$

using vector and tensor notations for the spinor index ζ and the α. Obviously, we have $\Phi u = u\Phi$. The matrix Λ is the usual one-particle operator occurring in the expression for the interaction Langrangian of the corresponding local theory which thus is a special case of the present formalism with

$$F = \delta(x' - x'')\,\delta(x' - x'''). \tag{6}$$

In the case of neutral pseudoscalar mesons, for instance, we have

$$\Lambda F = \left(ig_1\gamma_5 - i\frac{g_2}{m}\gamma_5\gamma_\mu\partial''_\mu\right)F(x',x'',x'''), \tag{7}$$

where g_1 and g_2 are the coupling constants of the pseudo-scalar and the pseudo-vector interactions, respectively. In the case of scalar mesons, we have simply $\Lambda = g\cdot 1$. When we deal with charged and neutral mesons in symmetrical interaction with the nucleons, these expressions should be multiplied by the isotopic spin operator τ^α, $\alpha = 1,2,3$.

As shown by C. Bloch[7], Yukawa's theory of non-local fields suggests the following expression for the form factor

$$F = (2\pi)^{-8}\int G(L,l)\exp i\left\{L\left(\frac{x'+x'''}{2} - x''\right) + l(x' - x''')\right\}dL\,dl, \tag{8}$$

where the Fourier transform $G(L,l)$ is a function only of the quantity Π^2 defined by

$$\Pi^2 = l^2 - \frac{(Ll)^2}{L^2}. \tag{9}$$

Here, $Ll = L_\mu l_\mu$ denotes the scalar product of the four-vectors L_μ and l_μ. For time-like L, the Fourier transform G is in this theory given by

$$G(L,l) = G(\Pi) = \frac{\sin\lambda\Pi}{\lambda\Pi}, \tag{10}$$

where λ is a constant of the dimension of a length.

As it will be seen later, the choice of the particular form factor (8), (10) does not lead to a convergent theory. We shall therefore try to develop the theory, as far as possible using a largely arbitrary form factor restricted only by general physical arguments.

In the first place, F must be an invariant by arbitrary displacements of the origin of the system of space-time coordinates. This condition is conveniently expressed in terms of the Fourier transform $F(l^1, l^2, l^3)$ of the function $F(x', x'', x''')$. One sees at once that this condition requires $F(l^1, l^2, l^3)$ to contain a factor $\delta(l^1+l^2+l^3)$. Accordingly, putting $F(l^1, l^2, l^3) = G(l^1, l^3)\,\delta(l^1+l^2+l^3)$, we get

$$\left.\begin{aligned} F(x', x'', x''') &= (2\pi)^{-8} \int G(l^1, l^3) \\ \cdot \exp i &\left\{ l^1 x' + l^3 x''' - (l^1 + l^3) x'' \right\} dl^1 dl^3. \end{aligned}\right\} \tag{11}$$

Next, $\int L_{\text{int}}\, dx' dx'' dx'''$ must be Hermitian, which requires

$$F(x', x'', x''') = F^*(x''', x'', x'). \tag{12}$$

In the Fourier representation, this is expressed by

$$G(l^1, l^3) = G^*(-l^3, -l^1). \tag{13}$$

Obviously, as F has to be an invariant with respect to Lorentz transformations, G must have the same property. Sometimes it is convenient to introduce new variables of integration

$$L = l^1 + l^3, \quad l = \frac{l^1 - l^2}{2} \tag{14}$$

into the expression (11), which gives

$$\left.\begin{aligned} F(x', x'', x''') &= (2\pi)^{-8} \int G(l^1, l^3) \\ \cdot \exp i &\left\{ L \left(\frac{x' + x'''}{2} - x'' \right) + l\,(x' - x''') \right\} dL\, dl. \end{aligned}\right\} \tag{15}$$

In this form, F appears as a function of the variables

$$R = \frac{x' + x'''}{2} - x'', \quad r = x' - x'''. \tag{16}$$

While the dependence of F on the variable r describes a type of internal coupling of the nucleon field to itself, which has no classical analogue, the dependence on R is just what one would

expect from analogy with a classical theory of extended interaction between the two types of particles. It will appear, however, that the dependence on r is actually most essential for the convergence of the theory.

Finally, it must be required that the theory of non-localized interaction is equivalent to the usual field theory for sufficiently slowly varying fields. This means that the form factor must have the same effect as the δ-functions of the local theory in any expressions containing slowly varying fields, only.

In Section 4, we shall give a precise definition of what we understand by slowly varying fields as well as a detailed discussion of the restrictions imposed on the form factor from the correspondence requirement mentioned above. The definition of slowly varying fields involves the introduction of a new constant λ into the theory, which conveniently may be taken of the dimension of a length and which one would expect to be of the order of magnitude of, or smaller than, the range of nuclear forces. It will appear that the function F can be chosen to depend on λ in such a way that the limiting cases of $\lambda \to 0$ and of slowly varying fields become identical. Hence, we have

$$\lim_{\lambda \to 0} F(x', x'', x''') = \delta(x' - x'')\, \delta(x' - x''') \tag{17}$$

and, for instance,

$$\int u(x'')\, \psi(x''')\, F(x', x'', x''')\, dx''dx''' = u(x')\, \psi(x') \tag{18}$$

for slowly varying u and ψ.

The equations of motion obtained from the variational principle (1) are

$$\left.\begin{aligned} (\gamma_\mu \partial'_\mu + M)\, \psi(x') &= -\int \Phi(x', x'', x''')\, u(x'')\, \psi(x''')\, dx''dx''' \\ (\Box'' - m^2)\, u(x'') &= \int \bar{\psi}(x')\, \Phi(x', x'', x''')\, \psi(x''')\, dx'dx'''. \end{aligned}\right\} \tag{19}$$

On account of the non-local character of the interaction, the four-current

$$i\bar{\psi}(x)\, \gamma_\mu\, \psi(x) \tag{20}$$

does not satisfy the continuity equation. In fact, by the usual procedure, one obtains from the first equation (19)

$$\left.\begin{aligned}\partial_\mu (i\,\overline{\psi}\gamma_\mu\psi) = -i\Big\{&\int \overline{\psi}(x)\,\Phi(x,x'',x''')\,u(x'')\,\psi(x''')\,dx''\,dx''' \\ &-\int \overline{\psi}(x')\,\Phi(x',x'',x)\,u(x'')\,\psi(x)\,dx'dx''\Big\}.\end{aligned}\right\} \quad (21)$$

Integrating this equation over the whole four-dimensional space, the right hand side vanishes identically. Hence, we get

$$\int \psi^\dagger(x)\,\psi(x)\,d^{(3)}\vec{x}\Big|_{t=-\infty} = \int \psi^\dagger(x)\,\psi(x)\,d^{(3)}\vec{x}\Big|_{t=+\infty}. \quad (22)$$

The quantity $\Delta N = \int \psi^\dagger\,\psi\,d^{(3)}\vec{x}$ is equal to the difference between the total number of nucleons and antinucleons, and equation (22) demonstrates that this number is strictly conserved over infinitely large time intervals. This is in general not the case for finite time intervals, where a conservation theorem holds in the limit of slowly varying fields, only. In fact, in this limit we may apply (18) on the right hand side of (21) and the two terms cancel.

The situation is somewhat similar in the case of energy and momentum conservation. The invariance of the Lagrangian with respect to displacements of the origin of the system of space-time coordinates leads again only to the identification of constants of collision. So far treating the field variables as c-numbers we obtain by the usual procedure

$$\left.\begin{aligned}\int \partial_\nu\, t^{(0)}_{\mu\nu}\,\partial x - \int\Big\{&\partial'_\mu\,\overline{\psi}(x')\cdot\Phi(x',x'',x''')\,u(x'')\,\psi(x''') \\ &+\overline{\psi}(x')\,\Phi(x',x'',x''')\,\partial''_\mu\,u(x'')\,\psi(x''') \\ &+\overline{\psi}(x')\,\Phi(x',x'',x''')\,u(x'')\,\partial'''_\mu\,\psi(x''')\Big\}\,dx'dx''dx''' = 0,\end{aligned}\right\} \quad (23)$$

where $t^{(0)}_{\mu\nu}$ is the usual energy-momentum tensor of the free fields*)

$$\left.\begin{aligned}t^{(0)}_{\mu\nu} = \frac{1}{2}\Big[&(\overline{\psi}\gamma_\nu\,\partial_\mu\psi - \partial_\mu\overline{\psi}\cdot\gamma_\nu\psi) - \delta_{\mu\nu}\,(\overline{\psi}\gamma_\lambda\,\partial_\lambda\psi - \partial_\lambda\overline{\psi}\cdot\gamma_\lambda\psi)\Big] \\ &- \delta_{\mu\nu}M\overline{\psi}\psi + \partial_\nu u\cdot\partial_\mu u - \frac{1}{2}\,\delta_{\mu\nu}\,(\partial_\lambda u\cdot\partial_\lambda u + m^2u^2).\end{aligned}\right\} \quad (24)$$

This result can also be verified directly from the equations (19), from which it follows that

*) For quantized fields, the term $\partial_\nu u\partial_\mu u$ should of course be replaced by the Hermitian expression $\frac{1}{2}\,(\partial_\nu u\partial_\mu u + \partial_\mu u\partial_\nu u)$, which involves a corresponding change in the second term on the right hand side of (25).

$$\left.\begin{aligned}\partial_\nu t^{(0)}_{\mu\nu}(x) = &\int \partial_\mu \bar{\psi}(x) \cdot \Phi(x, x'', x''') u(x'') \psi(x''') dx'' dx''' \\ &+ \int \bar{\psi}(x') \Phi(x', x, x''') \partial_\mu u(x) \psi(x''') dx' dx''' \\ &+ \int \bar{\psi}(x') \Phi(x', x'', x) u(x'') \partial_\mu \psi(x) dx' dx''.\end{aligned}\right\} \quad (25)$$

Integrating this equation over the whole domain of four-dimensional space, one obtains again (23). The invariance of the interaction Lagrangian density (3) now allows (23) to be written in the form of an integral of a four-dimensional divergence of a certain tensor $t_{\mu\nu}$. From the invariance of, for instance,

$$\mathcal{L}^{(2)} = -\int \bar{\psi}(x') \Phi(x', x, x''') u(x) \psi(x''') dx' dx''' \quad (26)$$

and from the fact that the form factor is form-invariant, it follows that

$$\left.\begin{aligned}\partial_\mu \mathcal{L}^{(2)} = -\int \Big\{ &\partial'_\mu \bar{\psi}(x') \cdot \Phi(x', x, x''') u(x) \psi(x''') \\ &+ \bar{\psi}(x') \Phi(x', x, x''') \partial_\mu u(x) \psi(x''') \\ &+ \bar{\psi}(x') \Phi(x', x, x''') u(x) \partial'''_\mu \psi(x''') \Big\} dx' dx'''\end{aligned}\right\} \quad (27)$$

and, hence, (23) can be written in the form

$$\int \partial_\nu t^{(2)}_{\mu\nu}(x) dx = 0, \quad (28)$$

where

$$t^{(2)}_{\mu\nu}(x) = t^{(0)}_{\mu\nu}(x) + \delta_{\mu\nu} \mathcal{L}^{(2)}(x). \quad (29)$$

Thus, the following Hermitian quantities are constants of collision

$$G_\mu = -i \int t^{(2)}_{\mu 4}(x) d^{(3)}\vec{x} = G^{(0)}_\mu - i\delta_{\mu 4} \int \mathcal{L}^{(2)}(x) d^{(3)}\vec{x} \quad (30)$$

and may be interpreted as the total momentum and energy of the field. If we had chosen, instead of (26), one of the two other possible interaction Lagrangian densities,

$$\left.\begin{aligned}\mathcal{L}^{(1)} &= -\int \bar{\psi}(x) \Phi(x, x'', x''') u(x'') \psi(x''') dx'' dx''' \\ \mathcal{L}^{(3)} &= -\int \bar{\psi}(x') \Phi(x', x'', x) u(x'') \psi(x) dx' dx''\end{aligned}\right\} \quad (31)$$

we would, instead of (28), have obtained

$$\int \partial_\nu t^{(1)}_{\mu\nu}\, dx = 0, \qquad \int \partial_\nu t^{(3)}_{\mu\nu}\, dx = 0, \tag{32}$$

respectively, where

$$t^{(1)}_{\mu\nu} = t^{(0)}_{\mu\nu} + \delta_{\mu\nu}\mathfrak{L}^{(1)}, \qquad t^{(3)}_{\mu\nu} = t^{(0)}_{\mu\nu} + \delta_{\mu\nu}\mathfrak{L}^{(3)}. \tag{33}$$

However, the requirement that the energy-momentum tensor must be Hermitian reduces the number of possible choices of this tensor to one of the two

$$\left.\begin{aligned} t_{\mu\nu} &= \frac{1}{2}(t^{(1)}_{\mu\nu} + t^{(3)}_{\mu\nu}) = t^{(0)}_{\mu\nu} + \delta_{\mu\nu}\frac{1}{2}(\mathfrak{L}^{(1)} + \mathfrak{L}^{(3)}) \\ t^{(2)}_{\mu\nu} &= t^{(0)}_{\mu\nu} + \delta_{\mu\nu}\mathfrak{L}^{(2)}. \end{aligned}\right\} \tag{34}$$

It may be remarked that any of these becomes identical with the usual expression of the energy-momentum tensor in the limits of $\lambda \to 0$ or of slowly varying fields.

From the preceding discussion it is clear that the present formalism is entirely different from the Hamiltonian scheme of ordinary quantum mechanics. This is obvious from the fact that the non-local quantities corresponding to the total energy and momentum of the system are in general not constants of motion. However, the fact that these quantities are conserved over the *infinite* time interval $-\infty \leqq t \leqq +\infty$ suggests that G_μ may be regarded as constants of collision in the sense of the S-matrix theory and that a consistent treatment of this formalism can be found inside the frame of HEISENBERG's S-matrix theory. The present theory thus offers an example of a case in which the S-matrix may be calculated without any reference to an underlying Hamiltonian scheme.

2. Derivation of the S-matrix.

For the derivation of the S-matrix we shall use the method developed by YANG and FELDMAN and by KÄLLÉN[10]. As shown in the Appendix A, the field equations (1.11) are equivalent to the integral equations

$$\left.\begin{aligned}\psi(x) &= \psi(x,\sigma) + \int S_M^\sigma(x,x')\,\Phi(x',x'',x''')\,u(x'')\,\psi(x''')\,dx'\,dx''\,dx''' \\ u(x) &= u(x,\sigma) - \int \bar{\psi}(x')\,\Phi(x',x'',x''')\,\Delta_m^\sigma(x,x'')\,\psi(x''')\,dx'\,dx''\,dx''',\end{aligned}\right\} \quad (1$$

where $\psi(x,\sigma)$ and $u(x,\sigma)$ are the free fields coinciding with $\psi(x)$ and $u(x)$ on a space-like surface σ. S_M^σ and Δ_m^σ are Green's functions defined by (A. 3) and (A. 32) and corresponding to the mass values M and m, respectively. Taking σ in the infinite past, the functions S_M^σ and Δ_m^σ become identical with the corresponding retarded Green's functions and the equations (1), in this limit, are

$$\left.\begin{aligned}\psi(x) &= \psi^{\text{in}}(x) + \int S_M^{\text{ret}}(x-x')\,\Phi(x',x'',x''')\,u(x'')\,\psi(x''')\,dx'\,dx''\,dx''' \\ u(x) &= u^{\text{in}}(x) - \int \bar{\psi}(x')\,\Phi(x',x'',x''')\,\Delta_m^{\text{ret}}(x-x'')\,\psi(x''')\,dx'\,dx''\,dx'''.\end{aligned}\right\} \quad (2$$

These equations may be considered as definitions of the in-fields ψ^{in} and u^{in}. As a consequence of (A. 7),

$$\left.\begin{aligned}\psi^{\text{in}}(x) &= \lim_{\sigma\to-\infty} \psi(x,\sigma) \\ u^{\text{in}}(x) &= \lim_{\sigma\to-\infty} u(x,\sigma)\end{aligned}\right\} \quad (3)$$

and the in-fields satisfy the free field equations.

Similarly, we may define the out-fields by

$$\left.\begin{aligned}\psi^{\text{out}}(x) &= \lim_{\sigma\to+\infty} \psi(x,\sigma) \\ u^{\text{out}}(x) &= \lim_{\sigma\to+\infty} u(x,\sigma)\end{aligned}\right\} \quad (4)$$

or, alternatively, by the equations

$$\left.\begin{aligned}\psi(x) &= \psi^{\text{out}}(x) + \int S_M^{\text{adv}}(x-x')\,\Phi(x',x'',x''')\,u(x'')\,\psi(x''')\,dx'\,dx''\,dx''' \\ u(x) &= u^{\text{out}}(x) - \int \bar{\psi}(x')\,\Phi(x',x'',x''')\,\Delta_m^{\text{adv}}(x-x'')\,\psi(x''')\,dx'\,dx''\,dx'''.\end{aligned}\right\} \quad (5)$$

Hence, in a certain sense, the in- and out-fields may be regarded as the free fields which coincide with the actual fields at $t = -\infty$ and $t = +\infty$, respectively, thus representing the ingoing and out-

going fields. By solving the equations (2) we obtain the actual fields in terms of the in-fields. Further, subtracting (5) from (2), we get an expression for the out-fields in terms of the in-fields and the actual fields and, eventually, in terms of the in-fields. Using (A. 20), the equations obtained from (5) and (2) are

$$\left.\begin{aligned} \psi^{\text{out}}(0) &= \psi^{\text{in}}(0) - \int S_M(0-1)\,\Phi(1,2,3)\,u(2)\,\psi(3)\,d(123) \\ u^{\text{out}}(0) &= u^{\text{in}}(0) + \int \bar{\psi}(1)\,\Phi(1,2,3)\,\Delta_m(0-2)\,\psi(3)\,d(123), \end{aligned}\right\} \quad (6)$$

where we use the symbols 0, 1, 2, 3, ... for x, x', x'', x''', ... and $d(123) = dx'\,dx''\,dx'''$.

Following YANG and FELDMAN[10] and BLOCH[7], the quantization of the field variables can now be performed by introduction of commutation relations for the in-field variables. It is then clear from the preceding discussion that also the commutation relations for the actual fields and the out-fields are determined. Since the in-fields satisfy the homogeneous wave equations, we may consistently assume the usual free field commutation relations to hold for these fields, viz.

$$\left.\begin{aligned} \left\{\psi^{\text{in}}_{\zeta}(x),\ \bar{\psi}^{\text{in}}_{\zeta'}(x')\right\} &= \frac{1}{i} S_{M\zeta\zeta'}(x-x') \\ [u^{\text{in}}(x),\ u^{\text{in}}(x')] &= i\Delta_m(x-x'). \end{aligned}\right\} \quad (7)$$

It has been shown by BLOCH[7] that then also the out-fields satisfy the commutation relations (7). Consequently, the in- and out-fields must be connected by a unitary transformation

$$\left.\begin{aligned} \psi^{\text{out}} &= S^{-1}\psi^{\text{in}}S \\ u^{\text{out}} &= S^{-1}u^{\text{in}}S \\ S^{\dagger}S &= SS^{\dagger} = 1. \end{aligned}\right\} \quad (8)$$

On account of the interpretation of the ψ^{out}, u^{out} and ψ^{in}, u^{in} as the variables describing the outgoing and ingoing fields, respectively, the unitary matrix S is the Heisenberg S-matrix of the system[9a].

It is convenient to introduce a Hermitian matrix η by

$$S = e^{i\eta} \tag{9}$$

and the problem is now to determine η from (8) and (9) and the field equations. To solve the field equations we have to take recourse to an iteration method in which the in-fields are chosen as the zero order approximation, and we shall take into account the interaction to the second order in the coupling constants contained in the function Φ. To the first order, we find from (6)

$$\left.\begin{aligned} \psi^{\text{out}}(0) &= \psi^{\text{in}}(0) - \int S_M(0-1)\,\Phi(1,2,3)\,u^{\text{in}}(2)\,\psi^{\text{in}}(3)\,d(123) \\ u^{\text{out}}(0) &= u^{\text{in}}(0) + \int \psi^{\text{in}}(1)\,\Phi(1,2,3)\,\Delta_m(0-2)\,\psi^{\text{in}}(3)\,d(123). \end{aligned}\right\} \tag{10}$$

However, on account of the conservation of energy and momentum, no real first order processes can occur. Consequently, the first order term in η and, therefore, also the first order corrections to the out-fields, must be zero. This can also easily be verified directly by evaluation of the integrals on the right hand side of (10) in momentum space. Therefore, since

$$\left.\begin{aligned} S_M^{\text{ret}} &= \overline{S}_M - \frac{1}{2} S_M \\ \Delta_m^{\text{ret}} &= \overline{\Delta}_m - \frac{1}{2}\Delta_m \end{aligned}\right\} \tag{11}$$

the actual fields calculated to the first order from (2) may be written

$$\left.\begin{aligned} \psi(0) &= \psi^{\text{in}}(0) + \int \overline{S}_M(0-1)\,\Phi(1,2,3)\,u^{\text{in}}(2)\,\psi^{\text{in}}(3)\,d(123) \\ u(0) &= u^{\text{in}}(0) - \int \overline{\psi}^{\text{in}}(1)\,\Phi(1,2,3)\,\overline{\Delta}_m(0-2)\,\psi^{\text{in}}(3)\,d(123). \end{aligned}\right\} \tag{12}$$

Using (12) in (6) we finally get the expressions for the out-fields in terms of the in-fields to the second order in the coupling constants

$$
\left.
\begin{aligned}
\psi^{\text{out}}(0) &= \psi^{\text{in}}(0) - \int S_M(0-1)\,\Phi(1,2,3)\,u^{\text{in}}(2)\,\bar{S}_M(3-4) \\
&\quad \times \Phi(4,5,6)\,u^{\text{in}}(5)\,\psi^{\text{in}}(6)\,d(1\ldots6) \\
&\quad + \int S_M(0-1)\,\Phi(1,2,3) \\
&\quad \times \{\bar{\psi}^{\text{in}}(4)\,\Phi(4,5,6)\,\bar{\Delta}_m(2-5)\,\psi^{\text{in}}(6)\}\,\psi^{\text{in}}(3)\,d(1\ldots6) \\
u^{\text{out}}(0) &= u^{\text{in}}(0) + \int \bar{\psi}^{\text{in}}(1)\,\Phi(1,2,3)\,\Delta_m(0-2) \\
&\quad \times \bar{S}_M(3-4)\,\Phi(4,5,6)\,u^{\text{in}}(5)\,\psi^{\text{in}}(6)\,d(1\ldots6) \\
&\quad + \int \bar{\psi}^{\text{in}}(4)\,\Phi(4,5,6)\,u^{\text{in}}(5) \\
&\quad \times \bar{S}_M(6-1)\,\Phi(1,2,3)\,\Delta_m(0-2)\,\psi^{\text{in}}(3)\,d(1\ldots6).
\end{aligned}
\right\} \quad (13)
$$

Since the first order term in η vanishes, the connection between the in-fields and out-fields expressed by (8) and (9) can, to the second approximation, be written

$$
\left.
\begin{aligned}
\psi^{\text{out}} &= \psi^{\text{in}} + \frac{1}{i}[\eta, \psi^{\text{in}}] \\
u^{\text{out}} &= u^{\text{in}} + \frac{1}{i}[\eta, u^{\text{in}}].
\end{aligned}
\right\} \quad (14)
$$

Comparing (13) and (14), and using the free field commutation relations (7) for the in-fields, it is easily verified that the η-matrix in this approximation is given by

$$
\left.
\begin{aligned}
\eta &= -\int \bar{\psi}^{\text{in}}(1)\,\Phi(1,2,3)\,u^{\text{in}}(2)\,\bar{S}_M(3-4) \\
&\qquad \times \Phi(4,5,6)\,u^{\text{in}}(5)\,\psi^{\text{in}}(6)\,d(1\ldots.6) \\
&\quad + \frac{1}{2}\int \bar{\psi}^{\text{in}}(1)\,\Phi(1,2,3) \\
&\quad \times \{\bar{\psi}^{\text{in}}(4)\,\Phi(4,5,6)\,\bar{\Delta}\ (2-5)\,\psi^{\text{in}}(6)\}\,\psi^{\text{in}}(3)\,d(1\ldots.6).
\end{aligned}
\right\} \quad (15)
$$

In this approximation,

$$
i\eta = S - 1. \qquad (16)
$$

According to the S-matrix theory[3],[9], the matrix $S-1$ is a product of two factors, the first of which is a δ-function taking care of the conservation of energy and momentum while the square of the second directly gives the cross-sections for the possible real processes.

3. Calculation of the matrix elements of η.

Since the η-matrix given by (2.15) contains in-fields only we shall, in this section, omit the subscript "in" attached to the field variables, and $\bar{\psi}$, ψ and u then denote free field wave functions satisfying the commutation relations (2.7). These functions may in a relativistically invariant way be decomposed into positive and negative frequency parts which then, in the usual way, are interpreted as annihilation and creation operators, respectively. The non-vanishing commutators (anticommutators) between these variables are the following

$$\left.\begin{aligned} \{\psi_\zeta^{(+)}(x),\ \bar{\psi}_{\zeta'}^{(-)}(x')\} &= -iS_{\zeta\zeta'}^{(+)}(x-x') \\ \{\psi_\zeta^{(-)}(x),\ \bar{\psi}_{\zeta'}^{(+)}(x')\} &= -iS_{\zeta\zeta'}^{(-)}(x-x') \\ [u_\alpha^{(+)}(x),\ u_{\alpha'}^{(-)}(x')] &= i\delta_{\alpha\alpha'}\Delta^{(+)}(x-x'), \end{aligned}\right\} \quad (1)$$

where, for simplicity, we use the notations S and Δ instead of S_M and Δ_m. For the definitions of the various Green's functions introduced here see Appendix A. Δ-functions referring to the nucleon mass will be explicitly written Δ_M. The vacuum state vector $|0\rangle$ is now defined by

$$\left.\begin{aligned} \psi^{(+)}|0\rangle &= 0 \\ \bar{\psi}^{(+)}|0\rangle &= 0 \\ u^{(+)}|0\rangle &= 0 \end{aligned}\right| \qquad \left|\begin{aligned} \langle 0|\psi^{(-)} &= 0 \\ \langle 0|\bar{\psi}^{(-)} &= 0 \\ \langle 0|u^{(-)} &= 0. \end{aligned}\right. \quad (2)$$

In the Appendix B, the matrix elements of the various combinations of wave functions occurring in η have been calculated.

From (B.5) it follows that the vacuum expectation value of the nucleon source density occurring in the interaction between nucleons and pseudoscalar mesons is zero. For instance,

$$\langle 0 \,|\, i\bar{\psi}(1)\gamma_5\psi(3) \,|\, 0\rangle = i \operatorname{Tr}\gamma_5 S^{(-)}(3-1) = 0, \tag{3}$$

where we have used $\operatorname{Tr}\gamma_5 = \operatorname{Tr}\gamma_5\gamma_\mu = 0$. This is a particularly simple feature of the pseudoscalar theory. In the scalar meson theory, for instance, the necessary vanishing of the vacuum expectation value of the source density creating the meson field would be obtained only by a suitable symmetrization procedure analogous to HEISENBERG's rule in quantum electrodynamics.

We shall now confine ourselves to the case of pseudoscalar neutral mesons in pseudoscalar interaction with the nucleons and our task will be first to derive the various matrix elements of η.

a) *The self-energy of the meson.* As is well known, the η-matrix contains non-vanishing matrix elements corresponding to transitions between two states in which only one meson and no nucleons are present. Denoting the momenta of the mesons in the initial and final states by p' and p'', respectively, one finds that the matrix element in question is of the form

$$-\pi \frac{\delta(p'-p'')}{\omega'} \delta m^2, \tag{4}$$

where δm^2 is an invariant constant and ω is defined by

$$\omega = \sqrt{\vec{p}^2 + m^2}. \tag{5}$$

A term of this form would also arise from an additional term in the interaction Lagrangian density

$$\delta L^{\text{int}} = \delta m^2 u^2. \tag{6}$$

Thus, δm^2 must be interpreted as the contribution to the square of the meson mass due to the interaction with the nucleons. In the local theory this contribution turns out to be infinite. However, as it will be shown below, it is possible to choose the form factor in accordance with the general requirements outlined in

Section 2 in such a way that the correction to the meson mass comes out finite and small compared with the actual meson mass.

To calculate δm^2 we consider the one particle part of the matrix element of η between the two states mentioned above with the corresponding state vectors $|\vec{p}'\rangle$ and $|\vec{p}''\rangle$. In the one particle part

$$\langle \vec{p}'' | \eta_{(1)} | \vec{p}' \rangle = \langle \vec{p}'' | (\eta - \langle 0 | \eta | 0 \rangle) | \vec{p}' \rangle \tag{7}$$

the contribution from the vacuum fluctuations, being of no physical significance, has been subtracted. In the case considered, the form factor can, according to (1.7), with $g_2 = 0$ be written

$$\Phi = ig\gamma_5 F(1,2,3) \tag{8}$$

and the η-matrix given by (2.15) becomes

$$\eta = \eta_{\mathrm{I}} + \eta_{\mathrm{II}}, \tag{9}$$

where

$$\left.\begin{aligned} \eta_{\mathrm{I}} &= g^2 \int F(1,2,3)\, F(4,5,6)\, d(1\ldots6) \\ &\quad \times \overline{\psi}(1)\, \gamma_5 \overline{S}(3-4)\, \gamma_5 \psi(6)\, u(2)\, u(5) \\ \eta_{\mathrm{II}} &= -\frac{1}{2} g^2 \int F(1,2,3)\, F(4,5,6)\, d(1\ldots6) \\ &\quad \times \overline{\psi}(1)\, \gamma_5 [\overline{\psi}(4)\, \gamma_5 \psi(6)]\, \psi(3)\, \overline{\Delta}(2-5). \end{aligned}\right\} \tag{10}$$

Since η_{II} does not contribute to (7), we get

$$\left.\begin{aligned} &\langle \vec{p}'' | \eta_{(1)} | \vec{p}' \rangle = g^2 \int F(1,2,3)\, F(4,5,6)\, d(1\ldots6) \\ &\times \langle 0 | \overline{\psi}(1)\, \gamma_5 \overline{S}(3-4)\, \gamma_5 \psi(6) | 0 \rangle \langle \vec{p}'' | [u(2)\, u(5)]_{(1)} | \vec{p}' \rangle. \end{aligned}\right\} \tag{11}$$

The nucleon vacuum expectation value can be evaluated, using (B. 5),

$$\left.\begin{aligned} &\langle 0 | \overline{\psi}(1)\, \gamma_5 \overline{S}(3-4)\, \gamma_5 \psi(6) | 0 \rangle \\ &\quad = \sum_{\zeta_1 \zeta_6} (\gamma_5 \overline{S}(3-4)\, \gamma_5)_{\zeta_1 \zeta_6} \left(-iS^{(1)}_{\zeta_6 \zeta_1}(6-1)\right) \\ &\quad = i\,\mathrm{Tr}\,(\gamma_\mu \partial^{(3)}_\mu + M)(\gamma_\nu \partial^{(6)}_\nu - M)\, \overline{\Delta}_M(3-4)\, \Delta^{(-)}_M(6-1) \\ &\quad = 4\, i\, (\partial^{(3)}_\mu \partial^{(6)}_\mu - M^2)\, \overline{\Delta}_M(3-4)\, \Delta^{(-)}_M(6-1). \end{aligned}\right\} \tag{12}$$

The one particle part of the meson matrix element is directly found in (B. 26)

$$\left.\begin{aligned} \langle \vec{p}'' \,|\, [u(2)\, u(5)]_{(1)} \,|\, \vec{p}' \rangle &= \frac{1}{2} (2\pi)^{-3} \frac{1}{\sqrt{\omega'' \omega'}} \\ &\times \{ e^{i(p'5 - p''2)} + e^{i(p'2 - p''5)} \}. \end{aligned} \right\} \quad (13)$$

Inserting (12) and (13) into (11), and using the Fourier expansions of $\overline{\Delta}_M$, $\Delta_M^{(-)}$ (A. 26), (A. 28), and F (1.15), we find that the first of the two parts of the matrix element (11) arising from the first of the two terms in (13) is

$$\left.\begin{aligned} &2 g^2 (2\pi)^{-26} \frac{1}{\sqrt{\omega'' \omega'}} \int d(1 \ldots 6)\, d(l^1 l^3 l^4 l^6)\, dK' dK \\ &\times G(l^1, l^3)\, G(l^4, l^6) \frac{K'K + M^2}{K'^2 + M^2} \delta(K^2 + M^2) \frac{1 - \varepsilon(K)}{2} \\ &\times \exp i \{ l^1 1 + l^3 3 - (l^1 + l^3) 2 + l^4 4 + l^6 6 - (l^4 + l^6) 5 \} \\ &\times \exp i \{ K'(3 - 4) + K(6 - 1) + p' 5 - p'' 2 \}. \end{aligned} \right\} \quad (14)$$

Performing the integration over all the variables except K we obtain

$$\left.\begin{aligned} &2 g^2 (2\pi)^{(-2)} \frac{\delta(p' - p'')}{\omega'} \int dK \cdot |\, G(K, -K - p') \,|^2 \\ &\times \frac{(p' + K) K + M^2}{(p' + K)^2 + M^2} \delta(K^2 + M^2) \frac{1 - \varepsilon(K)}{2}. \end{aligned} \right\} \quad (15)$$

The other part of (11), arising from the second term in (13), is obtained from (15) by the transformation

$$\left.\begin{aligned} p' &\to -p'' \\ p'' &\to -p'. \end{aligned} \right\} \quad (16)$$

Changing the variable of integration K into $-K$, one finds immediately, by means of the symmetry property (1.13) of G, that this part is identical with (15) except for a change of sign in $\varepsilon(K)$. Hence, we get

$$\langle \vec{p}'' \,|\, \eta_{(1)} \,|\, \vec{p}' \rangle = -\pi \frac{\delta(p' - p'')}{\omega'} \delta m^2, \tag{17}$$

where the correction to the square of the meson mass is

$$\left.\begin{aligned} \delta m^2 = -\frac{2g^2}{\pi}(2\pi)^{-2} \int dK \cdot |G(K, -K - p')|^2 \\ \times \frac{(p' + K)K + M^2}{(p' + K)^2 + M^2} \delta(K^2 + M^2). \end{aligned}\right\} \tag{18}$$

In the local limit $G = 1$ and we obtain the well known result that δm^2 is quadratically divergent. We also see that a $G(l^1, l^3)$, depending on $l^1 + l^3$ only, cannot bring about convergence, since in this case the form factor occurring in (18) is independent of the variable of integration. Finally, it is easily seen that the choice (1.10) of the form factor following from BLOCH's version of YUKAWA's theory only reduces the degree of divergence to a logarithmic one.

b) *The self-energy of the nucleon.* In the same way, we now consider the matrix elements of the one particle part of η corresponding to a transition from a state $|\sigma' P'\rangle$ with one nucleon present with wave vector P' and spin σ' to a state $|\sigma'' P''\rangle$ and we obtain a result of the form

$$\langle \sigma'' P'' \,|\, \eta_{(1)} \,|\, \sigma' P' \rangle = -2\pi \delta(P'' - P') \cdot \{ j_\mu \delta A_\mu + I \delta M \}. \tag{19}$$

Here, j_μ and I are defined in terms of the spinor plane wave amplitudes (p. 47) by

$$\left.\begin{aligned} j_\mu = j_\mu(\sigma'', \sigma'; \vec{P}') = i\bar{v}(\sigma'' \vec{P}')\gamma_\mu v(\sigma' \vec{P}') \\ I = I(\sigma'', \sigma'; \vec{P}') = \bar{v}(\sigma'' \vec{P}') v(\sigma' \vec{P}'). \end{aligned}\right\} \tag{20}$$

Further, δM and δA_μ are a scalar and a four-vector, respectively, given by

$$\left.\begin{aligned} \delta A_\mu &= \delta A_{\mathrm{I}\mu} + \delta A_{\mathrm{II}\mu} \\ \delta M &= \delta M_{\mathrm{I}} + \delta M_{\mathrm{II}}, \end{aligned}\right\} \tag{21}$$

where

$$\left.\begin{aligned}
\delta A_{\mathrm{I}\mu} &= \frac{1}{(2\pi)^3} g^2 \int dk \,\big|\, G(P', k-P') \,\big|^2 \\
&\quad \times \frac{(P'-k)_\mu}{(P'-k)^2 + M^2} \delta(k^2 + m^2) \frac{1+\varepsilon(k)}{2} \\
\delta M_{\mathrm{I}} &= \frac{1}{(2\pi)^3} g^2 \int dk \,\big|\, G(P', k-P') \,\big|^2 \\
&\quad \times \frac{M}{(P'-k)^2 + M^2} \delta(k^2 + m^2) \frac{1+\varepsilon(k)}{2} \\
\delta A_{\mathrm{II}\mu} &= \frac{1}{(2\pi)^3} g^2 \int dK \,\big|\, G(K, -P') \,\big|^2 \\
&\quad \times \frac{K_\mu}{(K-P')^2 + m^2} \delta(K^2 + M^2) \frac{1-\varepsilon(K)}{2} \\
\delta M_{\mathrm{II}} &= \frac{1}{(2\pi)^3} g^2 \int dK \,\big|\, G(K, -P') \,\big|^2 \\
&\quad \times \frac{M}{(K-P')^2 + m^2} \delta(K^2 + M^2) \frac{1-\varepsilon(K)}{2}.
\end{aligned}\right\} \quad (22)$$

A term of the type (19) would appear in the S-matrix from an additional term in the interaction part of the Lagrangian of the form

$$\delta L_{\mathrm{int}} = i\bar{\psi}\gamma_\mu \psi \delta A_\mu + \bar{\psi}\psi \delta M. \quad (23)$$

Such a term corresponds to an additional term in the energy of the free particle field

$$\delta H = \int \psi^* \left\{ -\vec{\alpha}\,\delta\vec{A} + \delta A_0 - \beta \delta M \right\} \psi \, d^{(3)}\vec{x}. \quad (24)$$

Hence, δM should be considered as the contribution to the nucleon mass due to the interaction with the meson field, while $\delta\vec{A}$ and δA_0 represent a constant self-potential.

4. General properties of the form factor. Convergence of the theory to the second order.

In this section, we shall investigate the general properties of the form factor following from the correspondence requirement briefly mentioned in Section 1, and we shall show that it is pos-

sible to choose the form factor in accordance with the result of this investigation in such a way that no divergencies occur in the theory to the second order approximation in the coupling constants. It will be our first task to give a precise formulation of what we understand by a slowly varying field. It is clear that a field variable which could be considered slowly varying at one time or, more generally, in the neighbourhood of a space-like surface σ will not retain this property throughout the whole space-time. Accordingly, the definition of the slowly varying field must be given with reference to a certain surface σ. The field variables will now be called slowly varying on σ if, in a suitably chosen Lorentz system, the free field functions $\psi(x,\sigma)$ and $u(x,\sigma)$ which coincide with $\psi(x)$ and $u(x)$ on σ may be regarded as built up of plane waves involving only momenta small compared with $\frac{1}{\lambda}$. In this way, the notion of slowly varying fields is given a relativistically invariant meaning, but it may be remarked that the expression slowly varying then is somewhat misleading, since it is obvious that slowly varying fields are not composed of waves corresponding to small momenta, only, in every Lorentz system.

The correspondence with the local theory now requires that the evolution of the thus defined slowly varying fields in the neighbourhood of the surface σ is the same as in the usual theory. The value of $\psi(x)$ for x on an infinitesimally displaced surface σ' is given by (2.1), and since

$$S^{\sigma}(x,x') \tag{1}$$

is zero if x' is outside the domain in four-space between the neighbouring surfaces σ and σ', the integral on the right hand side of (2.1) is small of the first order in the distance between σ and σ'. Neglecting terms of the second order in this distance, the usual iteration procedure for solving (2.1) gives for x in the neighbourhood of σ

$$\left.\begin{aligned}\psi(x) &= \psi(x,\sigma)+\int S^{\sigma}_{\mathrm{M}}(x,x')\,\Phi(x',x'',x''')\,u(x'',\sigma)\,\psi(x''',\sigma)\,dx'dx''dx'''\\ u(x) &= u(x,\sigma)-\int \bar{\psi}(x',\sigma)\,\Phi(x',x'',x''')\,\Delta^{\sigma}_{\mathrm{m}}(x,x'')\,\psi(x''',\sigma)\,dx'dx''dx'''.\end{aligned}\right\}\ (2$$

Comparing the first of these equations with the corresponding local equation we see that the form factor must satisfy the condition

$$\left.\int F(x', x'', x''')\, u(x'', \sigma)\, \psi(x'', \sigma)\, dx'\, dx'' = u(x', \sigma)\, \psi(x', \sigma)\right\} \quad (3)$$

for arbitrary, slowly varying ψ and u. Introducing the Fourier expansions of the function F (1.15) in (3), we obtain

$$\left.\begin{aligned} \int G(P+p, -P)\, u(p, \sigma)\, \psi(P, \sigma)\, e^{i(P+p)x'} dp dP = \\ = \int u(p, \sigma)\, \psi(P, \sigma)\, e^{i(P+p)x'} dp dP, \end{aligned}\right\} \quad (4)$$

where $u(p, \sigma)$, $\psi(P, \sigma)$ are the Fourier transforms of $u(x, \sigma)$, $\psi(x, \sigma)$, respectively.

Hence, G must satisfy the condition

$$G(P+p, -P) = 1 \quad (5)$$

whenever P and p are four-momenta entering in the Fourier expansions of the slowly varying ψ and u. From the Hermitian conjugate equation of (4) we get similarly, using (1.13),

$$G^*(l^1, l^3) = G(-l^3, -l^1)$$

and

$$u^*(p) = u(-p),$$

the further condition

$$G(P, p-P) = 1. \quad (6)$$

Finally, the second equation (2) leads to the condition

$$G(P', -P'') = 1 \quad (7)$$

which must hold for any two four-momenta P^{II} and P^{I} occurring in the Fourier expansions of the slowly varying nucleon wave function.

If the form factor G is assumed to be real we have the symmetry relation

$$G(l^1, l^3) = G(-l^3, -l^1) \quad (8)$$

and, since G must be an invariant, it can be a function of the three invariants

$$\left(\frac{l^1 - l^3}{2}\right)^2, \quad (l^1 + l^3)^2, \quad \left[(l^1 + l^3)\left(\frac{l^1 - l^3}{2}\right)\right]^2 \tag{9}$$

only. We shall show, however, that it is possible to obtain convergence with a G depending only on one variable. The calculation of the correction of the meson mass (3.18) shows that this variable cannot be $(l^1 + l^3)^2$. Similarly, the last variable in (9) is excluded since it is constant and in fact zero for the momenta entering in the last term of the expression for the self-energy of the nucleons (3.22). Accordingly, the only possibility left is to choose G as a function of $[(l^1 - l^3)/2]^2$ or a combination of the quantities (9) containing $[(l^1 - l^3)/2]^2$. It was found convenient to choose the combination

$$\Pi^2 = \left(\frac{l^1 - l^3}{2}\right)^2 - \frac{\left[(l^1 + l^3)\left(\frac{l^1 - l^3}{2}\right)\right]^2}{(l^1 + l^3)^2} \tag{10}$$

which is identical with Π^2 entering in (1.10).

For the l^1 and l^3 values in condition (7), we have

$$\Pi^2(l^1, l^3) = \left(\frac{P'' + P'}{2}\right)^2. \tag{11}$$

If P_0'' and P_0' have the same sign, i. e. if P'' and P' are wave vectors corresponding to the same type of particles, $P'' + P'$ is time-like. In the rest system of the two particles, where $\vec{P}'' = -\vec{P}' = \Delta\vec{P}$, Π^2 is

$$\Pi^2 = -\left[\left(\Delta\vec{P}\right)^2 + M^2\right]. \tag{12}$$

On the other hand, if P'' and P' are wave vectors of an anti-nucleon and a nucleon, $-P'' + P'$ is time-like and in the rest system of the two particles, where now $\vec{P}'' = \vec{P}' = \Delta\vec{P}$, Π^2 is

$$\Pi^2 = \left(\Delta\vec{P}\right)^2. \tag{13}$$

The condition (7) now requires that $G = 1$ for values of Π^2 corresponding to $(\Delta\vec{P})^2$ small compared with $1/\lambda^2$. This suggests

the following choice of a simple form factor depending on one variable, only,

$$G(\Pi^2) = 1 \quad \text{for} \quad \begin{cases} -M^2 - \dfrac{1}{\lambda^2} \leq \Pi^2 \leq -M^2 \\ 0 \leq \Pi^2 \leq \dfrac{1}{\lambda^2} \end{cases} \tag{14}$$

and zero outside these intervals. For the l^1 and l^3 occurring in the conditions (5) and (6), we have

$$\Pi^2 = -M^2 + \frac{(Pp)^2}{m^2}. \tag{15}$$

In the rest system of the nucleon, (15) becomes

$$\Pi^2 = \frac{M^2}{m^2}(\vec{p})^2. \tag{16}$$

Hence, the choice (14) of the form factor is also in accordance with the conditions (5) and (6). However, on account of the factor M/m in (16), we see that with the choice (14) the range of momenta for which we have correspondence to the usual theory is more restricted for the mesons than for the nucleons.

Using the explicit expression (14) for the form factor the self-energies of the meson and the nucleon derived in Section 3 may now be evaluated. The meson self-energy (3.18) contains a G-factor

$$\left| G(K, -K - p') \right|^2. \tag{17}$$

In the frame of reference where the meson is at rest, we have

$$\Pi^2 = \vec{K}^2. \tag{18}$$

Accordingly, the form factor restricts the domain of integration to

$$0 \leq \vec{K}^2 \leq \left(\frac{1}{\lambda}\right)^2.$$

In the meson rest system, we obtain from (3.18), performing the intergrations over K_0 and over all directions of $\vec{K}$,

$$\delta m^2 = -\frac{4}{\pi}\left(\frac{g^2}{4\pi}\right)\int_0^{\frac{1}{\lambda}} \frac{\sqrt{k^2+M^2}\cdot k^2\, dk}{k^2+M^2-\frac{m^2}{4}}. \tag{19}$$

Whence, to the first order in $\frac{1}{M\lambda}$

$$\frac{\delta m}{m} = \frac{\delta m^2}{2m^2} = -\frac{2}{3\pi}\left(\frac{g^2}{4\pi}\right)\frac{m}{M}\cdot\alpha^{-3}. \tag{20}$$

$\alpha = m\lambda$ is the ratio between λ and the meson Compton wavelength $\frac{1}{m}$ and may be expected to be of the order of magnitude of unity.

For the nucleon self-energy (3.22) we obtain in the rest system of the particle, in the same approximation as before,

$$\left.\begin{aligned} \frac{\delta M_{\mathrm{I}}}{M} &= -\frac{1}{6\pi}\left(\frac{g^2}{4\pi}\right)\left(\frac{m}{M}\right)^4\alpha^{-3} \\ \delta\vec{A}_{\mathrm{I}} &= 0 \\ \frac{\delta (A_{\mathrm{I}})_0}{M} &= \frac{\delta M_{\mathrm{I}}}{M} \end{aligned}\right\} \tag{21}$$

and

$$\left.\begin{aligned} \frac{\delta M_{\mathrm{II}}}{M} &= -\frac{2}{3\pi}\left(\frac{g^2}{4\pi}\right)\left(\frac{m}{M}\right)^3\alpha^{-3} \\ \delta\vec{A}_{\mathrm{II}} &= 0 \\ \frac{\delta (A_{\mathrm{II}})_0}{M} &= \frac{\delta M_{\mathrm{II}}}{M}. \end{aligned}\right\} \tag{22}$$

Introducing for m the mass of the π-meson, and putting $g^2/4\pi \sim \frac{1}{10}$, we obtain

$$\left.\begin{aligned} \frac{\delta m}{m} &\sim 10^{-2}\,\alpha^{-3} \\ \frac{\delta m}{m} &\sim 10^{-4}\,\alpha^{-3} \end{aligned}\right\} \tag{23}$$

which, for α of the order of magnitude of unity, means that the mass corrections are small fractions of the actual masses.

It is instructive by direct calculation to verify that the form factor (14), which was chosen in accordance with the correspondence requirement formulated in the beginning of this section, actually does not affect the cross-sections for nucleon-nucleon scattering and for the scattering of mesons by nucleons for sufficiently weak collisions. We shall not here give any detailed derivation of the corresponding matrix elements of the η-matrix. The calculation is quite straightforward, and the results will be quoted without proof. In the local limit, the matrix element of η for a transition from an initial state with one meson of momentum p' and one nucleon of momentum $P^{(+)\prime}$ present to a final state where the particles have momenta p'' and $P^{(+)\prime\prime}$, respectively, consists of two contributions corresponding to the two graphs

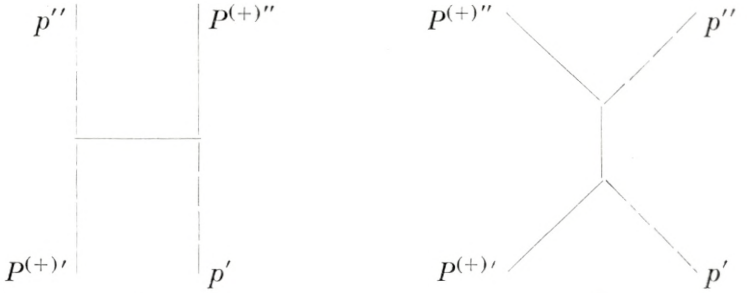

Let the contribution from the first graph be $\langle P^{(+)\prime\prime} p'' | A | P^{(+)\prime} p' \rangle$ and that from the second $\langle P^{(+)\prime\prime} p'' | B | P^{(+)\prime} p' \rangle$. Then, the corresponding matrix element in the theory of non-localized interaction can be written in the form

$$\left.\begin{aligned} &\langle P^{(+)\prime\prime} p'' | A | P^{(+)\prime} p' \rangle G(P^{(+)\prime\prime}, -P^{(+)\prime\prime} - p') G(P^{(+)\prime} + p'', -P^{(+)\prime}) \\ &+ \langle P^{(+)\prime\prime} p'' | B | P^{(+)\prime} p' \rangle G(P^{(+)\prime\prime}, -P^{(+)\prime\prime} - p'') G(P^{(+)\prime} + p', -P^{(+)\prime}). \end{aligned}\right\} \quad (26)$$

Also the matrix element determining the nucleon-nucleon scattering cross-section can in the local limit be written as a sum of two terms A and B. If P' and P''' denote the momenta of the incident nucleons, and P'' and P^{iv} those of the scattered nucleons, the corresponding matrix elements in the theory of non-localized interaction are

$$\left.\begin{aligned} &\langle P'' P^{\mathrm{iv}} \,|\, A \,|\, P' P''' \rangle \, G(P'', -P') \, G(P^{\mathrm{iv}}, -P''') \\ &+ \langle P'' P^{\mathrm{iv}} \,|\, B \,|\, P'' P''' \rangle \, G(P^{\mathrm{iv}}, -P') \, G(P'', -P''') . \end{aligned}\right\} \quad (27)$$

The two terms are the contributions from the following two graphs, respectively.

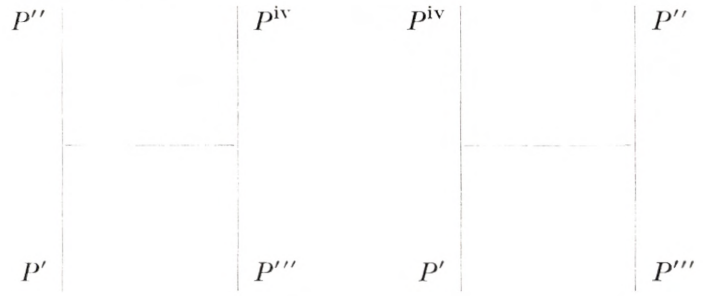

By comparing the G-factors in (26) and (27) with those in (5), (6), and (7) it becomes clear from the discussion on p. 26 and 27 that the scattering matrix elements (26) and (27) are identical with those of the corresponding local theory for all processes in which the momenta involved are small compared with $\frac{1}{\lambda}$ in the frame of reference where the center of gravity of the system is at rest.

5. Physical interpretation of the theory. Transformation theory.

In the general formalism developed in Section 1, the variables $\bar{\psi}(x)$, $\psi(x)$ and $u(x)$ play a role similar to that of the field variables in the usual theories, in as far as the connection between these variables in different space-time points is given by certain integro differential equations. However, the physical interpretation of the field variables is in general much more complicated than in the usual theory. In fact, a direct interpretation is given only for the in- and out-fields which are the quantities having a simple physical meaning. In the general case, the ψ and u variables may rather be regarded as a kind of auxiliary quantities giving the connection between the directly observable in- and out-fields and thus allowing of a determination of the S-matrix.

The usual interpretation of the field variables is possible only in the limit of slowly varying fields where the conventional theory is valid.

The present formalism offers an example of a theory which allows the S-matrix to be calculated for any system of interacting nucleons and mesons. The only arbitrariness still present in the theory is that involved in the choice of the invariant function $G(l^1, l^3)$. This function could in principle be determined by comparison of the results of high energy scattering experiments with the cross-sections following from the theory.

In order to obtain a convergent theory, it seems necessary to give up some of the general concepts of quantum mechanics and, to avoid paradoxes, it is important to realize the fundamental difference between a theory of the kind considered here and the usual quantum mechanical description. This difference was strikingly illustrated already in the first section, where it was pointed out that the quantities which in the local limit correspond to energy, momentum, and charge of the system cannot be considered constants of the motion. This should, however, not be considered a defect of the theory, since it is sufficient to require that these quantities in general are constants of collision.

On account of the non-Hamiltonian form of the present formalism it is clear that also the notion of canonical transformations loses its importance in this theory. There are other, more general transformations, however, which play a similar role as the canonical transformations do in ordinary quantum mechanics. In the local theory, a canonical transformation of the field variables $\varphi(x)$ can always be written in the form

$$\mathring{\varphi}(x) = T^{\dagger} \varphi(x)\, T, \tag{1}$$

where T is a unitary operator which may be regarded as an arbitrary functional of the field variables $\varphi(\vec{x}, t)$ on a space-like surface t = constant. This transformation has the property that the commutation relations for the transformed variables $\mathring{\varphi}$ are the same as those for the old variables on the surface t = constant. Further, the field equations in terms of the new variables have again the form of canonical equations of motion with the same Hamiltonian H, although of course H is a different function of the transformed variables than it is of the old variables.

In an S-matrix formalism where the S-matrix is defined as the unitary matrix connecting two sets of free field variables φ^{in} and φ^{out}, by the equation

$$\varphi^{\text{out}}(x) = S^{\dagger}\varphi^{\text{in}}(x)\,S, \tag{2}$$

one is led to consider canonical transformations of the in- and out-variables given by

$$\left.\begin{aligned} \overset{\circ}{\varphi}{}^{\text{in}}(x) &= T^{\text{in}\,\dagger}\varphi^{\text{in}}(x)\,T^{\text{in}} \\ \overset{\circ}{\varphi}{}^{\text{out}}(x) &= T^{\text{out}\,\dagger}\varphi^{\text{out}}(x)\,T^{\text{out}}, \end{aligned}\right\} \tag{3}$$

where T^{in} and T^{out} are certain functionals of $\varphi^{\text{in}}(x)$ and $\varphi^{\text{out}}(x)$, respectively, on the arbitrary surface $t =$ constant. From (3) we get

$$\overset{\circ}{\varphi}{}^{\text{out}} = \overset{\circ}{S}{}^{\dagger}\overset{\circ}{\varphi}{}^{\text{in}}\overset{\circ}{S}, \tag{4}$$

where

$$\overset{\circ}{S} = T^{\text{in}\,\dagger}ST^{\text{out}} \tag{5}$$

is a unitary matrix. If the transformation (3) is such that

$$T^{\text{out}} = S^{\dagger}T^{\text{in}}S, \tag{6}$$

which means that T^{out} is the same functional of out-variables as T^{in} is of the in-variables, we have

$$\left.\begin{aligned} \overset{\circ}{S} &= T^{\dagger}[\varphi^{\text{in}}]\cdot S\cdot T[\varphi^{\text{out}}]\,S^{\dagger}S \\ &= T^{\dagger}[\varphi^{\text{in}}]\cdot T[\varphi^{\text{in}}]\cdot S = S \end{aligned}\right\} \tag{7}$$

and the S-matrix is invariant. A transformation of this kind may be called a "collision transformation" and, in a pure S-matrix theory, such transformations play a similar role as the canonical transformations in the usual theory.

In a formalism like the present, which pretends to link up the pure S-matrix description with the usual quantum mechanical description, a certain class of transformations of the variables φ are of special importance. To any collision transformation corresponds a very wide class of transformations

$$\overset{\circ}{\varphi} = \overset{\circ}{\varphi}[\varphi(x)] \tag{8}$$

which have the property that $\overset{\circ}{\varphi}(x)$ asymptotically for $t \to \pm \infty$ coincides with $\overset{\circ}{\varphi}^{\text{in}}$ and $\overset{\circ}{\varphi}^{\text{out}}$, respectively. However, on account of the correspondence requirement, we are only interested in those transformations which in the limit of slowly varying fields reduce to canonical transformations. Transformations of this kind will be called quasi-canonical.

We shall now consider a special type of quasi-canonical transformations, viz. the gauge transformation

$$\left.\begin{aligned} \overset{\circ}{\varphi}(x) &= e^{i\chi(x)}\psi(x) \\ \overset{\circ}{u}(x) &= u(x) \end{aligned}\right\} \tag{9}$$

which transforms the field equations (1.19) into

$$\left.\begin{aligned} \{\gamma_\mu(\partial_\mu - i\partial_\mu\chi) + M\}\,\overset{\circ}{\psi} &= -\int \overset{\circ}{\Phi}(x, x'', x''')\, u(x'')\, \overset{\circ}{\psi}(x''')\, dx''dx''' \\ (\Box - m^2)\, u &= \int \overset{\circ}{\bar{\psi}}(x')\, \overset{\circ}{\Phi}(x', x, x''')\, \overset{\circ}{\psi}(x''')\, dx'dx''', \end{aligned}\right\} \tag{10}$$

where we have put

$$\overset{\circ}{F}(x', x'', x''') = e^{i\chi(x')} F(x', x'', x''') e^{-i\chi(x''')},\ \overset{\circ}{\Phi} = \Lambda \overset{\circ}{F}. \tag{11}$$

Since the transformed in- and out-fields are equal to the original in- and out-fields times $e^{i\chi}$, it is clear that the S-matrix connecting the in- and out-fields remains unchanged by this transformation. As is well known, the phase transformation of the free field variables is a canonical transformation of the type (3) with

$$\left.\begin{aligned} T^{\text{in}} &= T[\psi^{\text{in}}] = \exp\left\{i\int \psi^{\text{in}\,\dagger}(\vec{x}, t)\, \psi^{\text{in}}(\vec{x}, t)\, \chi(\vec{x}, t)\, d^{(3)}\vec{x}\right\} \\ T^{\text{out}} &= T[\psi^{\text{out}}]. \end{aligned}\right\} \tag{12}$$

In the case of slowly varying fields, both $\overset{\circ}{\Phi}$ and Φ are effectively equal to δ-functions, and we have complete gauge invariance in the usual sense. On the other hand, if the fields cannot be considered slowly varying, the form factor F must transform along with a phase transformation of the ψ's in accordance with (11).

If the nucleons are protons subject to an external electromagnetic field, a gauge invariant theory can again only be obtained if the form factor is considered as dependent on the four-potentials of the external field. As remarked by C. Bloch, a formally gauge invariant theory can be obtained in the case of an external electromagnetic field if the form factor is taken as

$$\Phi_A(x', x'', x''') = \exp\left(-i\int_{x'}^{x'''} A_\mu \, dx_\mu\right) \cdot \Phi(x', x'', x'''), \qquad (13)$$

where Φ is the form factor for $A_\mu = 0$, and the path of integration is taken as the straight line connecting the points x' and x''' in Minkowski space. The field equations can then be taken as

$$\left.\begin{aligned} \{\gamma_\mu(\partial_\mu - ieA_\mu) + M\}\psi &= -\int \Phi_A(x, x'', x''') u(x'') \psi(x''') dx'' dx''' \\ (\Box - m^2) u &= \int \bar{\psi}(x') \Phi_A(x', x, x''') \psi(x''') dx' dx''' . \end{aligned}\right\} \qquad (14$$

It is easily seen that the so defined form factor by the gauge transformation

$$\overset{\circ}{A}_\mu = A_\mu + \partial_\mu \Lambda \qquad (15)$$

of the potentials transforms as

$$\overset{\circ}{F}_A(x', x'', x''') = e^{ie\Lambda(x')} F_A(x', x'', x''') e^{-ie\Lambda(x''')}, \qquad (16)$$

which means that the transformation (16) is equivalent to a quasi-canonical transformation of the type (9).

Instead of this completely gauge invariant scheme with the complicated form factor (14) an alternative procedure would be to fix the gauge of the potentials by choosing these as the retarded potentials from external current and charge distributions. Since the retarded potentials in the limit of vanishing current and charge distribution tend to zero, it would be consistent to choose the same form factor as in the case of no external fields. For a different choice of gauge, the form factor should then be transformed in accordance with (11).

6. The polarization of the vacuum by an external meson field.

As is well known, the coupling of the meson field to the nucleon field in its vacuum state gives rise to a polarization effect which, in the language of perturbation theory, can be attributed to the virtual creation and annihilation of nucleon pairs. In this section, we shall confine ourselves to the approximation where the meson field can be treated as a classical field. Although the physical interpretation of an external meson field is not at all obvious, an investigation of this kind throws some light on the types of polarization effects which are caused by quantized meson fields.

To illustrate this effect, we shall calculate the vacuum expectation value of the source density

$$I(x) = ig \int \bar{\psi}(1)\, \gamma_5 F(1, x, 3)\, \psi(3)\, d(13) \tag{1}$$

to the second order in the coupling constant. To simplify the problem, we only treat the case of a meson field which is weak, in the sense that no real scattering and pair creation processes take place to the first order in the coupling constant g. Consequently, the first order correction to the out-fields obtained from the field equations (2.6) vanishes. Transforming the expression (2.10) for this correction to momentum space, it can be seen that the Fourier components $u(p)$ of a weak meson field vanish whenever pair creation is compatible with the conservation laws of energy and momentum, i. e. whenever

$$p = P - \bar{P}, \tag{2}$$

where P and $\bar{P}$ are nucleon wave vectors, $P^2 = \bar{P}^2 = -M^2$. Hence, the only non-vanishing Fourier components of u are those corresponding to wave vectors which could be considered as four-momenta of a particle with rest mass smaller than $2M$. In the same way as in Section 2, the vanishing of the first order correction to the out-fields allows one to simplify the expression of the first order correction $\psi^{(1)}$ to the ψ's to

$$\psi^{(1)}(0) = ig \int \bar{S}(0 - 1)\, \gamma_5 F(1, 2, 3)\, u(2)\, \psi^{\text{in}}(3)\, d(123) \tag{3}$$

given by (2.12). We can now calculate the vacuum expectation value of the source density (1). To the second order in the coupling constant g, we get

$$\left.\begin{aligned} \langle I\rangle_0 = {} & ig\int F(1\,x\,3)\langle \bar{\psi}^{\mathrm{in}}(1)\,\gamma_5\psi^{\mathrm{in}}(3)\rangle_0\, d(13) \\ & + ig\int F(1\,x\,3)\langle \bar{\psi}^{(1)}(1)\,\gamma_5\psi^{\mathrm{in}}(3)\rangle_0\, d(13) \\ & + ig\int F(1\,x\,3)\langle \bar{\psi}^{\mathrm{in}}(1)\,\gamma_5\psi^{(1)}(3)\rangle_0\, d(13). \end{aligned}\right\} \tag{4}$$

The first of the terms on the right hand side vanishes. The two other ones can be evaluated using standard methods given in the Appendix B and we obtain after a short calculation

$$\left.\begin{aligned} \langle I\rangle_0 = {} & -4\,g^2(2\pi)^{-3}\int dp dL\,|\,G(L+p,-L)\,|^2 \\ & \times\frac{pL}{2\,pL+p^2}\,\delta(L^2+M^2)\,u(p)\,e^{ipx}. \end{aligned}\right\} \tag{5}$$

Here, G is the Fourier transform of the form factor and $u(p)$ is defined by

$$u(x) = \int u(p)\,e^{ipx}dp. \tag{6}$$

(5) can conveniently be written in the form

$$\langle I\rangle_0 = \int \Phi(p)\,u(p)\,e^{ipx}dp \tag{7}$$

or, alternatively,

$$\langle I\rangle_0 = \Phi(-i\partial_\mu)\,u(x). \tag{8}$$

From (5) we obtain the expression for Φ,

$$\Phi = -4\,g^2(2\pi)^{-3}\int dL\,\frac{|\,G(L+p,-L)\,|^2\cdot(pL)\cdot\delta(L^2+M^2)}{2\,pL+p^2}. \tag{9}$$

According to our assumption about the external field, p is a time-like vector and we can introduce the variable of integration Λ defined as the magnitude of $\vec{L}$ in the frame of reference where the "meson is at rest", i.e. where $p=(\vec{0},\pm i\sqrt{-p^2})$. Using (4.18), and performing three of the integrations, we obtain

$$\left.\begin{aligned} \Phi = {} & -4\,g^2(2\pi)^{-2}\int_0^\infty d\Lambda\,|\,G(\Lambda^2)\,|^2\,\frac{\Lambda^2\sqrt{\Lambda^2+M^2}}{\Lambda^2+M^2+\frac{1}{4}p^2}. \end{aligned}\right\} \tag{10}$$

Making use of the covariant expansion

$$\left.\begin{aligned}\left(\Lambda^2+M^2+\frac{1}{4}p^2\right)^{-1} &= \left(\Lambda^2+M^2-\frac{1}{4}m^2\right)^{-1}\\ \times\left[1+\frac{1}{4}\frac{(-p^2-m^2)}{\left(\Lambda^2+M^2-\frac{1}{4}m^2\right)}+\frac{1}{16}\frac{(-p^2-m^2)^2}{\left(\Lambda^2+M^2-\frac{1}{4}m^2\right)^2}+\cdots\right]&\end{aligned}\right\} \quad (11)$$

we finally obtain the operator Φ introduced by (8) as a power series in the operator $(\Box - m^2)/M^2$,

$$\Phi = \delta m^2 + \varepsilon(\Box - m^2) + c^{(1)}\frac{\Box - m^2}{M^2}(\Box - m^2) + \ldots \quad (12)$$

It is convenient to express the induced source density $\langle I\rangle_0$ in terms of the external source density $I^{(e)}$ creating the external meson field due to

$$(\Box - m^2)\, u = I^{(e)}, \quad (13)$$

and by (8) and (12) the expression for $\langle I\rangle_0$ is

$$\langle I\rangle_0 = \delta m^2 u + \varepsilon I^{(e)} + c^{(1)}\frac{\Box - m^2}{M^2} I^{(e)} + \cdots . \quad (14)$$

The various constants introduced are easily obtained from (10) and (11). We get

$$\left.\begin{aligned}\delta m^2 &= -4g^2(2\pi)^{-2}\int_0^\infty \frac{|G(\Lambda^2)|^2\cdot\Lambda^2\sqrt{\Lambda^2+M^2}}{\Lambda^2+M^2-\frac{1}{4}m^2}\,d\Lambda\\ \varepsilon &= -\,g^2(2\pi)^{-2}\int_0^\infty \frac{|G(\Lambda^2)|^2\cdot\Lambda^2\sqrt{\Lambda^2+M^2}}{\left(\Lambda^2+M^2-\frac{1}{4}m^2\right)^2}\,d\Lambda\\ c^{(1)} &= -\frac{1}{4}g^2(2\pi)^{-2}\int_0^\infty \frac{|G(\Lambda^2)|^2\cdot M^2\Lambda^2\sqrt{\Lambda^2+M^2}}{\left(\Lambda^2+M^2-\frac{1}{4}m^2\right)^3}\,d\Lambda .\end{aligned}\right\} \quad (15)$$

Clearly, δm^2 represents the contribution to the square of the meson mass due to the interaction of the meson field with the

nucleons. In fact, δm^2 in (15) is identical to (4.19). The induced density $\varepsilon I^{(e)}$ is also unobservable in principle and gives rise to a change of the coupling constant by an amount εg. Thus, the first observable term in the series is the third one. It will be seen from (15) that the numerical values of the expansion coefficients are highly sensible to the choice of the form factor. In the local limit, the two first of these diverge, δm^2 quadratically and ε logarithmically, while with the choice (4.18) of the form factor we obtain the finite and small corrections

$$\left.\begin{aligned} \frac{\delta m}{m} &= -\frac{2}{3\pi}\left(\frac{g^2}{4\pi}\right)\frac{m}{M}\alpha^{-3} \\ \varepsilon &= -\frac{1}{3\pi}\left(\frac{g^2}{4\pi}\right)\left(\frac{m}{M}\right)^3\alpha^{-3}, \end{aligned}\right\} \tag{16}$$

where we have neglected higher powers in $1/\lambda M$.

Here, α is the product of λ with the meson mass m. Also the value obtained for the constant $c^{(1)}$ is considerably reduced by the introduction of the form factor. In fact, in the local limit, we obtain

$$c^{(1)}_{\text{local}} = -\frac{1}{12\pi}\left(\frac{g^2}{4\pi}\right) \tag{17}$$

while, using the form factor (4.18), $c^{(1)}$ becomes

$$c^{(1)} = -\frac{1}{12\pi}\left(\frac{g^2}{4\pi}\right)\left(\frac{m}{M}\right)^3\alpha^{-3}. \tag{18}$$

The ratio of the two values

$$\frac{c^{(1)}}{c^{(1)}_{\text{local}}} = \left(\frac{m}{M}\right)^3\alpha^{-3} \tag{19}$$

may be expected to be small. Thus, in the present theory, $c^{(1)}_{\text{local}}$ does not represent the true vacuum polarization, contrary to what would be expected from a renormalization point of view. This is in accordance with the point of view that the difficulties in quantum field theory should be overcome by a modification of the theories in the high energy region.

It is seen from (15) that the main contribution to $c^{(1)}_{\text{local}}$ comes from the region $\Lambda \sim 2M$. Hence, in meson theory, the vacuum polarization should be considered as a high energy phenomenon, contrary to what is the case in electrodynamics where the main contribution to the induced current comes from distances of the order of the Compton wavelength of the electron. This distance must be expected to be large compared with the constant λ' which must be expected to occur in a convergent electron theory.

Added in proof. Professor W. PAULI has kindly pointed out to us that it is possible to construct a tensor $t_{\mu\nu}$ and a four vector j_μ having the properties that a) for $\lambda \to 0$ $t_{\mu\nu}$ and j_μ become identical with the usual expressions for the energy-momentum tensor and the four current of the field, respectively, and b) that $t_{\mu\nu}$ and j_μ satisfy the strict continuity equations $\partial_\nu t_{\mu\nu} = 0$ and $\partial_\mu j_\mu = 0$. As shown by Professor PAULI, this opens the interesting possibility to introduce a Hamiltonian formalism and, hence, to perform a canonical quantization of the theory. We are greatly indebted to Professor PAULI for many illuminating discussions and comments on the subject of this papir.

References.

1. J. Schwinger, Phys. Rev. **74**, 1439 (1948); **75**, 651 (1949).
   S. Tomonaga, Progr. Theor. Phys. **1**, 27 (1946); Phys. Rev. **74**, 224 (1948).
   F. J. Dyson, Phys. Rev. **75**, 486, 1735 (1949).
   R. P. Feynmann, Rev. Mod. Phys. **20**, 367 (1948); Phys. Rev. **74**, 939, 1430 (1948).
2. A. Pais and G. E. Uhlenbeck, Phys. Rev. **79**, 145 (1950).
   P. T. Matthews and Abdus Salam, Rev. Mod. Phys. **23**, 311 (1951).
3. W. Heisenberg, ZS. f. Phys. **120**, 513, 673 (1943) and numerous later papers on the subject.

3a. W. Heisenberg, Göttingen, Festschrift, p. 50 (1951).

4. W. Pauli, Hdb. d. Phys., vol. 24, Chapter 2, p. 271 (Berlin 1933). — Meson Theory of Nuclear Forces. (New York 1946).
5. R. E. Peierls, 8^{me} Conseil de Physique, Institut Solvay, p. 291 (1948).
   H. McManus, Proc. Roy. Soc. A **195**, 323 (1949).
6. C. Bloch, Progress Theor. Phys. **5**, 606 (1950).
7. C. Bloch, Private communication. See also: forthcoming paper in Dan. Mat. Fys. Medd.
8. J. Rayski, Proc. Roy. Soc. A **206**, 575 (1951).
9. C. Møller, Dan. Mat. Fys. Medd. **23**, no. 1 (1945); **22**, no. 19 (1946).

9a. C. Møller, Recent Developments in Relativistic Quantum Theory. Lecture Notes. University of Bristol. Spring Term (1946).

10. G. Källén, Ark. f. Fys. **2**, 371 (1951).
    C. N. Yang and D. Feldman, Phys. Rev. **76**, 972 (1950).

Appendix A.

In this appendix*), we shall, for the purpose of reference, give the definition of the various Green's functions introduced in the text and their Fourier expansions. The singular function Δ can be defined as Green's function solving the initial value problem of the homogeneous wave equation. Let us consider that solution $\Phi(x, \sigma)$ of the equation

$$(\Box - \varkappa^2)\, \Phi(x, \sigma) = 0 \tag{1}$$

which, together with its normal derivative, is given on a space-like surface σ. Writing the solution in the form of a surface integral

$$\Phi(x, \sigma) = \int_\sigma \{\Delta(x - x')\, \partial'_\mu \Phi(x', \sigma) - \Phi(x', \sigma)\, \partial'_\mu \Delta(x - x')\}\, d\sigma_\mu, \tag{2}$$

$\Delta(x)$ obviously must satisfy

$$\left.\begin{aligned} (\Box - \varkappa^2)\, \Delta(x) &= 0 \\ \Delta(x) &= 0, \quad x_\mu x_\mu > 0 \\ \int_\sigma \partial_\mu \Delta(x)\, d\sigma_\mu &= 1 \end{aligned}\right\} \tag{3}$$

for any σ including the origin.

To solve the same boundary value problem of the inhomogeneous equation

$$(\Box - \varkappa^2)\, \Phi(x) = I(x) \tag{4}$$

we introduce one more Green's function $\Delta^\sigma(x, x')$ satisfying

* This appendix and the following contain no new results. For details and proofs the reader is referred to [1] and [10].

$$\left.\begin{aligned} (\Box - \varkappa^2)\, \Delta^\sigma(x, x') &= -\delta(x - x') \\ \Delta^\sigma(x/\sigma, x') &= 0 \\ n_\mu \partial_\mu \Delta^\sigma(x/\sigma, x') &= 0, \end{aligned}\right\} \tag{5}$$

where we have used the notation x/σ to indicate a point x lying on the surface σ. n_μ is the unit normal to σ in the point x/σ. The solution of the mentioned boundary value problem is then

$$\Phi(x) = \Phi(x, \sigma) - \int \Delta^\sigma(x, x')\, I(x')\, dx', \tag{6}$$

where the free field $\Phi(x, \sigma)$, coinciding with $\Phi(x)$ on σ, is given by (2). Taking in (5) for fixed x', σ in the infinite past, we obtain the retarded Green's function

$$\Delta^{\mathrm{ret}}(x - x') = \lim_{\sigma \to -\infty} \Delta^\sigma(x, x') \tag{7}$$

satisfying

$$\left.\begin{aligned} (\Box - \varkappa^2)\, \Delta^{\mathrm{ret}}(x - x') &= -\delta(x - x') \\ \lim_{x_0 \to -\infty} \Delta^{\mathrm{ret}}(x - x') &= 0 \\ \lim_{x_0 \to -\infty} \partial_0 \Delta^{\mathrm{ret}}(x - x') &= 0. \end{aligned}\right\} \tag{8}$$

Formally, Δ^{ret} solves the initial value problem, where the asymptotic form of $\Phi(x)$ and its derivative in the time direction are given at the infinite past. In the same way, we can define

$$\Delta^{\mathrm{adv}}(x - x') = \lim_{\sigma \to +\infty} \Delta^\sigma(x, x') \tag{9}$$

satisfying

$$\left.\begin{aligned} (\Box - \varkappa^2)\, \Delta^{\mathrm{adv}}(x - x') &= -\delta(x - x') \\ \lim_{x_0 \to +\infty} \Delta^{\mathrm{adv}}(x - x') &= 0 \\ \lim_{x_0 \to +\infty} \partial_0 \Delta^{\mathrm{adv}}(x - x') &= 0. \end{aligned}\right\} \tag{10}$$

Starting from the thus defined Green's functions Δ, Δ^{ret} and Δ^{adv}, we can define various other singular functions satisfying either the homogeneous equation

$$(\Box - \varkappa^2)\, \Phi(x) = 0 \tag{11}$$

or the inhomogeneous equation

$$(\Box - \varkappa^2)\, \Phi(x) = -\delta(x). \tag{12}$$

It is clear that the positive and negative frequency parts of Δ

$$\Delta^{(+)} = \text{positive frequency part of } \Delta \tag{13}$$

$$\Delta^{(-)} = \text{negative frequency part of } \Delta \tag{14}$$

satisfy (11). The same holds for the function

$$\Delta^{(1)} = i(\Delta^{(+)} - \Delta^{(-)}). \tag{15}$$

On the other hand, $\overline{\Delta}$ defined by

$$\overline{\Delta} = \frac{1}{2}(\Delta^{\text{adv}} + \Delta^{\text{ret}}) \tag{16}$$

is a solution of (12).

If we introduce the characteristic functions

$$\left.\begin{aligned} \varepsilon(x) &= \operatorname{sign} x_0 \\ \varepsilon(\sigma, x) &= \begin{cases} -1 \text{ for } x \text{ on the future side of } \sigma \\ +1 \text{ for } x \text{ on the past side of } \sigma \end{cases} \end{aligned}\right\} \tag{17}$$

the following relations can be shown to hold among the various functions introduced.

$$\Delta = \Delta^{(+)} + \Delta^{(-)} \tag{18}$$

$$\overline{\Delta} = -\frac{1}{2}\varepsilon(x)\, \Delta(x) \tag{19}$$

$$\Delta = \Delta^{\text{adv}} - \Delta^{\text{ret}} \tag{20}$$

$$\Delta^{\text{adv}} = \overline{\Delta} + \frac{1}{2}\Delta = -\frac{\varepsilon(x) - 1}{2}\Delta \tag{21}$$

$$\Delta^{\text{ret}} = \overline{\Delta} - \frac{1}{2}\Delta = -\frac{\varepsilon(x) + 1}{2}\Delta \tag{22}$$

$$\Delta^{\sigma}(x, x') = -\frac{1}{2}\{\varepsilon(x - x') - \varepsilon(\sigma, x')\}\, \Delta(x - x'). \tag{23}$$

From the well known Fourier expansions of Δ and $\overline{\Delta}$ and the relations given above, one can easily deduce the expansions for the other functions. We have

$$\Delta = -i(2\pi)^{-3}\int \varepsilon(k)\,\delta(k^2+\varkappa^2)\,e^{ikx}dk \tag{24}$$

$$\Delta^{(+)} = -i(2\pi)^{-3}\int \frac{1+\varepsilon(k)}{2}\,\delta(k^2+\varkappa^2)\,e^{ikx}dk \tag{25}$$

$$\Delta^{(-)} = i(2\pi)^{-3}\int \frac{1-\varepsilon(k)}{2}\,\delta(k^2+\varkappa^2)\,e^{ikx}dk \tag{26}$$

$$\Delta^{(1)} = (2\pi)^{-3}\int \delta(k^2+\varkappa^2)\,e^{ikx}dk \tag{27}$$

$$\overline{\Delta} = (2\pi)^{-4}\int \frac{1}{k^2+\varkappa^2}\,e^{ikx}dk \tag{28}$$

$$\Delta^{\mathrm{ret}} = (2\pi)^{-4}\int \left\{\frac{1}{k^2+\varkappa^2}+i\pi\varepsilon(k)\,\delta(k^2+\varkappa^2)\right\}e^{ikx}dk \tag{29}$$

$$\Delta^{\mathrm{adv}} = (2\pi)^{-4}\int \left\{\frac{1}{k^2+\varkappa^2}-i\pi\varepsilon(k)\,\delta(k^2+\varkappa^2)\right\}e^{ikx}dk\,. \tag{30}$$

Here, $\dfrac{1}{k^2+\varkappa^2}$ should be understood as Cauchy's principal value, so that, for instance,

$$\Delta^{\mathrm{ret}} = (2\pi)^{-4}\int_{-\infty}^{\infty} d^{(3)}\vec{k}\int_{C^{\mathrm{ret}}} dk_0\,\frac{1}{k^2+\varkappa^2}\,e^{ikx}, \tag{31}$$

where C^{ret} is taken along the k_0-axes below the poles at $k_0 = \pm\sqrt{\vec{k}^2+\varkappa^2}$. In this form it can easily be verified that Δ^{ret} has the required asymptotic form.

Let us denote any of the Green's functions introduced above by $\Delta^?$. The corresponding Green's functions belonging to the Dirac equation are then defined as

$$S^? = (\gamma_\mu\partial_\mu - \varkappa)\,\Delta^?. \tag{32}$$

For completeness, we give the expansions for the S-functions

$$S = (2\pi)^{-3}\int (\gamma_\mu k_\mu + i\varkappa)\,\varepsilon(k)\,\delta(k^2+\varkappa^2)\,e^{ikx}dk \tag{33}$$

$$^{(+)} = (2\pi)^{-3}\int(\gamma_\mu k_\mu + i\varkappa)\frac{1+\varepsilon(k)}{2}\delta(k^2+\varkappa^2)\,e^{ikx}dk \tag{34}$$

$$^{(-)} = -(2\pi)^{-3}\int(\gamma_\mu k_\mu + i\varkappa)\frac{1-\varepsilon(k)}{2}\delta(k^2+\varkappa^2)\,e^{ikx}dk \tag{35}$$

$$^{(1)} = i(2\pi)^{-3}\int(\gamma_\mu k_\mu + i\varkappa)\,\delta(k^2+\varkappa^2)\,e^{ikx}dk \tag{36}$$

$$= i(2\pi)^{-4}\int\frac{\gamma_\mu k_\mu + i\varkappa}{k^2+\varkappa^2}\,e^{ikx}dk \tag{37}$$

$$^{\text{ret}} = i(2\pi)^{-4}\int(\gamma_\mu k_\mu + i\varkappa)\left\{\frac{1}{k^2+\varkappa^2} + i\pi\varepsilon(k)\,\delta(k^2+\varkappa^2)\right\}e^{ikx}dk \tag{38}$$

$$^{\text{adv}} = i(2\pi)^{-4}\int(\gamma_\mu k_\mu + i\varkappa)\left\{\frac{1}{k^2+\varkappa^2} - i\pi\varepsilon(k)\,\delta(k^2+\varkappa^2)\right\}e^{ikx}dk\,. \tag{39}$$

Appendix B.

In this appendix, we shall derive the various matrix elements needed in the calculation of the S-matrix. All field variables considered here are in-field variables and will be written without the subscript "in". For simplicity, we also use the notation of § 3, i. e. instead of x', x'', ..., we write 1, 2, ... The spinor variables can, in a relativistically invariant way, be decomposed into a positive and a negative frequency part

$$\psi = \psi^{(+)} + \psi^{(-)}, \quad \bar{\psi} = \bar{\psi}^{(+)} + \bar{\psi}^{(-)}. \tag{1}$$

From the well known commutation relations for $\bar{\psi}$ and ψ one immediately finds that the only non-vanishing anticommutators are

$$\left.\begin{aligned} \{\psi_\alpha^{(+)}(3), \bar{\psi}_\beta^{(-)}(1)\} &= -iS_{\alpha\beta}^{(+)}(3-1) \\ \{\psi_\alpha^{(-)}(3), \bar{\psi}_\beta^{(+)}(1)\} &= -iS_{\alpha\beta}^{(-)}(3-1). \end{aligned}\right\} \tag{2}$$

The operation of any positive frequency operator on a state of the nucleon field lowers the energy of the system and the operation of the ψ-function lowers the value of the quantity ΔN*) while the negative frequency operators and $\bar{\psi}$ increase the energy and ΔN, respectively. Accordingly, $\bar{\psi}^{(-)}$ creates nucleons, $\psi^{(-)}$ creates antinucleons, while $\bar{\psi}^{(+)}$ and $\psi^{(+)}$ annihilate antinucleons and nucleons, respectively. The vacuum state vector $|0\rangle$, defined as the state in which no particles are present, then satisfies

$$\psi^{(+)}|0\rangle = 0, \quad \bar{\psi}^{(+)}|0\rangle = 0, \tag{3}$$

and the Hermitian conjugate equations

$$\langle 0|\bar{\psi}^{(-)} = 0, \quad \langle 0|\psi^{(-)} = 0. \tag{4}$$

*) $\Delta N = \int \psi^\dagger \psi \, d^{(3)}\vec{x}$.

(2), (3), and (4) allow us to calculate the vacuum expectation value of any product of $\overline{\psi}$ and ψ functions occurring in the S-matrix. For instance,

$$\langle 0 \,|\, \overline{\psi}_\alpha(1)\, \psi_\beta(3) \,|\, 0 \rangle = -iS^{(-)}_{\beta\alpha}(3-1). \tag{5}$$

Using (1), the vacuum definitions (3) and (4), and the relation (2), the proof is straightforward

$$\begin{aligned} \langle 0 \,|\, \overline{\psi}_\alpha(1)\, \psi_\beta(3) \,|\, 0 \rangle &= \langle 0 \,|\, \overline{\psi}^{(+)}_\alpha(1)\, \psi^{(-)}_\beta(3) \,|\, 0 \rangle \\ &= \langle 0 \,|\, \{\overline{\psi}^{(+)}_\alpha(1),\ \psi^{(-)}_\beta(3)\} \,|\, 0 \rangle \\ &= -iS^{(-)}_{\beta\alpha}(3-1), \end{aligned}$$

if we assume that the vacuum state vector is normalized. In a similar way, we can show that

$$\left.\begin{aligned} &\langle 0 \,|\, \overline{\psi}_\alpha(1)\, \overline{\psi}_\beta(4)\, \psi_\gamma(6)\, \psi_\delta(3) \,|\, 0 \rangle \\ &= S^{(-)}_{\gamma\alpha}(6-1)\, S^{(-)}_{\delta\beta}(3-4) - S^{(-)}_{\gamma\beta}(6-4)\, S^{(-)}_{\delta\alpha}(3-1). \end{aligned}\right\} \tag{6}$$

To define states in which nucleons are present, it will be convenient to work in the momentum representation. We introduce the following notations: $v^{(+)}(\sigma, \vec{P}) \exp(iP^{(+)}x)$, and $v^{(-)}(\sigma, \vec{P}) \exp(iP^{(-)}x)$ are the one particle eigenstates of energy and momentum satisfying the Dirac equation and corresponding to positive and negative states of energy, respectively. If the amplitudes $v^{(+)}$ and $v^{(-)}$ are normalized, the expansion coefficients a defined by

$$\left.\begin{aligned} \psi^{(+)}(x) &= (2\pi)^{-\frac{3}{2}} \sum_\sigma \int d^{(3)}\vec{P} \cdot v^{(+)}(\sigma, \vec{P})\, e^{iP^{(+)}x}\ a^{(+)}(\sigma, \vec{P}) \\ \overline{\psi}^{(-)}(x) &= (2\pi)^{-\frac{3}{2}} \sum_\sigma \int d^{(3)}\vec{P} \cdot \overline{v}^{(-)}(\sigma, \vec{P})\, e^{-iP^{(+)}x}\, \overline{a}^{(-)}(\sigma, \vec{P}) \\ \psi^{(-)}(x) &= (2\pi)^{-\frac{3}{2}} \sum_\sigma \int d^{(3)}\vec{P} \cdot v^{(-)}(\sigma, \vec{P})\, e^{iP^{(-)}x}\ a^{(-)}(\sigma, \vec{P}) \\ \overline{\psi}^{(+)}(x) &= (2\pi)^{-\frac{3}{2}} \sum_\sigma \int d^{(3)}\vec{P} \cdot \overline{v}^{(+)}(\sigma, \vec{P})\, e^{-iP^{(-)}x}\, \overline{a}^{(+)}(\sigma, \vec{P}) \end{aligned}\right\} \tag{7}$$

satisfy the following commutation relations (only the non-vanishing anticommutators are written)

$$\left.\begin{aligned}\left\{\overline{a}^{(+)}(\sigma'',\vec{P}''),a^{(-)}(\sigma',\vec{P}')\right\} &= \delta_{\sigma''\sigma'}\delta(\vec{P}''-\vec{P}')\\ \left\{\overline{a}^{(-)}(\sigma'',\vec{P}''),a^{(+)}(\sigma',\vec{P}')\right\} &= \delta_{\sigma''\sigma'}\delta(\vec{P}''-\vec{P}').\end{aligned}\right\} \quad (8)$$

In (7), $P^{(+)}$ is short for $(\vec{P}, i\sqrt{\vec{P}^2+M^2})$ and $P^{(-)}$ for $(\vec{P},-i\sqrt{\vec{P}^2+M^2})$ while σ is the spin quantum number. It is easily seen from (7) that

$$\overline{a}^{(+)} = a^{(-)\dagger}, \quad \overline{a}^{(-)} = a^{(+)\dagger}. \quad (9)$$

The one particle states are now defined in the following way

$$\left.\begin{aligned}|\,\sigma P^{(+)}\rangle &= \overline{a}^{(-)}(\sigma,\vec{P})\,|\,0\rangle, \quad \langle\,\sigma P^{(+)}| = \langle 0\,|\,a^{(+)}(\sigma,\vec{P})\\ |\,\sigma P^{(-)}\rangle &= a^{(-)}(\sigma,\vec{P})\,|\,0\rangle, \quad \langle\,\sigma P^{(-)}| = \langle 0\,|\,\overline{a}^{(+)}(\sigma,\vec{P}).\end{aligned}\right\} \quad (10)$$

By this definition the states with one particle present are automatically normalized. For instance,

$$\begin{aligned}\langle\,\sigma P^{(+)}|\,\sigma' P^{(+)\prime}\rangle &= \langle 0\,|\,a^{(+)}(\sigma,\vec{P})\,\overline{a}^{(-)}(\sigma',\vec{P}')\,|\,0\rangle\\ &= \langle 0\,|\left\{a^{(+)}(\sigma,\vec{P}),\overline{a}^{(-(}(\sigma',\vec{P}')\right\}|\,0\rangle\\ &= \delta_{\sigma\sigma'}\delta(\vec{P}-\vec{P}')\langle 0\,|\,0\rangle\\ &= \delta_{\sigma\sigma'}\delta(\vec{P}-\vec{P}').\end{aligned}$$

If an annihilation operator $a^{(+)}$ is applied to $|\,\sigma P^{(+)}\rangle$, we obtain

$$a^{(+)}(\sigma',\vec{P}')\,|\,\sigma P^{(+)}\rangle = \delta_{\sigma\sigma'}\delta(\vec{P}-\vec{P}')\,|\,0\rangle. \quad (11)$$

In the same way, states with two particles present are defined as

$$|\,\sigma'' P^{(+)\prime\prime},\sigma' P^{(+)\prime}\rangle = \overline{a}^{(-)}(\sigma'',\vec{P}'')\,\overline{a}^{(-)}(\sigma',\vec{P}')\,|\,0\rangle. \quad (12)$$

By this definition the states are automatically normalized and antisymmetric in the two particles, i. e.

$$|\,\sigma'' P^{(+)\prime\prime},\sigma' P^{(+)\prime}\rangle = -|\,\sigma' P^{(+)\prime},\sigma'' P^{(+)\prime\prime}\rangle \quad (13)$$

in accordance with the exclusion principle.

If an annihilation operator is applied to the state (12) one obtains

$$\left.\begin{aligned} &a^{(+)}(\vec{P}''', \sigma''')\,|\,\sigma'' P^{(+)''}, \sigma' P^{(+)'}\rangle = \\ &= \delta_{\sigma'''\sigma''}\delta(\vec{P}''' - \vec{P}'')\,|\,\sigma' P^{(+)'}\rangle - \delta_{\sigma'''\sigma'}\delta(\vec{P}''' - \vec{P}')\,|\,\sigma'' P^{(+)''}\rangle, \end{aligned}\right\} \quad (14)$$

a relation which can be verified most easily in the standard way by pushing the annihilation operator through to the right, using (8), (3), and (10).

We can now derive the matrix elements of the one particle part of the operator $\bar{\psi}_\alpha(1)\,\psi_\beta(6)$ obtained by subtraction of the vacuum expectation value times the unit operator, i. e.

$$\left[\bar{\psi}_\alpha(1)\,\psi_\beta(6)\right]_{(1)} = \bar{\psi}_\alpha(1)\,\psi_\beta(6) - \langle 0\,|\,\bar{\psi}_\alpha(1)\,\psi_\beta(6)\,|\,0\rangle. \quad (15)$$

For instance, if the initial and final states both are nucleon states, we obtain

$$\left.\begin{aligned} &\langle \sigma'' P^{(+)''}\,|\,\left[\bar{\psi}_\alpha(1)\,\psi_\beta(6)\right]_{(1)}\,|\,\sigma' P^{(+)'}\rangle = \\ &= (2\pi)^{-3}\,\bar{v}^{(-)}_\alpha(\sigma'', \vec{P}'')\,v^{(+)}_\beta(\sigma', \vec{P}')\exp i(P^{(+)'}6 - P^{(+)''}1). \end{aligned}\right\} \quad (16)$$

To prove this, we first remark that

$$\begin{aligned} &\langle \sigma'' P^{(+)''}\,|\,\bar{\psi}_\alpha(1)\,\psi_\beta(6)\,|\,\sigma' P^{(+)'}\rangle = \\ &= \langle \sigma'' P^{(+)''}\,|\,\bar{\psi}^{(+)}_\alpha(1)\,\psi^{(-)}_\beta(6)\,|\,\sigma' P^{(+)'}\rangle \\ &+ \langle \sigma'' P^{(+)''}\,|\,\bar{\psi}^{(-)}_\alpha(1)\,\psi^{(+)}_\beta(6)\,|\,\sigma' P^{(+)'}\rangle, \end{aligned}$$

which is a consequence of the fact that terms containing two creation or two annihilation operators vanish when the number of particles is the same in the two states considered. The first of the terms on the right hand side is easily identified as the matrix element of the operator subtracted in (15), and the second becomes identical with the right hand side of (16) if one introduces the expansion (7) of $\bar{\psi}^{(-)}$ and $\psi^{(+)}$ and uses (11).

Similarly, we find

$$\left.\begin{aligned} &\langle \sigma'' P^{(+)''}\,|\,\left[\bar{\psi}_\alpha(1)\,\bar{\psi}_\beta(4)\,\psi_\gamma(6)\,\psi_\delta(3)\right]_{(1)}\,|\,\sigma' P^{(+)'}\rangle = \\ -i(2\pi)^{-3}\Big\{ &\bar{v}^{(-)}_\beta(\sigma'', \vec{P}'')\,v^{(+)}_\gamma(\sigma', \vec{P}')\exp i(P^{(+)'}6 - P^{(+)''}4)\cdot S^{(-)}_{\delta\alpha}(3-1) \\ &+ \bar{v}^{(-)}_\alpha(\sigma'', \vec{P}'')\,v^{(+)}_\delta(\sigma', \vec{P}')\exp i(P^{(+)'}3 - P^{(+)''}1)\cdot S^{(-)}_{\gamma\beta}(6-4) \\ &- \bar{v}^{(-)}_\beta(\sigma'', \vec{P}'')\,v^{(+)}_\delta(\sigma', \vec{P}')\exp i(P^{(+)'}3 - P^{(+)''}4)\cdot S^{(-)}_{\gamma\alpha}(6-1) \\ &- \bar{v}^{(-)}_\alpha(\sigma'', \vec{P}'')\,v^{(+)}_\gamma(\sigma', \vec{P}')\exp i(P^{(+)'}6 - P^{(+)''}1)\cdot S^{(-)}_{\delta\beta}(3-4)\Big\} \end{aligned}\right\} \quad (17)$$

Finally, using the same type of arguments, we obtain the matrix elements of the two particle part of the product of four ψ-functions. In the derivation, due regard must be paid to the minus signs introduced by the annihilation processes as illustrated by (14). The result is

$$
\begin{aligned}
&\langle P''\sigma'', \sigma^{\mathrm{iv}} P^{(+)\,\mathrm{iv}} \big| \left[\bar{\psi}_\alpha(1)\,\bar{\psi}_\beta(4)\,\psi_{\gamma'}(6)\,\psi_\delta(3)\right]_{(2)} \big| \sigma' P^{(+)\prime}, \sigma''' P^{(+)\prime\prime\prime}\rangle = \\
&= (2\pi)^{-6}\Big\{ \bar{v}_\alpha^{(-)}(\sigma^{\mathrm{iv}}, \vec{P}^{\mathrm{iv}})\,\bar{v}_\beta^{(-)}(\sigma^{\mathrm{iv}}, \vec{P}^{\mathrm{iv}})\,v_{\gamma'}^{(+)}(\sigma', \vec{P}')\,v_\delta^{(+)}(\sigma''', \vec{P}''') \\
&\quad \times \exp i\left\{P^{(+)\prime} 6 + P^{(+)\prime\prime\prime} 3 - P^{(+)\prime\prime} 1 - P^{(+)\,\mathrm{iv}} 4\right\} \\
&\quad - \bar{v}_\beta^{(-)}(\sigma'', \vec{P}'')\,\bar{v}_\alpha^{(-)}(\sigma^{\mathrm{iv}}, \vec{P}^{\mathrm{iv}})\,v_{\gamma'}^{(+)}(\sigma', \vec{P}')\,v_\delta^{(+)}(\sigma''', \vec{P}''') \\
&\quad \times \exp i\left\{P^{(+)\prime} 6 + P^{(+)\prime\prime\prime} 3 - P^{(+)\prime\prime} 4 - P^{(+)\,\mathrm{iv}} 1\right\} \\
&\quad - \bar{v}_\alpha^{(-)}(\sigma'', \vec{P}'')\,\bar{v}_\beta^{(-)}(\sigma^{\mathrm{iv}}, \vec{P}^{\mathrm{iv}})\,v_\delta^{(+)}(\sigma', \vec{P}')\,v_{\gamma'}^{(+)}(\sigma''', \vec{P}'''') \\
&\quad \times \exp i\left\{P^{(+)\prime} 3 + P^{(+)\prime\prime\prime} 6 - P^{(+)\prime\prime} 1 - P^{(+)\,\mathrm{iv}} 4\right\} \\
&\quad + \bar{v}_\beta^{(-)}(\sigma'', \vec{P}'')\,\bar{v}_\alpha^{(-)}(\sigma^{\mathrm{iv}}, \vec{P}^{\mathrm{iv}})\,v_\delta^{(+)}(\sigma', \vec{P}')\,v_{\gamma'}^{(+)}(\sigma''', \vec{P}''') \\
&\quad \times \exp i\left\{P^{(+)\prime} 3 + P^{(+)\prime\prime\prime} 6 - P^{(+)\prime\prime} 4 - P^{(+)\,\mathrm{iv}} 1\right\}\Big\}.
\end{aligned}
\tag{18}
$$

The corresponding results for the free meson field are the following. The meson wave functions can be decomposed into a positive and a negative frequency part $u^{(+)}$ and $u^{(-)}$, where $u^{(-)}$ is the creation operator and $u^{(+)}$ the annihilation operator of the field. The meson vacuum is defined by

$$
u^{(+)}\big|0\rangle = 0, \quad \langle o\big| u^{(-)} = 0 \tag{19}
$$

and the non-vanishing commutators are

$$
\begin{aligned}
[u^{(+)}(2), u^{(-)}(5)] &= i\Delta^{(+)}(2-5) \\
[u^{(-)}(2), u^{(+)}(5)] &= i\Delta^{(-)}(2-5)
\end{aligned}
\tag{20}
$$

in accordance with $\Delta^{(+)}(x) = -\Delta^{(-)}(-x)$. From (19) and (20) we get immediately the following vacuum expectation value used in the text

$$
\langle 0\big| u(2)\,u(5)\big|0\rangle = i\Delta^{(+)}(2-5). \tag{21}
$$

Introducing the quantity

$$\omega(\vec{p}) = \sqrt{\vec{p}^2 + m^2}, \quad p = (\vec{p}, i\omega) \tag{22}$$

$u^{(-)}$ and $u^{(+)}$ can be expanded

$$\left.\begin{aligned} u^{(+)} &= (2\pi)^{-\frac{3}{2}} \int \frac{1}{\sqrt{2\omega}} \cdot b(\vec{p})\, e^{ipx} d^{(3)}\vec{p} \\ u^{(-)} &= (2\pi)^{-\frac{3}{2}} \int \frac{1}{\sqrt{2\omega}} \cdot b^{\dagger}(\vec{p})\, e^{-ipx} d^{(3)}\vec{p} \end{aligned}\right\} \tag{23}$$

and the b's are seen to satisfy the commutation relations

$$[b(\vec{p}'), b^{\dagger}(\vec{p})] = \delta(\vec{p}' - \vec{p}). \tag{24}$$

A state with one meson present of momentum $\vec{p}$ is defined as

$$|\vec{p}\rangle = b^{\dagger}(\vec{p})\,|0\rangle \tag{25}$$

and it follows that the one particle part of $u(2)\,u(5)$ has the matrix elements

$$\left.\begin{aligned} &\langle \vec{p}'' \,|\, [u(2)\,u(5)]_{(1)} \,|\, \vec{p}' \rangle = \\ &= \frac{1}{2}(2\pi)^{-3} \left\{ \omega(\vec{p}'')\,\omega(\vec{p}') \right\}^{-\frac{1}{2}} \\ &\times [e^{i\{p'5 - p''2\}} + e^{i\{p'2 - p''5\}}]. \end{aligned}\right\} \tag{26}$$

Indleveret til selskabet den 17. april 1952.
Færdig fra trykkeriet den 20. november 1952.

Det Kongelige Danske Videnskabernes Selskab

Matematisk-fysiske Meddelelser, bind **27**, nr. 8

Dan. Mat. Fys. Medd. **27**, no. 8 (1952)

ON FIELD THEORIES WITH NON-LOCALIZED INTERACTION

BY

CLAUDE BLOCH

København

i kommission hos Ejnar Munksgaard

1952

CONTENTS

Printed in Denmark
Bianco Lunos Bogtrykkeri

Summary.

A relativistic field theory with non-localized interaction is investigated. The field equations are deduced by the variational principle from a Lagrange function containing an interaction term involving a form function. The essential departure from conventional field theory is the lack of causality, or, in other words, the lack of propagation character of the field equations. It is shown, however, that under certain conditions which must be satisfied by the form function this property remains limited to small domains. Similarly there are no continuity equations, but conservation laws hold in the large. The quantization is performed according to an extension of the scheme developed by YANG and FELDMAN making use of the concept of incoming and outgoing fields. It is shown that this procedure is always consistent with the field equations. Assuming that the field equations can be solved by means of power series expansions it is possible to give rules generalizing Feynman's rules giving all the terms of the expansion of an outgoing operator in terms of the incoming operators. Every term is associated with a doubled graph. An investigation is made of the convergence of the integrals obtained in this way. It is shown that many terms converge automatically as soon as the Fourier transform of the form function is supposed to fall off rapidly at large momenta. Some divergences remain in the higher order terms. They can, however, be removed by assuming that the Fourier transform of the form function has only time-like components. It is finally shown that the gauge invariance requires the addition of a new interaction term in the Lagrange function, corresponding to a sort of exchange current.

1. Introduction.

It has been shown by PEIERLS and MACMANUS[1] that it is possible to introduce a smearing function in a field theory in a Lorentz-invariant way. YUKAWA[2], on the other hand, has proposed a theory involving non-local fields, which, as will be shown later, is equivalent to an ordinary field theory with an interaction containing a form function, if one takes a variation principle as a starting point[3]. These theories cannot be put into a Hamiltonian form and, consequently, have met with some difficulty in quantization. Recently, however, a new treatment of conventional field theory was developed by YANG and FELDMAN[4] and by KÄLLÉN[5], which can immediately be applied to field theories involving smearing functions[6, 7]. It has therefore become possible to build a complete Lorentz-invariant quantized field theory with a non-localized interaction, and it may be worth while to investigate the consistency of such a scheme, and the convergence of the results it yields.

If we take, for simplicity, the example of a nucleon field interacting with a neutral scalar meson field, the scalar non-localized interaction term reads(*)

$$L_i = g \int dx' dx'' dx''' F(x', x'', x''') \psi^+(x') u(x'') \psi(x'''), \qquad (1,1)$$

where the form function F must be Lorentz invariant and such that contributions to L_i come only from the volume elements for which the three points x', x'', x''' are very near each other. By points near each other is meant points whose coordinates differ by amounts of the order of a characteristic length λ. The interaction (1,1) is Hermitian if the form function satisfies the condi-

(*) In this formula x stands for $x^1, x^2, x^3, x^4 = t$, and dx for $dx^1 dx^2 dx^3 dx^4$. We shall use units such that $\hbar = c = 1$. We shall write ab for the scalar product $\Sigma a^i b^i$, where $a_i = a^i$ for $i = 1, 2, 3$, and $a_4 = -a^4$. The metric tensor $g_{\mu\nu}$ is defined by $g_{\mu\nu} = 0$ if $\mu \neq \nu$, $g_{\mu\mu} = 1$, if $\mu = 1, 2, 3$, and $g_{44} = -1$.

tion $F(x''', x'', x') = F^{*}(x', x'', x''')$. The introduction of a form function in L_i corresponds to a kind of interaction which has no propagation character, and it is important that such effects should remain limited to small domains. Because of its Lorentz invariance F will remain finite for arbitrarily large distances of the points x', x'', x''' as long as they remain near the light cones of one another. Under certain conditions, however, compensations can occur in the neighborhood of the light cones in such a way that the corresponding volume elements do not contribute appreciably to the integral (1,1)[1]. A quantitative study of this effect will be made in section 2, and the conditions which F must satisfy will be established.

It may be of some interest to show that YUKAWA's non-local field theory leads to an interaction of the form (1,1) with a particular form function F. We may take, for instance, a non-local field U interacting with a conventional field ψ. The field U is a function of two points x' and x''' in space-time[2], and the field equations can be deduced from a variation principle involving the interaction term

$$L_i = g \int dx' dx''' \psi^{+}(x') (x' \,|\, U \,|\, x''') \psi(x'''). \qquad (1,2)$$

The field U can be represented by the Fourier integral

$$(x' \,|\, U \,|\, x''') = \int dk\, a(k)\, e^{ikX}\, \delta(kr)\, \delta(r^2 - \lambda^2),$$

where $X = (1/2)(x' + x''')$ and $r = x' - x'''$. If we associate with the field U the local field

$$u(x'') = \int dk\, a(k)\, e^{ikx''},$$

we can write (1,2) in the form of (1,1) with

$$F(x', x'', x''') = (2\pi)^{-4} \int dk\, e^{ik(X - x'')}\, \delta(kr)\, \delta(r^2 - \lambda^2).$$

Detailed investigation of this form function, however, shows that it does not yield convergent self-energies[8].

The non-localized interaction is also connected with the field theories involving higher order equations considered by several authors and systematically investigated by PAIS and UHLENBECK[9]. The general type of these equations is

$$f(\Box)u(x) = \varrho(x), \tag{1,3}$$

where $\varrho(x)$ is the source of the field. If f is an analytical function it can be factorized and each factor corresponds to a possible mass of the particles described by the field u. Theories with more than one mass, however, should be rejected because they introduce negative energies. The only acceptable equations (1,3) are then of the form

$$e^{f(\Box)}(\Box - m^2)u(x) = \varrho(x). \tag{1,4}$$

The differential operator $e^{f(\Box)}$ has an inverse and we can write (1,4) in the equivalent form

$$(\Box - m^2)u(x) = e^{-f(\Box)}\varrho(x) = \int dx'\, G(x - x')\varrho(x'), \tag{1,5}$$

where

$$G(x) = (2\pi)^{-4}\int dk\, e^{-f(-k^2)}\, e^{ikx}. \tag{1,6}$$

This is the equation which would be obtained with the interaction (1,1) and a form function $F = G(x'' - x')\,\delta(x' - x''')$. The possibility of transforming an equation such as (1,3) into an equation of the form (1,5) shows that one has to eliminate certain types of form functions corresponding to the introduction of particles with different masses and negative energy. If the Fourier transform of G has poles, G can be written

$$G(x) = (2\pi)^{-4}\int dk\, e^{ikx}\, g(-k^2) \Big/ \prod_i (k^2 + m_i^2), \tag{1,7}$$

and the equation (1,5) is equivalent to the multi-mass equation

$$\prod_i (-\Box + m_i^2)(\Box - m^2)\, u(x) = g(\Box)\varrho(x).$$

The function (1,7), however, behaves for large x like $\left|x^2\right|^{-3/4}$ as does every propagation function (the flux of the square of the function through a given solid angle is independent of the distance). The occurrence of additional masses will then be avoided if it is specified that the form functions should fall off for large x faster than propagation functions.

The field equations are deduced from the Lagrange function by the variation principle. Because of the introduction of a form function in the interaction the field equations are not ordinary differential equations, and the values of the field functions at

$t + dt$ are not simply defined in terms of the values at t. Consequently, the conservation equations do not hold in their differential form. It will be shown, however, that conservation laws hold in the large, in the sense that energy, momentum, angular momentum and electric charge at a time t, before any collision has taken place, are equal to the corresponding quantities after collision.

The quantization can be performed by postulating that the

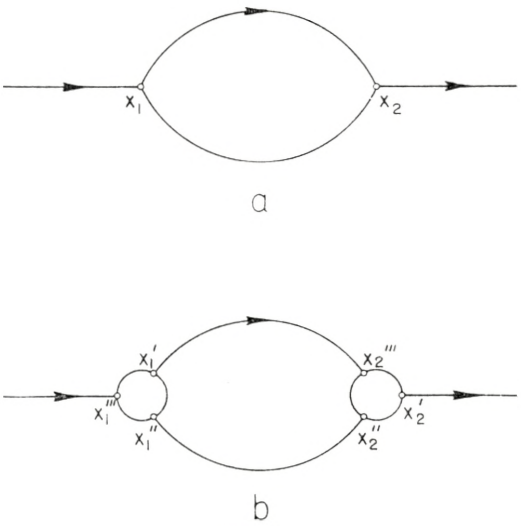

Fig. 1.

asymptotic values of the fields for $t = -\infty$ and $t = +\infty$ (called the incoming and the outgoing fields) satisfy the usual commutation relations of the free fields. It must then be shown that these commutation relations are consistent with the field equations. This can be done by using the fact that the constants of collision: energy, momentum, etc. . . . define the infinitesimal canonical transformations corresponding to the infinitesimal translations etc. . . . The S-matrix is then defined as the matrix which transforms the incoming fields into the outgoing fields.

Any outgoing operator can in principle be computed from the field equations as a power series of the incoming operators. The calculations are simplified by a set of rules similar to FEYNMAN's rules for electrodynamics[10]. These rules are used for an investigation of the convergence of the self-energies to all orders. The way in which convergence results from the introduction of

a form function in the interaction can easily be seen on the second order self-energy. The graph corresponding to the conventional field theory is represented on Fig. 1 a. To the lines going from x_1 to x_2 correspond functions of $x_1 - x_2$ which are singular on the light cone, and a divergence arises from the fact that the self-energy integral involves a product of two functions becoming singular at the same points. The small circles on Fig. 1 b correspond to the introduction of form functions $F(x', x'', x''')$, and it is seen that the divergence will disappear if F is a smooth function of $x' - x''$ and $x'' - x'''$. A rigorous treatment requires the use of the energy-momentum space. However, it can already be seen that the convergence of the self-energies of both types of particles requires that F be a smooth function of all three variables.

There is then a little difficulty when the interactions with the electromagnetic field are taken into account since the interaction term (1,1) is not gauge invariant. It will be shown, however, that a supplementary interaction term can be added to (1,1) in such a way that the sum is gauge invariant. This term describes the current due to the jumping of the charge between the points x_1''' and x_1', x_2''' and x_2'.

2. The form functions.

In this section we shall investigate under which conditions the non-localizability of the interaction is limited to dimensions of the order of a given length λ. We consider first a simple case:

A. *Functions of two points*[1]. In the conventional theory with a localized interaction the function F is a product of two four-dimensional Dirac functions: $F(x', x'', x''') = \delta(x' - x'')\,\delta(x'' - x''')$. As a first generalization we shall assume that F contains only one four-dimensional Dirac function: $F = \delta(\alpha' x' + \alpha'' x'' + \alpha''' x''')\,G$, where the scalar constants α', α'', α''' satisfy the relation $\alpha' + \alpha'' + \alpha''' = 0$. The factor G can be expressed as a function of two points only, x' and x'', for instance, if $\alpha''' \neq 0$. The invariance under translations and Lorentz transformations requires that G should be a function of $s = (x' - x'')^2$(*).

(*) For $s < 0$ the function G can also take two different values for the same value of s depending on whether $x_4' - x_4''$ is positive or negative. We shall come back to this later.

We shall now investigate under which conditions the form factor becomes very small as soon as x' and x'' are not very near one another. More precisely, considering the integral

$$I = \int dx' \, G(s) \, f(x'), \tag{2,1}$$

where $f(x')$ is an arbitrary smooth function, it should depend only on the values of $f(x')$ for x' very near x''. A first condition to be fulfilled is that $G(s)$ should fall off very rapidly as $|s|$ becomes much larger than λ^2. This condition, however, is not sufficient as $G(s)$ remains finite for x' near the light cone of x''. Thus, the contribution to I coming from the volume elements which are far from x'', but near the light cone of x'', requires a special investigation.

It is convenient to introduce the point x_0 of the light cone of x'' which is near x' and has the same three first coordinates. We call a the three-dimensional length of $x' - x''$ or $x_0 - x''$. We have $x_0^4 - x''^4 = \varepsilon a$, where ε is $+1$ or -1 depending on whether $x_0^4 - x''^4$ is positive or negative. The distance of x' to the light cone is conveniently defined by $\xi = \varepsilon (x_0^4 - x'^4)$. The relation between s and ξ is

$$s = 2 a \xi - \xi^2. \tag{2,2}$$

It shows that for large a a small variation of ξ corresponds to a large variation of s. As G is very small for large values of $|s|$, it follows that for large a we can expand the function f in powers of ξ around the light cone and extend the integration with respect to x'^4 or ξ from $-\infty$ to $+\infty$.

As we are interested in orders of magnitude only we shall omit all numerical coefficients. The Taylor expansion of f around the light cone reads

$$f(x') = f(\mathbf{x}_0, x_0^4 - \varepsilon\xi) \cong \sum_0^\infty \xi^k f_0^k,$$

where $f_0^k = (\partial/\partial x'^4)^k f(x')$ taken at the point $x' = x_0$. Finally, we replace the variable of integration x'^4 by s. We have

$$dx'^4 = ds/2\,(a - \xi) \cong (ds/a) \sum_0^\infty (\xi/a)^m,$$

and from (2,2) we deduce

$$\xi = a - (a^2 - s)^{1/2} \cong (s/a) \sum_0^\infty (s/a^2)^n .$$

Using all the preceding expansions the contribution to I of the neighborhood of the light cone of x'' can be written

$$\left.\begin{aligned} &\int dx' G(s) f(x') \cong \int d\boldsymbol{x}' ds \sum_0^\infty \xi^{k+m} G(s) f_0^k / a^{m+1} \cong \\ &\int d\boldsymbol{x}' ds \sum_0^\infty (s/a)^{k+m} (s/a^2)^n G(s) f_0^k / a^{m+1} \cong \int d\boldsymbol{x}' \sum_0^\infty M_{m+k} f_0^k / a^{2m+k+1} \end{aligned}\right\} \quad (2,3$$

where the M_n are the "moments" of the function G defined by

$$M_n = \int_{-\infty}^{+\infty} ds s^n G(s) .$$

The formula (2,3) shows how the contributions to I coming from the neighborhood of the light cone of x'' decrease with increasing distance a. Namely, if

$$M_0 = M_1 = M_2 = \cdots = M_{p-1} = 0 , \quad M_p \neq 0 , \qquad (2,4)$$

the contributions decrease as $(1/a)^{p+1}$. As the volume element $d\boldsymbol{x}'$ is proprotional to $a^2 da$, it is seen that the integral I extended to the whole space-time is convergent for any bounded function f with bounded derivatives if $p \geqslant 3$. The integral $\int dx' G(s)$ is convergent for $p \geqslant 2$.

It should be noted that integrals such as I are usually not absolutely convergent. The convergence is due to cancellations arising within the volume elements which are near the light cone of x''. In calculating such integrals, one must always use a method allowing these cancellations to take place. For instance, one can start by restricting the domain of integration to a finite part of space-time enclosed within a closed surface Σ, and then let Σ go to infinity. It is easily seen that the cancellations which make the integral I convergent will take place if the angle under which Σ cuts the light cone tends nowhere to zero. The possibility of defining in a Lorentz invariant way an integral which is not absolutely convergent clearly comes from the fact that the cancellations making the integral convergent take place within layers along the light cone which become infinitely narrow at infinity.

If for $s \leqslant 0$ the form function takes different values depending on the sign of x^4, it is convenient to write G as a sum of an even

function G_+ which is invariant under the substitution $x \to -x$, and of an odd function G_- which changes sign under the same substitution. It follows from the relativistic invariance that G_- must vanish for $s > 0$. It is easily seen that the functions G_+ and G_- must satisfy the conditions (2,4) independently.

For many calculations it is more appropriate to represent G by a Fourier integral

$$G(x) = \int dk\, e^{ikx} g(k), \tag{2,5}$$

where $g(k)$ is a function of the argument $q = k^2$, and can be represented by a sum of an even function g_+ and an odd function g_-. The Fourier transformation (2,5) gives then G_+ in terms of g_+, and G_- in terms of g_-. We shall now investigate which conditions must be satisfied by g_+ and g_- in order that the corresponding G should be an acceptable form function. This requires a closer investigation of the correspondence between G and g given by (2,5).

The integration in (2,5) with respect to the angular orientation of $\boldsymbol{k}$ yields

$$\begin{aligned} G(x) &= \frac{4\pi}{a} \int_{-\infty}^{+\infty} l\, dl \int_{-\infty}^{+\infty} dk^4 \operatorname{Sin} l a\, e^{-ik^4x^4} g(k) \\ &= -\frac{4\pi}{a} \frac{\partial}{\partial a} \int_{-\infty}^{+\infty} dl \int_{-\infty}^{+\infty} dk^4 \operatorname{Cos} l a\, e^{-ik^4x^4} g(k) \\ &= -\frac{2\pi}{a} \frac{\partial}{\partial a} \int_{-\infty}^{+\infty} dl \int_{-\infty}^{+\infty} dk^4\, e^{i(l a - k^4x^4)} g(k), \end{aligned}$$

where $a = |\boldsymbol{x}|$, and $|l| = |\boldsymbol{k}|$. Introducing now the decomposition of G and g into even and odd parts we get

$$\left.\begin{aligned} G_+(s) &= -\frac{2\pi}{a} \frac{\partial}{\partial a} \iint_{-\infty}^{+\infty} dl\, dk^4 e^{i(la - k^4x^4)} g_+(q), \\ G_-(s) &= -\frac{2\pi}{a} \frac{\partial}{\partial a} \iint_{-\infty}^{+\infty} dl\, dk^4 e^{i(la - k^4x^4)} \varepsilon(k^4)\, g_-(q), \end{aligned}\right\}$$

where $s = x^2$, $q = k^2$, and $\varepsilon(k^4) = k^4/|k^4|$. It should be noted that the precise definition of $G_-(s)$ is

$$G_-(x) = G_-(s) \text{ if } x^4 > 0, \quad G_-(x) = -G_-(s) \text{ if } x^4 < 0.$$

A similar definition holds for $g_-(q)$. Replacing the variables of integration l and k^4 by

$$\left.\begin{aligned} q = l^2 - (k^4)^2, \text{ and } \alpha = \frac{l - k^4}{a - x^4} \text{ if } a \neq x^4, \\ \text{or } \alpha = \frac{l + k^4}{a + x^4} \text{ if } a = x^4, \end{aligned}\right|$$

we get after some simple manipulations

$$\left.\begin{aligned} G_+(s) = -\frac{\pi}{a}\frac{\partial}{\partial a}\iint_{-\infty}^{+\infty}\frac{d\alpha\, dq}{\alpha}\,\varepsilon(\alpha)\, e^{(i/2)(\alpha s + q/\alpha)}\, g_+(q), \\ G_-(s) = -\frac{\pi}{a}\frac{\partial}{\partial a}\iint_{-\infty}^{+\infty}\frac{d\alpha\, dq}{\alpha}\, e^{(i/2)(\alpha s + q/\alpha)}\, g_-(q). \end{aligned}\right|$$

As $\frac{1}{a}\frac{\partial}{\partial a} = 2\frac{\partial}{\partial s}$, we can also write

$$\left.\begin{aligned} G_+(s) = -i\pi\iint_{-\infty}^{+\infty} d\alpha\, dq\, \varepsilon(\alpha)\, e^{(i/2)(\alpha s + q/\alpha)}\, g_+(q), \\ G_-(s) = -i\pi\iint_{-\infty}^{+\infty} d\alpha\, dq\, e^{(i/2)(\alpha s + q/\alpha)}\, g_-(q)^{(*)}. \end{aligned}\right| \quad (2,6)$$

The formulas (2,6) may be interpreted in the following manner. G is obtained from g by three successive transformations:

a) the Fourier transformation

$$\varphi(\beta) = \int_{-\infty}^{+\infty} dq\, e^{(i/2)\beta q}\, g(q),$$

b) the transformation

$$\psi_+(\alpha) = \varepsilon(\alpha)\varphi_+(1/\alpha), \text{ or } \psi_-(\alpha) = \varphi_-(1/\alpha),$$

c) the Fourier transformation

$$G(s) = -i\pi\int_{-\infty}^{+\infty} d\alpha\, e^{(i/2)\alpha s}\psi(\alpha).$$

(*) In this formula $g_-(q) = 0$ for $q > 0$. It follows then from Cauchy's theorem applied to the integration with respect to α that $G_-(s) = 0$ for $s > 0$.

We shall use this decomposition to find the properties of g sufficient that G defined by (2,5) shall be an acceptable form function.

The conditions which must be satisfied by G are:

$$\left.\begin{array}{l} 1)\ \text{to be continuous;} \\ 2)\ \text{to go to zero as } |s| \to \infty\ , \text{ for instance as } (1/s)^k; \\ 3)\ \int_{-\infty}^{+\infty} ds s^n G(s) = 0, \quad \text{for } n = 0, 1, \ldots, p-1. \end{array}\right\} \quad (2,7)$$

As regards the condition 2), one might require that $G(s)$ should tend to zero much faster than we assume here, exponentially for instance. It seems, however, natural to require only that G behaves for large s in such a way that its integral over the whole space-time is convergent. The condition 2) with $k \geq 3$ is then sufficient. The convergence of the moments involved in the condition 3) requires in fact $k \geq p + 1$(*). The condition assumed here seems natural in view of the fact that the contribution to the integral (2,1) coming from the neighborhood of the light cone never decreases faster than an inverse power of the distance.

Sufficient conditions for $\psi(\alpha)$ corresponding to (2,7) are that ψ must have k continuous derivatives such that

$$\left.\begin{array}{l} 1)\ \int_{-\infty}^{+\infty} d\alpha\, |\psi(\alpha)| < \infty\ ; \\ 2)\ \int_{-\infty}^{+\infty} d\alpha\, |\psi^{(n)}(\alpha)| < \infty\ , \text{ for } n = 1, 2, \ldots, k\text{(**)}; \\ 3)\ \psi^{(n)}(0) = 0, \qquad \text{for } n = 0, 1, \ldots, p-1. \end{array}\right\} \quad (2,8)$$

The derivatives of ψ (with respect to α) are given in terms of the derivatives of φ (with respect to β) by the formula

$$\psi^{(n)}(\alpha) \simeq \sum_{m=1}^{m=n} \beta^{m+n} \varphi^{(m)}(\beta), \quad (2,9)$$

where $\beta = 1/\alpha$, and where the numerical coefficients have been

(*) The expansion (2,3) requires the existence of moments of all orders i. e. an exponential decrease of G for large s. The whole argument, however, can be carried through by means of limited asymptotic expansions only. The condition we have assumed is then sufficient.

(**) Here we make use of a well-known theorem on the aysmptotic value of Fourier integrals; see for instance, S. Bochner, Fouriersche Integrale, Chelsea Publishing Co., New York, p. 11.

omitted. The presence in the relation between φ_+ and ψ_+ of the factor $\varepsilon(\alpha)$ which has a discontinuous variation at $\alpha = 0$ does not modify the equation (2,9) since the function ψ and all its derivatives involved here vanish at $\alpha = 0$ (this follows from 3 for the $p - 1$ first derivatives and for the derivatives of the order $p, p+1, \ldots, k$ from the behavior of $\varphi^{(m)}$ at infinity as indicated below).

It is seen from (2,9) that we must assume that φ has k continuous derivatives. From the condition 1) it follows that φ must be such that

$$\int_{-\infty}^{+\infty} \frac{d\beta}{\beta^2} |\varphi(\beta)| < \infty .$$

This condition is satisfied if we assume that φ is bounded for $\beta = \pm\infty$, is regular at $\beta = 0$, and that $\varphi(0) = \varphi'(0) = 0$. Finally, it is easily seen that the conditions 2) are satisfied if we assume that $\varphi^{(m)}(\beta)$ $(m = 1, 2, \ldots, k)$ behaves at infinity as $(1/\beta)^{m+k}$. The conditions 3) are then automatically satisfied. From the relations $\varphi(0) = \varphi'(0) = 0$ it follows that

$$\int_{-\infty}^{+\infty} dq g(q) = \int_{-\infty}^{+\infty} dq q g(q) = 0 . \tag{2,10}$$

On the other hand,

$$\varphi^{(m)}(\beta) \cong \int_{-\infty}^{+\infty} dq e^{(i/2)\beta q} q^m g(q);$$

and this function behaves at infinity as $(1/\beta)^{m+k}$ if $q^m g(q)$ has $m + k$ continuous derivatives absolutely integrable from $-\infty$ to $+\infty$ (Bochner loc. cit.). As m takes the values $1, 2, \ldots, k$ we are led to the following conditions:

$$\left.\begin{array}{l} g(q) \text{ is continuous and has } 2k \text{ continuous derivatives;} \\ g^{(n)}(q)\ (n = 0, 1, \ldots, 2k) \text{ goes to zero as } q \to \pm\infty \\ \quad \text{faster than } (1/q)^{k+1}. \end{array}\right\} \tag{2,11}$$

The condtitions (2,10 and 11) are sufficient to insure that $G(s)$ satisfies (2,7). The function $g_-(q)$ vanishes for $q > 0$. It follows then from the continuity of the $2k$ first derivatives that

$$g_-^{(n)}(0) = 0, \text{ for } n = 0, 1, \ldots, 2k. \tag{2,12}$$

The conditions (2, 10 and 11) allow us to choose functions $g(q)$ which vanish outside a certain interval. In such a case, $g(q)$ and its $2k$ first derivatives must vanish at the ends of the interval.

The function $G_-(s)$ can be expressed in terms of the usual function D of field theory. Performing in (2,5) first the integration at q constant, and then the integration over q, we get indeed

$$G_-(s) = (2\pi)^3 i \int_{-\infty}^{0} dq\, g_-(q) D(s, q), \qquad (2,13)$$

where $D(s, q)$ is the function corresponding to the mass $\sqrt{-q}$. If we assume that $g_+(q)$ is different from zero only if $q < 0$ (which implies that $g_+^{(n)}(0) = 0$, for $n = 0, 1, \ldots, 2k$), we can, similarly, express $G_+(s)$ in terms of $D^{(1)(11)}$:

$$G_+(s) = (2\pi)^3 \int_{-\infty}^{0} dq\, g_+(q) D^{(1)}(s, q). \qquad (2,14)$$

The expressions (2,13 and 14) are identical with those used in the theory of regularization[12]. The relations (2,10) also belong to the latter theory. They express the condition that the singularities of the functions D and $D^{(1)}$ at $s = 0$ should not appear in $G(s)$. The conditions (2,11), however, are in contradiction with the limiting process used in the idealistic renormalization, or with the introduction of a discrete set of masses. Consequently, the behavior for large s of a form function is essentially different from that of a regularized function.

It may be noted, finally, that the transformations considered in this section are special cases of the Fourier-Bessel transformation[13]. The transformation of the odd functions, for instance, can be written

$$r G_-(r) = 2 i \pi^2 \int_0^{+\infty} \varkappa d\varkappa J_1(\varkappa r) \varkappa g_-(\varkappa),$$

where $r = \sqrt{-s}$, and $\varkappa = \sqrt{-q}$.

B. *Functions of three points.* As it was shown in section 1, the form function should actually be a smooth function of all three variables. It will then be a function of the invariants(*)

$$s = (x'' - x''')^2, \qquad t = (x''' - x')^2, \qquad u = (x' - x'')^2.$$

(*) These invariants are not entirely independent. No triangle x', x'', x''' exists if s, t and u are negative and if $s^2 + t^2 + u^2 - 2st - 2tu - 2us < 0$.

First of all, the form function should fall off rapidly as s, t, or u becomes large (strictly speaking, one could also require that F falls off as any of two only of the quantities s, t, u becomes large). There are, however, large triangles x', x'', x''' for which s, t and u are small. The contribution to an integral such as

$$I = \int dx'\, dx''\, dx'''\, F\, f(x', x'', x''') \tag{2,15}$$

coming from such triangles can be investigated by the same method as for the functions of two variables. Let a, b and c be the lengths of the space parts of $x'' - x'''$, $x''' - x'$ and $x' - x''$, respectively, and suppose that $a \geqslant b \geqslant c$. For a large triangle a and b at least will be large compared with λ. Let x_0 and x_1 be the points of the light cone of x''' which are near x' and x'', and have the same space coordinates. We have

$$x_1^4 - x'''^4 = \varepsilon a, \qquad x_0^4 - x'''^4 = \varepsilon b, \quad \cdot \quad \varepsilon = \pm 1.$$

Introducing the distances of x' and x'' to the light cone of x''' by

$$\xi = \varepsilon (x_1^4 - x''^4), \qquad \eta = \varepsilon (x_0^4 - x'^4), \tag{2,16}$$

we have

$$s = 2a\xi - \xi^2, \qquad t = 2b\eta - \eta^2. \tag{2,17}$$

Again, we can carry out the integration in I with respect to x'^4 and x''^4 using Taylor expansions around the light cone of x'''. It is then convenient to replace the variables x'^4 and x'^4 by s and t with the help of (2,16) and (2,17). An additional complication comes from the fact that u is now a function of s and t since all three quantities are functions of x'^4 and x''^4 (or ξ and η). It is readily found that

$$u = c^2 - (a-b)^2 + (a-b)\left(\frac{s}{a} - \frac{t}{b}\right) + (a-b)\left(\frac{\xi^2}{a} - \frac{\eta^2}{b}\right) - (\xi - \eta)^2,$$

which shows that when the triangle becomes large the quantity $q = c^2 - (a-b)^2$ must remain finite. It is one of the parameters which define the way in which the triangle is increasing. As other parameter we can take $a/b = \mu$, and we have then

$$u = (1-\mu)(t - s/\mu) + q + \ldots,$$

where the omitted terms are quadratic in ξ and η. We can then expand F in Taylor series in ξ and η around $u = (1-\mu)(t-s/\mu)+q$. One finally finds for the contribution of the large triangles the expansion

$$I = \int d\boldsymbol{x}'\, d\boldsymbol{x}''\, dx''' \sum_{0}^{\infty} \frac{M^{(j+j')/2}_{m+j+k,\, m'+j'+k'}(\mu, q)\, f_0^{kk'}}{a^{2m+j+k+1}\, b^{2m'+j'+k'+1}}, \qquad (2{,}18)$$

where $f_0^{kk'} = (\partial/\partial x'^4)^k (\partial/\partial x'^4)^{k'} f(x', x'', x''')$ taken at $x' = x_0$, $x'' = x_1$, and $M^j_{n,n'}(\mu, q)$ is the derivative of the order j with respect to q of the moment

$$M_{n,n'}(\mu, q) = \int ds\, dt\, s^n\, t^{n'}\, F(s, t, (1-\mu)(t-s/\mu)+q).$$

It is seen from (2,18) that if F satisfies the conditions

$$M_{n,n'}(\mu, q) = 0, \quad \text{for } n + n' \leq p-1,$$

for all relevant values of μ and q, the contribution of the large triangles decreases as $(1/a)^{p+2}$. Thus, we have extended the result obtained for the form functions of two variables.

We shall not go any further into the analysis of the general case since it is much more complicated than for the functions of two points. Moreover, form functions of three points can be built by means of form functions of two points, and this procedure may be sufficient for practical purposes. For instance, we may take

$$F(x', x'', x''') = G^*(x'-x'')\, G(x''-x'''),$$

or, more symmetrically,

$$F(x', x'', x''') = \int dx\, G^*(x'-x)\, H(x''-x)\, G(x'''-x). \qquad (2{,}19)$$

The use of such a form function corresponds to replacing the field functions by "smeared fields", as defined by PEIERLS and MACMANUS[1].

The Fourier transform of the function (2,19) is particularly simple. It is the product of the Fourier transforms of the three functions G^*, H and G occurring in F and of the four-dimensional Dirac function $\delta(k'+k''+k''')$.

The results of this section show that the conditions under which a form function behaves like a smeared δ-function have nothing

to do with the condition that its Fourier transform should resemble that of a δ-function. This is due to the non-positive definite character of the distance in space-time. It follows that the behavior for $\lambda \to 0$ of the Fourier transform of a form function gives very little information about the behavior of the function itself. In particular, a form function defined by a Fourier transform $g(k)$ such that $\lim_{\lambda \to 0} g(k) = 1$ may very well give rise for λ small to undesirable interactions transmitted with the velocity of light over large distances, or having no propagation character.

3. Conservation equations.

Taking the usual expressions for the Lagrange functions of the free particles, and the expression (1,1) for the interaction term, we obtain from the variation principle the field equations

$$\left.\begin{aligned} &\left(\gamma^\mu \frac{\partial}{\partial x^\mu} + M\right)\psi(x) + g\int dx''dx'''F(x,x''x''')u(x'')\psi(x''') = 0, \\ &-\frac{\partial \psi^+(x)}{\partial x^\mu}\gamma^\mu + M\psi^+(x) + g\int dx'dx''F(x',x'',x)\psi^+(x')u(x'') = 0, \\ &(-\Box + m^2)u(x) + g\int dx'dx'''F(x',x,x''')\psi^+(x')\psi(x''') = 0. \end{aligned}\right\} \quad (3,1)$$

In order to prove the existence of conservation equations it is convenient to introduce the integral L_Ω obtained by restricting the domain of integration in L to a finite part Ω of space-time. In the interaction term L_i it is sufficient to restrict to Ω the integration of only one variable x'' for instance. We thus consider

$$L_\Omega = \int_\Omega dx\, H(x), \text{ where } H(x) = H_0(x) + H_i(x),$$

in which H_0 is the free particle term and

$$H_i(x) = g\int dx'dx'''F(x',x,x''')\psi^+(x')u(x)\psi(x''').$$

We call E_Ω the field equations deduced from L_Ω by the variational principle. The equations (3,1) will then be called E_∞. The difference between the equations E_Ω and E_∞ is that in the two first equations the integration with respect to x'' is extended to Ω in-

stead of the whole space-time. The difference is very small if x is inside Ω at a distance large compared with λ of the boundary Σ of Ω. This follows from the property of the form function $F(x', x'', x''')$ that it gives contributions to the integral L_i only if the points x', x'', x''' are at distances of the order of λ from one another.

In what follows we shall consider only collision problems. This means that we assume that very far in the past and very far in the future the particles do not interact. The equations E_Ω and E_∞ are then very nearly identical everywhere if Ω is so large that no collision takes place outside Ω or near its boundary.

It should be noted that it is not quite correct to neglect the interaction term outside Ω. Even if the particles do not interact, the existence of the interaction creates self-energies which modify the rest masses of the particles. This can be taken into account by adding to H_i a renormalization term $H_i' = -[\Delta M \psi^+ \psi + (\Delta m^2/2) u^2]$, where ΔM and Δm^2 should be chosen in such a way that the interaction $H_\mathrm{I} = H_i + H_i'$ does not give rise to any self-energy. With this modification the quantities M and m occurring in (3,1) are the real observed masses of the particles, and it is justified to neglect H_I if the particles described by the field are very far from each other.

Finally we see that considering a solution ψ, u of the equations E_∞, it is possible to find a domain Ω such that the equations E_Ω have a solution approximating ψ, u inside Ω and on Σ as closely as required. It follows that if a conservation equation on the boundary Σ of Ω holds for any solution of E_Ω, the same conservation equation will hold for the solutions of E_∞ on Σ if Ω is large enough.

Let us assume now that ψ and u are solutions of the equations E_Ω and consider an arbitrary variation of ψ and u; we have

$$\delta L_\Omega = \frac{1}{2} \int_\Sigma d\sigma_\mu \left(\psi^+ \gamma^\mu \delta\psi - \delta\psi^+ \gamma^\mu \psi + \frac{\partial u}{\partial x_\mu} \delta u + \delta u \frac{\partial u}{\partial x_\mu} \right), \quad (3,2)$$

where $d\sigma_\mu$ is the surface element on Σ pointing toward the outside. If the variations of the fields correspond to a displacement of the fields defined by δx^μ, the variation δL_Ω can be computed directly by making use of the invariance of the Lagrange function under

displacements. The difference between the integral of the displaced fields and the non-displaced fields is readily found

$$\delta L_{\Omega} = -\int_{\Sigma} d\sigma_{\mu} \delta x^{\mu} H(x). \tag{3,3}$$

From (3,2) and (3,3) we obtain the general conservation equation

$$\int_{\Sigma} d\sigma_{\mu} \left[\frac{1}{2} \left(\psi^{+} \gamma^{\mu} \delta\psi - \delta\psi^{+} \gamma^{\mu} \psi + \frac{\partial u}{\partial x_{\mu}} \delta u + \delta u \frac{\partial u}{\partial x_{\mu}} \right) + \delta x^{\mu} H \right] = 0. \tag{3,4}$$

If the displacement is an infinitesimal translation

$$\delta x_{\mu} = \varepsilon_{\mu}, \qquad \delta\psi = -\frac{\partial \psi}{\partial x_{\mu}} \varepsilon_{\mu}, \text{ etc. } \cdots\cdots$$

the equation (3,4) becomes

$$\int_{\Sigma} d\sigma_{\nu} T^{\mu\nu} = 0, \tag{3,5}$$

where

$$T^{\mu\nu} = \frac{1}{2} \left((\psi^{+} \gamma^{\nu} \frac{\partial \psi}{\partial x_{\mu}} - \frac{\partial \psi^{+}}{\partial x_{\mu}} \gamma^{\nu} \psi \right) + \frac{\partial u}{\partial x_{\mu}} \frac{\partial u}{\partial x_{\nu}} - g^{\mu\nu} H \tag{3,6}$$

can be identified as the energy-momentum tensor of the system. The same method applied to the infinitesimal Lorentz transformations leads to the conservation equation of angular momentum. The Lagrange function is also invariant under gauge transformations

$$\psi \to e^{i\alpha} \psi, \quad \psi^{+} \to e^{-i\alpha} \psi^{+}, \quad \alpha = \text{constant}.$$

The corresponding infinitesimal transformation

$$\delta\psi = i\delta\alpha\psi, \quad \delta\psi^{+} = -i\delta\alpha\psi^{+}, \quad \delta u = 0$$

gives $\delta L_{\Omega} = 0$. From (3,2) we obtain then the conservation equation

$$\int_{\Sigma} d\sigma_{\nu} j^{\nu} = 0, \tag{3,7}$$

where

$$j^{\nu} = i\varepsilon\psi^{+}\gamma^{\nu}\psi \tag{3,8}$$

is the four-vector current-charge.

It should be noted that in the conservation equations (3,5) and (3,7) the surface Σ is not arbitrary; it is the boundary surface

of the volume Ω occurring in L_Ω. It follows that the usual continuity equations

$$\frac{\partial T^{\mu\nu}}{\partial x^\nu} = 0, \qquad \frac{\partial j^\nu}{\partial x^\nu} = 0 \tag{3,9}$$

do not hold if the interaction is non-localized.

It may be of interest to show this more directly. The calculation is simpler for the conservation equation of electric charge. Let us multiply as usual the first of the equations (3,1) on the left-hand side by $\psi^+(x)$, the second on the right-hand side by $\psi(x)$ and subtract. This gives

$$\left.\begin{aligned}\frac{\partial}{\partial x^\nu}(\psi^+\gamma^\nu\psi) = g\Big[&\int dx'dx''F(x', x'', x)\psi^+(x')u(x'')\psi(x)\\ -&\int dx''dx'''F(x, x'', x''')\psi^+(x)u(x'')\psi(x''')\Big].\end{aligned}\right\} \tag{3,10}$$

The right-hand side of (3,10) vanishes of course if F is different from zero only if $x' = x'''$, as in the case of a localized interaction. It does not vanish, however, in general, but if we integrate equation (3,10) over a domain Ω the contribution of the right-hand side reads

$$\left.\begin{aligned}g\Big[&\int_{\Omega'} dx' \int dx''dx'''\\ -&\int_{\Omega'} dx''' \int dx'dx''\Big] F(x', x'', x''')\psi^+(x')u(x'')\psi(x'''),\end{aligned}\right\} \tag{3,11}$$

where Ω' is the part of space-time lying outside Ω. If the interaction term H_I vanishes outside Ω, then (3,11) vanishes and we obtain the conservation equation (3,7).

It will be useful to consider domains Ω limited by two space-like surfaces $\sigma_{(1)}$ and $\sigma_{(2)}$ very far in the past and in the future, respectively. Defining then the quantities

$$G^\mu = \int_\sigma d\sigma_\nu T^{\mu\nu}, \qquad Q = \int_\sigma d\sigma_\nu j^\nu, \tag{3,12}$$

where $d\sigma_\nu$ is the surface element on σ such that $d\sigma_4 > 0$; the equations (3,5) and (3,7) show that G^μ and Q have the same value if $\sigma = \sigma_{(1)}$ or if $\sigma = \sigma_{(2)}$. These quantities are thus constants of collision[14]; they represent the total energy-momentum and electric charge of the system.

4. Quantization.

If all the calculations of the preceding section are carried out in such a way that the order of the factors is always preserved, the results will still hold if the field functions are non-commuting operators. In order to complete the formulation of the theory, we must still define the commutation relations of the field functions. It is not easy to find directly commutation relations which are consistent with the field equations (3,1). In the conventional theory one postulates the commutation relations of the field functions at all points of a space-like surface, and one shows that these relations still hold on any other space-like surface. This is possible because the field equations have one and only one solution for any arbitrary initial conditions given on a space-like surface. It is not easy to see what the corresponding problem is for the field equations (3,1). On the one hand, the knowledge of the field functions on a space-like surface is not sufficient to define the field functions even in the neighborhood of the initial surface. On the other hand, it is not clear that the field functions can be given arbitrary values on a space-like surface. This makes the extension of the canonical method of quantization difficult.

The situation, however, simplifies if one considers a space-like surface very far in the past or very far in the future. Because of the assumption that the interactions are negligible in the distant past and future, the commutation relations on such a surface must in the limit be identical with the conventional commutation relations of free fields. This suggests that the quantization method to be used in the present case will be to postulate the commutation relations for the asymptotic values of the field functions for $x^4 \to \pm \infty$.

The most convenient mathematical method to find the solutions of a differential system with given boundary values is to transform the system into a system of integral equations by means of the Green's functions corresponding to the boundary values considered. The boundary values that we have here are the values for $x^4 \to -\infty$. The corresponding Green's functions are the retarded ones defined by

$$\left.\begin{aligned} &\left(\gamma^\mu \frac{\partial}{\partial x^\mu} + M\right) S_+(x) = -\delta(x), \\ &(-\Box + m^2) D_+(x) = -\delta(x), \\ &\text{and } S_+(x) = D_+(x) = 0 \text{ if } x^4 < 0. \end{aligned}\right\} (4,1)$$

As it will be important in what follows that the interaction term vanishes before and after the collision, it is necessary to use the renormalized interaction

$$L_I = L_i - \int dx \left(\Delta M \psi^+ \psi + \frac{\Delta m^2}{2} u^2\right);$$

and in order to simplify the writing we shall introduce the notation of variational derivatives. The field equations (3,1) read then

$$\left.\begin{aligned} &\left(\gamma^\mu \frac{\partial}{\partial x^\mu} + M\right) \psi(x) + \frac{\delta L_I}{\delta \psi^+(x)} = 0, \\ &-\frac{\partial \psi^+(x)}{\partial x^\mu} \gamma^\mu + M \psi^+(x) + \frac{\delta L_I}{\delta \psi(x)} = 0, \\ &(-\Box + m^2) u(x) + \frac{\delta L_I}{\delta u(x)} = 0, \end{aligned}\right\} (4,2)$$

where, for instance,

$$\frac{\delta L_I}{\delta \psi^+(x)} = g \int dx'' dx''' F(x, x'', x''') u(x'') \psi(x''') - \Delta M \psi(x), \text{ etc. } \cdots$$

Using now the retarded Green's functions we can transform the system (4,2) into the equivalent system of integral equations

$$\left.\begin{aligned} \psi(x) &= \psi^{in}(x) + \int dx' S_+(x - x') \frac{\delta L_I}{\delta \psi^+(x')} \\ \psi^+(x) &= \psi^{+in}(x) + \int dx''' \frac{\delta L_I}{\delta \psi(x''')} S_+^+(x - x''') \\ u(x) &= u^{in}(x) + \int dx'' D_+(x - x'') \frac{\delta L_I}{\delta u(x'')} \end{aligned}\right\} (4,3)$$

where the fields ψ^{in} and u^{in} satisfy the free field equations. The retarded Green's functions are different from zero only inside the past part of the light cone, and as we assume throughout that the interactions are negligible far in the past, we see that the second

term in equations (4,3) becomes very small as $x^4 \to -\infty$. It follows that the fields ψ^{in} and u^{in} represent asymptotically ψ and u as $x^4 \to -\infty$. They describe the incoming particles.

The integral equations (4,3) can formally be solved by iteration to all orders of approximation for arbitrary incoming fields. It is natural to postulate that the incoming fields satisfy the conventional commutation relations of free fields

$$\left.\begin{aligned} \left[\psi^{\text{in}}(x_1),\ \psi^{\text{in}}(x_2)\right]_+ &= \left[\psi^{+\,\text{in}}(x_1),\ \psi^{+\,\text{in}}(x_2)\right]_+ = 0, \\ i\left[\psi^{\text{in}}_{\varrho}(x_1),\ \psi^{+\,\text{in}}_{\sigma}(x_2)\right]_+ &= S_{\varrho\sigma}(x_1 - x_2), \\ \left[\psi^{\text{in}}(x_1),\ u^{\text{in}}(x_2)\right] &= \left[\psi^{+\,\text{in}}(x_1),\ u^{\text{in}}(x_2)\right] = 0, \\ i\left[u^{\text{in}}(x_1),\ u^{\text{in}}(x_2)\right] &= D(x_1 - x_2), \end{aligned}\right\} \quad (4,4)$$

where $[A, B] = AB - BA$, $[A, B]_+ = AB + BA$. The commutation relations (4,4) are clearly consistent with the field equations (4,3). The commutation relations of the fields ψ and u can in principle be deduced from the relations (4,4) with the help of the field equations (4,3).

The above considerations can be repeated with the boundary conditions for $x^4 \to +\infty$. We introduce the advanced Green's functions S_- and D_- which satisfy the same equations as the retarded Green's functions but vanish for $x^4 > 0$. They lead to the integral equations

$$\left.\begin{aligned} \psi(x) &= \psi^{\text{out}}(x) + \int dx'\, S_-(x - x')\frac{\delta L_{\text{I}}}{\delta \psi^+(x')}, \\ \psi^+(x) &= \psi^{+\,\text{out}}(x) + \int dx'''\, \frac{\delta L_{\text{I}}}{\delta \psi(x''')}\, S^+_-(x - x'''), \\ u(x) &= u^{\text{out}}(x) + \int dx''\, D_-(x - x'')\frac{\delta L_{\text{I}}}{\delta u(x'')}, \end{aligned}\right\} \quad (4,5)$$

where ψ^{out} and u^{out} are free fields, which are asymptotically identical with ψ and u as $x^4 \to +\infty$, and represent the outgoing particles. The outgoing fields should, of course, satisfy also the free field commutation relations. In fact the commutation relations of the outgoing fields can in principle be deduced from the commutation relations of the incoming fields with the help of the equations (4,3) and (4,5). We have to show that the relations obtained in this way are similar to the relations (4,4).

This can easily be done with the help of the constants of collision defined in the preceding section. These constants can be computed with the incoming or outgoing fields. For instance, the total electric charge before collision is given by

$$Q(\text{in}) = i\varepsilon \int_{\sigma} d\sigma_\nu \psi^{+\,\text{in}} \gamma^\nu \psi^{\text{in}},$$

where σ is any arbitrary space-like surface. The same applies to the energy-momentum and the angular momentum before and after collision, and the conservation equations read now

$$G^\mu(\text{in}) = G^\mu(\text{out}), \qquad Q(\text{in}) = Q(\text{out}), \cdots \tag{4,6}$$

It is a well known property that the commutator of any incoming field function with an incoming constant of collision is related to the corresponding infinitesimal transformation by the equations

$$\left.\begin{aligned} [A, G^\mu(\text{in})] &= -i\frac{\partial A}{\partial x^\mu} \\ [A, Q(\text{in})] &= -i\frac{\partial A}{\partial \alpha}, \cdots \end{aligned}\right\} \tag{4,7}$$

for any incoming field quantity A. In the second equation (4,7) α is the parameter occurring when use is made of an arbitrary gauge (ψ^{in} is proportional to $e^{i\varepsilon\alpha}$, $\psi^{+\,\text{in}}$ is proportional to $e^{-i\varepsilon\alpha}$ and u^{in} independent of α). A similar equation connects the angular momentum of the system and the infinitesimal Lorentz transformations. It is easily seen that if two quantities A and B satisfy the relations (4,7), $A + B$ and AB satisfy the same relations. It follows that any quantity which can be built by algebraic operations from quantities satisfying the relations (4,7) also satisfies these relations. In particular the outgoing fields satisfy the relations (4,7), and taking into account the conservation equations (4,6) we get

$$[A, G^\mu(\text{out})] = -i\frac{\partial A}{\partial x^\mu}, \text{ etc.} \cdots \text{ where } A = \psi^{+\,\text{out}}, u^{\text{out}}, \text{ or } \psi^{\text{out}}. \tag{4,8}$$

From these relations it can be deduced that the commutation relations of the outgoing fields are similar to the relations (4,4). The detailed proof is given in the appendix.

In the present theory we have been using the Heisenberg representation. The situation of the particles before a collision is described by certain operators, the incoming field functions, and by a certain state vector Ψ in Hilbert space. After the collision the operators are changed into the outgoing field functions, but the state vector remains the same. In the interaction representation the initial situation is described by operators which can be identified with the present incoming field functions and by a state vector $\Psi(\text{in})$ which can be identified with Ψ. The situation after the collision is described by the same operators, but by a different state vector $\Psi(\text{out})$. The unitary matrix S which transforms $\Psi(\text{in})$ into $\Psi(\text{out})$ according to $\Psi(\text{out}) = S\Psi(\text{in})$ is the collision matrix, and the squares of the absolute values of its elements give the transition probabilities. The situation after the collision could as well be described by the state vector $S^{-1}\Psi(\text{out}) = \Psi(\text{in})$ and the operators $S^{-1}\psi^{\text{in}}S$, $S^{-1}u^{\text{in}}S$, $\cdots$. In a theory with a localized interaction the formalisms using the Heisenberg representation or the interaction representation are of course equivalent, so we must have

$$\psi^{\text{out}} = S^{-1}\psi^{\text{in}}S, \qquad u^{\text{out}} = S^{-1}u^{\text{in}}S. \tag{4,9}$$

If the interaction is non-localized we do not know the interaction representation. However, as the outgoing fields satisfy the same commutation relations as the incoming fields, we know that there exists a unitary matrix S satisfying the relations (4,9). It is then natural to define this matrix as the collision matrix.

The equations (4,3), (4,4), (4,5) and (4,9) give a complete self-consistent formulation of the theory. These equations can, in principle, be solved by successive approximations. In fact, we need practical rules giving a way of computing any matrix element of S. Such rules will be given in the following sections.

5. Solution of the field equations.

We shall first consider the case where the interaction is a conventional local interaction

$$I_1 = \int dx H_{\text{I}}(x),$$

where

$$H_{\mathrm{I}}(x) = g\psi^{+}(x)u(x)\psi(x) - \Delta M\psi^{+}(x)\psi(x) - (\Delta m^2/2)u^2(x).$$

We assume that the solution of the field equations (4,3) can be expanded into powers of the constants g, ΔM and Δm^2, and we set

$$\psi(x) = \sum_0^{\infty}(-i)^n\psi^{(n)}(x), \qquad u(x) = \sum_0^{\infty}(-i)^n u^{(n)}(x), \quad (5,1)$$

where $\psi^{(n)}(x)$ and $u^{(n)}(x)$ are of the order n with respect to the constants g, ΔM and Δm^2. The zero order approximation is of course given by the incoming fields. The first order approximation is easily computed, and the value of $\psi^{(1)}$, for instance, is

$$\psi^{(1)}(x) = i\int dx'\, S_{+}(x-x')\frac{\delta L_{\mathrm{I}}^{\mathrm{in}}}{\delta\psi^{+}(x')}, \qquad (5,2)$$

where $L_{\mathrm{I}}^{\mathrm{in}}$ is equal to L_{I} with the field functions replaced by the corresponding incoming field functions.

It is well known that the function S occurring in the commutation relations is connected to the Green's functions by

$$S(x) = S_{-}(x) - S_{+}(x).$$

As $S_{+}(x)$ vanishes if $x^4 < 0$, and $S_{-}(x)$ vanishes if $x^4 > 0$, it follows that

$$\left.\begin{aligned} S_{+}(x) &= -S(x) \quad \text{if } x^4 > 0, \\ &= 0 \qquad\quad \text{if } x^4 < 0. \end{aligned}\right\} \quad (5,3)$$

Similarly

$$\left.\begin{aligned} S_{-}(x) &= 0 \qquad\quad \text{if } x^4 > 0, \\ &= S(x) \quad \text{if } x^4 < 0. \end{aligned}\right\} \quad (5,4)$$

Similar relations hold for the D functions.

The relations (5,3) show that the expression (5,2) can also be written

$$\psi^{(1)}(x) = \int_{x^4 > x'^4} dx'\,[\psi^{\mathrm{in}}(x),\ \psi^{+\mathrm{in}}(x')]_{+}\frac{\delta L_{\mathrm{I}}^{\mathrm{in}}}{\delta\psi^{+}(x')}$$

or still

$$\psi^{(1)}(x) = \int_{x^4 > x'^4} dx'\,[\psi^{\mathrm{in}}(x),\ H_{\mathrm{I}}^{\mathrm{in}}(x')]. \qquad (5,5)$$

Similar formulas hold for $\psi^{+(1)}(x)$ and $u^{(1)}(x)$. The generalization of these formulas to higher orders is obvious. Let $A(x)$ be any field function; the term of order n in its expansion is given by

$$A^{(n)}(x_0) = \int_{x_0 > x_1 > \cdots > x_n} dx_1 dx_2 \cdots dx_n \,[\cdots[[A^{\text{in}}(x_0),\, H_1,],\, H_2],\cdots H_n], \quad (5{,}6)$$

where H_n has been written for $H_{\text{I}}^{\text{in}}(x_n)$, and $x_i > x_j$ for $x_j^4 > x_j^4$. Formula (5,6) is well known in field theory, and is usually deduced from the Schrödinger equation. It can also be obtained from the field equations (4,3) by induction (see appendix III).

The next step is the calculation of the outgoing fields. We again assume expansions in power series

$$\psi^{\text{out}}(x) = \sum_0^\infty (-i)^n \psi^{\text{out}\,(n)}(x), \quad u^{\text{out}}(x) = \sum_0^\infty (-i)^n u^{\text{out}\,(n)}(x). \quad (5{,}7)$$

By subtraction of the equations (4,3) from the equations (4,5) we get for the outgoing fields the expressions

$$\psi^{\text{out}}(x) = \psi^{\text{in}}(x) - \int dx'\, S(x - x') \frac{\delta L_{\text{I}}}{\delta \psi^+(x')}, \text{ etc.} \cdots.$$

The zero order approximation is thus given by the incoming fields, and the first order approximation is readily found to be

$$\psi^{\text{out}\,(1)}(x) = \int dx' \,[\psi^{\text{in}}(x),\ H_{\text{I}}^{\text{in}}(x')], \quad (5{,}8)$$

and similar formulas for $\psi^{+\,\text{out}\,(1)}$ and $u^{\text{out}\,(1)}$. These formulas can be generalized by induction, and it can be shown that the term of order n of any outgoing field quantity A^{out} is given by

$$A^{\text{out}\,(n)}(x) = \int_{x_1 > x_2 > \cdots > x_n} dx_1 dx_2 \cdots dx_n \,[[\cdots[A^{\text{in}}(x),\, H_1],\, H_2],\cdots H_n\,]. \quad (5{,}9)$$

We shall now extend the preceding expressions to the case of a non-localized interaction. It will be convenient to write the interaction term in the form

$$L_{\text{I}} = \int dx' dx'' dx''' H_{\text{I}}(x', x'', x'''),$$

where

$$\left.\begin{aligned} H_{\text{I}}(x', x'', x''') &= gF(x', x'', x''')\psi^+(x')u(x'')\psi(x''') \\ -\delta(x' - x'')\delta(x'' - x''') &\{\Delta M \psi^+(x')\psi(x''') - (\Delta m^2/2)u^2(x'')\}. \end{aligned}\right\} \quad (5{,}10)$$

The first order terms can be computed as in the preceding case, and are given by

$$\left.\begin{aligned} \psi^{(1)}\ (x) &= \int_{x>x'} dx'dx''dx'''\,[\psi^{\text{in}}\ (x),\ H_1(x', x'', x''')], \\ \psi^{+(1)}(x) &= \int_{x>x'''} dx'dx''dx'''\,[\psi^{+\,\text{in}}(x),\ H_1(x', x'', x''')], \\ u^{(1)}\ (x) &= \int_{x>x''} dx'dx''dx'''\,[u^{\text{in}}\ (x),\ H_1(x', x'', x''')]. \end{aligned}\right\} \quad (5{,}11)$$

It should be noted in these formulas that the domain of integration of only one of the three variables occurring in H_1 is restricted by an inequality. This variable is different depending on the field function which is being computed; it is the variable of the field function which does not commute with the field function which is being computed. This is because the inequalities appear when a Green's function is replaced by a commutator (or anticommutator) of two field functions. This complication makes it impossible to extend directly the formulas (5,6) and (5,9).

It will be convenient in what follows to make use of some conventions and notations. We shall always call x' (sometimes provided with an index) the argument of a function ψ^+, x'' the argument of a function u, x''' the argument of a function ψ. We shall write ψ_n for $\psi^{\text{in}}(x_n''')$, u_n for $u^{\text{in}}(x_n'')$, ψ_n^+ for $\psi^{+\,\text{in}}(x_n')$, and H_n for $H_1^{\text{in}}(x_n', x_n'', x_n''')$. Finally, ξ_n will stand for the three points x_n', x_n'', x_n''', and $d\xi_n$ for $dx_n'dx_n''dx_n'''$.

We shall now try to extend the formulas (5,6) and (5,9) to the case of a non-localized interaction. These formulas are obtained from the field equations by a certain number of algebraic operations: additions, multiplications, integrations. The same operation can be performed as well with a non-localized interaction, and the result should be very similar. The only difference, in fact, lies in the inequalities.

This leads us to consider also in the case of non-localized interaction expressions such as

$$E_n = [\cdots[[\psi_0,\ H_1],\ H_2], \cdots H_n].$$

If we develop E_n by computing first the commutator of ψ_0 with H_1, then the commutator of the result with H_2, and so on, the

result is a sum of terms T, each of which is a product of form functions, of field functions, and of n "elementary" commutators or anticommutators such as $[\psi_i^+, \psi_j]_+$, or $[u_i, u_j]$. These commutators (or anticommutators) associate some of the variables $x_1', x_1'', \cdots x_n'''$ by groups of two. For instance, the two elementary commutators mentioned as examples associate x_i' with x_j''', and x_i'' with x_j'', respectively.

Let us call $I(T)$ the set of inequalities expressing that in all the groups of two variables associated by the elementary commutators or anticommutators of the term T, the variable with the lower index should correspond to a time later than the variable with higher index. There are n inequalities for each term T. They define a domain $D(T)$ which is different for every term. The same decomposition can be performed in the case of a localized interaction, with the only difference that the form functions disappear and that $x_i' = x_i'' = x_i''' = x_i$.

It can easily be seen by analyzing the way in which the successive approximations are obtained from the field equations in the case of a localized interaction, that the terms of the order n appear at first as sums of products of field functions and of n Green's functions. The next step consists in replacing the Green's functions by the corresponding commutators or anticommutators. The domains of integration must then be restricted by certain inequalities. The terms obtained in this way are precisely the terms T obtained by decomposition of E_n, and the inequalities associated with each term are clearly the inequalities $I(T)$. By a further transformation it is possible to replace the inequalities $I(T)$ by the inequalities $\mathrm{I}: x_0 > x_1 > \cdots > x_n$. Since the domain of integration is then the same for all the terms, it becomes possible to put the sum of all the terms T into the compact form E_n, and one gets the final formula (5,6). In the case of a non-localized interaction all the operations can be performed in the same way, except the last transformation. Thus, we must try to extend to the case of a non-localized interaction the expressions of the successive approximations as sums of T terms.

A few definitions will be useful.

We shall call $P(T)$ the set of all the permutations of the indexes 1, 2, . . . n such that in every inequality of $I(T)$ the variable indicated as corresponding to the later time keeps an index lower than the index of the other variable.

$N(T)$ will be the number of the permutations of $P(T)$ (unity included).

Finally we shall call terms equivalent to T the terms deduced from T by a permutation of the indexes belonging to $P(T)$.

These definitions apply as well to localized and non-localized interactions.

As an example, let us consider the following term of E_4 (the form functions have not been written down):

$$T = g^3(-\Delta m^2/2)\,[\psi_0, \psi_1^+]_+\,[\psi_1, \psi_2^+]_+\,[u_1, u_3]\,[u_2, u_4]\,u_3\,\psi_4^+\psi_4\psi_2,$$

which is one of the terms coming from the terms in g of H_1, H_2 and H_4, and from the term in $(-\Delta m^2/2)$ of H_3. The inequalities $I(T)$ are

$$I(T) : x_0''' > x_1', \quad x_1''' > x_2', \quad x_1'' > x_3'', \quad x_2'' > x_4''.$$

The permutations $P(T)$ are besides unity the permutations (2,3) and (3,4) which transform the inequalities $I(T)$ into

$$(2,3) : x_0''' > x_1', \quad x_1''' > x_3', \quad x_1'' > x_2'', \quad x_3'' > x_4'',$$
$$(3,4) : x_0''' > x_1', \quad x_1''' > x_2', \quad x_1'' > x_4'', \quad x_2'' > x_3''.$$

The following properties are easily shown:

a) Equivalent terms integrated over their associated domains give identical results.

b) If T belongs to the development of E_n, all the terms equivalent to T also belong to the development of E_n.

c) In the case of a localized interaction ($x' = x'' = x'''$), the domain $D(T)$ is the sum of the domain D defined by $I : x_0 > x_1 > \cdots > x_n$, and of the domains deduced from D by the permutations of $P(T)$.

As an example of property c), the domain

$$D(T) : x_0 > x_1, \quad x_1 > x_2, \quad x_1 > x_3, \quad x_2 > x_4$$

is the sum of the domains

$$D : x_0 > x_1 > x_2 > x_3 > x_4, \qquad (2,3)D : x_0 > x_1 > x_3 > x_2 > x_4,$$
$$(3,4)D : x_0 > x_1 > x_2 > x_4 > x_3.$$

It will now be possible to make a precise comparison of the expression (5,6) with the development of E_n. According to b)

the terms in the development of E_n can be collected into families of $N(T)$ equivalent terms. From a) and c) it follows that the sum of $N(T)$ equivalent terms integrated over the domain D is equal to any one of the terms of the family integrated over its associated domain. As we know from (5,6) that $\psi^{(n)}(x_0)$ is the sum of all T terms integrated over the domain D, we see that

$$\psi^{(n)}(x_0) = \sum_T (1/N(T)) \int_{D(T)} dx_1 dx_2 \cdots dx_n \; T, \qquad (5,12)$$

where the summation is extended to all the terms T of the development of E_n. One could also omit the factor $1/N(T)$ and instead say that only one term in each family of equivalent terms should be taken into account, and it is easily seen that this is exactly the expression obtained by a straightforward calculation from the field equations.

The extension to the case of a non-localized interaction is now obvious, and we shall write symbolically

$$\psi^{(n)}(x_0) = \int_t d\xi_1 d\xi_2 \cdots d\xi_n [\cdots [[\psi^{\text{in}}(x_0'''), H_1], H_2] \cdots H_n], \quad (5,13)$$

where $\int_t$ is a "time ordered integration" and should be computed in the following way:

a) The integrand must be developed into a sum of T terms.
b) Each term should be integrated over the domain $D(T)$.
c) Each integral should be multiplied by $1/N(T)$.

The formulas (5,11) are clearly particular cases of (5,13). The general formula can be obtained directly from the field equations by induction (see appendix III). The outgoing fields are given by formulas differing from (5,13) only by the fact that all inequalities involving x_0', x_0'', or x_0''' should be omitted. In order that the indexes should remain specifically connected with time ordering, it is convenient then to suppress the index 0 and to write

$$\psi^{\text{out}(n)}(x''') = \int_t d\xi_1 d\xi_2 \cdots d\xi_n [\cdots [[\psi^{\text{in}}(x''), H_1], H_2], \cdots H_n]. \quad (5,14)$$

The domains of integrations are now independent of the points at which the field functions are being computed. This gives the

possibility of a useful generalization of the equations (5,14). Let A^{in} be a polynomial of the incident field functions or, more generally, a power series. The field functions can be taken at different points, and A will depend on a certain number of points in space-time. The value of the same polynomial (or series) of the outgoing field functions taken at the same points is given by

$$A^{\text{out}} = \sum_{n=0}^{\infty} (-i)^n A^{\text{out}(n)}, \tag{5,15}$$

where

$$A^{\text{out}(n)} = \int_l d\xi_1 d\xi_2 \cdots d\xi_n [\cdots [A^{\text{in}}, H_1], H_2], \cdots H_n]. \tag{5,16}$$

The proof is given in appendix III. As an example, let us take for A^{in} the expressions $[\psi^{+\text{in}}(x'), \psi^{\text{in}}(x''')]_+$, $[\psi^{+\text{in}}(x'), u^{\text{in}}(x'')]$, etc. $\cdots$ As these quantities are c-numbers, all terms in the expansions (5,15) vanish, except the first term. Thus, $A^{\text{out}} = A^{\text{in}}$, and this proves again that the commutation relations of the outgoing fields are the same as those of the incoming fields.

A few remarks should be added to the results of this section.

1. *Lorentz invariance.* The domains $D(T)$ are not Lorentz invariant. If the vector joining x_i and x_j is space-like, the time ordering of the two points has no invariant meaning. This time ordering matters for a term T only if T has as a factor a commutator (or anticommutator) of two field functions at the points x_i and x_j. As this commutator (or anticommutator) vanishes if $x_i - x_j$ is space-like, it is seen that the integrated formula is Lorentz invariant.

2. *The Schrödinger equation.* Let us consider in the case of a localized interaction the field functions taken at arbitrary points on a space-like surface σ. In the equations (5,6) the inequality $x_0 > x_1$ can without changing the value of the integral be replaced by the condition that x_1 should be in the past region of space-time with respect to σ. Thus, the domain of integration in (5,6) can be chosen in such a way that it is the same for all the field functions on all points of σ. It follows that if A^{in} is a polynomial of the incoming fields taken at various points of σ, the same polynomial of the fields ψ^+, u and ψ taken at the same points is given by an expansion similar to (5,15), where the term of the order n is given by

$$A^{(n)} = \int_{\sigma > x_1 > x_2 > \cdots > x_n} dx_1 dx_2 \cdots dx_n \left[\cdots \left[[A^{\text{in}}, H_1], H_2 \right], \cdots H_n \right].$$

If A is a commutator (or anticommutator) of two field functions, it is seen that $A = A^{\text{in}}$. Thus, the commutation relations of the field functions *on a space-like surface* σ are identical with those of the incoming field functions. Hence, a unitary matrix $S(-\infty, \sigma)$ exists such that

$$A(x_0) = S^{-1}(-\infty, \sigma) A^{\text{in}}(x_0) S(-\infty, \sigma), \qquad (5,17)$$

where A is ψ^+, u or ψ and x_0 any point on σ. The Schrödinger equation is (in the Tomonaga—Schwinger form[15]) the differential equation giving the variations of $S(-\infty, \sigma)$ corresponding to infinitesimal variations of the surface σ.

In the case of a non-localized interaction, it is not possible to use the same domains of integration for computing all the field functions on a space-like surface. The equations (5,11), for instance, show that for the first order terms already, the domain of integration unavoidably depends on which field function is being computed. Then the commutation relations of the field functions on a space-like surface are not the same as those of the incoming fields, and there is no matrix satisfying the equations (5,17). This explains why there cannot be any Schrödinger equation if the interaction is non-localized, and shows that one has to use a formalism giving directly the matrix $S = S(-\infty, +\infty)$.

6. Outgoing operators.

Before starting any actual calculation, it is necessary to antisymmetrize the Lagrange function in ψ and ψ^+ so as to introduce the correct interpretation of the negative energy states as antiparticles. Thus, the expression (5,10) for the interaction term should be replaced by

$$\left.\begin{aligned} & H_{\text{I}}(x', x'', x''') = \\ & (g/2) F(x', x'', x''') \left(\psi^+(x') u(x'') \psi(x''') - \psi(x''') u(x'') \psi^+(x')\right) \\ & - \delta(x' - x'') \delta(x'' - x''') \left\{ (\Delta M/2) \left(\psi^+(x') \psi(x''') - \psi(x''') \psi^+(x')\right) \right. \\ & \left. - (\Delta m^2/2) u^2(x'') \right\}. \end{aligned}\right\} \qquad (6,1)$$

This clearly does not modify the general conclusions of the preceding sections. In particular the rules given for the calculation of the outgoing fields still apply.

The Fourier expansion of any free field is a superposition of plane waves e^{iKx}, where K is always a time-like vector. Hence, it is possible to split in a Lorentz invariant way any field function in two parts for which K^4 is positive or negative, respectively. Thus, we can write for the incoming fields (in what follows the incoming fields will be called ψ and u without the subscript in)

$$\left.\begin{aligned} \psi(x) &= \psi^{(+)}(x) + \psi^{(-)}(x), \\ \psi^{+}(x) &= \psi^{+(+)}(x) + \psi^{+(-)}(x), \\ u(x) &= u^{(+)}(x) + u^{(-)}(x). \end{aligned}\right\} \quad (6,2)$$

In the decomposition (6,2), $\psi^{(+)}$ and $\psi^{+(-)}$ are annihilation and creation operators of nucleons, respectively; $\psi^{+(+)}$ and $\psi^{(-)}$ are annihilation and creation operators of antinucleons; $u^{(+)}$ and $u^{(-)}$ are annihilation and creation operators of mesons[11]. These operators are related to one another by the equations

$$(\psi^{(+)})^{+} = \psi^{+(-)}, \quad (\psi^{(-)})^{+} = \psi^{+(+)}, \quad u^{(+)*} = u^{(-)}. \quad (6,3)$$

The operators introduced in (6,2) commute or anticommute except creation and annihilation operators of the same particles. For these pairs of operators the commutation relations are

$$\left.\begin{aligned} i\left[\psi_{\varrho}^{(+)}(x_1), \psi_{\sigma}^{+(-)}(x_2)\right]_{+} &= S_{\varrho\sigma}^{(+)}(x_1 - x_2), \\ i\left[\psi_{\varrho}^{(-)}(x_1), \psi_{\sigma}^{+(+)}(x_2)\right]_{+} &= S_{\varrho\sigma}^{(-)}(x_1 - x_2), \\ i\left[u^{(+)}(x_1), u^{(-)}(x_2)\right] &= D^{(+)}(x_1 - x_2), \\ i\left[u^{(-)}(x_1), u^{(+)}(x_2)\right] &= D^{(-)}(x_1 - x_2), \end{aligned}\right\} \quad (6,4)$$

where $S^{(+)}$ and $S^{(-)}$, $D^{(+)}$ and $D^{(-)}$ are the positive and negative frequency parts, respectively, of S and D.

An important notion in field theoretical calculations is that of "ordered product" of operators[16]. It is defined as follows:

a) The ordered product: $abc\cdots$: of the creation or annihilation operators a, b, $c\cdots$ is equal to the product $abc\cdots$ re-ordered in such a way that all annihilation operators are at the right-hand

side of the creation operators, multiplied by $(-)^p$, where p is the number of permutations of nucleon operators involved in the reordering procedure.

b) The definition is extended to products of field functions by decomposing the various factors into sums of creation and annihilation operators, and by postulating the distributivity of the ordered product with respect to addition.

The importance of the ordered products comes from the fact that when an ordered product acts on a state vector a particle cannot be created by one of the factors and reabsorbed by another factor. Thus, all virtual particles have been eliminated, and it is easy to select the relevant terms for a particular problem. In this connection it is important to be able to transform any product of operators into a sum of ordered products. This is most conveniently done by introducing the notion of "contractions."

For two field functions a and b the contraction $a^{\cdot}b^{\cdot}$ is defined as the difference between the regular and the ordered products by(*)

$$ab = :ab: + a^{\cdot}b^{\cdot}. \tag{6,5}$$

The only non-vanishing contractions are given by the following relations which are easily deduced from (6,4)

$$\left.\begin{aligned} \psi_\varrho^{\cdot}(x_1)\psi_\sigma^{+\cdot}(x_2) &= (-i)S_{\varrho\sigma}^{(+)}(x_1 - x_2), \\ \psi_\varrho^{+\cdot}(x_2)\psi_\sigma^{\cdot}(x_1) &= (-i)S_{\varrho\sigma}^{(-)}(x_1 - x_2), \\ u^{\cdot}(x_1)u^{\cdot}(x_2) &= (-i)D^{(+)}(x_1 - x_2). \end{aligned}\right\} \tag{6,6}$$

A contraction within an ordered product is defined by

$$:a \cdots bc^{\cdot}d \cdots ef^{\cdot}g \cdots: = (-)^p c^{\cdot}f^{\cdot} :a \cdots bd \cdots eg \cdots:, \tag{6,7}$$

where p is the number of permutations of nucleon operators necessary in order to bring the factors c and f beside one another.

The transformation of a product of field functions into a sum of ordered products is now given by the following identity[16]:

$$abcd \cdots = :abcd \cdots: + \sum :a^{\cdot}b^{\cdot}cd \cdots:, \tag{6,8}$$

where the summation is extended to all possible contractions of the factors a, b, c, $\cdots$

(*) This definition is that of HOURIET and KIND[16].

It should be noted finally that the order of the factors in an ordered product can be changed arbitrarily, with only a change of sign if an odd permutation of the nucleon operators has been performed.

The results of the preceding section together with the identity (6,8) make it possible to express any function of the outgoing operators as a sum of ordered products of incoming operators. Each term may be associated with a doubled Feynman graph. The rules will now be given for a single outgoing operator. These rules generalize some of the results obtained by DYSON[17].

Graph. A graph consists of directed lines (nucleon lines), of undirected lines (meson lines), and of vertices of the following types:

a) g-vertices consisting of three points x', x'', x''' on a small circle with an undirected line arriving at x'', and two directed lines arriving at x' and x''', directed away from x' and toward x''';

b) Δm^2-vertices and ΔM-vertices consisting of a single point with two undirected lines or two directed lines of different directions, respectively;

c) one incoming vertex consisting of p points with a line arriving at each of them;

d) one outgoing vertex consisting of one point with one line. The line arriving at the outgoing vertex is an undirected line, a line directed toward the vertex or a line directed away from the vertex, depending on whether the field function which is being computed is u^{out}, ψ^{out} or $\psi^{+\,\text{out}}$.

Doubled graph. Some of the lines of the graph must be considered as doubled lines. The doubled lines should be drawn in such a way that it is possible to go from any vertex (the incoming vertex excepted) to the outgoing vertex by a uniquely defined path consisting of doubled lines only. This can be pictured by saying that all vertices except the incoming vertex are lying on the branches of a "tree" having its root at the outgoing vertex and forks at some of the g-vertices. It follows that all graphs are connected, and it is easily seen that the number of doubled lines is equal to the number of vertices, incoming and outgoing vertices excluded. The lines arriving at the incoming or outgoing vertices will be called incoming or outgoing lines.

Orientation of the graph. The doubled lines and the incoming lines are oriented toward the outgoing vertex. Every g-vertex should be oriented in the following sense. At every g-vertex arrive one double line oriented away from the vertex and two other lines l_1, l_2. To orient the vertex means to draw an arrow from one of the lines l_1, l_2 toward the other, in an arbitrary way. Consider finally an undoubled line joining two vertices a and b. It is possible to go from a and b to the outgoing vertex by following doubled lines only. The two paths meet at a vertex ξ. The line ab is then oriented according to the orientation of ξ.

Examples of such graphs will be given in the next section (see Fig. 2).

To each graph corresponds a term in the development of the outgoing operator. It is an integral of a product of terms associated with each line and each vertex of the graph. It is convenient to use the energy-momentum variables. A four-vector k is then associated with every line of the graph, and the various factors will be listed now.

We shall write only the factors corresponding to the undirected lines from which the factors corresponding to the directed lines can be deduced by replacing m by M and by multiplying by $(ik^\mu\gamma_\mu - M)$ or $(-ik^\mu\gamma_\mu - M)$ depending on whether the orientation and the direction are parallel or antiparallel.

a) For the doubled lines (except the outgoing line) the factor is

$$D_+(k) = (-1)/(k^2 + m^2), \text{ or } S_+, \text{ or } S_+^{\pm}, \tag{6,9}$$

where the integration with respect to k^4 should be taken in the complex plane along a contour passing above the two singularities.

b) For the undoubled lines the factor is

$$D^{(+)}(k) = (-\pi)\,(1 + \varepsilon(k))\,\delta(k^2 + m^2), \text{ etc. } \cdots, \tag{6,10}$$

where $\varepsilon(k)$ is $+1$ or -1 depending on whether k^4 is positive or negative.

c) For the outgoing line the factor is

$$D(k) = (-2i\pi)\,\varepsilon(k)\,\delta(k^2 + m^2), \text{ etc. } \cdots. \tag{6,11}$$

d) Finally, to the incoming lines is associated an ordered product of factors $u(k)\,\delta(k^2 + m^2)$, $\psi^+(k)\,\delta(k^2 + M^2)$, or $\psi(k)\ \delta(k^2 + M^2)$, where

$$u(k)\delta(k^2 + m^2) = \int dx\, u^{\text{in}}(x) e^{-ikx}, \text{ etc.} \cdots.$$

To each undirected line, to each directed line with direction and orientation parallel or antiparallel corresponds a factor u, ψ or ψ^+, respectively.

The factors corresponding to Δm^2-, ΔM-, and g-vertices are in the case where all lines are oriented toward the vertex

$$\left.\begin{aligned} &(-\Delta m^2/2)\delta(k_1 + k_2), \quad -\Delta M \delta(k_1 + k_2), \text{ and} \\ &(g/2)\Phi(k', k'', k''')\delta(k' + k'' + k''') = \\ &(g/2)(2\pi)^{-6}\int d\xi F(x', x'', x''') e^{i(k'x' + \cdots)}, \end{aligned}\right\} \quad (6{,}12)$$

where k', k'', k''' are the vectors associated with the lines arriving at x', x'', x'''. For every line oriented away from the vertex, k should be replaced by $-k$ in (6,12).

Finally, summation should be made over the spinor indexes, the term should be multiplied by $1/N(T)$ and a certain power of i, and integrated over all variables. The outgoing operator is obtained by taking into account all possible graphs and all possible orientations of the vertices.

As for the justification of the preceding rules we only mention that the doubled lines correspond to the elementary commutators, and the undoubled lines to the contractions. The orientation of a vertex corresponds to the effect of the choice of a term $\psi^+ u \psi$ or $\psi u \psi^+$ in the interaction term (6,1) on the order of the operators occurring in the T-term.

The extension to products of outgoing operators is obvious. The only change is that there will be an outgoing line corresponding to every factor of the product. These lines are oriented with respect to one another in the following way: the orientation goes from the line a to the line b when the factor corresponding to a in the product is at the left of the factor corresponding to b.

7. Self-energies.

It has been assumed throughout that ΔM and Δm^2 are chosen in such a way that the interaction term is negligible when the particles described by the field are far apart. We shall now com-

pute the values of ΔM and Δm^2 for which this assumption holds.

An equivalent, but more precise formulation of the same assumption is to state that the interaction term should be rigorously negligible if the system contains zero or one particle. In the interaction representation this fact is described by the equation

$$S|) = |), \tag{7,1}$$

where $|)$ is the vacuum state or a state in which only one particle is present. The corresponding properties of the incoming and outgoing fields follow from

$$A^{\text{out}} = S^* A^{\text{in}} S, \tag{7,2}$$

where A is any field function. In order to avoid complicated notations we shall use a simplified model in which states are characterized only by the number of particles. Moreover, we shall assume the existence of only one kind of particles. The basic vectors may then be represented by $|0), |1), \cdots |n), \cdots$, where $|n)$ is the state in which n particles are present. In this representation the conditions (7,1) read

$$(n|S|0) = \delta_{0n}, \quad (n|S|1) = \delta_{1n}, \tag{7,3a}$$

where δ_{mn} is 0 if $m \neq n$ and 1 if $m = n$. From the unitarity condition of S it follows that

$$(0|S|n) = \delta_{0n}, \quad (1|S|n) = \delta_{1n}. \tag{7,3b}$$

The relation (7,2) can be written

$$(i|A^{\text{out}}|j) = \sum_{m,n} (i|S^*|m)\,(m|A^{\text{in}}|n)\,(n|S|j). \tag{7,4}$$

For $j = 0$, the equation (7,4) specializes into

$$(i|A^{\text{out}}|0) = \sum_{m} (i|S^*|m)\,(m|A^{\text{in}}|0), \tag{7,5}$$

where the conditions (7,3) have been taken into account. If A is a pure annihilation operator $A^{(+)}$, then $A^{(+)\text{in}}|0) = 0$, and from (7,5) it follows that

$$A^{(+)\text{out}}|0) = 0, \tag{7,6}$$

which is the equation of conservation of vacuum. If A is a creation operator $A^{(-)}$, its only non-vanishing matrix element is $(1\,|\,A^{(-)\,\mathrm{in}}\,|\,0)$, and from (7,3) and (7,5) it follows that

$$A^{(-)\,\mathrm{out}}\,|\,0) = A^{(-)\,\mathrm{in}}\,|\,0). \tag{7,7}$$

Putting now $j = 1$ into (7,4) we get

$$(i\,|\,A^{\mathrm{out}}\,|\,1) = \sum_m (i\,|\,S^*\,|\,m)\,(m\,|\,A^{\mathrm{in}}\,|\,1), \tag{7,8}$$

and a simple relation is obtained only if A is an annihilation operator. It follows then from (7,3) and (7,8) that

$$A^{(+)\,\mathrm{out}}\,|\,1) = A^{(+)\,\mathrm{in}}\,|\,1). \tag{7,9}$$

No simple relation is obtained for $j > 1$. The relation (7,9) is in fact a consequence of (7,6) and (7,7), and of the commutation relations

$$[A^{(+)\,\mathrm{in}},\ A^{(-)\,\mathrm{in}}] = [A^{(+)\,\mathrm{out}},\ A^{(-)\,\mathrm{out}}] = 1. \tag{7,10}$$

On multiplying (7,10) on the right-hand side by $|0)$ and on taking (7,6) into account we get

$$A^{(+)\,\mathrm{out}}\,A^{(-)\,\mathrm{out}}\,|\,0) = A^{(+)\,\mathrm{in}}\,A^{(-)\,\mathrm{in}}\,|\,0). \tag{7,11}$$

The equation (7,9) follows from (7,11) if one takes into account (7,7) and the fact that $A^{(-)\,\mathrm{in}}\,|\,0)$ is a multiple of $|\,1)$. Thus, the basic relations are (7,6) and (7,7). It is in fact a matter of simple algebra to show that, conversely, these relations have the relations (7,3) as consequences (apart from an irrelevant phase factor).

For the actual system, equations similar to (7,6) and (7,7) should hold with $A = \psi^+$, u or ψ. We shall see that the equations (7,6) are identically satisfied, whereas the equations (7,7) define the self-energies ΔM and Δm^2.

Let A be any of the field functions. The Fourier component $A^{\mathrm{out}}(k)$ is, according to the results of the preceding section, given by a sum of terms

$$A^{\mathrm{out}}(k) = \sum_n \int dk_1 \cdots dk_j K_n(k_1, \cdots k_j) : a_1(k_1) \cdots a_j(k_j) :, \tag{7,12}$$

where K_n is a c-number function, and where the k_i satisfy

$$k = \sum k_i, \quad (k_i)^2 + m_i^2 = 0. \tag{7,13}$$

Only the creation parts of the operators a will give contributions to $A^{\text{out}}|0)$. Thus we may in (7,12) restrict the domain of integration to the vectors k such that

$$k_i^4 < 0. \tag{7,14}$$

If $A = A^{(+)}$ is an annihilation operator all its Fourier components are such that $k^4 > 0$. It follows then from (7,13 and 7,14) that $A^{(+)\,\text{out}}|0)$ vanishes identically.

We consider now the case where $A = A^{(-)}$ is a creation operator. Then K_n vanishes except for k such that

$$k^2 + \mu^2 = 0, \quad k^4 < 0,$$

where μ is the mass of the particles described by the field A. From $k = \sum k_i$ it follows that

$$|\boldsymbol{k}| \leqslant \sum |\boldsymbol{k}_i|, \text{ and}$$
$$(k^4)^2 \geqslant \sum (k_i^4)^2 + 2 \sum_{i<k} m_i m_k,$$

where it has been taken into account that all k_i^4 are negative and have m_i as minimum absolute values. From these two inequalities it is easily deduced that

$$\mu \geqslant \sum m_i. \tag{7,15}$$

Finally, we shall also need the remark that if $A = u$, there will be among the operators a as many ψ as ψ^+; if $A = \psi$ (or ψ^+) there will be as many ψ as ψ^+ plus one odd ψ (or ψ^+).

It follows that if $A = \psi$ (or ψ^+), one of the m_i in (7,15) must be equal to $M = \mu$, and we get a contradiction if we assume the existence of more than one m_i. Thus, contributions to $\psi^{(-)\,\text{out}}|0)$ come only from the terms in which there is only one operator $a_1 = \psi$.

If $A = u$ and if we assume that an a is equal to u, the same argument applies and there cannot be any other factor a. The possibility of all a being nucleon operators is ruled out by (7,15) if $m < 2M$(*).

(*) If $m > 2M$, spontaneous decay of a meson into a pair of nucleons becomes possible, and one cannot expect the equation (7,1) to hold for a state in which there is one meson.

Thus, in all cases, the only terms in (7,12) giving contributions to $A^{(-)\,\mathrm{out}}|0)$ are those which contain only one $a = A$. For these terms K_n is a Lorentz invariant function of one argument k only, satisfying the equations

$$(k^2 + m^2)K = 0, \quad \text{or } (ik^\mu \gamma_\mu + M)K = 0, \text{ etc. } \cdots.$$

Hence K_n is proportional to

$$D^{(-)}(k) \cong (1 - \varepsilon(k))\delta(k^2 + m^2), \text{ or } S^{(-)}(k), \text{ etc. } \cdots,$$

and if we write $K_n(k) = K_n D^{(-)}(k)$, etc. $\cdots$ we obtain, corresponding to the equation (7,7), the scalar equations

$$\sum K_n = 0. \tag{7,16}$$

As the equations corresponding to ψ and ψ^+ are not distinct, we have two equations defining ΔM and Δm^2.

We shall now investigate the convergence of the integrals occurring in the K_n. Each K_n corresponds to a self-energy graph (graph with one incoming line and one outgoing line) and is given by the rules of paragraph 6.

First of all some of the integrations should be carried out in order to eliminate all the δ functions introduced at the vertices except one $\delta(k^{\mathrm{in}} - k^{\mathrm{out}})$ which expresses the conservation of energy and momentum between the incoming and the outgoing lines. These lines can be considered as associated with a fixed vector $k_0 = k^{\mathrm{in}} = k^{\mathrm{out}}$. There is some arbitrariness in the choice of the variables which should be conserved. We shall show that one can always take as independent variables of integration the vectors p_i associated with the undoubled lines. We have to show

a) that no relation such as $\sum \pm p_i = 0$ can exist,

b) that every vector k associated with a doubled line can be expressed as $k = \sum \pm p_i$, or $k = k_0 + \sum \pm p_i$.

It is easily seen that every relation $\sum \pm k_i \pm p_j = 0$ can be represented on the graph by a closed curve C leaving the incoming and the outgoing vertices outside and cutting the lines associated with the k_i and the p_i involved in the relation.

The assertion a) follows then from the fact that no line C can cut undoubled lines only (the vertices inside could not be connected with the outgoing vertex by means of doubled lines).

The assertion b) follows from the fact that it is always possible to draw a line C which cuts a given doubled line and no other doubled line except, maybe, the incoming line (this is a consequence of the tree-like structure of the doubled lines).

Divergences in the self-energy terms arise from two causes: divergences coming from the large values of the variables of integration and divergences due to the coincidence of several poles of the integrand. The latter type of divergence appears in the terms coming from graphs containing one or more self-energy graphs as sub-graphs. It can be seen that these divergences cancel in the sum (7,16).

The real self-energy divergences come from the large values of the variables p_i. At every g-vertex, the form function introduces a convergence factor Φ (6,12). We can assume that Φ which is a function of k'^2, k''^2 and k'''^2 falls off very rapidly as any of these arguments becomes large. Consequently, we can consider that the domain of integration of the variables p_i is practically limited to the values for which all vectors k associated with the various lines of the graph have bounded four-dimensional lengths k^2.

The following property will be useful: if a time-like vector k has a bounded scalar product with a fixed time-like vector k', its four components are bounded. This is easily seen in a frame of reference where k' reduces to a time component. More precisely, it can be shown that

$$\left|\boldsymbol{k}\right| < A\left(\left|\boldsymbol{k}'\right| + \left|k'^4\right|\right)/\left|(k')^2\right| \tag{7,17}$$

if $\left|kk'\right| < A$.

In every graph the undoubled lines will form a certain number of connected arcs. If there are two such arcs connected with the incoming and the outgoing lines, we shall call them L^{in} and L^{out}; the other arcs will be called L_n.

We shall first consider a term which has no other undoubled lines than L^{in} and L^{out}. Let $p_1, p_2, \cdots$ be the vectors associated with the lines forming L^{in}, starting from the incoming line, and $p'_1, p'_2, \cdots$ be the corresponding quantities associated with L^{out}. The functions Φ limit then the domain of integration to values of the variables p_i and p'_i such that the scalar products

$$k_0 p_1,\ p_1 p_2,\ p_2 p_3, \cdots \qquad k_0 p'_1,\ p'_1 p'_2,\ p'_2 p'_3, \cdots$$

are bounded. As k_0 is a fixed time-like vector and the p satisfy equations such as $p^2 + m^2 = 0$, it follows from the inequality (7,17) that the corresponding domain of integration is bounded. Thus, the corresponding terms are convergent, such as, for instance, the second-order self-energies.

We consider now the case where there are other undoubled

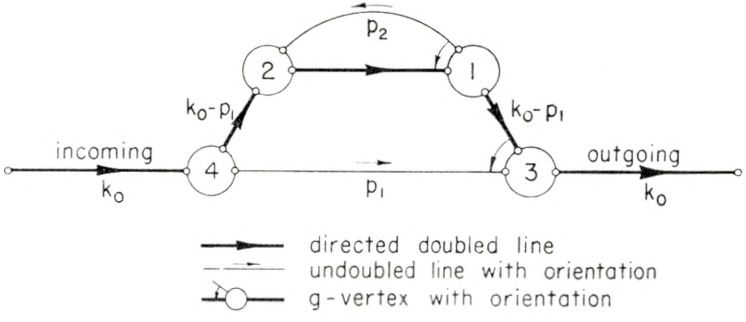

Fig. 2.

lines besides L^{in} and L^{out}. First of all, we know that the vectors associated with L^{in} and L^{out} have bounded components. The same holds for those vectors associated with the doubled lines which are linear combinations of the vectors of L^{in} and L^{out} only. Moreover, if one vector of a line L_n is kept fixed, all other vectors of the same line have bounded components. Some other scalar products will be kept bounded by the effect of the functions Φ. However, for certain graphs these conditions are not sufficient, due to the fact that the vectors associated with the doubled lines are not always time-like vectors. Fig. 2 shows an example of such a case. It is seen that the vertices 1 and 2 give the condition that the scalar product of p_2 with $k_0 - p_1$ should be bounded. The vector $k_0 - p_1$ has bounded components, but as it may be a space-like vector, the components of p_2 are not bounded, and the corresponding divergence remains.

A tentative way out of this difficulty is to assume that the function Φ should be different from zero only if the three vectors k', k'', k''' are time-like vectors. Moreover, we can assume that Φ vanishes if $|k'^2|$, $|k''^2|$ or $|k'''^2|$ are less than a fixed number which may be chosen arbitrarily small. The inequality (7,17) can then be applied to all vectors, and it is clear that all integrals become convergent. The assumption made here does not contradict any

condition previously formulated for the form functions which limits the non-localizability to small domains. It is, however, a very large departure from conventional field theory, especially since it makes many virtual transitions impossible, and its physical consequences should be investigated more completely.

So far, we have been concerned only with the self-energies. However, the matrix elements of any operator lead to integrals very similar to the self-energy integrals, and the investigation of convergence we have made is of quite general validity.

8. Final remarks.

a) *Electromagnetic interactions.*

When the interactions with the electromagnetic field are introduced, new terms have to be added to the Lagrange function so as to make it gauge invariant. The situation in the present theory differs from that in the conventional theory by the fact that the interaction term is not gauge invariant in itself.

A gauge transformation is defined by

$$\bar{A}_\mu(x) = A_\mu(x) + \frac{\partial \Lambda}{\partial x^\mu}, \quad \bar{\psi}(x) = \psi(x) e^{i\varepsilon\Lambda}, \quad \bar{\psi}^+(x) = \psi^+(x) e^{-i\varepsilon\Lambda}, \quad (8,1$$

where $\Lambda(x)$ is any function such that $\Box \Lambda(x) = 0$. It follows that

$$\bar{\psi}^+(x')\,\bar{\psi}(x''') = \psi^+(x')\,\psi(x''')\,e^{i\varepsilon(\Lambda(x''')-\Lambda(x'))}, \qquad (8,2)$$

which shows the lack of gauge invariance if the form function allows x' to be different from x'''. On using (8,1), however, one can write

$$\Lambda(x''') - \Lambda(x') = \int_C \frac{\partial \Lambda}{\partial x^\mu}\, dx^\mu = \int_C (\bar{A}_\mu - A_\mu)\, dx^\mu, \qquad (8,3)$$

where C is an arbitrary path going from x' to x'''. Substitution of (8,3) into (8,2) yields

$$\bar{\psi}^+(x')\, e^{-i\varepsilon\int_C \bar{A}_\mu dx^\mu}\, \bar{\psi}(x''') = \psi^+(x')\, e^{-i\varepsilon\int_C A_\mu dx^\mu}\, \psi(x'''). \qquad (8,4)$$

This equation expresses a gauge invariance property which holds for any path C although the invariant expression depends on the

choice of the path. Considerations of invariance and of simplicity suggest taking as path C the straight line joining x' and x'''. The final expression for the corresponding Hermitian gauge invariant interaction term reads then

$$(g/2)\int dx'dx''dx''' F(x', x'', x''')\psi^{+}(x')\left[u(x''),\ e^{-i\varepsilon\int_{x'}^{x'''}A_\mu dx^\mu}\right]_{+}\psi(x'''), \qquad (8,5)$$

where the integral $\int_{x'}^{x'''}$ is taken along a straight line.

The problem of finding a gauge invariant interaction term which in the limit $A_\mu = 0$ reduces to (1,1) has no unique solution. A very general expression is obtained on replacing in (8,5) the exponential function by an integral in the functional space of all paths going from x' to x''' which may be written

$$\int dC\,\varrho(C)\,e^{-i\varepsilon\int_C A_\mu dx^\mu}. \qquad (8,6)$$

In this expression dC is the volume element in the functional space. The weighting function $\varrho(C)$ must be normalized according to

$$\int dC\,\varrho(C) = 1,$$

and such that (8,6) is invariant under all displacements.

The introduction of exponential factors into the interaction term can be pictured as describing the effect of the electric charge jumping between the points x' and x'''. The path C can be considered as the path followed by the electric charge between the two points and $\varrho(C)$ as a sort of probability distribution of all possible paths. The function $\varrho(C)$, however, need not be positive everywhere.

The interpretation of the extra interaction term as describing the motion of the charge between x' and x''', that is over distances of the order of λ, shows that its effects will, presumably, be small. It was, however, important to show that no contradiction with the requirement of gauge invariance arises from the introduction of form functions. It is remarkable that the electromagnetic properties of charged particles are modified by the interaction with a neutral field when the interaction is of a non-localized type.

b) *Transition probabilities.*

The transition probability between a state a and a state b can, in principle, be computed as the average value in state a of the projection operator on state b, or conversely. The projection operators can be computed by the methods developed above, and the convergence proof holds. Practically, however, it is simpler to guess the lowest order terms of the S-matrix from the equations (4,9) (7,8). In connection with the difficulty of solving the latter equations, it can be asked whether another method of quantization would not give the S-matrix more directly. In fact, the Lagrangian formulation of quantum mechanics developed by FEYNMAN[18] can be applied to the present problem. The result is quite simple: the only modification to the Feynman rules is the introduction of form functions at every vertex of the graphs. This solution, however, cannot be accepted since the corresponding matrix is not unitary. A calculation, for instance, of the second order unitarity condition yields after some manipulations an irreducible sum of terms involving factors such as

$$F(x_1', x_1'', x_1''')S_+(x_1''' - x_2')S_-(x_1' - x_2''')F(x_2', x_2'', x_2'''),$$

which clearly vanish in the limit of a local interaction, due to the properties of the retarded and advanced Green's functions, but do not vanish in the more general case.

In conclusion, I should like to express my gratitude to Professor C. MØLLER for his advice and encouragement, and to Professor N. BOHR for the hospitality of the Institute of Theoretical Physics during my stay. I am indebted to Dr. R. GLAUBER for many helpful comments on the manuscript. The foregoing work was supported by the Direction des Mines et de la Sidérurgie in Paris.

Appendix I.

Definition of some singular functions.

The singular functions used in field theory are conveniently defined by the Fourier integral

$$D(x) = -(2\pi)^{-4} \int dk\, e^{ikx}/(k^2 + m^2).$$

Since the integrand is singular for $k^2 + m^2 = 0$, it is convenient to perform the integration with respect to k^4 in the complex plane

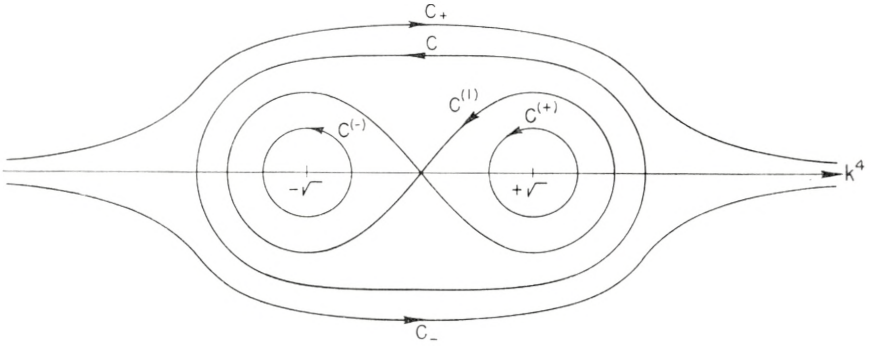

Fig. 3.

along a contour avoiding the singularities. The integrand has two poles at $k^4 = \sqrt{k^2 + m^2}$, and $k^4 = -\sqrt{k^2 + m^2}$. The contours C_+ and C_- (Fig. 3) yield the retarded and advanced Green's functions D_+ and D_-. The contour $C = C_- - C_+$ yields the function D occurring in the commutation relations. The decomposition $C = C^{(+)} + C^{(-)}$ corresponds to the decomposition of D into the positive and negative frequency parts $D^{(+)}$ and $D^{(-)}$. Finally, the contour $C^{(1)}$ yields the function $D^{(1)}$.

If we call $\Delta(x)$ the functions similar to the D functions where the mass m is replaced by M, the functions S are given by

$$S(x) = \left(-\gamma^\mu \frac{\partial}{\partial x^\mu} + M\right) \Delta(x).$$

Appendix II.

Commutation relations of the outgoing fields.

The outgoing fields are solutions of the free field equations. Assuming that the fields are enclosed in a large cube of volume V, we can expand them in Fourier series as

$$\left.\begin{aligned} \psi^{\text{out}}(x) &= V^{-1/2} \sum_{\boldsymbol{K},r} a^r_{\boldsymbol{K}} \psi^r_+(K) e^{iKx} + b^{*r}_{\boldsymbol{K}} \psi^r_-(K) e^{-iKx}, \\ u^{\text{out}}(x) &= V^{-1/2} \sum_{\boldsymbol{k}} (2k^4)^{-1/2} (v_{\boldsymbol{k}} e^{ikx} + v^*_{\boldsymbol{k}} e^{-ikx}), \end{aligned}\right\} \quad \text{(II,1)}$$

where $\boldsymbol{K}$ is the space part of the vector K ($K^4 = +\sqrt{\boldsymbol{K}^2 + M^2}$), $\boldsymbol{k}$ is the space part of k^μ ($k^4 = +\sqrt{\boldsymbol{k}^2 + m^2}$), and $\psi^r_\pm(K)$ ($r = 1,2$) are the positive and negative energy solutions, respectively, of the equations $(\pm iK_\mu \gamma^\mu + M)\psi^r_\pm(K) = 0$, orthonormalized according to

$$\psi^{*r}_+(K)\psi^s_+(K) = \delta^{rs}, \qquad \psi^{*r}_-(K)\psi^s_-(K) = \delta^{rs}.$$

Substituting these developments into the expressions of the constants of collision we get

$$\left.\begin{aligned} G^\mu &= \sum_{\boldsymbol{K},r} K^\mu (a^{*r}_{\boldsymbol{K}} a^r_{\boldsymbol{K}} - b^r_{\boldsymbol{K}} b^{*r}_{\boldsymbol{K}}) + (1/2) \sum_{\boldsymbol{k}} k^\mu (v^*_{\boldsymbol{k}} v_{\boldsymbol{k}} + v_{\boldsymbol{k}} v^*_{\boldsymbol{k}}), \\ Q &= \varepsilon \sum_{\boldsymbol{K},r} a^{*r}_{\boldsymbol{K}} a^r_{\boldsymbol{K}} + b^r_{\boldsymbol{K}} b^{*r}_{\boldsymbol{K}}, \end{aligned}\right\} \quad \text{(II,2)}$$

and a similar expression for the angular momentum. Substitution of the developments (II,1) and (II,2) into the relations (4,8) gives

$$\left.\begin{aligned} [a^r_{\boldsymbol{K}}, H^{+r}_{\boldsymbol{K}}] &= a^r_{\boldsymbol{K}}, & [a^{*r}_{\boldsymbol{K}}, H^{+r}_{\boldsymbol{K}}] &= -a^{*r}_{\boldsymbol{K}}, \\ [b^{*r}_{\boldsymbol{K}}, H^{-r}_{\boldsymbol{K}}] &= b^{*r}_{\boldsymbol{K}}, & [b^r_{\boldsymbol{K}}, H^{-r}_{\boldsymbol{K}}] &= -b^r_{\boldsymbol{K}}, \\ [v_{\boldsymbol{k}}, H_{\boldsymbol{k}}] &= v_{\boldsymbol{k}}, & [v^*_{\boldsymbol{k}}, H_{\boldsymbol{k}}] &= -v^*_{\boldsymbol{k}}, \end{aligned}\right\} \quad \text{(II,3)}$$

where $H^{+r}_{\boldsymbol{K}} = a^{*r}_{\boldsymbol{K}} a^r_{\boldsymbol{K}}$, $H^{-r}_{\boldsymbol{K}} = b^r_{\boldsymbol{K}} b^{*r}_{\boldsymbol{K}}$ and $H_{\boldsymbol{k}} = (1/2)(v^*_{\boldsymbol{k}} v_{\boldsymbol{k}} + v_{\boldsymbol{k}} v^*_{\boldsymbol{k}})$: every other commutator of a quantity a, b or v with an H vanishes.

The incoming fields can be developed in the same way as the outgoing fields. The coefficients in the Fourier series will be operators a^{in}, b^{in} and v^{in} which not only satisfy commutation relations similar to (II,3), but also the following ones which result from (4,4)

$$[a_{\boldsymbol{K}}^{\mathrm{in},r},\ a_{\boldsymbol{K}}^{*\mathrm{in},r}]_+ = 1\,,\quad [b_{\boldsymbol{K}}^{\mathrm{in},r},\ b_{\boldsymbol{K}}^{*\mathrm{in},r}]_+ = 1\,,\quad [v_{\boldsymbol{k}}^{\mathrm{in}},\ v_{\boldsymbol{k}}^{*\mathrm{in}}] = 1\,;\ (\mathrm{II},4)$$

all other commutators (or anticommutators if two operators a or b are involved) vanish.

The field equations give expressions of the outgoing operators as power series of the coupling constants. Each term of these series is a polynomial of the incoming operators. Thus the outgoing operators are continuous functions of the coupling constants, and have the incoming operators as limit if the coupling vanishes.

The problem now is to show that, as a consequence of (II,3), the outgoing operators satisfy commutation relations identical with (II,4).

WIGNER[19] has given the general form of the operators satisfying the relations

$$[v,\ H] = v,\quad [v^*,\ H] = -v^*,\quad H = (1/2)\,(v^*v + vv^*)\,. \qquad (\mathrm{II},5)$$

His method can be applied with very little change (although the result is very different) to the case of operators satisfying the relations

$$[a,\ H] = a,\quad [a^*,\ H] = -a^*,\quad H = a^*a\,. \qquad (\mathrm{II},6)$$

One finds in this case an infinite number of irreducible representations with 0, 1, 2, 3, $\cdots$ or ∞ dimensions. Only in the case of a two-dimensional representation do the operators satisfy the relations

$$[a,\ a]_+ = 0\,,\quad [a^*,\ a^*]_+ = 0\,,\quad [a,\ a^*]_+ = 1\,. \qquad (\mathrm{II},7)$$

However, as there is only a discrete set of possibilities, and as the outgoing operators go continuously over to the incoming operators as the coupling goes to zero, it follows that the outgoing operators satisfy the relations (II,7). The same applies to any operator a or b.

Next, we take two operators a_1 and a_2. They satisfy besides the relations (II,7) the relations

$$[a_1,\ H_2] = [a_1^*,\ H_2] = [a_2,\ H_1] = [a_2^*,\ H_1] = 0\,. \qquad (\mathrm{II},8)$$

It is easily seen that these relations have as consequences the relations

$$a_1a_2 = ca_2a_1\,,\quad a_1a_2^* = c^*a_2^*a_1\,,\quad a_1^*a_2 = c^*a_2a_1^*\,,\quad a_1^*a_2^* = ca_2^*a_1^*\,, \qquad (\mathrm{II},9)$$

where c is any number such that $|c|^2 = 1$. The relations (II,9) are not symmetrical in a_1 and a_2. In order to make it more obvious we can write, for instance,

$$a_1 a_2 = c_{12} a_2 a_1, \qquad a_2 a_1 = c_{21} a_1 a_2.$$

We have then $c_{21} = c_{12}^*$. The operators a_1 and a_2 appear in fact as Fourier coefficients of two plane waves with propagation vectors $\boldsymbol{K}_1$ and $\boldsymbol{K}_2$ and spin orientations r_1 and r_2, and c must then be an invariant function of these quantities. As all invariant functions of two propagation vectors and two spin orientations are symmetrical we must have $c_{12} = c_{21}$. It follows that $c = +1$ or -1, and by continuity we see that $c = -1$. The same applies to any couple of operators a or b. Thus, we have shown that the fields $\psi^{+\,\mathrm{out}}$ and ψ^{out} satisfy the same commutation relations as the incoming fields.

The case of the operators v can be treated by very similar considerations. A slight complication comes from the fact shown by WIGNER that the representations of the operators satisfying the relations (II,5) depend on a continuous parameter which fixes in particular the zero-point energy. So the continuity argument does not apply here. It is, however, easily seen that the zero—point energy must be the same for the outgoing fields as for the incoming fields as a consequence of the conservation equation

$$G^4(\mathrm{out}) = G^4(\mathrm{in}).$$

The proof is then easily completed.

Appendix III.

On the solution of the field equations.

1. *Localized interaction.*

We assume that the formulas (5,6) hold up to the order $n-1$. The terms of order n can then be computed from the field equations (4,3). For ψ, for instance, one finds

$$\psi^{(n)}(x_0) = i \int dx_1 S_+(x_0 - x_1) \{ g A(x_1) - \Delta M \psi^{(n-1)}(x_1) \}, \qquad \text{(III,1)}$$

where

$$A(x_1) = \sum_{p=0}^{n-1} u^{(p)}(x_1)\,\psi^{(n-p-1)}(x_1).$$

Explicitly $A(x_1)$ reads

$$A(x_1) = \sum_{p=0}^{n-1} \int_{\substack{x_1 > x'_1 > x'_2 > \cdots > x'_p \\ x_1 > x''_1 > x''_2 > \cdots > x''_{n-p-1}}} dx'_1 dx'_2 \cdots dx'_p dx''_1 dx''_2 \cdots dx''_{n-p-1}$$

$$[\cdots[u^{\mathrm{in}}(x_1),\ H'_1],\cdots H'_p]\,[\cdots[\psi^{\mathrm{in}}(x_1),\ H''_1],\cdots H''_{n-p-1}].$$

If we call $x_2, x_3, \cdots x_n$ the points $x'_1, \cdots x'_p, x''_1, \cdots x''_{n-p-1}$ chronologically reordered, we can write for $A(x_1)$

$$A(x_1) = \int_{x_1 > x_2 > \cdots > x_n} dx_2 \cdots dx_n \sum \Big[\cdots\big[u^{\mathrm{in}}(x_1),\ H_{j_1}\big],\cdots H_{j_p}\Big] \Big[\cdots\big[\psi^{\mathrm{in}}(x_1),\ H_{j_{p+1}}\big],\cdots H_{j_{n-1}}\Big]$$

where the summation $\sum$ is extended to all permutations $j_1, j_2, \cdots j_{n-1}$ of $2, 3, \cdots n$ such that $j_1 < j_2 < \cdots < j_p$ and $j_{p+1} < j_{p+2} < \cdots < j_{n-1}$. It is now easily seen that

$$A(x_1) = \int_{x_1 > x_2 > \cdots > x_n} dx_2 dx_3 \cdots dx_n\,[\cdots[u^{\mathrm{in}}(x_1)\psi^{\mathrm{in}}(x_1),\ H_2],\cdots H_n]. \qquad \text{(III,2)}$$

After substitution in (III,1) of (III,2) and of the expression of $\psi^{(n-1)}$, we get

$$\psi^{(n)}(x_0) = i\int_{x_1 > x_2 > \cdots > x_n} dx_1 dx_2 \cdots dx_n S_+(x_0 - x_1)\left[\cdots\left[\frac{\delta L_{\mathrm{I}}^{\mathrm{in}}}{\delta\psi^+(x_1)},\ H_2\right]\cdots H_n\right]$$

$$= \int_{x_1 > x_2 > \cdots > x_n} dx_1 dx_2 \cdots dx_n\,[\cdots[\psi^{\mathrm{in}}(x_0),\ H_1],\ H_2],\ \cdots H_n]$$

where use has been made of the relation

$$\left.\begin{aligned} iS_+(x_0 - x_1)\frac{\delta L_{\mathrm{I}}^{\mathrm{in}}}{\delta\psi^+(x_1)} &= [\psi^{\mathrm{in}}(x_0),\ H_1] \quad \text{if} \quad x_0 > x_1, \\ &= 0 \qquad\qquad\quad \text{if} \quad x_0 < x_1. \end{aligned}\right\}$$

A similar treatment applies to the other field functions. Thus, (5,6) holds to all orders.

As for the outgoing fields, the term of order n of ψ, for instance, is given by

$$\psi^{\text{out}\,(n)}(x) = i\int dx_1 S(x - x_1)\{gA(x_1) - \Delta M\psi^{(n-1)}(x_1)\},$$

and on using (III,2) and the relation

$$iS(x - x_1)\frac{\delta L_{\text{I}}^{\text{in}}}{\delta\psi^{+}(x_1)} = [\psi^{\text{in}}(x),\ H_1],$$

we get

$$\psi^{\text{out}\,(n)}(x) = \int_{x_1 > x_2 > \cdots > x_n} dx_1 dx_0 \cdots dx_n [\cdots [\psi^{\text{in}}(x),\ H_1], \cdots H_n].$$

2. *Non-localized interaction.*

The preceding proof can be extended immediately to the case of a non-localized interaction. The only delicate point is the transformation of the expression called $A(x_1)$. Presently, we have to show the identity

$$\left.\begin{aligned}\sum_{p=0}^{n-1}\int_t d\xi'_1 \cdots d\xi'_n [\cdots [u^{\text{in}}(x''_0),\ H'_1], \cdots H'_p]\int_t d\xi''_1 \cdots d\xi''_{n-p-1}\\ [\cdots [\psi^{\text{in}}(x'''_0),\ H''_1], \cdots H''_{n-p-1}] =\\ = \int_t d\xi_1 \cdots d\xi_n [\cdots [u^{\text{in}}(x''_0)\psi^{\text{in}}(x'''_0),\ H_1],\ H_2], \cdots H_n].\end{aligned}\right\} \quad \text{(III,3}$$

In the left-hand side the variables ξ' on the one hand, and the variables ξ'' on the other hand, are ordered in time independently. We have to develop both sides of (III,3) and to compare the results. The integrand in the right-hand side can first be expanded as

$$\sum [\cdots [u^{\text{in}}(x''_0),\ H_{j'_1}], \cdots H_{j'_p}] [\cdots [\psi^{\text{in}}(x'''_0),\ H_{j''_1}], \cdots H_{j''_{n-p-1}}], \quad \text{(III,4}$$

where the summation is extended to all permutations of 1, 2, 3, $\cdots n$ such that $j'_1 < j'_2 < \cdots < j'_p$, and $j''_1 < j''_2 < \cdots < j''_{n-p-1}$. Then, the term in u^{in} and the term in ψ^{in} have to be developed. Thus a term T of (III,4) is the product of a term T_u coming from the first factor, and a term T_ψ coming from the second factor. The term T_u will also appear in the development of the first factor in the left-hand side of (III,3), and T_ψ will appear in the development of the second factor. The associated domains are clearly the same in both sides. Finally, the rule that each term T should be multiplied by $1/N(T)$ is conveniently replaced here by the

rule that only one term in each family of equivalent terms should be taken into account. It follows that each term appears the same number of times in both sides of (III,3), and this completes the proof.

The formulas for the outgoing fields and the products of outgoing fields are merely generalizations of (III,3).

References.

(1) R. E. Peierls and H. MacManus, Proc. Roy. Soc. A **195**, 323, (1948).
(2) H. Yukawa, Phys. Rev. **76**, 300, 1731, (1949), **77**, 219, (1950).
(3) C. Bloch, Dan. Mat. Fys. Medd. **26**, no. 1, (1950).
(4) C. N. Yang and D. Feldman, Phys. Rev. **79**, 972, (1950).
(5) G. Källen, Arkiv för Fysik, **2**, 371, (1950).
(6) C. Bloch, Prog. theor. Phys. **5**, 606, (1950.)
(7) J. Rayski, Phil. Mag. **42**, 1289, (1951).
(8) C. Møller, Communication at the Conference on Nuclear Physics, Copenhagen, (1951).
(9) A. Pais and G. E. Uhlenbeck, Phys. Rev. **79**, 145, (1950).
(10) R. P. Feynman, Phys. Rev. **76**, 749, 769, (1949).
(11) J. Schwinger, Phys. Rev. **75**, 651, (1949).
(12) W. Pauli and F. Villars, Rev. Mod. Phys. **21**, 434, (1949).
(13) G. N. Watson, Theory of Bessel functions, (Cambridge).
(14) C. Møller, Dan. Mat. Fys. Medd. **23**, no. 1, (1945).
(15) J. Schwinger, Phys. Rev. **74**, 1439, (1948).
(16) A. Houriet and A. Kind, Helv. Phys. Acta, **22**, 319; (1949) G. C. Wick, Phys. Rev. **80**, 268, (1950).
(17) F. J. Dyson, Phys. Rev. **82**, 428, (1951).
(18) R. P. Feynman, Phys. Rev. **80**, 440, (1950).
(19) E. P. Wigner, Phys. Rev. **77**, 711, (1950).

Indleveret til selskabet den 26. juni 1952.
Færdig fra trykkeriet den 6. november 1952.

Errata.

P. 29, line 13, instead of x' read x'''.
P. 29, line 15, instead of x''' read x'.
P. 32, eq. (5,13), left side, instead of (x_0) read (x_0''').
P. 32, eq. (5,14), right side, instead of (x'') read (x''').

Det Kongelige Danske Videnskabernes Selskab
Matematisk-fysiske Meddelelser, bind **27**, nr. 9

Dan. Mat. Fys. Medd. **27**, no. 9 (1953)

ON THE RELATION BETWEEN PHASE SHIFT ENERGY LEVELS AND THE POTENTIAL

BY

RES JOST AND WALTER KOHN

København
i kommission hos Ejnar Munksgaard
1953

Printed in Denmark
Bianco Lunos Bogtrykkeri

A method recently developed by GEL'FAND and LEVITAN is adapted to the problem of determining a central potential from the "spectral function" corresponding to a given angular momentum. (The spectral function incorporates the phase shift, binding energies and m additional free parameters if there are m bound states). Two applications are given: An explicit expression is deduced for the totality of potentials with the same phase shift and binding energies as a given potential. Further it is shown that for a given phase shift the position of the bound states is entirely arbitrary and an explicit example is given which illustrates this fact. Implications for the interpretation of scattering data are discussed.

Introduction.

It was shown in a previous paper [1] that a short range central potential is uniquely determined by the phase shift and binding energies for any given angular momentum plus as many additional parameters C_i as there are bound states. For boundary conditions $h\,\varphi(0) + \varphi'(0) = 0$ GEL'FAND and LEVITAN have in a beautiful paper [2] combined phase shift binding energies and the C_i's into one so-called spectral function $\varrho(E)$ and reduced the problem of determining h and the potential to the solution of a linear integral equation. Their method can easily be adopted to the physically interesting case $\varphi(0) = 0$, which will be done in § 1. The resulting integral equation thus provides a method for constructing the totality of potentials corresponding to given phase shift and binding energies.

In § 2 we first exhibit the dependence of these potentials on the parameters C_i. We have solved this problem in a previous paper [3] by elementary means. The present method yields in a simple way the same results in an improved form.

It is a consequence of the theory of GEL'FAND and LEVITAN that the positions of the bound states are independent of the phase shift. This is proved and illustrated by an example in the second part of § 2.

In § 3 we discuss the implications of these results for the interpretation of scattering experiments.

§ 1. Derivation of the Integral Equation.

We consider potentials for which $\int_0^\infty r \,|V(r)|\, dr < \infty$ and $\int_0^\infty r^2 \,|V(r)|\, dr < \infty$. The Schroedinger equation for S-states is

$$\psi''(E, r) + E\,\psi(E, r) = V\psi(E, r). \tag{1.1}$$

We will make use of the following solutions of this equation:

$$\varphi(E, r):\ \varphi(E, 0) = 0;\quad \varphi'(E, 0) = 1 \tag{1.2}$$

and

$$f(k, r):\ \lim_{r\to\infty} e^{ikr} f(k, r) = 1, \tag{1.3}$$

where

$$k^2 = E. \tag{1.4}$$

$\varphi(E, r)$ is for a fixed r an entire function of E, whereas $f(k, r)$ is regular for $Im(k) < 0$ and continuous for $Im(k) \leqq 0$.
For large $|k|$

$$\varphi(k^2, r) \sim \frac{\sin kr}{k}, \tag{1.5}$$

and for large $|k|$ in $Im(k) \leq 0$

$$f(k, r) \sim e^{-ikr}. \tag{1.6}$$

The function $f(k) \equiv f(k, 0)$ determines and is determined by the phase shift and the binding energies, which latter are given by

$$E_l = -\varkappa_l^2;\quad f(-i\varkappa_l) = 0,\quad \varkappa_l > 0\,. \tag{1.7}$$

For real k

$$\varphi(k^2, r) = \frac{1}{2ik}\,[f(k)\,f(-k, r) - f(-k)\,f(k, r)]\,. \tag{1.8}$$

Further we introduce the spectral function $\varrho(E)$ defined by

$$\left.\begin{aligned} \varrho(-\infty) &= 0 \\ \frac{d\varrho}{dE} &= \sum C_l \delta(E - E_l), \quad E < 0 \\ \frac{d\varrho}{dE} &= \frac{1}{\pi}\frac{\sqrt{E}}{|f(\sqrt{E})|^2}, \qquad E \geqslant 0 \end{aligned}\right\} \tag{1.9}$$

where

$$\left.\begin{aligned} C_l &= \left[\int_0^\infty [\varphi(E_l, r)]^2\, dr\right]^{-1} = \frac{2\, i\varkappa_l f'(i\varkappa_l, 0)}{\dot{f}(-i\varkappa_l)}, \\ \dot{f}(-i\varkappa_l) &\equiv \left[\frac{df(k)}{dk}\right]_{k=-i\varkappa_l}. \end{aligned}\right\} \quad (1.10)$$

The spectral function has the property that we have for every square integrable function $F(r)$ the completeness relation

$$\int_0^\infty [F(r)]^2\, dr = \int d\varrho(E) \left[\int_0^\infty dr\, F(r)\, \varphi(E, r)\, dr\right]^2. \quad (1.11)$$

We now consider two potentials $V_1(r)$ and $V(r)$ and the corresponding solutions φ_1, f_1 and φ, f. In analogy with GEL'FAND and LEVITAN we shall establish the equation

$$\varphi(E, r) = \varphi_1(E, r) + \int_0^r dt\, K(r, t)\, \varphi_1(E, t), \quad (1.12)$$

where

$$K(r, t) = -\int d\,[\varrho(E) - \varrho_1(E)]\, \varphi(E, r)\, \varphi_1(E, t). \quad (1.13)$$

For this purpose we first consider the integral

$$\left.\begin{aligned} I &= \int d\varrho(E')\, \varphi(E', r) \int_0^r dt\, \varphi_1(E^1, t)\ \varphi_1(E, t) \\ &= \sum C_l\, \varphi(E_l, r) \int_0^r dt\, \varphi_1(E_l, t)\, \varphi_1(E, t) \\ &+ \frac{1}{\pi} \int_{-\infty}^\infty \frac{k'^2\, dk'}{f(k')\, f(-k')}\, \varphi(k'^2, r) \int_0^r dt\, \varphi_1(k'^2, t)\, \varphi_1(E, t). \end{aligned}\right\} \quad (1.14)$$

We substitute in the first term

$$\varphi(E_l, r) = \frac{f(-i\varkappa_l, r)}{f'(-i\varkappa_l, r)}, \quad (1.15)$$

and in the second term we use Eq. (1.8):

$$\left.\begin{aligned} I &= \sum_l \frac{2\, i\varkappa_l}{\dot{f}(-i\varkappa_l)} f(-i\varkappa_l, r) \int_0^r dt\, \varphi_1(-\varkappa_l^2, t)\, \varphi_1(E, t) \\ &+ \frac{1}{\pi i} \int_{-\infty}^\infty \frac{k'\, dk'}{f(-k')} f(-k', r) \int_0^r dt\, \varphi_1(k'^2, t)\, \varphi_1(E, t). \end{aligned}\right\} \quad (1.16)$$

The second term can be transformed into an integral over a large semicircle in the upper half plane and a sum of residues which cancel the first term. The remaining integral can be evaluated by using the asymptotic expressions (1.5) and (1.6) (compare ref. 1 Eqs. (A 2.26) — (A 2.30)) giving the final result

$$\frac{1}{2}\varphi_1(E,r) = \int d\varrho(E')\,\varphi(E',r)\int_0^r dt\,\varphi_1(E',t)\,\varphi_1(E,t). \quad (1.17)$$

Next, consider the integral

$$J = \int d\varrho_1(E')\,\varphi(E',r)\int_0^r dt\,\varphi_1(E',t)\,\varphi_1(E,t). \quad (1.18)$$

Using the Schroedinger equation we can write

$$\left.\begin{aligned}&\int_0^r dt\,\varphi_1(E',t)\,\varphi_1(E,t)\\ &= \frac{1}{-E'+E}\left[\varphi_1'(E',r)\,\varphi_1(E,r) - \varphi_1(E',r)\,\varphi_1'(E,r)\right].\end{aligned}\right\} \quad (1.19)$$

Substituting $d\varrho_1(E')$ from Eq. (1.9) and eliminating $\varphi_1(E',r)$ by (1.8) and (1.15), respectively, gives, for E not on the positive real axis,

$$\left.\begin{aligned}J = &\sum_l \frac{2i\varkappa_{1l}}{\dot{f}_1(-i\varkappa_{1l})}\,\varphi(-\varkappa_{1l}^2,r)\,\frac{1}{\varkappa_{1l}^2+E}\\ &\times\left[f_1'(-i\varkappa_{1l},r)\,\varphi_1(E,r) - f_1(-i\varkappa_{1l},r)\,\varphi_1'(E,r)\right]\\ &-\frac{1}{\pi i}\int_{-\infty}^{\infty}\frac{k'\,dk'}{f_1(-k')}\,\varphi(k'^2,r)\,\frac{1}{k'^2-E}\left[f_1'(-k',r)\,\varphi_1(E,r)\right.\\ &\left.-f_1(-k',r)\,\varphi_1'(E,r)\right].\end{aligned}\right\} \quad (1.20)$$

Shifting the path of integration in the second term into the upper half plane gives residues cancelling the first term plus an integral over a large semicircle and a residue at $k' = \sqrt{E}$. The integral over the semicircle can be evaluated by using the asymptotic expression (1.5) and (1.6). The final result is

$$\left.\begin{aligned}&\varphi(E,r) - \frac{1}{2}\varphi_1(E,r)\\ &= \int d\varrho_1(E')\,\varphi(E',r)\int_0^r dt\,\varphi_1(E',t)\,\varphi_1(E,t).\end{aligned}\right\} \quad (1.21)$$

Combining (1.17) and (1.21) and interchanging the order of integration leads to (1.12), (1.13). The same result can be similarly derived when E is on the positive real axis.

From (1.13) one can deduce the following properties of the function $K(r, t)$:

$$\left.\begin{aligned} \frac{\partial^2 K}{\partial r^2} - V(r)\,K &= \frac{\partial^2 K}{\partial t^2} - V_1(t)\,K, \\ K(r, 0) &= 0. \end{aligned}\right\} \tag{1.22}$$

Furthermore substituting (1.12) into the Schroedinger equation and using (1.22) leads to

$$\frac{dK(r, r)}{dr} = \frac{1}{2}\,[V(r) - V_1(r)]. \quad [4]. \tag{1.23}$$

The equations (1.22) and (1.23) characterize $K(r, t)$ uniquely in terms of $V(r)$ and $V_1(r)$.

On the other hand, multiplying (1.12) with $\varphi_1(E, s)$ and integrating with the weight $\varrho(E) - \varrho_1(E)$ gives the Gel'fand-Levitan integral equation

$$K(r, s) + g(r, s) + \int_0^r dt\, K(r, t)\, g(s, t) = 0 \tag{1.24}$$

whose kernel is

$$g(s, t) = \int d\,[\varrho(E) - \varrho_1(E)]\,\varphi_1(E, s)\,\varphi_1(E, t). \tag{1.25}$$

The construction of a potential can now be carried out in the following steps: Phase shift and bound states determine the function $f(k)$ (ref. 1, Eqs. (2.16)—(2.18)). $|f(k)|^2$ and the constants C_l determine by (1.9) the spectral function $\varrho(E)$. Deriving $\varrho_1(E)$ and $\varphi_1(E, r)$ from any convenient comparison potential one can now construct $g(s, t)$ by (1.25). One must then solve the linear integral equation (1.24) for all values of the parameter $r \geqslant 0$ to obtain $K(r, s)$.

Finally the potential is calculated from (1.23).

In order that the integral equation can be solved it is necessary that the corresponding homogeneous equation has no solution. To show this we write down the homogeneous equation, using (1.25):

$$\chi(s) + \int d\,[\varrho(E) - \varrho_1(E)]\,\varphi_1(E, s) \int_0^r dt\, \varphi_1(E, t)\,\chi(t) = 0. \tag{1.26}$$

Multiplying by $\chi(s)$ and integrating over s from 0 to r leads to

$$\left.\begin{aligned} &\int_0^r [\chi(s)]^2\, ds + \int d\varrho(E) \left[\int_0^r ds\, \varphi_1(E, s)\, \chi(s)\right]^2 \\ &- \int d\varrho_1(E) \left[\int_0^r ds\, \varphi_1(E, s)\, \chi(s)\right]^2 = 0. \end{aligned}\right\} \tag{1.27}$$

Applying the completeness relation (1.11) to the function

$$\left.\begin{aligned} F(s) &= \chi(s) \qquad 0 \leqslant s \leqslant r \\ F(s) &= 0 \qquad\quad s > r \end{aligned}\right\} \tag{1.28}$$

reduces (1.27) to

$$\sum_l C_l \left[\int_0^\infty ds\, \varphi_1(E_l, s)\, F(s)\right]^2 + \frac{2}{\pi} \int_0^\infty \frac{k^2 dk}{|f(k)|^2} \left[\int_0^\infty ds\, \varphi_1(k^2, s)\, F(s)\right]^2 = 0. \tag{1.29}$$

Therefore $F(s)$ is orthogonal to all the continuum eigenfunctions of the potential $V_1(r)$ and hence a superposition of the discrete eigenfunctions. Consequently it cannot vanish for $s > r$ in contradiction with (1.28). [5].

The fact that the integral equation (1.24) has a solution is not sufficient to insure the existence of the potential Eq. (1.23). It may not be out of place to indicate here how conditions sufficient for the construction of the potential from the spectral function can be obtained.

The only difficulty in justifying the construction occurs in Eq. (1.22) involving second derivatives of $K(r, t)$. It can be dealt with by using a limiting process. We introduce an auxiliary function $\varrho^M(E)$, $M > 0$, defined by

$$\left.\begin{aligned} \varrho^M(E) &= \varrho(E), \qquad E \leqslant M, \\ \frac{d\varrho^M(E)}{dE} &= \frac{d\varrho_1(E)}{dE}, \quad E > M. \end{aligned}\right\} \tag{1.30}$$

Assuming e. g. a comparison potential $V_1(r)$ continuous for $r > 0$ we have no difficulties with the second derivatives of the function

$$g^M(s, t) = \int_{-\infty}^{\infty} d\left[\varrho^M(E) - \varrho_1(E)\right] \varphi_1(E, s)\, \varphi_1(E, t) \tag{1.31}$$

which satisfies the differential equation

$$\frac{\partial^2 g^M}{\partial s^2} - V_1(s)\, g^M = \frac{\partial g^M}{\partial t^2} - V_1(t)\, g^M. \tag{1.32}$$

The function $K^M(r, t)$ constructed by (1.24) using the $g^M(s, t)$ is twice differentiable.

It is easy to verify that the expression

$$\left.\begin{aligned}\chi^M(r,t) \equiv \frac{\partial K^M(r,t)}{\partial r^2} - 2\left(\frac{dK^M(r,r)}{dr}\right) K^M(r,t) \\ -V_1(r)\,K^M(r,t) - \frac{\partial^2 K^M(r,t)}{\partial t^2} + V_1(t)\,K^M(r,t)\end{aligned}\right\} \tag{1.33}$$

satisfies the homogeneous integral equation

$$\chi^M(r,s) + \int_0^r \chi^M(r,t)\,g^M(s,t)\,dt = 0 \tag{1.34}$$

and therefore vanishes identically, so that we have established the equations

$$\left.\begin{aligned}\frac{\partial^2 K^M(r,t)}{\partial r^2} - 2\left(\frac{dK^M(r,r)}{dr}\right) K^M(r,t) - V_1(r)\,K^M(r,t) \\ = \frac{\partial^2 K^M(r,t)}{\partial t^2} - V_1(t)\,K^M(r,t), \\ K^M(r,0) = 0.\end{aligned}\right\} \tag{1.35}$$

It is a consequence of (1.35) that the function

$$\varphi^M(E,r) = \varphi_1(E,r) + \int_0^r K^M(r,t)\,\varphi_1(E,t)\,dt \tag{1.36}$$

satisfies a Schroedinger equation with the potential

$$V^M(r) = V_1(r) + 2\frac{dK^M(r,r)}{dr} \tag{1.37}$$

or, what amounts to the same, the integral equation

$$\varphi^M(E,r) = \varphi_1(E,r) + 2\int_0^r G(E,r,t)\frac{dK^M(t,t)}{dt}\varphi^M(E,t)\,dt, \tag{1.38}$$

where $G(E,r,t)$ is the appropriate Green's function.

We now assume that $\partial g^M(s,t)/\partial t$ is uniformly bounded for all M and in every closed region of the (s,t) plane and that, furthermore,

$$\lim_{M\to\infty} \frac{\partial g^M(s,t)}{\partial t} = \Omega(s,t) \tag{1.39}$$

exists. Then $\Omega(s,t)$ is integrable and

$$\int_0^t \Omega(s,\eta)\,d\eta = \lim_{M\to\infty}\int_0^t \frac{\partial g^M(s,\eta)}{\partial \eta}\,d\eta = \lim_{M\to\infty} g^M(s,t) = g(s,t) \tag{1.40}$$

exists also, and we have

$$\Omega(s,t) = \frac{\partial g(s,t)}{\partial t}. \tag{1.41}$$

The existence of

$$K(r,t) = \lim_{M\to\infty} K^M(r,t) \tag{1.42}$$

which is now a solution of (1.24) is a consequence of simple theorems on integral equations. From the explicit solution of (1.24) follows the existence of

$$\frac{dK(r,r)}{dr} = \lim_{M\to\infty} \frac{dK^M(r,r)}{dr} \tag{1.43}$$

and its integrability. Obviously

$$\lim_{M\to\infty} \varphi^M(E,r) = \varphi(E,r) = \varphi_1(E,r) + \int_0^r K(r,t)\,\varphi_1(E\,t)\,dt \tag{1.44}$$

exists and satisfies

$$\varphi(E,r) = \varphi_1(E,r) + 2\int_0^r G(E,r,t)\,\frac{dK(t,t)}{dt}\,\varphi_1(E,t)\,dt. \tag{1.45}$$

This concludes the verification.

The following conditions on the difference $\varrho(E) - \varrho_1(E)$ and on $V_1(r)$ are sufficient to insure the above conditions and hence the applicability of the construction procedure. They cover most of the physically interesting cases:

$$\int_0^r r^\alpha\,|V_1(r)|\,dr + \int_1^\infty r\,|V_1(r)|\,dr < \infty\ ,\quad 0<\alpha<1 \tag{1.46}$$

$$\left.\begin{aligned} \frac{d}{dE}[\varrho(E) - \varrho_1(E)] &= \frac{\sqrt{E}}{\pi}\left[\frac{\Gamma}{E} + \frac{F(E)}{E^{1+\varepsilon}}\right], \\ E > E_0 > 0,&\quad \varepsilon > 0, \end{aligned}\right\} \tag{1.47}$$

where

$$|F(E)| < \gamma < \infty \tag{1.48}$$

and Γ is constant.

The extension of the foregoing considerations to higher angular momenta, $l>0$, is straightforward. We define the solution $f(k,r)$ as before by

$$\lim_{r\to\infty} e^{ikr} f(k,r) = 1 \tag{1.49}$$

and call

$$f(k) = (2l+1)\lim_{r\to 0} r^l f(k,r). \tag{1.50}$$

Further we define the solution $\varphi(E,r)$ by

$$\lim_{r\to 0} \varphi(E,r)/r^{l+1} = 1. \tag{1.51}$$

Then, for real k,

$$\varphi(k^2, r) = \frac{1}{2ik}[f(k)f(-k, r) - f(-k)f(k, r)] \qquad (1.52)$$

while, in the bound states, $k = -i\varkappa_m$,

$$f(-\varkappa_m, r) = \lim_{l \to 0}\left[\frac{f(-i\varkappa_m, l)}{l^{l+1}}\right]\varphi(-\varkappa_m^2, r). \qquad (1.53)$$

Appendix II of ref. 1 can now be worked through for $l > 0$ (dropping, however, the distinction between φ and $\bar{\varphi}$) and gives for $d\varrho/dE$ (cf. Eq. (1.11) and ref. 1, Eq. (A 2.37))

$$\left.\begin{aligned} \frac{d\varrho}{dE} &= \sum C_m \delta(E - E_m), \quad E < 0 \\ \frac{d\varrho}{dE} &= \frac{\sqrt{E}}{\pi |f(\sqrt{E})|^2} \quad , \quad E \geqslant 0 \end{aligned}\right\} \qquad (1.54)$$

where

$$C_m = \int_0^\infty [\varphi(-\varkappa_m^2, r)]^2 \, dr = \frac{2i\varkappa_m}{\dot{f}(-i\varkappa_m)} \lim_{r \to 0}[f(-i\varkappa_m, r)/r^{l+1}]. \qquad (1.55)$$

With these new definitions one arrives again at the basic equations (1.23), (1.24) and (1.25). [6].

§ 2. Two Applications of the Integral Equation.

(a) *Equivalent Potentials.*

We first want to exhibit the dependence of the manifold of equivalent potentials (i. e. potentials with the same S-phase shift and bound states) on the parameters C_l. We choose for $V_1(r)$ an arbitrary potential out of this manifold corresponding to the values C_{1l}. Since equivalent potentials have the same $f(k)$, we get

$$\frac{d[\varrho(E) - \varrho_1(E)]}{dE} = 0, \quad E > 0 \qquad (2.1)$$

and

$$\frac{d[\varrho(E) - \varrho_1(E)]}{dE} = \sum_{l=1}^{m} [C_l - C_{1l}]\,\delta(E - E_l), \quad E < 0. \qquad (2.2)$$

The kernel (1.25) then reduces to a finite bilinear series

$$g(s, t) = \sum_{l=1}^{m} (C_l - C_{1l})\ \varphi_{1l}(s)\, \varphi_{1l}(t), \tag{2.3}$$

where we have used the abbreviation

$$\varphi_{1l}(r) \equiv \varphi_1(E_l, r) \tag{2.4}$$

for the bound state wave functions. To solve the integral equation (1.24) we make the Ansatz

$$K(r, s) = \sum_{l=1}^{m} a_l(r)\, \varphi_{1l}(s). \tag{2.5}$$

The $a_l(r)$ are then determined by the linear equations

$$\sum_{l=1}^{m} M_{kl}(r)\, a_l(r) = (C_k - C_{1k})\, \varphi_{1k}(r), \tag{2.6}$$

where

$$M_{kl}(r) = -\delta_{kl} - (C_k - C_{1k}) \int_0^r \varphi_{1k}(t)\, \varphi_{1l}(t)\, dt. \tag{2.7}$$

As we have seen at the end of § 1, the matrix M_{kl} has an inverse, so that

$$a_j(r) = \sum_{k=1}^{m} M_{jk}^{-1}(r)\, (C_k - C_{1k})\, \varphi_{1k}(r) \tag{2.8}$$

and

$$\left.\begin{aligned} K(r, s) &= \sum_{j,k} \varphi_{1j}(s)\, M_{jk}^{-1}(r)\, (C_k - C_{1k})\, \varphi_{1k}(r) \\ V(r) &= V_1(r) - 2\, \frac{d^2}{dr^2} \log \operatorname{Det} \| M_{jk}(r) \|. \end{aligned}\right| \tag{2.9}$$

Examples of equivalent potentials have been given in ref. 3.

(b) *Independence of Binding Energies from the Phase Shift.*

The independence of the binding energies from the phase shift is a simple consequence of the Gel'fand-Levitan theory. We consider the S-phase shift as given and assume that there exists a potential $V_1(r)$ reproducing this phase shift and having a bound state at the position $k = -i\varkappa_1$. We now make the assumption that $V_1(r)$ satisfies Eq. (1.46) from which it follows easily that

$$\frac{1}{|f_1(k)|^2} = 1 + \frac{F(k)}{k^{1-\alpha}}, \quad |F(k)| < N < \infty . \tag{2.10}$$

(2.10) is satisfied in all physically interesting cases.

Next we construct the $f(k)$ corresponding to the same phase, but the bound state at a different position, $k = -i\varkappa$:

$$f(k) = f_1(k)\frac{k^2+\varkappa^2}{k^2+\varkappa_1^2} \tag{2.11}$$

so that

$$\left.\begin{aligned} \frac{d}{dE}[\varrho(E)-\varrho_1(E)] &= C\delta(E+\varkappa^2) - C_1\delta(E+\varkappa_1^2), \\ & \qquad\qquad E<0; \\ \frac{d}{dE}[\varrho(E)-\varrho_1(E)] &= \frac{\sqrt{E}}{\pi}\frac{1}{|f_1(\sqrt{E})|^2}\frac{(2E+\varkappa_1^2+\varkappa^2)(\varkappa_1^2-\varkappa^2)}{(E+\varkappa^2)^2}, \\ & \qquad\qquad E>0. \end{aligned}\right\} \tag{2.12}$$

Evidently the conditions (1.46) and (1.48) are satisfied so that a potential corresponding to the same phase shift, arbitrary position of the bound state and arbitrary constant C can be constructed.

For the case when the position of a bound state is changed from $-i\varkappa_1$ to $-i\varkappa$ the $g(s,t)$ can be explicitly calculated.

By (1.25) and (2.12) we have

$$g(s,t) = C\varphi_1(-\varkappa^2,s)\varphi_1(-\varkappa^2,t) - C_1\varphi_1(-\varkappa_1^2,s)\varphi_1(-\varkappa_1^2,t) + g^{(c)}(s,t), \tag{2.13}$$

where the contribution $g^{(c)}(s,t)$ from the continuum is

$$g^{(c)}(s,t) = \frac{1}{\pi}\int_{-\infty}^{\infty}\frac{k^2dk}{|f_1(k)|^2}\left(\frac{2(\varkappa_1^2-\varkappa^2)}{k^2+\varkappa^2} + \frac{(\varkappa_1^2-\varkappa^2)^2}{(k^2+\varkappa^2)^2}\right)\varphi_1(k^2,s)\varphi_1(k^2,t). \tag{2.14}$$

By (1.8) and use of contour integration this becomes, for $s \geqslant t$,

$$\left.\begin{aligned} g^{(c)}(s,t) &= \frac{i}{\pi}\int_{-\infty}^{\infty}\frac{k\,dk}{f_1(k)}\left(\frac{2(\varkappa_1^2-\varkappa^2)}{k^2+\varkappa^2} + \frac{(\varkappa_1^2-\varkappa^2)^2}{(k^2+\varkappa^2)^2}\right) f_1(k,s)\varphi_1(k^2,t) \\ &= \sum_{l=1}^{m} C_l \frac{(\varkappa_1^2-\varkappa^2)(2\varkappa_l^2-\varkappa^2-\varkappa_1^2)}{(\varkappa_l^2-\varkappa^2)^2}\varphi_1(-\varkappa_l^2,s)\varphi_1(-\varkappa_l^2,t) \\ &\quad + \frac{i}{2\varkappa}\frac{\partial}{\partial k}\left[\frac{(k^2+\varkappa_1^2)^2}{f_1(k)} f_1(k,s)\varphi_1(k^2,t)\right]_{k=-i\varkappa}. \end{aligned}\right\} \tag{2.15}$$

For $s < t$, $g(s, t)$ can be determined from the symmetry relation $g(s, t) = g(t, s)$.

It is interesting to calculate the derivative of the potential with respect to the variation of one of the binding energies. From (1.23) and (1.24) we have

$$\left.\begin{aligned}\left[\frac{\partial}{\partial \varkappa} V(r;\varkappa)\right]_{\varkappa=\varkappa_1} &= 2\frac{\partial}{\partial r}\left[\frac{\partial}{\partial \varkappa} K(r, r;\varkappa)\right]_{\varkappa=\varkappa_1} \\ &= -2\frac{\partial}{\partial r}\left[\frac{\partial}{\partial \varkappa} g(r, r;\varkappa)\right]_{\varkappa=\varkappa_1}\end{aligned}\right\} \tag{2.16}$$

and by (2.15)

$$\left.\begin{aligned}\left[\frac{\partial}{\partial \varkappa} g(r, r;\varkappa)\right]_{\varkappa=\varkappa_1} &= -\frac{1}{4}\sum_{l=1}^{m} A_l [f_1(-i\varkappa_l, r)]^2 \\ &\quad - \frac{2 i\varkappa_1}{\dot{f}_1(-i\varkappa_1) f_1'(-i\varkappa_1, 0)}\left[\frac{\partial}{\partial \varkappa}[f(-i\varkappa, r)]^2\right]_{\varkappa=\varkappa_1}.\end{aligned}\right\} \tag{2.17}$$

Thus $[\partial V(r;\varkappa)/\partial\varkappa]_{\varkappa=\varkappa_1}$, has the form

$$\left.\begin{aligned}\left[\frac{\partial V(r;\varkappa)}{\partial \varkappa}\right]_{\varkappa=\varkappa_1} &= \sum_{l=1}^{m} A_l \dot{f}_1(-i\varkappa_l, r) f_1'(-i\varkappa_l, r) \\ &+ \frac{8 i\varkappa_1}{\dot{f}_1(-i\varkappa_1) f_1'(-i\varkappa_1, 0)}\left[\frac{\partial}{\partial \varkappa}(f_1(-i\varkappa, r) f_1'(-i\varkappa, r)\right]_{\varkappa=\varkappa_1}.\end{aligned}\right\} \tag{2.18}$$

This expression can be checked in an elementary way. We consider the infinitesimal change of potential

$$\delta V(r) = \delta\varkappa\left[\frac{\partial V(r;\varkappa)}{\partial \varkappa}\right]_{\varkappa=\varkappa_1} \tag{2.19}$$

and shall verify that to first order in $\delta\varkappa$ it changes only the binding energy $-\varkappa_1^2$, to $-(\varkappa_1 + \delta\varkappa)^2$, leaving the other binding energies and phase shift unaltered.

We have seen in ref. 3, Eq. (2,3), that the first term of (2.18) does not change the eigenvalues or phase shift; it merely leads one to a neighbouring "equivalent" potential. Next we calculate the change of the eigenvalues due to the second term in (2.18). Let ψ_l be the normalized eigenfunction of V_1, belonging to binding energy E_l. Then

$$\left.\begin{aligned}\delta E_l &= \int_0^\infty \delta V(r)\,[\psi_l(r)]^2\,dr \\ &= \delta\varkappa\,\frac{8 i\varkappa_1}{\dot{f}_1(-i\varkappa_1) f_1'(-i\varkappa_1, 0)}\int_0^\infty\left[\frac{\partial}{\partial \varkappa}(f_1(-i\varkappa, r) f_1'(-i\varkappa, r)\right]_{\varkappa=\varkappa_1}\psi_l^2(r)\,dr.\end{aligned}\right\} \tag{2.20}$$

With the help of the Schroedinger equation we find (cf. ref. 3, Eq. (2.3))

$$\int_0^\infty f_1(-i\varkappa, r)\, f_1'(-i\varkappa, r)\, \psi_e^2(r)\, dr = \frac{1}{4}(\varkappa^2 + E_m)\left[\int_0^\infty f_1(-i\varkappa, r)\, \psi_l(r)\, dr\right]^2. \quad (2.21)$$

Differentiating with respect to $\varkappa$ and substituting into (2.20) gives, with the help of (1.10) and (1.15),

$$\left.\begin{aligned} \delta E_e &= \delta\varkappa \frac{8 i\varkappa_1}{\dot{f}_1(-i\varkappa_1)\, f_1'(-i\varkappa_1, 0)} \frac{\varkappa_1}{2}\left[\int_0^\infty \frac{f_1'(-i\varkappa, 0)}{C_1^{1/2}} \psi_1(r)\, \psi_l(r)\, dr\right] \\ &= \delta_{l1}\left[(\varkappa_1 + \delta\varkappa)^2 - \varkappa_1^2\right]. \end{aligned}\right\} \quad (2.22)$$

Similarly one can check that $\delta V(r)$ does not alter the phase shift, which completes the verification.

As an illustration, we shall explicitly construct the potentials corresponding to the phase shift $\eta(k)$ given by

$$\left.\begin{aligned} k \cot \eta(k) &= -\alpha + \frac{1}{2} r_0 k^2 \\ \alpha > 0, \quad r_0 > 0, \quad 2\alpha r_0 &< 1, \end{aligned}\right\} \quad (2.23)$$

and a bound state located at the arbitrary negative energy $E_1 = \varkappa_1^2$. Eq. (2.23) has been used for an approximate description of low energy neutron proton scattering in the triplet state. According to Eq. (6.19) of ref. 1 this leads to

$$f(k) = \frac{4k^2 + 4\varkappa_1^2}{[2k - i(\varrho - \sigma)]\,[2k - i(\varrho + \sigma)]}, \quad (2.24)$$

where

$$\varrho = \frac{2}{r_0}, \qquad \sigma = \frac{2}{r_0}\sqrt{1 - 2\alpha r_0}. \quad (2.25)$$

As auxiliary potential $V_1(r)$ we chose the potential corresponding to

$$f_1(k) = \frac{(2k - 2i\varkappa_1)^2}{[2k - i(\varrho - \sigma)]\,[2k - i(\varrho + \sigma)]}. \quad (2.26)$$

This potential has no bound state and is uniquely defined. It is contained among the examples of BARGMANN [7]. Since

$$|f_1(k)|^2 = |f(k)|^2 \quad (2.27)$$

the kernel $g(s, t)$ of Eq. (1.25) reduces to a single bilinear term so that the solution of the integral equation (1.24) becomes trivial and $V(r)$ can be determined.

To obtain an expression for $V_1(r)$ we express $\varkappa_1$ by means of a new parameter λ as

$$\varkappa_1 = \frac{1}{2}(\varrho+\sigma)\frac{1+\lambda}{1-\lambda}, \quad -1<\lambda<1. \text{ [8]}. \tag{2.28}$$

Then $V_1(r)$ can be written as

$$\left.\begin{aligned} V_1(r) = {} & 2\varrho\sigma\{(\varrho+\lambda\sigma)^2(\sigma+\lambda\varrho)^2(\varrho-\sigma)^2[e^{\frac{1}{2}(\varrho+\sigma)r}-\lambda^2 e^{-\frac{1}{2}(\varrho+\sigma)r}]^2 \\ & -\lambda^2(\varrho+\sigma)^2[(\varrho+\lambda\sigma)^2 e^{\frac{1}{2}(\varrho-\sigma)r}-(\sigma+\lambda\varrho)^2 e^{-\frac{1}{2}(\varrho-\sigma)r}]^2\} \\ & \times\{(\varrho+\lambda\sigma)^2[(\sigma e^{\varrho r}+\varrho\lambda^2 e^{-\sigma r}]-(\sigma+\lambda\varrho)^2[\varrho e^{\sigma r}+\sigma\lambda^2 e^{-\varrho r}]\}^{-2} \end{aligned}\right\} \tag{2.29}$$

and the corresponding $\varphi_1(E_1, r)$ is

$$\left.\begin{aligned} \varphi_1(E_1, r) = {} & e^{\varkappa_1 r}(1-\lambda^2) \\ & \times\frac{(\varrho+\lambda\sigma)[\sigma e^{\varrho r}+\varrho\lambda e^{-\sigma r}]-(\sigma+\lambda\varrho)[\varrho e^{\sigma r}+\lambda\sigma e^{-\varrho r}]}{(\varrho+\lambda\sigma)^2[\sigma e^{\varrho r}+\varrho\lambda^2 e^{-\sigma r}]-(\sigma+\lambda\varrho)^2[\varrho e^{\sigma r}+\lambda^2\sigma e^{-\varrho r}]}. \end{aligned}\right\} \tag{2.30}$$

The integral equation for $K(r, t)$ is

$$\left.\begin{aligned} & K(r, s)+C\,\varphi_1(E_1, r)\,\varphi_1(E_1, s) \\ & +C\,\varphi_1(E_1, s)\int_0^r K(r, t)\,\varphi_1(E_1, t)\,dt = 0 \end{aligned}\right\} \tag{2.31}$$

with the solution

$$K(r, t) = \frac{C\varphi_1(E_1, r)\,\varphi_1(E_1, t)}{1+C\int_0^r[\varphi_1(E_1, t')]^2\,dt'}, \quad 0<C<\infty\,. \tag{2.32}$$

The family of potentials with the phase shift (2.10) and the bound state at the arbitrary energy $E_1<0$ is therefore given by

$$V(r) = V_1(r)-2C\frac{\partial}{\partial r}\frac{[\varphi_1(E_1, r)]^2}{1+C\int_0^r[\varphi_1(E_1, t)]^2\,dt}. \tag{2.33}$$

Summarizing we may note that we have here a four parameter manifold of potentials; ϱ and σ are determined by the phase shift, λ by the position of the bound state and C by the normalization of the bound state function $\varphi(E_1, r)$.

§ 3. Remarks on the Interpretation of Scattering Data.

In some of the early investigations of the S-matrix, it was believed that the zeros of the S-matrix determine the bound states. Counter-examples showed, however, that in some cases, at the so-called false zeros, no bound states occur. Still, the idea survived that at least the S-matrix must always vanish at the points of the discrete spectrum. For instance, this idea was used in one of the justifications of the so-called effective range theory [9], to establish the connection between the neutron proton triplet S-phase and the binding energy of the deuteron. We have seen that such a connection does not exist, in general. We shall show that only for sufficiently short-range potentials do bound states necessarily coincide with the zeros of the S-matrix. (It should be noted that the original derivation of the effective range formalism by SCHWINGER [10] does not make use of this connection, but is based only on the assumption that the range of the potential is short compared to the size of the deuteron).

Thus consider the case where the S-matrix, $S(k) = e^{2i\eta(k)}$, is known and has zeros at $k = -i\varkappa_l$, $l = 1, 2, \cdots m$. Suppose further we know *a priori* that the underlying potential is short range in the sense that

$$\lim_{r\to\infty} e^{2\varkappa r} V(r) = 0 \tag{3.1}$$

for some $\varkappa > 0$. Then $f(k)$ is regular in $Im(k) < \varkappa$ so that in the strip, $-\varkappa < Im(k) < 0$, there is a one to one correspondence between zeros of the S-matrix and binding energies. On the other hand, no bound states need occur at those zeros $-i\varkappa_l$ which lie below this strip. For suppose there exists a potential V_1 reproducing the phase shift and having bound states at $-i\varkappa_l$. According to (2.19) and (2.18) one can add an infinitesimal increment $\delta V = \varepsilon\,[(\partial/\partial\varkappa)\,(f_1(-i\varkappa, r)\,f_1'(-i\varkappa, r))]_{\varkappa=\varkappa_l}$, which changes only the position of the l'th bound state. Since it behaves asymptotically like $\delta V \sim \varepsilon\,(2\varkappa_l r - 1)\exp(-2\varkappa_l r)$ it does not violate (3.1), provided that $\varkappa_l > \varkappa$, and hence leads to an acceptable potential with the same S-matrix, but a displaced bound state.

For the neutron proton system $\varkappa$, Eq. (3.1) may be estimated by meson theory and is substantially larger than the smallest

zero, $-i\varkappa_1$, of the S-matrix ($\varkappa/\varkappa_1 \sim 1{\cdot}5$). From this additional information it follows that this zero corresponds to the deuteron binding energy.

It is a great pleasure to express our thanks to Professor Niels Bohr for the opportunity to carry out this work at his institute and to the Rask Ørsted Foundation for financial support.

Institute for Theoretical Physics, University of Copenhagen, Denmark.

References & Footnotes.

[1] R. Jost and W. Kohn, Phys. Rev. **87**, 977 (1952).
[2] I. M. Gel'fand and B. M. Levitan, Doklady Akad. Nauk. S.S.S.R. n Ser. 77, 557 (1951); we are indebted to Professor Lars Gårding for bringing this paper to our attention.
[3] R. Jost and W. Kohn, Phys. Rev. **88**, 382 (1952); See also B. Holmberg, Nuovo Cimento **9**, 597 (1952).
[4] The derivation of (1.23) by means of (1.22) is not mathematically strict, because of the occurrence of second derivatives in (1.22). Conditions for the validity of (1.23) will be given on page 8 ff.
[5] One can verify the completeness of the functions $\varphi(E, r)$ defined by (1.12) with the aid of (1.11), (1.12), and (1.13).
[6] The connection of $f(k)$ and $\eta(k)$, in the absence of bound states, is given by

$$f(k) = \frac{1 \cdot 1 \cdot 3 \cdots (2l+1)}{(ik)^l} \exp\left[-\frac{1}{\pi}\int_{-\infty}^{+\infty} \frac{\eta(k')}{k'-k'} dk'\right],$$

with obvious modifications when bound states are present ([1], Eqs. (2.15)—(2.18)).
[7] V. Bargmann, Rev. Mod. Phys. **21**, 488 (1949), Eqs. (4.1)—(4.6).
[8] The connection between our parameter λ and Bargmann's α and β (ref. 5, Eq. (4.3)) is $\beta = \lambda^2$, $\alpha = \left(\frac{\sigma + \lambda\varrho}{\varrho + \lambda\sigma}\right)^2$.
[9] J. M. Blatt and J. D. Jackson, Phys. Rev. **76**, 18 (1949).
[10] J. Schwinger, Unpublished lectures at Harvard University (1947).

Note added in proof.

After completion of this manuscript the existence of a more detailed paper by I. M. Gel'fand and B. M. Levitan (Isvestiia Akad. Nauk. S.S.S.R. **15**, 309, 1951) was brought to our attention. This paper contains all the proofs and treats, also the case of boundary conditions $\varphi(0) = 0$. No application to scattering theory is discussed.

Indleveret til selskabet den 27. september 1952.
Færdig fra trykkeriet den 12. marts 1953.

Det Kongelige Danske Videnskabernes Selskab
Matematisk-fysiske Meddelelser, bind **27**, nr. 10

Dan. Mat. Fys. Medd. **27**, no. 10 (1953)

EXPANDING UNIVERSE AND THE ORIGIN OF GALAXIES

BY

G. GAMOW

København
i kommission hos Ejnar Munksgaard
1953

Printed in Denmark
Bianco Lunos Bogtrykkeri

§ 1. According to the general theory of relativity, the time-behaviour of homogeneous isotropic Universe is described by the equation (1)

$$\frac{dR}{dt} = \sqrt{\frac{8\pi G}{3}\varrho R^2 - c^2}, \tag{1}$$

where G is the Newtonian constant, c the velocity of light, ϱ the total mean density in space, and R the curvature radius[1]. If l is the distance between any two material points in the expanding Universe standing in a constant ratio α to the curvature radius, we can rewrite (1) as:

$$\frac{dl}{dt} = \sqrt{\frac{8\pi G}{3}\varrho l^2 - c^2\alpha^2}. \tag{2}$$

As it is well known, this equation simply states the law of conservation of mechanical energy (kinetic plus potential) for the masses enclosed within a sphere of the radius l. Generally speaking, the total mean density ϱ is composed of two terms: the density of matter ϱ_{mat} which is inversely proportional to l^3, and the mass-density of thermal radiation given by aT^4/c^2. At the present state of the universe, the mass-density of thermal radiation is presumably negligibly small as compared with the density of matter which can be assumed to be of the order of magnitude of $10^{-30}\,\text{g/cm}^3$.

Dividing (2) by l we get

$$\frac{1}{l}\frac{dl}{dt} = \sqrt{\frac{8\pi G}{3}\varrho - \frac{\alpha^2 c^2}{l^2}}. \tag{3}$$

[1] R. C. Tolman. Relativity, Thermodynamics, and Cosmology. Clarendon Press. Oxford. 1934 p. 396. We have assumed the cosmological constant Λ to be zero since the cosmological term is not needed in the expanding model, and since, in fact, the new value of Hubble's constant leads to the correct age of the universe without the help of cosmological terms.

The present value of $\frac{dl}{dt}/l$ is known as HUBBLE's constant, and is numerically equal to the inverse age of the universe. We have

$$\left(\frac{1}{l}\frac{dl}{dt}\right)_{\text{pres.}} = \frac{1}{3.5 \cdot 10^9 \text{ years}} = \frac{1}{10^{17} \text{ sec.}} = 10^{-17} \text{ sec.}^{-1}. \qquad (4)$$

Substituting this value, along with that for the present mean density, in the equation (3), we find that, for the present epoch, the first term under the radical is negligibly small as compared with the second term, indicating that l is now increasing linearly with time. For the curvature radius the equation (3) leads to an imaginary quantity: $R_{\text{pres.}} = ic\,10^{+17} = i\,3 \cdot 10^{27}$ cm $= i \cdot 3 \cdot 10^9$ light-years, meaning, geometrically, that the space of our universe is hyperbolic (infinite), and ever-expanding. Physically our result means that, just as in the case of a space rocket which had escaped from the terrestrial field of gravity, the galaxies are now flying away from each other without being hindered by the forces of mutual gravitational attraction. For that free expansion period we can apparently write:

$$\varrho_{\text{mat}} = 10^{-30}\left(\frac{10^{17}}{t}\right)^3 = \frac{10^{21}}{t^3} \text{ g/cm}^3. \qquad (5)$$

For earlier periods of time, when the deceleration by gravity could not be neglected, the equation (3) should be integrated analytically. The result of integration indicates, however, that, down to one hundredth of the present age, the deviations of calculated matter density from the simple expression (5) are less than by a factor of three. Since in future consideration we will not be interested in the behaviour of matter-universe for still earlier dates, and since the present value of density used in the derivation of (5) is not known anyway within a factor of three, we will not use this refinement in our calculations.

Since in an adiabatically expanding thermal radiation the energy density changes as the inverse fourth power of linear dimensions, in contrast to the inverse third power in the case of matter density, we should expect that, for sufficiently early stages of expansion, mass density of thermal radiation plays a more important role than the density of matter. In this case the equation (3) can be rewritten in the form

$$\sqrt{\frac{8\pi G}{3}\frac{a}{c^2}}\,T^4 = \frac{1}{l}\frac{dl}{dt} = -\frac{1}{T}\frac{dT}{dt}. \tag{6}$$

The last equality holds because in an adiabatically expanding thermal radiation the temperature varies inversely proportionally to linear dimensions. Equation (6) can be integrated as

$$T = \sqrt[4]{\frac{3c^2}{32\pi aG}}\frac{1}{t^{1/2}} = \frac{1.5\cdot 10^{10}}{t^{1/2}}\,^{\circ}K, \tag{7}$$

giving, for the mass density of radiation during the radiation period of the expansion,

$$\varrho_{\mathrm{rad}} = \frac{4.4\cdot 10^{5}}{t^2}\,\mathrm{g/cm^3}. \tag{8}$$

Density functions given by (5) and (8) are shown by two straight lines marked "matter late", and "radiation early" in the logarithmic plot of Fig. 1. We see that these two lines intersect at the point corresponding to

$$\left.\begin{aligned} t &= 2.2\cdot 10^{15}\ \mathrm{sec}\\ \varrho &= 1\cdot 10^{-25}\ \mathrm{g/cm^3}\\ T &= 320\ ^{\circ}K. \end{aligned}\right\} \tag{9}$$

Thus we may conclude that, during the first two hundredths of its history, the expansion of the universe was ruled by radiation, whereas during the remaining time the matter was of primary importance. During the radiation epoch, matter density was changing as $l^{-3} \sim T^3 \sim t^{-\frac{3}{2}}$, so that we can write

$$\varrho_{\mathrm{mat.\ early}} = \frac{\varrho_0}{t^{3/2}} = \frac{10^{-2}}{t^{3/2}}\,\mathrm{g/cm^3}, \tag{10}$$

where the numerical value of the coefficient is adjusted so that the line passes through the intersection point obtained before. During the matter epoch, radiation density is changing as $l^{-4} \sim t^{-4}$, and we have

$$\varrho_{\mathrm{rad.\ late}} = \frac{2.5\cdot 10^{36}}{t^4}\,\mathrm{g/cm^3}. \tag{11}$$

These variations are shown by lines marked "matter early" and "radiation late" in Fig. 1. It is interesting to notice that (11)

leads to the radiation mass density $2 \cdot 10^{-32}$ g/cm^3, and the temperature 7 °K, for the present epoch.

§ 2. Some time ago[1] it was indicated by the author that the assumption of the predominantly radiative, and predominantly

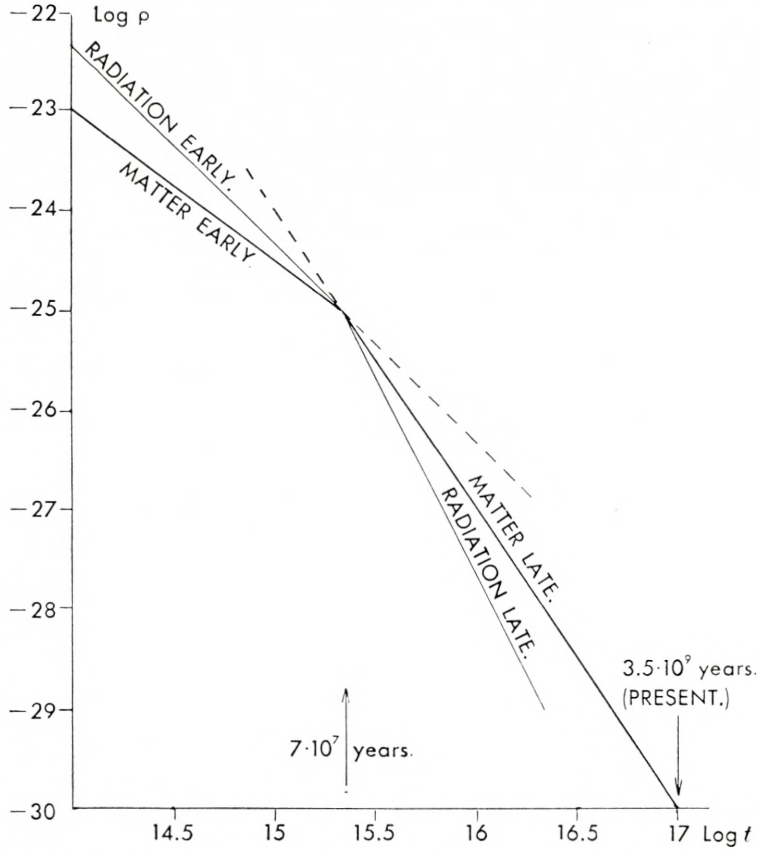

Fig. 1. Variation of matter—and radiation—densities in the expanding Universe.

material states of the universe can be very helpful for the understanding of the formation of "protogalaxies" (i. e. the initial gaseous galaxies before their condensation into individual stars) from the originally uniform gaseous material which presumably existed during the very early stages of the evolution. In fact, as long as thermal radiation was the predominant factor in the

[1] G. Gamow. Nature. Vol. 162, p. 680 (1948).

universe, the particles of matter submerged into it must have been constantly kicked around by light quanta, and should have maintained a uniform distribution through the space. As soon, however, as material density became the main factor, Newtonian forces between the elements of gas must have caused a break-up of the formerly uniform distribution into the individual gas clouds (protogalaxies) the size of which was determined by the well known JEANS' formula for gravitational instability. The present mean density of individual galaxies, being of the order of magnitude 10^{-24} or 10^{-25} g/cm^3, suggests indeed that the separation process must have taken place near the intersection or radiation- and matter-curves in Fig. 1. Substituting the density and temperature values from (9) into the JEANS' formula

$$D_{\min} = \sqrt{\frac{5\,\pi\varkappa\,T}{3\,G m_H \bar{\mu} \varrho}} \tag{12}$$

for the minimum diameter of gravitational condensation[1], we obtain

$$D_{\min} = 5 \cdot 10^{21}\,\text{cm} = 5000 \text{ light-years.} \tag{13}$$

For the minimum mass of the condensation we obtain

$$M_{\min} = 10^{40}\,\text{g} = 5 \cdot 10^6 \text{ sun masses.} \tag{14}$$

We can now compare this theoretical lower limit with HOLMBERG's data[2] concerning mass distribution among the galaxies, shown in Fig. 2. We see that the theoretical minimum mass-value, being certainly of galactic order of magnitude, falls short by a factor of ten from the observed lower limit of galactic masses. This may be due, of course, to the approximate nature of the theory, but may also be a real effect caused by not taking into account the possibility of turbulent motion in the primordial gas. In fact, according to recent calculations of S. CHANDRASEKHAR[3],

[1] The value for the mean molecular weight $\bar{\mu}$ may range from 2.7 for a half and half (by mass) mixture of molecular hydrogen and atomic helium, to 0.7 for the same mixture in completely ionised state. Evaluating (12) we have assumed $\bar{\mu} = 1$.

[2] HOLMBERG. Lund. Medd. Ser. II. No. 128 (1950). The curve shown in Fig. 2 is redrawn from HOLMBERG's original luminosity curve under the assumption that the luminosities of different galaxies are proportional to their masses.

[3] S. CHANDRASEKHAR. Proc. Roy. Soc. A. Vol. 210, p. 26 (1951).

JEANS' expression for minimum radius of gravitational condensation in turbulent medium must be multiplied by a factor

$$\left(1+\frac{1}{3}M^2\right)^{1/2}, \tag{15}$$

where M is the mean Mach number of turbulence. Thus, the assumption of Mach number 4 would bring the calculated lower limit of galactic masses to its observed value.

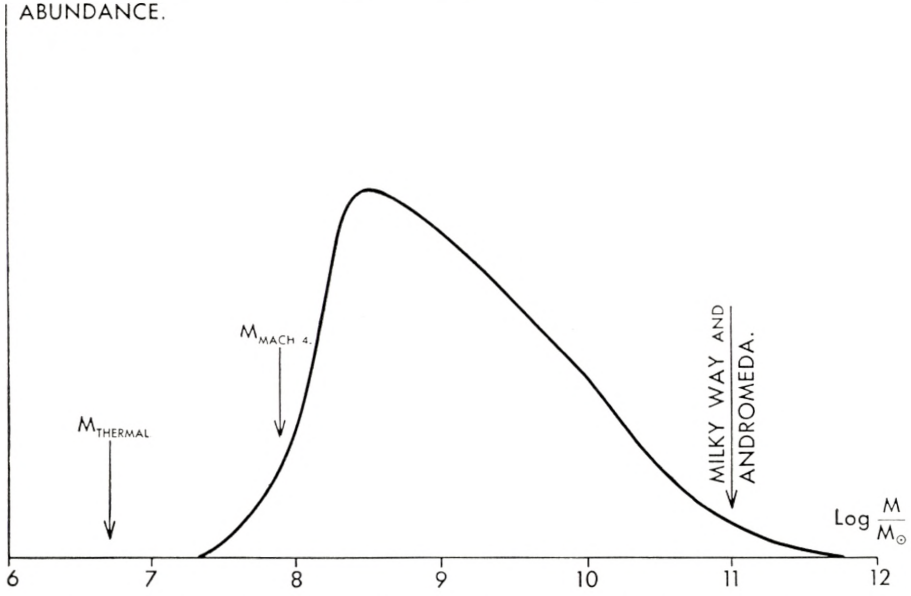

Fig. 2. Comparison of HOLMBERG's curve for the distribution of galactic masses with the calculated lower limit.

Apart from reasonable numerical agreement between the observed minimum value of galactic masses, and the value given by JEANS' formula, we want to stress the point that the shape itself of HOLMBERG's curve, with its steep descent on the side of lower masses, and a long tail extending into the region of exceptionally massive systems (such as our Milky way, and Andromeda), strongly supports the point of view that the formation of protogalaxies proceeded under the conditions characterised by the existence of a certain lower threshold for their mass.

§ 3. We have mentioned above the possible role of turbulence in determining the sizes and masses of gravitational condensations

in the expanding primordial gas. As it was first suggested by WEIZSÄCKER[1], the assumption of turbulent motion in the primordial gas might be also absolutely necessary for the correct description of the condensation process itself. In fact, as it is in the case of many instability problems, JEANS' gravitational condensations will develop within a finite time only if there are present some rudimentary local compressions and expansions which can be further augmented by the action of gravity forces. It seems in fact that, unless we have extensive density fluctuations by a factor of two or three in the primordial gas, no gravitational condensations could develop within the time period permitted by the age of the universe. It is clear that no such fluctuations could be expected in the original gas on the basis of the simple statistical theory. On the other hand, since the RAYNOLD's number may become arbitrarily large in an infinite gas medium, we may expect the formation of large size turbulent eddies. Since, in this case, the velocity of turbulent streamings could well have been larger than the velocity of thermal motion (as it is the case for interstellar gas in our Galaxy), one could easily expect the formation of local compressions and rarefactions of all possible sizes. And the compression eddies exceeding the minimum mass given by JEANS' formula must have been prevented from subsequent expansion by the Newtonian forces between their parts. According to this point of view, HOLMBERG's distribution of galactic masses may reflect the state of turbulent motion in the primordial gas, and it would be interesting to see whether this distribution is indeed in accordance with KOLMOGOROFF's spectral law for isotropic homogeneous turbulence.

Much larger, and correspondingly much weaker, compression and rarefaction eddies would have no time to change considerably since the separation time, as would be noticeable at present only as certain inhomogeneities in the space distribution of individual galaxies. Such deviations from the uniform distribution of galaxies through the space of the universe were actually observed and studied by H. SHAPLEY[2], and C. D. SHANE[3]. In Fig. 3 we give, as an example, one of SHANE's diagrams showing the isolines for

[1] C. VON WEIZSÄCKER. Astrophys J. Vol. 14, p. 165 (1951) and earlier publications.
[2] H. SHAPLEY. Proc. Nat. Acad. Sc. Vol. 37, p. 191 (1951), and previous publications.
[3] C. D. SHANE. Proc. Amer. Phil. Soc. Vol. 94, p. 13. (1950).

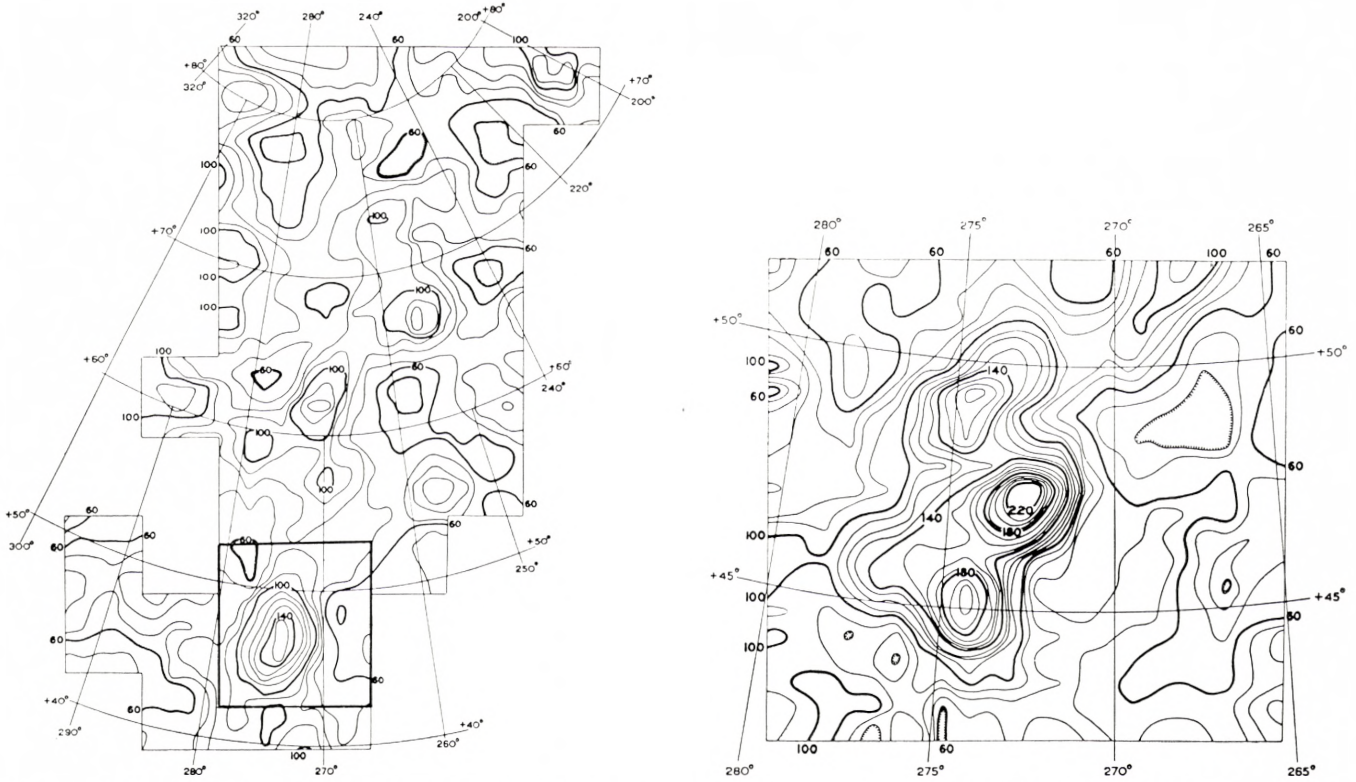

Fig. 3. Irregularities in the distribution of galaxies according to C. D. SHANE. Numbers indicate the number of galaxies per square degree of the celestial sphere. Picture on the right represents the result of more detailed study of the region squared in the left picture. Notice the appearance of smaller condensations within the original large condensation, in accordance with the expectations of the theory of turbulent motion. (The author is grateful to Dr. SHANE for the permission to reproduce these, as yet unpublished, diagrams.)

the projected distribution density of galaxies in a certain region of celestial sphere. The distribution shown in this diagram does indeed resemble a density distribution which might be expected in the case of turbulent motion in a compressible fluid.

The study of the observed space distribution of galaxies from the point of view of the theory of turbulence is now being carried out by the author in collaboration with Dr. F. N. FRENKIEL and Mrs. VERA RUBEN, and may lead to some interesting conclusions concerning the early state of the expanding universe, and the problem of the formation of galaxies.

§ 4. Accepting the ideas expressed in the previous section, we can now inquire about the conditions which must have existed very early in the history of the universe, close to the singular point at $t = 0$. For the temperature variations, and the variations of matter density during these very early stages, we may use the expressions (7) and (10) derived above.

During the first few seconds of expansion, the temperature of space must have been of the order of billions of degrees, corresponding to kinetic energy of thermal motion of the order of millions of electron volts, and the density of matter was comparable to that of the atmospheric air. Thus we may expect that at this time matter must have existed in completely dissociated state, being composed entirely of neutrons, protons, and electrons. As the temperature was dropping in the process of expansion, nucleons forming this primordial material, or *ylem*, must have started to aggregate, forming composite atomic nuclei of various degrees of complexity. The process must have come to an end after about half an hour when most of the neutrons present in the original mixture have either decayed or been captured by protons and other nuclei, and the temperature dropped to $4 \cdot 10^8$ °K (60 Kev), being too low for most thermonuclear reactions between charged particles. The result of the process must have depended critically on the assumed value of the coefficient in (10). If the assumed density is too low, most of the neutrons will decay into protons before being captured by other particles, and the resultant material will be almost exclusively hydrogen. If, on the contrary, the density is taken too high, everything would be built into helium and heavier elements and no hydrogen

will be left. The problem was first investigated by the author[1] with the result that, in order to obtain the observed half-and-half hydrogen-helium ratio, one should choose $\varrho_0 = 0.7 \cdot 10^{-2}$. Subsequent more detailed calculations were carried out by FERMI and TURKEVICH[2], who took into account all possible thermonuclear reactions up to the formation of He^4. The result of their calculations, carried out with $\varrho_0 = 1.7 \cdot 10^{-3}$, are shown in Fig. 4,

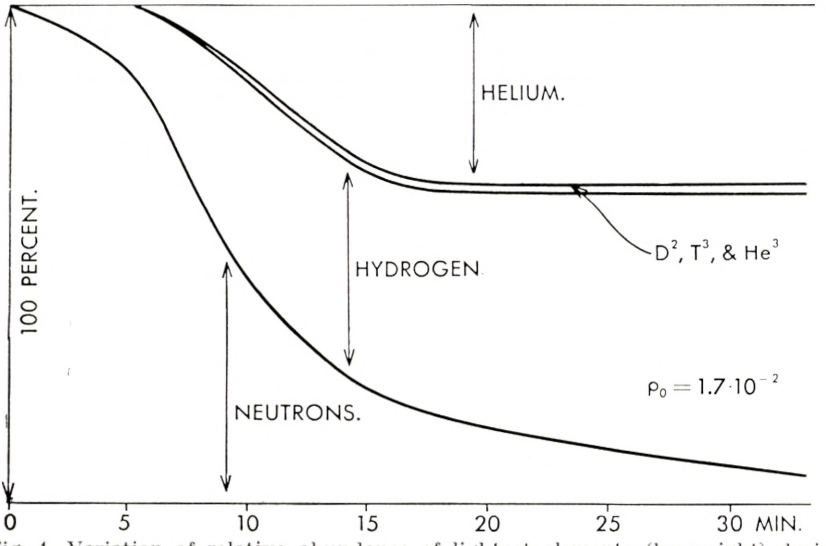

Fig. 4. Variation of relative abundance of lightest elements (by weight) during first half hour of expansion, calculated by FERMI & TURKEVICH.

and are in good agreement with the observed relative amount of Hydrogen and Helium in the universe. Attempts by the same authors to carry the detailed calculations of the element formation beyond He^4 have failed, mostly because of the non-existence of any nucleus with mass 5, and this difficulty is not as yet removed.

On the other hand, a general theory of the formation of heavier elements by the process of neutron capture, developed by the author in collaboration with ALPHER[3], and later extended by ALPHER and HERMAN[4], shows that the amount of heavy ele-

[1] G. GAMOW, *l. c.*

[2] E. FERMI and A. TURKEVICH. Unpublished. For more details on these calculations, see the review by R. A. ALPHER and R. C. HERMAN. Rev. Mod. Phys. vol. 22, p. 153 (1950).

[3] ALPHER, BETHE, and GAMOW. Phys. Rev. vol. 73, p. 803 (1948).

[4] R. ALPHER and R. HERMAN. Phys. Rev. vol. 84, p. 60 (1951).

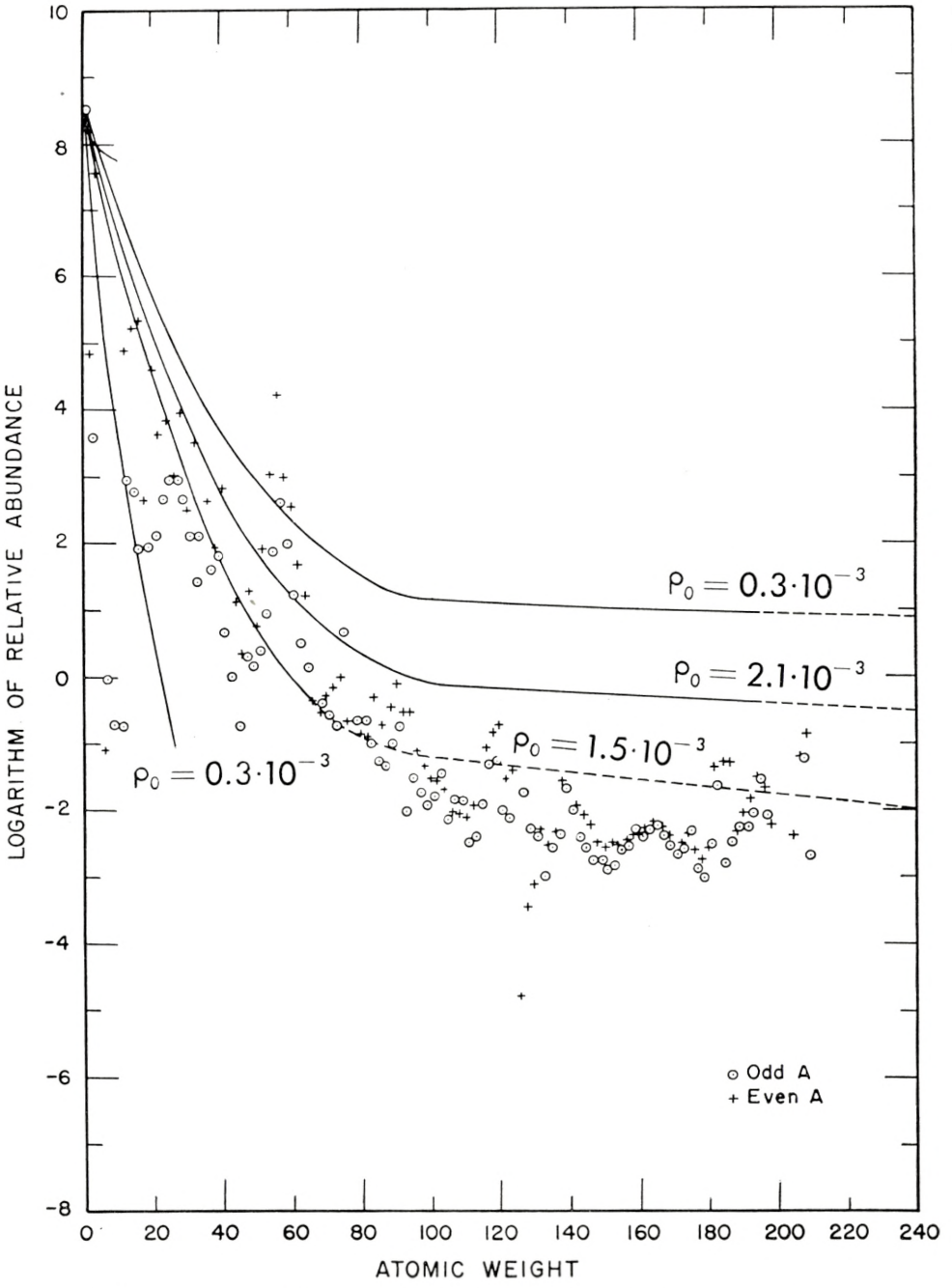

Fig. 5. Comparison of the observed relative abundance of elements (circles and crosses) with theoretical curves calculated with different values of ϱ_0 by ALPHER and HERMAN.

ments formed is also very sensitive to the assumed value of ϱ_0. Fig. 5 shows the theoretical abundance curves calculated for different ϱ_0's in the recent work by ALPHER and HERMAN[1]. The curves faithfully represent general variation of the relative abundances, and we find that the best fit with observed data is obtained by assuming $\varrho_0 = 1.2 \cdot 10^{-3}$, in good agreement with the results obtained by FERMI and TURKEVICH.

It is quite remarkable that the calculations pertaining to the formation of atomic species lead to about the same density as is obtained from purely cosmological considerations pertaining to the formation of galaxies. This agreement can be even improved if one assumes that the concentration of neutrons in ylem was lower than that ($\sim$ 100 per cent) assumed in the above calculations, since lower concentration of neutrons will call for higher total density necessary for the formation of elements.

[1] R. ALPHER and R. HERMAN. Phys. Rev. vol. 84, p. 60 (1951).

Conclusions.

Considering the very preliminary nature of the theory described in the present paper, and the exceptionally broad scope of the phenomena which it attempts to tie together into one consistent cosmogonical picture, one should agree that the proposed point of view may be accredited with a certain degree of success, even though there are still many difficulties standing in its way. In the author's opinion, the most promising feature of the theory is the possibility of binding together such seemingly non-related observational data as the relative abundance of chemical elements, on the one hand, and the sizes, masses, and space distribution of stellar galaxies, on the other. It seems to the author that the agreement between density functions obtained from direct observations at the present time ($t = 3 \cdot 10^{17}$ sec), from the conditions necessary for the formation of protogalaxies (at $t \simeq 2 \cdot 10^{15}$sec), and from the theory of the origin of atomic species (at $t \simeq 10^{3}$sec), cannot be entirely coincidental.

The George Washington University.
Washington D. C., U. S. A.
October 1952.

Indleveret til selskabet den 21. oktober 1952.
Færdig fra trykkeriet den 12. februar 1953.

Det Kongelige Danske Videnskabernes Selskab
Matematisk-fysiske Meddelelser, bind **27**, nr. 11

Dan. Mat. Fys. Medd. **27**, no. 11 (1953)

THE FUTURE ORBIT OF COMET 1898 VII (CODDINGTON–PAULY)

BY

ERIK SINDING

København
i kommission hos Ejnar Munksgaard
1953

Printed in Denmark
Bianco Lunos Bogtrykkeri

About 20 calculations back in time of nearly parabolic comet orbits have been carried out according to the principles set out by E. STRÖMGREN[1], in order to determine the eccentricities of these orbits when the comets were moving at a great distance from the Sun. In Publ. 146 from Cop. Obs. (1948) a list of the results of these calculations is given showing the changes in $\frac{1}{a}$, the reciprocal semi-major axis. It is seen that the great majority of the orbits have changed in the elliptical direction by the backward-computation, and on an average we find:

$$\Delta\left(\frac{1}{a}\right)_m = +0.000552 \text{ with a standard error of } \pm 0.000055,$$

considering the distribution as random. Including v. BIESBROECK's calculation for Comet 1908 III[2] we find:

$$\Delta\left(\frac{1}{a}\right)_m = +0.000568 \pm 0.000054$$

and for an individual orbit:

$$\Delta\left(\frac{1}{a}\right) = +0.00057 \pm 0.00025.$$

Considering the conditions in the solar system in a simplified way and using a Jacobian integral for the Sun, Jupiter, and a comet it is shown that on an average we get:

$$\Delta\left(\frac{1}{a}\right)_m = \frac{1}{\bar{a}} - \frac{1}{a} = \frac{2\,m_1}{\varrho} - \frac{m_1}{r_1^3}(r^2 - \varrho^2).$$

Here $\bar{a}$ is the semi-major axis in the original orbit of the comet relative to the common centre of gravity of the Sun and Jupiter, and a is the same element of orbit in the osculating

orbit relative to the Sun (at an epoch near the time of perihelion). Furthermore m_1 and r_1 are the mass and radius of orbit of Jupiter, Jupiter's orbit being considered as circular, and r and ϱ are the distances comet-Sun and comet-Jupiter, respectively, at the moment of osculation. Introducing an average value of ϱ equal to $r_1 = 5.203$, $r = 1$, and $m_1 = \frac{1}{1047}$, we find:

$$\Delta\left(\frac{1}{a}\right)_m = + 0.000544.$$

These considerations show that the phenomenon that nearly parabolic orbits change systematically in the elliptical direction when epochs further and further back in time are considered is plausibly explained by the dominating influence of Jupiter.

In 1906 G. Fayet published a great investigation[3] showing the result of an approximate backward-calculation of 146 nearly parabolic cometary orbits. J. H. Oort has computed $\Delta\left(\frac{1}{a}\right)_m$ for these orbits[4] and found + 0.000500. I have made a new computation excluding Comets 1844 III and 1897 I, as Fayet in those cases used erroneous elements. The result is:

$$\Delta\left(\frac{1}{a}\right)_m = + 0.000498 \pm 0.000056,$$

corresponding to:

$$\Delta\left(\frac{1}{a}\right) = + 0.00050 \pm 0.00067$$

for an individual comet. (This standard deviation is different from Oort's value.)

In comparison with the standard deviation found by the 22 rigorous calculations backwards we find that this is essentially smaller, and in Oort's opinion the reason must be that by chance no great perturbations take place for these 22 comets. The real reason is undoubtedly another. The 'original elements' of Fayet are determined relative to the Sun while the same elements in the case of the rigorous calculations are computed relative to the gravity centre of the system Sun-Jupiter-Saturn (possibly

more planets), and this circumstance is the cause of the great standard deviation in FAYET's case.

This is easily shown by a simple reasoning. H. SEELIGER has derived the following Jacobian integral for the motion relative to the Sun[5]:

$$V^2 = 2\gamma + \frac{2k^2}{r} + \frac{2k^2 m_1}{\varrho} + 2n_1 k\sqrt{p}\cos i - \frac{k^2 m_1}{r_1^3}(r^2 - \varrho^2)$$

or:

$$\frac{1}{a} = -2C - \frac{2m_1}{\varrho} - \frac{2n_1}{k}\sqrt{p}\cos i + \frac{m_1}{r_1^3}(r^2 - \varrho^2).$$

V is the velocity of the comet, 2γ and $2C$ constants, n_1 is the mean motion of Jupiter, and p and i the parameter and inclination, respectively, of the orbit of the comet. If we consider now the motion of the comet at greater and greater distances from the Sun the term $\frac{2m_1}{\varrho}$ is decreasing towards zero, while the last term is oscillating about zero with increasing amplitude. A great material with elements relative to the Sun will on an average yield:

$$\Delta\left(\frac{1}{a}\right)_m = \frac{2m_1}{\varrho} - \frac{m_1}{r_1^3}(r^2 - \varrho^2),$$

i. e. the same expression as given above but with a greater scattering.

The expression may be used as a matter of course, if we take into consideration the changes in $\frac{1}{a}$ in nearly parabolic orbits in forward-calculations. Now it is a well-known fact that not one decidedly hyperbolic orbit is found in backward-calculations, and that consequently all these comets originate in the solar system. But the result of the forward-calculations is that among the known, near perihelion nearly parabolic orbits there are some which are hyperbolic at a great distance from the Sun, and consequently these comets are leaving the solar system.

In accordance with the principles used for the above-mentioned 146 approximate backward-calculations FAYET has carried out forward-calculations for 36 nearly parabolic orbits[6]. A computation of $\Delta\left(\frac{1}{a}\right)_m$ in this case yields:

$$\Delta\left(\frac{1}{a}\right)_m = +0.000409 \pm 0.000110,$$

corresponding to:

$$\Delta\left(\frac{1}{a}\right) = +0.00041 \pm 0.00066$$

for an individual comet, in good agreement with the expected result. Among these comets FAYET found 7 with hyperbolic orbits. He made a new calculation of these 7 orbits, computing by numerical integration perturbations of the first order in the eccentricity caused by Jupiter 15—20 years forward in time, in conclusion referring the eccentricity to the centre of gravity of the system Sun-Jupiter and obtaining the same result.

In order to check FAYET's approximate calculations I have carried out a rigorous calculation of the perturbations for Comet 1898 VII. The definitive orbit has been determined by C. J. MERFIELD[7] on the basis of 414 observations during the time 1898 Jun. 11—1899 Dec. 6, and perturbations by Venus, the Earth, Mars, Jupiter, and Saturn have been taken into account.

Osculation: 1898 Jun. 21.0 G. M. T.

$$\begin{aligned} T &= 1898\ \text{Sept. } 14.0442056\ \text{G. M. T.} \\ \omega &= 233^\circ 15' 18''.66 \\ \Omega &= 74\ \ 0\ 58.17 \quad 1900.0 \\ i &= 69\ 56\ \ 0.37 \\ \log q &= 0.2308587 \pm 0.0000009 \\ e &= 1.0010336 \pm 0.0000164 \\ \frac{1}{a} &= -0.00006074 \pm 0.0000096 \end{aligned}$$

Reducing to 1950.0 we find:

$$\begin{aligned} \omega &= 233^\circ.26204 \\ \Omega &= 74.71189 \quad 1950.0 \\ i &= 69.93455 \end{aligned}$$

The corresponding equatorial constants are as follows:

$$\begin{aligned} P_x &= +0.1075006 & Q_x &= +0.4092631 \\ P_y &= -0.2963618 & Q_y &= +0.8831024 \quad 1950.0 \\ P_z &= -0.9490065 & Q_z &= -0.2294208 \end{aligned}$$

The orbit was traced forward through 27 years by direct numerical integration of the rectangular co-ordinates, and attractions by the Sun, Jupiter, and Saturn were taken into account. To some extent perturbations by Mercury, Venus, and the Earth have been taken into account, including the masses of these planets in the constant of attraction. The calculation was carried out to 7 decimal places and COMRIE's 'Planetary Co-ordinates' was used. My thanks are due to Mr. P. NAUR, M. Sc., for some checking.

Perturbed, equatorial co-ordinates of Comet 1898 VII.

	x	y	z
1898 May 10.5	−0.744165	−2.164022	−0.521978
20.5	0.678990	2.066691	0.631351
30.5	0.612088	1.964098	0.739110
Jun. 9.5	0.543456	1.855944	0.844768
19.5	0.473115	1.741948	0.947759
29.5	0.401126	1.621875	1.047434
Jul. 9.5	0.327594	1.495550	1.143059
19.5	0.252678	1.362889	1.233831
29.5	0.176597	1.223930	1.318886
Aug. 8.5	0.099637	1.078857	1.397338
18.5	−0.022149	0.928023	1.468316
28.5	+0.055460	0.771966	1.531016
Sep. 7.5	0.132743	0.611396	1.584756
17.5	0.209232	0.447178	1.629032
27.5	0.284468	0.280281	1.663554
Oct. 7.5	0.358030	−0.111727	1.688264
17.5	0.429548	+0.057471	1.703333
27.5	0.498733	0.226366	1.709131
Nov. 6.5	0.565371	0.394113	1.706190
16.5	0.629331	0.560000	1.695150
26.5	0.690550	0.723456	1.676716
Dec. 6.5	0.749028	0.884045	1.651614
16.5	0.804809	1.041458	1.620556
26.5	0.857976	1.195491	1.584225
1899 Jan. 5.5	+0.908633	+1.346031	−1.543251

		x	y	z
1899	Jan. 15.5	+ 0.956898	+ 1.493032	— 1.498210
	25.5	1.002902	1.636506	1.449621
	Feb. 4.5	1.046774	1.776503	1.397945
	14.5	1.088641	1.913101	1.343588
	24.5	1.128631	2.046399	1.286910
	Mar. 6.5	1.166861	2.176509	1.228222
	16.5	1.203446	2.303550	1.167799
	26.5	1.238490	2.427644	1.105879
	Apr. 5.5	1.272095	2.548915	1.042671
	15.5	1.304350	2.667483	0.978355
	25.5	1.335343	2.783469	0.913090
	May 5.5	1.365151	2.896986	0.847014
	25.5	1.421501	3.117049	0.712893
	Jun. 14.5	1.473920	3.328497	0.576788
	Jul. 4.5	1.522851	3.532070	0.439305
	24.5	1.568672	3.728433	0.300918
	Aug. 13.5	1.611710	3.918180	0.161989
	Sep. 2.5	1.652244	4.101838	— 0.022802
	22.5	1.690515	4.279879	+ 0.116420
	Oct. 12.5	1.726734	4.452724	0.255506
	Nov. 1.5	1.761085	4.620751	0.394318
	21.5	1.793729	4.784296	0.532751
	Dec. 11.5	1.824808	4.943663	0.670722
	31.5	1.854446	5.099127	0.808165
1900	Jan. 20.5	1.882755	5.250936	0.945030
	Feb. 9.5	1.909835	5.399313	1.081281
	Mar. 1.5	1.935773	5.544463	1.216886
	21.5	1.960651	5.686572	1.351825
	Apr. 10.5	1.984538	5.825811	1.486083
	May 20.5	2.029600	6.096284	1.752518
	Jun. 29.5	2.071407	6.356984	2.016153
	Aug. 8.5	2.110334	6.608847	2.276992
	Sept. 17.5	2.146694	6.852676	2.535069
	Oct. 27.5	2.180753	7.089163	2.790434
	Dec. 6.5	+ 2.212736	+ 7.318912	+ 3.043151

		x	y	z
1901	Jan. 15.5	+ 2.242840	+ 7.542453	+ 3.293288
	Feb. 24.5	2.271231	7.760248	3.540920
	Apr. 5.5	2.298057	7.972712	3.786120
	May 15.5	2.323446	8.180212	4.028962
	Jun. 24.5	2.347512	8.383073	4.269521
	Aug. 3.5	2.370355	8.581593	4.507868
	Sep. 12.5	2.392064	8.776036	4.744074
	Dec. 1.5	2.432389	9.153632	5.210326
1902	Feb. 19.5	2.469033	9.517536	5.668786
	May 10.5	2.502436	9.869145	6.119922
	Jul. 29.5	2.532966	10.209639	6.564162
	Oct. 17.5	2.560926	10.540022	7.001896
1903	Jan. 5.5	2.586573	10.861160	7.433483
	Mar. 26.5	2.610125	11.173798	7.859248
	Jun. 14.5	2.631772	11.478590	8.279490
	Sep. 2.5	2.651676	11.776109	8.694482
	Nov. 21.5	2.669979	12.066858	9.104475
1904	Feb. 9.5	2.686808	12.351288	9.509700
	Apr. 29.5	2.702273	12.629797	9.910370
	Jul. 18.5	2.716477	12.902744	10.306681
	Dec. 25.5	2.741453	13.433210	11.086943
1905	Jun. 3.5	2.762370	13.944921	11.851796
	Nov. 10.5	2.779763	14.439737	12.602377
1906	Apr. 19.5	2.794093	14.919228	13.339689
	Sep. 26.5	2.805757	15.384742	14.064621
1907	Mar. 5.5	2.815101	15.837451	14.777968
	Aug. 12.5	2.822426	16.278385	15.480447
1908	Jan. 19.5	2.827990	16.708454	16.172704
	Jun. 27.5	2.832018	17.128472	16.855329
	Dec. 4.5	2.834697	17.539167	17.528858
1909	May 13.5	2.836188	17.941196	18.193783
	Oct. 20.5	2.836626	18.335153	18.850552
1910	Mar. 29.5	2.836119	18.721576	19.499582
	Sep. 5.5	2.834756	19.100956	20.141252
1911	Feb. 12.5	+ 2.832605	+ 19.473738	+ 20.775916

	x	y	z
1911 Jul. 22.5	+ 2.829718	+ 19.840329	+ 21.403899
Dec. 29.5	2.826131	20.201098	22.025502
1912 Jun. 6.5	2.821863	20.556382	22.641004
Nov. 13.5	2.816921	20.906484	23.250662
1913 Apr. 22.5	2.811302	21.251675	23.854712
Sep. 29.5	2.804992	21.592198	24.453372
1914 Mar. 8.5	2.797978	21.928261	25.046839
Aug. 15.5	2.790223	22.260047	25.635292
1915 Jan. 22.5	2.781725	22.587706	26.218895
Jul. 1.5	2.772469	22.911365	26.797791
Dec. 8.5	2.762459	23.231127	27.372112
1916 May 16.5	2.751713	23.547080	27.941976
Oct. 23.5	2.740270	23.859302	28.507496
1917 Apr. 1.5	2.728186	24.167867	29.068776
Sep. 8.5	2.715532	24.472853	29.625918
1918 Feb. 15.5	2.702389	24.774344	30.179025
Jul. 25.5	2.688842	25.072435	30.728200
1919 Jan. 1.5	2.674978	25.367229	31.273547
Jun. 10.5	2.660876	25.658840	31.815172
Nov. 17.5	2.646610	25.947387	32.353181
1920 Apr. 25.5	2.632242	26.232996	32.887682
Oct. 2.5	2.617824	26.515792	33.418778
1921 Mar. 11.5	2.603394	26.795905	33.946575
Aug. 18.5	2.588983	27.073458	34.471173
1922 Jan. 25.5	2.574605	27.348576	34.992672
Jul. 4.5	2.560268	27.621377	35.511166
Dec. 11.5	2.545968	27.891974	36.026746
1923 May 20.5	2.531689	28.160476	36.539502
Oct. 27.5	2.517410	28.426982	37.049515
1924 Apr. 4.5	2.503096	28.691584	37.556864
Sep. 11.5	2.488708	28.954364	38.061623
1925 Feb. 19.0	2.474196	29.215392	38.563858
Jul. 29.0	2.459507	29.474725	39.063630
1926 Jan. 5.0	+ 2.444586	+ 29.732404	+ 39.560990

Perturbed equatorial co-ordinates and velocities x, y, z, and $\frac{dx}{dt}$, $\frac{dy}{dt}$, $\frac{dx}{dt}$ for 1925 Feb. 19.0 are given below. The reductions ξ, η, ζ, and $\frac{d\xi}{dt}$, $\frac{d\eta}{dt}$, $\frac{d\zeta}{dt}$ to the centre of gravity of the system Sun-Jupiter-Saturn are also given together with co-ordinates and velocities $\bar{x}$, $\bar{y}$, $\bar{z}$, and $\frac{d\bar{x}}{dt}$, $\frac{d\bar{y}}{dt}$, $\frac{d\bar{z}}{dt}$ relative to the said centre of gravity.

$x = +2.474196$	$y = +29.215392$	$z = +38.563858$
$\xi = +0.001637$	$\eta = +0.006221$	$\zeta = +0.002562$
$\bar{x} = +2.475833$	$\bar{y} = +29.221613$	$\bar{z} = +38.566420$
$\frac{dx}{dt} = -0.0145909$	$\frac{dy}{dt} = +0.2601723$	$\frac{dz}{dt} = +0.5009939$
$\frac{d\xi}{dt} = -0.0012790$	$\frac{d\eta}{dt} = +0.0000067$	$\frac{d\zeta}{dt} = +0.0000341$
$\frac{d\bar{x}}{dt} = -0.0158699$	$\frac{d\bar{y}}{dt} = +0.2601790$	$\frac{d\bar{z}}{dt} = +0.5010280$

From this we find the reciprocal semi-major axis with the aid of the following equation:

$$V^2 = w^2 k^2 (1 + \Sigma m) \left(\frac{2}{\bar{r}} - \frac{1}{\bar{a}} \right)$$

or:

$$\frac{1}{\bar{a}} = \frac{2}{\bar{r}} - \frac{V^2}{w^2 k^2 (1 + \Sigma m)}.$$

We get:

$$\frac{1}{\bar{a}} = -0.0007747.$$

Finally we get:

$$\bar{e} = 1.001321.$$

FAYET's result for 1924 Dec. 24 was:

$$\bar{e} = 1.001514$$

relative to the centre of gravity for the system Sun-Jupiter. The rigorous calculation thus confirms FAYET's result. *Hence it is certain that this comet will leave the solar system.*

The backward-calculation for this comet[8] shows that $\frac{1}{\bar{a}}$ in the

original orbit (1886) was -0.0000157. Considering the standard deviation of $\frac{1}{a}$, this hyperbolic residual is illusory and it may be taken for granted that the comet has its origin in the solar system.

A rigorous calculation of the change in the eccentricity when tracing a nearly parabolic orbit forward has been carried out also in the case of Comet 1904 I[9]. The main result was as follows. In the definitive orbit we had:

$$\frac{1}{a} = -0.0005040 \pm 0.0000079 \text{ (1904 May)}.$$

With the aid of a calculation of the perturbations by Jupiter and Saturn we got:

$$\frac{1}{a} = +0.0005096 \text{ for 1917 Apr.}$$

Hence this comet remains in the solar system. The backward-calculation for this comet[10] showed that in the original orbit (before perihelion passage):

$$\frac{1}{\bar{a}} = +0.0002165 \text{ (1891 Mar.)}.$$

Hence the passage through the inner parts of the solar system has made the orbit more elliptical.

Even if FAYET's calculations are not absolutely convincing in the individual cases they show that rather a great diffusion of comets out of the solar system takes place. A rigorous calculation has to be carried out in the same way as the investigation of original orbits to provide evidence in the particular cases regarding the question whether a comet remains in the solar system or not. In accordance with the above considerations a special interest is connected with the orbits with $\frac{1}{a} <$ about -0.0005 at an epoch near the time of perihelion, on condition that the orbits have been well determined on the basis of observations distributed over several months. From the expression $q = a(1 - e)$ we deduce that this corresponds to $e > 1 + 0.0005 \cdot q$, where q is the perihelion distance.

References.

1. Publ. Cop. Obs. 19, 1914.
2. Publ. Yerkes Obs., **8**, 1943.
3. G. FAYET, Recherches concernant les excentricités des comètes, Paris 1906.
4. B. A. N., **11**, 102, 1950.
5. A. N., **124**, 209. 1890.
6. Ann. Bur. Long., **10**, B. 1, 1933.
7. A. N., **154**, 229, 1901.
8. Publ. Cop. Obs. 19, 1914.
9. Mat. Tidsskrift B, 124, 1945.
10. Publ. Cop. Obs. 105, 1935.

Indleveret til selskabet den 13. december 1952.
Færdig fra trykkeriet den 20. februar 1953.

Det Kongelige Danske Videnskabernes Selskab
Matematisk-fysiske Meddelelser, bind **27**, nr. 12

Dan. Mat. Fys. Medd. **27**, no. 12 (1953)

ON THE MAGNITUDE OF THE RENORMALIZATION CONSTANTS IN QUANTUM ELECTRODYNAMICS

BY

GUNNAR KÄLLÉN

København
i kommission hos Ejnar Munksgaard
1953

Printed in Denmark.
Bianco Lunos Bogtrykkeri.

With the aid of an exact formulation of the renormalization method in quantum electrodynamics which has been developed earlier, it is shown that not all of the renormalization constants can be finite quantities. It must be stressed that this statement is here made without any reference to perturbation theory.

Introduction.

In a previous paper[1], the author has given a formulation of quantum electrodynamics in terms of the renormalized Heisenberg operators and the experimental mass and charge of the electron. The consistency of the renormalization method was there shown to depend upon the behaviour of certain functions ($\Pi(p^2)$, $\Sigma_1(p^2)$ and $\Sigma_2(p^2)$) for large, negative values of the argument p^2. If the integrals

$$\int^{\infty} \frac{\Pi(-a)}{a}\, da, \quad \int^{\infty} \frac{\Sigma_i(-a)}{a}\, da \quad (i = 1, 2) \tag{1}$$

converge, quantum electrodynamics is a completely consistent theory, and the renormalization constants themselves are finite quantities. This would seem to contradict what has appeared to be a well-established fact for more than twenty years, but it must be remembered that all calculations of self-energies etc. have been made with the aid of expansions in the coupling constant e. Thus what we know is really only that, for example, the self-energy of the electron, considered as a function of e, is not analytic at the origin. It has even been suggested[2] that a different scheme of approximation may drastically alter the results obtained with the aid of a straightforward application of perturbation theory. It is the aim of the present paper to show—without any attempt at extreme mathematical rigour—that this is actually not the case in present quantum electrodynamics. The best we can

[1] G. Källén, Helv. Phys. Acta **25**, 417 (1952), here quoted as I.

[2] *Cf., e. g.*, W. Thirring, Z. f. Naturf. **6a** 462 (1951). N. Hu, Phys. Rev. **80**, 1109 (1950).

hope for is that the renormalized theory is finite or, in other words, that the integrals

$$\int^{\infty} \frac{\Pi(-a)}{a^2}\, da, \quad \int^{\infty} \frac{\Sigma_i(-a)}{a^2}\, da, \tag{2}$$

appearing in the renormalized operators, do converge. No discussion of this point, however, will be given here.

General Outline of the Method.

We start our investigation with the assumption that all the quantities K, $(1-L)^{-1}$ and $\frac{1}{N}$ (for notations, cf. I) are finite or that the integrals (1) converge. This will be shown to lead to a lower bound for $\Pi(p^2)$ which has a finite limit for $-p^2 \to \infty$, thus contradicting our assumption. In this way it is proved that not all of the three quantities above can be finite. Our lower bound for $\Pi(p^2)$ is obtained from the formula (cf. I, Eqs. (32) and (32 a))

$$\Pi(p^2) = \frac{V}{-3p^2} \sum_{p^{(z)}=p}{}' |\langle 0 | j_\nu | z \rangle|^2 (-1)^{N_1^{(z)}}.^{1}) \tag{3}$$

It was shown in I that, in spite of the signs appearing in (3), the sum for $\Pi(p^2)$ could be written as a sum over only positive terms. Thus we get a lower bound for $\Pi(p^2)$, if we consider the following expression

$$\Pi(p^2) > \frac{V}{-3p^2} \sum_{q+q'=p}{}' |\langle 0 | j_\nu | q, q' \rangle|^2. \tag{4}$$

In Eq. (4), $\langle 0 | j_\nu | q, q' \rangle$ denotes a matrix element of the current (defined in I, Eq. (3)) between the vacuum and a state with one electron-positron pair (for $x_0 \to -\infty$). The energy-momentum vector of the electron is equal to q and of the positron is equal to q'. The sum is to be extended over all states for which $q + q' = p$. We can note here that, if we develop the function $\Pi(p^2)$ in powers of e^2 and consider just the first term in this expansion, only the states included in (4) will give a contribution. For this case, the sum is easily computed, *e. g.* in the following way:

---

[1]) $\Sigma' |\langle 0 | j_\nu | z \rangle|^2 = \sum{}' \left(\sum_{k=1}^{3} |\langle 0 | j_k | z \rangle|^2 - |\langle 0 | j_4 | z \rangle|^2 \right)$

$$\left.\begin{aligned} \Pi^{(0)}(p^2) &= \frac{V}{-3p^2}\sum_{q+q'=p}{}' |\langle 0|j_\nu^{(0)}|q, q'\rangle|^2 \\ &= \frac{Ve^2}{-3p^2}\sum_{q+q'=p}{}' \langle 0|\bar{\psi}^{(0)}|q'\rangle\gamma_\nu\langle 0|\psi^{(0)}|q\rangle\langle q|\bar{\psi}^{(0)}|0\rangle\gamma_\nu\langle q'|\psi^{(0)}|0\rangle \\ &= \frac{e^2}{12\pi^2}\left(1-\frac{2m^2}{p^2}\right)\sqrt{1+\frac{4m^2}{p^2}}\frac{1}{2}\left[1-\frac{p^2+4m^2}{|p^2+4m^2|}\right]. \end{aligned}\right\} \quad (5)$$

The function $\Pi^{(0)}(p^2)$ has the constant limit $\frac{e^2}{12\pi^2}$ for large values of $-p^2$. This corresponds, of course, to the well-known divergence for the first-order charge-renormalization. We shall see, however, that with the assumptions we have made here the lower bound for the complete $\Pi(p^2)$, obtained from (4), is rather similar to $\Pi^{(0)}(p^2)$.

An Exact Expression for the Matrix Element of the Current.

Our next problem is to obtain a formula for $\langle 0|j_\nu|q, q'\rangle$ with which we can estimate the matrix element for large values of $-(q+q')^2$. For this purpose we first compute

$$\left.\begin{aligned} [j_\mu(x), \psi^{(0)}(x')] &= -N\int_{-\infty}^{x} S(13)\,[j_\mu(x), f(3)]\,dx''' \\ &\quad -iN\int_{x_0'''=x_0} S(13)\,\gamma_4\,[j_\mu(x), \psi(3)]\,d^3x'''. \end{aligned}\right\} \quad (6)$$

(Cf. I, Eq. (54).) The last commutator can be computed without difficulty if we introduce the following formula for $j_\mu(x)$

$$j_\mu(x) = \frac{ieN^2}{1-L}\xi_{\mu\lambda}s_\lambda(x) + \frac{L}{1-L}\xi_{\mu\lambda}\frac{\partial^2 A_\nu(x)}{\partial x_\lambda \partial x_\nu} - L\delta_{\mu 4}\Box A_4(x) \quad (7)$$

with

$$\xi_{\mu\lambda} = \delta_{\mu\lambda} - L\delta_{\mu 4}\delta_{\lambda 4} \quad (7\,a)$$

and

$$s_\lambda(x) = \frac{1}{2}[\bar{\psi}(x), \gamma_\lambda\psi(x)]. \quad (7\,b)$$

The expression (7) is written in such a way that the second time-derivatives of all the A_μ's drop out. With the aid of I, Eqs. (4)—(7) we now get

$$\left.\begin{aligned}[j_\mu(x), \psi(3)]_{x_0'''=x_0} &= \frac{ieN^2}{1-L}\xi_{\mu\lambda}[s_\lambda(x), \psi(3)] \\ &= -\frac{ie}{1-L}\xi_{\mu\lambda}\gamma_4\gamma_\lambda\psi(x)\,\delta(\bar{x}-\bar{x}''').\end{aligned}\right\} \quad (8)$$

It thus follows that

$$\left.\begin{aligned}[j_\mu(x), \psi^{(0)}(x')] &= -N\int_{-\infty}^{x} S(13)\,[j_\mu(x), f(3)]\,dx''' \\ &\quad -\frac{eN}{1-L}\xi_{\mu\lambda}S(1x)\gamma_\lambda\psi(x).\end{aligned}\right\} \quad (9)$$

We then proceed by computing

$$\left.\begin{aligned}&\langle 0\,|\,\{[j_\mu(x), \psi^{(0)}(x')], \bar{\psi}^{(0)}(x'')\}\,|\,0\rangle \\ &= \frac{ieN}{1-L}\xi_{\mu\lambda}S(1x)\gamma_\lambda S(x2) - N\int_{-\infty}^{x} S(13)\,dx''' \\ &\times[\langle 0|[j_\mu(x), \{\bar{\psi}^{(0)}(2), f(3)\}]\,|\,0\rangle - \langle 0\,|\,\{[j_\mu(x), \bar{\psi}^{(0)}(2)], f(3)\}\,|\,0\rangle].\end{aligned}\right\} \quad (10)$$

If this expression is considered as an identity in x' and x'' it will obviously give us a formula for $\langle 0\,|\,j_\mu\,|\,q, q'\rangle$ and for $\langle q\,|\,j_\mu\,|\,q'\rangle$. (Cf. I, Eqs. (68) and (77).) We transform the right-hand side of (10) in the following way:

$$\{\bar{\psi}^{(0)}(2), f(3)\} = N\int_{-\infty}^{x'''}\{f(3), \bar{f}(4)\}\,S(42)\,dx^{\mathrm{IV}} - \frac{i}{N}[ie\gamma A(3) + K]\,S(32) \quad (11)$$

and, hence,

$$\left.\begin{aligned}\langle 0\,|\,[j_\mu(x), \{\bar{\psi}^{(0)}(2), f(3)\}]\,|\,0\rangle &= \frac{e}{N}\gamma_\lambda S(32)\langle 0\,|\,[j_\mu(x), A_\lambda(3)]\,|\,0\rangle \\ &\quad + N\int_{-\infty}^{x'''} dx^{\mathrm{IV}}\langle 0\,|\,[j_\mu(x), \{f(3), \bar{f}(4)\}]\,|\,0\rangle S(42).\end{aligned}\right\} \quad (12)$$

The last term in (10) can be treated in a similar way:

$$[j_\mu(x), \bar{\psi}^{(0)}(2)] = N\int_{-\infty}^{x}[j_\mu(x), \bar{f}(4)]\,S(42)\,dx^{\mathrm{IV}} + \frac{eN}{1-L}\bar{\psi}(x)\gamma_\lambda S(x2)\,\xi_{\lambda\mu} \quad (13)$$

and

$$\left.\begin{aligned}N\int_{-\infty}^{x} S(13)\,dx'''\langle 0\,|\,\{\bar{\psi}(x), f(3)\}\,|\,0\rangle &= -\langle 0\,|\,\{\bar{\psi}(x), \psi^{(0)}(x') \\ &\quad + iN\int_{x_0'''=x_0} S(13)\,\gamma_4\psi(3)\,d^3x'''\}\,|\,0\rangle = iS(1x)\left[1-\frac{1}{N}\right].\end{aligned}\right\} \quad (14)$$

Collecting (12), (13) and (14) we get

$$\left.\begin{aligned}
&\langle 0\,|\,\{[j_\mu(x),\psi^{(0)}(x')],\bar{\psi}^{(0)}(x'')\}\,|\,0\rangle \\
&\quad=\frac{ie}{1-L}[1+2(N-1)]\,\xi_{\mu\lambda}S(1x)\gamma_\lambda S(x2) \\
&\quad-e\int_{-\infty}^{x}S(13)\gamma_\lambda S(32)\,dx'''\,\langle 0\,|\,[j_\mu(x),A_\lambda(3)]\,|\,0\rangle \\
&-N^2\int_{-\infty}^{x}dx'''\int_{-\infty}^{x'''}dx^{\mathrm{IV}}S(13)\,\langle 0\,|\,[j_\mu(x),\{f(3),\bar{f}(4)\}]\,|\,0\rangle\,S(42) \\
&+N^2\int_{-\infty}^{x}dx'''\int_{-\infty}^{x}dx^{\mathrm{IV}}S(13)\,\langle 0\,|\,\{f(3),[j_\mu(x),\bar{f}(4)]\}\,|\,0\rangle\,S(42).
\end{aligned}\right\}\tag{15}$$

The second term in (15) can be rewritten with the aid of the functions $\Pi(p^2)$ and $\overline{\Pi}(p^2)$.

$$\left.\begin{aligned}
\langle 0\,|\,[j_\mu(x),A_\lambda(3)]\,|\,0\rangle&=\int D_R(34)\,\langle 0\,|\,[j_\mu(x),j_\lambda(4)]\,|\,0\rangle\,dx^{\mathrm{IV}} \\
&=\frac{-1}{(2\pi)^3}\int dp e^{ip(3x)}\,\varepsilon(p)\,[p_\mu p_\lambda-p^2\delta_{\mu\lambda}]\,\frac{\Pi(p^2)}{p^2}.
\end{aligned}\right\}\tag{16}$$

We are, however, more interested in the expression

$$\left.\begin{aligned}
\frac{1}{2}[1+\varepsilon(x3)]\,\langle 0\,|\,[j_\mu(x),A_\lambda(3)]\,|\,0\rangle&=\frac{i\delta_{\mu\lambda}}{(2\pi)^4}\int dp e^{ip(x3)}\,[\overline{\Pi}(p^2) \\
+i\pi\varepsilon(p)\,\Pi(p^2)]+\frac{1}{2}[1+\varepsilon(x3)]\,&\frac{\partial^2\Phi(3x)}{\partial x_\mu\,\partial x_\lambda},
\end{aligned}\right\}\tag{17}$$

where

$$\Phi(x)=\frac{1}{(2\pi)^3}\int dp e^{ipx}\,\varepsilon(p)\,\frac{\Pi(p^2)}{p^2}.\tag{17 a}$$

Obviously, we have

$$\Phi(3x)=0\tag{18 a}$$

$$\frac{\partial\Phi(3x)}{\partial x_0'''}=-i\overline{\Pi}(0)\,\delta(\bar{x}-\bar{x}''')\tag{18 b}$$

for $x_0'''=x_0$. It thus follows

$$\varepsilon(x3)\,\frac{\partial^2\Phi(3x)}{\partial x_\mu\,\partial x_\lambda}=\frac{\partial^2}{\partial x_\mu\,\partial x_\lambda}[\varepsilon(x3)\,\Phi(3x)]+2i\overline{\Pi}(0)\,\delta_{\mu 4}\delta_{\lambda 4}\delta(x3).\tag{19}$$

Using the equation

$$\frac{\partial}{\partial x_\lambda'''} S(13)\gamma_\lambda S(32) = 0, \tag{20}$$

we get

$$\left.\begin{aligned} &-e\int_{-\infty}^{+\infty}\frac{1}{2}[1+\varepsilon(x3)]\,S(13)\gamma_\lambda S(32)\langle 0|[j_\mu(x), A_\lambda(3)]|0\rangle dx''' \\ &= -\frac{ie}{(2\pi)^4}\int dx'''\int dp e^{ip(x3)} S(13)\gamma_\mu S(32)[\bar{\Pi}(p^2)+i\pi\varepsilon(p)\Pi(p^2)] \\ &\qquad + i\delta_{\mu 4}\frac{L}{1-L} S(1x)\gamma_4 S(x2). \end{aligned}\right\} \tag{21}$$

Introducing (21) into (15) we obtain

$$\left.\begin{aligned} &\langle 0|\{[j_\mu(x), \psi^{(0)}(x')], \bar{\psi}^{(0)}(x'')\}|0\rangle \\ &= ie\int dx'''\int\frac{dp}{(2\pi)^4} e^{ip(x3)} S(13)\gamma_\mu S(32)[1-\bar{\Pi}(p^2) \\ &\qquad + \bar{\Pi}(0) - i\pi\varepsilon(p)\Pi(p^2)] \\ &-N^2\int_{-\infty}^{x} dx'''\int_{-\infty}^{x'''} dx^{\mathrm{IV}} S(13)\langle 0|[j_\mu(x), \{f(3), \bar{f}(4)\}]|0\rangle S(42) \\ &+N^2\int_{-\infty}^{x} dx'''\int_{-\infty}^{x} dx^{\mathrm{IV}} S(13)\langle 0|\{f(3), [j_\mu(x), \bar{f}(4)]\}|0\rangle S(42) \\ &\qquad + \frac{2ie(N-1)}{1-L}\xi_{\mu\lambda} S(1x)\gamma_\lambda S(x2). \end{aligned}\right\} \tag{22}$$

The first term in (22) describes the vacuum polarization and is quite similar to the corresponding expression for a weak external field (cf. I, Appendix). The remaining terms contain the anomalous magnetic moment, the main contribution to the Lamb shift etc. Introducing the notation

$$\left.\begin{aligned} &-N^2\theta(x3)\theta(34)\langle 0|[j_\mu(x), \{f(3), \bar{f}(4)\}]|0\rangle \\ &+N^2\theta(x3)\theta(x4)\langle 0|\{f(3), [j_\mu(x), \bar{f}(4)]\}|0\rangle \\ &\qquad -\frac{2ie(N-1)}{1-L} L\delta_{\mu 4}\gamma_4\delta(x3)\delta(34) \\ &\qquad = \frac{ie}{(2\pi)^8}\iint dpdp' e^{ip'(3x)+ip(x4)} A_\mu(p', p) \end{aligned}\right\} \tag{23}$$

$$\theta(x) = \frac{1}{2}[1 + \varepsilon(x)], \tag{23 a}$$

we obtain from (22)

$$\left.\begin{aligned} &\langle 0 | j_\mu | q, q' \rangle \\ &= \langle 0 | j_\mu^{(0)} | q, q' \rangle \left[1 - \bar{\Pi}((q+q')^2) + \bar{\Pi}(0) - i\pi\Pi((q+q')^2) \right. \\ &\left. + 2\frac{N-1}{1-L} \right] + ie \langle 0 | \bar{\psi}^{(0)} | q' \rangle \Lambda_\mu(-q', q) \langle 0 | \psi^{(0)} | q \rangle . \end{aligned}\right\} \tag{24}$$

This is the desired formula for the matrix element of the current.

Analysis of the Function $\Lambda\mu(p', p)$.

We now want to investigate the function $\Lambda\mu(p', p)$ in some detail, especially studying its behaviour for large values of $-(q+q')^2$ in (24). For simplicity, we put $\mu = k \neq 4$ and study

$$\left.\begin{aligned} ie\Lambda_k(p', p) = \iint dx''' dx^{\mathrm{IV}} e^{-ip'(3x) - ip(x4)} N^2 \{ &\theta(x3)\theta(x4) \langle 0 | \{ f(3), \\ [j_k(x), \bar{f}(4)] \} | 0 \rangle - \theta(x3)\theta(34) \langle 0 | [j_k(x), \{ f(3), \bar{f}(4) \}] | 0 \rangle \}. \end{aligned}\right\} \tag{25}$$

We treat the two terms in (25) separately. The first vacuum expectation value can be transformed to momentum space with the aid of the functions

$$A_k^{(+)}(p', p) = V^2 \sum_{\substack{p^{(z)} = p \\ p^{(z')} = p'}} \langle 0 | f | z' \rangle \langle z' | j_k | z \rangle \langle z | \bar{f} | 0 \rangle \tag{26}$$

$$A_k^{(-)}(p', p) = V^2 \sum_{\substack{\cdots \\ \cdots}} \langle 0 | \bar{f} | z' \rangle \langle z' | j_k | z \rangle \langle z | f | 0 \rangle \tag{27}$$

$$B_k^{(+)}(p', p) = V^2 \sum_{\substack{\cdots \\ \cdots}} \langle 0 | f | z' \rangle \langle z' | \bar{f} | z \rangle \langle z | j_k | 0 \rangle \tag{28}$$

$$B_k^{(-)}(p', p) = V^2 \sum_{\substack{\cdots \\ \cdots}} \langle 0 | j_k | z' \rangle \langle z' | \bar{f} | z \rangle \langle z | f | 0 \rangle . \tag{29}$$

It then follows that

$$\left.\begin{aligned} \langle 0 | \{ f(3), [j_k(x), \bar{f}(4)] \} | 0 \rangle = \frac{1}{V^2} \sum_{p, p'} \{ &e^{ip'(3x) + ip(x4)} A_k^{(+)}(p', p) \\ - e^{ip'(34) + ip(4x)} B_k^{(+)}(p', p) &+ e^{ip'(x4) + ip(43)} B_k^{(-)}(p', p) \\ - e^{ip'(4x) + ip(x3)} A_k^{(-)}(p', p) \}. \end{aligned}\right\} \tag{30}$$

Our discussion started with the assumption that all the renormalization constants and, of course, all the matrix elements of the operators $j_\mu(x)$ and $f(x)$ are finite. As this is a condition on the behaviour of, for example, the function $\Pi(p^2)$ for large values of $-p^2$, and as this function is defined as a sum of matrix elements, it is clear that we also have a condition on the matrix elements themselves, *i. e.* on the functions A and B defined in (26)—(29) for large values of $-p^2, -p'^2$ and $-(p-p')^2$. To get more detailed information on this point we consider the expression

$$\left.\begin{aligned} &\langle z|[j_\mu(x), A_\nu^{(0)}(x')]|z\rangle \\ &= -i\frac{L}{1-L}\frac{\partial^2 D(x'-x)}{\partial x_\mu \partial x_\nu} + \int dx'' F_{\mu\nu}(x-x'') D(x'-x'') \end{aligned}\right\} \quad (31)$$

with

$$F_{\mu\nu}(x-x'') = \theta(x-x'')\langle z|[j_\mu(x), j_\nu(x'')]|z\rangle \quad (32)$$

(cf. I, Eq. (A. 8) and the equation of motion for $A_\mu(x)$). Supposing, for simplicity, that $|z\rangle$ does not contain a photon with energy-momentum vector k, we have

$$\left.\begin{aligned} &\langle z|j_\mu(x)|z,k\rangle \\ &= -\frac{L}{1-L}k_\mu k_\nu \langle 0|A_\nu^{(0)}(x)|k\rangle + i\int dx'' F_{\mu\nu}(x-x'')\langle 0|A_\nu^{(0)}(x'')|k\rangle. \end{aligned}\right\} \quad (33)$$

Writing

$$F_{\mu\lambda}(x-x'') = \theta(x-x'')\frac{-1}{(2\pi)^3}\int dp e^{ip(x-x'')} F_{\mu\lambda}(p) \quad (34)$$

and using the formula

$$\varepsilon(x-x'') = \frac{1}{i\pi} P\int \frac{d\tau}{\tau} e^{i\tau(x_0-x_0'')} \quad (35)$$

we get

$$iF_{\mu\lambda}(x-x'') = \frac{-1}{(2\pi)^4}\int dp e^{ip(x-x'')}\{\overline{F}_{\mu\lambda}(p) + i\pi F_{\mu\lambda}(p)\} \quad (36)$$

with

$$\overline{F}_{\mu\lambda}(p) = P\int \frac{d\tau}{\tau} F_{\mu\lambda}(\overline{p}, p_0+\tau). \quad (37)$$

We further note that from (34) it follows that

$$F_{\mu\lambda}(p) = V \sum_{p^{(z')} = p^{(z)} + p} \langle z | j_\lambda | z' \rangle \langle z' | j_\mu | z \rangle - V \sum_{p^{(z')} = p^{(z)} - p} \langle z | j_\mu | z' \rangle \langle z' | j_\lambda | z \rangle . \quad (38)$$

If every expression appearing in our formalism is finite, the integral in (37) must converge. This means that[1])

$$\lim_{p_0 \to \pm\infty} F_{\mu\lambda}(\bar{p}, p_0) = 0 . \quad (39)$$

Putting $\mu = \lambda = k$ we then get from (38) and (39)

$$\lim_{p_0 \to \infty} \sum_{p^{(z')} = p^{(z)} + p} |\langle z | j_k | z' \rangle|^2 (-1)^{N_4^{(z)} + N_4^{(z')}} = 0 \quad (40\,a)$$

and

$$\lim_{p_0 \to -\infty} \sum_{p^{(z')} = p^{(z)} - p} |\langle z | j_k | z' \rangle|^2 (-1)^{N_4^{(z)} + N_4^{(z')}} = 0 . \quad (40\,b)$$

If we first consider a state $|z\rangle$ with no scalar or longitudinal photons, it can be shown with the aid of the gauge-invariance of the current operator (cf. I, p. 426. Eq. (47) there can be verified explicitly with the aid of (32) and (33) above) that only states $|z'\rangle$ with transversal photons will give a non-vanishing contribution to (40 a) and (40 b), and these contributions are all positive. We thus obtain the result

$$\lim_{|p_0^{(z)} - p_0^{(z')}| \to \infty} |\langle z | j_k | z' \rangle|^2 = 0 \quad (41)$$

if none of the states $|z\rangle$ and $|z'\rangle$ contains a scalar or a longitudinal photon. Because of Lorentz invariance which requires that Eq. (41) is valid in every coordinate system, it follows, however, that (41) must be valid for all kinds of states. If we make a Lorentz transformation, the "transversal" states in the new coordinate system will in general be a mixture of all kinds of states in the old system. If (41) were not valid also for the scalar and longitudinal states in the old system, it could not hold for the transversal states in the new system.

[1]) The case in which the integrals converge without the functions vanishing will be discussed in the Appendix.

From equation (41) we conclude that

$$\lim_{-(p-p')^2 \to \infty} A_k^{(\pm)}(p', p) = 0 \tag{42 a}$$

$$\lim_{-p^2 \to \infty} B_k^{(+)}(p', p) = 0 \tag{42 b}$$

$$\lim_{-p'^2 \to \infty} B_k^{(-)}(p', p) = 0. \tag{42 c}$$

It is, of course, not immediately clear that the sum over all the terms in (26)—(29) must vanish because every term vanishes. What really follows from (40) is, however, that the sum of all the absolute values of $\langle z | j_\mu | z' \rangle$ must vanish. If the limits in A and B are then performed in such a way that p^2 and p'^2 are kept fixed for A and $(p-p')^2$ and one of the p^2's are kept fixed for the B's, equations (42) will follow.

To summarize the argument so far, we have shown that if we write

$$\langle 0 | \{f(3), [j_k(x), \bar{f}(4)]\} | 0 \rangle = \frac{1}{(2\pi)^6} \iint dp dp' e^{ip'(3x) + ip(x4)} F_k(p', p) \tag{43}$$

we have

$$\lim_{-(p-p')^2 \to \infty} F_k(p', p) = 0. \tag{44}$$

Introducing the notations

$$\bar{F}_k(p', p) = \int \frac{d\tau}{\tau} F_k(p' - \varepsilon\tau, p) \tag{45 a}$$

and

$$\tilde{F}_k(p', p) = \int \frac{d\tau}{\tau} F_k(p', p + \varepsilon\tau) \tag{45 b}$$

(ε is a "vector" with the components $\varepsilon_k = 0$ for $k \neq 4$ and $\varepsilon_0 = 1$) we find from (44) and the assumption that the integrals in (45) converge that

$$\lim_{-(p-p')^2 \to \infty} \bar{F}_k(p', p) = \lim_{-(p-p')^2 \to \infty} \tilde{F}_k(p', p) = 0 \tag{46}$$

(cf. the Appendix). With the aid of the notations (45) we can now write

$$\left.\begin{aligned}&\theta(x3)\,\theta(x4)\,\langle 0\,|\,\{f(3),[j_k(x),\bar{f}(4)]\}\,|\,0\rangle\\&=\frac{-1}{(2\pi)^8}\iint\!\!\int dpdp'\,e^{ip'(3x)+ip(x4)}\,[\tilde{\bar{F}}_k(p',p)\\&-\pi^2 F_k(p',p)+i\pi(\bar{F}_k(p',p)+\tilde{F}_k(p',p))].\end{aligned}\right\}\quad(47)$$

In quite a similar way it can be shown that the second term in (25) can be written in a form analogous to (47) with the aid of a function $G_k(p',p)$ which also has the properties (44) and (46). It thus follows

$$\lim_{-(p-p')^2\to\infty} A_k(p',p)=0. \tag{48}$$

It must be stressed that this property of the function $A_k(p',p)$ is a consequence of (41) and thus essentially rests on the assumption that all the renormalization constants are finite quantities.

It is clear from (24) that the function A_μ transforms as the matrix γ_μ under a Lorentz transformation. The explicit verification of this from (23) is somewhat involved but can be carried through with the aid of the identity

$$\left.\begin{aligned}&\theta(x3)\,\theta(x4)\,\{f(3),[j_\mu(x),\bar{f}(4)]\}-\theta(x3)\,\theta(34)\,[j_\mu(x),\{f(3),\bar{f}(4)\}]\\&=\theta(x4)\,\theta(x3)\,\{\bar{f}(4),[j_\mu(x),f(3)]\}-\theta(x4)\,\theta(43)\,[j_\mu(x),\{\bar{f}(4),f(3)\}]\end{aligned}\right\}\quad(49)$$

and the canonical commutators. Eq. (49) can also be used to prove the formula

$$-C^{-1}A_\mu(-q',q)\,C=A_\mu^T(-q,q') \tag{50}$$

which is, however, also evident from (24) and the charge invariance of the formalism. From the Lorentz invariance it follows that we can write

$$A_\mu(p',p)=\sum_{\varrho'=0,1}\sum_{\varrho=0,1}(i\gamma p'+m)^{\varrho'}\,[\gamma_\mu F^{\varrho'\varrho}+p_\mu G^{\varrho'\varrho}+p'_\mu H^{\varrho'\varrho}]\,(i\gamma p+m)^{\varrho} \tag{51}$$

where the functions F, G and H are uniquely defined and depending only on p^2, p'^2, $(p-p')^2$ and the signs $\varepsilon(p)$, $\varepsilon(p')$ and $\varepsilon(p-p')$. From (50) it then follows

$$F^{\varrho\varrho'}(-p,p') = F^{\varrho'\varrho}(-p',p) \tag{52 a}$$

$$G^{\varrho\varrho'}(-p,p') = H^{\varrho'\varrho}(-p',p). \tag{52 b}$$

Utilizing (51) and (52) we get

$$\left.\begin{aligned} ie\langle 0|\overline{\psi}^{(0)}|q'\rangle \Lambda_\mu(-q',q)\langle 0|\psi^{(0)}|q\rangle &= \langle 0|j_\mu^{(0)}|q,q'\rangle R((q+q')^2) \\ &+ \frac{e}{2m} S((q+q')^2)(q_\mu - q'_\mu)\langle 0|\overline{\psi}^{(0)}|q'\rangle\langle 0|\psi^{(0)}|q\rangle \end{aligned}\right\} \tag{53}$$

where, in view of (48),

$$\lim_{-(q+q')^2\to\infty} R((q+q')^2) = \lim_{-(q+q')^2\to\infty} S((q+q')^2) = 0. \tag{54}$$

The equations (53) and (54) are the desired result of this paragraph.

Completion of the Proof.

We are now nearly at the end of our discussion. From the assumptions made about $\Pi(p^2)$ (and its consequences for $\overline{\Pi}(p^2)$, cf. the Appendix), Eqs. (53) and (54), the limit of Eq. (24) reduces to

$$\left.\begin{aligned} \lim_{-(q+q')^2\to\infty}\langle 0|j_\mu|q,q'\rangle &= \langle 0|j_\mu^{(0)}|q,q'\rangle\left[1+\overline{\Pi}(0)+2\frac{N-1}{1-L}\right] \\ &= \langle 0|j_\mu^{(0)}|q,q'\rangle\frac{2N-1}{1-L}. \end{aligned}\right\} \tag{55}$$

Our inequality (4) now gives

$$\left.\begin{aligned} \Pi(p^2) &> \frac{V}{-3p^2}\sum_{q+q'=p}{}'|\langle 0|j_\mu|q,q'\rangle|^2 \\ &\to \frac{V}{-3p^2}\sum_{q+q'=p}{}'|\langle 0|j_\mu^{(0)}|q,q'\rangle|^2\left(\frac{2N-1}{1-L}\right)^2 \\ &= \Pi^{(0)}(p^2)\left(\frac{2N-1}{1-L}\right)^2 \to \frac{e^2}{12\pi^2}\left(\frac{2N-1}{1-L}\right)^2. \end{aligned}\right\} \tag{56}$$

Except for the possibility of N being exactly $\frac{1}{2}$ $\left(\text{independent of } e^2 \text{ and } \frac{m^2}{\mu^2}\right)$ we have then proved that, if all the renormaliza-

tion constants K, $\frac{1}{N}$ and $\frac{1}{(1-L)}$ are finite, the function $\Pi(p^2)$ cannot approach zero for $-p^2 \to \infty$. This is an obvious contradiction and the only remaining possibility is that at least one (and probably all) of the renormalization constants is infinite.

The case $N = \frac{1}{2}$ is rather too special to be considered seriously. We can note, however, that N must approach 1 for $e \to 0$ and that one of the integrals in I Eq. (75) will diverge at the lower limit for $\mu \to 0$, independent of the value of e. The constant N could thus at the utmost be equal to $\frac{1}{2}$ for some special combination (or combinations) of e^2 and $\frac{m^2}{\mu^2}$. As μ is an arbitrarily small quantity it is hardly possible to ascribe any physical significance to such a solution, even if it does exist.

The proof presented here makes no pretence at being satisfactory from a rigorous, mathematical point of view. It contains, for example, a large number of interchanges of orders of integrations, limiting processes and so on. From a strictly logical point of view we cannot exclude the possibility that a more singular solution exists where such formal operations are not allowed. It would, however, be rather hard to understand how the excellent agreement between experimental results and lowest order perturbation theory calculations could be explained on the basis of such a solution.

Appendix.

It has been stated and used above that: if

$$\bar{f}(x) = P\int_0^\infty \frac{f(y)}{y-x}\,dy \quad (f(0) = 0) \tag{A. 1}$$

where $f(x)$ is bounded and continuous for all finite values of x and fulfills

$$|f(x+y) - f(x)| < M|y| \quad \text{for all } x \tag{A. 2}$$

and if the integral converges, both $f(x)$ and $\bar{f}(x)$ will vanish for large values of the argument. This is not strictly true, and in this appendix we will study that point in some detail.

We begin by proving that if the integral in (A. 1) converges absolutely and if

$$\lim_{x \to \infty} \log x \, |f(x)| = 0 \tag{A. 3}$$

it follows that

$$\lim_{x \to \pm \infty} \bar{f}(x) = 0 . \tag{A. 4}$$

(Note that the integral $\int_{\cdot}^{\infty} \frac{dx}{x \cdot \log x}$ is *not* convergent and that the vanishing of $f(x)$ is already implicit in (A. 3).) To get an upper bound for $\bar{f}(x)$ when $x > 0$ we write

$$\bar{f}(x) = P \int_0^{\infty} \frac{f(y)}{y - x} \, dy = \left(\int_0^{x/2} + P \int_{x/2}^{3x/2} + \int_{3x/2}^{\infty} \right) \frac{f(y)}{y - x} \, dy . \tag{A. 5}$$

(The limit $x \to -\infty$ is simpler and need not be discussed explicitly.) The absolute value of the first term in (A. 5) is obviously less than

$$\frac{2}{x} \int_0^{x/2} |f(y)| \, dy < \text{const.} \, \frac{2}{x} \int_0^{x/2} \frac{dy}{\log y} \to 0 . \tag{A. 6}$$

The last term can be treated in a similar way and yields the result

$$\left| \int_{3x/2}^{\infty} \frac{f(y)}{y - x} \, dy \right| \leqq \int_{3x/2}^{\infty} \frac{|f(y)|}{y/3} \, dy \to 0 . \tag{A. 7}$$

The remaining term can be written

$$\left. \begin{aligned} \left| P \int_{x/2}^{3x/2} \frac{f(y)}{y - x} \, dy \right| &= \left| \int_0^{x/2} \frac{dy}{y} \left[f(x + y) - f(x - y) \right] \right| \\ \leq \int_0^{\varepsilon} \frac{dy}{y} \left| f(x + y) - f(x - y) \right| &+ \int_{\varepsilon}^{x/2} \frac{dy}{y} \left| f(x + y) \right| + \int_{\varepsilon}^{x/2} \frac{dy}{y} \left| f(x - y) \right| . \end{aligned} \right\} \tag{A. 8}$$

In view of (A. 2) and (A. 3), the three terms in (A. 8) vanish separately for large values of x. It thus follows

$$\lim_{x \to \infty} \bar{f}(x) = 0$$

q. e. d.

As the function $\Pi(p^2)$ is positive the condition (A. 3) seems rather reasonable from a physical point of view. On the other hand, the functions F_k in (45) are not necessarily positive. It is, however, also possible to construct a more general argument where (A. 3) is not used, and where even the vanishing of $f(x)$ is not needed. Instead, we then require that from

$$\bar{f}(x) = P \int_0^{\infty} \frac{f(y)}{y-x}\, dy; \; f(y) = 0 \quad \text{for} \quad y \leqq 0 \tag{A. 9}$$

will follow

$$f(x) = -\frac{1}{\pi^2} P \int_{-\infty}^{+\infty} \frac{\bar{f}(y)}{y-x}\, dy \tag{A. 10}$$

where both $f(x)$ and $\bar{f}(x)$ are finite.

Note that

$$\left.\begin{aligned} &\frac{1}{\pi^2} P \int_{-\infty}^{+\infty} \frac{dz}{(z-x)(z-y)} \\ &= \frac{-1}{4\pi^2} \iint dw_1 dw_2 \int dz e^{i(w_1+w_2)z} \cdot e^{-iw_1 x - iw_2 y} \frac{w_1 w_2}{|w_1 w_2|} \\ &= \frac{1}{2\pi} \int dw_1 e^{iw_1(y-x)} = \delta(y-x). \end{aligned}\right\} \tag{A. 11}$$

It then follows that the integral

$$\int_{x}^{\infty} \frac{|1+\bar{f}(x)+i\pi f(x)|^2}{x}\, dx > \int_{x}^{\infty} \frac{|1+2\bar{f}(x)|}{x}\, dx$$

is divergent, because the second term is convergent in view of (A. 10). This is everything that is needed for the proof.

It is, of course, possible to construct functions $f(x)$ where (A. 10) does not follow from (A. 9). In that case we are not allowed to interchange the order of the integrations in (A. 11); but we have already excluded such cases from our discussion.

For simplicity, the statement that the functions "vanish" for large values of the variables has been used in the text. If a more careful argument is wanted the phrase

"the functions have the property that the integral

$$\int^{\infty} \frac{f(x)}{x}\, dx$$

converges" should be substituted for the word "vanish" in many places.

The author wishes to express his gratitude to Professor NIELS BOHR, Professor C. MØLLER, and Professor T. GUSTAFSON for their kind interest. He is also indebted to Professor M. RIESZ for an interesting discussion of the problems treated in the appendix.

CERN (European Council for Nuclear Research)
Theoretical Study Group at the
Institute for Theoretical Physics, University of Copenhagen,
and
Department of Mechanics and Mathematical Physics,
University of Lund.

Indleveret til selskabet den 28. februar 1953.
Færdig fra trykkeriet den 27. maj 1953.

Det Kongelige Danske Videnskabernes Selskab
Matematisk-fysiske Meddelelser, bind **27**, nr. 13

Dan. Mat. Fys. Medd. **27**, no. 13 (1953)

PROTON STOPPING POWER AND ENERGY STRAGGLING OF PROTONS

BY

C. B. MADSEN

København
i kommission hos Ejnar Munksgaard
1953

Printed in Denmark
Bianco Lunos Bogtrykkeri

Introduction.

The energy loss of protons in foils of various substances has been determined as a function of the proton energy. The sharp resonances for proton reactions have been used for analyzing the energy distribution of a beam of protons after its passage through a thin layer of various substances. Because of the energy loss in such a layer, the resonance curves are found at a higher voltage when a foil is inserted in the beam than when no foil is inserted. The shift of proton energy gives the energy loss in the foil.

Moreover, a broadening of the resonance curves obtained when a foil is inserted in the beam makes it possible to determine the energy straggling. Some measurements, concerning mainly beryllium and mica, have been published earlier[1),2),3)]. In the present paper, experimental results are reported for other materials of higher atomic numbers and the range of proton energy is extended to 2 MeV.

Experimental.

The experiments were carried out at the Institute for Theoretical Physics in Copenhagen with the pressure insulated van de Graaff generator[4)]. The rotating compensation voltmeter was calibrated by the proton capture resonance in aluminum at 503 keV and the linearity was checked by measuring the 503 keV resonance with protons and molecular ions.

The proton current was of the order of 2 μA when no foil was inserted in the beam; when a foil was used the current was adjusted to about 0.2 μA. The current integrator[5)] consists of a recorder, which counted the pulses of a neon lamp, discharging a condensor constantly charged by the target current. At the lowest energies where the stopping power and, consequently, the

heating of the foil are greatest, and especially for thicker foils, the integrator could not be used. In such cases, the beam current was measured with a sensitive galvanometer and kept constant by means of small variations of the voltage of the probe in the source.

As γ-ray counter a Geiger-Müller tube, 10 mm in diameter and 40 mm long, was used. It was placed in a lead box as close to the target as possible and connected to a scale-of-32. The neutrons were detected by means of boron neutron counters surrounded by paraffin wax. An electronic switch[4] blocked the counting of both γ-rays and neutrons when the acceleration voltage differed by more than about 2 keV from the desired value. This blocking of the counting arrangement makes it possible to obtain sharper resonance peaks.

The foils were placed in a small disk with six circular openings, some of which were covered by foils. The disk was mounted in the acceleration tube at a distance of 35 cm from the target in order to reduce the background radiation from reactions in the foil as far as possible. The disk could rotate on an axis through its center, and all openings were placed in the same distance from the axis. With the aid of a magnet the different openings of the disk could be brought into the path of the protons. Foils of different thicknesses were used as listed in the tables. They were cut into small round pieces of a diameter of 11 mm after their thickness had been determined by measuring the weights and areas of larger pieces.

Because of the stop in the Faraday cage the scattering in the foil decreases the current to the target. Moreover, the straggling in the foil causes a broadening of the resonance peak and a consequent diminishing of the peak intensity. For these reasons only the strongest peaks could be used as energy indicators. The following peaks have been used: Proton-capture resonance, in fluorine at 339 and 660 keV[7], in aluminum at 630, 986, and 1255 keV[4], and in chlorine at 860 keV[8]. Due to the great density of the levels none of the capture processes can be used at higher potentials. The measurements about 2 keV are based on the (p, n) resonance at 1974 keV[8] in the process Cl^{35} (p, n) A^{35}. Measurements at the lowest proton energies were carried out with the molecular beam, since focussing was unstable at low

generator voltages; however, this should not influence the results, as the molecules are split up as soon as they hit the foil.

Targets were prepared by evaporation of calcium fluoride, aluminum or lead chloride in vacuum on small disks of silver or copper. Copper backings were used for γ-ray observations from proton capture reactions with a proton energy smaller than 0.9 keV, and for the (p, n) reaction at 2 MeV. Silver targets were used for γ-rays from capture reactions with a proton energy higher than 0.9 MeV. The small width of the resonance levels indicates that a target with a stopping power of 1—2 keV, giving saturation intensity, is suitable. However, the broadening of the peaks due to the energy straggling in the foil, especially at lower energies, necessitates a thicker target. Accordingly, many targets of different thicknesses were used.

Most of the measurements were performed on foils. Both commercial foils which are rolled out and foils prepared in the laboratory by evaporation in vacuum were used. The commercial foils are rather inhomogeneous and are only convenient for the determination of the stopping power, because the broadening of the resonance curve in these cases is not only due to the straggling in the foil. Foils produced by evaporation seem to be rather homogeneous. In a previous paper[3] the straggling in foils of beryllium and mica has been described.

Besides foils also sandwich targets have been used. They were prepared in the following way. On 3—4 disks of the support material (copper or silver) a layer, containing the energy indicator (fluorine, aluminum or chlorine), is evaporated. One or two disks are removed from the evaporation chamber, while the stopping substance (Be, Al, Cu, Ag or Bi) is evaporated on the energy indicator layer of the remaining targets*.

In this way, heating of the foil is avoided and a greater beam current can be used. Moreover, a decrease in the beam current caused by scattering is prevented. However, some difficulties arose from the determination of the thickness of the stopping layer. The increase in weight of the target caused by the stopping layer was often too small as to be measured with sufficient accuracy.

* Thanks are due civilengineer Mr. O. B. NIELSEN for preparing sandwich targets.

Before evaporation of the stopping substance, the targets were placed on pieces of glass. Both the targets and the glass around the targets were covered with stopping material. After removal of the targets the thickness of the stopping layer was found by measurements of the interference between the rays coming from the clean surface of the glass behind the target and the rays from the surface of the stopping layer. In many cases, however, the thicknesses found in this way disagreed with results obtained in other ways. This may be due to different reflections of the molecular particles from the metal surface of the target itself and from the surface of the glass.* Therefore the thickness of a stopping layer was determined by comparing the energy loss of the layer with that of a foil with known thickness. Thus, a value of the stopping power found by means of the sandwich targets is determined relative to measurement with foils. However, the principal value of such targets lies in their homogeneity and in the possibility of obtaining better resonance peaks for the determination of the straggling.

In order to find the energy loss ΔE and the straggling Ω in a foil or in a sandwich target, the energy distribution of the peaks is approximated by the Gaussian, even though this should not always be the correct shape, at least not for the peaks measured without foil or stopping layer, where the width is due mainly to the thickness of the target.

As it was shown in greater detail in the previous paper[3], the resonance curves are transformed into straight lines by means of tables[9] or probability paper. The energy loss ΔE is the difference between the energies corresponding to the mid point of the straight lines (probits = 5) found with and without a foil, respectively.

Since the standard deviations are added geometrically the true straggling Ω is found by means of the formula $\Omega = \sqrt{\Omega_2^2 - \Omega_1^2}$, where Ω_2 and Ω_1 are the standard deviations corresponding to the measurements with and without foil, respectively. These deviations can be found from the slopes of the straight lines.

ΔE and Ω are thus determined in a rather unambiguous way. In most cases, the resonance curves are symmetrical and

* The author is indebted to mag. scient. Rahbek for carrying out the interference measurements.

the transformed curves are straight lines. In such cases, the most probable energy loss and the mean energy loss are the same. By far the greatest number of the resonance curves could be transformed to straight lines. The shift could be found with an accuracy of less than 1 keV and the slope was determined accurate to ten per cent.

In some cases a transformed curve was not a straight line because of a long tail of the resonance curve. In such a case the most probable energy loss and the mean energy loss are not identical; however, the difference is small, about 1 keV. In comparison with a shift of 30—50 keV this uncertainty does not influence considerably the value of the stopping power. The value for the straggling is greatly affected by the deviations from a straight line. In a few of these cases, an attempt was made to determine the straggling by determining that Gaussian distribution which, folded with the resonance curve found without foil, gave the best fit to the curve obtained with a foil inserted in the proton beam. However, no greater accuracy could be obtained in this way. These values of the straggling may thus be rather uncertain (cf. the spread of the points on fig. 3).

Results.

The results obtained are presented in the following tables, which also include the values published in previous papers[1, 2, 3]).

The columns show:

1) Thickness t of the stopping material in mg per cm^2. The areas of the foils are calculated from measurements with a travelling microscope and their weights are determined with a microbalance. The thicknesses obtained in this way are believed to be correct within a few per cent. After the measurements the thicknesses were checked and found to be unchanged. When a sandwich target was used, further details are given in a footnote.
2) The energy shift ΔE in keV.
3) The proton energy E in keV. The energy given in the table is the mean value of the proton energies of the peaks of the resonance curves found with and without stopping material.

4) Stopping power of the substance measured in keV per mg per cm^2.
5) Standard deviation Ω_1 in keV, without stopping layer.
6) Standard deviation Ω_2 in keV, with stopping layer.
7) Straggling Ω in keV.

The straggling is determined neither for commercial foils nor for cases where the resonance peak is too small to give a tolerable accuracy in the value for the standard deviation.

Beryllium. Only foils prepared by evaporation have been used and the total contamination of other metals was found, by spectral analysis, to be less than 0.1 per cent.

In a previous paper[1] two curves found without and with foil are shown.

TABLE I. *Beryllium.*

t thickness	ΔE shift	E proton energy	s stopping power	Ω_1 standard deviations	Ω_2	Ω straggling
mg/cm²	keV	keV	keV/mg/cm²	keV	keV	keV
1	2	3	4	5	6	7
0.609	230	455	377	4.2	9.5	7.2
0.222	73	540	329	4.4	6.1	4.2
0.222	62	661	279	1.5	5.1	4.9
0.222	64	662	288	4.2	5.3	3.3
0.245	69	665	282	—	a)	—
0.222	53	798	239	—	a)	—
0.222	48	1010	216	1.4	5.0	4.8
0.222	48	1010	216	1.7	4.2	3.9
0.245	53	1013	216	1.3	4.2	4.0
0.609	126	1049	207	2.5	6.6	6.1
0.222	42	1133	189	2.9	5.3	4.5
0.222	45	1135	203	2.9	5.5	4.7
0.222	42	1276	189	1.7	4.9	4.6
0.609	108	1310	177	—	b)	—
0.222	39.5	1392	178	—	b)	—
0.609	101	1422	166	—	b)	—
0.610	85	2016	139	4.2	8.2	6.6

a) the intensity of the resonance is too low to determine Ω_2.
b) the two peaks Al 1372 and Al 1379 are superposed, Ω_2 cannot be determined.

Mica. The foils were prepared by splitting mica into thin pieces. On account of the optical transparency of a mica foil, information about the homogeneity can be obtained by interferometer measurements, according to the method of Tolansky. Details of these measurements are published in the earlier paper[3]. Thus, only for the mica foils it has been possible to check the homogeneity directly.

TABLE II. *Mica*.

t thickness	ΔE shift	E proton energy	s stopping power	Ω_1 standard deviations	Ω_2	Ω straggling
mg/cm²	keV	keV	keV/mg/cm²	keV	keV	keV
1	2	3	4	5	6	7
0.336	101	389	300	3.6	5.8	4.5
0.336	75,4	668	225	3.4	5.6	4.4
0.336	59	1016	176	1.7	5.2	4.9
0.336	59	1016	176	1.7	5.0	4.7
0.441	76	1024	172	1.6	6.4	6.2
0.441	76	1024	172	1.6	6.1	5.9
0.441	76	1024	172	1.6	5.9	5.7
0.441	76	1024	172	1.5	6.3	6.1
0.665	111	1041	168	1.7	7.6	7.4
0.665	113	1042	171	1.7	8.0	7.8
0.73	115	1047	158	3.5	7.2	8.3
0.78	131	1051	168	3.7	7.7	6.8
0.76	130	1051	171	3.5	8.0	7.2
0.76	130	1051	171	3.6	6.7	5.7
1.02	169	1070	166	1.9	9.4	9.2
1.02	173	1072	170	2.1	9.5	9.3
1.02	172	1072	168	2.1	9.1	8.9
1.02	172	1072	168	1.9	9.0	8.8
1.02	175	1073	171	1.7	8.7	8.5
1.23	212	1092	172	3.0	9.5	9.0
1.71	284	1140	166	3.8	12.5	11.9
1.06	155	1180	146	2.5	9.5	9.2
0.336	48	1279	143	3.0	4.8	3.8
0.336	36	1992	107	4.8	5.9	3.5
0.730	79	2014	108	4.8	8.5	7.0

Aluminum. In most measurements commercial foils were used. The total contamination of other substances was found

by chemical analysis to be less than 1 per cent*. No value for the straggling is determined for the commercial foils. Sandwich

TABLE III. *Aluminum.*

t thickness	ΔE shift	E proton energy	s stopping power	Ω_1 standard deviations	Ω_2	Ω straggling
mg/cm²	keV	keV	keV/mg/cm²	keV	keV	keV
1	2	3	4	5	6	7
0.23 a)	58	368	252	—	—	—
0.38 a)	95	387	250	—	—	—
0.23 a)	42	681	182	—	—	—
0.38 a)	70	695	185	—	—	—
0.23 a)	38.5	1005	167	—	—	—
0.38 a)	59.5	1016	157	—	—	—
0.48	72	1020	150	3.5	6.9	6.0
0.50	82	1025	164	3.5	7.0	6.0
0.23 a)	31	1270	135	—	—	—
0.38 a)	53	1281	139	—	—	—
0.23 a)	23	1986	100	—	—	—
0.38 a)	37	1993	98	—	—	—
0.37 b)	37	1993	100	4.8	7.2	5.4
0.37 b)	39	1994	105	4.8	6.2	4.0

a) commercial foil.
b) sandwich target. Thickness found from the width of the (p, γ) resonance radiation of the stopping layer at 986 keV.

targets can only be used at the (p, n) resonance of chlorine at 1974 keV because the aluminum itself will give rise to disturbing radiation if (p, γ) reactions are used as energy indicators.

Copper. Only commercial foils and two sandwich targets have been used. The contamination of other substances was found by chemical analysis to be about 5 per cent. As, however, the main part of the other substances was zinc, whose atomic number differs only by one unit from that of copper, this contamination does not influence the results appreciably.

* Thanks are due amanuensis T. LANGVAD for carrying out the analysis.

TABLE IV. *Copper.*

t thickness	ΔE shift	E proton energy	s stopping power	Ω_1 standard deviations	Ω_2	Ω straggling
mg/cm²	keV	keV	keV/mg/cm²	keV	keV	keV
1	2	3	4	5	6	7
0.49 a)	73	376	149	—	—	—
0.58 a)	90	384	155	—	—	—
0.49 a)	60	690	122	—	—	—
0.58 a)	70	695	121	—	—	—
0.59 b)	64	892	—	—	—	—
0.84 b)	91	905	—	2.5	6.5	6.0
0.49 a)	53.5	1012	109	—	—	—
0.50 a)	53.0	1012	106	—	—	—
0.58 a)	56.5	1014	98	—	—	—
0.49 a)	46	1278	94	—	—	—
0.58 a)	51	1281	88	—	—	—
0.49 a)	35	1991	72	—	—	—
0.58 a)	46	1997	79	—	—	—
0.59 b)	41.4	1994	70	5.4	7.5	5.2
0.84 b)	54	2001	64	4.8	8.1	6.5
0.84 b)	56	2002	67	4.3	7.0	5.6

a) commercial foil.
b) sandwich target. (Chlorine as indicator) thickness determined from the shift of the (p, γ) resonance at 860 keV.

Silver. Commercial foils, foils prepared by evaporation, and sandwich targets were used. The contamination was found by chemical analysis to be less than 1 per cent.

TABLE V. *Silver.*

t thickness	ΔE shift	E proton energy	s stopping power	Ω_1 standard deviations	Ω_2	Ω straggling
mg/cm²	keV	keV	keV/mg/cm²	keV	keV	keV
1	2	3	4	5	6	7
0.432 b)	59	369	137	4.8	6.3	4.1
0.42 a)	60	370	143	—	—	—
0.42 a)	60	370	143	—	—	—
0.36 a)	51	365	142	—	—	—

(continued)

TABLE V. *Silver.* (continued)

t thickness	ΔE shift	E proton energy	s stopping power	Ω_1 standard deviations	Ω_2	Ω straggling
mg/cm²	keV	keV	keV/mg/cm²	keV	keV	keV
1	2	3	4	5	6	7
0.59 a)	84	381	142	—	—	—
1.51	209	445	138	3.8	8.9	8.0
0.225 c)	22.8	641	101	2.2	3.7	3.0
0.235 c)	22.6	641	96	2.1	3.6	2.9
0.285 c)	32.5	646	114	2.7	4.7	3.8
0.36 a)	36	678	100	—	—	—
0.432 b)	45	682	—	5.5	7.0	4.4
0.442 a)	44	683	100	—	—	—
0.59 a)	64	692	108	—	—	—
0.51 e)	47.5	880	93	2.2	6.0	5.6
0.81 d)	75	885	—	—	—	—
0.225 c)	18.6	995	—	2.1	3.7	3.1
0.235 c)	19.5	996	—	2.0	3.7	3.1
0.285 c)	24.4	998	—	2.5	4.3	3.5
0.434 c)	36.2	1002	—	2.4	6.2	5.7
0.36 a)	33	1003	91	—	—	—
0.42 a)	34.7	1004	82	—	—	—
0.48 a)	38.5	1005	80	—	—	—
0.49 a)	40	1006	82	—	—	—
0.59 a)	53	1012	90	—	—	—
1.51	130	1051	86	3.4	8.0	7.2
0.225 c)	15.9	1263	71	2.3	3.8	3.0
0.225 c)	15.9	1263	71	1.8	3.2	2.7
0.434 c)	29.6	1270	68	2.3	4.3	3.6
0.28 e)	23	1986	—	6.0	8.3	5.7
0.49 a)	29	1989	59	—	—	—
0.51 e)	30	1989	—	3.8	6.8	5.6
0.81 d)	47.5	1998	59	6.5	7.7	4.1
0.91 e)	66	2007	—	6.0	8.7	6.3
1.51	90	2019	60	—	—	—

a) commercial foil.

b) sandwich target, fluorine as indicator, thickness determined from the shift of the (p, γ) resonance at 660 keV.

c) sandwich target, aluminum as indicator, thickness from the shift of the (p, γ) resonance at 986 keV.

d) sandwich target, chlorine as indicator, thickness from the shift of the (p, γ) resonance at 860 keV.

e) sandwich target, chlorine as indicator, thickness from the shift of the (p, n) resonance at 1974 keV.

Gold. Commercial gold foils have been used. As the production of sandwich targets covered with gold did not succeed, sandwich targets covered with bismuth were used. The stopping power varies with $Z^{\frac{1}{2}}$ and thus a value of the stopping power found by means of a sandwich target covered with bismuth must be increased by 2 % when compared with the stopping power of gold. When the thickness of a sandwich target is found from the shift of a resonance curve this factor must also be taken into account. In the table the measured stopping powers

TABLE VI. *Gold.*

stopping substance	t thickness	ΔE shift	E proton energy	S_{Bi}	S_{Au} stopping powers	Ω_1	Ω_2 standard deviations	Ω straggling
	mg/cm²	keV	keV	keV/mg/cm²		keV	keV	keV
1	2	3	4	5	6	7	8	9
Au	0.45 a)	38.5	359	—	85	—	—	—
Au	0.52 a)	42	360	—	81	—	—	—
Bi	0.55 b)	44	366	80	82	4.8	6.0	3.6
Bi	0.61 c)	41.9	651	69	71	2.1	5.0	4.6
Bi	0.61 c)	42.9	652	70	72	2.1	5.3	4.9
Bi	0.66 c)	49.4	655	74	76	2.3	6.8	6.4
Bi	0.55 b)	38	679	—	—	4.6	7.2	5.5
Bi	0.69 d)	42.3	881	—	—	2.5	6.0	5.5
Bi	0.69 d)	43.3	881	—	—	2.5	5.9	5.4
Au	0.45 a)	27	999	—	60	—	—	—
Au	0.52 a)	30	1000	—	58	—	—	—
Au	0.51 a)	31	1001	—	61	—	—	—
Bi	0.61 c)	35.4	1004	—	—	2.2	5.8	5.4
Bi	0.66 c)	38.7	1005	—	—	2.0	6.0	5.7
Bi	0.68 c)	39.4	1006	—	—	2.2	6.1	5.7
Au	0.84 a)	49.5	1009	—	59	—	—	—
Bi	0.61 c)	29.6	1270	49	50	2.0	6.0	5.7
Bi	0.69 d)	29	1988	42	43	5.8	7.6	5.0
Bi	0.69 d)	28.7	1988	42	43	4.8	6.5	4.4
Au	0.84 a)	34	1991	—	41	—	—	—

a) commercial foil.

b) sandwich target, fluorine as indicator, thickness determined from the shift of resonance at 660 keV.

c) sandwich target, aluminum as indicator, thickness determined from the shift of resonance at 986 keV.

d) sandwich target, chlorine as indicator, thickness determined from the shift of resonance at 860 keV.

for bismuth are given in column 5, and in column 6 are given the two per cent higher values valid for the stopping power of gold.

The values found for the stopping power $\left(\text{in } \frac{\text{keV}}{\text{mg/cm}^2}\right)$ are plotted as a function of the proton energy in fig. 1. Also the results obtained by WARSHAW[10] at lower energies are plotted on the figure. It is seen that, for each substance, the points can be connected by a smooth curve.

Discussion.

The energy loss per cm path is given by BETHE's formula[11]:

$$-\frac{dE}{dx} = \frac{4\pi e^4 Z_1^2}{mv^2} \cdot NZ_2 \cdot \log \frac{2mv^2}{I}. \qquad (1)$$

Here, e and m are the electronic charge and mass, v is the velocity, and Z_1 the atomic number of the incident atom, N is the number of atoms per cm^3, Z_2 is the atomic number and I the average excitation potential of the stopping substance.

A relativistic treatment shows that another term has to be added to the logarithm. At the velocities used in the present investigation this term can be omitted. The formula (1) is only valid if the velocity of the incident particle is much higher than the velocity of the electrons of the stopping substance.

In a previous paper[1] concerning the stopping power of solid beryllium, the formula (1) has been used in the form

$$S = \frac{4\pi e^4}{Em} \cdot \frac{Z_2}{A_2} \cdot \left\{\log\left(\frac{4E}{I} \cdot \frac{m}{M}\right) - \frac{C_K}{Z_2}\right\}, \qquad (2)$$

where S is the stopping power for unit thickness, E the proton energy, M the proton mass, and C_K is a correction due to the strong binding of the K-electrons, which has been calculated by BETHE[10] for the lightest elements.

The value of I was found to be equal to 64 ± 5 eV, in good agreement with a theoretical estimate of A. BOHR[12], who gives I to be about 60 eV. Recently, BAKKER and SEGRÈ[13] and MATHER and SEGRÈ[14], using 340 MeV protons whose energies are so high

that the C_K-corrections may be omitted, found values of I very close to 60 eV.

For the heavier substances, the velocities of the most firmly bound electrons may be comparable with or exceed the velocity of the incident particles. As no C_K-corrections are available for the heavier elements and, moreover, corrections due to the L and M shells are also necessary, the formulas (1) and (2) no longer apply.

For such cases, N. Bohr[15], using a simplified atomic model, gives an approximate expression and finds that the specific energy loss is proportional to $Z_2^{\frac{1}{3}} \cdot v^{-1}$. This dependence on v is found to hold approximately in the present experiments, but the numerical value given by Bohr is about 1.5 times the experimental results.

Recently, Lindhard and Scharff[16] have calculated energy losses for lower velocities. By means of a statistical argument they derive the quantity $L(x) = (\Delta E \cdot mv^2/4\,NZ_2e^4\,\Delta R)$ as a common function of the variable $x = Z_2^{-1}\left(\frac{v}{v_0}\right)^2$ for heavier substances.

For higher velocities, Bloch[17] has obtained the formula $L(x) = \log(2mv^2/Z_2I_0)$, where I_0 is a constant.

In order to compare the measurements with these formulas, the stopping powers at 350, 650, 1000, 1500, and 2000 keV found from fig. 1 are given in table VII.

Table VII. Specific Stopping Power (keV/mg/cm^2).

Substance \ Proton energy	350	650	1000	1500	2000 keV
Beryllium	386	285	215	167	138
Mica	310	220	170	134	107
Aluminum	270	190	158	119	99
Copper	170	125	105	84	70
Silver	138	104	83	68	58
Gold	83	70	59	50	42

From these five values for each element (mica excluded) the experimental values of $L(x)$ have been found and are plotted

against $x^{\frac{1}{2}} = Z_2^{-\frac{1}{2}} \frac{v}{v_0}$ on fig. 2. On this figure, a straight line through the origin would correspond to a specific stopping power proportional to $Z_2^{\frac{1}{2}} \cdot \frac{1}{v}$; this is seen to hold, in first approximation,

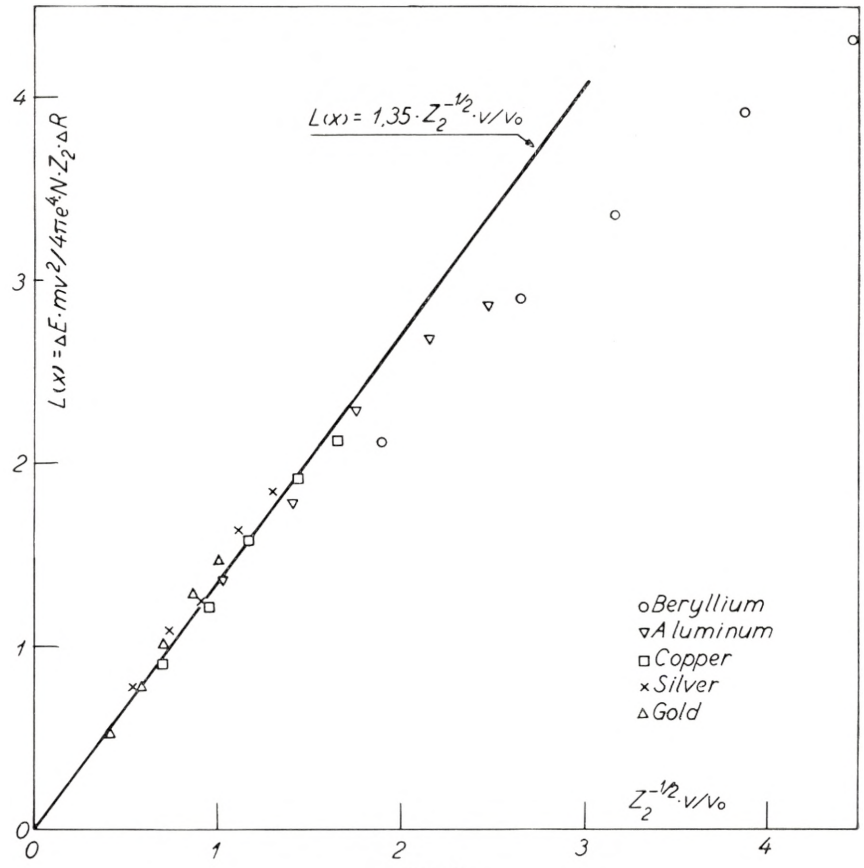

Fig. 2.

for the experimental points corresponding to the four heaviest elements.

The experimental points of beryllium do not fit with a straight line, because the velocities of the protons are so high that the formula of BLOCH is valid. The value of the Bloch constant $\frac{I}{Z_2}$ is 16 ± 1 eV in agreement with the results of BAKKER and SEGRÈ[13].

Several authors have tried to find an empirical formula for the variation of the stopping power with the atomic number Z. BRAGGS and KLEMANS[19] assumed that the stopping power S was proportional to $A^{\frac{1}{2}}$, where A is the mass number. RAUSCH v. TRAUBENBERG[18] adopted $S \cdot Z_2^{-\frac{1}{2}} = \text{const.}$ and GLASSON[20] found that $S \cdot Z_2^{-\frac{2}{3}} = \text{const.}$ gave the best fit.

The formula of BOHR[15] and that of LINDHARD and SCHARFF[16] may be written

$$L(x) = k_1 \cdot Z_2^{-\frac{2}{3}} \cdot \frac{2v}{v_0} \tag{3}$$

and

$$L(x) = k_2 \cdot Z_2^{-\frac{1}{2}} \cdot \frac{v}{v_0}. \tag{4}$$

From the values of $L(x)$ used on fig. 2 and from corresponding values of Z and v, the constants k_1 and k_2 have been calculated for the five energies of the four heaviest elements whose points are lying on a straight line. From these twenty values of k_1 and k_2 the mean values are found to be 1.20 and 1.35 with mean errors 10 % and 3 %, respectively. The value 1.35 is in agreement with an estimate of LINDHARD and SCHARFF[21], who find

$$L(x) = 1.36 \cdot x^{\frac{1}{2}} - 0.016 \cdot x^{\frac{3}{2}}$$

where $x = Z_2^{-1} \cdot v^2/v_0^2$.

As is well known, the factor Z_1^2 in the specific energy loss implies that the stopping of an α-particle is the same as that of a proton with an energy one quarter that of the α-particle. Therefore, the stopping power for protons at 1.5 MeV can be compared with earlier measurements for 6 MeV α-particles by MARSDEN and RICHARDSON, GEIGER, MANO and, ROSENBLUM. The values quoted by BETHE and LIVINGSTON[11] have been used. The values of the present investigation are, for all substances, 5—10 % lower than the average values of the four mentioned authors. It may be added that their results are obtained only relative to air, which demands an accurate knowledge of the stopping power of this substance. A general comparison of empirical ranges and specific energy loss is given in the paper of LINDHARD and SCHARFF[21], where it is found that the present results are not at variance with the recent accurate range curve in air by BETHE[22].

An extensive discussion of the fluctuations in the energy loss on a given path length ΔR has been given by BOHR[15]. It was shown by BOHR that for high velocities of the penetrating particle, where all electrons in the atoms contribute to the stopping, the average square of the fluctuations in energy loss is simply given by

$$\Omega^2 = 4\pi Z_1^2 \cdot e^4 \cdot Z_2 \cdot N \Delta R. \tag{5}$$

Since the energy loss can be written

$$\frac{\Delta E}{\Delta R} = \frac{4\pi Z_1^2 \cdot e^4 Z_2 \cdot N}{mv^2} L(x),$$

where $L(x)$ is the function shown in fig. 2, we may write, instead of (3),

$$u^2 = \frac{\Omega^2}{E \cdot \Delta E} = \frac{m}{M} \frac{2}{L(x)}, \tag{6}$$

where M is the proton mass.

For lower velocities of the particle, where only a part of the atomic electrons contribute to the energy loss, a reduction in straggling takes place. Here, we shall refer only to the calculations by LINDHARD and SCHARFF[21] who find:

$$u^2 = \frac{m}{M}. \tag{7}$$

The two formulas (6) and (7) should be joined smoothly.

In order to compare the measurements of the straggling with the theoretical estimate, the values of $u = \left(\frac{\Omega^2}{E \Delta E}\right)^{\frac{1}{2}}$ are plotted versus $x^{\frac{1}{2}} = Z_2^{-\frac{1}{2}} \cdot \frac{v}{v_0}$ in fig. 3. The points are found from the measured values of Ω, E and ΔE. The curves are drawn according to the value $\frac{m}{M} = 0.00055$ and to the semi-empirical value of $L(x) = 1.35 \cdot Z_2^{-\frac{1}{2}} \frac{v}{v_0}$ from equation (4).

In the case of mica, an effective atomic number has been found by interpolation between the values of the stopping powers of beryllium and aluminum. A value of $Z_2 = 10.5$ is used for mica.

From the spread of the points corresponding to the homogeneous mica foils the uncertainty in the values of Ω can be estimated to about $10\,^0/_0$. For the other substances the spread is a little greater. This may be due to small inhomogeneities in the foils

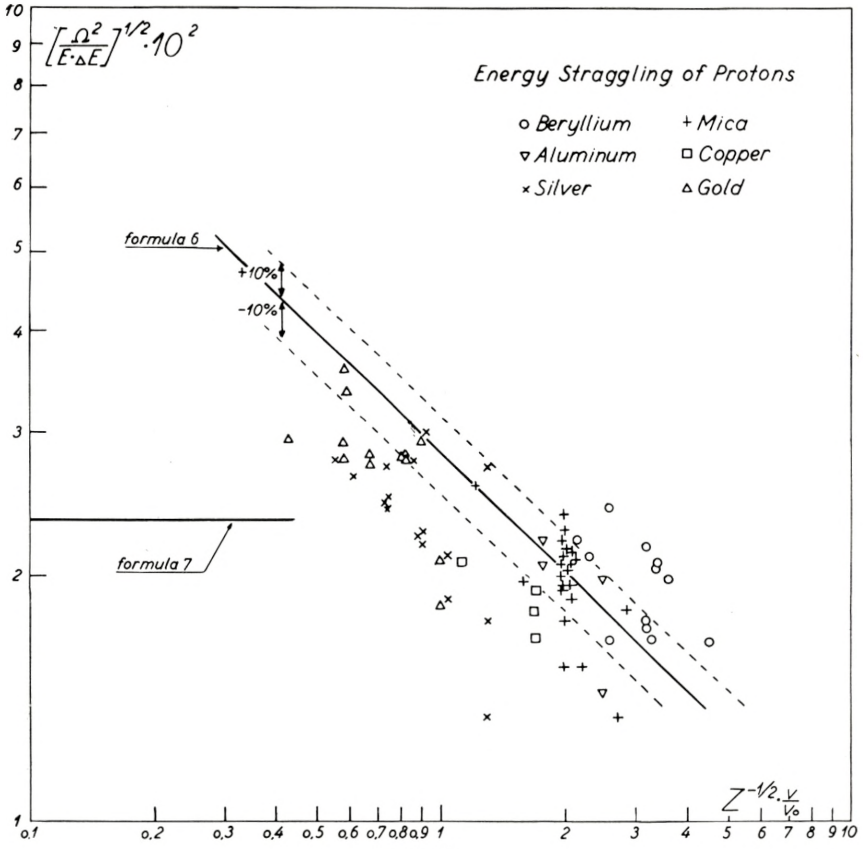

Fig. 3.

and sandwich targets. For the two heaviest substances, the values are about 1.3 times those corresponding to formula (7).

The author (on leave from the Physical Institute, University of Aarhus, Denmark), wishes to thank Professor NIELS BOHR for his continuous interest in this work and for the great hospitality at the Institute for Theoretical Physics in Copenhagen. Moreover, thanks are due the members of the VAN DE GRAAFF staff of this institute, cand. mag. K. J. BROSTRÖM and mag. scient.

T. Huus, and to mag. scient. J. Lindhard and mag. scient. M. Scharff for valuable help and discussions. The Carlsberg Foundation and the Research Foundation of the University of Aarhus have supported the work financially.

After the completion of this paper, a communication has been received from Dr. S. A. Allison, Chicago, concerning some measurements of the stopping power, performed by Mr. David Kahn and to be published in the Physical Review. In case of the lightest and the heaviest elements, the agreement between this author's and our results is good; however, for medium elements, Kahn has found the stopping power to be higher than the present results. The largest deviations (20 per cent) are found for Copper, and they are much too large to be explained by impurities in the foils. The copper foils used in our investigation have been rolled or beaten, whereas Kahn's foils were prepared by evaporation. Since the method of foil preparation might be significant in explaining the difference in the results, a few remarks about the inhomogeneity of the foils may be useful.

When a commercial foil is inserted in the beam, contributions to the broadening of the resonance curve arise from 1) the width of the resonance curve without foil, 2) the straggling, and 3) the inhomogeneity of the foil. The width of the resonance curve without foil and that of the curve with foil can be found in the usual way. The contribution of the straggling can be estimated from the present measurements. Assuming the deviations to be added geometrically a standard deviation of the inhomogeneity of the foil can be found. In case of the 0,50 mg/cm^2 copper foil this quantity is 7 keV. The energy shift is found to 53 keV. The thickness is 0,50 $\pm$ 0,065 mg/cm^2, so that the inhomogeneity is 13 per cent. All the commercial foils showed an inhomogeneity of this magnitude.

A further communication has been received from Dr. J. N. Cooper, Ohio State University, whose results for copper foils, which have been prepared by an electrolytical process, lie between those of Kahn and those of the present author.

References.

1. C. B. Madsen and P. Venkateswarlu, Phys. Rev. **74**, 648, 1948.
2. T. Huus and C. B. Madsen, Phys. Rev. **76**, 323, 1949.
3. C. B. Madsen and P. Venkateswarlu, Phys. Rev. **74**, 1782, 1948.
4. K. J. Broström, T. Huus, R. Tangen, Phys. Rev. **71**, 661, 1947.
5. R. Tangen, K.N.V.S. Skrifter 1946, nr. 1.
6. T. Huus, Dan. Mat. Fys. Medd. **26**, no. 4, 1951.
7. L. R. Hafstad and M. A. Tuve, Phys. Rev. **48**, 306, 1935.
8. K. J. Broström, B. Madsen and C. B. Madsen, Phys. Rev. **83**, 1265, 1951.
9. R. A. Fischer and N. Yates, Statistical Tables, London 1938.
10. S. D. Warshaw, Phys. Rev. **76**, 1759, 1950.
11. M. S. Livingston and H. A. Bethe, Revs. Mod. Phys. **9**, 263, 1937.
12. Å. Bohr, Dan. Mat. Fys. Medd. **24**, no. 19, 1948.
13. C. J. Bakker and E. Segrè, Phys. Rev. **81**, 489, 1951.
14. R. Mather and E. Segrè, Phys. Rev. **84**, 191, 1951.
15. N. Bohr, Dan. Mat. Fys. Medd. **18**, no. 8, 1948.
16. J. Lindhard and M. Scharff, Phys. Rev. **85**, 1058, 1952.
17. F. Bloch, Zs. f. Phys. **81**, 363, 1933.
18. W. H. Braggs and R. D. Klemanns, Phil. Mag. **11**, 406, 1906.
19. R. Rausch v. Traubenberg, Zs. f. Phys. 396, 404, 1921 & Phys. Zs. **21**, 588, 1920.
20. J. L. Glasson, Phil. Mag. **43**, 477, 1922.
21. J. Lindhard and M. Scharff, Dan. Mat. Fys. Medd. **27**, no. **15**, 1953.
22. H. A. Bethe, Revs. Mod. Phys. **22**, 233, 1950.

Indleveret til selskabet den 13. februar 1953.
Færdig fra trykkeriet den 4. juli 1953.

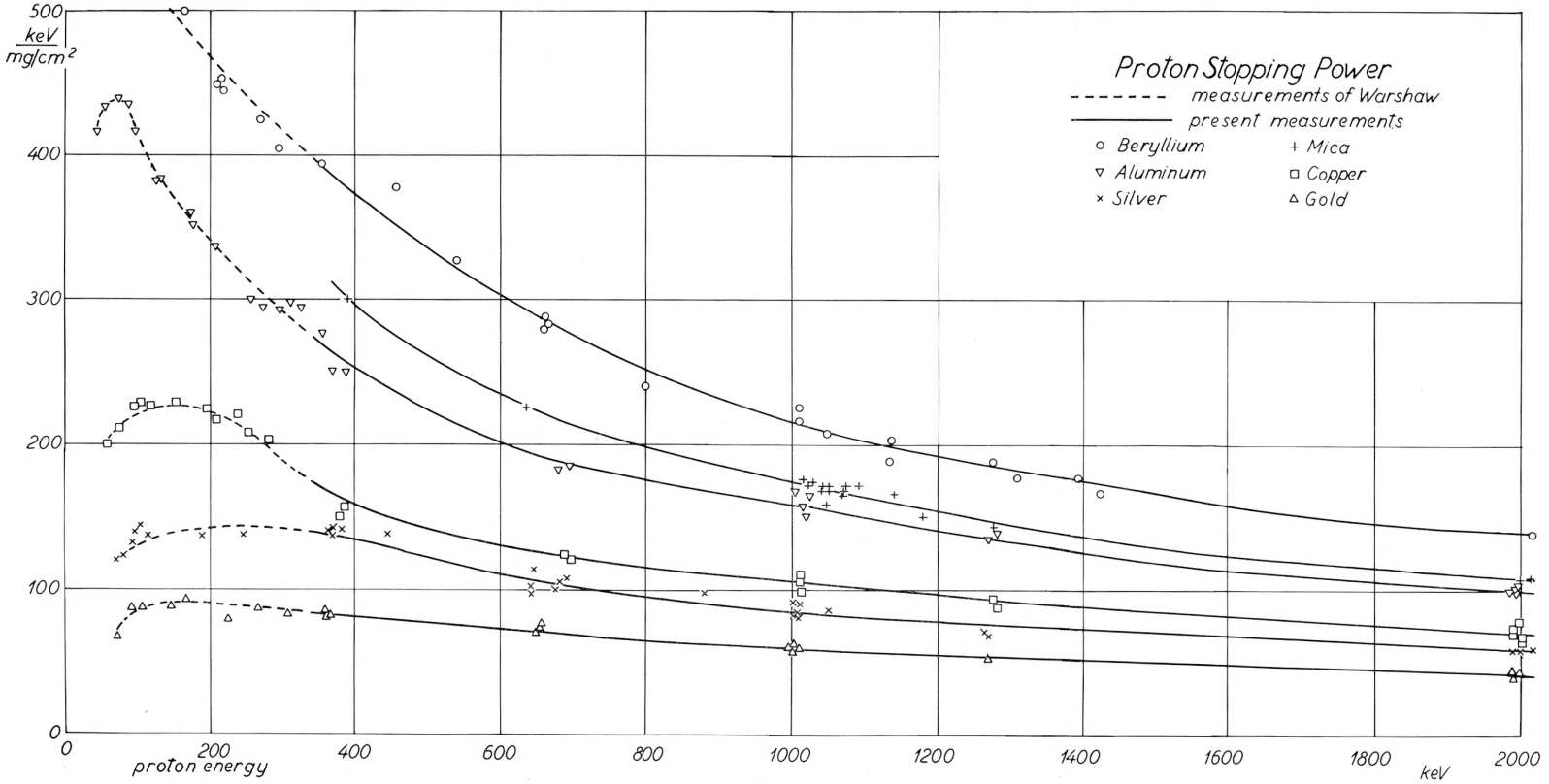
Proton Stopping Power
measurements of Warshaw
present measurements
Beryllium
Aluminum
Silver
Mica
Copper
Gold
500
keV
mg/cm²
400
300
200
100
0
0
200
400
600
800
1000
1200
1400
1600
1800
2000
proton energy
keV

Fig. 1.

Det Kongelige Danske Videnskabernes Selskab
Matematisk-fysiske Meddelelser, bind **27**, nr. 14

Dan. Mat. Fys. Medd. **27**, no. 14 (1953)

ON THE COUPLING CONSTANTS IN β-DECAY. EVIDENCE FROM ALLOWED TRANSITIONS

BY

AAGE WINTHER AND O. KOFOED-HANSEN

København
i kommission hos Ejnar Munksgaard
1953

Printed in Denmark.
Bianco Lunos Bogtrykkeri.

1. Introduction.

It is the aim of the present paper to discuss the information on the coupling in β-decay which can be gained from the allowed transitions. At the present stage of experimental information, it seems that the best determination of the coupling is achieved by comparing the experimental ft-values with the calculated nuclear matrix elements. In the following, we consider the mirror transitions and a few other favoured transitions, since methods for estimating matrix elements for unfavoured transitions are more uncertain. The precise investigation of the shape of β-spectra and the angular correlation in β-decay (recoil experiments) is also valuable for the determination of the coupling and will be discussed in relation to the present considerations. Information may also be obtained from polarization experiments which have already been discussed in detail by de Groot and Tolhoek[1].

In the following, we shall consider an arbitrary mixture of the five linearly independent invariants in β-theory (Table 1), which, for allowed transitions $\Delta I = \begin{cases} 0 \\ 1 \end{cases}$ no, leads to the following β-spectrum[1)*]:

$$
\left.
\begin{aligned}
P_{\pm}(E) &= \frac{m^5 c^4}{2\pi^3 \hbar^7} F(Z,E)\, pE\,(E_{\max}-E)^2 \\
&\quad \left[(g_1^2+g_2^2)\left|\int 1\right|^2+(g_3^2+g_4^2)\left|\int \vec{\sigma}\right|^2 \mp \frac{2\gamma}{E}\,(g_1 g_2\left|\int 1\right|^2+g_3 g_4\left|\int \vec{\sigma}\right|^2)\right] \\
&= \frac{m^5 c^4}{2\pi^3 \hbar^7} F(Z,E)\, pE\,(E_{\max}-E)^2 \\
&\quad [g_F^2(1 \mp b_F/E)\left|\int 1\right|^2+g_{GT}^2(1 \mp b_{GT}/E)\left|\int \vec{\sigma}\right|^2] \\
&= \frac{m^5 c^4}{2\pi^3 \hbar^7} F(Z,E)\, pE\,(E_{\max}-E)^2\,(1+b/E) \\
&\quad [g_F^2\left|\int 1\right|^2+g_{GT}\left|\vec{\sigma}\right|^2],
\end{aligned}
\right\} \quad (1)
$$

*) In formula (1), we have omitted the pseudoscalar term which, according to its selection rules, contributes to allowed transitions only through higher order terms[22]).

where we have used the notation from ref. 1, with

$$\left.\begin{aligned} & g_1^2 + g_2^2 = g_F^2 \quad \text{and} \quad g_3^2 + g_4^2 = g_{GT}^2 \\ & b_F = \frac{2\gamma g_1 g_2}{g_1^2 + g_2^2} \qquad b_{GT} = \frac{2\gamma g_3 g_4}{g_3^2 + g_4^2} \\ & b = \mp \frac{2\gamma \left[g_1 g_2 \left| \int 1 \right|^2 + g_3 g_4 \left| \int \vec{\sigma} \right|^2 \right]}{g_F^2 \left| \int 1 \right|^2 + g_{GT} \left| \int \vec{\sigma} \right|^2} \\ & \gamma = \sqrt{1 - (\alpha Z)^2}. \end{aligned}\right\} \quad (1\,a)$$

The cross terms $g_1 g_2$ and $g_3 g_4$ are the so-called Fierz terms. They are in general assumed to vanish. In section 2, where we shall discuss the information on the coupling, which can be gained from experimental *ft*-values in combination with calculated matrix elements, these terms are neglected. In section 3,

TABLE 1.

Invariant	Coupling constant	Nuclear matrix element. Allowed transitions	Selection rules
Scalar	g_1 } g_F	$\int 1$	$\Delta I = 0$ no
Vector	g_2 } g_F	$\int 1$	$\Delta I = 0$ no
Tensor	g_3 } g_{GT}	$\int \vec{\sigma}$	$\Delta I = \begin{cases} 0 \\ 1 \end{cases}$ no no $0 \to 0$
Pseudovector	g_4 } g_{GT}	$\int \vec{\sigma}$	$\Delta I = \begin{cases} 0 \\ 1 \end{cases}$ no no $0 \to 0$
Pseudoscalar	g_5	$\int \gamma_5$	$\Delta I = 0$ yes

however, it will be shown how uncertain is the usual argument against the existence of cross terms, and a discussion of the influence of cross terms on the results obtained in section 2 will be given, together with a few remarks on the interpretation of angular correlation experiments in view of the possible existence of cross terms.

2. Information from *ft*-values and matrix elements.

If we neglect cross terms the total disintegration probability is given by

$$\lambda = \frac{m^5 c^4}{2\pi^3 \hbar^7} \left[g_F^2 \left| \int 1 \right|^2 + g_{GT}^2 \left| \int \vec{\sigma} \right|^2 \right] f$$

or

$$B = ft \left[(1-x) \left| \int 1 \right|^2 + x \left| \int \vec{\sigma} \right|^2 \right], \tag{2}$$

where

$$B = \frac{2\pi^3 \hbar^7 ln\, 2}{(g_F^2 + g_{GT}^2)\, m^5 c^4} \quad \text{and} \quad x = \frac{g_{GT}^2}{g_F^2 + g_{GT}^2}. \tag{2 a}$$

It is seen that the experimental *ft*-value combined with calculated matrix elements determines a straight line in a B-x diagram for each allowed β-transition. The common intersection point for such lines determines g_F^2 and g_{GT}^2.

For mirror transitions, we can neglect the change in the radial wave functions and thus compute $\left| \int 1 \right|^2$ and $\left| \int \vec{\sigma} \right|^2$ from the angular wave functions alone. In this case, the Fermi matrix element is given by

$$\left.\begin{aligned} \left| \int 1 \right|^2 &= \sum_{M'} \left| \langle JM' \left| \sum_i Q_i \right| JM \rangle \right|^2 \\ &= \left| \langle JM \left| \sum_i Q_i \right| JM \rangle \right|^2 \end{aligned}\right\} \tag{3}$$

where Q_i changes the i'th neutron into a proton. We have specified the total angular momentum J and its z component M only.

The Gamow-Teller matrix element is, correspondingly,

$$\left.\begin{aligned} \left| \int \vec{\sigma} \right|^2 &= \sum_{M'} \sum_k \left| \langle JM' \left| \sum_i \sigma_{ki} Q_i \right| JM \rangle \right|^2 \\ &= \frac{J(J+1)}{M^2} \left| \langle JM \left| \sum_i \sigma_{zi} Q_i \right| JM \rangle \right|^2 \end{aligned}\right\} \tag{4}$$

according to the general rules for matrix elements of vector components[2].

If the state of the mirror nuclei in question can be described in terms of a single particle outside a core, coupled to an angular momentum zero, one obtains

$$\left.\begin{aligned} \left|\int 1\right|^2 &= \left|\langle 1\rangle\right|^2 = 1 \\ \left|\int \vec{\sigma}\right|^2 &= \frac{J(J+1)}{M^2}\left|\langle\sigma_z\rangle_{J_z=M}\right|^2 \\ &= \frac{J(J+1)}{M^2}\left|\langle\frac{\vec{\sigma}\cdot\vec{J}}{J^2}\rangle\langle J_z\rangle\right|^2 \\ &= \begin{cases} \dfrac{J}{J+1} & \text{for} \quad J = l - {}^1/_2 \\ \dfrac{J+1}{J} & \text{for} \quad J = l + {}^1/_2 \end{cases} \end{aligned}\right\} \quad (5)$$

where l is the orbital angular momentum of the odd particle.

In Table 2, we have listed the experimental ft-values for all mirror transitions together with spins and magnetic moments for the daughter nuclei. In the table we have also listed the shell model configuration assignments for the particles outside closed configurations and the corresponding magnetic moments.

a) Closed shell $\pm$ 1 nuclei[4].

It is generally believed that single-particle states are most purely realized for those mirror nuclei which have closed shells of 0, 2, 8, 20 protons and neutrons $\pm$ one nucleon. This assumption is supported by the fact that the experimental magnetic moments generally agree rather well with those calculated from single-particle wave functions. In Table 2, under the heading closed shell $\pm$ 1, we have listed the matrix elements for these transitions found from formula (5). Using these together with the ft-values one obtains the $B(x)$-lines in Fig. 1. These lines are inside the experimental errors consistent with a common intersection point of $(B_0, x_0) = (2650 \pm 85,\ .50 \pm .05)$, where the errors are mean square deviations found from internal consistency of the data. However, these errors should not be taken too literally and some remarks in this connection will be given later*).

*) In a paper by LANGER and MOFFAT[20], which came to our knowledge after the conclusion of this paper, a redetermination of the H^3 ft-value is given. The result is $ft = 1014 \pm 20$, which is in clearcut disagreement with a common intersection point in Fig. 1. LANGER's value for $E_{max} = 17.95 \pm .10$ disagrees also with another recent value given by HAMILTON, i.e. $E_{max} = 19.4 \pm .4$ keV[19]).

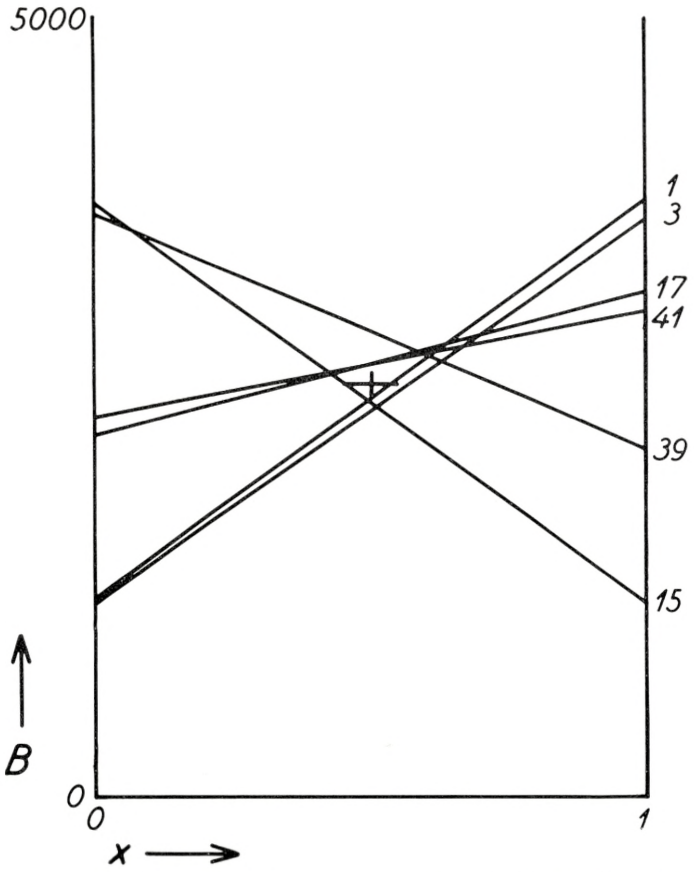

Fig. 1. $B(x)$ lines for closed shell $\pm$ one nucleon transitions. Mass numbers are indicated.

b) Other mirror transitions.

Also in other cases than those discussed under a) the shell model predicts closed configurations $\pm$ one single nucleon (i.e. for mass numbers 11, 13, 19, 27, 29, 31, 33). In these cases, the matrix elements may also be calculated from formula (5).

For several particles outside closed configurations the *ft*-value depends sensitively on the coupling scheme.

If one assumes that the even structures couple to zero angular momentum, as is often done in shell model calculations of mag-

TABLE 2. The E_{max} quoted are often taken from reaction data (ref. 1 where the formulas of FEENBEF

	Transition	E_{max} (MeV)	t	ft-value	spin	μ_{exp} daug ter
1	n → p	0.782 ± 0.001[15])	12.8^{m} ± 2.5	1280 ± 250	$^1/_2$	2.7
3	H → He	0.0191 ± 0.0005[14]) [18])	12.45^{y} ± 0.2	1240 ± 120	$^1/_2$	—2.1
7	Be → Li	0.863 ± 0.002[15])	52.9^{d} ± 0.2	2240 ± 40	$^3/_2$	3.2
11	C → B	0.958 ± 0.003[15])	20.39^{m} ± 0.06	3840 ± 70	$^3/_2$	2.6
13	N → C	1.200 ± 0.005[15])	10.1^{m} ± 0.1	4560 ± 100	$^1/_2$	0.7
15	O → N	1.683 ± 0.005[14])	2.1^{m} ± 0.1	3800 ± 200	$^1/_2$	—0.2
17	F → O	1.745 ± 0.006[16])	65^{s} ± 2	2320 ± 100	$^5/_2$	—1.8
19	Ne → F	2.234 ± 0.005[16])	19.5^{s} ± 1.0	1970 ± 100	$^1/_2$	2.6
21	Na → Ne	2.50 ± 0.03[14])	22.8^{s} ± 0.5	3700 ± 200	$(^3/_2)$	<0
23	Mg → Na	3.073 ± 0.010[16])	12.0^{s} ± 0.2	4780 ± 150	$^3/_2$	2.2
25	Al → Mg	..	7.3^{s}	..	$(^5/_2)$	—0.8
27	Si → Al	3.48 ± 0.10[17])	5.0^{s} ± 0.4	3350 ± 600	$^5/_2$	3.6
29	P → Si	3.60 ± 0.15[14])	4.6^{s} ± 0.2	3510 ± 700	$^1/_2$	—0.5
31	S → P	4.06 ± 0.12[17])	3.1^{s} ± 0.2	4020 ± 600	$^1/_2$	1.1
33	Cl → S	4.43 ± 0.13[17])	2.0^{s} ± 0.2	3800 ± 650	$^3/_2$	0.6
35	A → Cl	4.4 ± 0.2[14])	1.90^{s} ± 0.05	3420 ± 800	$^3/_2$	0.8
37	K → A	4.57 ± 0.13[17])	1.2^{s} ± 0.2	2520 ± 600	..	..
39	Ca → K	5.13 ± 0.15[17])	1.06^{s} ± 0.03	3740 ± 500	$^3/_2$	0.3
41	Sc → Ca	4.9 ± 0.2[14])	0.87^{s} ± 0.03	2430 ± 800	..	..

*) probably in strong admixture with $d^2_{5/2}\, s_{1/2}$ which would make $|\int 1|^2$ and

netic moments, etc., the j—j coupling scheme leads to unique wave functions. The matrix elements are easily calculated using the formulae (3) and (4) together with the rules for matrix elements of sums of single-particle operators[3]). The result is shown

ıd 16). The *ft*-values are calculated numerically except for $Z < 7$, ıd TRIGG[18] have been used.

ɔnfiguration	$\mu_{\text{theor.}}$	closed shell ± 1		*j-j* coupling even structure 0		*T*-multiplet		semi-empirical	
		$\lvert\int 1\rvert^2$	$\lvert\int \vec{\sigma}\rvert^2$	$\lvert\int 1\rvert^2$	$\lvert\int \vec{\sigma}\rvert^2$	$\lvert\int 1\rvert^2$	$\lvert\int \vec{\sigma}\rvert^2$	$\lvert\int 1\rvert^2$	$\lvert\int \vec{\sigma}\rvert^2$
$s_{1/2}$	2.79	1	3	..	..	..	..	1	
$s^3_{1/2}$	−1.91	1	3	..	..	..	..	1	
$p^3_{3/2}$	3.79	..	..	$^1/_4$	$^5/_{12}$	..	..	1	0.98
$(p^3_{3/2})^{1/2,\,1/2}_{3/2}$	3.03	..	..	..	..	1	$^{121}/_{135}$		
$p^5_{3/2}$	3.79	..	..	..	..	1	$^5/_3$	1	0.45
$p_{1/2}$	0.64	..	..	..	..	1	$^1/_3$	1	0.40
$p^3_{1/2}$	−0.26	1	$^1/_3$	..	..	..	..	1	0.35
$d_{5/2}$	−1.91	1	$^7/_5$	..	..	..	..	1	1.37
$s^3_{1/2}$ *)	2.79	..	..	..	..	1	3	1	2.59
$(d^5_{5/2})_{3/2}$	−1.14	..	..	0	0	1	not	1	—
$(d^7_{5/2})_{3/2}$	2.89	..	..	0	0	1	unique	1	0.16
$d^9_{5/2}$	−1.91	..	..	$^1/_9$	$^7/_{45}$	..	..	1	0.28
$(d^9_{5/2})^{1/2,\,1/2}_{5/2,\,5/2}$	−1.04	..	..	..	..	1	0.784		
$d^{11}_{5/2}$	4.79	..	..	..	..	1	$^7/_5$	1	0.35
$s_{1/2}$	−1.91	..	..	..	..	1	3	1	0.25
$s^3_{1/2}$	2.79	..	..	..	..	1	3	1	0.23
$d_{3/2}$	1.15	..	..	..	..	1	$^3/_5$	1	0.19
$d^3_{3/2}$	0.13	..	..	$^1/_4$	$^3/_{20}$	..	..	1	0.15
$(d^3_{3/2})^{1/2,\,1/2}_{3/2}$	0.27	..	..	..	..	1	$^{121}/_{375}$		
$d^5_{3/2}$	1.15	..	..	$^1/_4$	$^3/_{20}$	..	..	1	—
$(d^5_{3/2})^{1/2,\,1/2}_{3/2}$	1.01	..	..	..	..	1	$^{121}/_{375}$		
$d^7_{3/2}$	0.13	1	$^3/_5$	..	..	..	..	1	0.39
$f_{7/2}$	−1.91	1	$^9/_7$	..	..	..	..	1	—

$\lvert\int \vec{\sigma}\rvert^2$ smaller without altering μ.

in Table 2 under the heading "*j*—*j* coupling, even structure 0". The *ft*-values calculated from these numbers, using the $B_0\, x_0$ value given in a), are in very poor agreement with the experimental *ft*-values. This is not surprising since the wave functions

used are not consistent with the charge independence of nuclear forces.

In general, the wave function will depend on the nuclear forces. However, in some cases (i.e. mass number 7, 25, 35, 37), the wave functions may be uniquely constructed from the assumption that the ground state has the lowest possible value of the total isotopic spin T[5].

The wave function for Li^7, where $J = M = {}^3/_2$ and $T = T_\zeta = {}^1/_2$ is thus given by[23]

$$\left(p^3_{{}^3/_2}\right)^{{}^1/_2,\,{}^1/_2}_{{}^3/_2,\,{}^3/_2} = \sqrt{\frac{4}{15}}\, p^N_{{}^3/_2,\,{}^1/_2}\, p^N_{{}^3/_2,\,-{}^1/_2}\, p^P_{{}^3/_2,\,{}^3/_2} - \sqrt{\frac{9}{15}}\, p^N_{{}^3/_2,\,{}^3/_2}\, p^N_{{}^3/_2,\,-{}^3/_2}\, p^P_{{}^3/_2,\,{}^3/_2}$$
$$+ \sqrt{\frac{1}{15}}\, p^N_{{}^3/_2,\,{}^3/_2}\, p^N_{{}^3/_2,\,-{}^1/_2}\, p^P_{{}^3/_2,\,{}^1/_2} - \sqrt{\frac{1}{15}}\, p^N_{{}^3/_2,\,{}^3/_2}\, p^N_{{}^3/_2,\,{}^1/_2}\, p^P_{{}^3/_2,\,-{}^1/_2}$$

where we have left out the antisymmetrization operator

$$\frac{1}{\sqrt{3!}} \sum_P (-1)^P P,$$

where P means the permutation of all three particle coordinates. For mass numbers 21 and 23, where $j = {}^5/_2$, the wave functions are not uniquely determined from the assumption $T = {}^1/_2$.

If the total isotopic spin T is a good quantum number, one can easily show that the Fermi matrix element for a transition between a state T, T_ζ and a state $T', T_\zeta - 1$ is given by[6]

$$\left|\int 1\right|^2 = (T + T_\zeta)(T - T_\zeta + 1)\,\delta_{TT'}. \tag{8}$$

For mirror transitions, where $T' = T = {}^1/_2$ and $T_\zeta = {}^1/_2$, we get $\left|\int 1\right|^2 = 1$.

The Gamow-Teller matrix element may be calculated using explicit wave functions inserted in Eq. (4). The results are listed in Table 2, under the heading "T-multiplet", together with the matrix elements for the above mentioned cases, where we have to do with closed configurations $\pm$ one particle. In Fig. 2, the corresponding $B(x)$ lines are plotted. The $B_0 x_0$ value from section a) is indicated by a cross. It is seen that the agreement with this

value of B,x (or any other value) is very poor. However, it should be noted that the lines which deviate most from B_0,x_0 correspond to transitions between nuclei for which the theoretical

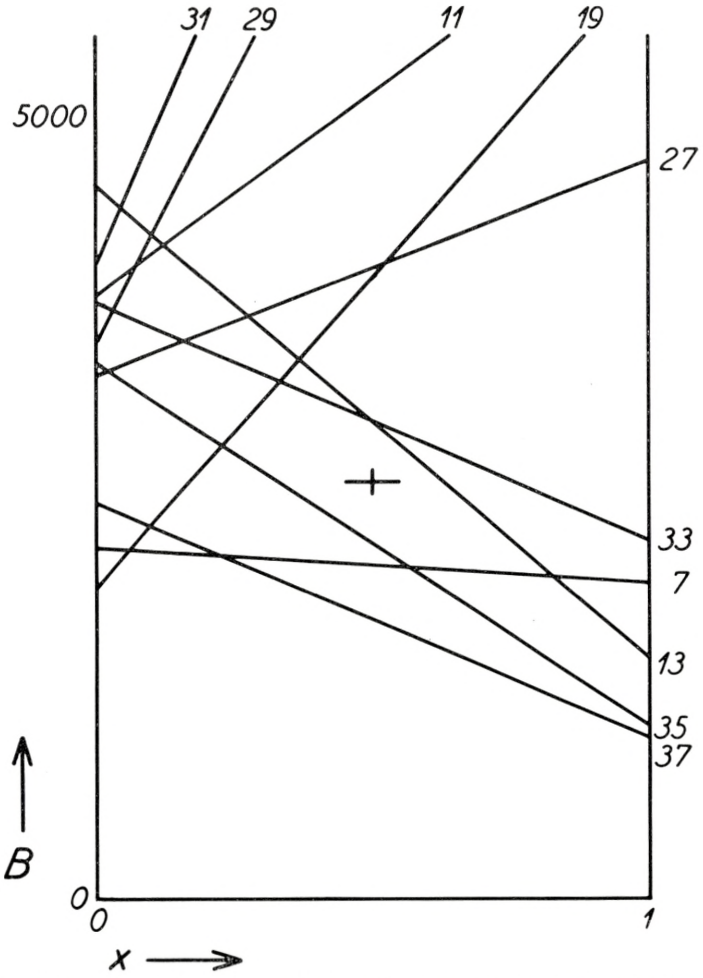

Fig. 2. B (x) lines for mirror transitions with unadjusted matrix elements. Mass numbers are indicated.

magnetic moments deviate essentially from the empirical ones. It thus seems interesting to try to find whether any simple correlation exists between the ft-values and the deviations of the magnetic moments from the Schmidt lines. Such correlations have actually been found by TRIGG[12] who evaluates the matrix

elements from an interpolation between the Schmidt lines and the Margenau-Wigner lines for the magnetic moments.

In the following, we shall try to give an argument for an evaluation of the Gamow-Teller matrix element which is essentially an interpolation between the two Schmidt lines.

If one assumes that the deviation of the magnetic moments from the Schmidt lines arises from an interaction between the odd particle and some other particles in the nucleus, which take over part of the angular momentum, e.g., as in the model used by A. BOHR and B. MOTTELSON[7], one may write the magnetic moment

$$\begin{aligned}\mu &= g_s \langle s_z \rangle_{J_z = J} + g_l \langle l_z \rangle_{J_z = J} + g_R \langle R_z \rangle_{J_z = J} \\ &= (g_s - g_l) \langle s_z \rangle_{J_z = J} + g_l J + (g_R - g_l) \langle R_z \rangle_{J_z = J}.\end{aligned}$$

Here, $\vec{J} = \vec{s} + \vec{l} + \vec{R} = \vec{j} + \vec{R}$. s and l are the spin and orbital angular momenta of the single particle, and R is the angular momentum of the system of particles to which it is coupled. $\langle\ \rangle$ means average value and the g's are the gyromagnetic ratios.

The success of the shell model in predicting spins of the light nuclei leads one to believe that $\langle j_z \rangle_{J_z = J}$ is not very different from J, that is $\langle R_z \rangle_{J_z = J}$ is small compared with J. As the factor $(g_R - g_l)$ is small also compared with $(g_s - g_1)$, g_R being perhaps of the order $^1/_2$, one may in first order neglect the last term in (9). This result in fact also turns out if one uses the model by AAGE BOHR[7].

For the Gamow-Teller matrix element, we get from (4)

$$\left| \int \vec{\sigma} \right|^2 = 4 \frac{J+1}{J} \left| \langle s_z \rangle_{J_z = J} \right|^2.$$

$\langle s_z \rangle$ may be inserted from (9) after neglect of the last term and we thus get the following approximate formula

$$\left| \int \vec{\sigma} \right|^2 \approx 4 \frac{J+1}{J} \left(\frac{\mu - g_l J}{g_s - g_l} \right)^2. \tag{10}$$

For the Fermi matrix element we find from (8)

$$\left| \int 1 \right|^2 = 1.$$

Using the magnetic moments listed in Table 2, we can thus obtain the matrix elements listed under the heading "semi-empirical". The results are plotted in Fig. 3. The full-drawn lines

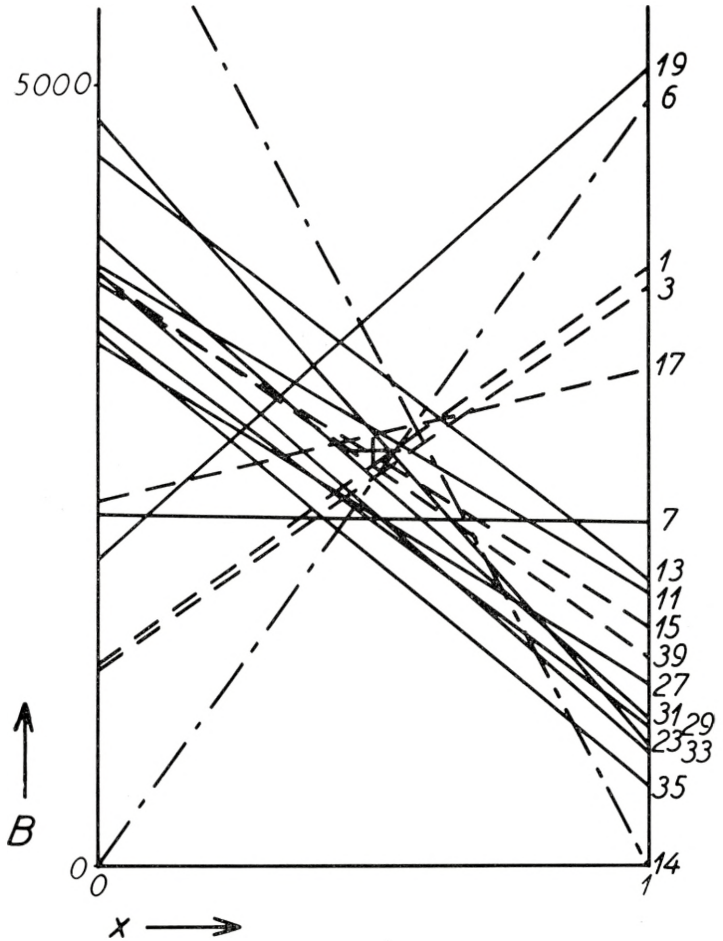

Fig. 3. $B(x)$ lines for mirror transitions with adjusted matrix elements and for He^6 and O^{14} decay. Mass numbers are indicated.
— — — closed shell $\pm$ 1 transitions.
——— other mirror transitions.
— · — He^6 and O^{14} decay.

are essentially the same transitions as those plotted in Fig. 2. The dotted lines are those transitions which were used in Fig. 1 for the determination of B_0, x_0. The use of formula (10) instead of

(5) has changed these lines only by small amounts. The semi-empirical method does not work, however, in the case of the triton decay ($|\langle s_z \rangle| > 1/2$) where we have used the value 3†).

The deviations of the full-drawn lines from the B_0, x_0 value are, in several cases, larger than the experimental uncertainty. We have tried to evaluate the magnitude of the term $(g_R - g_l) \langle R_z \rangle_{J_z = J}$ which would be necessary to explain this deviation. It turns out that $|g_R - g_l| \approx 1/2$ and $|\langle R_z \rangle_{J_z = J}| \lesssim 1/2$ will suffice to explain the deviations in all cases. One might thus hope that a theory which in detail explains the magnetic moments will at the same time explain the matrix elements for mirror transitions.

c) Even-A transitions and unfavoured transitions.

Among the allowed even-A transitions only those which are of the type $0 \rightarrow 0$ no are very simple. For transitions of this type, the Gamow-Teller matrix elements vanish. The Fermi matrix element may be calculated from formula (8) which is based on the assumption of charge independence of nuclear forces only. Until now, two cases of $0 \rightarrow 0$ no transitions are known with some certainty, namely $C^{10} \rightarrow B^{10*}$ and $O^{14} \rightarrow N^{14*}$. The experimental data are listed in Table 3.

TABLE 3.

Decay	E_{max} (MeV)	t	Branching ratio	ft-value	$\lvert \int 1 \rvert^2$	$\lvert \int \vec{\sigma} \rvert^2$
$C^{10} \rightarrow B^{10*}$	1.15 ± 0.10	$19.1^s \pm 0.8$	0.021 ± 0.006	$6000 + 3000$	2	0
$O^{14} \rightarrow N^{14*}$	1.8 ± 0.1	$76.5^s \pm 0.2$	1	3300 ± 900	2	0
$He^6 \rightarrow Li^6$	3.50 ± 0.05	$0.823^s \pm 0.013$	1	815 ± 70	0	6

The O^{14} decay has been used by BLATT[9] to determine the coupling in β-decay, but, with the present experimental uncertainty, both this transition and the C^{10} decay are consistent with our values for B_0 and x_0.

†) A more detailed estimation of the Gamow-Teller matrix element has been given recently by BLATT[8] who finds $|\int \vec{\sigma}|^2 \approx 2.84$. As mentioned by BLATT, this result is rather uncertain. The value 3 which we have used is, according to BLATT, an upper limit.

Also the decay of He^6, the experimental data of which are listed in Table 3, has been used for the determination of the coupling[10]. It seems, however, that the Gamow-Teller matrix element for this transition is rather ambiguous (the Fermi matrix element is certainly 0). The matrix element obtained by using j—j coupling is definitely too small. The matrix element quoted in the table is obtained by L—S coupling. Although this value is probably an upper limit; we have used it for the $B(x)$ line for He^6 in Fig. 3.

A few other even-A transitions with "superallowed" ft-values exist, but matrix elements for these are even more uncertain than for the He^6 decay.

For all other allowed transitions the ft-value is a factor 50—100 larger than the ft-value for mirror transitions; they are so-called unfavoured transitions. The "unfavoured factor" may partly be understood by noting that, in all other cases than the mirror transitions, the quantum number T is different for the ground states of mother and daughter nuclei, i.e. the Fermi matrix element vanishes[6]. This will, however, only explain a part of the unfavoured factor and probably one has to take into account other differences between the nuclei than the states for the odd nucleons[7].

3. Cross terms[11].

Until now we have assumed that the products $g_1 g_2$ and $g_3 g_4$ vanish. In this section, we shall investigate in how far this assumption can be verified experimentally.

a) Spectrum shape.

As seen from Eq. (1), the cross terms are energy dependent, i.e. they will show up in a β-spectrum. If we consider a Kurie plot

$$K = \sqrt{\frac{P}{F(Z,E)\,pE}} = C\,(E_{\max} - E)\sqrt{1 + b/E}, \qquad (11)$$

the most important effect of the cross term b/E for low and medium maximum energies is a change of the slope of the plot. This

change is, however, not detected since it is equivalent to a change of C. What remains is a curvature which appears as a small deviation from a straight line the slope of which is adjusted to the experimental points.

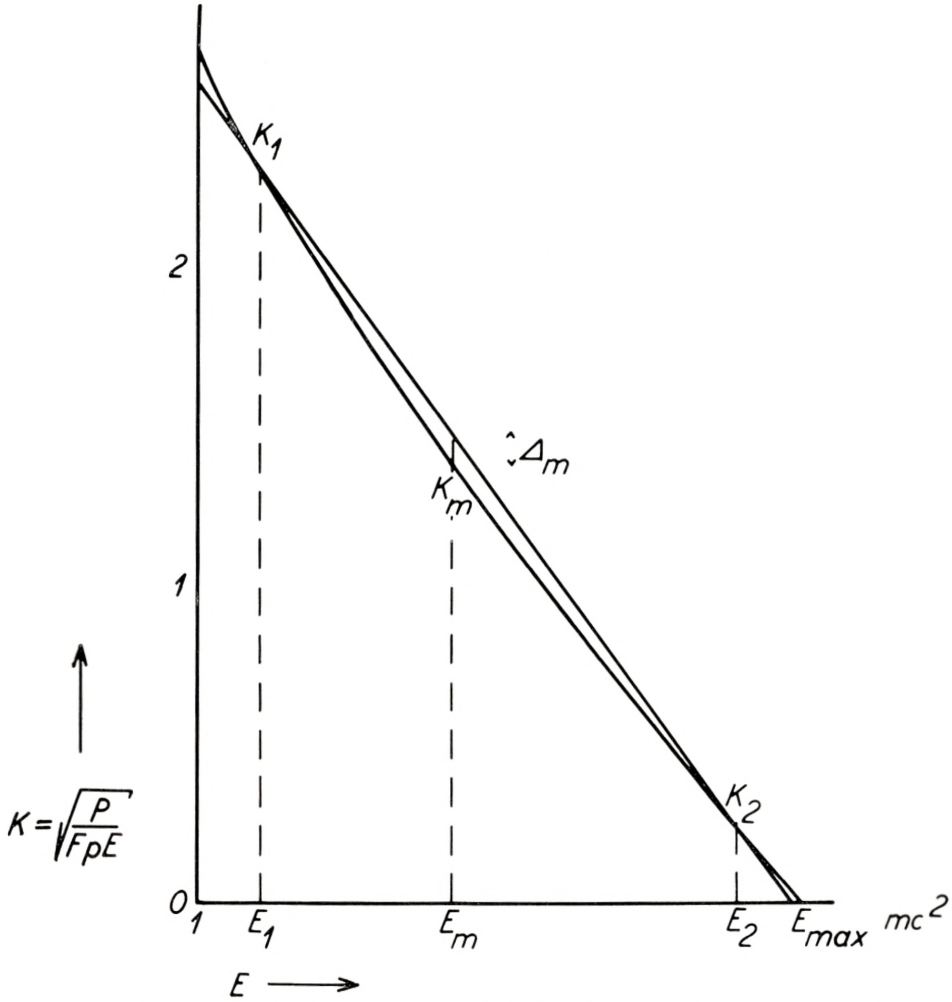

Fig. 4. Kurie plot with cross terms compared with straight line adjusted to the points E_1 and E_2.

In Fig. 4 we have illustrated an example where the straight line is adjusted to the curved Kurie plot[11] in the points E_1 and E_2. The maximum deviation Δ_m will appear at a point $E_m \approx \sqrt{E_1 E_2}$. To illustrate the magnitude of the curvature, we have plotted in

Fig. 5 Δ_m/K_m as a function of the maximum energy for different values of b in the case where $E_1 = 1.2$ and $E_2 = E_{\max} - 0.2$.

It is seen from Fig. 5 that even large values of b ($-1 \leqslant b \leqslant 1$) give only small deviations and that, consequently, it is difficult to obtain narrow limits for b. In fact, an analysis of the published

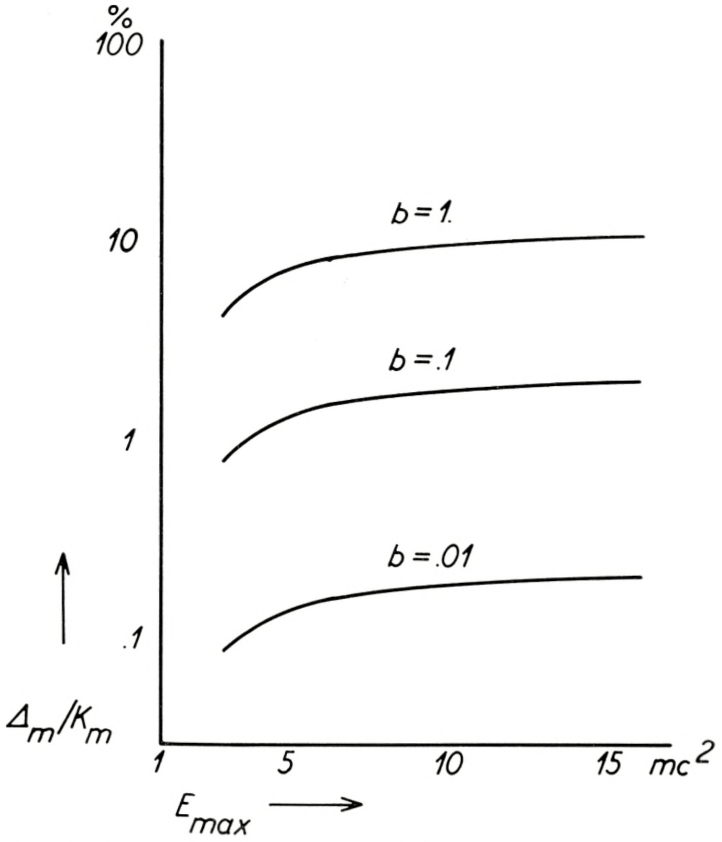

Fig. 5. Maximum deviation Δ_m/K_m of curved Kurie plot from straight line for different values of cross terms b.

β-spectra indicates that, in no case, b-values as large as 0.4 can be excluded. In such experimental comparison it should, of course, be remembered that b has opposite sign for positon and negaton emission*).

*) Recently, MAHMOUD and KONOPINSKI[21] have given a careful analysis of the shapes of some allowed β-spectra in order to set a limit on the cross terms. Their result $|b| < 0.2$ is based on a statistical treatment of all the experimental data.

Furthermore, it should be noted that experimenters usually apply the straightness of the Kurie plot as a control on their spectrometers.

The information about the coupling constants which can be obtained from a determination of b is contained in Eq. (1a). Since b depends on the nuclear matrix elements, it is of course most valuable to determine b in cases where the ratio $|\int 1|^2/|\int \vec{\sigma}|^2$ is known. As an example, we have in Fig. 7 plotted the dependence of b on the ratio g_4/g_3 in the simple case where $|\int 1|^2$ is known to vanish.

b) *ft*-values.

The cross terms will also have some influence on the ft-values as the new f-value will be given by

$$f = f_0 (1 + b\delta),$$

where f_0 is the usual Fermi integral and

$$\delta = \int F(Z, E)\, p\, (E_{\max} - E)^2\, dE/f_0.$$

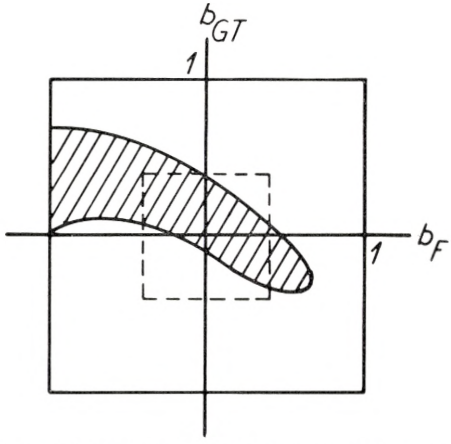

Fig. 6. Area in b_F, b_{GT} plane which is allowed according to the assumption of consistent $B(x)$ lines for closed shell $\pm$ 1 transitions.

To see what influence this will have on our considerations in section 2, we derive from Eq. (1) that

$$\frac{1}{t} = \frac{m^5 c^4}{2\pi^3 \hbar^7 \ln 2} f_0 \left[g_F^2 (1 \mp b_F \delta) \left|\int 1\right|^2 + g_{GT} (1 \mp b_{GT} \delta) \left|\int \vec{\sigma}\right|^2\right].$$

With the notation (2a) we get

$$B = f_0 t \left[(1-x)(1 \mp b_F \delta) \left| \int 1 \right|^2 + x(1 \mp b_{GT} \delta) \left| \int \vec{\sigma} \right|^2\right]$$

which shows that the $B(x)$ lines will still be straight lines, only they will be shifted by an amount depending on b_F and b_{GT}. This now provides us with another tool for the determination of the cross terms. If we assume that the $B(x)$ lines for the simple closed shell ± 1 nuclei have to pass through a common point within their experimental uncertainty, we can estimate limits for b_F and b_{GT}. In Fig. 6, we have indicated the area in the b_F, b_{GT} plane which is allowed according to this condition.

c) Recoil experiments.

If cross terms exist, the angular correlation between β-particle and neutrino for allowed transitions is given by[1)]

$$W(\theta_{\beta\nu}) = 1 + \alpha p/E \cos\theta_{\beta\nu} + b/E$$

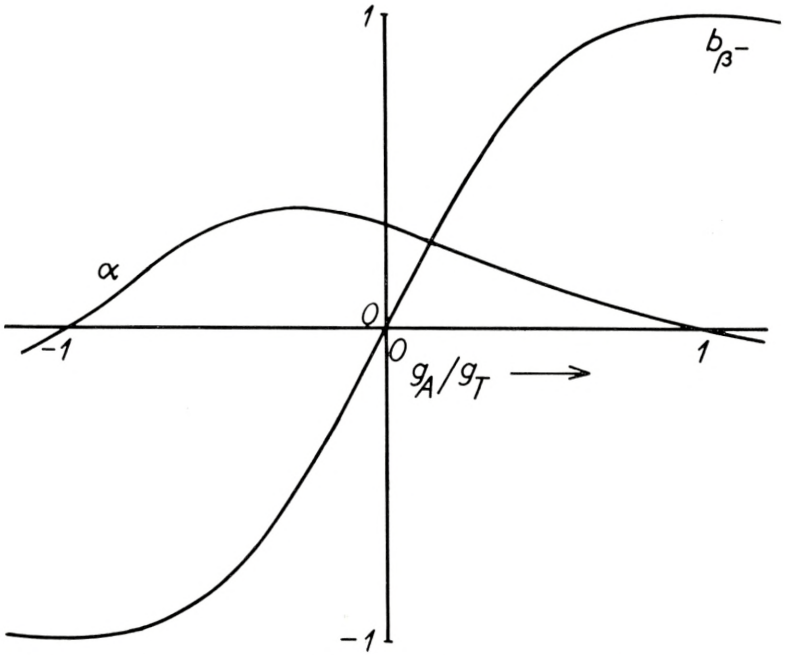

Fig. 7. The experimental angular correlation parameter α and the cross term parameter b_{β^-} for allowed GT transitions.

where

$$a = -\frac{(g_1^2 - g_2^2)\left|\int 1\right|^2 - {}^1/_3\,(g_3^2 - g_4^2)\left|\int \vec{\sigma}\right|^2}{g_F^2\left|\int 1\right|^2 + g_{GT}^2\left|\int \vec{\sigma}\right|^2}$$

and b is given in (1a).

In angular correlation experiments, one usually determines the ratio between the cosine-dependent term and the constant term

$$\alpha = a/(1 + b/E),$$

where E is the energy of those electrons for which the angular correlation is measured.

To illustrate what information on the coupling constants can be obtained from a determination of α, we have plotted in Fig. 7 a α as a function of g_4/g_3 for $E = 2$ in the simple case where $\left|\int 1\right|^2$ is known to vanish. It is seen that a determination of α in general does not permit a unique determination of g_4/g_3. It thus seems valuable to combine angular correlation experiments with β-spectroscopic measurements, especially in those cases where the ratio $\left|\int 1\right|^2/\left|\int \vec{\sigma}\right|^2$ can be estimated.

4. Summary.

In the present paper, an investigation of nuclear matrix elements has been combined with the experimental ft-values in order to determine the coupling constants for Fermi- and Gamow-Teller interaction in β-decay. It is shown that the mirror transitions between nuclei with closed shells $\pm$ one nucleon are consistent with approximately equal amounts of the two couplings. Within the limits of error, this result agrees with similar calculations carried out by TRIGG[12], BOUCHEZ and NATAF[13], and BLATT[9]. For the remaining mirror transitions, the matrix elements derived from the shell model are not consistent with this result. However, as pointed out by TRIGG[12], considerable improvement can be obtained by adjusting the wave functions to the observed magnetic moments. In the present paper, it is shown that, on the assumption of an interaction between the single particle and the nuclear core, an approximate correlation exists between the Gamow-Teller

matrix elements and the magnetic moments of the nuclei involved in the transitions. The results for the adjusted matrix elements thus obtained are, within the uncertainties and the approximation, in agreement with the above mentioned coupling constants.

The possible existence of cross terms in the β-decay coupling is also discussed. It is shown that the present experimental data do not provide very narrow limits for these terms, and further experiments on this matter are therefore desirable.

We wish to thank Professor NIELS BOHR for his interest in our work and we are indebted to Mr. AAGE BOHR and Dr. BEN MOTTELSON for many valuable discussions and suggestions.

References.

1. S. R. de Groot and H. A. Tolhoek, Physica **16**, 456, 1950.
2. E. Wigner, Gruppentheorie. Braunschweig 1931, p. 264.
3. E. U. Condon and G. H. Shortley, The Theory of Atomic Spectra. Cambridge 1935, p. 169 ff.
4. O. Kofoed-Hansen and A. Winther, Phys. Rev. **86**, 428, 1952.
5. E. Wigner, Phys. Rev. **51**, 106, 1937.
6. E. Wigner and E. Feenberg, Rep. Prog. Phys. **8**, 274, 1941.
7. A. Bohr and B. Mottelson, Dan. Mat. Fys. Medd. **27**, no. 16 (1953).
8. J. Blatt, Phys. Rev. **89**, 86, 1953.
9. J. Blatt, Phys. Rev. **89**, 83, 1953.
10. S. A. Moszkowski, Phys. Rev. **82**, 118, 1951.
11. O. Kofoed-Hansen and A. Winther, Phys. Rev. **89**, 526, 1953.
12. G. L. Trigg, Phys. Rev. **86**, 506, 1952.
13. R. Bouchez and R. Nataf, C. R. **234**, 86, 1952.
14. Nuclear Data, N. B. S. Circ. 499.
15. C. W. Li et al., Phys. Rev. **83**, 512, 1951.
16. C. W. Li, Phys. Rev. **88**, 1038, 1952.
17. F. J. Boley and D. J. Zaffarano, Phys. Rev. **84**, 1059, 1951.
18. E. Feenberg and G. L. Trigg, Revs. mod. Phys. **22**, 399, 1950.
19. D. R. Hamilton et al., Phys. Rev. **83**, 215, 1951.
20. L. M. Langer and R. J. D. Moffat, Phys. Rev. **88**, 689, 1952.
21. H. M. Mahmoud and E. J. Konopinski, Phys. Rev. **88**, 1266, 1952.
22. G. Alaga, O. Kofoed-Hansen and A. Winther, in preparation.
23. M. Mizushima and M. Umezawa, Phys. Rev. **85**, 37, 1952.

Indleveret til selskabet den 13. februar 1953.
Færdig fra trykkeriet den 27. juni 1953.

Det Kongelige Danske Videnskabernes Selskab
Matematisk-fysiske Meddelelser, bind **27**, nr. 15

Dan. Mat. Fys. Medd. **27**, no. 15 (1953)

ENERGY LOSS IN MATTER BY FAST PARTICLES OF LOW CHARGE

BY

J. LINDHARD AND M. SCHARFF

København
i kommission hos Ejnar Munksgaard
1953

Printed in Denmark
Bianco Lunos Bogtrykkeri A/S

§ 1. Introduction.

In the discussion of the energy loss by swift charged particles passing through matter one may conveniently distinguish between two extreme cases. When a penetrating particle has a sufficiently high charge, or low velocity, it will carry electrons which to some extent will screen the field of the particle. The problem of its energy loss is then quite involved, even though it may be treated essentially on classical mechanics. But as soon as the velocity of the particle is high compared with the orbital velocity of an electron carried by it in the ground state, the energy loss can be computed rather accurately using a quantum mechanical perturbation treatment. In the present paper we shall be concerned with the latter simple case, and in particular with the slowing down of protons and α-particles. We shall try to build up a simple and consistent picture of the atomic processes displayed in stopping problems for atoms containing many electrons. But it may be useful to make first a few remarks regarding the different treatments and points of view on the subject.

We consider then the energy loss suffered by a heavy particle of velocity v and charge ze, passing through a substance of atomic number Z and with a density N atoms per unit volume. As long as v remains large compared with the velocity of the more strongly bound electrons in the substance, the average specific energy loss of the particle is with good approximation given by the general formula of Bethe (Bethe (1930), Bethe and Livingston (1937))

$$\frac{dE}{dR} = \frac{4\pi z^2 e^4}{mv^2} \cdot NZ \log \frac{2mv^2}{I}, \tag{1}$$

where I is a constant characteristic of the substance, often denoted as the average excitation potential. This constant was by Bethe found to be determined by

$$L = \log \frac{2mv^2}{I} = \frac{1}{Z} \sum_{i,k}{}' f_{ik} \log \frac{2mv^2}{\hbar\omega_{ik}}, \qquad (1')$$

where f_{ik} is the atomic oscillator strength corresponding to the transition (i, k) with frequency ω_{ik}; a similar formula applies when chemical bindings come into play. The equation (1) holds for non-relativistic velocities. For very fast particles the relativistic term $(-\log(1 - v^2/c^2) - v^2/c^2)$ is to be added to the logarithm in (1). It is well known that half of this term arises from close collisions with the electrons in the substance, while the other half is due to distant collisions. It should be mentioned that the relativistic formula is not always quoted correctly in the literature, and also that some authors introduce a potential I defined in a manner different from that used here. A correction to the above relativistic term, depending on the density of the material, was introduced by FERMI (1940). We shall not be concerned with relativistic cases where this effect is important.

In connection with (1) it is worth recalling that for an analysis of stopping problems it can be of advantage to use a simple idealized picture of the energy transfer. The collision may then be described by a classical impact parameter, p, and a collision time, $\tau = p/v$. For a particle of high velocity the collisions can be divided into the close and the distant ones. In the violent close collisions the binding and mutual interaction of the electrons will not be important. In the more distant collisions the average energy transfer is equivalent to that in free classical impacts. It is now decisive for the magnitude of the total energy loss by the particle that the energy transfer becomes negligible for collision frequencies, $1/\tau = v/p$, less than the adiabatic frequency ω characterizing the dynamical properties of the atomic system. The value of ω is connected with I by the relation $I = \hbar\omega$. We shall repeatedly make use of the above simple concepts.

The energy loss suffered by electrons passing through matter cannot, for several reasons, be contained in formulae of type of (1). In the following we shall treat only heavier particles, but the estimates of the average excitation potentials, which involve only distant collisions for fast penetrating particles, can of course be used as well in the description of the stopping of electrons.

In BETHE's deduction I is determined by the transition fre-

quencies and corresponding oscillator strengths in the atomic system. A direct calculation of I on these lines is simple in the case of hydrogen, but becomes complicated for substances of high atomic number. A considerable simplification of the problem for heavier substances was achieved by BLOCH (1933), when he applied the Thomas-Fermi model of the atom. Making some simplifying approximations in the Thomas-Fermi model when extending it to dynamical problems, BLOCH found that the average excitation potential $I = I(Z)$ in Bethe's formula (1) could be written as

$$I = I_0 \cdot Z, \tag{2}$$

I_0 being a constant independent of Z. BLOCH did not calculate the value of I_0; in fact, it seemed difficult to compute this quantity from his model with sufficient accuracy, an empirical determination being preferable. A calculation of I_0 was carried through later by JENSEN (1937), but with a picture of the atom too simplified to allow quantitative comparisons.

The numerous data on the slowing-down of protons and α-particles in substances of medium and high atomic number have shown that Bloch's relation (2) is rather well satisfied for sufficiently high velocities v. The values of $I_0 = I/Z$ found empirically are about 10 eV, with only slight variations between the different elements.

When the velocity of the particle becomes comparable with those of the more strongly bound electrons in the substance—as is usually the case for natural α-rays—the energy loss is no longer well represented by the constant potential in equations (2) or (1). The potential will then vary with velocity because the logarithmic expressions in (1′) apply only when the arguments are large. BETHE has here introduced corrections of the contributions from the electrons in the K-shell (BETHE and LIVINGSTON (1937)). In the following we shall be particularly interested in this velocity region, and also in the stopping for still lower velocities, where N. BOHR (1948) has accounted in a simple manner for the empirical v^3-relation for the range of α-rays.

It is the aim of this paper to bring out general relationships, embracing results like that of BLOCH (2). We shall rely on simplified descriptions of atoms, where the main features of atomic

dynamics are most easily recognized. It may be that more than due emphasis is given to the comparison with a free electron gas and the description based on polarization. But we found this way of approach preferable; although less common it is perhaps the simplest one.

In order to get a first insight into the phenomena we shall, in § 2, try to arrive at a simple qualitative picture of the stopping in heavier substances, and in § 3 discuss in how far this picture can be said to agree with the data. These questions were treated briefly in a recent note (LINDHARD and SCHARFF (1952)). A more detailed discussion of different kinds of approach employed in atomic dynamics is attempted in § 4. We shall endeavour to show the significance of the revolution frequencies of the electrons in these problems, and their connection with the adiabatic frequency. Moreover, the electronic interaction appearing in the polarization is found to be of decisive influence for the dynamics of heavier atoms. A formula with rather general applicability is derived for the energy loss in matter, and more quantitative results are then obtained in § 5. Among the questions there to be treated are the magnitude of the polarization effects and the reduction in energy loss for low velocities of the particle. Finally, the straggling phenomena are discussed briefly in § 6 on similar lines.

§ 2. Stopping by Heavier Substances in a Qualitative Description.

As well known the statistical description of THOMAS and FERMI gives a surprisingly good account of the atomic structure and binding, in particular for electrons in the intermediate region of an atom. In the problem of the energy loss of a particle penetrating through atomic systems this method will seem especially well suited, because the atomic electrons all give comparable contributions to the stopping, so that the total effect is due mainly to the majority of the electrons with medium binding. Neither the individual characteristics of the atoms or molecules, determined by the outer electrons, nor the precise magnitude of the binding of the innermost electrons will be of importance in first approximation.

In the Thomas-Fermi model the electronic density distri-

butions for different atoms are similar, and the common unit of length is proportional to $Z^{-1/3}$. The charge density $e\varrho$ is therefore proportional to Z^2, and the total binding energy of the atom behaves as $Z^{7/3}$. Since, thus, the binding per electron is proportional to $Z^{4/3}$ the electrons may be said to have velocities proportional to $Z^{2/3}$.

In the present connection we are interested in the dynamics rather than the statics of the atom. When the dynamical treatment is based on the Thomas-Fermi model the motions can be described on classical mechanics, only with due regard to the exclusion principle in the initial state of the system. Suppose now that a small disturbance is set up in the atom. The development in time of this disturbance can be governed by only two kinds of frequencies. Of these, one is the frequency $\omega_0 = (4\pi e^2\varrho/m)^{1/2}$, determined by the densities of mass and charge and corresponding to the classical resonance frequency of an extended gas of charged particles. For heavy atoms the spectrum of classical resonance frequencies ω_0, behaving as $\varrho^{1/2}$, is thus contained in a single distribution with a scale proportional to Z. The second kind of frequencies can be pictured in the following manner. The disturbance will be propagated and at the same time damped with certain velocities, and since all velocities in the static model behave as $Z^{2/3}$ the velocities of propagation and damping must show this dependence on the atomic number. Now, the linear dimensions of the system are proportional to $Z^{-1/3}$, and accordingly the frequencies of damping and revolution are proportional to Z. Thus, we have found that all frequencies entering in the dynamical description show the same dependence on the atomic number. This result was first obtained by Bloch (1933) on the basis of his simplified hydrodynamical model of atomic dynamics.

The general behaviour of the frequencies in the atom may also be accounted for by noting that the unit of time in the Thomas-Fermi model is proportional to Z^{-1}. It follows that in a perturbation treatment, i.e. in the approximation of linear field equations, where one can speak of a set of proper frequencies of the system, these frequencies must behave as Z.

As to the approximations involved in this picture of atomic dynamics, the use of a perturbation treatment was just a charac-

teristic of the stopping problem for fast particles of low charge. Moreover, the description by a classical approximation is appropriate here, partly because we are concerned with a calculation of the screening in distant collisions, where the classical treatment gives the same average result as the quantum mechanical calculations, and partly since we have described the atom by the semi-classical Thomas-Fermi model.

From the above results we can obtain a qualitative picture of the stopping of a heavy particle, with velocity v and charge ze. One may for instance argue as follows. The specific energy loss will always be of the same form as equation (1), i.e. equal to $(4\pi z^2 e^4 ZN/mv^2)$ times a dimensionless function, L, independent of the charge ze of the particle. This function is in Bethe's formula an average over the atomic system of quantities of the characteristic logarithmic type. The logarithms depend on the maximum energy transfer $2mv^2$ —or the corresponding frequency $\omega_{\max} = 2mv^2/\hbar$— and on the transition frequencies in the atomic system. In the semi-classical description of Thomas and Fermi we must thus expect that the only frequencies which can enter in the function L are $\omega_{\max}$ and the atomic frequencies proportional to Z, even when L is no longer of the logarithmic type. The dimensionless function L will therefore depend on Z and v only through the ratio of the frequencies, proportional to Z/v^2, and we can write

$$\frac{1}{N}\cdot\frac{dE}{dR}\cdot\frac{mv^2}{4\pi z^2 e^4 Z} = L = L\left(\frac{v^2}{v_0^2 Z}\right), \tag{3}$$

where the so far unspecified function $L(x)$ is determined by the distribution of the frequencies in the atom. In order to obtain a suitable dimensionless parameter in the function L in (3) we have introduced $v_0 = e^2/\hbar$ as a measure for the velocities. The equation (3), as it stands, is applicable only for non-relativistic velocities, and normally the familiar term $(\log(1 - v^2/c^2) + v^2/c^2)$ must be added on the left hand side of (3) if v is comparable with c.

It is clear from the above deduction that, if the atomic frequencies entering in the description were, for instance, the binding frequencies of the electrons, proportional to $Z^{4/3}$, the function L

would instead depend on the ratio $Z^{4/3}/v^2$. But, as we have seen, the dynamic frequencies in the Thomas-Fermi atom are not of this kind. A quite different question is the limitations of the Thomas-Fermi description, mentioned in the beginning of this paragraph. In the first place, due to the individual variations in the binding of the outermost electrons in the atom, one will expect small fluctuations from one element to another, but on the average the formula should remain valid. We shall return to the problem of these fluctuations in § 5. In the second place, the binding of the innermost electrons is not well accounted for by the Thomas-Fermi model, and the corresponding frequencies do not behave as Z. While the most loosely bound electrons primarily give rise to fluctuations, the presence of the strongly bound electrons imply instead systematic deviations from the dependence of L on the single variable $v^2/v_0^2 Z$. Still, since the individual contributions and the number of these electrons both are small, it is to be expected that they will not have an appreciable influence on the variation of the total stopping with Z and v.

A few simple results may be derived immediately from equation (3). If the velocity v of the particle is large compared with the electronic velocities in the atom, the dependence of the function L on v must be approximately as $\log(v^2)$, as in Bethe's formula (1). Equation (3) then leads to Bloch's formula (2), again with an undetermined value of the constant I_0. In § 5 will be given an approximate estimate of this constant. It may here be noted that the mentioned replacement of Z/v^2 by $Z^{4/3}/v^2$ in L would in this case give a formula deduced by SOMMERFELD (1932), where Z in Bloch's formula (2) is replaced by $Z^{4/3}$, at variance with the measured stopping.

For low velocities of the particle, or values of v comparable with the velocities of the majority of the electrons in the atom, the more strongly bound electrons no longer contribute appreciably to the stopping, and the function L will not behave as in the Bloch formula. In the lower part of this region the specific energy loss is approximately proportional to $1/v$, corresponding to Geiger's formula for the range of α-rays. With this dependence on v it follows from (3) that the energy loss is proportional to $Z^{1/2}$, in fair agreement with the classical rule according to which the stopping behaves as $A^{1/2}$. We shall presently give a more quanti-

tative discussion of the region of low velocities on the basis of recent measurements.

The above-mentioned reduction in the contribution of the strongly bound electrons has been discussed by BETHE from a somewhat different point of view. For velocities comparable with the electron velocities in the K-shell BETHE estimates the decrease in stopping due to these electrons (BETHE and LIVINGSTON (1937), BROWN (1950), WALSKE (1952)). This correction sets in at quite high velocities of the particle, and changes initially only rather slowly with velocity. It will therefore seem that a separate correction for the K-shell is a somewhat doubtful procedure, and it is of course not in line with the statistical treatment of the atom. Although further corrections for the L-shell and even higher states can be made, such an attack becomes highly complicated.

For extremely low velocities, as in the case of canal rays, the present description no longer applies. This is partly because there is a high probability that the particle will carry an electron when its velocity is of the order of that of an electron bound to it in the ground state, and partly because the stopping is then mainly due to the outermost electrons which do not follow the statistical model. The deviations set in for values of x somewhat lower than 1, depending on the substance and the charge of the penetrating particle. For values of x of the order z^2/Z the deviations are expected to be considerable.

Instead of the above formulation where L in (3) is a function only of v^2/Z, one might say that the specific energy loss itself is a function of v^2/Z, because dE/dR differs from L only by a factor proportional to Z/v^2. This formulation can be useful, but it is no longer valid when relativistic corrections set in. Moreover, if one wants to study the empirical justification of a picture of the kind suggested here, it is a better criterion to plot L, which function will show more clearly the presence of small deviations from the picture.

As to the range of the particle we may similarly write, for not too high energies,

$$R = \frac{M}{m} \cdot \frac{Z}{z^2} \cdot \frac{1}{8\pi a_0^2 N} \cdot f\left(\frac{v^2}{v_0^2 Z}\right), \tag{4}$$

where R is the range, M the mass of the particle, and a_0 the radius of the hydrogen atom. The function $f(x)$ is connected with $L(x)$ by

$$f(x) = \int_0^x \frac{x'\,dx'}{L(x')}. \tag{5}$$

For higher velocities the relativistic corrections of magnitude about v^2/c^2 destroy the validity of (4); these corrections are primarily due to the kinetic energy being no longer $\frac{1}{2}Mv^2$. One might then attempt a more precise formulation in analogy to (3), but unfortunately this is not feasible on the same simple lines.

The formula (4) applies strictly for range differences only. The above-mentioned deviations from the description of stopping for extremely low velocities imply the presence of very small differences in range, depending on the substance and the particle. These differences we shall call differences in excess range, and their values will be found in § 3.

§ 3. Comparison with Experiments.

Let us compare the formula (3) with experimental data available at present. In Fig. 1 we have plotted $L(x)$ as a function of the variable $x = (v/v_0)^2 \cdot Z^{-1}$, using a number of absolute measurements of the stopping of protons of energy between 1—200 keV and 340 MeV, for metals ranging from uranium to the extreme case of beryllium. The values of $L(x)$ are obtained by introducing the measured stopping on the left hand side of (3), and afterwards adding the relativistic correction if the velocity is high. As mentioned no correction should be made for the K-shell. The points on the figure are based on measurements of specific energy loss of protons, performed by the following authors: Bakker and Segrè (1951), Mather and Segrè (1951), 340 MeV. Sachs and Richardson (1951), 18 MeV. Warshaw (1949), 100–300 keV. Madsen (1953), 0.2–2 MeV. See, further, the note on page 14.

The points in Fig. 1 appear to give a rather well-defined curve. The fluctuations around the average are small, as was to be expected. In the present connection it is more significant that the different groups of elements, arranged according to atomic number, do not show a tendency to separate out into consecutive curves. The points for Be should of course not properly be included in this comparison based on the statistical model.

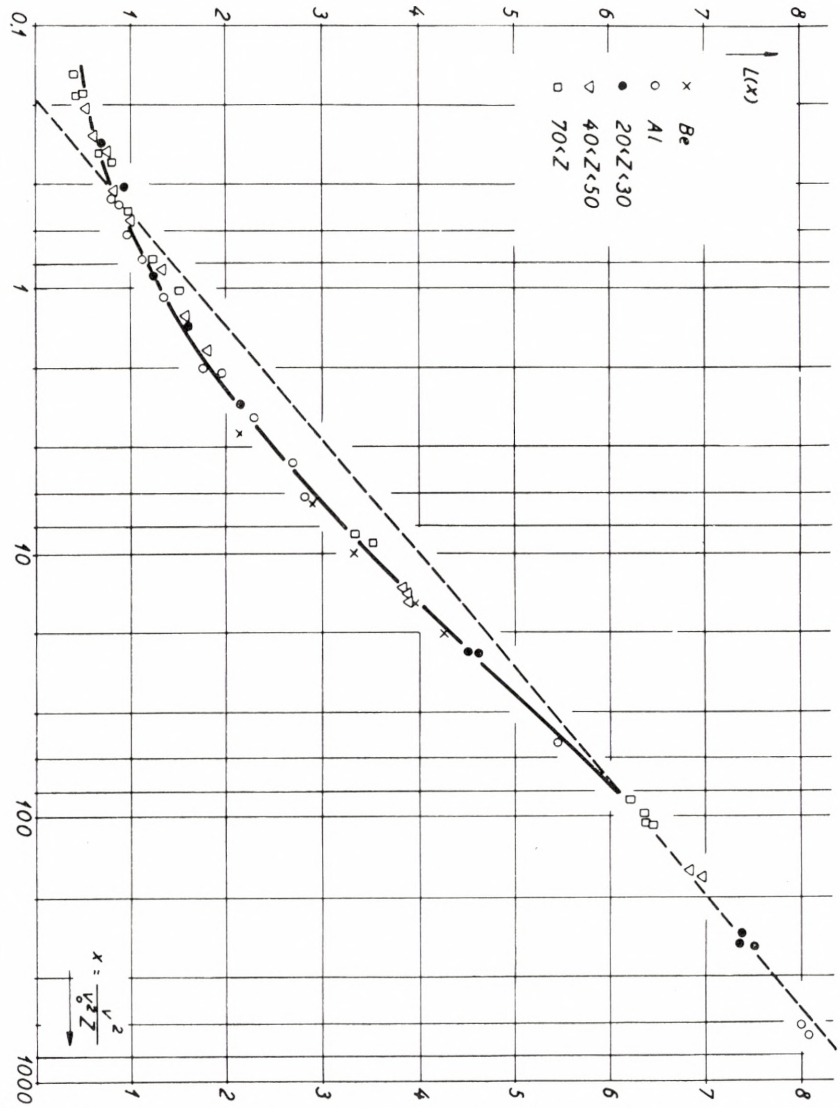

Fig. 1. Comparison between experiments on stopping power according to the statistical treatment. The points represent experimental values, for metals, of the quantity L given by equ. (3). The abscissa is the variable x, in a logarithmic scale. The dotted straight line gives the inclination in Bloch's asymptotic formula, and it corresponds to $I_0 = 10$ eV.

In order to cover a wide range of x-values we have used a logarithmic scale for the abscissa in Fig. 1. This has the advantage that points with the same value of $I_0 = I/Z$ lie on a straight line. The common inclination of such lines is given

by the dotted line on the figure, which corresponds to $I_0 = 10$ eV. For high values of x, i.e. high velocities, it is seen that Bloch's formula with constant I_0 has approximate validity. The value of I_0 thus obtained is about 10 eV, determined essentially by the measurements of BAKKER and SEGRÈ, and of MATHER and SEGRÈ. For decreasing values of x the curve dips gradually towards

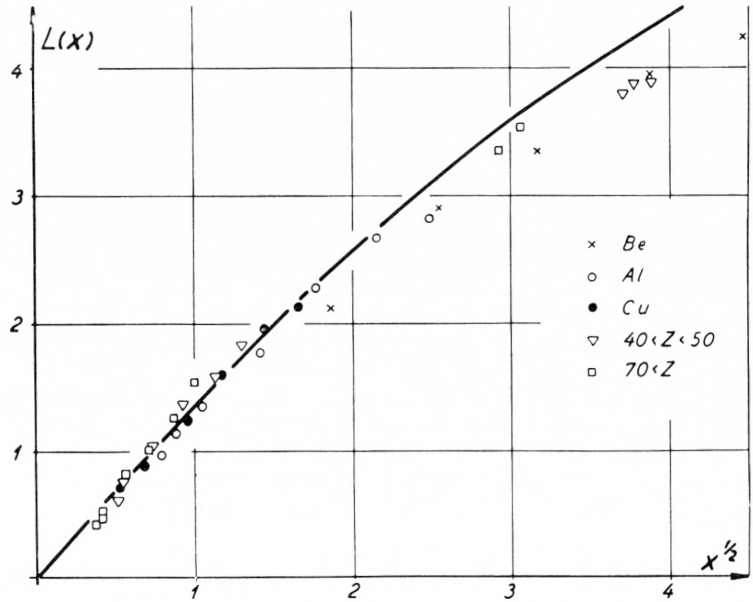

Fig. 2. Comparison between experiments according to the statistical treatment, for low values of $x = v^2/Zv_0^2$. As abscissa is used $x^{1/2}$. The curve represents formula (11), to be discussed in § 5.

higher values of $I = I(v)$. When x is about 5 a maximum in I is reached, and this potential is here almost twice as large as for high velocities. Eventually, for x decreasing below 5, the value of I decreases again and passes through the original high velocity value when x is of the order 0.5. It should be mentioned here that for x-values between 1 and 5 the curve shown on the figure lies somewhat below the semi-empirical curve for air given by BETHE and LIVINGSTON (1937).

If one measures the specific energy loss in matter for a particle of a certain velocity it is possible to find the limiting ionization potential at high velocities by multiplying the measured values of I by the proper factor corresponding to the variation of the

potential along the curve in Fig. 1. It is difficult to estimate the accuracy of such a semi-empirical procedure. A correction of this kind has been suggested by SACHS and RICHARDSON (1951), whose measurements cover a considerable part of the curve in Fig. 1. These authors, however, did not emphasize that for lower velocities the correction reaches a maximum, whereupon it decreases again.

The behaviour of the curve for low values of x is more apparent from Fig. 2, covering the interval $0.2 < x < 20$. As abscissa is used $x^{1/2}$, because a v^3-law for the range in this representation gives a straight line through the origin. In the first approximation the points on the figure may be said to correspond to this law, but the resulting curve is curved slightly downwards. This is particularly so for higher x-values. It should be noted that the figure includes quite high particle energies, e.g. 18 MeV protons in Ag, and that the v^3-law has been suggested only for considerably lower velocities.

The approximate result that the present parameter x even for low velocities collects the experimental points on a single curve was expected from the qualitative considerations in § 2, but its significance will be seen more directly in the discussion in § 5. It is here interesting that, if one uses instead of x the previously mentioned parameter $v^2/Z^{4/3}$, the measurements will separate out into a succession of curves for the different separate elements.

When this paper had been sent to press it came to our notice that KAHN in Chicago has investigated the specific energy loss by protons in Be, Al, mica, Cu, and Au, in the energy interval 0.5–1.3 MeV. His measurements for Be, mica, and Au agree well with MADSEN (1953), whereas for Al and Cu KAHN finds values about 10 to 20 % higher than those of MADSEN, the deviations being largest for Cu. The reason for the discrepancies is, as yet, not known. Further, measurements of the stopping in Cu have been made by COOPER in Ohio, whose results are about 5 % lower than those of KAHN. The x-values involved in the new measurements are 0.6–2 for Cu and 1–4 for Al. Since, in the region around $x = 1$ on Figs. 1 and 2, the points for Au and Ag are somewhat higher than those for Al and Cu, a possible increase in the latter values should not impair the description by a single function depending only on x. However, for $x < 6$ the deviation from the straight Bloch line on Fig. 1 would be less, and the curve would lie closer to that for air. The maximum deviation from the Bloch line would not be changed

essentially, but instead occur at a somewhat higher value of x ($x \sim 10$). The above-mentioned discrepancies may serve to emphasize the uncertainties prevailing in present determinations of energy loss, excepting, perhaps, energy loss in air and in photographic plates.

The measurements shown in Figs. 1 and 2 refer only to the specific energy loss in metals. As regards other substances—and in particular gases—the evidence is mostly relative measurements of ranges, or differences in range. The range observations even have the advantage of being more accurate than direct measurements of the specific energy loss. These two cannot immediately be compared, but instead a separate discussion of the ranges may be made. We shall therefore attempt to plot ranges as a function of the single variable x, in the manner prescribed by equation (4). As mentioned in § 2, this method of comparing ranges can only be applied in the non-relativistic region. There is another difference from the treatment of specific energy loss, because in the very last part of the range the stopping will no longer show the common behaviour assumed above. Even though the resulting range deviations are small they must be taken into account in an accurate representation of the data.

The procedure used in obtaining a range curve is now the following. The measured ranges in mg/cm² are according to equation (4) multiplied by the factor $(1/AZ)\cdot(z^2M_p/M)$, where M_p is the mass of the proton, and M that of the particle. This will, apart from a constant factor, correspond to finding the quantity f on the right side of equation (4). As a first approximation the results are plotted as a function of the variable x. One finds roughly a common curve, but the sets of points for the separate elements will not precisely follow the trend of the common curve. There will be deviations which are significant only for the shortest range values. We then try to subtract a small individual amount—call it the excess range—from the ranges in order to obtain a curve on which all the measurements are collected. This amount will depend both on the substance and on the charge of the particle. The excess ranges are then so far determined apart from a common additive constant, the fixation of which is given below. The resulting points are shown in Fig. 3 in a double logarithmic scale, together with the values of the excess ranges. We have employed the extensive measurements by

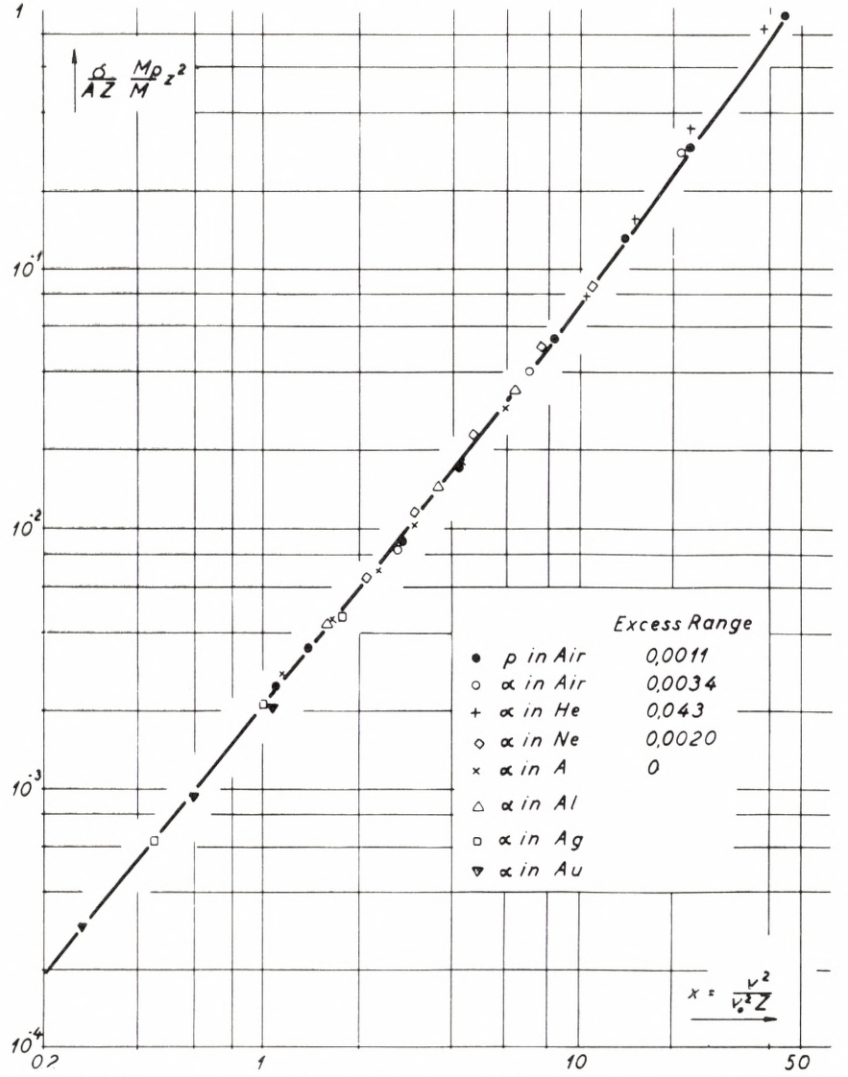

Fig. 3. Ranges plotted according to the statistical formula (4). The ordinate gives, in a logarithmic scale, ranges in mg/cm² multiplied by $(1/AZ)\cdot(z^2 M_p/M)$. The ranges used are experimental ranges minus the excess ranges (see text). The full-line curve was obtained by integration of the averaged curve in Fig. 1.

Mano (1934) of ranges of natural α-rays in He, air, Ne and A. Further are used the accurate semi-empirical range curves for α-particles and protons in air by Bethe (1950)[1]. Included on the

[1] Recent measurements by Reynolds et al. (cf. Bull. Am. Phys. Soc. **27**, No. 6 (1952)) with protons of low energies appear to deviate somewhat from the curve by Bethe. For higher energies, 2—8 MeV protons, Burcham (1953) has obtained results in good agreement with Bethe.

figure are moreover the measurements by ROSENBLUM (1928) of range differences for α-rays in the metals Al, Ag and Au. From these range differences one does not, of course, obtain the values of the excess ranges. On the figure is included He where the statistical considerations in § 2 do not apply and the average excitation potential is much higher than the value given by the Bloch formula. As seen from the figure, this gas cannot either be made to follow the common curve for higher values of the variable x. For air the charge value $Z = 7.22$ can be used, since the expressions in question vary only with a low power of Z.

The ranges in Fig. 3 can be compared with the specific energy loss from Figs. 1 and 2. For this purpose we integrate according to equations (4) and (5) the averaged experimental specific energy loss given by the full-line curve in Fig. 1. However, the specific energy loss is not accurately known for x-values below ~ 0.2. We have here made the plausible choice of continuing the curve to the origin by a straight line on Fig. 2. The integration can then be performed, and the resulting curve is shown by the full-line curve in Fig. 3. There is good agreement with the range measurements.

Using the integrated curve we have fixed the additive constant in the excess ranges. This gives the not unreasonable result that the excess range for α-rays is highest in He and vanishes in A. Moreover, the excess ranges are of the order of magnitude to be expected from the previously mentioned effects. For α-rays they are higher than for protons, corresponding to the screening of the charge appearing for higher values of x.

The description in § 2 has thus been found to apply rather well for the average specific energy loss. Similarly, the ranges seem to show mutual agreement on this picture, and further to be consistent with the specific energy loss in metals. But one should not, of course, be deluded as to the accuracy obtained from the procedure used here in discussing the ranges and comparing them with the specific energy losses.

§ 4. Collective and Independent Particle Descriptions.

In the following we shall consider the mechanisms involved in the present problems of atomic dynamics, and discuss the connection between the independent particle and collective de-

scriptions as they appear in statistical models of atoms. For a further justification of the present line of argument, the reader is referred to LINDHARD (1953).

A detailed description of an atom is afforded by the Hartree model, where the wave function of the total system is the product of one-particle wave functions. When the system is disturbed by an external field these wave functions will of course not develop independently in time. Still, since the one-particle wave functions are governed by the same one-particle Hamiltonian, they will automatically remain orthogonal. This has the advantage that the exclusion principle need not be taken into account in the dynamical treatment.

Now, in actual treatments of atomic dynamics, one usually has recourse to the so-called independent particle model. By the independent particle model we shall here understand a description of the system as particles moving independently of each other in a fixed atomic field. This differs from the Hartree description in that the dynamics is governed only by the action of the external forces, the internal forces being regarded as unchanged. It is apparent that in this simplified description too the exclusion principle may be disregarded.

Let us apply the general expression for the average energy loss given by BETHE, where the logarithmic term in equation (1) has the form

$$L = \frac{1}{Z} \sum_{i,k}' f_{ik} \log \frac{2mv^2}{\hbar \omega_{ik}}. \tag{1'}$$

For the present we assume that the velocity of the particle is high compared with the electronic velocities in the atom, and ask for the corresponding limiting value of the average excitation potential I. If we were concerned with only one electron bound in a static potential it would be the spacing between neighbouring quantum states which determined I, equal to $\hbar$ times the effective adiabatic frequency limiting the energy transfer. For high quantum numbers these quantities are then simply given by the frequency of revolution of the electron.

When the Hartree model or the independent particle model is introduced in (1') we may, according to the above, sum over

all final states k for each electron, without regard to the exclusion principle. We can then write, instead of (1′),

$$L = \frac{1}{Z} \sum_i{}' \log \frac{2mv^2}{\hbar\omega_i}, \quad \log \omega_i = \sum_k{}' f_{ik} \log \omega_{ik}, \tag{6}$$

where L contains only one simple summation over frequencies attributed to completely independent electrons. This formulation allows a direct application of correspondence arguments, as for one electron, and in the independent particle model the frequencies ω_i will for high quantum numbers represent essentially the revolution frequencies for the electronic states in question. It is clear that, if one took the same electronic states in the independent particle model as in the Hartree model, the formula would lead to different results in the two instances, on account of the neglect of polarization effects in the former model.

The picture with independently moving electrons is thus characterized by certain frequencies of revolution in the classical limit, and it is based on an analogy with a single electron in a fixed potential. Now, we found in § 2 that the two kinds of frequencies one may imagine in the atom—the classical resonance frequency determined by the interaction, and the frequencies of revolution—behave in the same manner in the statistical description. It even appeared that a distinction between the two was rather artificial in the present dynamical problem. On account of this equivalence of the two kinds of frequencies it seems possible to picture the dynamical behaviour of the atom as being governed only by the interaction and inertia of the electron cloud, instead of by the frequencies of the independent particle model.

In order to appreciate the consequences of the interaction picture we shall first consider the effect of interaction in the simple case of an extended homogeneous electron gas. It has been shown by Kramers (1947) that the specific energy loss by a heavy charged particle in a gas of free electrons at rest is given by

$$\frac{dE}{dR} = \frac{4\pi z^2 e^4}{mv^2} \cdot \varrho \cdot \log \frac{2mv^2}{\hbar\omega_0}, \tag{7}$$

where ϱ is the density of electrons, and $\omega_0 = (4\pi e^2 \varrho/m)^{1/2}$ the classical resonance frequency of the medium.

Equation (7) shows that the frequency determining the adiabatic limit is just ω_0. This result may be obtained directly when considering in more detail the competition between the polarization in the gas and the direct force from the penetrating particle (A. Bohr (1948)). In fact, for a collision with impact parameter p between an electron and the particle, the force on the electron will be approximately ze^2/p^2, and since the collision time is p/v the displacement in space of the electron during the impact must be $(ze^2/mp^2)\cdot(p/v)^2 = ze^2/mv^2$. The electronic displacements give rise to a polarization force $4\pi\varrho ze^4/mv^2$, and accordingly the force from the particle will be compensated by the polarization for an impact parameter $p = v/\omega_0$, from which follows the formula of Kramers.

In this deduction the electrons were supposed to be at rest before the collision. But it can be shown easily that, even for a degenerate gas, the formula (7) remains valid for a penetrating particle of velocity high compared with the velocities of the electrons in the gas. Indeed, we may, as mentioned, neglect the exclusion principle in the calculation of the perturbed motion of the electrons, and it is then seen that the displacements of the individual electrons during the collision will be just as above. We thus find the same adiabatic limit as before, and, since the average energy transfer for a given impact parameter is to the first order independent of the electron velocities, we arrive again at formula (7).

In calculations of the effects of polarization, where one is concerned primarily with large impact parameters, the behaviour of the electrons can be described on classical mechanics when their quantum numbers are sufficiently high. Already from this circumstance it could be foreseen that for a free electron gas the adiabatic limit is determined by the classical resonance frequency, which is the only frequency defined in a classical description of the system.

For lower velocities of the particle the energy loss differs from that given by the equation (7). In the limit for very slow particles, Fermi and Teller (1947) have shown that the energy loss in a degenerate gas is approximately proportional to v. We shall here use a similar estimate by Lindhard (1953), where the logarithmic term per electron, L, is found to be approximately

$$L \approx \frac{1}{20}\left(\frac{2mv^2}{\hbar\omega_0}\right)^{3/2} \qquad (7')$$

instead of the value $L = \log(2mv^2/\hbar\omega_0)$ in (7). The two formulae are to be joined for an argument somewhat larger than ten.

In this discussion of polarization effects we have used the conventional picture of a free electron gas. It may be that this picture does not represent closely an actual extended system of electrons. Still, it does seem to give a sufficient indication of the behaviour to be expected in atomic systems, when combined properly with the corresponding ideas regarding the orbital motions and revolution frequencies of the electrons.

We have seen that for the present purpose the extended electron gas may be described essentially as a compressible classical liquid of a given density of mass and charge. It is clear that, if the density of the system—and consequently also the classical resonance frequency ω_0—varies only slowly in space, we can compute the total stopping of the particle by averaging (7) over space. But if we try to extend this liquid picture to the case of an atom we meet with the apparent difficulty that here the density varies quite rapidly in space. Still, let us tentatively apply the procedure of averaging (7) over the atom. This leads to the following expression for the logarithmic term in the stopping formula

$$L = \frac{1}{Z}\int d^3r \cdot \varrho(r) \log\frac{2mv^2}{\hbar\omega_0}, \qquad (8)$$

where $\omega_0^2 = 4\pi e^2\varrho(r)/m$ varies in space proportionally to the electron density $\varrho(r)$. It is now seen from the structure of formula (8) that it may be expected approximately to account for the stopping by heavier atoms. Indeed, in formula (7) a summation is supposed already to have been made over the distribution in momentum space. When we now average over ordinary space this will correspond to an integration over phase space. More precisely, we can consider (8) as an outcome of the Bethe formula (1′) with generalized oscillator strengths, when the statistical model is applied in a literal manner and only the electronic interaction is included in the dynamics.

In order to illustrate the connection between the two pictures

used above we shall compare them for the case of an extremely simple statistical model of atoms. Let the orbital velocity and radius of the n'th electron in an atom be given by

$$\left.\begin{aligned} a_n &= a_0 \frac{\nu^2}{n}, \\ & \qquad n = 1, 2, \cdots, Z. \\ v_n &= v_0 \frac{n}{\nu}, \end{aligned}\right\} \tag{9}$$

where the effective quantum number ν is supposed to be the same for all the electrons, and equal to a constant, γ, times $Z^{1/3}$. In this description the atoms have the same similarity as in the Thomas-Fermi model, and if γ is slightly less than 1, formula (9) even gives approximately the same density distribution as the Thomas-Fermi model for the major part of the atom. For the n'th electron we now find that the revolution frequency $\omega_n = v_n/a_n = (v_0/a_0)\cdot(n^2/\nu^3)$ is exactly equal to the classical resonance frequency ω_0 for the density given by (9) at the distance a_n from the nucleus. The frequencies ω_i and $\omega_0(r)$ entering in (6) and (8), respectively, are thus the same and the two formulae give equal results.

Thus far, we have treated separately the revolution frequencies of the independent particle model and the classical resonance frequencies. As mentioned, it will seem difficult to distinguish between the two, and it is possible to describe the dynamics of the atom using only one of the two concepts. Nevertheless, for any particular model of the atom the magnitude of the separate contributions of the two frequencies is prescribed. When trying to find the total effect on the stopping we note that the force constants involved will be proportional to the squares of the frequencies. The total effective frequency squared is then the sum of the two squares. Since the two kinds of contributions behave in the same manner we can write

$$L = \frac{1}{Z}\int d^3r \cdot \varrho(r) \log \frac{2mv^2}{\chi \hbar \omega_0}, \tag{8'}$$

where χ is a constant. The value of χ we estimate from the simplified model (9) where ω_n and ω_0 are equal in magnitude. On the basis of this result we assume in the following, for simplicity,

the value $\chi = 2^{1/2}$ for heavier substances. For the very lightest substances, where the polarization in the atom is of minor importance, the quantity χ will be expected to approach the value 1.

The formula (8′), as it stands, should give an account of non-relativistic polarization phenomena in dense substances, and from the deduction of (7) it is clear that the formula will give a fair representation also of the stopping contribution from free electrons. An interesting question is here the effect of damping by resistance, due to random collisions of the freely moving electrons with the lattice. If the collision frequency were comparable with the resonance frequency an essential change would result in the stopping formula. However, in all known cases the collision frequencies are small, and the effects of resistance can be neglected. This circumstance was not recognized by HALPERN and HALL (1948) in their treatment of polarization effects in carbon. The damping introduced by these authors leads to an anomalously high effective value of I in graphite ($\sim$ 190 eV). Their result is at variance with recent measurements (BAKKER and SEGRÈ (1951), $I = 76$ eV).

§ 5. Theoretical Estimates of Stopping Power.

On the basis of equation (8′) we can compute the excitation potential per electron, I_0, in Bloch's formula (2). The results for various atomic models are listed in Table 1. For the constant χ we have chosen the value $2^{1/2}$ introduced above. One finds approximate agreement with the empirical value of the Bloch constant, about 10 eV. The result of the Lenz-Jensen description appears to be a fairly good average of the Hartree model. The value for the Thomas-Fermi model is a little lower; it is characteristic that, while the average binding in the Thomas-Fermi model is closely equal to that in the Lenz-Jensen descrip-

TABLE 1. Values of the Bloch constant $I_0 = I/Z$ (in eV), calculated from (8′) with $\chi = 2^{1/2}$.

	Thomas-Fermi	Lenz-Jensen	Hartree	
			A	atomic Hg
I_0	8.9	10.7	11.0	9.6

tion, averages of the kind (8′) are better represented by the latter model. Regarding the value of I_0 for mercury we note that in the metallic state it will be slightly higher than for free atoms.

The agreement in Table 1 with the empirical values may be regarded as fortuitous, but it gives a useful guidance in the further treatment. The above results apply in the case of particles of velocity so high that the potential I remains velocity-independent. We shall now consider some of the aspects of the rather involved case presented for lower velocities, and in particular treat the simpler question of stopping for the lowest velocities covered by the statistical model, or $0.1 \lesssim x \lesssim 5$. As before, it can be useful to apply the less familiar picture of polarization when estimating the energy loss.

Formulae such as (6) show that I is no longer independent of velocity when the arguments $2mv^2/\hbar\omega_i$ in the logarithmic terms are not large compared with unity. The resulting gradual change in I with velocity may just as well be calculated from the electron gas description corresponding to (7). In this picture the energy loss will be much reduced if $\omega_{\max} = 2mv^2/\hbar$ is of the order ω_0, as seen from (7′). The reduction in the contribution to the energy loss from the individual electrons, or from the different regions in the atom, does not set in at all abruptly, but the summation over electrons with widely different revolution frequencies makes it natural to proceed at first as if the change were abrupt. We then assume that the low frequencies in the atom contribute in the usual manner to the energy loss, while the high frequencies give no contribution, the division between high and low frequencies being given by $\omega_{\max}/C$, where C is a constant. The effect of this cut-off procedure can be seen most directly from the simplified atomic model (9). Indeed, the more refined statistical models of the atom lead in this case essentially to the same result. Using (9) we now sum in (8′) over the frequencies less than $\omega_{\max}/C$ and find

$$L = \frac{(2\gamma)^{3/2} v}{v_0 Z^{1/2}} \cdot \frac{1 + \log C^{1/2}}{C^{1/2}}, \tag{10}$$

where the effective quantum number ν is written as $\gamma \cdot Z^{1/3}$. The specific energy loss thus becomes proportional to $Z^{1/2}/v$, corresponding to the simple law for α-rays mentioned earlier. This

derivation is similar to that used by N. BOHR (1948), equ. (3.5.7), but the resulting formula is somewhat different.

As to the value of the constant of proportionality in (10), we see that it varies only slowly with the cut-off C. The parameter γ is now so adjusted as to give for high velocities the correct value of $I_0 = 10$ eV; this requires $\gamma = 0.71$. We can then compare with the approximate value of L determined from the experiments at low velocities, which lead to $L = 1.35 \cdot x^{1/2}$ (see Fig. 2). The value required for C from this is $C = 5.6$. Such a high value for the cut-off in the energy loss is in line with the discussion by BETHE for hydrogen, or K-shells in general, where the reduction is considerable when v is of the order of the electron velocity, i.e. for a value of the argument in the logarithm much larger than unity.

A similar result is obtained when formula (7′) is applied. In the atomic model (9) the integration is performed over the electrons for which respectively (7) and (7′) are applicable. This gives

$$L = 1.36 \cdot x^{1/2} - 0.016 \cdot x^{3/2}, \qquad (11)$$

and it so happens that formula (11) for lower values of x is in close agreement with the experiments shown in Fig. 2. The full-line curve on the figure represents (11). If one allows for an uncertainty by a factor 2 in (7′) a latitude will result of about 10 % in the formula (11). The formula joins smoothly to the one which applies for high velocities at a value of x equal to 19.

The variation of (11) with x is qualitatively of the kind found on Fig. 1. For increasing x the effective potential defined by $(11) = \log (2mv^2/I)$ increases from low values to a maximum of about 16–17 eV, occurring at $x \sim 5$, and then decreases to 10 eV. The gradual cut-off (7′) is in this respect superior to the abrupt one leading to (10), because it is effective for considerably higher values of x. But even though the initial part of the curve (11) is not wrong the maximum in I is too narrow, and for x between about 6 and 30 the curve should lie somewhat lower.

One might suppose that the shortcomings of formula (11) for higher values of x are due to the defects of the simplified atomic model (9), where the firmest electron bindings are not properly accounted for. One could then attempt to use, e.g., the Lenz-

Jensen model. This leads to a slight improvement for higher velocities, but only part of the experimental deviation from the Bloch formula can be accounted for. For low velocities the Lenz-Jensen description gives even worse agreement with the experiments, which indicates that the good agreement of (11) is somewhat accidental.

We shall not attempt further improvements of the present treatment, which would appear to demand not merely a more detailed picture of the electronic states, but rather a description of the adiabatic effects and the polarization considerably more elaborate than in the present discussion.

Let us return to the question of the calculation of the average excitation potential I in the limit of high velocity of the particle. In the first part of this paragraph we found values of I from various atomic models. As soon as a more detailed atomic description as the Hartree model is used there will appear minor individual deviations from the relation of Bloch (2). This is indicated in Table 1, for argon and atomic mercury. Similar differences occur when the bindings in molecules or solids are taken into account. One can attempt to evaluate such differences on the basis of equation (8′). However, estimates of this kind are not expected to be very accurate, since they involve the most loosely bound electrons in atoms.

In order to see how much the formula (8′) can be in error for the most loosely bound electrons we use it in the case of the lightest elements, where it should be least applicable. We introduce the actual density distributions in the light atoms and find then from (8′) a corresponding potential I. For these substances it will be natural to put $\chi = 1$, because in the dynamics each electron moves in a nearly static atomic field, the separate effects of polarization being small. The results are shown in Table 2, where for molecular hydrogen we have simply put $Z = 1.2$. For helium we have used hydrogen wave functions, with $Z = 1.69$. The valence electrons in metallic lithium are assumed to be distributed with constant density in space. These rough descriptions of the lightest elements will be accurate enough for our purpose.

The approximate correctness of the results in Table 2 and Table 1 seems to indicate that one can estimate the changes ΔI

TABLE 2. Comparison between the measured I (in eV), and the value given by (8′) with $\chi = 1$. The measurements are by MANO (1934), and BAKKER and SEGRÈ (1951).

	Formula (8′)	Bethe's formula	Exp.
$\frac{1}{2}H_2$	16	17.6[2]	15—16
He	37	43	35
solid Li	36	45[1]	34—37

[1] Estimate by A. BOHR (1948).
[2] PLATZMAN (1952) quotes the value 19 eV.

in I due to chemical bindings, or due to deviations from the statistical model for different atoms, by introducing the density changes in formula (8′). The calculated values of ΔI can hardly be more in error than corresponding to the latitude in the values of χ. The changes ΔI, thus obtained, can never become very large, so that only minor deviations from the Bragg rule will occur for a particle of high velocity. We note that this conclusion disagrees with some of the measurements concerning liquid water and water vapour, where considerable deviations from the Bragg rule have been reported (cf. PLATZMAN (1952)).

§ 6. Straggling in Energy Loss and Range.

The straggling in energy loss, or straggling in range, can be calculated in a direct manner when the cross sections for the individual possible energy transfers are known (N. BOHR (1948)). We shall for the present consider only the case where the particle has penetrated a layer of thickness sufficient to ensure that the distribution in energy loss is approximately Gaussian. The average square fluctuation in energy loss then determines the distribution completely, and it is given by the familiar formula

$$\Omega^2 = \langle (dE - \langle dE \rangle)^2 \rangle = NdR \sum_i T_i^2 \sigma_i, \tag{12}$$

where σ_i is the cross section for energy loss T_i. The contributions to the straggling are thus weighted towards the close collisions, and the effect becomes independent of the screening

in the distant collisions if the velocity v is large. For a fast particle the cross section for energy transfer T in close collisions is

$$d\sigma = \frac{2\pi z^2 e^4}{mv^2} \cdot \frac{dT}{T^2}\left(1 - \beta^2 \frac{T}{T_{\max}}\right), \tag{13}$$

where relativistic effects are included, and $\beta = v/c$. We assume that the particle is so heavy that the maximum energy transfer to an electron is $T_{\max} = 2\,mv^2/(1 - \beta^2)$. The straggling in energy loss is accordingly

$$\Omega^2 = 4\pi z^2 e^4 N \cdot dR \cdot Z \frac{1 - \frac{\beta^2}{2}}{1 - \beta^2}, \tag{14}$$

which leads to an average square fluctuation in range given by

$$(\Delta R)^2 = 4\pi z^2 e^4 NZ \int_0^E \left(\frac{dE'}{dR'}\right)^{-3} \frac{1 - \frac{\beta^2}{2}}{1 - \beta^2}\, dE', \tag{15}$$

where $\beta = \beta(E')$.

For lower velocities the problem is more involved and, as for the average energy loss, one will expect that the more strongly bound electrons give reduced contributions. The discussion here is in line with that in the preceding paragraphs, but of a more qualitative kind. Of course, the same holds for the measurements where the straggling cannot be determined as accurately as the range or specific energy loss.

While the absolute value of the straggling per unit path is a constant for high, but non-relativistic, velocities it will for lower velocities decrease towards zero. Since this is true for each separate frequency in the atom, one may introduce a cut-off for a suitable value of $2\,mv^2/\hbar\omega_0$, and in this way estimate the straggling in collisions with atoms. The important question is then the place at which the reduction sets in. This can be estimated by taking, for instance, the result for the case of a free gas. It is here convenient to quote the value of the straggling relative to the energy loss, which quantity is a measure for the magnitudes of the energy transfers in the collisions. For a free Fermi gas of high density one finds roughly, in the limit of low velocities (Lindhard (1953)),

$$\frac{\Omega^2}{dE} = v\,(5\,m\hbar\omega_0)^{1/2}, \tag{16}$$

corresponding to an effective cut-off at about $2\,mv^2/\hbar\omega_0 \cong 3$.

In collisions with atoms sufficiently heavy for the statistical model to apply, the relative straggling is according to (16) of the form

$$\frac{\Omega^2}{EdE} = \frac{m}{M}\cdot u\,(x), \tag{17}$$

where M is the mass of the particle. When integrating over the atom, using the formulae (14) and (16) in the atomic model (9), it is found that for low values of x the function u tends to a constant value, given approximately by

$$u(x) \cong 1, \qquad x \lesssim 3. \tag{17'}$$

This result for the relative straggling coincides with that found by N. Bohr (1948). For higher velocities the straggling approaches smoothly the value given by (14), and one may write

$$u\,(x) = \frac{2}{L\,(x)}\,, \tag{17''}$$

where the formula holds when relativistic corrections can be neglected.

The straggling in range for lower velocities can be found directly from (17'). We obtain here

$$\frac{(\Delta R)^2}{R^2} = \frac{3}{4}\frac{m}{M}, \qquad x \lesssim 5. \tag{18}$$

For higher values of x one can derive from (15) the approximate formula (cf. N. Bohr (1948), equ. (5.2.7))

$$\frac{(\Delta R)^2}{R^2} = \frac{2}{L\,(x)}\frac{m}{M}\left(1 - \frac{2}{5}\frac{v^2}{c^2}\right), \tag{19}$$

where terms in v/c are included up to second order. The simple formula (19) is not much in error for proton energies even as high as those used in the measurements of Mather and Segrè (1951). It should be mentioned that these authors employed an

essentially non-relativistic formula for the straggling in range, different from (15) and (19).

The measurements of straggling in energy loss are mainly in the region of high values of x. As regards a comparison with experiments for cases where also smaller values of x enter, and equation (17′) should apply, the reader is referred to a recent publication by C. B. MADSEN (1953).

We are much indebted to Professor N. BOHR and M. Sc. A. BOHR for numerous enlightening discussions and comments on the subject of the present paper. Dr. C. B. MADSEN has kindly placed at our disposal the results of his experiments before publication, which has been of great value in this investigation. Further, we wish to thank Mr. KNUD H. HANSEN for help with numerical calculations.

Institute for Theoretical Physics,
University of Copenhagen,
Denmark.

References.

Bakker and Segrè (1951), Phys. Rev. **81**, 489.
Bethe (1930), Ann. d. Phys. **5**, 325.
Bethe and Livingston (1937), Revs. Mod. Phys. **9**, 245.
Bethe (1950), Revs. Mod. Phys. **22**, 213.
Bethe and Walske (1951), Phys. Rev. **83**, 457.
Bloch (1933), ZS. f. Phys. **81**, 363.
Bohr, A. (1948), Dan. Mat. Fys. Medd. **24**, no. 19.
Bohr, N. (1948), Dan. Mat. Fys. Medd. **18**, no. 8.
Brown (1950), Phys. Rev. **79**, 297.
Burcham (1953), Phil. Mag. (7) **44**, 211.
Fermi (1940), Phys. Rev. **57**, 485.
Fermi and Teller (1947), Phys. Rev. **72**, 399.
Halpern and Hall (1948), Phys. Rev. **73**, 477.
Jensen (1932), ZS. f. Phys. **77**, 722.
— (1937), ZS. f. Phys. **106**, 620.
Kramers (1947), Physica **13**, 401.
Lindhard and Scharff (1952), Phys. Rev. **85**, 1058.
Lindhard (1953), to appear in Dan. Mat. Fys. Medd.
Madsen (1953), Dan. Mat. Fys. Medd. 27, no. 13; see further Madsen and Venkateswarlu, Phys. Rev. **74**, 648 (1948), Madsen and Huus, Phys. Rev. **76**, 323 (1949).
Mano (1934), Annales de Phys. **1**, 407; J. Phys. Radium **5**, 628; Thesis, Paris 1934.
Mather and Segrè (1951), Phys. Rev. **84**, 191.
Platzman (1952), Symposium on Radiobiology, p. 139; J. Wiley and Sons.
Rosenblum (1928), Annales de Phys. **10**, 408.
Sachs and Richardson (1951), Phys. Rev. **83**, 834.
Sommerfeld (1932), ZS. f. Phys. **78**, 283.
Walske (1952), Phys. Rev. **88**, 1283.
Warshaw (1949), Phys. Rev. **76**, 1759.

Indleveret til selskabet den 13. februar 1953.
Færdig fra trykkeriet den 24 juni 1953.

Det Kongelige Danske Videnskabernes Selskab
Matematisk-fysiske Meddelelser, bind **27**, nr. 16

Dan. Mat. Fys. Medd. **27**, no. 16 (1953)

COLLECTIVE AND INDIVIDUAL-PARTICLE ASPECTS OF NUCLEAR STRUCTURE

BY

AAGE BOHR AND BEN R. MOTTELSON

København
i kommission hos Ejnar Munksgaard
1953

CONTENTS

INDEX OF TABLES

INDEX OF FIGURES

I. Introduction.

Great progress has been achieved in recent years in the exploration of nuclear properties, and an extensive body of data is now available, giving information on many aspects of nuclear structure.

Strong evidence has been accumulated that the nucleons may be considered as occupying states of binding characteristic of independent particle motion in the averaged nuclear field. This recognition has led to the development of a nuclear shell model, which exhibits many similarities with the description of atomic constitution (MAYER, 1950; HAXEL, JENSEN and SUESS, 1950, 1952). The shell model has been an important guide in the interpretation of nuclear phenomena; besides the numerous features of the nuclear systematics associated with the discontinuities of binding energies at closed shells, the model especially explains many regularities of nuclear spins and parities.

There are, however, also essential differences between atomic and nuclear structures, arising from the fact that the nuclear field is generated by the nucleons themselves, while the atomic field, responsible for the electronic binding, is largely governed by the attraction from the central nucleus. The large mass of the atomic nucleus, as compared with the electrons, makes it possible to a first approximation to treat the atomic field as a static quantity, but, in the nuclear case, the dynamic aspects of the field, associated with collective oscillations of the structure as a whole, must be expected to play an essential role. The significance of collective features in a system where the cohesion is a result of the mutual attraction of the particles has earlier found expression in the liquid drop nuclear model (N. BOHR, 1936; N. BOHR and F. KALCKAR, 1937).

The importance of taking into account the collective aspects of the nuclear structure is clearly evidenced in the empirical

data, and ordered types of motion of the nucleons are strikingly exhibited by a number of phenomena:

1) The occurrence of the fission reaction, many features of which can be understood on the basis of the liquid drop model (MEITNER and FRISCH, 1939; BOHR and WHEELER, 1940).

2) The large quadrupole moments observed for many nuclei, which in some cases are more than 20 times larger than single-particle estimates (CASIMIR, 1936; TOWNES, FOLEY and LOW, 1949; cf. also Fig. 9 on page 55 below). It has been pointed out by RAINWATER (1950) that the magnitude of the quadrupole moments can be accounted for by the tendency of the particle structure to deform the nuclear surface.

3) The occurrence of nuclear gamma transitions of electric quadrupole type with lifetimes about a hundred times shorter than single-particle estimates (GOLDHABER and SUNYAR, 1951). The existence of collective transitions with such short lifetimes is a characteristic feature of the excitation spectra of strongly deformed nuclei (BOHR and MOTTELSON, 1953).

One is thus led to describe the nucleus as a shell structure capable of performing oscillations in shape and size. These collective oscillations involve variations of the nuclear field and are therefore strongly coupled to the particle motion. The general dynamics of such a coupled system of individual particle motion and collective oscillations has previously been considered*, **. The system exhibits many analogies to molecular structures with the interplay between electronic and nuclear motion.

In the present paper, we consider the further development of such a unified nuclear model incorporating collective and individual-particle features, and pursue its consequences, especially for the nuclear properties pertaining to the ground state and the low energy region of excitation. The available empirical evidence is analyzed in an attempt to ascertain to what extent a comprehensive interpretation is possible on the basis of such a description of the nucleus.

* A. BOHR (1951, 1952). In the following, we refer to sections and equations of the latter paper as (A. § V. 4), (A 39), etc.

** Such a unified description of nuclear structure has also been discussed by HILL and WHEELER (1953) ("the collective nuclear model").

In Chapter II, the formulation of the coupled particle-collective model and its general dynamical features are considered. The subsequent three chapters discuss the properties of nuclear ground states (spins, magnetic moments, and quadrupole moments) which yield information on the nuclear coupling scheme. Chapter VI treats the level structure of the low energy region, resulting from the interplay of the particle and collective types of excitation. Important evidence on the interpretation of nuclear excitations is afforded by the analysis of gamma and beta transitions (Chapters VII and VIII). A summary of main conclusions is given in Chapter IX.

Some details, mostly of a mathematical nature, are deferred to appendices (Ap. I—IV). In Appendix V, a description of nuclear reactions is formulated, which embodies features of single-particle scattering as well as the formation of the compound nucleus, and which assumes the same couplings as those operating in the low energy phenomena. In Appendix VI, a discussion is given of the excitation of nuclei by the electrostatic field of an incident particle, which should be a valuable tool, especially in the study of collective types of excitation.

The present investigation has been carried out at the Institute for Theoretical Physics of the Copenhagen University*, and we have greatly benefited from numerous discussions with members and guests of the Institute, as well as with members of the Theoretical Study Group of CERN (European Council of Nuclear Research), which for the last year has been assembled at the Institute. Especially, we are indebted to Professor NIELS BOHR for his continued interest in this work and for many enlightening discussions on the combination of the evidence on nuclear collective and individual-particle motion in a consistent description of nuclear dynamics. We would also like to acknowledge our many stimulating contacts over a period of years with Professors V. F. WEISSKOPF and J. A. WHEELER, who have given valuable comments on many problems of nuclear structure.

* One of us (B.R.M.) wishes to acknowledge the grant of an A.E.C. postdoctoral fellowship, held during the years 1951—53.

II. The Coupled System of Particles and Collective Oscillations.

a) Formulation of the Model.

i. *Collective coordinates.*

The nuclear collective properties may be described by a set of coordinates α characterizing the spatial distribution of the nucleon density which, in turn, defines the nuclear field. Such collective coordinates are symmetric functions of the individual nucleon coordinates.

For a system with a small compressibility, the collective degrees of freedom which have the lowest energies are associated with deformations in shape with approximate preservation of volume. Assuming the system to have a sharp surface, the normal coordinates of these oscillations would be the expansion parameters $\alpha_{\lambda\mu}$ of the nuclear surface defined by (cf., e. g., (A. 1))

$$R(\vartheta, \varphi) = R_0 \left[1 + \sum_{\lambda\mu} \alpha_{\lambda\mu} Y_{\lambda\mu}(\vartheta, \varphi)\right], \tag{II.1}$$

where R_0 is the equilibrium radius, and $Y_{\lambda\mu}$ the normalized spherical harmonic, of order λ, μ. Such surface oscillations are associated with a collective flow with the same velocity field as for the oscillations of an incompressible classical liquid drop (cf., e. g., (A.31)). This leads to the expression

$$\alpha_{\lambda\mu} = \frac{4\pi}{3A} \sum_{p=1}^{A} \left(\frac{r_p}{R_0}\right)^{\lambda} Y^*_{\lambda\mu}(\vartheta_p, \varphi_p) \tag{II.2}$$

for the collective parameters in terms of the polar coordinates $(r_p, \vartheta_p, \varphi_p)$ of the individual particles.

The nuclear compressibility* implies a non-constant radial

* For estimates of the nuclear compressibility, cf. FEENBERG (1947) and SWIATECKI (1951).

density distribution, and the proper modes can no longer be characterized as pure surface oscillations, but are also accompanied by density changes in the nucleus. The degrees of freedom associated with the compressibility imply that, for a given angular dependence, there is a set of normal oscillations with different radial density variations. The lowest among these has no radial nodes and corresponds, in the limit of vanishing compressibility, to the surface oscillations. This mode is in general the most important for the low energy nuclear properties; its coordinates will be of the form (2)* with some modification of the radial function resulting from the compressibility.

For a small compressibility, one can obtain corrections to the proper oscillations by considering only first order terms in the deviation from a uniform density distribution (FLÜGGE and WOESTE, 1952; WOESTE, 1952). In the case of an essentially non-uniform radial equilibrium distribution, major modifications in the collective properties may be expected.

The existence of two kinds of nucleons implies additional types of oscillations in which neutrons and protons move with respect to each other (GOLDHABER and TELLER, 1948; STEINWEDEL and JENSEN, 1950). These oscillations are of special interest for the nuclear photo-effect but, because of their large frequencies, are in general of lesser importance for the low energy phenomena.

The types of collective motion considered correspond to an irrotational flow of nuclear matter, which is the collective response to variations in the nuclear field. Vorticity effects are already contained in the description of the particle structure for a fixed field and do not occur as collective phenomena provided the independent-particle approximation is adequate to describe this structure. It is also seen that vortex motion cannot be described in terms of parameters, such as the $\alpha_{\lambda\mu}$, which are symmetric functions of the particle coordinates and thus, due to the exclusion principle, cannot in a simple way be separated from the state of the particle structure.**

* A single number refers to an equation in the chapter in which the reference is made.

** For a discussion of the implications of the exclusion principle for the quantum rotations of a quasi-rigid system, cf. TELLER and WHEELER (1938).

ii. *Oscillations of a shell structure.*

The relationship of the particle and collective motion is especially simple if the frequencies ω_p for particle excitation are large compared with the frequencies ω_c of a collective type of motion. The nucleus can then be treated, in analogy to molecules, on the basis of the adiabatic approximation, and the appropriate wave function is of the type

$$\Psi_{n\nu}(x) = \Phi_\nu(\alpha)\,\psi_n(x, \alpha), \tag{II.3}$$

where x represents the coordinates, including spin variables, of all the particles in the nucleus. The wave function $\psi_n(x, \alpha)$, specified by a set of quantum numbers n, is the shell model wave function for a fixed field specified by the parameters α. The wave function $\Phi_\nu(\alpha)$ describes oscillations of the nucleus as a whole, characterized by additional quantum numbers, ν*.

In the approximation $\omega_p \gg \omega_c$ underlying (3), there corresponds to a state n of the particle structure a set of states with different quantum numbers ν, corresponding to a Hamiltonian of the form

$$H_c = T(\alpha) + E_n(\alpha), \tag{II.4}$$

where the potential energy $E_n(\alpha)$ is the energy of the particle structure n, calculated for fixed α. The existence of a collective kinetic energy T is contained in the implicit dependence of the wave function on x through α and may be obtained by writing the nucleon velocity as a sum of a velocity with respect to the nuclear field and a velocity of the collective flow. For small amplitudes of oscillation, T is a quadratic expression in the $\dot{\alpha}$.

If the particle structure prefers spherical symmetry, the deformation energy may be expanded around the equilibrium ($\alpha_{\lambda\mu} = 0$), and the surface Hamiltonian reduces to (cf. A.(2 and 3))

$$H_S = \sum_{\lambda\mu}{}' \left\{ \frac{1}{2} B_\lambda \left| \dot{\alpha}_{\lambda\mu} \right|^2 + \frac{1}{2} C_\lambda \left| \alpha_{\lambda\mu} \right|^2 \right\} \tag{II.5}$$

* A wave function describing the adiabatic oscillation of a shell structure has also been given by HILL and WHEELER (1953; eq. (5)), but this expression appears to differ essentially from (3) above. The procedure employed by these authors of incorporating the collective motion both through the exponential factor involving the velocity potential and in the oscillator function $h(\alpha)$ seems difficult to interpret; it appears that in the resultant wave function, obtained by integration over the α-variable, the function h does not directly represent the probability amplitude for a given deformation.

which represents a set of harmonic oscillators with frequencies

$$\omega_\lambda = \sqrt{\frac{C_\lambda}{B_\lambda}}. \tag{II.6}$$

The coefficient B_λ is associated with the mass transported by the collective flow and depends on the velocity field. For pure surface oscillations described by the coordinates (2), one obtains the classical hydrodynamical expression (cf., e. g., (A. 4)),

$$B_\lambda = \frac{1}{\lambda}\frac{3}{4\pi} A M R_0^2, \tag{II.6a}$$

where M is the nucleon mass. The coefficient C_λ represents the nuclear deformability; one may attempt to estimate C_λ from the empirically determined surface energy and the assumption of a uniform charge distribution. This leads to (cf., e. g., (A. 5))

$$C_\lambda = (\lambda-1)(\lambda+2) R_0^2 S - \frac{3}{2\pi}\frac{\lambda-1}{2\lambda+1}\frac{Z^2 e^2}{R_0} \tag{II.6b}$$

where S is the surface tension and Ze the nuclear charge. The analysis of nuclear binding energies leads to the estimate $4\pi R_0^2 S = 15.4\ A^{2/3}$ MeV (cf. ROSENFELD, 1948, p. 24).

While the form of (5) has a rather general validity, it must be stressed that the analogy with the hydrodynamics of a classical liquid drop is of limited scope, and characteristic effects of the quantum structure of the nucleus are to be expected. Thus, the deformability will depend on the particle state in question* and the value of C_λ will be especially large for closed-shell nuclei which owe their particular stability to their spherical form.** The nuclear compressibility may also have an important effect on the value of B_λ and on the relation (2) between $\alpha_{\lambda\mu}$ and the multipole moments.

When, in the following, we often make numerical estimates on the basis of the hydrodynamic approximation (2, 6a and 6b), it will be in order to gain a first orientation and to have a convenient reference with which to compare the evidence on the

* Features of the deformability of a quantum shell structure have been discussed by GALLONE and SALVETTI (1953) and by HILL and WHEELER (1953). Some comments on this problem from the point of view of the present formulation are given in Appendix I.

** We are indebted to Dr. W. J. SWIATECKI for valuable suggestions concerning this point.

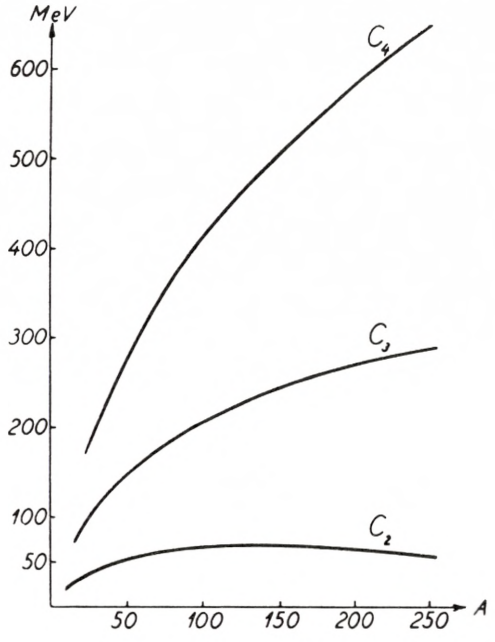

Fig. 1.

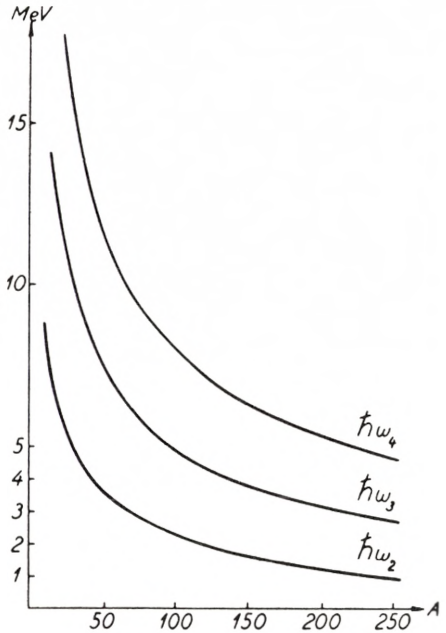

Fig. 2.

Fig. 1. *Nuclear deformability in the hydrodynamic approximation.* The deformability coefficients C_λ of the first three proper modes of the surface (cf. (5); $\lambda = 2$, 3, and 4) are plotted as a function of the atomic number A. The nuclear deformation energy is assumed to arise from a surface tension estimated from empirical binding energies and from the influence of a uniformly distributed electric charge (cf. (6b)).

Fig. 2. *Frequencies of surface oscillations in the hydrodynamic approximation.* The phonon energies $\hbar\omega_\lambda$ of the first three proper modes of the surface (cf. (6)) are plotted as a function of the atomic number A. The deformabilities C_λ of Fig. 1 are used, and the mass parameters B_λ are taken from (6a) which assumes a velocity field of the type associated with surface oscillations of an incompressible fluid.

nuclear collective properties deduced from empirical data. In Figs. 1 and 2 are plotted the hydrodynamical values of C_λ and of the phonon energies $\hbar\omega_\lambda$ for an assumed nuclear radius of

$$R_0 = 1.44 \times A^{1/3}\, 10^{-13} \text{ cm}. \tag{II.7}$$

iii. *Coupling to particle motion.*

The simple separation between collective and particle types of excitations, corresponding to stationary states of the type (3), is no longer possible if the particles possess modes of excitation

with frequencies smaller than, or comparable with, the collective frequencies. The particle structure may then be non-adiabatically excited by the collective oscillations, and the nucleus must be described in terms of a coupled system of collective and particle degrees of freedom.

The particle degrees of freedom represent the low frequency modes of excitation of the particle structure, associated with the particles in the last filled levels. The bulk of the nucleons, whose energies are well below the maximum for the occupied levels, manifest themselves at moderate nuclear excitations only through the collective properties of the nucleus.

For the coupled system of surface oscillators, with coordinates $\alpha_{\lambda\mu}$, and particle degrees of freedom, with appropriate coordinates x, the Hamiltonian may be written in the form

$$H = H_S(\alpha_{\lambda\mu}) + H_p(x) + H_{\text{int}}(x, \alpha_{\lambda\mu}), \tag{II.8}$$

where H_S is given by (5) and H_p represents the particle energy for a spherical nucleus. The coupling term H_{int} gives the energy dependence of the particles on the surface deformation.*, **

Expanding H_{int} in powers of $\alpha_{\lambda\mu}$ we get for the first term

$$H_{\text{int}} = -\sum_p k(r_p) \sum_{\lambda\mu} \alpha_{\lambda\mu} Y_{\lambda\mu}(\vartheta_p, \varphi_p), \tag{II.9}$$

where the sum p extends over the particles included in H_p.*** The assumption of a sharp nuclear boundary implies that $k(r_p)$ has the form of a delta function at the surface with matrix elements given by (cf. FEENBERG and HAMMACK, 1951)

$$< nl \,|\, k(r_p) \,|\, n'l' > = V_0 R_0^3 \Re_{nl}(R_0)\, \Re_{n'l'}(R_0), \tag{II.10}$$

where n and l label the radial and orbital angular momentum quantum numbers of the particle with radial wave function $\Re_{nl}$.

* The existence of an important coupling between particle motion and the nuclear deformation, associated with the centrifugal pressure exerted by the particle on the surface, was first recognized by RAINWATER (1950).

** It is interesting to note that a somewhat similar effect has been discussed for the atomic spectra where a small level shift for non-penetrating orbits has been ascribed to a polarization of the atomic core (BORN and HEISENBERG, 1924; cf. also DOUGLAS, 1953).

*** There may also be a contribution to H_{int} from the spin orbit force, but its dependence on $\alpha_{\lambda\mu}$ is more ambiguous (PFIRSCH, 1952; DAVIDSON and FEENBERG, 1953).

The nuclear potential is denoted by V_0. For binding energies in the region 5—10 MeV, the matrix elements of k are approximately independent of n and l and are of the order of 40 MeV, assuming a kinetic energy inside the nucleus of 25 MeV. In the following, we therefore treat k as a constant. If particles are replaced by holes in a closed-shell structure, the sign of k is reversed.

In the following paragraphs, we shall discuss some approximate solutions for the nuclear Hamiltonian (8) for various types of particle configurations. For most physical problems involving low nuclear excitations, the collective motion associated with surface deformations of quadrupole type ($\lambda = 2$) are of primary importance. We especially consider the effect of these deformations and usually drop the index λ.

The coupled system of particles, obeying Fermi statistics, and surface oscillators, which are equivalent to a Boson field, is in many respects analogous to the dynamical system considered, for instance, in electromagnetic theory. The coupling term (9) is of a similar form as in the electrodynamic system, with the coupling constant k playing the role of the charge e. Thus, many effects characteristic of field theories, such as the influence of the field on the motion of a particle in an external potential (Lamb-Retherford effect), the interaction of particles through the intermediate field, etc., have their counterpart in the unified nuclear model. The formal analogies also imply that many methods of solution are common to the two systems.

b) Coupling of Single Particle to Nuclear Surface.

An especially simple case of the coupled system occurs when the particle configuration can be described in terms of a single particle outside of a fairly stable structure of spherical symmetry. In this paragraph, we consider methods of treating this system, appropriate to different strengths of the coupling.

i. *Perturbation approximation.*

For sufficiently weak coupling, the motions of the particle and the surface are approximately independent. The state of the

particle is then characterized by the same quantum numbers as in the shell model. The surface oscillations* are described by the number of phonons, N, each having an angular momentum of two units, the total angular momentum of the surface R, and its z-component m_R. In general, two additional quantum numbers are required to specify completely the state of the surface, but, for small values of $N (N \leq 3)$, the above quantum numbers are sufficient.

The effect of the coupling implies a certain interweaving of particle and surface motion, which for weak coupling is conveniently treated by expanding the wave function in the representation of uncoupled motion**, ***

$$\Psi = |> = \sum_{jNR} |j;\ NR;\ IM> <j;\ NR;\ IM|>, \qquad \text{(II.11)}$$

where j stands for the particle quantum numbers, while the total nuclear angular momentum and its z-component are denoted by I and M.

In the absence of coupling, the ground state is given by $|j;\ 00;\ I = j,\ M>$ and, to first order, H_{int}, which is linear in α_μ (cf. (9)), only introduces the states $|j';\ 12;\ I, M>$, where the particle state j' has the same parity as the state j and differs by at most two units in the total angular momentum. The relevant matrix element for the creation of the one-phonon state is obtained from (9) and (A. § III.1), and is given by

$$\left.\begin{aligned} &<j;\ 00;\ I = j, M \,|\, H_{\text{int}} \,|\, j';\ 12;\ I, M> \\ &\qquad = -k \sqrt{\frac{\hbar\omega}{2C}} <j \,|\, h \,|\, j'> \end{aligned}\right\} \qquad \text{(II.12)}$$

in terms of the coupling constant k, and the surface frequency ω and deformability C. The coefficients $<j \,|\, h \,|\, j'>$ can be expressed in terms of Racah coefficients and are given in Appendix II.

These matrix elements determine to first order the nuclear

* The quantization of free surface waves has been discussed by Nogami (1948), A. Bohr (1952), and Jekeli (1952).

** The coupling between particle motion and surface oscillations has been considered in such a phonon representation by Foldy and Milford (1950).

*** We use the bracket notation of Dirac (1947). The proper vectors are given by $|\ j;\ NR;\ IM>$, while the expansion coefficients are $<j;\ NR;\ IM\,|>$.

wave function from which the various nuclear properties can be obtained. Thus, the coupling leads to a sharing of angular momentum between the particle and the surface, which is reflected in a reduction of the expectation value of j_z. If j remains a constant of the motion, we get

$$<j_z> = \left(1 - \frac{15}{128\,\pi}\,\frac{(2j-1)(2j+3)}{j^2(j+1)^2}\,\frac{k^2}{\hbar\omega C}\right) M. \qquad \text{(II.13)}$$

The more general case in which particle states having a different angular momentum are admixed is considered in Appendix II.

For the following, it will be convenient to introduce the dimensionless parameter

$$x = \sqrt{\frac{5}{16\,\pi}}\,\frac{1}{\sqrt{j}}\,\frac{k}{\sqrt{\hbar\omega C}} \qquad \text{(II.14)}$$

as a measure of the strength of the coupling. From (13) one sees that the validity of the perturbation approximation is essentially determined by the smallness of x. The relevant parameter for the perturbation expansion is actually $x\sqrt{j}$, which represents the order of magnitude of the amplitude of the one-phonon state.

ii. *Strong coupling approximation.*

For $x\sqrt{j} \gtrsim 1$, the perturbation treatment is no longer valid, but for $x \gg 1$ one can obtain another type of approximate solution to the coupled system (A. § V.3).* For such strong couplings, the nuclear surface acquires a large deformation and, therefore, a certain stability in its spatial orientation. One then obtains an approximate solution by considering, first, the relatively fast motion of the particle with respect to the deformed nuclear surface and, subsequently, the relatively slow vibration and rotation of the entire system.**

* Apart from factors involving j, the parameter x corresponds to the ratio of total nuclear deformation to zero point oscillation amplitude used in A to characterize the strength of the coupling (cf., e. g., (II. 22)).

** This solution of the coupled nuclear system is in some respects similar to the strong coupling treatment of the nucleon-meson coupling, the $\vec{j}$ of the particle playing the role of the nucleon spin, or isotopic spin (cf., e. g., Tomonaga, 1946). The nucleon isobars are the analogue of the nuclear rotational states.

The surface will in general acquire an axially symmetric shape under the influence of the centrifugal pressure exerted by the particle. The resulting nuclear coupling scheme (A. Bohr, 1951), illustrated in Fig. 3, is thus analogous to that of linear molecules.

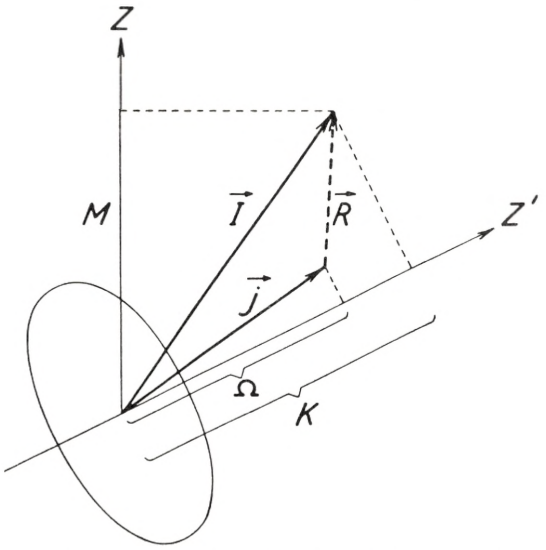

Fig. 3. *Coupling scheme for strong particle-surface interaction.* In strong coupling, the surface acquires an axially symmetric deformation. The angular momentum $\vec{j}$ of the particle precesses around the nuclear axis with a constant projection Ω. The total angular momentum $\vec{I}$ is the sum of $\vec{j}$ and the angular momentum $\vec{R}$ of the surface. The coupled system of particle and surface rotates like a symmetric top with quantum numbers I, K (projection of $\vec{I}$ on nuclear axis), and M (projection of $\vec{I}$ on space fixed axis).

The angular momentum vector $\vec{j}$ of the particle precesses rapidly around the nuclear symmetry axis z' with a constant projection Ω. The nuclear surface performs small vibrations, both with respect to magnitude and shape of the deformation. The rotational motion is like that of a symmetric top and is characterized by the three quantum numbers I, K, and M, representing the total nuclear angular momentum, its projection on the symmetry axis z' and on the fixed z-axis, respectively.

From the analysis which follows, one finds that the particle precession frequency is of order $x^2\omega$, while the vibrational frequencies are of order ω. The rotational frequencies about the

symmetry axis and an axis perpendicular to z' are of order ω and $x^{-2}\omega$, respectively. (Cf. also A. § V.3 and Appendix IV).

The strongly coupled system is conveniently described by introducing the Eulerian angles θ_i specifying a coordinate system fixed in the nucleus, and the two additional surface coordinates β and γ defining the nuclear shape (cf. A. § II.2). The total deformation parameter β is given by

$$\beta^2 = \sum_{\mu} |\alpha_\mu|^2, \tag{II.14a}$$

while γ is an angular coordinate characterizing the eccentricity of the nuclear shape. Thus, for $\gamma = 0$ and π, the deformation is symmetric about the z'-axis, and is of prolate and oblate shape, respectively (cf. A. Fig. 1).

The strong coupling wave function has the form (A. 118)

$$\left.\begin{aligned} &|\Omega;\ n_\beta n_\gamma;\ IKM> \\ &= \sqrt{\frac{2I+1}{16\pi^2}} \cdot \varphi_{n_\beta n_\gamma}(\beta, \gamma) \left\{ \chi_\Omega \mathfrak{D}^I_{MK}(\theta_i) + (-)^{I-j} \chi_{-\Omega} \mathfrak{D}^I_{M-K}(\theta_i) \right\} \end{aligned}\right\} \tag{II.15}$$

where χ_Ω describes the motion of the particle with respect to the deformed nucleus, while $\varphi_{n_\beta, n_\gamma}$ represents vibrations in β and γ characterized by the quantum numbers n_β and n_γ. Finally, the $\mathfrak{D}^I_{MK}$ are the proper functions for the symmetric top, and describe the nuclear rotations. The normalization is such that $\mathfrak{D}$ gives the unitary transformation from the fixed coordinate system to the nuclear coordinate system (cf. WIGNER, 1931). The simultaneous occurrence in (15) of both signs for Ω and K reflects the invariance of the surface with respect to a rotation of 180° about an axis perpendicular to z',* and is similar to the symmetrization of wave functions for homonuclear molecules (cf. HERZBERG, 1950, p. 128 ff.). The symmetrization ensures that the total parity of the strong coupling wave function equals the parity of the particle state. The sign of the symmetrization term in (15) depends on j, and if j is not a good quantum number, each part of χ must be symmetrized with the appropriate sign.

The wave function (15), apart from the symmetrization, is actually of the form (3), corresponding to the fact that the pre-

* Cf. A. § V.2 for a discussion of the symmetry requirements for the strong coupling wave function.

cession frequency of the particle is large compared to the collective frequencies of the system. This contrasts with the weak coupling situation where the degeneracy with respect to spatial orientation of $\vec{j}$ provides a very easily excitable degree of freedom. Thus, (11) is in general not of the type (3).

The sharing of angular momentum between particle and surface approaches a definite limit with the realization of the strong coupling scheme of Fig. 3. The expectation value of $\vec{j}$ is given by

$$<\vec{j}> = \frac{<\vec{j}\cdot\vec{I}>}{I(I+1)}<\vec{I}>, \tag{II.16}$$

and for $\vec{j}\cdot\vec{I}$ we may write

$$\vec{j}\cdot\vec{I} = j_1 I_1 + j_2 I_2 + j_3 I_3, \tag{II.17}$$

where the components of the two vectors refer to the coordinate system fixed in the nucleus. One thus finds, for the state (15),

$$<\vec{j}\cdot\vec{I}> = \Omega K + (-)^{I-j}\frac{1}{2}\left(j+\frac{1}{2}\right)\left(I+\frac{1}{2}\right)\delta_{\Omega,\frac{1}{2}}\,\delta_{K,\frac{1}{2}} \tag{II.18}$$

where the last term arises from the symmetrization and only contributes for $\Omega = K = \frac{1}{2}$ (cf. also DAVIDSON and FEENBERG, 1953). Therefore, from (16),

$$<j_z> = \frac{\Omega K M}{I(I+1)}\left\{1 + (-)^{I-j}\,2\left(j+\frac{1}{2}\right)\left(I+\frac{1}{2}\right)\delta_{\Omega,\frac{1}{2}}\,\delta_{K,\frac{1}{2}}\right\}. \tag{II.19}$$

For the ground state we have $I = K = \Omega$, except for $K = \Omega = \frac{1}{2}$ (cf. below), and thus

$$<j_z> = \frac{I}{I+1}M. \tag{II.20}$$

For each particle state Ω, we have a spectrum of vibrational and rotational states, as in the case of molecules (cf. (3)). The nuclear potential energy is a sum of the surface energy and of the particle energy as a function of the deformation and, if j is a good quantum number, is given by (cf. A. 77 and 98)

$$W_{\text{pot}}(\beta, \gamma) = \left. \begin{aligned} & \\ H_p + \frac{1}{2} C \beta^2 + \sqrt{\frac{5}{4\pi}} k \beta \cos \gamma \frac{1}{4j(j+1)} (3\Omega^2 - j(j+1)), \end{aligned} \right\} \quad \text{(II.21)}$$

where H_p is the particle energy for an undeformed nucleus.

It is seen from (21) that, for $j > 3/2$, the lowest minimum of W_{pot} and, therefore, the lowest state of the nucleus, occurs for $\Omega = j$ and a cylindrically symmetric equilibrium deformation with $\gamma = \pi$ (oblate shape). The equilibrium value of β is given by

$$\beta = \sqrt{\frac{5}{4\pi}} \frac{k}{C} \frac{2j-1}{4(j+1)} = x \sqrt{j} \frac{2j-1}{2(j+1)} \sqrt{\frac{\hbar\omega}{C}} \quad \text{(II.22)}$$

in terms of the coupling parameter x (cf. (14)).

The kinetic energy of the surface motion consists of a vibrational and a rotational part. For strong coupling, the dominant term is the vibrational energy (A. 48)

$$T_{\text{vib}} = -\frac{\hbar^2}{2B} \left\{ \frac{1}{\beta^4} \frac{\partial}{\partial \beta} \beta^4 \frac{\partial}{\partial \beta} + \frac{1}{\beta^2} \frac{1}{\sin 3\gamma} \frac{\partial}{\partial \gamma} \sin 3\gamma \frac{\partial}{\partial \gamma} \right\}. \quad \text{(II.23)}$$

The Hamiltonian obtained by adding (23) to (21) describes oscillations around the equilibrium positions of β and γ (cf. (4)). Since the zero point amplitude of β is of order $(\hbar\omega/C)^{1/2}$, which is small compared to (22) for $x > 1$, one obtains approximately independent harmonic oscillations in the β and γ variables with states labeled by n_β, n_γ.

The rotational energy can be expressed in terms of the angular momentum quantum numbers, and is given by*

$$W_{\text{rot}} = \left. \begin{aligned} & \frac{\hbar^2}{2\Im_3} (K-\Omega)^2 + \left(\frac{\hbar^2}{4\Im_1} + \frac{\hbar^2}{4\Im_2} \right) \left\{ I(I+1) - K^2 \right. \\ & \left. + j(j+1) - \Omega^2 - (-)^{I-j} \left(j + \frac{1}{2} \right) \left(I + \frac{1}{2} \right) \delta_{\Omega, \frac{1}{2}} \delta_{K, \frac{1}{2}} \right\} \end{aligned} \right\} \quad \text{(II.24)}$$

where the moments of inertia are given by (A. 27)

$$\Im_\varkappa = 4B\beta^2 \sin^2 \left(\gamma - \varkappa \frac{2\pi}{3} \right) \qquad \varkappa = 1, 2, 3. \quad \text{(II.25)}$$

* Cf. (A. 98); the last term in (24) arises from U_1 (cf. A. 96) which contributes a diagonal term in the special case of $\Omega = K = 1/2$ (cf. also DAVIDSON and FEENBERG, 1953).

For $\Omega = j$, the lowest rotational state occurs, according to (24), for $I = K = \Omega = j$.

The case of $j = 3/2$ requires special consideration, since the last term in (21) has the same value for $\Omega = 3/2$ and $\gamma = \pi$ as for $\Omega = 1/2$ and $\gamma = 0$. In this case, the potential surface has no pronounced minimum in γ, which has the consequence that there is no exact limiting solution of the type (15). The strong coupling wave function has then a somewhat more complex form and requires the solution of a set of coupled differential equations. Still, it can be shown that the ground state is always $I = 3/2$ (cf. Appendix III.ii).

For $j = 1/2$ there is no coupling between particle and surface. Actually, in this case, the strong coupling wave function (15) reduces to the uncoupled wave function.

The Hamiltonian consisting of the three terms (21), (23), and (24) does not represent the total energy of the nucleus. There are additional terms (cf. A. 96) which are non-diagonal in the representation (15) and which cause the breakdown of the strong coupling solution for $x \lesssim 1$. An estimate of these perturbation terms provides a measure of the accuracy of the strong coupling solution and can be used to obtain correction terms when x has intermediate values (A. § V.4; FORD, 1953; cf. also Appendix III.ii).

The non-spherical character of the nuclear field implies that the j of the particle is not an exact constant of the motion. Major modifications in χ_Ω may occur if there are close-lying single-particle levels which are coupled by the surface. In such cases, χ_Ω may be considered as a superposition of particle states with different j, however all with the same Ω. The last term in the potential energy (21) is then to be replaced by (cf. (9) and (A.12))

$$W_{\text{coupl}} = -k\beta \cos\gamma Y_0(\vartheta'), \tag{II.26}$$

which is a non-diagonal matrix in the particle quantum numbers j whose elements are given in Appendix III.i. The coordinate ϑ' of the particle is referred to the nuclear z'-axis. The rotational energy remains of the form (24), which is diagonal in j.

The potential energy matrix must now be diagonalized and its proper values determined as a function of the deformation.

The minimum of the lowest potential energy surface corresponds to the ground state equilibrium and the ground state χ_Ω is determined as the proper vector of W at equilibrium.

Such effects are of importance in causing a partial decoupling of the particle $\vec{l}$ and $\vec{s}$ and also occur in regions where there are near-lying levels of the same parity (e. g. $s_{1/2}-d_{3/2}$; $p_{3/2}-f_{5/2}$). In the case of $j = 1/2$ states, the non-diagonal terms are of special interest in making possible a strong coupling to the surface. Calculations of this type are employed in particular in the Addendum to Chapters IV and V.

iii. *Intermediate coupling.*

The treatments of the coupled system discussed above apply in the limiting cases of weak and strong coupling. It is of interest, however, to follow the transition between the two coupling regions. This is of special importance for large j, since the perturbation approximation is valid for $x\sqrt{j} \ll 1$, while the strong coupling approximation demands $x \gg 1$. This gap between the regions of validity of the two solutions reflects the increasing number of phonons necessary to achieve the strong coupling situation for increasing j.

In the intermediate coupling region, one may employ the weak coupling representation (11), carrying the expansion sufficiently far to give an adequate representation of the nuclear state. The determination of the coefficients of the wave function requires the solution of the corresponding secular determinant.*

As an illustration of this procedure, the solution has been worked out for the case of $I = j = 3/2$, including all states with phonon number N up to 4. The expansion coefficients are plotted in Fig. 4 as a function of x.**

Further information about the intermediate coupling region can be obtained by considering the case of very large j for which one can obtain a semi-classical solution valid for all x. (Cf. Appendix IV). From this solution, one can calculate (Ap. IV.10)

* Cf. the non-adiabatic treatment of the meson-nucleon system discussed by TAMM (1945) and DANCOFF (1950).

** Note added in proof: The intermediate coupling treatment, based on the uncoupled representation, has been extended by D. C. CHOUDHURY (cf. forthcoming publication), who has studied level structures, as well as magnetic moments and quadrupole moments, for a number of configurations.

$$< j_z > = \left(1 - \frac{1}{I+1} \frac{x^2}{\sqrt{x^4 + 4/9}}\right) M \qquad \text{(II.27)}$$

correct to terms of order M/I. To this order, (27) coincides for small x with the perturbation result (13); for large x, the value of (27) equals the strong coupling result (20).

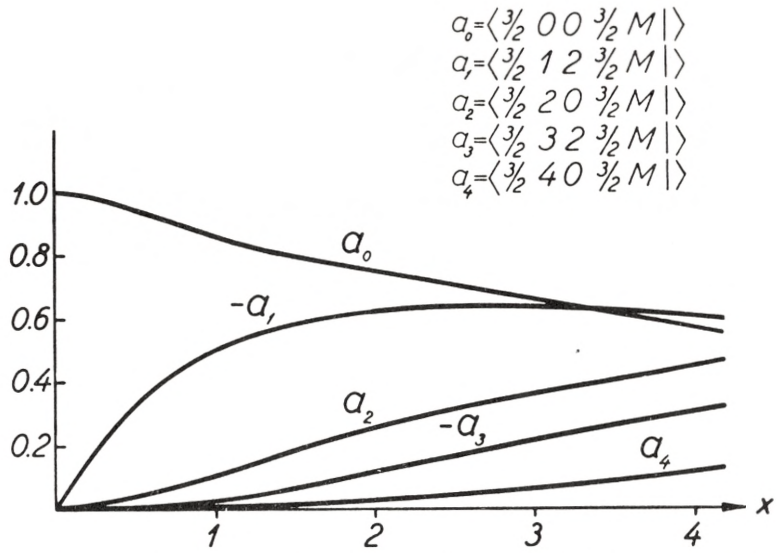

Fig. 4. *Wave function in intermediate coupling for* $I = j = 3/2$. The wave function for the ground state ($I = 3/2$) of the system consisting of a $j = 3/2$ particle coupled to the nuclear surface oscillations is expanded in the representation of uncoupled motion (11). The Hamiltonian is diagonalized including all states with up to four phonons, and the probability amplitudes are plotted as functions of the coupling parameter x (cf. (14)). In the particular case considered, only a single state occurs for each value of the phonon number.

The process of transfer of angular momentum to the surface, as a function of x, is illustrated in Fig. 5 for the various solutions considered in this chapter.

In the hydrodynamic approximation (cf. Figs. 1 and 2), one obtains from (14), assuming $k = 40$ MeV, a coupling strength of $x = 0.9\, j^{-1/2}$ for $A = 20$ increasing rather slowly with A to a value of $x = 1.4\, j^{-1/2}$ for $A = 200$. From Fig. 5 one sees that this would correspond to an intermediate region in which neither the perturbation nor the strong coupling approximation would be very reliable.* Besides the contribution of H_{int} that is diagonal

* Similar conclusions have been drawn (Davidson and Feenberg, 1953;

in j, there is also in general a contribution to the coupling energy from the interaction between states of different j. In some cases, this latter coupling may considerably increase the effective value of x.

For a single particle moving with respect to a closed-shell core of great stability, the expected large value of C, as compared with the hydrodynamic estimate (cf. § II a.ii and Ap. I), may

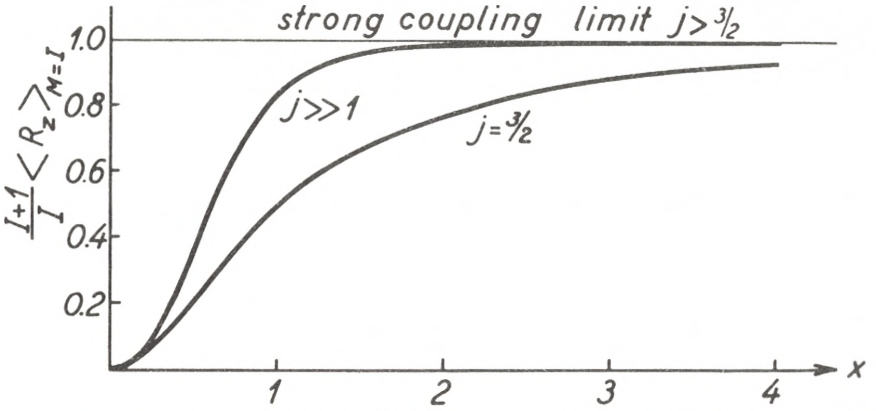

Fig. 5. *Sharing of angular momentum between particle and surface motion.* The particle-surface coupling implies a transfer of angular momentum from the particle motion to the surface oscillators, which, in the limit of strong coupling, approaches the value (20) for $j > 3/2$. For $j = 3/2$, the limiting ordinate in the figure is somewhat in excess of unity (cf. Ap. III.8). The gradual transfer of angular momentum as a function of the coupling parameter x (14) is shown for the case of $j = 3/2$ (obtained from Fig. 4) and $j \gg 1$ (cf. (27) and Ap. IV).

lead to a considerable reduction in the value of x. In such a situation, the particle-surface coupling may have only a minor effect on the properties of the system.

c) Many-Particle Configurations.

In the case of configurations involving several particles, the coupled system can be treated by methods similar to those discussed in the previous paragraph. While the surface coupling effects considered there may be described as nucleon self-energy

Ford, 1953) from a comparison of the proper values of the strong coupling Hamiltonian with those of the uncoupled system. In the procedure employed, however, corrections to the vibrational energy (A. 108 and 113) of the same order as the rotational energies have been neglected. If these are included, the comparison is somewhat more favourable to the strong coupling solution.

effects arising from the coupling to the phonon field, this coupling also produces mutual interactions between particles.

An additional feature which may affect the coupling scheme arises from the nuclear forces acting between the particles. The resultant coupling scheme will in general depend on a competition between the two effects. We first consider the surface coupling in the absence of direct forces between the particles.

i. *Weak surface coupling.*

For sufficiently weak coupling, one can employ the usual perturbation procedure of field theory to obtain effective two-particle interactions, resulting from the surface coupling. These interactions remove the degeneracy of many-particle configurations and may thus be important in determining the ground state spin.

If j_1 and j_2 of the particles are constants of motion, one may use a simplified form of H_{int} in terms of the operators $\vec{j}_1$ and $\vec{j}_2$ (A. 76, 77, 78), and one finds the two-body potential

$$\left.\begin{aligned} V(1,2) = -\frac{5}{64\pi}\frac{k^2}{C}\frac{1}{j_1(j_1+1)\,j_2(j_2+1)}\,[6(\vec{j}_1\vec{j}_2)^2 \\ +3(\vec{j}_1\vec{j}_2)-2j_1(j_1+1)\,j_2(j_2+1)]\,. \end{aligned}\right\} \quad \text{(II.28)}$$

More general expressions may be derived if the surface introduces states with other j values. The interaction (28) is of the type well known from quadrupole couplings in atoms and molecules and is attractive if the two particles have parallel or antiparallel angular momenta and repulsive for perpendicular orientations. Since the coupling constant for a hole has opposite sign to that for a particle, two holes interact as given by (28), while a particle and a hole have an interaction with opposite sign.

ii. *Strong surface coupling.*

For increasing coupling strengths, one obtains more complicated two-body interactions in addition to many-particle interactions. However, for strong coupling, the surface effect again becomes simple if viewed in the appropriate coordinate system. Under the combined action of the particles, the surface in general

acquires an equilibrium deformation of cylindrically symmetric character*; and, relatively to the deformed nucleus, the particles move independently of each other as long as the direct nuclear forces can be neglected.**

The wave function is of the type (15), where the particle state χ_Ω now stands for an appropriately antisymmetrized product of individual particle wave functions, each characterized by a quantum number Ω_p. The total Ω equals the sum of the individual Ω_p (cf. Fig. 6a). The symmetrization of the wave function follows the same lines as (15), except that the exponent j in the phase of the symmetrization term is replaced by $\sum_p j_p$.

Corresponding to (21) and (26), the potential energy is given by

$$W_{\text{pot}}(\beta, \gamma) = \sum_p H_p + \frac{1}{2} C \beta^2 - \beta \cos \gamma \sum_p k_p Y_0(\vartheta'_p). \qquad \text{(II.29)}$$

If not only the Ω_p, but also the j_p, are good quantum numbers, simpler interaction terms of the type used in (21) replace the last term in (29).

We first consider a group of n equivalent particles with a definite j. If n is smaller than half the number of states in the shell, the equilibrium shape of the nucleus has $\gamma = \pi$. The part-

* In special cases, an asymmetric equilibrium deformation may be favoured, or the potential energy surface may have no pronounced minimum in γ. The quantities Ω_p and K are then no longer constants of the motion, and a more complex rotational spectrum arises (cf. the case of asymmetric molecules; cf. also Ap. III.ii).

** The strong coupling solution for many-particle configurations has also been considered by FORD (1953).

Fig. 6. *Coupling schemes for many-particle configurations.* In many-particle configurations, the coupling scheme results from a competition between surface coupling and particle forces. Two extreme cases are shown.

a) Surface coupling dominates over particle forces. The particles move independently of each other in the deformed nucleus, each having a constant component Ω_p of angular momentum along the symmetry axis. The total Ω equals $\sum_p \Omega_p$ and the nuclear ground state has $I = K = \Omega$. The figure illustrates the coupling scheme for a $(j)^3$ configuration. The three lowest particle states have $\Omega_p = j, -j, j-1$, leading to $I = \Omega = j - 1$.

b) Particle forces dominate over surface coupling. The particles are coupled to a resultant $\vec{J}$ which is then coupled to the surface as a single particle (cf. Fig. 3). The figure refers to a $(j)^3$ configuration, where the particle forces in general favour the state $J = j$ (cf. p. 34). The resultant ground state has $I = \Omega = J = j$.

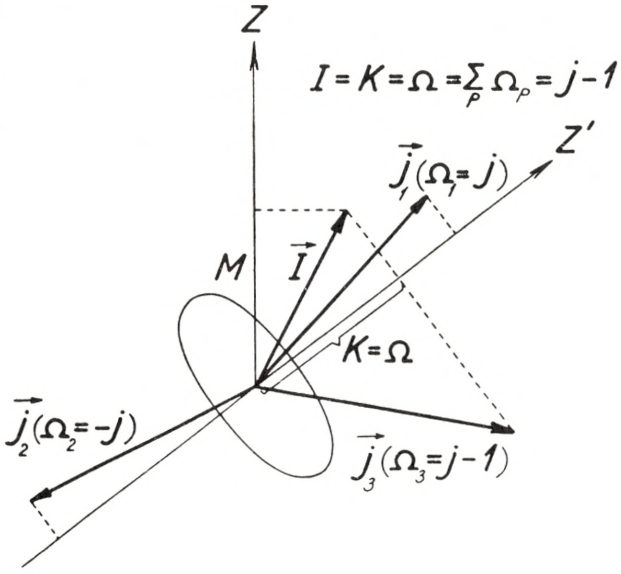
Z
$I = K = \Omega = \sum_p \Omega_p = j-1$
Z'
$\vec{j}_1(\Omega_1 = j)$
M
$\vec{I}$
$K = \Omega$
$\vec{j}_2(\Omega_2 = -j)$
$\vec{j}_3(\Omega_3 = j-1)$

Fig. 6 a.

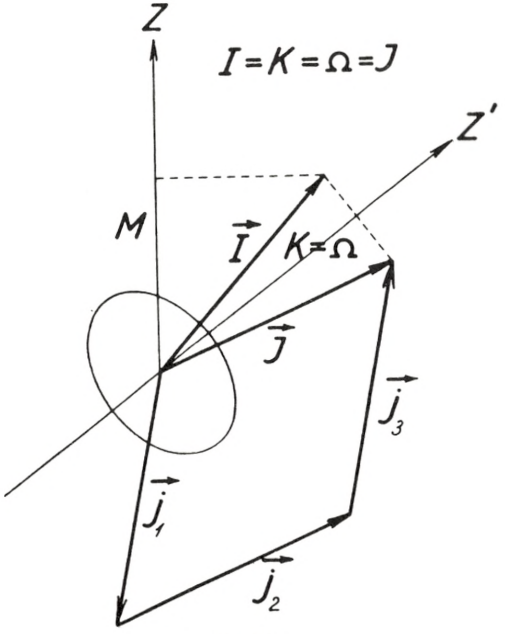
Z
$I = K = \Omega = J$
Z'
M
$\vec{I}$
$K = \Omega$
$\vec{J}$
$\vec{j}_3$
$\vec{j}_1$
$\vec{j}_2$

Fig. 6 b.

icles fill pairwise in states of opposite Ω_p; for n even, the ground state has $\Omega = 0$, while, for n odd, we get $\Omega = j - 1/2$ $(n-1)$. If n is greater than $j + 1/2$, it is more convenient to consider the holes in the shell. The preferred shape now has $\gamma = 0$, and one gets the same rules for Ω of the ground state if n is replaced by the number of holes. In the special case of a half filled shell, the nucleus spends equal time around the positions $\gamma = 0$ and $\gamma = \pi$. For nuclei of this type, the total Hamiltonian is invariant with respect to a replacement of particles by holes together with the substitution $k \to -k$ or $\gamma \to \gamma + \pi$ (self charge conjugate configurations).

If we have two groups a and b of equivalent particles, there is again in general a definite preference for either $\gamma = 0$ or $\gamma = \pi$. For an even group, the states are occupied pairwise with a resultant $\Omega_a = 0$, while an odd group contributes a finite Ω_a. If both groups are odd, the energy (29) is degenerate, corresponding to $\Omega = |\Omega_a \pm \Omega_b|$. In special cases, such as when one group is obtained from the other by replacing particles by holes, the positions $\gamma = 0$ and $\gamma = \pi$ may be equally preferred and the Hamiltonian possesses the same symmetry as discussed above.

The rotational contribution to W has the form

$$\left.\begin{aligned} W_{\text{rot}} = \frac{\hbar^2}{2\,\Im_3}(K-\Omega)^2 + \left(\frac{\hbar^2}{4\,\Im_1} + \frac{\hbar^2}{4\,\Im_2}\right)[I(I+1) - K^2 \\ + D\vec{J}^2 - \Omega^2 - 2D(J_1 I_1 + J_2 I_2)], \end{aligned}\right\} \quad \text{(II.30)}$$

where $\vec{J} = \sum_p \vec{j}_p$ and where the operator D picks out the part which is diagonal in the strong coupling representation (cf. FORD, 1953). The last term in (30) contributes only for configurations with $\Omega = K = 1/2$ and if equivalent particles are filled pairwise with opposite Ω_p; the term is then equal to the last term of (24) for the remaining odd particle. Apart from this special case of $\Omega = 1/2$ the nuclear ground state has $I = K = \Omega$.

In odd-odd nuclei, there are, as mentioned above, two families of states with $\Omega = |\Omega_a \pm \Omega_b|$, whose energies are degenerate in first order. This degeneracy is removed by the rotational terms (30), and the ground state has $I = K = \Omega = |\Omega_a - \Omega_b|$ in the limit of strong coupling.

The validity of the strong coupling approximation depends on the magnitude of the total deformation, as compared with the zero point oscillations. Since the particles act coherently in producing the deformation, the effective coupling increases with the addition of particles until the next closed-shell configuration is approached. Thus, for two equivalent particles, the relevant parameter measuring the strength of the coupling is $2x$ rather than x. The hydrodynamic estimate of the coupling strength for a single particle, given on p. 25, therefore implies a rather fully developed strong coupling situation in regions removed from closed shells.*

iii. *Influence of particle forces.*

The influence of nuclear two-body forces, with the neglect of surface coupling, has been considered for the (*jj*) coupling scheme along lines similar to those employed in atomic spectra (MAYER, 1950a; KURATH, 1950, 1952, 1953; FLOWERS, 1952, 1952a, 1952b; EDMONDS and FLOWERS, 1952, 1952a; TALMI, 1952; HITCHCOCK, 1952, 1952a; RACAH and TALMI, 1952). The choice of the forces is somewhat uncertain, since the present knowledge of the nuclear two-body system only partially defines the interaction. Moreover, the problem of nuclear saturation as well as the existence of shell regularities has raised the question whether these forces are appropriate to the description of interactions of nucleons in nuclei (cf., e. g., WEISSKOPF, 1952). The analysis of coupling schemes for nuclear many-particle configurations may provide evidence on these important questions.

The competition between the particle forces and the surface interactions determines the resultant nuclear coupling scheme. If the forces are weak compared to the coupling of the individual particles to the nuclear axis of deformation, the coupling scheme is that discussed in § II c.ii and illustrated by Fig. 6a. The effect of the particle forces is then to contribute a small energy shift which depends on the Ω_p quantum numbers. Such effects may be significant if there are near-lying states of different Ω, such as in odd-odd nuclei.

* Numerical examples illustrating the improvement of the strong coupling approximation for several particles have been given by FORD (1953) (cf. also the footnote on p. 25—26).

With increasing strength, the particle forces tend to destroy the above type of strong coupling solution by introducing non-diagonal terms in the Ω_p and, if the particle forces and the surface coupling are comparable, a rather complex situation may arise. For very strong forces, the particle structure is coupled to a resultant angular momentum $\vec{J}$. This vector is then coupled to the surface in the same manner as a single particle (cf. Fig. 6b) with an effective coupling constant (cf. Table VIII)

$$k_J = \frac{2(J+1)}{2J-1} \sum_p k_p < 3\cos^2\vartheta_p - 1 >_{J_z = J}. \qquad \text{(II.31)}$$

In this case, the nuclear ground state spin $I = J$ is determined by the particle forces.

A simple comparison of the strength of the surface coupling relative to that of the particle forces is obtained by considering that the former results from the interaction of the nucleons with the total displaced matter of the nuclear deformation. While the particle forces may play an important role in light nuclei, the surface coupling should thus become increasingly dominant in heavier nuclei and especially for the large deformations encountered in regions removed from closed shells.

III. Ground State Spins.

The interpretation of ground state spins and parities is most unambiguous in regions with large separations between neighbouring single-particle levels, where the lowest particle configuration can be uniquely assigned. The ordering of levels within this configuration is determined by the forces acting between the particles and by their coupling to the surface (cf. § IIc), and the observed ground state spin may give evidence on the resulting coupling scheme. The parity follows directly from the configuration.

In regions with close-lying particle levels, the lowest state of the system may be affected by relatively small shifts in the configuration energies, arising from surface or particle interactions,* as well as by configuration mixings produced by these interactions.

In the present chapter, we restrict ourselves to the problem of the lowest state for a given configuration. Some aspects of the configuration interactions are considered in connection with magnetic moments (cf. Addendum to Chapters IV and V) and level structures (§ VIb).

i. *Single-particle configurations.*

For a single-particle configuration, it follows from the considerations in § IIb that, for the lowest state, I equals j of the particle, irrespective of the strength of the surface coupling. Indeed, for this important class of nuclei, the observed spins and parities are successfully accounted for by the strong spin orbit coupling shell model (MAYER, 1950; HAXEL, JENSEN and SUESS, 1950).

* Cf., e. g., the shell model pairing energy (MAYER, 1950a).

ii. *Configurations of two equivalent particles. Even structures.*

The calculations based on the assumption of attractive two-body forces have shown that such forces will couple two equivalent particles to a ground state of spin zero (MAYER, 1950a; FLOWERS, 1952b; EDMONDS and FLOWERS, 1952a; RACAH and TALMI, 1952).

The same result is obtained for the influence of the surface coupling. In weak coupling, this effect may be considered in terms of equivalent two-body interactions given by (II.28), which favour the state $I = 0$. In strong coupling, the particles fill pairwise in states of opposite Ω_p and the ground state has $I = K = \Omega = 0$.

Empirically, one has always found $I = 0$ for these configurations, but the rule is far more general, applying to all even-even nuclei. For configurations involving only protons or neutrons, this result can be obtained for short range attractive forces (MAYER, 1950a; FLOWERS, 1952b). It is apparent that the surface, in strong coupling, leads to $I = 0$ quite generally for even-even nuclei (cf. § II.ii).

Since, in the strong coupling picture, an even group of equivalent particles has no influence on the angular momentum properties of the nuclear ground state, aside from the tendency to favour prolate or oblate deformations, one has a certain basis for treating any odd-A nucleus in terms of the odd group of particles alone. Thus, if the odd group contains only a single particle (or hole) with an angular momentum j, one obtains the same ground state spin ($I = j$) as for a single-particle configuration (cf. § III.i). The observed spins of these nuclei have been found to be consistent with such a simplification of the model (MAYER, 1950; HAXEL, JENSEN and SUESS, 1950). The possibility exists, however, that the even group of particles produces a deformation of the opposite shape to that preferred by the odd group and thereby affects the ground state spin.

iii. *Configurations of three equivalent particles.*

Several calculations have been carried out to determine the ground state spin resulting from two-body forces acting in $(j)^{\pm 3}$ configurations (MAYER, 1950a; KURATH, 1950; TALMI, 1952;

Edmonds and Flowers, 1952a; Flowers, 1952a; Racah and Talmi, 1952). These calculations have shown that, for sufficiently short range attractive forces, one obtains $I = j$ for the ground state; when the range is no longer negligible compared to the nuclear radius, the ground state may have other spin values. The range at which cross-overs occur depends somewhat on the shape and exchange nature of the two-body potential.

For the $(5/2)^3$ and $(7/2)^3$ configurations, the state $I = j - 1$ will, for sufficiently long range forces, become the ground state, but the necessary range seems to be considerably in excess of that deduced from two-body data. For the $(9/2)^3$ configurations, a ground state of $I = 7/2$ not only requires an excessively long range, but also a rather implausible exchange nature of the potential.

Thus, it appears that, for forces consistent with the known properties of the two-body system, the state $I = j$ remains the ground state. It may be added that particle forces of sufficiently long range to produce cross-overs in the $(j)^3$ configurations would also strongly affect the predicted ground state spins of other configurations. In particular, high ground state spins may result for even-even nuclei, and the even group of particles no longer remains inert with respect to the spins of odd-A nuclei (Edmonds and Flowers, 1952a).

The effect of the surface coupling on the splitting of the $(j)^{\pm 3}$ configuration may be treated in weak and strong coupling. In the former case, the effective two-body interaction (II.28) can be shown to lead to a ground state spin of $I = j$ for $j = 5/2$, $7/2$, and $9/2$.

In strong coupling, however, three particles produce an oblate deformation and fill the three lowest levels $\Omega_p = j$, $-j$, $j - 1$, with a resultant $\Omega = j - 1$ and $I = K = \Omega = j - 1$ for the ground state (cf. Fig. 6a). For a $(j)^{-3}$ configuration, a prolate deformation results with the same angular momentum quantum numbers as for $(j)^3$. The special case of three $j = 5/2$ particles, which constitute a half filled shell, possesses the symmetry in γ discussed in § IIc.ii, aside from the stabilizing influence of an even non-closed configuration.

Evidence on the level order for $(j)^{\pm 3}$ configurations has been obtained from spectroscopic measurements of ground state spins

and from the analysis of nuclear disintegration schemes. The observed spin for the lowest state within these configurations is given in Table I which shows that the values $I = j$ and $I = j - 1$ occur about equally frequently.

TABLE I. Lowest spins of $(j)^{\pm 3}$ configurations.

Nucleus	Configuration	I_{lowest}
$_{10}Ne^{21}$	$(d_{5/2})^3$	3/2 *g*
$_{11}Na^{23}$	,,	3/2 *g*
$_{20}Ca^{43}$	$(f_{7/2})^3$	7/2 *g**
$_{23}V^{51}$	,,	7/2 *g*
$_{25}Mn^{55}$	$(f_{7/2})^{-3}$	5/2 *g*
$_{32}Ge^{75}$	$(g_{9/2})^3$	7/2 **
$_{34}Se^{77}$	,,	7/2
$_{36}Kr^{79}$	,,	7/2 *g*
$_{34}Se^{81}$	$(g_{9/2})^{-3}$	7/2
$_{36}Kr^{83}$	,,	9/2 *g*
$_{38}Sr^{85}$	,,	9/2 *g*
$_{43}Tc^{95}$	$(g_{9/2})^3$	9/2 *g*
$_{43}Tc^{97}$	,,	9/2 *g*
$_{43}Tc^{99}$	,,	9/2 *g*
$_{47}Ag^{107}$	$(g_{9/2})^{-3}$	7/2
$_{47}Ag^{109}$	,,	7/2

The table includes available evidence on the spin of the lowest state in $(j)^{\pm 3}$ configurations in those regions where the configuration assignment is relatively unambiguous. This assignment, for the odd group of particles, is given in the second column, while the third column gives the observed spin of the lowest state of the configuration. The letter *g* indicates ground state of the nucleus. The spin values come from spectroscopic data (MACK, 1950) and from the analysis of decay schemes (GOLDHABER and HILL, 1952), except where otherwise noted.

* JEFFRIES (1953) (added in proof). ** SMITH et. al. (1952).

The empirical data may be interpreted in a straightforward manner by assuming that the surface coupling dominates over the particle interactions and produces a lowest spin $I = j$ or $I = j - 1$, depending on the strength of the coupling. It is also possible that the occurrence of $I = j$ reveals a significant influence of the particle forces (cf. Fig. 6b).

This interpretation would imply that $I = j$ is more likely in regions near a closed shell in the even structure, while $I = j - 1$

would be preferred for more deformed nuclei. Such a trend is indeed discernible in the data. Thus, in the $f_{7/2}$ shell, $I = 7/2$ is observed for $_{20}Ca^{43}$ and $_{23}V^{51}$ with the closed-shell even structures, while the more deformed $_{25}Mn^{55}$ gives $I = 5/2$. In the $g_{9/2}$ shell, $I = 7/2$ is, for the odd-neutron nuclei, favoured for $Z = 32$, 34, and 36, while $I = 9/2$ lies lowest for $Z = 36$ and 38, corresponding to the approach to the closed subshell at 38. For the odd-proton nuclei, $I = 9/2$ is favoured for $N = 52$, 54, and 56 in the region of the closed shell at 50, while the more deformed nuclei with $N = 60$ and 62 have $I = 7/2$. Such trends could be tested in more detail if the separation between the $I = 7/2$ and $I = 9/2$ levels were known for a sequence of isotopes or isotones.

In this discussion, the even structure has been considered only in its influence on the magnitude of the nuclear deformation. As mentioned on p. 34, more specific effects may occur if the even structure has a strong preference for a shape opposite to that produced by the odd structure. In those cases in Table I where the even configurations are sufficiently well known for such considerations, it is verified that no such anomalies are expected.

Evidence is also available on the level order for $(g_{9/2})^5$ configurations which are expected to occur for 45 particles. For the known nuclei of this type, the lowest state of the configuration has been found to be $I = 7/2$. No calculations have been reported on the effect of particle forces in these configurations. The weak coupling approximation of the effect of surface coupling has not been worked out either but, in the limit of strong coupling, the state $I = 5/2$ would be favoured. It seems not implausible that $I = 7/2$ could result from an intermediate coupling. Considerable interest would attach to the location of the lowest $(5/2+)$ state.

iv. *Odd-odd nuclei.*

The ground state spins resulting from two-body forces have been considered for various types of odd-odd nuclei (Kurath, 1952, 1953; Hitchcock, 1952, 1952a; Edmonds and Flowers, 1952a). The results appear to be more sensitive to the range and exchange nature of the forces than in the case of odd-A nuclei.

The coupling scheme arising from the surface interaction can be derived from (II.28) for weak coupling and from the considerations in § IIc.ii for strong surface coupling. In the latter case, there are two families with $\Omega = |\Omega_{\text{prot}} \pm \Omega_{\text{neut}}|$, whose energies differ only by amounts of the order of rotational energies. In the strong coupling limit, the ground state corresponds to the lower value, but the order may be altered by deviations from strong coupling or by even a minor influence of particle forces.

TABLE II. Spins of simple odd-odd nuclei.

Nucleus	Configuration		I_{obs}	$I\binom{\text{weak}}{\text{coupl.}}$	$I\binom{\text{strong}}{\text{coupl.}}$
	protons	neutrons			
$_5B^{10}$	$(p_{3/2})^{-1}$	$(p_{3/2})^{-1}$	3	0	0,3
$_{17}Cl^{36}$	$d_{3/2}$	$(d_{3/2})^{-1}$	2	2	1,2
$_{17}Cl^{38}$	$d_{3/2}$	$f_{7/2}$	2	2	2,5
$_{19}K^{40}$	$(d_{3/2})^{-1}$	$f_{7/2}$	4	4	3,4
$_{37}Rb^{86}$	$(f_{5/2})^{-1}$	$(g_{9/2})^{-1}$	2	2	2,7

The table lists odd-odd nuclei whose proton and neutron configurations may be described in terms of a single particle or hole with $j > 1/2$. The observed spins, in column four, are taken from the references in Table XXI, except for Cl^{38} whose spin is derived from its observed beta spectrum (cf. Table XXXII).

The spins expected for weak and strong surface coupling are given in the two last columns. The weak coupling results coincide with those obtained for attractive spin-independent particle forces of zero range. For strong coupling, two values are listed, corresponding to the degenerate Ω-values implied by (II.29) ($\Omega = |\Omega_{\text{prot}} \pm \Omega_{\text{neut}}|$). The rotational energy (II.30) favours the smaller of the two spin values, but the relative position of the two states may be shifted by deviations from strong coupling or by even rather weak particle forces.

The measured spins of odd-odd nuclei with simple two-particle configurations are listed in Table II, which also gives the calculated values for weak and strong surface coupling.* We have confined ourselves to regions of relatively pure configurations and have omitted nuclei for which one or both of the odd particles have $j = 1/2$. These latter particle states are affected by the sur-

* In the present discussion, we restrict ourselves to nuclei with $A > 8$, since the division into particle and collective degrees of freedom loses its significance for the very lightest nuclei. Moreover, for the light nuclei, the analysis is complicated by the fact that the particle forces in general lead to a situation intermediate between (jj) and (LS) coupling (cf. INGLIS, 1952).

face only through their coupling to neighbouring states, and are also somewhat special as regards the effect of particle forces, since spin dependent interactions become decisive. For the cases in Table II, the ground state spin resulting from spin independent interactions of zero range (KURATH, 1952) coincide with the weak coupling values in column five. Results of other forces have been considered by the above mentioned authors.

It appears that both particle forces and surface interactions are capable of accounting for the data in Table II.* An interesting feature is the empirical evidence for a different coupling of particle-particle from that of particle-hole. This can be understood in terms of two-body forces of the Wigner or Majorana type (KURATH, 1953) and also follows from the opposite signs of the surface coupling associated with particles and holes.

The coupling scheme in some more complex odd-odd nuclei is considered in the Addendum to Chapters IV and V, in connection with a discussion of nuclear moments.

v. *Summary.*

The ground state spin is determined in general by a competition between particle forces and surface coupling. Often the two effects favour the same value of I, but, especially in the case of $(j)^3$ configurations, the predictions are different and the empirical evidence can be used to obtain information about the nuclear coupling scheme (cf. also footnote below).

The available data can be interpreted in a consistent manner in terms of the expected dominance of the surface coupling over the direct particle forces (cf. p. 32). The observed spins confirm the approach to the strong coupling scheme in regions removed

* Note added in proof: A level scheme for $_{17}Cl^{34}$ has recently been given (ARBER and STÄHELIN, 1953), in which the ground state has $I = 0$ (even parity) and in which there appears an isomeric level at 145 keV with $I = 3$ (even parity). For weak surface coupling the lowest state of this $(d_{3/2}; d_{3/2})$ configuration has $I = 0$, while for strong coupling one finds two states $I = 0,3$ with the former favoured by the rotational energy. Attractive particle forces of the expected range yield $I = 3$ for the ground state (KURATH, 1953).

Additional evidence on the ground state spins of self-mirrored odd-odd nuclei could provide further information on the competition between the direct particle forces and the coupling to the surface deformations, since the former in general favour $I = 2j$, while the latter gives $I = 0$ (cf., especially, $_{13}Al^{26}$, $_{19}K^{38}$, $_{21}Sc^{42}$, and $_{27}Co^{54}$).

from closed shells, with a relatively weaker coupling acting in the neighbourhood of closed shells.

In the immediate vicinity of major closed shells, the expected weak surface coupling implies the most favourable conditions for the study of particle forces. Important evidence on the strength and nature of these forces could be provided by further experimental data on ground state spins and moments in this region, especially when combined with a knowledge of the excitation spectrum and lifetimes of excited states (cf. § VIb).

IV. Magnetic Moments.

The sharing of angular momentum between particles and surface implies that both particle and surface motion contribute to the nuclear magnetic moment. Because of the large intrinsic moment of the nucleons, the particle aspect of nuclear moments is in general the more conspicuous, and indeed the empirical moments have provided a valuable guide in the formulation of the shell model (SCHMIDT, 1937; FEENBERG and HAMMACK, 1949; NORDHEIM, 1949; MAYER, 1950; HAXEL, JENSEN and SUESS, 1950).

In a more quantitative analysis, however, the surface coupling plays an important role. Appreciable shifts from the single-particle values can arise from the modified nuclear coupling scheme produced by the surface interaction; additional effects result from the tendency of the surface coupling to admix near-lying particle states, which may have very different magnetic properties (FOLDY and MILFORD, 1950; A. BOHR, 1951; DAVIDSON and FEENBERG, 1953).

The analysis of magnetic moments may also provide evidence on the extent to which the magnetic properties of nucleons may be affected by their interaction with nuclear matter (cf., e. g., VILLARS, 1947; SACHS, 1948; MIYAZAWA, 1951 a).

a) Shell Model Moments.

For a single particle moving in a spherical potential, the magnetic moment is given by

$$\mu = j g_j = j\left(g_l \pm \frac{1}{2\,l+1}\,(g_s - g_l)\right) \qquad j = l \pm 1/2, \qquad \text{(IV.1)}$$

where g_j is the total g-factor and

$$g_s = \left\{ \begin{matrix} 5.585 \\ -3.826 \end{matrix} \right\} \quad \text{and} \quad g_l = \left\{ \begin{matrix} 1 \\ 0 \end{matrix} \right\} \qquad \text{(IV.2)}$$

the intrinsic and orbital g-factors in units of nuclear magnetons. In the bracket, the upper values refer to a proton, the lower to a neutron.

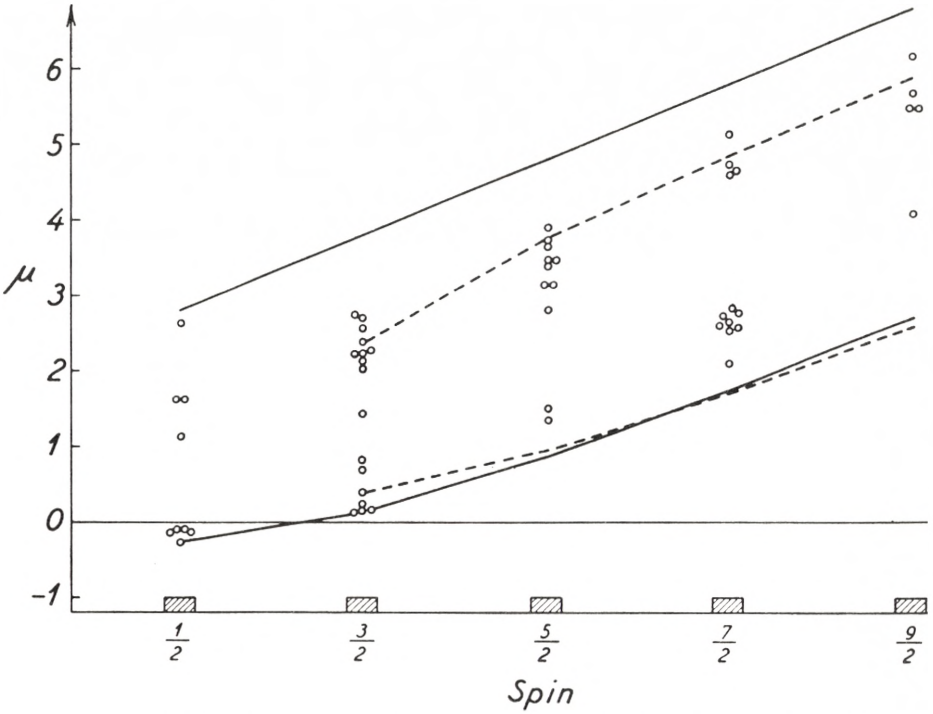

Fig. 7. *Magnetic moments of odd-proton nuclei.* The moments of odd-proton nuclei with $A > 8$ are plotted against the nuclear spin. This type of diagram was first used by SCHMIDT (1937). The experimental values are taken from the references given in the Addendum. The full-drawn curves give the single-particle values (1 and 2), while the dotted curves give the moment values obtained in the limit of strong surface coupling, assuming the particle j to remain a constant of the motion (cf. (6) and Ap. III.9). The surface coupling may further influence the magnetic moment through the tendency to admix neighbouring particle orbitals. This effect, however, depends sensitively on the level order and the shape and magnitude of the deformation, and must therefore be considered separately for the individual nuclei (cf. Table VII and the Addendum).

The empirical moments for odd-A nuclei are plotted in Figs. 7 and 8, in which also the single-particle values (1 and 2) are shown by the solid lines. In spite of the appreciable scatter of the empirical moments, they show a tendency to cluster in two groups, for given I, which can be related to the single-particle values. This correlation has been successfully employed in the

determination of nuclear parities (cf., e. g., MAYER, MOSZKOWSKI and NORDHEIM, 1951). Also the trends of the moments with I give support to the value (2) for the orbital g-factor.

For many-particle configurations, the magnetic moment depends on the coupling scheme which leads to the total angular momentum J. For a group of equivalent particles, one has, in

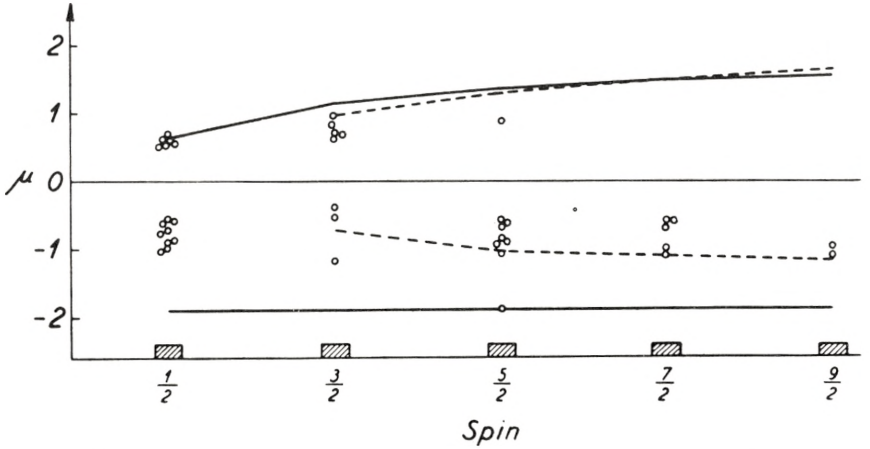

Fig. 8. *Magnetic moments of odd-neutron nuclei.* The moments of odd-neutron nuclei with $A > 8$ are plotted against the nuclear spin (cf. also the caption to Fig. 7).

the (jj) coupling model, $g_J = g_j$, but changes in the g-factor may arise for odd-A nuclei when the even structure is not a closed shell. In such cases, the nuclear state for a given J will in general depend on the interparticle forces; for three or five nucleons in $j = 3/2$ orbitals, the assumption of charge independent forces, however, suffices to determine the nuclear wave function. The magnetic moments for these cases are listed in Table III. For odd-odd nuclei, the magnetic moment is in general unique only when the proton—as well as the neutron—configuration is that of a single particle. By making more explicit assumptions about the character of the forces, one can obtain magnetic moments for more complicated many-particle configurations (HITCHCOCK, 1952; FLOWERS, 1952c).

A comparison of the shell model magnetic moments with the empirical data is given in Table IV. Nuclei are listed for which magnetic moments are known, and for which the (jj) coupling

TABLE III. Properties of charge symmetrized states of type $(j = 3/2)^3_{J=3/2}$ with $T = 1/2$.

Configuration		Magnetic moments		Quadrupole moments	Mirror β-decay
protons	neutrons	μ_j	μ_J	$Q_J/\lvert Q_j \rvert$	$(D_{GT})_J/(D_{GT})_j$
$(p_{3/2})^{\pm 1}$	$(p_{3/2})^2$	3.79	3.03	$\mp$ 11/15	121/225
$(p_{3/2})^2$	$(p_{3/2})^{\pm 1}$	— 1.91	—.1.15	$\mp$ 2/3	121/225
$(d_{3/2})^{\pm 1}$	$(d_{3/2})^2$	0.12	0.26	$\mp$ 11/15	121/225
$(d_{3/2})^2$	$(d_{3/2})^{\pm 1}$	1.15	1.01	$\mp$ 2/3	121/225

The table compares magnetic moments, quadrupole moments, and β-decay transition probabilities for the charge symmetrized state J with the corresponding quantities for the single-particle state j. Magnetic moments have been given by MIZUSHIMA and UMEZAWA (1952), quadrupole moments by HORIE and YOSHIDA (1951) and FLOWERS (1952c), and β-decay matrix elements by KOFOED-HANSEN and WINTHER (1952).

shell model provides a unique prediction μ_p. It is seen that, in most cases, the deviations from μ_p are of the order of a half to one magneton. The cases of agreement between μ_p and μ_{obs} are principally the $p_{1/2}$-nuclei and the self-mirrored odd-odd nuclei (cf. pp. 67 and 81).

b) Moments of the Coupled System.

For the coupled system consisting of a single particle and the nuclear surface, the magnetic moment is given by

$$\mu = < g_s s_z + g_l l_z + g_R R_z >_{M=I} \qquad \text{(IV.3)}$$

where g_R is the g-factor for the angular momentum carried by the surface. For a uniformly charged nucleus, we have*

$$g_R = Z/A. \qquad \text{(IV.4)}$$

If j remains a good quantum number, (3) reduces to

$$\left.\begin{aligned} \mu &= < g_j j_z + g_R R_z >_{M=I} \\ &= g_j I - (g_j - g_R) < R_z >_{M=I}. \end{aligned}\right\} \qquad \text{(IV.5)}$$

* In the discussion of the empirical data we employ for simplicity the fixed value $g_R = 0.45$, except for the self-mirrored odd-odd nuclei for which $g_R = 0.5$.

TABLE IV. Comparison of magnetic moments with shell model values.

Nucleus	Configurations		I	μ_{obs}	μ_p
	protons	neutrons			
$_4Be^9$	$(p_{3/2})^2$	$(p_{3/2})^{-1}$	3/2	−1.18	−1.15
$_5B^{10}$	$(p_{3/2})^{-1}$	$(p_{3/2})^{-1}$	3	1.80	1.88
$_5B^{11}$	$(p_{3/2})^{-1}$	—	3/2	2.69	3.79
$_6C^{13}$	—	$p_{1/2}$	1/2	0.70	0.64
$_7N^{14}$	$p_{1/2}$	$p_{1/2}$	1	0.40	0.37
$_7N^{15}$	$p_{1/2}$	—	1/2	−0.28	−0.26
$_8O^{17}$	—	$d_{5/2}$	5/2	−1.89	−1.91
$_9F^{19}$	$s_{1/2}$	—	1/2	2.63	2.79
$_{11}Na^{22}$	$(d_{5/2})^3$	$(d_{5/2})^3$	3	1.75	1.73
$_{13}Al^{27}$	$(d_{5/2})^{-1}$	—	5/2	3.64	4.79
$_{14}Si^{29}$	—	$s_{1/2}$	1/2	−0.56	−1.91
$_{15}P^{31}$	$s_{1/2}$	—	1/2	1.13	2.79
$_{16}S^{33}$	—	$d_{3/2}$	3/2	0.64	1.15
$_{17}Cl^{35}$	$d_{3/2}$	$(d_{3/2})^2$	3/2	0.82	0.26
$_{17}Cl^{37}$	$d_{3/2}$	—	3/2	0.68	0.12
$_{19}K^{39}$	$(d_{3/2})^{-1}$	—	3/2	0.39	0.12
$_{19}K^{40}$	$(d_{3/2})^{-1}$	$f_{7/2}$	4	−1.30	−1.68
$_{23}V^{51}$	$(f_{7/2})^3$	—	7/2	5.15	5.79
$_{37}Rb^{86}$	$(f_{5/2})^{-1}$	$(g_{9/2})^{-1}$	2	−1.69	−2.13
$_{37}Rb^{87}$	$(p_{3/2})^{-1}$	—	3/2	2.75	3.79
$_{38}Sr^{87}$	—	$(g_{9/2})^{-1}$	9/2	−1.1	−1.91
$_{39}Y^{89}$	$p_{1/2}$	—	1/2	−0.14	−0.26
$_{40}Zr^{91}$	—	$d_{5/2}$	5/2	−1.1	−1.91
$_{82}Pb^{207}$	—	$p_{1/2}$	1/2	0.59	0.64
$_{83}Bi^{209}$	$h_{9/2}$	—	9/2	4.08	2.62

The table lists the nuclei with measured magnetic moments, for which the shell model yields unique μ-values, without specific assumptions about the nuclear forces other than charge independence. For references to the empirical data, cf. Addendum to Chapters IV and V. The odd-A nuclei are single-particle configurations, except for Be^9 and Cl^{35} for which cf. Table III. The odd-odd nuclei mostly have two-particle configurations, in which case the measured spin uniquely determines the state. For Na^{22} the total g-factor follows from the symmetry of the configuration, even though the state is not unique.

For the ground state with $I = j$, the dependence of $< R_z >$ on the coupling strength has been discussed in § IIb and is illustrated in Fig. 5. In the limit of large x, we get from (II.20), for $I = j > 3/2$, the strong coupling value (cf. A. BOHR, 1951)

$$\mu_c = \mu_{sp} - (g_j - g_R) \frac{I}{I+1}. \qquad \text{(IV.6)}$$

For $I = j = 3/2$, the limiting value μ_c differs somewhat from (6) (cf. Ap. III.9); for $I = j = 1/2$, there is no coupling to the surface and $\mu = \mu_{sp}$.

The values of μ_c for j a constant ($j = I$) are plotted as dotted lines in Figs. 7 and 8.

If there are neighbouring single-particle states j', which are admixed by the surface coupling, the magnetic moment may be strongly influenced. In the perturbation approximation, one obtains from (Ap. II.3 and 4)

$$\left.\begin{aligned} \mu &= \mu_{sp} \\ &+ x^2 \sum_{j'} \{ -\alpha_{jj'} (g_j - g_R) + \beta_{jj'} (g_{j'} - g_R) \} \left(\frac{\hbar\omega}{\hbar\omega + \Delta_{jj'}} \right)^2, \end{aligned} \right\} \quad \text{(IV.7)}$$

where the coefficients α and β are given in Table V, and where $\Delta_{jj'}$ represents the spacing between the particle states j and j'.

TABLE V. Coefficients in magnetic moment shifts produced by weak surface coupling.

I	$j' = j-2$		$j' = j-1$		$j' = j$		$j' = j+1$		$j' = j+2$	
	α	β	α	β	α	β	α	β	α	β
1/2	—	—	—	—	—	—	$\frac{1}{5}$	$-\frac{1}{5}$	$\frac{3}{10}$	$\frac{7}{10}$
3/2	—	—	$\frac{9}{10}$	$\frac{9}{50}$	$\frac{18}{25}$	—	$\frac{27}{70}$	$\frac{117}{350}$	$\frac{81}{35}$	$\frac{729}{175}$
5/2	$\frac{5}{2}$	$\frac{1}{2}$	$\frac{5}{7}$	$\frac{13}{49}$	$\frac{48}{49}$	—	$\frac{10}{21}$	$\frac{74}{147}$	$\frac{125}{21}$	$\frac{1375}{147}$
7/2	$\frac{63}{10}$	$\frac{27}{10}$	$\frac{7}{10}$	$\frac{37}{90}$	$\frac{10}{9}$	—	$\frac{35}{66}$	$\frac{115}{198}$	$\frac{245}{22}$	$\frac{3185}{198}$
9/2	$\frac{81}{7}$	$\frac{45}{7}$	$\frac{54}{77}$	$\frac{414}{847}$	$\frac{144}{121}$	—	$\frac{81}{143}$	$\frac{981}{1573}$	$\frac{5103}{286}$	$\frac{76545}{3146}$

The magnetic moment shift in a state $I = j$, arising from the sharing of angular momentum between the particle and the surface, and from the admixture of neighbouring orbitals j', is given in the weak coupling region by (IV.7). The table lists the coefficients $\alpha_{jj'}$, and $\beta_{jj'}$, occurring in this equation.

If the surface admixes the spin orbit partner, there is an additional contribution to μ from cross terms in j, j' giving (cf. Ap. II.5)

$$\left.\begin{aligned}\delta\mu = \pm x^2 (g_s - g_l) \frac{3}{4(2l+1)} \frac{(2j-1)(2j+3)}{(j+1)^2} \\ \left(\frac{\hbar\omega}{\hbar\omega + \Delta_{jj'}}\right),\end{aligned}\right\} \quad \text{(IV.8)}$$

where the upper and lower signs refer to the cases of a particle and a hole, respectively.

In strong coupling, the magnetic moment of a state with $I = K = \Omega \geqslant 3/2$ is given by

$$\mu_c = \frac{I^2}{I+1} g_\Omega + \frac{I}{I+1} g_R, \quad \text{(IV.9)}$$

where

$$g_\Omega = \frac{1}{\Omega} < g_s s_3 + g_l l_3 > \quad \text{(IV.10)}$$

is the g-factor associated with the particle motion in the deformed nucleus and can be evaluated for wave functions χ_Ω of the type discussed in § IIb.

For the special case of $\Omega = K = 1/2$, the value of μ_c is most easily obtained from (3) by means of the expectation values of j_z, given by (II.19), and of s_z given by (Ap. III.2).

For many-particle configurations, magnetic moments can be derived for the different coupling schemes discussed in § IIc. In the strong coupling scheme, in which the state is characterized by the Ω_p of the individual particles (cf. Fig. 6a), formula (9) still holds where, for odd-A nuclei, g_Ω is the g-factor for the last odd particle. For odd-odd nuclei, we have

$$g_\Omega = \frac{1}{\Omega} (\Omega_a g_a + \Omega_b g_b). \quad \text{(IV.11)}$$

If the nuclear forces first couple the particle to a resultant J (cf. Fig. 6b), the magnetic moment is obtained as for a single particle with a g-factor equal to g_J.

c) Comparison with Empirical Data.

A detailed application of the coupled model to the interpretation of moments of individual nuclei is given in the Ad-

dendum to Chapters IV and V. In the present section, we consider some of the general trends of the empirical data and summarize the conclusions that can be drawn from the more detailed analysis.

The surface coupling may affect the magnetic moment in two ways, by the transfer of angular momentum to the surface

TABLE VI. Magnetic moments in strong coupling.

Nucleus	Configuration		I	μ_{obs}	μ_c	μ_p
	protons	neutrons				
$_4Be^9$	$(p_{3/2})^2$	$(p_{3/2})^{-1}$	3/2	−1.18	−0.73	−1.15
$_5B^{11}$	$(p_{3/2})^{-1}$	—	3/2	2.69	2.37	3.79
$_8O^{17}$	—	$d_{5/2}$	5/2	−1.89	−1.04	−1.91
$_{12}Mg^{25}$	$(d_{5/2})^{-2}$	$(d_{5/2})^{-1}$	5/2	−0.86	−1.04	
$_{13}Al^{27}$	$(d_{5/2})^{-1}$	—	5/2	3.64	3.75	4.79
$_{21}Sc^{45}$	$f_{7/2}$	$(f_{7/2})^4$	7/2	4.76	4.86	
$_{22}Ti^{49}$	$(f_{7/2})^2$	$(f_{7/2})^{-1}$	7/2	−1.10	−1.14	
$_{27}Co^{57}$	$(f_{7/2})^{-1}$	$(p_{3/2}, f_{5/2})^2$	7/2	4.6	4.86	
$_{27}Co^{59}$	$(f_{7/2})^{-1}$	$(p_{3/2}, f_{5/2})^4$	7/2	4.65	4.86	
$_{38}Sr^{87}$	—	$(g_{9/2})^{-1}$	9/2	−1.1	−1.20	−1.91
$_{41}Nb^{93}$	$g_{9/2}$	$(d_{5/2}, g_{7/2})^2$	9/2	6.17	5.93	
$_{49}In^{113}$	$(g_{9/2})^{-1}$	$(d_{5/2}, g_{7/2}, h_{11/2})^{14}$	9/2	5.49	5.93	
$_{49}In^{115}$	$(g_{9/2})^{-1}$	$(d_{5/2}, g_{7/2}, h_{11/2})^{16}$	9/2	5.50	5.93	

The table lists the relatively simple nuclei whose odd structure is of $(j)^{\pm 1}$ type with a j larger than that of neighbouring orbitals. The last three columns give the observed moments, those calculated for strong surface coupling, and those resulting from particle forces with the neglect of surface coupling. The latter are only listed where the particle forces lead to a unique coupling scheme. For reference to experimental data, cf. the Addendum.

and by the admixture of near-lying particle orbitals. In a special class of nuclei, the former effect can be studied alone, provided the coupling is strong. Thus, if the odd-particle j is the largest in the corresponding shell, the strong coupling solution with $\Omega = j$ will have no other orbitals admixed.

Nuclei of this type, whose odd configuration consists of a single particle or a single hole, are listed in Table VI. The three last columns give the empirical moments and those calculated for strong and vanishing surface coupling.

It is seen that the assumption of a rather strong surface coupling makes possible an approximate interpretation of these moments. The principal exception is ${}_8O^{17}$, for which many properties attest the expected undeformability of the very stable ${}_8O^{16}$ core (cf. § Vc). In some cases, the magnitude of μ_{obs} is a few tenths of a magneton below that of μ_c, which may possibly arise from an interaction effect on the nucleon moment (cf. p. 51).

The rather fully developed strong coupling situation indicated by the empirical values in Table VI implies, according to (5) and Fig. 5, that coupling strengths of $x \geqslant 1.5$ are required if the nuclei are described in terms of a single particle coupled to the surface. Such values of x are somewhat larger, by about a factor two, than those estimated for a single particle in the hydrodynamic approximation (cf. p. 25), but may be understood in terms of the increased coupling expected from the influence of the even structures (cf. p. 31). In cases where an even structure, for a spherical nucleus, would form a closed sub-shell, it may still be active, provided the energy gap to the next higher levels is not too large (cf. Ap. I).

A similar effect on the magnetic moment is expected for all nuclei with $I \geqslant 3/2$, and the strong coupling value μ_c (cf. 6 and Ap. III.9) corresponding to $j = I$ is plotted in Figs. 7 and 8 as broken lines. However, for nuclei other than those listed in Table VI, there are additional contributions to μ, arising from the interaction between neighbouring particle orbitals.

This effect is of special interest for $I = 1/2$ nuclei, where it provides a mechanism for strong surface coupling. Thus, for $(1/2+)$ nuclei, the strong interaction between $s_{1/2}$ and the $d_{5/2}$ and $d_{3/2}$ states may lead to a large deformation. The effect on the moment depends especially on the sign of the deformation (cf. Fig. 11). Thus, the expected prolate shape of F^{19} leads to a very small moment shift, while the expected oblate shape of Si^{29} and P^{31} explains the observed large deviations of the moment from that of a single-particle $s_{1/2}$ state (cf. Ad. i).

For the $(1/2-)$ nuclei, the admixed states have relatively little effect on the moment. In the first p-shell, the large $p_{1/2}$ —$p_{3/2}$ splitting in addition leads to rather small amplitudes of admixture. In higher p-shells, there is a considerable tendency for the moment deviations, caused by the $p_{3/2}$ and $f_{5/2}$ admixtures, to

cancel, which provides an understanding of the strikingly small spread of the moments of this group (cf. Ad. ii).

Another effect of the interconfiguration admixtures can be studied for the (3/2+) nuclei. Due to the $d_{3/2} - d_{5/2}$ interference, the magnetic moment depends, as for the (1/2+) nuclei, on the sign of the deformation (cf. Fig. 12) and thus distinguishes be-

TABLE VII. Summary of magnetic moments for $A < 50$.

Nucleus	Configurations		I	μ_{obs}	μ_p	μ_c
	protons	neutrons				
$_4Be^9$	$(p_{3/2})^2$	$(p_{3/2})^{-1}$	3/2	−1.18	−1.15	−0.7
$_5B^{10}$	$(p_{3/2})^{-1}$	$(p_{3/2})^{-1}$	3	1.80	1.88	1.79
$_5B^{11}$	$(p_{3/2})^{-1}$	—	3/2	2.69	3.79	2.3
$_6C^{13}$	—	$p_{1/2}$	1/2	0.70	0.64	0.64 to 0.75
$_7N^{14}$	$p_{1/2}$	$p_{1/2}$	1	0.40	0.37	0.40 to 0.47
$_7N^{15}$	$p_{1/2}$	—	1/2	−0.28	−0.26	−0.27 to −0.41
$_8O^{17}$	—	$d_{5/2}$	5/2	−1.89	−1.91	−1.04
$_9F^{19}$	$s_{1/2}$	—	1/2	2.63	2.79	2.5 to 2.8
$_{11}Na^{22}$	$(d_{5/2})^3$	$(d_{5/2})^3$	3	1.75	1.73	1.71 to 1.78
$_{11}Na^{23}$	$(d_{5/2})^3$	$(d_{5/2})^{-2}$	3/2	2.22		2.2 to 2.5
$_{11}Na^{24}$	$(d_{5/2})^3$	$(d_{5/2})^{-1}$	4	1.69		1.4 to 1.8
$_{12}Mg^{25}$	$(d_{5/2})^{-2}$	$(d_{5/2})^{-1}$	5/2	−0.86		−1.04
$_{13}Al^{27}$	$(d_{5/2})^{-1}$	—	5/2	3.64	4.79	3.75
$_{14}Si^{29}$	—	$s_{1/2}$	1/2	−0.56	−1.91	−1.2 to −0.6
$_{15}P^{31}$	$s_{1/2}$	—	1/2	1.13	2.79	1.9 to 1.2
$_{16}S^{33}$	—	$d_{3/2}$	3/2	0.64	1.15	0.8 to 0.2
$_{17}Cl^{35}$	$d_{3/2}$	$(d_{3/2})^2$	3/2	0.82	0.26	0.5 to 1.2
$_{17}Cl^{37}$	$d_{3/2}$	—	3/2	0.68	0.12	0.5 to 1.2
$_{19}K^{39}$	$(d_{3/2})^{-1}$	—	3/2	0.39	0.12	0.3 to −0.1
$_{19}K^{40}$	$(d_{3/2})^{-1}$	$f_{7/2}$	4	−1.30	−1.68	−1.0 to −0.3
$_{19}K^{41}$	$(d_{3/2})^{-1}$	$(f_{7/2})^2$	3/2	0.22		0.3 to −0.1
$_{19}K^{42}$	$(d_{3/2})^{-1}$	$(f_{7/2})^3$	2	−1.14		−0.7 to −0.9
$_{21}Sc^{45}$	$f_{7/2}$	$(f_{7/2})^4$	7/2	4.76		4.86
$_{22}Ti^{49}$	$(f_{7/2})^2$	$(f_{7/2})^{-1}$	7/2	−1.10		−1.14

The table compares the observed magnetic moment μ_{obs} with the moment μ_p given by the shell model, with neglect of surface coupling, and the moment μ_c obtained for strong surface coupling. The value of μ_p is given only where it is independent of special assumptions about the nuclear forces. In cases where the strong coupling state contains several values of j, the moment may be rather sensitive to the equilibrium value of β, and the values given for μ_c correspond to deformations in the range $0.1 < \beta < 0.4$. For a more detailed discussion of μ_c, and for references to the empirical data, cf. the Addendum.

tween particles and holes. Such differences are indeed apparent in the empirical data (cf. Table XIV).

Further effects of the interaction of neighbouring particle states are discussed in the Addendum. The states often have very different magnetic moments, and their interaction may lead to large moment shifts.

The analysis of magnetic moments for nuclei with $A < 50$ is summarized in Table VII. The table compares the observed moments with those calculated for vanishing and strong surface coupling (columns six and seven, respectively). In those cases where the strong coupling state contains particle orbitals of different j, the magnetic moment may depend rather sensitively on the magnitude of the deformation, and the table lists moments appropriate to deformations in the range $0.1 < \beta < 0.4$. The expected values of β vary considerably from nucleus to nucleus, and estimates of values appropriate to the individual nuclei are given in the Addendum.

It is seen from the data collected in Tables VI and VII, and from the discussion in the Addendum, that the unified description of the nucleus, in terms of the coupled system of particles and collective oscillations, makes possible a rather systematic interpretation of the magnetic moments of nuclei with sufficiently simple configurations. The empirical data give evidence for the expected approach to the strong coupling scheme, except in the immediate vicinity of major closed shells.

An interpretation is also possible of the moments of many heavier nuclei not included in Tables VI and VII, wherever the configurations are sufficiently well known (cf. the Addendum). An important anomaly is the as yet unexplained large moment shift of $_{83}Bi^{209}$ with its single-particle configuration. The stability of the $_{82}Pb^{208}$ core with its closed-shell structure implies a rather negligible effect of the surface coupling, as confirmed by the small quadrupole moment. The observed moment shift thus probably reflects some unexpected feature of the particle structure.

Besides the contributions to the nuclear magnetic moment from the individual particles and from the surface, there may be an additional effect arising from the interaction of the nucleons. Such interaction effects have been described as exchange magnetic moments, and have sometimes been considered as a partial

quenching of the meson cloud responsible for the nucleon moments (Villars, 1947; Sachs, 1948; Osborn and Foldy, 1950; Spruch, 1950; Miyazawa, 1951, 1951a; Bloch, 1951; de-Shalit, 1951; Schiff, 1951; Jensen and Mayer, 1952; Russek and Spruch, 1952; Ross, 1952).

It is of interest to employ the analysis of the empirical moments to obtain evidence on the possible magnitude of these phenomena. In the $j = l - 1/2$ nuclei, there are small residual moment shifts which may perhaps be interpreted as arising from interaction effects. For the $p_{1/2}$ and $d_{3/2}$ configurations, the data are consistent with a reduction of the intrinsic nucleon moment by about 0.3 magnetons (cf. pp. 69 and 74). Somewhat larger effects may be present in the $f_{5/2}$ and possibly also in the $g_{7/2}$ nuclei (cf. pp. 78 og 79). It seems somewhat difficult, however, to interpret the moment shift of Bi^{209} ($h_{9/2}$) in this way, since an effect five times larger would be required (cf. p. 81). The moments of the $j = l + 1/2$ nuclei, with the exception of O^{17}, do not seem inconsistent with a reduction of the nucleon moment by a few tenths of a magneton (cf. Table VI).

That interaction contributions to the moment are in general small compared to the effects of the surface coupling is further supported by the correlations of magnetic moments with quadrupole moments (cf. p. 70) and especially with beta decay *ft*-values. Thus, for all the nuclei in Table VII with $Z = N - 1$, for which there are major discrepancies between μ_{obs} and μ_p, the *ft*-values of the corresponding mirror transitions give strong evidence that these discrepancies are associated with modifications in the nuclear coupling scheme rather than in the intrinsic nucleon moments (cf. § VIIIc.i). In these cases, the coupled model simultaneously improves the agreement with both the magnetic moments and the beta decay data (cf. Table XXIX).

V. Quadrupole Moments.

The magnitude of the electric quadrupole moments reveals directly their collective origin (CASIMIR, 1936). At the same time, the trends are strongly correlated with the nuclear shell structure (GORDY, 1949; HILL, 1949; TOWNES, FOLEY and LOW, 1949; ROSENFELD, 1951). These dual aspects of the quadrupole moments find their explanation in the coupling between the particle motion and the surface deformations (RAINWATER, 1950).

The importance of the deformations for the whole dynamics of nuclear states implies intimate correlations between quadrupole moments and many other nuclear properties.

a) Shell Model Moments.

A single proton contributes a quadrupole moment

$$Q_j = < r^2 \, (3 \cos^2 \vartheta - 1) >_{m=j} = - \frac{2j-1}{2\,(j+1)} < r^2 >, \qquad \text{(V.1)}$$

where the mean value of r^2, although depending somewhat on n and l, is of the order of $3/5\, R_0^2$. A single hole in a proton shell yields a quadrupole moment equal to (1), but of opposite sign. For a single-neutron state, the quadrupole moment comes only from the recoil and is Z/A^2 times the above value.

For configurations with several equivalent protons coupling to a total J, the quadrupole moment is usually somewhat smaller than the single-particle value. Examples of such configurations are listed in Table VIII. For configurations involving both neutrons and protons, the values of Q_J are given in Table III for those configurations which lead to unique charge symmetrized wave functions.

TABLE VIII. Quadrupole moments for $(j)^3$ proton configurations.

J \ $(j)^3$	$(5/2)^3$	$(7/2)^3$	$(9/2)^3$
3/2	0	−3/5	−1/5
5/2	0	13/14	−1/42
7/2		1/3	121/90
9/2	0	−5/11	+0.58 −0.73
11/2		5/49	2/39
13/2			11/60
15/2		5/7	−7/102
17/2			7/15
21/2			7/6

The table lists the ratio of the quadrupole moment Q_J of the state $(j)^3_J$ to the value of Q_j (cf. V.1). The configuration $(9/2)^3$ has two states with $J = 9/2$ and the quadrupole moments listed are the extreme values obtainable by combination of the two states. From the values of Q_J one can also calculate the effective particle-surface coupling constants k_J given by (II.31).

In Fig. 9 are plotted the measured quadrupole moments of odd-A nuclei in units of $|Q_j|$. In the case of odd-neutron nuclei, the value of $|Q_j|$ for a corresponding proton is used as a unit. The most conspicuous feature of the figure is the magnitude of $|Q/Q_j|$ which, in most cases, exceeds 2 and which, in some regions, reaches values of 20 or more. Moreover, odd-neutron nuclei have Q-values comparable to those of corresponding odd-proton nuclei. Shell structure is also apparent in Fig. 9, especially in the expected change from positive to negative Q at the major shell closings.

b) Moments of the Coupled System.

In the coupled model, the total nuclear quadrupole moment becomes

$$Q = Q_p + Q_S \tag{V.2}$$

of which the first part is associated with the particle structure. The second part is due to the surface deformation and is given by (cf. II.2)

$$Q_S = \frac{3}{\sqrt{5\pi}} Z R_0^2 < \alpha_0 >_{M=I} \tag{V.3}$$

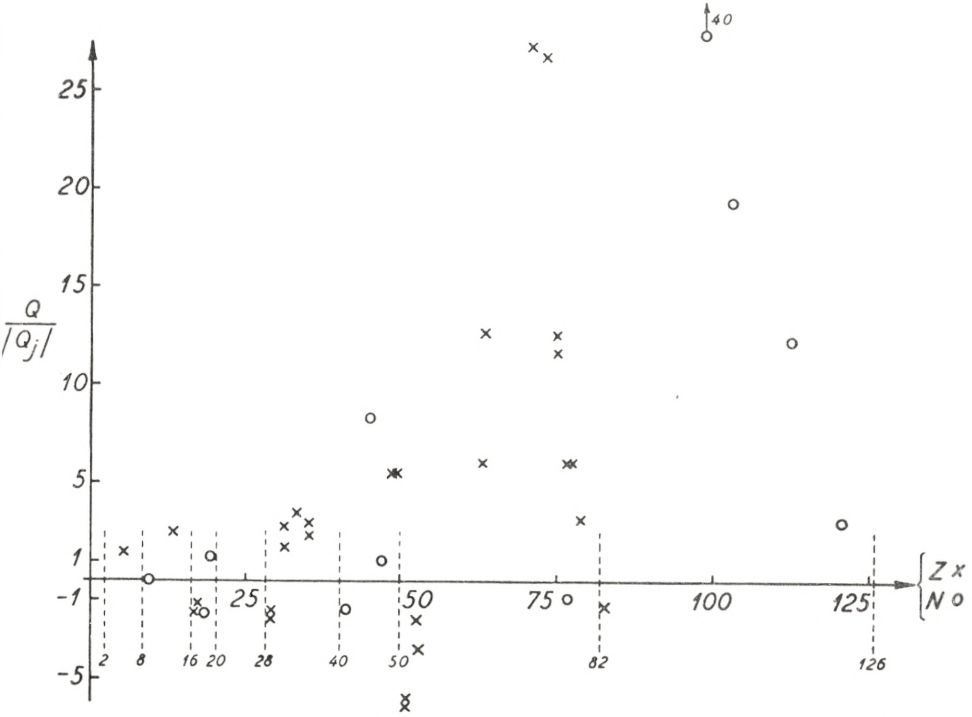

Fig. 9. *Quadrupole moments of odd-A nuclei.* Quadrupole moments, measured in units of the moment Q_j of a single-proton state with $j = I$ (cf. (1)), are plotted for odd-A nuclei with $A > 8$ as a function of Z (odd-proton nuclei) or N (odd-neutron nuclei). Similar diagrams have been given by GORDY (1949) and by TOWNES, FOLEY and LOW (1949). The experimental data are taken from the references given in the Addendum.

in the hydrodynamic approximation, where the nucleus is considered as an incompressible uniformly charged structure.

Quadrupole moments can be obtained from the various solutions of the coupled system considered in § IIb and § IIc. Thus, in first order perturbation approximation, the value of Q_S induced by a single particle may be found from (II.9) and (V.3) by considering only the α_0-part of the interaction. The matrix elements of α_0 and Y_0 are given by (A.38, 76, 77, and 78) and one obtains

$$Q_S = -\frac{3}{4\pi}\frac{2I-1}{2(I+1)}\frac{k}{C}ZR_0^2. \qquad \text{(V.4)}$$

The presence of near-lying single-particle levels does not influence this result to first order in k.

In strong coupling, we have (cf. A. 11 and 12)

$$\alpha_0 = \beta \cos\gamma \left(\frac{3}{2}\cos^2\theta - \frac{1}{2}\right) + \frac{\sqrt{3}}{2}\beta \sin\gamma \sin^2\theta \cos 2\psi. \qquad \text{(V.5)}$$

For the wave function (II.15), only the first term in (5) contributes to Q_S, and one obtains

$$Q_S = \frac{3K^2 - I(I+1)}{(I+1)(2I+3)} Q_0, \qquad \text{(V.6)}$$

where

$$Q_0 = \frac{3}{\sqrt{5\pi}} ZR_0^2 < \beta \cos\gamma > \qquad \text{(V.7)}$$

gives the intrinsic quadrupole moment, measured with respect to the nuclear axis (cf. (Ap. III.10) for the special case of $j = 3/2$).

In the limit of strong coupling, we may replace β and γ by their equilibrium values. From the estimate (II.22) for β we get, for the ground state, $I = K = \Omega$; $\gamma = \pi$, (cf. FEENBERG and HAMMACK, 1951; GALLONE and SALVETTI, 1951, 1951a)

$$Q_0 = -\frac{3}{4\pi} \frac{2I-1}{2(I+1)} \frac{k}{C} ZR_0^2 \qquad \text{(V.8)}$$

for the intrinsic quadrupole moment. This result is just equal to the perturbation value (4) for the total surface moment.

The factor preceding Q_0 in (6) is a projection factor P_Q relating the quadrupole moment of a given rotational state of a symmetric top to its intrinsic moment. For the ground state, $I = K$, its value is (cf. A. BOHR, 1951)

$$P_Q = \frac{I}{I+1} \frac{2I-1}{2I+3}. \qquad \text{(V.9)}$$

In a similar way, the contribution of the particles in strong coupling is reduced by the factor P_Q. The significance of P_Q is apparent for states of $I = 0$ or $1/2$, where the nucleus, although it may possess an intrinsic asymmetry Q_0, exhibits a spherically symmetric charge distribution ($Q = 0$).

In intermediate coupling, it is convenient to write the quadrupole moment as

$$Q_S = P_Q(x)\, Q_0, \qquad \text{(V.10)}$$

where Q_0 is given by (8) for a one-particle configuration with $j = I$. The projection factor $P_Q(x)$ is then unity for $x \ll 1$ and approaches the value (9) for $x \gg 1$.

The behaviour of the quadrupole moment for intermediate coupling may be studied for the case $I = j = 3/2$ by means of the wave function illustrated in Fig. 4. Moreover, from the solution of the coupled system valid for $I = j \gg 1$ (cf. Ap. IV), one obtains

$$P_Q(x) = 1 - 3\frac{2I+1}{(I+1)(2I+3)}\frac{x^2}{\sqrt{x^4+\frac{4}{9}}} \qquad \text{(V.11)}$$

correct to terms of order I^{-1}.

The gradual transition from weak to strong coupling is illustrated in Fig. 10.

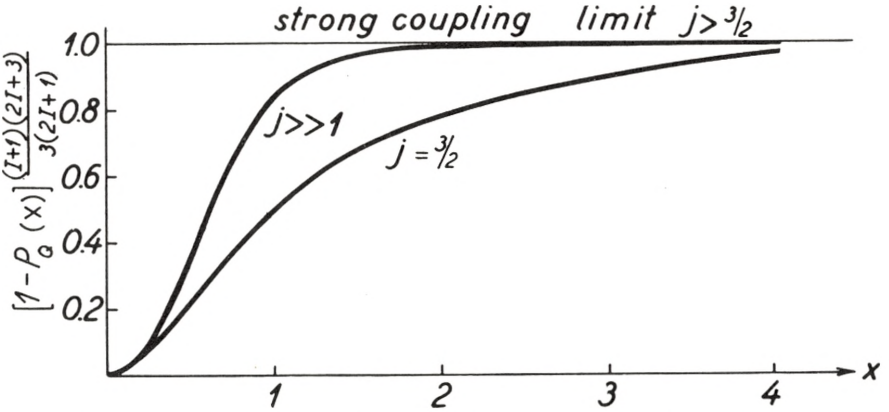

Fig. 10. *Projection factor for quadrupole moments in the coupled system.* The modification in the nuclear coupling scheme, arising from the interaction of the particle with the surface, implies a reduction in the surface quadrupole moment, as compared with that induced by a particle with $m_j = j$. This reduction is expressed by the projection factor $P_Q(x)$ (cf. (10)) which depends on the coupling strength x (cf. (II.14)). For weak coupling ($x \ll 1$), $P_Q \approx 1$ while, in the limit of strong coupling, P_Q approaches the value (9) for $j > 3/2$. In strong coupling, the particle has $\Omega = j$ (cf. Fig. 3) and thus induces the full quadrupole moment with respect to the nuclear coordinate system. The projection factor P_Q then gives the reduction of this intrinsic quadrupole moment Q_0 caused by the deviation of the nuclear axis from the fixed z-axis.

The figure illustrates the gradual development of the projection factor for $j \gg 1$ (cf. (11) and Ap. IV) and for $j = 3/2$ (obtained from Fig. 4). The strong coupling solution for $j = 3/2$ discussed in Ap. III.ii indicates that the curve for $j = 3/2$ may approach a value somewhat in excess of unity, for large x.

c) Discussion of Empirical Data.

The coupling between particle motion and surface deformations provides a mechanism capable of producing nuclear quadrupole moments of the observed order of magnitude (RAINWATER, 1950). In this way, one can account for important trends in the empirical data, in particular the rapid increase of quadrupole moments with A, and the comparable magnitudes of moments of neighbouring odd-proton and odd-neutron nuclei. Also the increase of the moments, as one moves away from closed-shell configurations, which leads to maximum values in the middle of shells, is a direct consequence of the increase in the coupling associated with many-particle configurations (cf. § IIc.ii).*

The empirical quadrupole moments provide valuable evidence on the nuclear deformability and its dependence on shell structure. Thus, it is found that closed-shell nuclei, as expected (cf. Ap. I), possess a much greater stability against surface deformations than is indicated by the hydrodynamic surface tension. For both ${}_8O^{17}$ and ${}_{83}Bi^{209}$, the empirical quadrupole moments are of the order of the single-particle moments and more than ten times smaller than the values estimated from the surface deformation.

The interpretation of these moments as reflecting a sharply decreased deformability is supported by other evidence. Thus, the first excited state of ${}_{82}Pb^{208}$ has an energy about twice the hydrodynamical phonon energy, and the first excited state of ${}_8O^{17}$ has the anomalous $(0+)$ character (cf. § VIc.i). Moreover, the magnetic moment of ${}_8O^{17}$ is very close to the single-particle value; in this respect, ${}_{83}Bi^{209}$ forms an exception, exhibiting a large moment shift of still unexplained origin (cf. p. 81).

The quantitative estimate of quadrupole moments depends sensitively on the assumed surface properties as well as on the details of the particle configuration. However, even a rather crude analysis of the empirical data reveals significant shortcomings of the hydrodynamical model. Thus, for nuclei whose

* PFIRSCH (1952) has discussed the trends of quadrupole moments, but it appears that the states considered do not in general represent nuclear ground states, both because $\Omega \neq I$ and because the chosen configurations do not fill the lowest particle orbitals.

odd structure is that of a single particle, it is found that the hydrodynamical estimate of the quadrupole moment produced by this single particle, with neglect of the deforming influence of the even structure, is already considerably in excess of the observed value.

The comparison* is shown in Table IX. The values of Q_0, listed in column five, are obtained from (8), using the deformabilities of Fig. 1. For a single-particle configuration, the hydrodynamical estimate leads to an intermediate coupling situation (cf. p. 25), and the values of the projection factor $P_Q(x)$, in column seven, are therefore not the full strong coupling values (9), but have been estimated from Fig. 10.** The resultant Q_{hydr} in the next to last column includes the contribution from the particle moment listed in column eight.

The assumption of a single-particle configuration with a constant j in most cases considerably underestimates the deformation; thus, the interaction of neighbouring particle orbitals may increase the coupling strength, and the even structures also in general contribute to the deformation. The resulting approach to the strong coupling scheme, which is also indicated by many other nuclear properties, at the same time implies a decrease in the projection factor.

In spite of the difficulty of a detailed estimate of these effects, it seems clear from the comparison in Table IX that the hydrodynamical values of Q are in general larger than the empirical ones by at least a factor two.

This deficiency of the hydrodynamical model is consistently exhibited by all nuclear properties related to quadrupole moments (cf. § VIc.ii and also p. 75), and gives an important indication as to how the collective properties of the nucleus differ from those of an idealized liquid drop. It seems most likely that

* A comparison of empirical quadrupole moments with those induced by a single particle has been given by VAN WAGENINGEN and DE BOER (1952). These authors find similar Q_0-values to those listed in Table IX, but have used the limiting values (9) for P_Q and thereby obtained appreciably smaller values for Q, than those resulting from the consistent one-particle hydrodynamical approximation employed in Table IX.

** Note added in proof: The projection factors employed in Table IX are in agreement with the recent, more detailed, intermediate coupling calculations by D. C. CHOUDHURY (cf. footnote on p. 24).

TABLE IX. Comparison of quadrupole moments with hydrodynamic estimates.

Nucleus	Configuration		I	Q_0	x	$P_Q(x)$	Q_{sp}	Q_{hydr}	Q_{obs}
	protons	neutrons							
$_5B^{11}$	$(p_{3/2})^{-1}$	—	3/2	+0.07	0.71	0.7	+0.023	+0.06	+0.06
$_8O^{17}$	—	$d_{5/2}$	5/2	−0.20	0.56	0.8	−0.0013	−0.16	−0.005
$_{13}Al^{27}$	$(d_{5/2})^{-1}$	—	5/2	+0.32	0.56	0.8	+0.065	+0.30	+0.16
$_{16}S^{33}$	—	$d_{3/2}$	3/2	−0.31	0.73	0.7	0	−0.22	−0.08
$_{16}S^{35}$	—	$(d_{3/2})^{-1}$	3/2	+0.31	0.73	0.7	0	+0.22	+0.06
$_{17}Cl^{35}$	$d_{3/2}$	$(d_{3/2})^2$	3/2	−0.32	0.73	0.7	−0.055	−0.26	−0.084
$_{17}Cl^{37}$	$d_{3/2}$	—	3/2	−0.32	0.73	0.7	−0.055	−0.26	−0.066
$_{29}Cu^{63}$	$p_{3/2}$	$(p_{3/2}, f_{5/2})^{-4}$	3/2	−0.61	0.76	0.7	−0.08	−0.48	−0.13
$_{29}Cu^{65}$	$p_{3/2}$	$(p_{3/2}, f_{5/2})^{-2}$	3/2	−0.61	0.76	0.7	−0.08	−0.48	−0.12
$_{31}Ga^{69}$	$(p_{3/2})^{-1}$	—	3/2	+0.67	0.77	0.7	+0.08	+0.53	+0.24
$_{31}Ga^{71}$	$(p_{3/2})^{-1}$	—	3/2	+0.67	0.77	0.7	+0.08	+0.53	+0.15
$_{32}Ge^{73}$	$(p_{3/2}, f_{5/2})^4$	$g_{9/2}$	9/2	−1.3	0.45	0.9	0	−1.2	−0.2
$_{49}In^{113}$	$(g_{9/2})^{-1}$	$(d_{5/2}, g_{7/2}, h_{11/2})^{14}$	9/2	+2.4	0.51	0.9	+0.21	+2.4	+1.18
$_{49}In^{115}$	$(g_{9/2})^{-1}$	$(d_{5/2}, g_{7/2}, h_{11/2})^{16}$	9/2	+2.4	0.51	0.9	+0.21	+2.4	+1.20
$_{51}Sb^{121}$	$d_{5/2}$	$(d_{5/2}, g_{7/2}, h_{11/2})^{20}$	5/2	−2.1	0.68	0.7	−0.17	−1.5	−1.0
$_{51}Sb^{123}$	$g_{7/2}$	$(d_{5/2}, g_{7/2}, h_{11/2})^{22}$	7/2	−2.4	0.58	0.8	−0.20	−2.1	−1.2
$_{83}Bi^{209}$	$h_{9/2}$	—	9/2	−6.7	0.68	0.8	−0.32	−5.6	−0.4

The table lists nuclei with measured quadrupole moments, whose odd structure is that of a single particle or hole. The intrinsic quadrupole moment Q_0 in column five is calculated from (V.8). In column six are listed the coupling strengths obtained from (II.14), while in column seven is given an estimate of the projection factor, based upon Fig. 10. The resultant hydrodynamic estimate of Q appears in column nine; in this estimate, the contribution from the particle moment, listed in column eight, has been included. For reference to Q_{obs}, cf. the Addendum.

the empirical data are to be interpreted as indicating that the quadrupole moment associated with a given deformation is overestimated by the hydrodynamical formula (3). Part of the discrepancy may also arise from an underestimate of the mass parameter B (cf. p. 13), in which case the coupling situation for a given deformation would be closer to the strong coupling limit with a resultant smaller projection factor P_Q.

Ratios of quadrupole moments of neighbouring isotopes often do not depend on the specific properties of the collective deformations, and may provide direct evidence on nuclear coupling schemes. Thus, for example, the decrease of Q from $_{17}Cl^{35}$ to

$_{17}Cl^{37}$, the latter with a closed neutron structure, indicates a coupling scheme in $_{17}Cl^{35}$ rather closer to the strong surface coupling than to that produced by particle forces (cf. p. 74).

d) Correlations with Other Nuclear Properties.

The important role of the surface deformation for the structure of nuclear states implies that many nuclear properties follow trends similar to the quadrupole moments and in particular reflect the increasing deformations as one moves away from closed shells. In some cases, there exist simple quantitative correlations.

Intimately connected with the large quadrupole moments are the low-lying nuclear rotational states with their characteristic properties (cf. § VI c.ii). From the lifetimes of these states (§ VII c.iii) or their excitation cross-sections (Ap. VI) one can directly determine the intrinsic quadrupole moment Q_0. The values obtained are just of the magnitude deduced from the spectroscopic Q-values (cf. Table XXVII). The comparison shows that the relationship between Q and Q_0 corresponds to a rather fully developed strong coupling (cf. 9), as is expected for the large deformations in question.

The study of transition probabilities between rotational states thus provides an additional means of determining nuclear quadrupole moments. Since the method also makes possible the determination of deformations in nuclei whose ground states have $I = 0$ or $1/2$, and therefore $Q = 0$, it may add considerably to our knowledge of nuclear deformations.

The excitation energies of the rotational states also depend on the nuclear deformation (§ VI c.ii) and have been observed to exhibit trends parallel to those of the quadrupole moments (Ford, 1953; cf. also Table XXIII).

There is a tendency for large quadrupole moments to be associated with relatively large deviations of the magnetic moments from single-particle values (cf., e. g., Kopfermann, 1951; Miyazawa, 1951 a). The observed correlations can be understood in terms of the magnetic moment shifts arising from the surface coupling (cf. discussion on p. 71).

Certain anomalies in the effective radius of the nuclear charge distribution, derived from spectroscopic isotope shifts, can be related to the observed quadrupole moments (BRIX and KOPFERMANN, 1949). In particular in Eu, the exceptionally large isotope shifts can be attributed to the great difference in the quadrupole moments of the two isotopes (BRIX and KOPFERMANN, 1952). The analysis indicates a relation between Q and Q_0 rather close to that of the strong coupling limit (cf. p. 77).

Addendum to Chapters IV and V.

Details of the Analysis of Nuclear Moments.

In this Addendum, we shall attempt a somewhat detailed analysis of nuclear moments on the basis of the coupled model. The main conclusions of this analysis have been summarized in the preceding chapters (§ IVc and § Vc).

Many of the features of the moments are specific to the configuration in question, and we therefore divide the odd-A nuclei according to spin and parity and consider each group separately. The discussion is confined to nuclei with $A > 8$ (cf. footnote on p. 38).

The tables of empirical moments are based on MACK (1950) and KLINKENBERG (1952) whose compilations we have attempted to bring up to date. The values listed represent what appears to be the most accurate determination, but at the most two significant decimals are quoted. Unless otherwise noted, references to the original experiments can be found in the above compilations.

The magnetic moments include diamagnetic corrections (DICKINSON, 1950) and the quadrupole moments have been corrected for the polarization effect (STERNHEIMER, 1951, 1952). As an aid in the assessment of the reliability of the quoted quadrupole moments, the method of determination is indicated by the letters A, M, and C, referring to atoms, molecules, and crystals, respectively.

i. $(1/2+)$ *nuclei.*

Although states of $I = 1/2$ have no spectroscopically measurable quadrupole moment to reveal directly the deformation of the nucleus, the magnetic moments as well as other nuclear properties (level order, cf. below, and β-decay, cf. § VIIIc) give

Table X. Moments of $(1/2+)$ nuclei).

odd proton ($\mu_{sp} = 2.79$)		odd neutron ($\mu_{sp} = -1.91$)	
nucleus	μ	nucleus	μ
$_{9}F^{19}$	2.63	$_{14}Si^{29}$	−0.56
$_{15}P^{31}$	1.13	$_{48}Cd^{111}$	−0.59
$_{81}Tl^{203}$	1.61	$_{48}Cd^{113}$	−0.62
$_{81}Tl^{205}$	1.63	$_{50}Sn^{115}$	−0.92
		$_{50}Sn^{117}$	−1.00
		$_{50}Sn^{119}$	−1.05
		$_{52}Te^{123}$	−0.74
		$_{52}Te^{125}$	−0.89
		$_{54}Xe^{129}$	−0.78

evidence of the influence of the surface coupling. Direct information on the intrinsic nuclear deformation could be obtained from energies, and especially from lifetimes or excitation cross-sections, for rotational states in these nuclei (cf. § VI c.iii).

The empirical moments of nuclei of this type show peculiar variations, as seen from Table X. Thus, for F^{19}, $\mu \approx \mu_{sp}$, while for P^{31} and Si^{29} in the same shell, very pronounced moment shifts are observed. In this region, the available single-particle orbitals are $d_{5/2}$, $s_{1/2}$ and, a little higher, $d_{3/2}$.

The interaction of these states gives rise to a large surface coupling which makes it appropriate to consider the nuclei in the strong coupling approximation.* The state χ_Ω of the last odd particle with $\Omega_p = 1/2$ then corresponds to the lowest proper value of the matrix (cf. II.26 and Ap. III.1),

$$W' = \begin{pmatrix} 0 & 0 & 0 \\ 0 & \Delta_{3/2} & 0 \\ 0 & 0 & \Delta_{5/2} \end{pmatrix} + k\beta\cos\gamma \sqrt{\frac{5}{4\pi}} \frac{1}{35} \begin{pmatrix} 0 & 7\sqrt{2} & -7\sqrt{3} \\ 7\sqrt{2} & -7 & \sqrt{6} \\ -7\sqrt{3} & \sqrt{6} & -8 \end{pmatrix} \quad \text{(Ad. 1)}$$

where $\Delta_{3/2}$ and $\Delta_{5/2}$ are the energies of the $d_{3/2}$ and $d_{5/2}$ states with respect to the $s_{1/2}$ level. There are additional terms in the nuclear potential energy arising from the surface tension and from the coupling energies of even groups of particles. While these terms are needed for the determination of the equilibrium

* The moment shift arising from the $s_{1/2} - d_{3/2}$ interaction in strong coupling has also been considered by DAVIDSON and FEENBERG (1953).

deformation, they do not otherwise influence the magnetic moment of the nucleus. There are also rotational energy terms (II.30) which may be of significance, especially in light nuclei; they may here be considered as giving additional contributions to the diagonal elements Δ in (1).

The magnetic moment of the state may be written

$$\mu = a_s^2 \mu_s + a_d^2 \mu_d, \tag{Ad. 2}$$

where a_s^2 and a_d^2 are the probabilities of the s and d states, respectively, ($a_d^2 = a_{3/2}^2 + a_{5/2}^2$). The moments μ_s and μ_d are given by (cf. IV.3, II.19, and Ap. III.2; cf. also footnote on p. 44).

$$\left.\begin{aligned} \mu_s = \mu_{sp} &= \begin{Bmatrix} 2.79 \\ -1.91 \end{Bmatrix} \\ \mu_d = a_d^{-2} \Bigg[&\begin{Bmatrix} 1.94 \\ -1.19 \end{Bmatrix} a_{5/2}^2 - \begin{Bmatrix} 2.98 \\ -2.50 \end{Bmatrix} a_{5/2} a_{3/2} + \begin{Bmatrix} 0.41 \\ -0.07 \end{Bmatrix} a_{3/2}^2 \Bigg] \end{aligned}\right\} \tag{Ad. 3}$$

where, in the curly brackets, the upper value refers to a proton, the lower value to a neutron. In Fig. 11, the value of μ_d is plotted as a function of

$$y = \frac{a_{3/2}}{a_{5/2}}. \tag{Ad. 4}$$

The asymmetry with respect to $y = 0$ is due to the interference terms in (3).

In the region just after O^{16}, the value of $\Delta_{5/2}$ is small compared to the surface coupling (cf., e. g., the level inversion of F^{19}, discussed below) and will therefore be neglected in (1). On the other hand, $\Delta_{3/2}$ is large (~ 5 MeV; cf. KOESTER, JACKSON and ADAIR, 1951). If we ignore the influence of the $d_{3/2}$ state, the resultant state χ_Ω is independent of the parameters of the model and corresponds to $a_s^2 \approx 0.5\, a_d^2$ and $y = 0$.

Even a small $d_{3/2}$ admixture may, however, have a rather large effect on μ_d, due to the interference term. The effect depends essentially on the sign of y (cf. Fig. 11), which is determined by the sign of $\cos\gamma$. In the beginning of the combined $d_{5/2} - s_{1/2}$ shell, it is found that the lowest state has $\Omega = 1/2$ and $\gamma = 0$, corresponding to negative y, and one therefore expects $\mu \approx \mu_{sp}$. At the end of the shell, we have $\gamma = \pi$ and

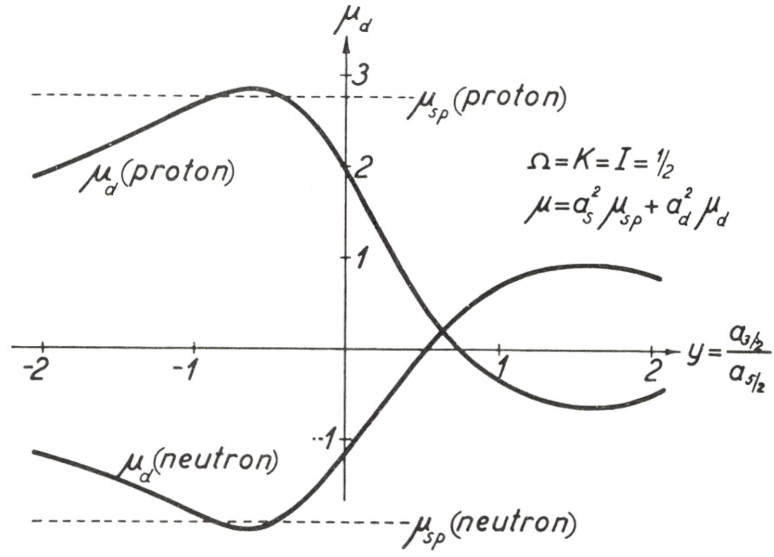

Fig. 11. *Magnetic moments arising from d-state admixture in* $I = \Omega = 1/2$ *states.* In the absence of surface coupling, these states would be pure $s_{1/2}$, but the coupling may introduce large amplitudes of neighbouring particle orbitals, especially d states. In the region after O^{16}, the $s_{1/2}$ and $d_{5/2}$ states are close-lying and one obtains, in strong coupling, $a_s^2 \sim \frac{1}{3}$ and $a_d^2 \sim \frac{2}{3}$. The $s_{1/2}$ state part of the magnetic moment remains equal to the single-particle value, but the d state moment is very sensitive to a small admixture of $d_{3/2}$ state. The figure gives μ_d as a function of the relative amplitude y of the $d_{3/2}$ state, which can be obtained from (1). The strong asymmetry of μ_d with respect to $y = 0$ implies that the moment is especially sensitive to the sign of y, which again depends on the sign of the deformation ($y < 0$ for $\gamma = 0$; $y > 0$ for $\gamma = \pi$).

positive y, and very large moment shifts, of one or two magnetons, may occur.

Thus, the striking difference between the F, and the Si and P moments may be understood in terms of the opposite shapes of the nuclear surface. The moment of F^{19} with a single proton ($y < 0$) can be approximately accounted for by any deformation $\beta \gtrsim 0.1$. In the case of P^{31} and Si^{29}, where the odd configuration is that of a single hole, the μ-values are more sensitive to y, and the empirical moments indicate $y \approx 0.5$. Such a value of y would be obtained, if $\Delta_{3/2} \sim 5$ MeV, for a deformation of $\beta \sim 0.4$ (cf. Table VII). A deformation of this order of magnitude is consistent with the hydrodynamical values for the surface parameters.

A perturbation calculation of the effects of the surface coupling on the magnetic moments gives similar characteristic differences between F^{19} and P^{31}, due to the influence of the $d_{5/2} - d_{3/2}$ interference. However, the magnitude of the observed shifts shows that we are outside the perturbation region and indicates that the strong coupling situation may be approximately realized.

The level shifts arising from the coupling of the $s_{1/2}$ and $d_{5/2}$ levels to the surface may explain the difference in ground state spin between F^{17} ($I = 5/2$) and F^{19} ($I = 1/2$). The comparison of the coupling energy (1) for $\Omega = 1/2$ with that corresponding to $\Omega = 5/2$ shows that the surface coupling favours the spin $I = 1/2$. Thus, the increased deformation in F^{19} as compared with F^{17}, resulting from the addition of the two neutrons, depresses the $I = 1/2$ level with respect to the $I = 5/2$ level.

In the case of Tl^{203} and Tl^{205}, the $s_{1/2}$ and $d_{3/2}$ states are near-lying, while the $d_{5/2}$ state is about an MeV lower. The equilibrium shape is expected to be $\gamma = \pi$ and, if one first ignores the influence of the $d_{5/2}$ state, one finds $a_s^2 = 0.5\, a_d^2$, which corresponds to a magnetic moment $\mu = 1.20$. However, the presence of the $d_{5/2}$ state will tend to increase the moment somewhat (leads to large negative values of y). Similarly, the expected small negative value of $\Delta_{3/2}$ increases a_s^2 and thereby also the moment.

The remaining nuclei, listed in Table X, cannot be studied in as much detail as the above cases due to lack of knowledge of configuration assignments.

ii. $(1/2-)$ *nuclei.*

A striking feature of the empirical moments of this type of nuclei, as compared with all other types, is the close grouping of the values (cf. also Figs. 7 and 8). Apart from the two lightest nuclei, N^{15} and C^{13}, the moments are closely clustered around the values $\mu = -0.12$ for odd proton nuclei, and $\mu = +0.56$ for odd neutron nuclei.

This characteristic feature is a simple consequence of the present model and is largely independent of the coupling. The main interacting states which produce the coupling to the surface are here $p_{3/2}$ and $f_{5/2}$. In perturbation approximation one obtains, from (IV. 7) and Table V, the resulting shift

$$\delta\mu = \begin{Bmatrix} -0.22 \\ +0.18 \end{Bmatrix} \left(\frac{\hbar\omega}{\hbar\omega + |\Delta_{3/2}|}\right)^2 x^2 + \begin{Bmatrix} 0.22 \\ -0.18 \end{Bmatrix} \left(\frac{\hbar\omega}{\hbar\omega + |\Delta_{5/2}|}\right)^2 x^2. \quad \text{(Ad. 5)}$$

Except for N^{15} and C^{13}, one expects $\Delta_{3/2} \sim \Delta_{5/2} \lesssim \hbar\omega$, and so the moment shift practically vanishes.

A similar situation is found when the coupling is strong. The potential energy matrix is then the same as (1), and $\delta\mu$ takes the form

$$\delta\mu = -\begin{Bmatrix} 0.55 \\ -0.45 \end{Bmatrix} a_{3/2}^2 + \begin{Bmatrix} 0.37 \\ -0.30 \end{Bmatrix} a_{5/2}^2. \quad \text{(Ad. 6)}$$

Diagonalizing W' under the assumption $\Delta_{3/2} \sim \Delta_{5/2}$, one finds that, irrespective of Δ, the ground state has $a_{3/2}^2 \sim 0.67\ a_{5/2}^2$, so that $\delta\mu$ practically vanishes.

The absence of a near-lying $f_{5/2}$ state in C^{13} and N^{15} implies a small moment shift outwards from the main group, as is observed. For these nuclei, the large separation of the $p_{1/2}$ level from the combining $p_{3/2}$ level implies a rather weak coupling and from (5) one obtains shifts of the order of 0.1 magneton, assuming $\Delta_{3/2} \sim -5$ MeV and hydrodynamical surface parameters. A similar effect would be obtained in strong coupling (cf. Table VII).

Although the surface coupling thus accounts for the relative values of the observed moments, the position of the main group of empirical values does not quite coincide with the single-particle moment, which might be expected from the above calculations. There thus exists a small residual moment shift, common to all these nuclei, and it is tempting to consider the pos-

TABLE XI. Moments of (1/2 —) nuclei.

odd proton ($\mu_{sp} = -0.26$)		odd neutron ($\mu_{sp} = +0.64$)	
nucleus	μ	nucleus	μ
$_{7}N^{15}$	−0.28	$_{6}C^{13}$	0.70
$_{39}Y^{89}$	−0.14	$_{34}Se^{77}$	0.53 **
$_{45}Rh^{103}$	−0.10 *	$_{70}Yb^{171}$	0.5
$_{47}Ag^{107}$	−0.11	$_{78}Pt^{195}$	0.61
$_{47}Ag^{109}$	−0.13	$_{80}Hg^{199}$	0.50
		$_{82}Pb^{207}$	0.59

* KUHN and WOODGATE (1951).
** DHARMATTI and WEAVER (1952a).

sibility that we may here be observing an interaction effect of the type mentioned on p. 51. This interpretation would require that the individual nucleons embedded in nuclear matter suffer a reduction in the magnitude of their intrinsic magnetic moments of $\delta\mu_s \sim 0.3$ nuclear magnetons.

iii. (3/2 —) *nuclei.*

TABLE XII. Moments of (3/2 —) nuclei.

odd proton ($\mu_{sp} = 3.79$)			odd neutron (μ_{sp}) $= -1.91$		
nucleus	μ	Q	nucleus	μ	Q
$_5B^{11}$	2.69	+0.06 (M) *	$_4Be^9$	−1.18	
$_{29}Cu^{63}$	2.23	−0.13 (C)	$_{24}Cr^{53}$	−0.47 §§§	
$_{29}Cu^{65}$	2.38	−0.12 (C)	$_{28}Ni^{61}$	$\lesssim(\pm)0.2$ §	
$_{31}Ga^{69}$	2.02	+0.24 (A)	$_{76}Os^{189}$	+0.7 §§	+2 (A) §§
$_{31}Ga^{71}$	2.56	+0.15 (A)	$_{80}Hg^{201}$	−0.56	+0.5 (A)
$_{33}As^{75}$	1.44	+0.3 (A) †			
$_{35}Br^{79}$	2.11	+0.34 (A) ††			
$_{35}Br^{81}$	2.27	+0.28 (A) ††			
$_{37}Rb^{87}$	2.75				

* DEHMELT (1952).
† MURAKAWA and SUWA (1952).
†† KING and JACCARINO (1953).
§ KESSLER (1950).
§§ MURAKAWA and SUWA (1952 a).
§§§ ALDER and HALBACH (1953) (added in proof).

In the first $p_{3/2}$ shell, the moments seem to give some indication of deviations from (*jj*) coupling (cf. also INGLIS, 1952 and KURATH, 1952 a). The description of B^{11} as a single $p_{3/2}$ hole, coupled to the surface, does imply a rather large moment shift, but in order to account for the observed moment, a coupling strength of $x \sim 3$ is required (cf. Fig. 5 and (IV.5)). This value of x is several times larger than the hydrodynamical estimate, which may reflect a partial breaking up of the $p_{3/2}$ shells. For Be^9, with a $((p_{3/2})^{-2}; (p_{3/2})^{-1})$ configuration, the observed moment is close to that expected in the absence of surface coupling ($\mu_p = -1.15$; cf. Table III). However, a perturbation estimate as well as the strong coupling treatment (cf. Ap. III.ii) indicate that the surface coupling should produce a reduction in the magnitude of the moment by a few tenths of a magneton (cf. Table VII).

In the higher $p_{3/2}$ shells, a strong interaction is expected between the neighbouring $p_{3/2}$ and $f_{5/2}$ levels. While a pure $j = 3/2$ state has the anomalous strong coupling behaviour, considered in Ap. III.ii, the $p_{3/2} - f_{5/2}$ interaction may lead to a stabilization of the surface shape and the usual strong coupling scheme. For a single $p_{3/2} - f_{5/2}$ particle, the $\Omega = 3/2$ state with

$$W' = \begin{pmatrix} 0 & 0 \\ 0 & \Delta_{5/2} \end{pmatrix} + k\beta \cos\gamma \sqrt{\frac{5}{4\pi}} \frac{1}{35} \begin{pmatrix} 7 & 6 \\ 6 & -2 \end{pmatrix} \qquad \text{(Ad. 7)}$$

is expected to represent the ground state if $\Delta_{5/2} > 0$. For small values of $\Delta_{5/2}$, one finds for this state $a_{3/2} \approx 2\,a_{5/2}$. A similar situation is found for a $p_{3/2} - f_{5/2}$ hole if $\Delta_{5/2} < 0$. The magnetic moment for this state is $\mu_c \approx \left\{ \begin{matrix} 2.15 \\ -0.55 \end{matrix} \right\}$. Thus, a rather fully developed strong coupling may account for the moments of Cr^{53}, $Cu^{63, 65}$, and Rb^{87}, whose odd configurations are those of a single particle or hole.

A contribution to the moment may also arise from a small admixture of $f_{7/2}$, due to interference with the $f_{5/2}$ state. This effect may shift the moment by about 0.1 magneton, inwards for a single-particle configuration (Cu and Cr) and outwards for a hole (Rb), and may thus be partly responsible for the relatively large moment of Rb^{87}. The largeness of this moment may also in part reflect the closed neutron structure which is expected to give rise to a lower deformability and thus to a less developed strong coupling situation.

For the other nuclei in this group, which are essentially many-particle configurations, the analysis is more complex. However, it is expected that, during the simultaneous filling of the $p_{3/2}$ and $f_{5/2}$ levels, $\Omega = 3/2$ ground states will occur in which the last odd particle is predominantly of $f_{5/2}$ character. The large moment shift of As^{75} may indicate such a configuration. It is of interest that the corresponding odd-neutron nucleus, Ni^{61}, seems also to have an especially large moment shift.

The (3/2 —) group of nuclei provides interesting evidence on the correlation between quadrupole moments and magnetic moment shifts. This relationship can especially be studied for

isotopic pairs for which the spectroscopic data are most unambiguously compared. It has been suggested that there is, in such cases, an approximate proportionality between $\delta\mu$ and Q (KOPFERMANN, 1951). The examples of this rule among the (3/2 —) nuclei are listed in Table XIII. The existence of an approximate relationship of this type can be understood from the fact that the major part of $\delta\mu$ is attributed to the approach of the moment to the strong coupling value μ_c and that also Q is relatively insensitive to the coupling strength x. While the deformation in-

TABLE XIII. Correlations between magnetic moments and quadrupole moments for (3/2 —) nuclei.

Element	$\delta\mu_A / \delta\mu_{A+2}$	Q_A / Q_{A+2}
$_{29}Cu^{63,\ 65}$	1.11	1.08 *
$_{31}Ga^{69,\ 71}$	1.44	1.59
$_{35}Br^{79,\ 81}$	1.10	1.20 **

* KRÜGER and MEYER-BERKHOUT (1952).
** DEHMELT and KRÜGER (1951).

creases, the projection factor decreases with x (cf. Fig. 10) and the two effects tend to compensate each other in the relevant coupling region. Thus, for two isotopes, the ratios of the $\delta\mu$'s and the Q's are usually both of order unity and differ from this value in the same direction. From this interpretation it is expected, however, that this particular correlation is not of a general character, and, in fact, counterexamples are anticipated (cf. K, p. 75).

Further evidence for a correlation between $\delta\mu$ and Q may be seen in the general tendency, among the (3/2 —) nuclei in the region $29 \leq Z \leq 37$, for large quadrupole moments to accompany large magnetic moment shifts (cf. MIYAZAWA, 1951 a). Moreover, certain trends in the moments can be understood in terms of the expected deformability of the configurations in question. Thus, the two largest magnetic moments are those of Rb^{87} and Ga^{71}, both with closed neutron shells.

iv. $(3/2+)$ *nuclei.*

TABLE XIV. Moments of $(3/2+)$ nuclei.

odd proton ($\mu_{sp} = 0.12$)			odd neutron ($\mu_{sp} = 1.15$)		
nucleus	μ	Q	nucleus	μ	Q
$_{17}Cl^{35}$	0.82	−0.084 (A)	$_{16}S^{33}$	0.64	−0.08 (M)
$_{17}Cl^{37}$	0.68	−0.066 (A)	$_{16}S^{35}$		+0.06 (M)
$_{19}K^{39}$	0.39		$_{54}Xe^{131}$	0.68 †	−0.12 (A) †
$_{19}K^{41}$	0.22		$_{56}Ba^{135}$	0.83	
$_{77}Ir^{191}$	0.16 *	+1 (A) *	$_{56}Ba^{137}$	0.94	
$_{77}Ir^{193}$	0.17 *	+1 (A) *			
$_{79}Au^{197}$	0.14 **	+0.5 (A) ***			
$_{11}Na^{23}$	2.22		$_{10}Ne^{21}$	< 0	

* MURAKAWA and SUWA (1952 a). *** SIEMENS (1951).
** KELLY (1952). † BOHR, KOCH and RASMUSSEN (1952).

The coupling of a pure $d_{3/2}$ state to the nuclear surface has only little effect on the magnetic moment, due to the rather small value of $(g_j - g_R)$. In intermediate coupling, the moment shift can be obtained from Fig. 5 and (IV.5), and in strong coupling, the approximate treatment in Ap. III.ii indicates a limiting moment shift inwards of only a few tenths of a magneton (cf. Figs. 7 and 8).

While a pure $j = 3/2$ state leads to the anomalous strong coupling scheme with no definite equilibrium shape γ (cf. Ap. III.ii), the interaction of neighbouring orbitals or the presence of an even non-closed structure may lead to a stabilization of the nuclear shape at the positions $\gamma = 0$ or π.

If the shape is such that the ground state has $\Omega = 3/2$ ($\gamma = \pi$ for $(d_{3/2})^{+1}$, or $\gamma = 0$ for $(d_{3/2})^{-1}$), the W' matrix is the same as (7), where $\Delta_{5/2}$ is now negative and represents the spin-orbit splitting. In Fig. 12 is plotted the magnetic moment as a function of $z = a_{5/2}/a_{3/2}$, and one sees the characteristic asymmetry resulting from the interference between the spin-orbit partners. With increasing deformation, the moment moves rapidly away from μ_{sp} for a single-particle configuration ($\gamma = \pi$; $z < 0$) and the opposite way for a hole in the $d_{3/2}$ shell ($\gamma = 0$; $z > 0$).

For the opposite shape ($\gamma = 0$ for $(d_{3/2})^{+1}$, or $\gamma = \pi$ for

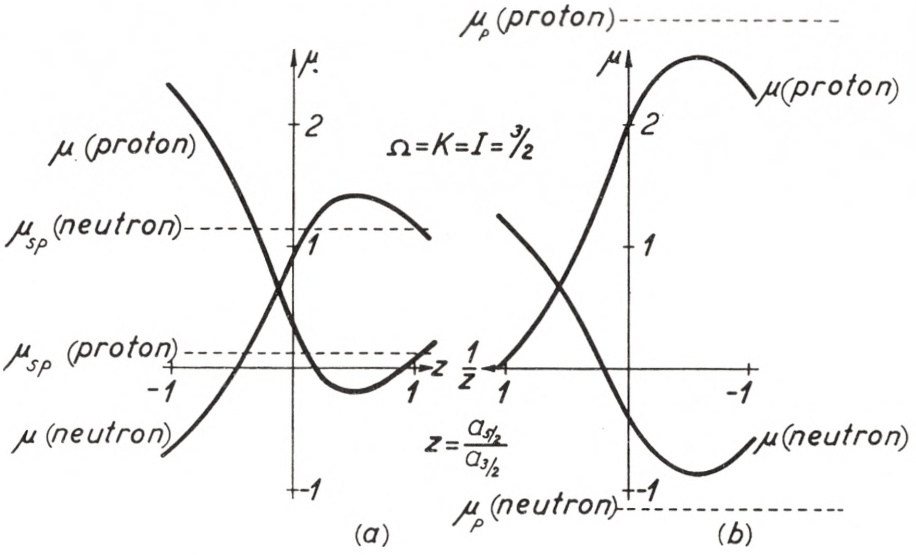

Fig. 12. *Magnetic moments arising from decoupling of spin and orbit in d-states with* $I = \Omega = 3/2$. In states of (3/2+) character, the surface deformation leads to a particle state which is a combination of $d_{3/2}$ and $d_{5/2}$. The figure shows the nuclear magnetic moment for the $I = K = \Omega = 3/2$ state as a function of the ratio of the $d_{5/2}$ and $d_{3/2}$ amplitudes. Fig. 12a gives the moment in the region of predominantly $d_{3/2}$ state and the values μ_{sp} correspond to an uncoupled $d_{3/2}$ nucleon. Fig. 12b gives the moment for a predominantly $d_{5/2}$ state with $\Omega = 3/2$, such as may occur for $(d_{5/2})^3$ configurations. The value of μ_p corresponds to an uncoupled $(d_{5/2})^3{}_{3/2}$ configuration.

$(d_{3/2})^{-1}$), one obtains $K = \Omega = 1/2$, but the ground state still has $I = 3/2$ (cf. II.24). Also the sign of the quadrupole moment is the usual one ($Q < 0$ for $(d_{3/2})^{+1}$ and $Q > 0$ for $(d_{3/2})^{-1}$), since the reversed sign for Q_0 is compensated by a change of sign of the projection factor (V.6). The W' matrix is the same as (1) and the magnetic moment exhibits the same difference between particles and holes as for the $\Omega = 3/2$ state, but the effect is somewhat smaller in magnitude.

The expected trends are found in the empirical magnetic moments which, for the $(d_{3/2})^{+1}$ configurations (S^{33}, $Cl^{35, 37}$, and Xe^{131}), are appreciably shifted inwards with respect to the moments of the $(d_{3/2})^{-1}$ configurations ($K^{39, 41}$, $Ba^{135, 137}$, $Ir^{191, 193}$, and Au^{197}).

In the first $d_{3/2}$ shell, where the level orders are best known, one finds that the coupling to the $d_{5/2}$ and $s_{1/2}$ states favours

the shape $\gamma = \pi$ for the isotopes of S and Cl as well as of K. The presence of two $f_{7/2}$ neutrons in K^{41} further stabilizes this shape. For S^{33} and $Cl^{35, 37}$, the moment values μ_c, listed in Table VII, are obtained from Fig. 12, using $\Delta_{5/2} \sim -5$ MeV, and the observed moments are consistent with a deformation of about $\beta = 0.2$. For $K^{39, 41}$, the μ_c values in Table VII refer to the state ($\gamma = \pi$, $\Omega = 1/2$, $I = 3/2$) and include the influence of the $s_{1/2}$ admixture ($\Delta_{1/2} \sim -5$ MeV).

The influence of a small interaction effect on the nucleon moment, of similar magnitude as that discussed for the (1/2—) nuclei (cf. p. 69), may be indicated by the moment of K^{39}, which is larger by about a tenth of a magneton than the estimated values.

The interpretation of the $K^{39} - K^{41}$ moment differences, as arising from interference with the $d_{5/2}$ level, receives some further support from the measured hyperfine structure anomaly (Ochs, Logan and Kusch, 1950), which gives information on the distribution of the magnetic moment over the nuclear volume (Bohr and Weisskopf, 1950; A. Bohr, 1951a; Eisinger, Bederson and Feld, 1952).

The quadrupole moment ratios in the (3/2+) group provide further interesting information on the coupling scheme. Thus, the decrease of Q from Cl^{35} to Cl^{37} is, as expected, due to the extra deformation caused by the unfilled neutron shell in Cl^{35}, which is also indicated by the observed magnetic moments of these nuclei. The opposite trend would have resulted if the particle forces dominated over the surface coupling, in which case the particle structure in Cl^{35} would have had a quadrupole moment and an effective coupling constant 11/15 times that of Cl^{37} (cf. II.31 and Table III).*

The quadrupole moments of the odd-neutron S isotopes are of the same order of magnitude as those of the neighbouring Cl isotopes, thus confirming the collective nature of these moments. The change of sign of Q from S^{33} to S^{35} is as expected, and the reduction in magnitude can also be understood in terms of the smaller deformability of a shell of 20 than a shell of 16. A determ-

* This conclusion is opposite to that drawn by Flowers (1952c). However, in this case, as well as in others in Table II of this reference, it appears necessary to allow for the difference between adding neutrons at the beginning and end of a shell.

ination of the magnetic moment of S^{35} would be of interest, since its configuration $(d_{3/2})^{-1}$, implies that it should be about a third of a magneton larger than the moment of S^{33}.

As already mentioned, the absolute values of the quadrupole moments of the Cl and S isotopes are considerably smaller than the hydrodynamical estimates (cf. Table IX and the discussion on p. 59). In this connection, it is of interest that the interpretation of the magnetic moments of these nuclei provide independent evidence for appreciable deformations, of the order of those estimated in the hydrodynamical approximation.

Evidence on the quadrupole moments of the K isotopes would be of interest. They are expected to be positive and Q (K^{41}) should be larger than Q (K^{39}) because of the deforming influence of the $f_{7/2}$ neutrons. The larger deformation is also indicated by the magnetic moments which, for these nuclei, decrease with increasing deformation. Such a correlation between Q and $\delta\mu$ is opposite to that usually observed (cf. p. 71).

The two last nuclei in Table XIV, Na^{23} and Ne^{21}, occur during the filling of the $d_{5/2}$ shell and have been classified by the shell model as $(d_{5/2})^3_{3/2}$, The spin $I = j - 1$ indicates that the surface coupling dominates over the particle forces (cf. § III.iii). The strong coupling state is then described by $\Omega = 3/2$ and has a limiting magnetic moment of $\mu_c = \left\{ \begin{matrix} 2.00 \\ -0.42 \end{matrix} \right\}$ for a pure configuration. Small admixtures of the $d_{3/2}$ state will produce shifts from this value, depending on the nuclear shape. For $\gamma = 0$, the moments increase in magnitude, while they decrease for $\gamma = \pi$. From considerations of the level filling in this region, Na^{23} is expected to prefer the $\gamma = 0$ shape (positive Q)*, in accordance with the indication from the observed μ-value (cf. Table VII).

v. $(5/2+)$ *nuclei.*

The magnetic moments of the nuclei in the first $d_{5/2}$ shell may, as already mentioned (cf. Table VI), be interpreted in terms of the coupling of a $d_{5/2}$ state to the nuclear surface. In

* Note added in proof: Recently, P. SAGALYN, working with F. BITTER, has found evidence for a positive quadrupole moment of Na^{23}. (Private communication from Professor BITTER).

TABLE XV. Moments of $(5/2+)$ nuclei.

odd proton ($\mu_{sp} = 4.79$)			odd neutron ($\mu_{sp} = -1.91$)		
nucleus	μ	Q	nucleus	μ	Q
$_{13}Al^{27}$	3.64	+0.16 (A)	$_{8}O^{17}$	−1.89	−0.005 (M)
$_{51}Sb^{121}$	3.36	−1.0 (A)***	$_{12}Mg^{25}$	−0.86	
$_{53}I^{127}$	2.81	−0.6 (A)	$_{40}Zr^{91}$	−1.1 ††	
$_{55}Cs^{131}$	3.48 *		$_{42}Mo^{95}$	−0.91	
$_{59}Pr^{141}$	3.9 **		$_{42}Mo^{97}$	−0.93	
$_{63}Eu^{151}$	3.6	+1.2 (A)	$_{46}Pd^{105}$	−0.6 §	
$_{63}Eu^{153}$	1.6	+2.6 (A)	$_{48}Cd^{111}$ †	−0.7 †	
$_{75}Re^{185}$	3.17	+2.9 (A)			
$_{75}Re^{187}$	3.20	+2.7 (A)			

* BELLAMY and SMITH (1953).
** LEW (1953); BRIX (1953).
*** DEHMELT and KRÜGER (1951 a).
† Refers to excited state ($E = 247$ keV); AEPPLI et al. (1952).
†† SUWA (1952).
§ STEUDEL (1952).

strong coupling, one obtains $\mu_c = \begin{cases} 3.75 \\ -1.04 \end{cases}$, which accounts approximately for the moments of Mg^{25} and Al^{27}.

For O^{17}, the magnetic moment and quadrupole moment are very little affected by the surface coupling, as is expected due to the high stability of the closed-shell core. The Q-value is comparable with the recoil moment (cf. § IVa; see also GESCHWIND et al., 1952), which is about -0.0013. Another measure of the quadrupole moment induced in the core by the odd neutron would be provided by the lifetime of the $(1/2+)$ excited state of O^{17} at 0.8 MeV (cf., e. g., AJZENBERG and LAURITSEN, 1952). The decay is of $E2$ character and, for a pure shell model state, will be determined by the small recoil quadrupole moment. This would lead to a lifetime of $\tau \sim 10^{-7}$ sec., which is longer than for a corresponding single-proton transition by a factor of 10^3 (cf. VII.7). However, the lifetime is very sensitive to impurities in the state.

In the region just beyond nucleon number 50, the $d_{5/2}$ and $g_{7/2}$ levels are near-lying, and nuclei of $(5/2+)$ character are expected to contain components of both orbitals. The ratio of the two orbitals in a state with $\Omega = 5/2$ depends rather sensitively on the spacing $\Delta_{7/2}$ of the $g_{7/2}$ level with respect to the $d_{5/2}$ level.

The spin of Sb^{121} indicates a positive $\Delta_{7/2}$ for this single-proton nucleus. A calculation of the type carried out in the preceding pages then shows that the content of $g_{7/2}$ is quite small ($a_{7/2}^2 \sim 0.1$), corresponding to the rather small deviation of $\mu(Sb^{121})$ from μ_c. While again the moment of Mo^{95} with 3 valence neutrons is consistent with a rather pure $d_{5/2}$, $\Omega = 5/2$ state, the small moment of I^{127} could be interpreted in terms of a negative $\Delta_{7/2}$. Already for small negative $\Delta_{7/2}$ (~ -0.5 MeV), additional moment shifts of the order of a magneton may be obtained.

The remaining $(5/2+)$ nuclei have more complex configurations. An exceptionally large shift is observed for Eu^{153}. It seems possible to account for such large moment shifts in terms of a state with $\Omega = 5/2$, but predominantly of $g_{7/2}$ character. A test of the strong coupling interpretation of this moment would be provided by a measurement of the $M1$ transition probability from the expected $(7/2+)$ rotational state (cf. VI c.iii and VII.20). An analogous situation is found for Yb^{173} (cf. Table XVI).

Further information on the coupling scheme in Eu comes from the anomalously large isotope shift which has been interpreted in terms of the large change in the quadrupole moments of the two isotopes (Brix and Kopfermann, 1949, 1952). Such an effect contributes to the isotope shift an amount δE given by*

$$\frac{\delta E}{\delta E_0} = \frac{15\,A}{8\pi}\frac{\Delta\beta^2}{\Delta A}\left(1 - 0.09\left(\frac{Ze^2}{\hbar c}\right)^2\right) \qquad \text{(Ad. 8)}$$

in units of the normal isotope shift δE_0, corresponding to an increase in the nuclear radius by the amount $\Delta R/R = 1/3\,\Delta A/A$. The change in β^2 is related to that of the intrinsic quadrupole moment (cf. V.7) and, for the contribution to the isotope shift between Eu^{153} and Eu^{151}, one obtains

$$\delta E = 0.056\;\; \Delta Q_0^2\;\; \delta E_0, \qquad \text{(Ad. 9)}$$

where Q_0 is measured in units of 10^{-24} cm^2. Deriving Q_0 from the measured Q by assuming the strong coupling projection factor (V.9), one obtains $\delta E = 2.4\,\delta E_0$, while the omission of the

* This expression is equivalent to formula (4) of Brix and Kopfermann (1949), except for the small relativistic correction which has been calculated by Mr. Jens Bang, to whom we are indebted for informing us of his results.

projection factor gives $\delta E = 0.3\,\delta E_0$. The measured isotope shift of about $2.2\,\delta E_0$ (Brix and Kopfermann, 1952) gives support to the assumption of a rather fully developed strong coupling in these nuclei.

vi. (5/2 —) *nuclei.*

Table XVI. Moments of (5/2 —) nuclei.

odd proton ($\mu_{sp} = 0.86$)		odd neutron ($\mu_{sp} = 1.37$)		
nucleus	μ	nucleus	μ	Q
$_{37}Rb^{85}$	1.35	$_{30}Zn^{67}$	0.88 *	
		$_{70}Yb^{173}$	−0.65	+4.0 (A)
$_{25}Mn^{55}$	3.47			

* Dharmatti and Weaver (1952).

In the first $f_{5/2}$ shell, the main influence of the surface on the magnetic moment is expected from the interference of the $f_{7/2}$ state. The Rb and Zn isotopes, containing a single $f_{5/2}$ hole, should resemble K rather than Cl (cf. p. 73). Thus, the inward moment shift of 0.4 — 0.5 magnetons is somewhat difficult to explain. It may be partly due to the influence of the near-lying $p_{3/2}$ level which, for weak or intermediate couplings, would cause inward moment shifts. Partly it may reveal an interaction effect on the intrinsic nucleon moment, possibly of somewhat larger magnitude than that considered for $p_{1/2}$ and $d_{3/2}$ nuclei.

Some further information on the structure of the Rb^{85} moment may be obtained from the observed hyperfine structure anomaly in the Rb isotopes (Bitter, 1949; Ochs and Kusch, 1952). Previous estimates of the effect (Bohr and Weisskopf, 1950; A. Bohr, 1951 a) are somewhat improved by including an interaction contribution to the nucleon moment (cf. Eisinger, Bederson and Feld, 1952).

The nucleus Mn^{55} occurs during the filling of the $f_{7/2}$ shell and has been classified by the shell model as $(f_{7/2})^{-3}{}_{5/2}$, which would correspond to a magnetic moment of $\mu_p = 4.13$ neglecting the neutron-proton forces. The spin anomaly suggests a rather fully developed strong coupling (cf. § III.iii), for which the magnetic moment is $\mu_c = 3.27$.

vii. (7/2—) *nuclei.*

TABLE XVII. Moments of (7/2—) nuclei.

odd proton ($\mu_{sp} = 5.79$)		odd neutron ($\mu_{sp} = -1.91$)		
nucleus	μ	nucleus	μ	Q
		$_{20}Ca^{43}$	−1.32 §	
$_{21}Sc^{45}$	4.76	$_{22}Ti^{49}$ **	−1.10 **	
$_{23}V^{51}$	5.15	$_{60}Nd^{143}$	−1.0	
$_{27}Co^{57}$	4.6 *	$_{60}Nd^{145}$	−0.6	
$_{27}Co^{59}$	4.65	$_{62}Sm^{147}$	(±) 0.7 †	
		$_{62}Sm^{149}$	(±) 0.6 †	
		$_{68}Er^{167}$		(±) 10 (C) ††

* BAKER et al. (1953).
** JEFFRIES et al. (1952); the mass assignment as well as the spin of the detected Ti isotope are in doubt.
† ELLIOT and STEVENS (1952).
†† BOGLE et al. (1952).
§ JEFFRIES (1953). (Added in proof).

The moments of the nuclei in the first $f_{7/2}$ shell may all be accounted for in terms of the coupling of an $f_{7/2}$ state to the surface. The moments of Sc^{45}, $Co^{57, 59}$, and Ti^{49} are all close to the strong coupling limit $\mu_c = \left\{ \begin{matrix} 4.86 \\ -1.14 \end{matrix} \right\}$, while the larger moment of Ca^{43} and V^{51} may indicate a somewhat weaker coupling, associated with the closed shells in the even structures. This smaller coupling may also be indicated by the fact that the ground state spin equals j rather than $j - 1$ for these $(j)^3$ configurations (cf. § III.iii).

viii. (7/2+) *nuclei.*

Due to the simultaneous filling of the $d_{5/2}$, $g_{7/2}$, and $h_{11/2}$ shells, most of the nuclei in this group possess complex configurations. One may attempt, however, a more detailed discussion of Sb^{123} with its single-proton configuration. In strong coupling, the main influence of the surface on the magnetic moment is expected from the small admixture of $g_{9/2}$ to the predominantly $g_{7/2}$ state. For a pure $g_{7/2}$ state, the strong coupling moment is very close to μ_{sp} (cf. Fig. 7). Since Sb^{123} with a single particle is analogous to Cl rather than to K (cf. p. 73), the interference of the spin orbit partner will increase the moment. The effect

TABLE XVIII. Moments of (7/2 +) nuclei.

odd proton ($\mu_{sp} = 1.72$)			odd neutron ($\mu_{sp} = 1.49$)	
nucleus	μ	Q	nucleus	Q
$_{51}Sb^{123}$	2.55	−1.2 (A)	$_{34}Se^{79}$	+1.2 (M) †
$_{53}I^{129}$	2.62	−0.44 (A)		
$_{55}Cs^{133}$	2.58	<0.3 (A)		
$_{55}Cs^{135}$	2.73			
$_{55}Cs^{137}$	2.84			
$_{57}La^{139}$	2.78			
$_{71}Lu^{175}$	2.9	+6.5 (A)		
$_{73}Ta^{181}$	2.1 *	+6.5 (A) *		

* BROWN and TOMBOULIAN (1952). † HARDY et al. (1952).

depends on the relative magnitude of $k\beta$ and $\Delta_{9/2}$, and assuming values of $\beta \approx 0.2$ and $\Delta_{9/2} \approx -2$ MeV, one obtains $\mu = 2.3$.

The nuclei having neutron configurations in the neighbourhood of the closed shell at 82 are expected to have relatively small deformability and there is evidence for a small quadrupole moment of the stable Cs isotope, Cs^{133}. For these nuclei, the surface should play a lesser role in causing magnetic moment shifts. However, the complex configurations in question make it difficult to decide whether the observed moment shifts can be explained by the particle structure itself or whether some additional effects are operating.

In Se^{79}, one expects a predominantly $(g_{9/2})^5$ neutron configuration. Such a half filled shell will in itself generate no quadrupole moment, although it may produce a large nuclear deformation (cf. § II c.ii and § III.iii). The observed positive sign of Q may be the result of the proton structure which is expected to favour a prolate shape.

ix. (9/2 +) *nuclei.*

The major part of the magnetic moment shifts for these nuclei may be accounted for in terms of the coupling between a $g_{9/2}$ state and the surface, which leads to the strong coupling moment $\mu_c = \left\{ \begin{matrix} 5.93 \\ -1.20 \end{matrix} \right\}$. In some cases, such as In, additional effects must be present, possibly in part due to interaction contributions to the nucleon moment.

TABLE XIX. Moments of (9/2 +) nuclei.

odd proton ($\mu_{sp} = 6.79$)			odd neutron ($\mu_{sp} = -1.91$)		
nucleus	μ	Q	nucleus	μ	Q
$_{41}Nb^{93}$	6.17		$_{32}Ge^{73}$		−0.2 (M)
$_{43}Tc^{99}$	5.68 *		$_{36}Kr^{83}$	−0.97	+0.16 (A)
$_{49}In^{113}$	5.49	+1.18 (A)	$_{38}Sr^{87}$	−1.1	
$_{49}In^{115}$	5.50	+1.20 (A)			

* WALCHLI et al. (1952).

x. (9/2 —) *nuclei.*

TABLE XX. Moments of (9/2 —) nuclei.

odd proton ($\mu_{sp} = 2.62$)		
nucleus	μ	Q
$_{83}Bi^{209}$	4.08	−0.4 (A)

The closed-shell structure of the Pb^{208} core implies a very small deformability, as is confirmed by the observed quadrupole moment of Bi^{209}, which is of the order of the single-particle value (cf. Table IX). However, in contrast to the case of O^{17}, the magnetic moment of Bi^{209} is very strongly shifted from the single-particle value. This moment shift is even larger than would have been expected for a normally deformable nucleus (cf. the case of Sb^{123}, p. 79). Since the observed quadrupole moment supports the expected negligible effect of the surface on the coupling scheme of this nucleus, it is probable that the magnetic moment reveals some as yet unexplained aspect of the particle structure. If the shift is interpreted as an interaction effect, the intrinsic proton moment is reduced to one magneton, a reduction many times larger than that indicated by the magnetic moments of other nuclei (cf. p. 52).

xi. *Odd-odd nuclei.*

For the self-mirrored nuclei ($N = Z$), the symmetry between neutrons and protons implies that the total g-factor will almost always be close to 0.5 and be insensitive to the detailed coupling

TABLE XXI. Moments of odd-odd nuclei.

Nucleus	Configurations		I	μ	Q
	protons	neutrons			
$_5B^{10}$	$(p_{3/2})^{-1}$	$(p_{3/2})^{-1}$	3	1.80	+0.13 (M) §§
$_7N^{14}$	$p_{1/2}$	$p_{1/2}$	1	0.40	+0.02 (M)
$_{11}Na^{22}$	$(d_{5/2})^3$	$(d_{5/2})^3$	3	1.75	
$_{11}Na^{24}$	$(d_{5/2})^3$	$(d_{5/2})^{-1}$	4	1.69 *	
$_{17}Cl^{36}$	$d_{3/2}$	$(d_{3/2})^{-1}$	2		−0.018 (M,A)
$_{19}K^{40}$	$(d_{3/2})^{-1}$	$f_{7/2}$	4	−1.30 **	
$_{19}K^{42}$	$(d_{3/2})^{-1}$	$(f_{7/2})^3$	2	−1.14 *	
$_{23}V^{50}$	$(f_{7/2})^3$	$(f_{7/2})^{-1}$	6 §	3.35 ***	
$_{27}Co^{58}$	$(f_{7/2})^{-1}$	$(p_{3/2}, f_{5/2})^3$	2	3.5 †	
$_{27}Co^{60}$	$(f_{7/2})^{-1}$	$(p_{3/2}, f_{5/2})^5$	5	3.3 † ††	
$_{37}Rb^{86}$	$(p_{3/2}, f_{5/2})^{-1}$	$(g_{9/2})^{-1}$	2	−1.69 *	
$_{55}Cs^{134}$			4	2.96 * †††	
$_{71}Lu^{176}$			$\geqslant 7$	4.2	+8 (A)

* BELLAMY and SMITH (1953).
** EISINGER et al. (1952).
*** WALCHLI et al. (1952 a).
† DANIELS et al. (1952).
†† GORTER at al. (1952).
††† JACCARINO et al. (1952).
§ KIKUTCHI et al. (1952).
§§ DEHMELT (1952).

scheme (cf. TALMI, 1951). For nuclei of this type, it is indeed found that μ_c and μ_p are nearly the same and agree closely with the observed moments.

For B^{10}, the μ_c value listed in Table VII refers to a state with $\Omega_{\text{prot}} = \Omega_{\text{neut}} = 3/2$ $(I = K = \Omega = 3)$ and pure $p_{3/2}$ configurations. In the case of N^{14}, the listed μ_c values refer to the state $\Omega_{\text{prot}} = \Omega_{\text{neut}} = 1/2$ $(I = K = \Omega = 1)$, and take into account the $p_{3/2}$ admixture.

For Na^{22}, the strong surface coupling leads to a state with $\Omega_{\text{prot}} = \Omega_{\text{neut}} = 3/2$ $(I = K = \Omega = 3)$. For pure $d_{5/2}$ orbitals, one obtains $\mu_c = 1.67$. For the expected nuclear shape $(\gamma = 0)$, the interference of the $d_{3/2}$ state tends slightly to increase μ, but, due to the neutron-proton symmetry, the effect is small, amounting to only 0.1 magneton for a deformation of $\beta \sim 0.3$ (cf. Table VII).

The corresponding interference effect is much larger in Na^{24} $(\Omega_{\text{prot}} = 3/2,\ \Omega_{\text{neut}} = 5/2)$, since it does not affect the neutron state. Neglecting the $d_{3/2}$ admixture, the strong coupling moment is $\mu_c = 1.13$, but the observed moment can be accounted for by a deformation of the same magnitude as considered for Na^{22}

(cf. Table VII). The shell model magnetic moment of Na^{24} depends upon the nuclear forces and is not made unique by the assumption of charge symmetry.

For K^{40} ($\Omega_{prot} = 1/2$, $\Omega_{neut} = 7/2$), the strong coupling magnetic moment for a pure configuration is $\mu_c = -1.14$, while the interference of the $d_{3/2}$ orbital and the admixture of $s_{1/2}$ in the proton state decreases the magnitude of the moment (cf. Table VII). The shell model gives $\mu_p = -1.68$. The observed moment thus indicates an intermediate coupling situation, consistent with the proximity to the doubly closed shell at Ca^{40}.

In K^{42}, the extreme strong coupling ($\Omega_{prot} = -1/2$, $\Omega_{neut} = 5/2$) with pure configurations gives $\mu_c = -0.65$. Additional shifts arise from admixtures of $f_{5/2}$ orbital to the neutron state, and $d_{5/2}$ and $s_{1/2}$ orbitals to the proton state. The μ_c values in Table VII are based on $\Delta(f_{5/2}) \sim 5$ MeV, $\Delta(d_{5/2}) \sim -5$ MeV, and $\Delta(s_{1/2}) \sim -5$ MeV.

For V^{50}, the coupling scheme arising from particle forces has been discussed and for forces of zero range a ground state of $I = 6$ has been obtained (Hitchcock, 1952) with $\mu_p = 3.21$*. However, forces of the expected range appear to favour $I = 5$. The effect of the surface coupling is somewhat complicated, since in strong coupling the neutrons and protons favour different surface shapes, with the result that neither $\gamma = 0$ nor π are stable positions.

The two Co isotopes can be accounted for by the strong coupling states ($\gamma = 0$, and $\Omega_{prot} = 7/2$; $\Omega_{neut} = \pm 3/2$), the upper sign referring to Co^{60}, the lower to Co^{58}. However, the great difference in the observed g-factors indicates a difference in the nature of the $|\Omega| = 3/2$ neutron states. Thus, for Co^{58}, the observed moment indicates a predominantly $f_{5/2}$ neutron state which leads to a strong coupling moment of $\mu_c = 3.61$, while, for Co^{60}, a predominantly $p_{3/2}$ neutron state, giving $\mu_c = 3.60$, is indicated. It is of interest that similar effects in the filling of the $p_{3/2}$, $f_{5/2}$ shells seem to occur in the $I = 3/2$ odd-A nuclei in this region (cf. p. 70).

The Rb^{86} nucleus can be described in terms of a single proton and a single neutron (cf. Table II). The observed spin of 2 suggests a $f_{5/2}$ assignment for the proton hole, which leads to the

*) Private communication from Dr. A. Hitchcock.

strong coupling moment $\mu_c = -1.56$. The shell model value for this configuration is $\mu_p = -2.13$.

Additional evidence on the nuclear states in question may be obtained from the observed quadrupole moments.

For the case of B^{10}, although the absolute magnitude of Q is probably rather uncertain, the observed ratio $Q(B^{10})/Q(B^{11}) = 2.08$ (DEHMELT, 1952) is significant. According to the (jj) coupling shell model, this ratio should be unity, whereas the surface coupling gives a ratio of about two.

The evidence for a moderate quadrupole moment for N^{14} indicates appreciable impurities in the listed configuration (cf. also the β-decay of C^{14}).

The Cl^{36} nucleus has the symmetry associated with the fact that the neutron structure is obtained from the proton structure by replacing particles with holes (cf. § IIc.ii). Neglecting inter-configuration effects, the quadrupole moment therefore vanishes, as also for the shell model state. The influence of the coupling to the $d_{5/2}$ and $s_{1/2}$ states favours the shape $\gamma = \pi$, and gives rise to a small negative Q value.

VI. Nuclear Level Structure.

a) General Features of Levels in the Coupled System.

The nuclear level spectrum, resulting from the interplay of particle and collective motion, depends essentially on the strength of the coupling. For weak coupling, there is associated with each particle level a spectrum of excited states with a spacing corresponding to the phonon energy (cf. Fig. 2 for the hydrodynamic estimate of $\hbar\omega$, which yields about 2 MeV for the quadrupole oscillations of a medium heavy nucleus). With increasing coupling, the two level structures become essentially interwoven. For intermediate coupling strength, a rather complicated spectrum may result but, in the limit of strong coupling, the low energy nuclear spectrum acquires a relative simplicity which bears some analogy to molecular spectra.

The strongly coupled nucleus thus exhibits two different types of excitation: The first corresponds to a change of state of the particle motion relative to the deformed surface and is in general associated with a readjustment of the surface. Such particle excitations are analogous to electronic transitions in molecules. The second type of excitation is a collective excitation corresponding to vibration or rotation of the coupled particle-surface system, and is the analogue of vibrational and rotational molecular transitions. While the energies of particle excitations depend on the configuration energies in the deformed nucleus, the vibrational quanta are of the order of the phonon energy. The rotational energies decrease strongly with increasing nuclear deformation and may become much smaller than the phonon energy.

The collective and particle excitations possess very distinct properties. Thus, it is characteristic of the collective excitations that levels of the same family have the same parity and small spin changes between neighbouring states ($\Delta I = 1$ or 2). In

contrast, particle excitations may involve change of parity as well as large spin changes. Further, the character of a given excitation reveals itself in the transition probability. While the particle transitions are in general slowed down by the differences in the surface shape of the combining states, the large electric quadrupole of the oscillating surface may greatly enhance the radiative probability for collective transitions.

With increasing excitation energy, the spacing of both particle and collective states rapidly decreases, and even a small perturbation in the ordered motion is sufficient to destroy any simple coupling scheme. In such a situation, the only remaining constants of the motion are the parity and total angular momentum. Still, provided the interactions are not so strong that they prevent the system from completing even a few periods of the simple particle or surface motion between energy exchanges, some of the gross features of the unperturbed level spectrum are preserved.

In the region of high excitation, additional types of collective motion, such as surface oscillations of higher order and compressive oscillations, may play an important role. Further, the number of excitable particle degrees of freedom increases. Finally, for the very high energies, at which an appreciable fraction of the nucleons is simultaneously excited, the distinction between particle and collective degrees of freedom ceases to have a simple significance.

b) Particle Excitations.

For each particle configuration there exists a lowest level in the coupled system which, as discussed in Chapter III, usually has the same spin and parity as the pure particle state. If the nucleus possesses several neighbouring configurations, there will thus be corresponding states in the low energy spectrum which, as regards spin and parity, may be classified by means of the shell model.

Striking evidence for such particle excitations is afforded by the occurrence of low-lying states with a spin very different from that of the ground state and often with different parity. These states give rise to the long lived isomers, whose interpretation has provided such an important support for the shell model (Gold-

HABER and SUNYAR, 1951; MOSZKOWSKI, 1951). The transition probabilities of these states, however, are found to be smaller than shell model estimates by a considerable factor, indicating that the excitations cannot be described in terms of particles moving in a fixed potential, but involve the surface readjustments characteristic of the particle transitions in the strongly coupled system (BOHR and MOTTELSON, 1952; cf. also § VII d.i).

The β-decays constitute another group of particle transitions in the classification of which the shell model has been a valuable guide (MAYER, MOSZKOWSKI and NORDHEIM, 1951; NORDHEIM, 1951). Again the observed transition probabilities are in general reduced as compared with shell model estimates, indicating the influence of a rather strong surface coupling (§ VIIIc.ii and iv).

The particle transitions also exhibit other features which may be attributed to the influence of the surface coupling. Thus, selection rules appropriate to the motion of particles in a spherical potential are often violated (l- and j-forbiddenness, cf. § VIIIc.iii and § VIIc.ii). The occurrence of such transitions provides evidence for configuration admixtures of a similar type as discussed for the magnetic moments (cf. § IVc).

The relative position of particle levels may depend on the nuclear deformation which can cause level shifts of the order of a few MeV* (cf., e. g., the spin difference of the F-isotopes, p. 67). Also the level order of the particle states within a many-particle configuration depends in an important way on the surface coupling (cf. § III.iii).

In the strong coupling scheme, particle modes of excitation which do not involve change of configuration, but only changes in the Ω_p quantum numbers, in general require a rather large energy. In cases where there are special degeneracies, however, they may occur among the lowest states. Thus, in strong coupling, the ground states of odd-odd nuclei are expected to be close doublets, the members of which have the same parity, but may differ appreciably in spin (cf. § IIc.ii). There seems to be evidence in spectra of odd-odd nuclei for a rather general occurrence

* Such a contribution to the nuclear energy may be interesting in connection with the estimates of the spin-orbit energy and pairing effects obtained from the analysis of binding energies (HARVEY, 1951; SUESS and JENSEN, 1952). Moreover, it may be significant in influencing the trends in the separations of isomeric levels (HILL, 1950; MITCHELL, 1951; GOLDHABER and HILL, 1952).

of such doublets (cf., e. g., GOLDHABER and HILL, 1952). Since the two members of the doublet have approximately the same shape, the γ-transition between them should be somewhat faster than most other particle transitions of similar type (cf. § VII d.i).

While in regions removed from closed shells, the particle excitation spectrum is thus essentially modified by the coupling to the nuclear deformation, the particle-surface coupling is expected to be rather ineffective in the immediate vicinity of major closed shells. These regions should offer relatively favourable conditions for studying the particle level order in a spherical nucleus and the effects of particle forces (cf., e. g., INGLIS, 1952; PRYCE, 1952).

In the light nuclei, the study of excited states by means of nuclear reactions has revealed levels, especially in the neighbourhood of He^4, C^{12}, and O^{16}, which correspond approximately to single-particle excitations in the uncoupled system (cf., e. g., KOESTER, JACKSON and ADAIR, 1951; and also AJZENBERG and LAURITSEN, 1952). These levels are identified by their reduced widths which are comparable to those of single-particle scattering in a fixed potential.

In the region around Pb^{208}, pure particle transitions may also be encountered (PRYCE, 1952; HARVEY, 1953). Lifetimes are here an important guide in interpreting the level scheme (cf. Chapter VII, and especially pp. 117 and 112, for comments on the Pb^{204} and Pb^{207} isomeric transitions).

c) Collective Excitations.

i. *Excitation of closed-shell nuclei.*

The weak coupling situation expected in the immediate vicinity of major closed-shells implies that the collective excitations are essentially of the simple phonon character.

The closed-shell nuclei themselves are of special interest. One here expects among the first excited states a $(2+)$ level, representing an approximately free surface oscillation of the quadrupole type. States of $(2+)$ character have been observed in ${}_8O^{16}$ and ${}_{82}Pb^{208}$ (the 3.8 MeV state in ${}_{20}Ca^{40}$ is also a possible example) and are difficult to interpret as particle excita-

tions (cf. PRYCE, 1952). Lifetime measurements for these states would provide crucial evidence regarding the nature of the excitation, since the phonon decay probability is much larger than that of a particle transition (cf. § VII b.i).

The fact that the first excited state of Pb^{208} ($E = 2.62$ MeV; $I = 2(+)$) is considerably in excess of the phonon energy ($\hbar\omega = 1.3$ MeV), calculated in the hydrodynamic approximation, supports the expectation of a very low deformability for such a doubly closed-shell structure (cf. Ap. I).

The O^{16} nucleus has, as one of the very few exceptions among even-even nuclei, a $(0+)$ first excited state. This state is difficult to account for as a particle excitation, especially because of its parity. One is driven to assume a two-particle excitation from $p_{1/2}$ into $d_{5/2}$ or $s_{1/2}$ orbits, which cannot, however, account for the observed rather large transition probability for pair emission (cf. AJZENBERG and LAURITSEN, 1952). It is possible that we here encounter a compressive oscillation of lowest order*. That such an excitation mode, in this special case, lies lower than the lowest surface excitation is perhaps not surprising, considering the large ratio of surface to volume energy for such a light nucleus and the fact that its closed-shell structure favours excitation modes which do not destroy its spherical symmetry.

ii. *Rotational states in even-even nuclei.*

For the strongly deformed nuclei, encountered in regions away from closed shells, the collective excitations can be characterized as vibrations and rotations**.

Especially characteristic of the strong coupling spectrum are the rotational states which may have energies much smaller than the phonon energy. These low-lying states correspond to rotations about an axis perpendicular to the nuclear symmetry

* This interpretation is rather similar to that of the α-particle model which describes the excitation of the $(0+)$ state as due to a radial oscillation of the whole structure (DENNISON, 1940).

** FORD (1953) has calculated excitation energies for a number of configurations, using the strong coupling representation. For the states considered, involving one or a few particles outside of closed shells, the limiting strong coupling situation is not well developed, and the spectra do not exhibit the regularities discussed in the present paragraph. In such cases, it seems necessary to employ methods appropriate to an intermediate coupling situation (cf. the more detailed calculations of D. C. CHOUDHURY, referred to in footnote on p. 24).

axis (cf. Fig. 3) and are labeled by varying I, for fixed values of Ω, K, n_β, and n_γ. Rotations about the nuclear axis, labeled by varying K, have energies which, in most cases, remain of the order of the phonon energy, and these excitations are considered together with the vibrational states (§ VIc.iv).

A special regularity in the collective spectrum occurs for the even-even nuclei, which have in their ground state $I = K = \Omega = 0$ (cf. § III.ii). The expected cylindrically symmetric deformation ($\gamma = 0$ or π) leads to rotational states with even I and with $K = \Omega = 0$. The odd values of I do not occur, since such states would have odd parity (cf. § IIc.ii for the appropriate symmetry properties of the wave function). From (II.30) we get for the rotational excitation energies

$$E_I = \frac{\hbar^2}{2\Im} I(I+1) \quad \underset{\text{even parity}}{I = 0, 2, 4 \cdots} \tag{VI.1}$$

where the moment of inertia $\Im$ is given by (cf. II.25)

$$\Im = 3 B \beta^2 \tag{VI.2}$$

in terms of the nuclear equilibrium deformation β and the mass parameter B (cf. II.5).

The spectrum (1) is the same as that for the rotation of a rigid body, but the rotational motion arises in essentially different ways in the two cases. The collective motion in the nucleus is of irrotational character (cf. p. 11), and the angular momentum is carried only by the surface waves. The effective moment of inertia associated with this motion depends on the square of the amplitude of the waves (cf. (2)), in a similar manner as the momentum in a sound wave is proportional to the square of the amplitude of oscillation.

Deviations from the limiting strong coupling scheme imply corrections to the spectrum (1). Some of these have the same I-dependence as (1) and give rise to corrections to the moment of inertia (2). Others involve higher powers of I and produce a distortion of the spectrum. Thus, the rotation-vibration interaction (cf., e. g., Herzberg 1950; Nielsen, 1951), which implies that β increases somewhat with I due to centrifugal distortions, gives to first order the energy shift

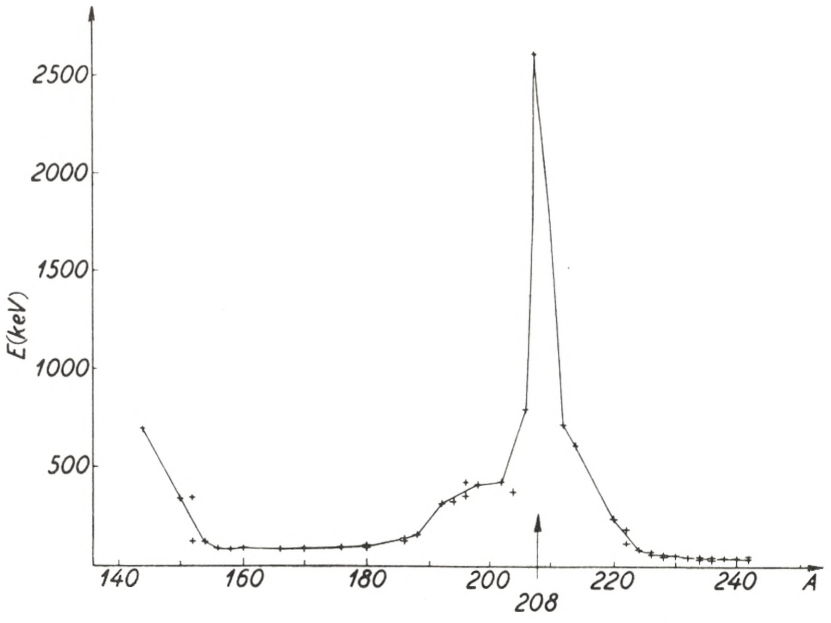

Fig. 13. *First excited states in even-even nuclei with* $A > 140$. The energy of the first excited state is plotted as a function of A. The data is taken from HOLLANDER, PERLMAN and SEABORG (1952) and from SCHARFF-GOLDHABER (1953). The evidence is consistent with a (2+) assignment for all the levels. Similar curves have been given by STÄHELIN and PREISWERK (1951), ROSENBLUM and VALADARES (1952), ASARO and PERLMAN (1952), and SCHARFF-GOLDHABER (1952, 1953).

$$(\Delta E_I)_1 = -2\frac{E_I}{C\beta^2}E_I = -\frac{3}{2}\left(\frac{1}{\hbar\omega_\beta}\right)^2\left(\frac{\hbar^2}{\Im}\right)^3 I^2(I+1)^2, \quad \text{(VI. 3a)}$$

where $\hbar\omega_\beta$ is the excitation energy of the β-vibration (cf. § VIc.iv). Another term of the same order of magnitude as (3a) arises from the influence of the γ-vibrations which imply a departure from the rotational spectrum of a symmetric top. The effect can be found as a second order perturbation produced by the operator U_3 (cf. A. 96), and one obtains

$$(\Delta E_I)_2 = -\frac{1}{2}\left(\frac{1}{\hbar\omega_\gamma}\right)^2\left(\frac{\hbar^2}{\Im}\right)^3 I^2(I+1)^2, \quad \text{(VI. 3b)}$$

where $\hbar\omega_\gamma$ is the energy of the γ-vibration.

Rotational states in regions of large deformations have recently been identified by their very striking properties: regu-

TABLE XXII. Energies of (2+) and (4+) states in even-even nuclei with $A > 140$.

Nucleus	E_2	E_4	$E_4:E_2$	Ref.
$_{62}Sm^{150}$	337	777	2.3	*
$_{72}Hf^{176}$	89	289	3.2	** †††
$_{72}Hf^{180}$	93	307	3.3	**
$_{82}Pb^{208}$	2614	3200	1.2	*
$_{88}Ra^{226}$	67	217	3.2	***
$_{90}Th^{228}$	58	187	3.2	†
$_{90}Th^{230}$	50	167	3.3	††
$_{94}Pu^{238}$	43	146	3.4	††

* SCHARFF-GOLDHABER (1953).
** GOLDHABER and HILL (1952).
*** BOUISSIÈRES et al. (1953), (added in proof).
† BLACK (1924).
†† HOLLANDER, PERLMAN and SEABORG (1952).
††† ARNOLD and SUGIHARA (1953), (added in proof).

The table lists the energies (in keV) of the (2+) and of the tentatively assigned (4+) states. While these assignments are consistent with the available empirical evidence, they are in many cases in need of further examination. For rotational states, the ratio $E_4:E_2$ is expected to approach the value 10:3 for large deformations (cf. 1).

larities of spins and parities, characteristic energy trends, simplicity of the excitation spectrum, and very large $E2$ transition probabilities (BOHR and MOTTELSON, 1952, 1953, 1953a; FORD, 1953; ASARO and PERLMAN, 1953).

Systematic studies of the first excited states of even-even nuclei (GOLDHABER and SUNYAR, 1951; HORIE, UMEZAWA, YAMAGUCHI and YOSHIDA, 1951; STÄHELIN and PREISWERK, 1951; PREISWERK and STÄHELIN, 1952; ASARO and PERLMAN, 1952; ROSENBLUM and VALADARES, 1952; WAPSTRA, 1952, 1953; SCHARFF-GOLDHABER, 1952, 1953*), have revealed that, with very few exceptions, the first excited state is of (2+) character**, and that the excitation energy exhibits definite trends with respect to

* We are indebted to Dr. G. SCHARFF-GOLDHABER for making available to us these results in advance of publication.

** It has been suggested that the excited states of even-even nuclei can be interpreted as a recoupling of the particles outside of closed shells (cf., e. g., HORIE et al., 1951; FLOWERS, 1952b). While this description may, for many configurations, explain the (2+) nature of the first excited levels, it has not provided an explanation of the many other striking features of the levels discussed in the present paragraph.

the shell structure, reaching maxima around the closed-shell configurations and minima as much as fifty times smaller in the middle of shells.

This trend is especially conspicuous in the region of the heavier nuclei where the shell structure is dominated by the doubly closed shells at Pb^{208} (cf. Fig. 13). Similar regularities are also observed for the lighter elements, but the trends are somewhat more complicated due to the fact that neutrons and protons form closed shells for different A-values (cf especially SCHARFF-GOLDHABER, 1953).

While the excitations of closed-shell nuclei may represent simple phonon states (cf. § VI c.i), a decreasing energy, as we move away from closed shells, results from the coupling with the particle structure, which leads to increasing nuclear deformations. The rapid decrease for the first few particles added to closed configurations, which develops into a rather flat minimum, can be understood from the fact that the particle states with large deformative power are the first to be filled, while in the middle of shells the last added particles are less coupled to the deformed nucleus.

The small excitation energies encountered in the regions $155 < A < 185$ and $A > 225$ imply that, in these cases, the coupling is very strong and that the rotational energies should be rather accurately represented by the simple formula (1), corrections of magnitude (3a and b) being small.

A direct measure of the validity of the strong coupling approximation is afforded by the location of the expected higher members of the rotational family. The available evidence on energies of the (4+) state, in the region covered by Fig. 13, is listed in Table XXII. It is seen that the energy ratio $E_4 : E_2$ shows the expected trend, approaching the strong coupling value 10:3 (cf. 1) in the regions of large deformation.*

* Note added in proof: ASARO and PERLMAN (1953), from a study of the α-spectra of the heavy elements, have recently obtained evidence for the systematic occurrence of a rotational spectrum in even-even nuclei in the region well beyond Pb^{208}. With the approach to Pb^{208}, deviations from the energy spectrum (1) are observed, which can be interpreted as distortions of the type (3a and b), corresponding to a vibrational energy of about one MeV, which is of the same magnitude as indicated by the hydrodynamical estimate (cf. Fig. 2). We are indebted to these authors for having informed us of their results in advance of publication.

TABLE XXIII Deformations deduced from properties of rotational states.

Nucleus	E (keV)	F	β_E	β_Q
$_{66}Dy^{160}$	85	140	0.65	0.28
$_{68}Er^{166}$	80	180	0.65	0.31
$_{70}Yb^{170}$	84	140	0.62	0.27
$_{72}Hf^{176}$	89	120	0.58	0.24
$_{76}Os^{186}$	137	55	0.45	0.15
$_{80}Hg^{198}$	411	6	0.25	0.05
$_{84}Po^{212}$	719	5	0.18	0.04
$_{84}Po^{214}$	606	7	0.19	0.05

The table lists the first excited states of even-even nuclei, classified as collective excitations on the basis of measured lifetimes (cf. Table XXVII). The factor F in the third column gives the enhancement of the transition probability over that expected for a particle transition (cf. Table XXVII). From a rotational interpretation of the states, the deformation β_E may be calculated from the excitation energy by means of (VI.1 and 2), and is listed in column four. The last column gives the deformation β_Q estimated from the intrinsic deformation Q_0 by means of (V.7). The value of Q_0 is obtained from the observed transition probability (cf. Table XXVII).

The large excitation energies, as well as the relatively small F-factors, for the last three cases in the table indicate an intermediate coupling situation, in which the rotational description is less appropriate.

The spin of 4 for the second rotational excitation and the $E_4:E_2$ ratios confirm the expected axial symmetry of the nuclear deformation (cf. p. 28). For a nucleus with an asymmetric equilibrium shape, the rotational spectrum would exhibit a sequence of I-values and energy ratios different from (1).

It is a characteristic of the rotational spectrum that the excitation of a high member is followed by a cascade of $E2$ gamma transitions with energy values in the ratio $\cdots$ 15:11:7:3, and with no cross-overs. There is indeed evidence (BOHR and MOTTELSON, 1953a) for such cascades involving states up to $I = 8$ with energies closely given by (1).*

The observed very short γ-ray lifetimes of low-lying excited states in even-even nuclei clearly indicate the collective nature of the excitation (GOLDHABER and SUNYAR, 1951). The ratio of

* Note added in proof: The recent measurement (ARNOLD and SUGIHARA, 1953) of the γ-spectrum following the β-decay of Lu^{176} considerably improves the agreement with the rotational spectrum in Hf^{176}.

the observed transition probabilities to those expected for particle transitions increases as one moves away from closed-shell configurations and reaches values of more than a hundred in regions far removed from closed shells (cf. Table XXIII).

The $E2$ transition probability of a rotational state is directly related to the intrinsic nuclear quadrupole moment Q_0 (cf. § Vb and § VIIc.ii), and the values derived from the observed lifetimes are just of the magnitude deduced from spectroscopic data for neighbouring odd-A isotopes (cf. Table XXVII on p. 116).

Another measure of the deformation is provided by the excitation energies which yield, by (1), the nuclear moment of inertia. Assuming the hydrodynamic value (II.6a) for B, the deformation β_E can be obtained from (2). This estimate of the deformation is compared, in Table XXIII, with the deformation β_Q estimated from the $E2$ transition probability, assuming the hydrodynamic relation (V.7) for Q_0.

It is seen that, although β_E and β_Q show parallel trends, β_E exceeds β_Q by about a factor of two in the region of the fully developed strong coupling. This effect is quite similar to the overestimate of the static quadrupole moments by the hydrodynamic model (cf. p. 59), and lends support to the view that the simple model of the collective deformations underlying (V. 7) is inadequate. As in the case of the static Q, it is also possible that some part of the discrepancy arises from an underestimate of B.

A general correlation has been found (Ford, 1953) between the energies of the first excited states of even-even nuclei, interpreted as rotational states, and the magnitude of the quadrupole moments of odd-A nuclei. The quantitative comparison shows the same feature encountered above, that, although the two estimates of the deformation exhibit similar trends, the β-values derived from quadrupole moments are several times smaller than those derived from excitation energies.

For the smaller deformations encountered in the regions of closed shells, perturbation terms of the magnitude (3a and b) may essentially modify the spectrum and also particle forces may have an important influence. The expected intermediate coupling situation is clearly revealed by the deviations of the $E_4 : E_2$ ratio (cf. Table XXII) from the strong coupling value of 10:3, with the approach to closed-shell configurations.

iii. *Rotational states in odd-A nuclei.*

The rotational spectrum in odd-A nuclei depends on the angular momentum I_0 of the ground state. If $I_0 = \Omega = K \geqslant 3/2$, we get a series of states with energies

$$E_I = \frac{\hbar^2}{2\Im}[I(I+1) - I_0(I_0+1)] \quad \underset{\text{same parity as ground state}}{I = I_0, I_0+1, I_0+2, \cdots} \qquad \text{(VI.4)}$$

If the system does not strongly prefer the symmetric shape ($\gamma = 0$ or π), as for a single particle with $j = 3/2$, a more complicated rotational spectrum may arise (cf. Ap. III.ii).

In the case $\Omega = K = 1/2$, there is the additional contribution to the rotational energy (cf. II.30)

$$\Delta E_I = (-)^{I-j+1} \frac{\hbar^2}{2\Im}(j+1/2)(I+1/2), \qquad \text{(VI.5)}$$

where j refers to the odd particle with $\Omega_p = 1/2$. In this case, the ground state spin is in general no longer 1/2, and a less regular sequence of rotational states appears.

Since the odd-A rotational states depend more specifically on the properties of the ground state, they do not exhibit the same simple trends as those in even-even nuclei. Moreover, since consecutive levels have $\Delta I = 1$, except in some cases with $\Omega = 1/2$, they may decay by $M1$ radiation, for which the transition probability is not enhanced.

A specially suited method for identifying and studying the rotational states in odd-A nuclei may be provided by the Coulomb excitation which directly measures the $E2$ transition probability (cf. Ap. VI). The collective excitations therefore manifest themselves by their especially large cross-sections.*

Measurements of the γ-decay probabilities of the rotational states are also of interest, since the $M1$ transition probability can be directly compared with the static magnetic moment of the ground state (cf. VII.20). The strong enhancement of the $E2$ radiation implies that appreciable $E2$ admixtures may be expected in many cases, although for a single-particle γ-transition

* Note added in proof: Recently, rotational states in odd-A nuclei have been identified by the method of Coulomp excitation (Huus and Zupančič, 1953; cf. also note on p. 166).

with $\Delta I = 1$ (no), the $E2$ radiation is extremely weak in comparison with $M1$. Moreover, it is expected that cross-over transitions ($\Delta I = 2$) may in some cases compete with the cascade.

iv. *Vibrational excitations.*

The vibrational states are characterized by the quantum numbers n_β and n_γ, and in the limit of strong coupling the excitation energies approach the phonon energy (cf. A. 108 and 113). A comparable energy is associated with changes in the quantum number K. Due to the symmetry of the surface, the n_γ- and K-excitations only occur in definite combinations, since n_γ must have the same parity as $1/2\ (K - \Omega)$ (cf. A. 92).

The vibrational states have strongly enhanced $E2$ decay probabilities, characteristic of collective excitations, and could be especially studied by the method of Coulomb excitation (cf. Ap. VI). In an even-even nucleus, an $E2$ transition from the ground state can lead to the vibrational states ($n_\beta = 1$; $n_\gamma = 0$; $I = 2$; $K = \Omega = 0$) and ($n_\beta = 0$; $n_\gamma = 1$; $I = K = 2$; $\Omega = 0$). In an odd-A nucleus, several rotational states can be reached for each type of vibrational excitation, and in addition there are two vibrational excitations with $n_\gamma = 1$, having $\Delta K = \pm 2$.

d) Higher Excitation. The Compound Nucleus.

The more highly excited states, produced in nuclear reaction processes, though characterized by a somewhat greater complexity than the low energy spectrum, can provide further insight into the dynamics of the nuclear system. Since the present discussion is concerned principally with the phenomena occurring in the low energy region, we shall attempt only a rather brief description of the properties of the coupled system for higher excitations.

In the present paragraph, we consider the general features of the level structure in this region, and summarize some of the consequences for nuclear reactions*, **. A more detailed formu-

* We are indebted to Professor N. Bohr for illuminating discussions on the influence of single-particle motion on the compound nucleus formation.

** Cf. also Hill and Wheeler (1953), who have pointed out many important consequences of the strong interaction between the nucleonic and surface motion for various nuclear processes, and especially the fission reaction.

lation of nuclear reaction theory, incorporating individual-particle as well as collective features, is attempted in Appendix V.

With increasing nuclear excitation, the level spacing rapidly decreases and any simple coupling scheme will be destroyed by even relatively small perturbations, which result in a sharing of properties between neighbouring levels of the same spin and parity. A simplified picture of the level structure may be obtained by characterizing the rate of exchange of energy in the system by an energy interval W within which the sharing of properties among levels is more or less complete. This energy is related to the mean free path λ_a of single-particle motion by

$$W = \frac{\hbar v}{\lambda_a}, \tag{VI.6}$$

where v is the particle velocity*. The coupling thus tends to obscure finer features in the level structure, associated with simple types of motion with frequencies smaller than $W/\hbar$.

The significance of single-particle motion depends on the relative magnitude of W and the single-particle level spacing Δ given by

$$\Delta = \pi K R_0 \frac{\hbar^2}{M R_0^2}, \tag{VI.7}$$

where K is the nucleon wave-number in the average potential. For W larger than Δ ($\sim 110\, A^{-1/3}$ MeV), the interactions destroy the effects of undisturbed single-particle motion, and the properties of the individual configurations are uniformly distributed over the whole energy spectrum. Such a situation corresponds to the strong interaction theory of nuclear reactions, according to which the incident particle shares its energy with many degrees of

* The energy exchange between surface and nucleonic motion has been discussed by HILL and WHEELER (1953) from a somewhat different point of view. These authors attempt a rather detailed description of the nuclear state in the region of high excitation by assuming the nucleus to occupy, at any given moment, a strong coupling state with a definite division of the energy between nucleonic, vibrational and rotational motion. The surface motion is treated in the semi-classical approximation appropriate to large quantum numbers. Exchanges of energy between nucleonic and vibrational motion occur with a frequency (the slippage or damping frequency) closely related to the quantity $W/\hbar$. It is found that the validity of this description requires W to be small compared with the energies of vibration and rotation. The estimate given in the present paragraph indicates that, in general, W is of the order of the vibrational energies, in accordance with tentative estimates by HILL and WHEELER.

freedom of the compound system in a time short compared to that required for a traversal of the nucleus (N. BOHR, 1936; cf. also FESHBACH and WEISSKOPF, 1949).

The existence of nuclear shell structure suggests a value of W small compared to Δ. If the main interaction is due to the particle-surface coupling, one obtains, for energies of the incident particle small compared with the nuclear potential, estimates of W which are on the average about 2–3 MeV, but depend on A and on the nuclear deformation (cf. Ap. Vc). For such values of W, the existence of relatively undisturbed single-particle motion is expected to manifest itself in the properties of the nuclear spectrum.

Thus, in a nuclear reaction, the first stage will be the action of the average nuclear field on the incident particle. The coupling between the particle and the internal degrees of freedom of the target nucleus may, in subsequent stages, lead to energy exchanges which may eventually result in the complex types of motion characteristic of the compound system.

Recent measurements of total neutron cross-sections (BARSCHALL, 1952; MILLER, ADAIR, BOCKELMAN and DARDEN, 1952; NERESON and DARDEN, 1953; WALT et al., 1953) confirm the expectation that the limit of strong interaction is not quite reached, and that single-particle effects are still discernible in the scattering process (WEISSKOPF, 1952). The measured cross-sections represent averages over levels and the data below 3 MeV have been accounted for in terms of single-particle scattering in a complex potential (FESHBACH, PORTER, and WEISSKOPF, 1953)*. The imaginary part of the potential represents the absorption into the compound nucleus and is closely related to the quantity W. The empirical data indicate an absorption which corresponds to $W \sim 2$ MeV. It thus appears that the properties of the higher excitation region may be understood in terms of the same couplings which operate at lower energies (cf. Ap. Vc).

A coupling energy W small compared with Δ has important implications for the whole course of nuclear reaction processes. Thus, the scattering widths of the individual states of the compound system depend on the distance from the nearest

* We are indebted to these authors for making available their results in advance of publication. Cf. also p. 158 ff. below for further discussion of this analysis, and of the conditions under which nuclear cross-sections can be described in terms of the scattering in a complex potential.

virtual level for single-particle potential scattering. The reduced width of the single-particle level is mainly distributed over the compound states within a distance W. Outside of this region, the compound states are much narrower, and appear as a fine structure on a background of potential scattering (cf. Ap. Vb)*.

Moreover, for $W < \Delta$, direct couplings between entrance and exit channels may lead to nuclear reactions which do not pass through the compound stage (direct ejection of particles or direct excitation of rotational or vibrational modes). The coupling energy W would also reveal itself in the relative probability of the various modes of decay of the compound state, which often depend on the amplitude of a few simple types of motion (cf. Ap. Vc).

* A formulation of the nuclear dispersion theory, incorporating single-particle features as well as the compound nucleus formation, has also recently been considered by FESHBACH, PORTER, and WEISSKOPF. We are indebted to these authors for a private communication of results of their investigation.

VII. Electromagnetic Transitions.

An essential part of the present knowledge of the low energy nuclear spectrum has been obtained from the study of γ-transitions. The determination of multipole orders is a valuable tool in assigning spins and parities to the nuclear states, and the measurement of transition probabilities yields further important information on the nature of the excitations involved.

The general implications of the empirical evidence for the nuclear level structure have already been considered in Chapter VI. In the present chapter, we give the calculation of electromagnetic transition probabilities in the coupled system and the more detailed analysis of the available empirical data.

a) Transition Operators.

The transition probability for radiation of a photon of multipole order λ and of frequency ω is given by (WEISSKOPF, 1951; MOSZKOWSKI, 1951, 1953; STECH, 1952; BLATT and WEISSKOPF, 1952, p. 595)

$$T(\lambda) = \frac{8\pi(\lambda+1)}{\lambda[(2\lambda+1)!!]^2}\frac{1}{\hbar}\left(\frac{\omega}{c}\right)^{2\lambda+1} B(\lambda) \qquad \text{(VII.1)}^*$$

where the reduced transition probability $B(\lambda)$ can be written as

$$B(\lambda) = \sum_{\mu, M_f} |<i|\mathfrak{M}(\lambda,\mu)|f>|^2 \qquad \text{(VII.2)}$$

in terms of the matrix elements of the multipole operator $\mathfrak{M}(\lambda,\mu)$ of order λ,μ between an initial state i and a final state f, with magnetic quantum number M_f.

* $(2\lambda+1)!! \equiv 1\cdot 3\cdot 5\ldots(2\lambda+1)$.

The electric and magnetic multipole operators are given by*

$$\mathfrak{M}_e(\lambda, \mu) = \sum_{p=1}^{A} e_p r_p^\lambda Y_{\lambda\mu}(\vartheta_p, \varphi_p) \tag{VII.3}$$

and

$$\mathfrak{M}_m(\lambda, \mu) = \frac{e\hbar}{2Mc} \sum_{p=1}^{A} \left(g_s \vec{s} + \frac{2}{\lambda+1} g_l \vec{l} \right)_p \cdot \vec{\nabla}_p \left(r_p^\lambda Y_{\lambda\mu}(\vartheta_p, \varphi_p) \right), \tag{VII.4}$$

respectively, where e_p, $(g_l)_p$, and $(g_s)_p$ refer to the charge, orbital and spin g-factors of the particle p.

In the unified description of the nuclear dynamics, the state of the nucleus is described in terms of collective and particle degrees of freedom. The former represent the bulk of the nucleons, which are strongly bound, while the latter represent the most loosely bound particles, which may be individually excited (cf. § IIa.iii). In the coordinates appropriate to this description, the multipole operators (3) and (4) take the form

$$\mathfrak{M}_e(\lambda, \mu) = \sum_p \left(e_p - \frac{Ze}{A^\lambda} \right) r_p^\lambda Y_{\lambda\mu}(\vartheta_p, \varphi_p) + \frac{3}{4\pi} ZeR_0^\lambda \alpha^*_{\lambda\mu} \tag{VII.5}$$

and

$$\left.\begin{aligned} \mathfrak{M}_m(\lambda, \mu) = {} & \frac{e\hbar}{2Mc} \sum_p \left(g_s \vec{s} + \frac{2}{\lambda+1} g_l \vec{l} \right)_p \cdot \vec{\nabla}_p \left(r_p^\lambda Y_{\lambda\mu}(\vartheta_p, \varphi_p) \right) \\ & + \frac{e\hbar}{Mc} \frac{1}{\lambda+1} g_R \int \vec{R}(r) \cdot \vec{\nabla} \left(r_\lambda Y_{\lambda\mu}(\vartheta, \varphi) \right) d\tau, \end{aligned}\right\} \tag{VII.6}$$

where the sums over p include the particle degrees of freedom, while the last terms refer to the multipole moments generated by the collective motion of the nucleons.

The particle part of the electric moment (5) includes the effect of the recoil of the nuclear core, which is of special importance for dipole transitions; for $\lambda \geqslant 2$, the recoil term also contains many-particle operators, which have been omitted in (5).

The coefficient of $\alpha^*_{\lambda\mu}$ in (5) is obtained from (II.2), which is based upon a hydrodynamical description of the collective motion. Inadequacies of this approximation of the kind indicated by the nuclear quadrupole moments (cf. § Vc) would imply a

* In (3), we neglect the contribution of the intrinsic magnetic moment of the particle, which is of the same order as that of the magnetic multipole of one higher order.

somewhat smaller value of the coefficient. The density of angular momentum in the collective motion is denoted by $\vec{R}(\vec{r})$ and may be expressed as a quadratic form in the α-coordinates.

The reduced transition probability $B(\lambda)$, which is related by (1) to the lifetime for γ-emission, can also be determined from the cross-section for Coulomb excitation by impact of heavy ions (TER-MARTIROSYAN (1952); cf. also Appendix VI; e. g. (Ap. VI.17)).

The two methods for determining B complement each other in the sense that the lifetime measurements are most easily performed when B is small, while large excitation cross-sections are obtained when B is large. Moreover, the relative intensity of the different multipole components in the field of the impinging particle is very different from that of the radiation field produced by a source of nuclear dimensions.

b) Transitions in the Weakly Coupled System.

i. *Particle transitions.*

In the case of a single particle moving in a spherical potential, a transition between states of angular momenta j_i and j_f is electric of order $\lambda = |j_i - j_f|$, if the spins and orbits are parallel in the initial as well as the final states, or if they are antiparallel in both cases. The value of B is given by (STECH, 1952; BLATT and WEISSKOPF, 1952; MOSZKOWSKI, 1953)

$$B_e(\lambda) = \frac{1}{4\pi}\left(e_p - \frac{Ze}{A^\lambda}\right)^2 |<i|r^\lambda|f>|^2 c(j_>, j_<) \frac{2j_f+1}{2j_<+1}, \qquad \text{(VII.7)}$$

where $<i|r^\lambda|f>$ is the radial matrix element, and where the $c(j_>, j_<)$ are numerical coefficients of order unity, which can be expressed in terms of Racah coefficients*. Values of $c(j_>, j_<)$ are listed in Table XXIV. The arguments $j_>$ and $j_<$ denote the larger and smaller, respectively, of j_i and j_f.

If $j_>$ has parallel spin and orbit, while $j_<$ has antiparallel spin and orbit, the transition is magnetic, of order $\lambda = |j_i - j_f|$, and (cf. the references of (7))

* STECH (1952) uses a corresponding quantity $\overline{|F(j_A, j_B)|^2}$ equal to $(j_< + 1/2)^{-1}\, c(j_>, j_<)$. MOSZKOWSKI (1953) uses the quantity $S(I_i, L, I_f)$ which, for $|I_i - I_f| = \lambda$, equals $(2j_f + 1)(2j_< + 1)^{-1}\, c(j_>, j_<)$.

TABLE XXIV. Coefficients $c(j_>, j_<)$ in transition probabilities.

$j_<$ \ $j_>$	3/2	5/2	7/2	9/2	11/2	13/2
1/2	1	1	1	1	1	1
3/2	1	$\frac{6}{5}$	$\frac{9}{7}$	$\frac{4}{3}$	$\frac{15}{11}$	$\frac{18}{13}$
5/2		1	$\frac{9}{7}$	$\frac{10}{7}$	$\frac{50}{33}$	$\frac{225}{143}$
7/2			1	$\frac{4}{3}$	$\frac{50}{33}$	$\frac{700}{429}$
9/2				1	$\frac{15}{11}$	$\frac{225}{143}$
11/2					1	$\frac{18}{13}$
13/2						1

The transition probability for a single particle transition $j_i \to j_f$ of multipole order $\lambda = |j_i - j_f|$ involves the coefficients $c(j_>, j_<)$ tabulated above. (Cf. equations (VII.7 and 8) and footnote on p. 103). The larger and smaller of j_i, j_f are denoted by $j_>$ and $j_<$, respectively.

$$B_m(\lambda) = \frac{\lambda^2}{4\pi}\left(\frac{e\hbar}{2Mc}\right)^2\left(g_s - \frac{2}{\lambda+1}g_l\right)^2 |\langle i|r^{\lambda-1}|f\rangle|^2 c(j_>, j_<)\frac{2j_f+1}{2j_<+1}. \quad \text{(VII.8)}$$

Finally, if $j_>$ has antiparallel while $j_<$ has parallel spin and orbit, the transition is forbidden in order $\lambda = |j_i - j_f|$. For a pure configuration, the transition would be electric of order $\lambda = |j_i - j_f| + 1$, but small admixtures of other configurations may suffice to produce a predominantly magnetic transition of order $\lambda = |j_i - j_f|$.

For many-particle configurations, similar expressions may be obtained, provided the coupling scheme is known (cf., e. g., MOSZKOWSKI, 1953). Thus, for two equivalent protons, the transition $(j^2)_{J=2} \to (j^2)_{J=0}$ is of electric quadrupole type with a reduced transition probability

$$B_e(2) = \frac{1}{16\pi}e^2|\langle i|r^2|f\rangle|^2\frac{(2j-1)(2j+3)}{j(j+1)}. \quad \text{(VII.9)}$$

In the estimates of transition probabilities in § VII d, we use the simple estimate

$$< i | r^\lambda | f > = \frac{3}{3+\lambda} R_0^\lambda \qquad \text{(VII.10)}$$

which would be obtained for a radial wave-function constant within the nuclear volume and vanishing outside. More detailed calculations have been made (Moszkowski, 1953) which yield similar results.

ii. *Phonon transitions.*

The radiation emitted by the freely oscillating nuclear surface is of electric multipole type of the same order λ as the surface deformation. For the decay of a one-phonon state to a no-phonon state, one finds from (5) and (A. 38) (cf. Flügge, 1941; Lowen, 1941; Fierz, 1943; Berthelot, 1944; Jekeli, 1952)*

$$B_e(\lambda) = \left(\frac{3}{4\pi} Ze R_0^\lambda\right)^2 \frac{\hbar\omega_\lambda}{2 C_\lambda} \qquad \text{(VII.11)}$$

for the reduced transition probability in terms of the frequency ω_λ and deformability C_λ of the λ^{th} surface mode (cf. Figs. 1 and 2). The cooperative nature of such a transition, as expressed in the appearance of the factor Z^2 in (11), in general leads to a much faster decay than for a corresponding particle transition.

iii. *Surface moments induced by particle transitions.*

In weak coupling, a transition between two different particle states induces a moment in the surface which may be calculated in the perturbation approximation. Although the admixture of collective excitation is small, its influence may be important in the case of electric multipole transitions, due to the larger charge involved in the surface motion. The induced surface moment is proportional to the mass moment of the particle transition, and the operator (5) becomes (cf. II. 5 and 9)

$$\left.\begin{aligned} \mathfrak{M}_e(\lambda, \mu) &= R_0^\lambda \sum_p Y_{\lambda\mu}(\vartheta_p, \varphi_p) \\ &\left\{ e_p \left(\frac{r_p}{R_0}\right)^\lambda + \frac{3}{4\pi} Ze \, \frac{k}{C_\lambda} \, \frac{(\hbar\omega_\lambda)^2}{(\hbar\omega_\lambda)^2 - (E_i - E_f)^2} \right\} \end{aligned}\right\} \qquad \text{(VII.12)}$$

* The results of the quoted authors differ somewhat from each other in numerical coefficients. Also the matrix element quoted by Blatt and Weisskopf (1952, p. 628) appears to lead to a transition probability too small by a factor four.

for a transition between particle states with energies E_i and E_f. It is of significance that the particle part of $\mathfrak{M}_e$ depends on the charge of the particles, while the surface part involves only the coupling constant k, which is the same for neutrons and protons. The hydrodynamic estimate of the second term in (12) (cf. Figs. 1 and 2) indicates that it is somewhat larger than the first term (by about a factor of four for a medium heavy nucleus).

c) Transitions in the Strongly Coupled System.

i. *Particle transitions.*

In the strong coupling representation (II.15), it is convenient to expand the multipole operators along the nuclear axis

$$\mathfrak{M}(\lambda, \mu) = \sum_{\nu} \mathfrak{M}'(\lambda, \nu)\, \mathfrak{D}^{\lambda}_{\mu\nu}(\theta_i), \qquad \text{(VII.13)}$$

where $\mathfrak{M}'(\lambda, \nu)$ is expressed in the nuclear coordinate system, and where the $\mathfrak{D}$-functions are the same as used in (II. 15).

For a particle transition between states with $I_i = K_i = \Omega_i$ and $I_f = K_f = \Omega_f$ one obtains, for $\lambda = |I_i - I_f|$,

$$B(\lambda) = \left| \int \chi^*_{\Omega_i} \mathfrak{M}'(\lambda, \pm\lambda)\, \chi_{\Omega_f} \right|^2 \left| \int \varphi_i^*(\beta, \gamma)\, \varphi_f(\beta, \gamma) \right|^2 \frac{2I_f + 1}{2I_> + 1}. \qquad \text{(VII.14)}$$

In special cases, the symmetrization of the wave function (II.15) may introduce additional terms.

In the strong coupling scheme, where the particles move independently with respect to the nuclear axis, the particle transitions are always one-particle transitions. Thus, the first factor in (14) is simply related to the transition probability for a single uncoupled particle, provided the particle wave functions χ have a definite j, and provided the collective part of the multipole moments (5 and 6) can be neglected. For a transition from $j_i = \Omega_i = I_i$ to $j_f = \Omega_f = I_f$, one then obtains

$$B(\lambda) = B_{\mathrm{sp}}(\lambda) \left| \int \varphi_i^* \varphi_f \right|^2 \frac{2I_< + 1}{2I_> + 1}, \qquad \text{(VII.15)}$$

where $B_{\mathrm{sp}}(\lambda)$ is given by (7) or (8). However, in some cases, important differences between (14) and (15) may arise from the

modification of the particle wave function caused by the non-spherical character of the potential, and from the collective contributions to the multipole operators.

Thus, the tendency of the surface coupling to admix certain neighbouring orbitals in the particle state may, in particular, cause transitions to occur, even when B_{sp} vanishes due to shell model selection rules (l-forbiddenness; j-forbiddenness).

An important contribution to electric transitions with $\lambda > 2$ may arise from the coupling to the surface mode of order λ. Since the coupling to these higher order modes may be considered as weak, the effect can be included by using the form (12) for the multipole operator. This contribution to the transition may be particularly significant in leading to comparable lifetimes for electric multipole transitions of odd-neutron and odd-proton nuclei.

The last factors in (15) imply reductions in the transition probability of the type known in molecular spectroscopy (Franck-Condon principle; (cf., e. g., HERZBERG, 1950, p. 199)). The factor involving the vibrational wave functions gives the reduction arising from the partial orthogonality of two states with differing magnitude or shape of deformation. This effect depends on the difference of the two equilibrium deformations as compared with the zero point amplitude. The dependence is exponential, and great reductions may result when the coupling is strong. If the two states have different shapes (strong coupling solutions centered on different values of γ), it is necessary to consider the full symmetry of the wave function (A.118), since it may be easier for the surface to oscillate from oblate to prolate form along different intrinsic nuclear axes (cf. HILL and WHEELER, 1953, fig. 28). The last factor in (15) involving the spins is a projection factor associated with the fact that only the projection of the particle multipole along the nuclear axis is effective.

The reduction in transition probability due to the surface coupling is illustrated in Fig. 14 for an $M1$ transition of $p_{3/2} \rightarrow p_{1/2}$ type. From the $I = j = 3/2$ wave function given in Fig. 4 (p. 25), the transition probability to an uncoupled $p_{1/2}$ state may be simply obtained. The "unfavoured factor", F, representing the ratio of B and B_{sp}, is plotted as a function of x. As an example of the effect due to differences in shape, we have also plotted

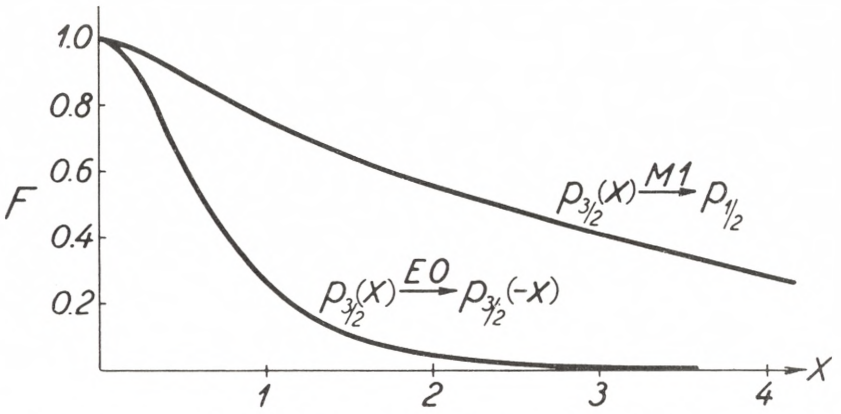

Fig. 14. *Unfavoured factors in intermediate coupling.* The coupling between particle and surface motion implies that particle transitions are in general slowed down by the partial orthogonality of the surface states of the combining levels. The ratio of the resulting transition probability to that for an uncoupled particle is referred to as the unfavoured factor, F. The figure illustrates the behaviour of F as a function of the dimensionless coupling constant x (II.14).

The upper curve corresponds to a $p_{3/2} \rightarrow p_{1/2}$ $M1$ transition; the $p_{3/2}$-state appropriate to a given x is obtained from Fig. 4, while the pure $p_{1/2}$-state has no coupling to the surface. The lower curve gives the square of the overlap integral between two $p_{3/2}$-states with equal magnitude, but opposite sign of the coupling parameter. This quantity would correspond to the F-factor for a hypothetical $E0$ transition.

the square of the overlap integral (F-factor for a hypothetical $E0$ transition) for two $p_{3/2}$ states with opposite sign, but same magnitude of the coupling constant.

One may also employ the strong coupling solutions (A. § V.3) to calculate the F-factors for large couplings. For a transition $j \rightarrow j$ between states with coupling strengths x and x', one finds that F contains the factor

$$F \sim \exp\left\{ -\frac{1}{2}\left(\frac{2j-1}{2j+2}\right)^2 j\,(x-x')^2 \right\} \qquad \text{(VII.16)}$$

which exhibits the exponential decrease of F with increasing coupling.

ii. *Collective transitions.*

In collective transitions of the strongly coupled system, the last term in (5) may give rise to strongly enhanced $E2$ transition probabilities.

Of special interest are the rotational excitations, which, in even-even nuclei, form a spectrum with $I = 0, 2, 4, \cdots$ (cf. VI.1). The γ-decay proceeds in cascades of $E2$ radiation, and for the transition $I + 2 \rightarrow I$, the reduced transition probability, which may be obtained by using (V. 5), is given by

$$B_e(2) = \frac{15}{32\pi} e^2 Q_0^2 \frac{(I+1)(I+2)}{(2I+3)(2I+5)}, \qquad \text{(VII.17)}$$

where Q_0 is the intrinsic quadrupole moment (V.7). The expression (17) exceeds the one-phonon decay probability (11) by a factor of the order of the average number of phonons present in the strong coupling state.

In odd-A nuclei, the rotational levels form a sequence with $I = K, K + 1, K + 2, \cdots$ (cf. VI.4), except for the case of $K = \Omega = 1/2$. For a transition $I + 1 \rightarrow I$, one obtains

$$B_e(2) = \frac{15}{16\pi} e^2 Q_0^2 \frac{K^2 (I+1-K)(I+1+K)}{I(I+1)(2I+3)(I+2)}, \qquad \text{(VII.18)}$$

while for the cross-over transitions $I + 2 \rightarrow I$

$$B_e(2) = \frac{15}{32\pi} e^2 Q_0^2 \frac{(I+1-K)(I+1+K)(I+2-K)(I+2+K)}{(I+1)(2I+3)(I+2)(2I+5)}. \qquad \text{(VII.19)}$$

For the $I + 1 \rightarrow I$ transitions, $M1$ radiation is also present, with a reduced transition probability given by

$$B_m(1) = \frac{3}{4\pi} \left(\frac{e\hbar}{2Mc}\right)^2 (g_\Omega - g_R)^2 \frac{\Omega^2 (I+1-K)(I+1+K)}{(I+1)(2I+3)}, \qquad \text{(VII.20)}$$

in terms of the g-factors of the particle and collective motion, g_Ω and g_R, respectively (cf. IV.4 and 10). While, for a similar sequence of particle excitations, the decay would proceed by a cascade of almost pure $M1$ radiation, the considerable enhancement of the $E2$ radiation produced by the collective deformation

may, in some cases, give rise to an appreciable admixture of $E2$ radiation, and also to cross-overs of the type (19).

For odd-A nuclei with $K = \Omega = 1/2$, the rotational spectrum is more complicated (cf. § VI c.iii). The electric radiation is still given by (18) and (19), but the matrix element for $M1$ transitions cannot be related so simply to the magnetic moment of the ground state as in (20).

Transitions involving a change of vibrational quantum numbers (cf. § VI c.iv) are of pure $E2$ type in the limit of strong coupling. The decay of a higher vibrational state may in general proceed to several rotational levels of the lower vibrational state. The transition probabilities can be obtained from (5), using the vibrational wave functions (A. 109 and 114). The matrix elements are of the same order of magnitude as for a single phonon decay (11) and thus are larger than for a particle transition, although smaller than for a rotational transition.

d) Discussion of Empirical Data.

The classification of the isomeric transitions, as well as the empirical decay energies, lifetimes, and the conversion coefficients used in this paragraph are, except where otherwise noted, taken from the articles by GOLDHABER and SUNYAR (1951) and GOLDHABER and HILL (1952).

In a field of such rapid development, it may be expected that improved experiments will modify some of the data considered here. Without evaluating the individual experiments, we have tried to confine ourselves to those classes of transitions which, at the present time, seem to provide the most reliable and significant information.

i. *$M4$ transitions; unfavoured factors.*

The strong spin-orbit coupling shell model predicts low-lying isomeric states of long lifetime in the regions before the closed shells at 50, 82, and 126. In these regions, particle levels of high spin ($g_{9/2}$, $h_{11/2}$, and $i_{13/2}$, respectively) are being filled simultaneously with levels of low spin and opposite parity ($p_{1/2}$, $d_{3/2}$, and $f_{5/2}$) and isomeric states decaying by $M4$ radiation are

TABLE XXV. $M4$ transitions in odd-A nuclei.

Nucleus	E (keV)	$-\log T$ ($\sec^{-1}$)	F	Nucleus	E (keV)	$-\log T$ ($\sec^{-1}$)	F
	$g_{9/2} \leftrightarrow p_{1/2}$				$h_{11/2} \leftrightarrow d_{3/2}$		
$_{30}Zn^{69}$	439	4.88	.060	$_{50}Sn^{117}$	159	7.95	.120
$_{36}Kr^{85}$	305	5.18	.101	$_{50}Sn^{119}$	65	11.13	.234
$_{38}Sr^{87}$	390	4.27	.089	$_{52}Te^{121}$	82	10.67	.082
$_{39}Y^{87}$	384	4.97	.055	$_{52}Te^{123}$	88	10.35	.086
$_{39}Y^{89}$	913	1.31	.098	$_{52}Te^{125}$	110	9.43	.094
$_{39}Y^{91}$	555	3.68	.037	$_{52}Te^{127}$	88	10.36	.080
$_{40}Zr^{89}$	588	2.61	.092	$_{52}Te^{129}$	106	9.34	.156
$_{41}Nb^{91}$	104	8.90	.73	$_{52}Te^{131}$	183	7.00	.236
$_{41}Nb^{95}$	216	6.39	.061	$_{54}Xe^{129}$	196	7.39	.056
$_{41}Nb^{97}$	747	1.94	.024	$_{54}Xe^{131}$	163	7.91	.086
$_{43}Tc^{95}$	39	~ 13.22	~ .046	$_{54}Xe^{133}$	232	6.42	.105
$_{43}Tc^{97}$	96	9 67	.046	$_{54}Xe^{135}$	520	3.22	.116
$_{43}Tc^{99}$	142	8.03	.057	$_{56}Ba^{133}$	275	6.05	.054
$_{49}In^{113}$	390	4.14	.038	$_{56}Ba^{135}$	269	5.77	.121
$_{49}In^{115}$	335	4.67	.044	$_{56}Ba^{137}$	661	2.40	.085
					$i_{13/2} \leftrightarrow f_{5/2}$		
				$_{78}Pt^{195}$	129	8.64	.049
				$_{78}Pt^{197}$	337	4.86	.053
				$_{80}Hg^{197}$	165	7.67	.048
				$_{80}Hg^{199}$	368	4.50	.054
				$_{82}Pb^{207}$	1063	0.113*	.084

The F-factor gives the ratio of the observed transition probability to that of a single-particle transition between the states indicated at the head of the column (cf. (8) and (10)).

* HOPKINS (1952).

expected. These expectations have been strikingly confirmed (GOLDHABER and SUNYAR, 1951; MOSZKOWSKI, 1951).

The lifetimes of these isomeric transitions yield further evidence on the properties of the combining states. The known $M4$ transition probabilities are listed in Table XXV. The last column gives the ratio F (the unfavoured factor) of the observed transition probability to that calculated for the appropriate single-particle transition (cf. (8) and (10), and (II.7))†. The F-factors are sensitive to the assumed value of the nuclear radius.

† The F-factors are analogous to the quantities $|M|^2$ listed by GOLDHABER and SUNYAR (1951), but are obtained by comparison with a somewhat more detailed theoretical estimate. In the notation of MOSZKOWSKI (1953), F equals the ratio of $|M|^2$ and M^2_{ML}, for magnetic transitions of order L.

Thus, a decrease of 10 % in the value (II.7) leads to an increase by about a factor two in the F-values of Table XXV.

Despite this uncertainty, it is evident that the transitions are consistently slower than expected for an uncoupled particle by a significant factor. This reduction provides evidence that the particle transitions are associated with an appreciable readjustment of the collective field. The observed unfavoured factors correspond to a nuclear coupling scheme resulting from an intermediate to strong particle-surface coupling (cf. § VII c.i).

From such an interpretation of the transitions, one can also correlate some of the observed trends of the unfavoured factor with the expected surface deformations. Thus, one notices that, for the nuclei possessing closed shells, and especially for those possessing double closed shells ± 1 particle, the F-factors are among the largest*. Moreover, for a series of isotopes of the same element, the F-values decrease as we move away from a closed-shell nucleus (cf. Bohr and Mottelson, 1952; Moszkowski, 1953). These trends can be understood in terms of the increased deformation, produced by the added particles and reflected in many nuclear properties (cf., e. g., § III.iii; § V c; § VI c.ii).

In the estimate of the F-factor, the transitions are compared with one-particle transitions, although many of the nuclei in question have several particles outside of closed shells. In the strong coupling approximation, where the particles are coupled separately to the nuclear axis, the transitions do indeed only involve changes in the quantum numbers of a single particle, and the F-factor can be directly related to the change in the vibrational state (cf. 15). If, however, the interparticle forces influence the coupling scheme in the nucleus (cf. Fig. 6), there will be an additional effect contributing to the F-factor (cf. Moszkowski. 1953). Still, it seems excluded that this latter effect gives the main part of F, since in Table XXV there are several nuclei with single-particle configurations, and also for these the transition probabilities are considerably reduced as compared with shell model estimates.

Reduction in the transition probability, associated with the

* In view of the marked stability of $_{82}Pb^{208}$, it may be significant that the F-factor for $_{82}Pb^{207}$ is as small as 0.08.

partial orthogonality of the vibrational states of different particle configurations, is expected as a very general feature of nuclear particle transitions. This is indeed observed and, besides the $M4$ isomeric transitions, especially the allowed unfavoured and the pure GT forbidden β-transitions provide evidence for the effect (cf. § VIIIc.ii and iv).

A consequence of this interpretation of the unfavoured factor is its absence in certain special cases where the combining states have similar surface shapes. Thus, the mirror β-transitions which, due to the symmetry in the particle configurations, have almost identical deformations are known to be conspicuously faster than other allowed β-transitions (cf. § VIIIc.i).

Another class of unretarded particle transitions is expected for the γ-transitions between the two members of the ground state doublet in an odd-odd nucleus, where the deformations are expected to be rather similar (cf. § VIb). There is some evidence that the low energy $M1$ transitions in odd-odd nuclei are faster than in odd-A nuclei (GRAHAM and BELL, 1953). Some of the long lived $M3$ isomers in odd-odd nuclei (cf. GOLDHABER and HILL, 1952) may also be of this type, but uncertainties in the spin assignments as well as in the conversion coefficients prevent as yet a quantitative analysis of the lifetimes.

It would also be of interest to compare β- or γ-transitions to different members of a rotational family, since the vibrational integral in F does not affect the branching ratio.

ii. *$E3$ transitions; j-forbiddenness.*

In the region before the closed shell at 50, another important group of long lived isomers has been found. These have been identified as $E3$ transitions of the $(7/2+) \leftrightarrow (1/2-)$ type and occur for the nucleon numbers 43, 45, and 47. The $(7/2+)$ states have been classified on the basis of the shell model as $(g_{9/2})^{3,5,7}_{7/2}$ (GOLDHABER and SUNYAR, 1951; MOSZKOWSKI, 1951). For pure configurations of this type, the transitions would be forbidden to order $E3$ (j-forbiddenness). For odd-neutron nuclei, there is an additional forbiddenness for these transitions which require an electric multipole moment. Both these types of forbiddenness are removed by the surface coupling which is expected to be rather large in these nuclei, as evidenced by the energy

TABLE XXVI. $E3$ transitions of $(7/2+) \leftrightarrow (1/2-)$ type.

Nucleus	E (keV)	$-\log T$ ($\sec^{-1}$)	F
$_{34}Se^{77}$	160	1.68	.013
$_{34}Se^{79}$	80	3.89	.0025
$_{34}Se^{81}$	98	4.64	.0004
$_{36}Kr^{79}$	127	2.47	.0026
$_{36}Kr^{81}$	187	1.45	.0017
$_{36}Kr^{83}$	32.2	~ 7.39	$\sim .0004$
$_{45}Rh^{103}$	40	~ 6.95	$\sim .0007$
$_{45}Rh^{105}$	130	2.55	.0010
$_{47}Ag^{107}$	93.9	3.03	.013
$_{47}Ag^{109}$	87	3.04	.021
$_{74}W^{183}$	80	~ 3.02	$\sim .014$

The shell model assigns a $(g_{9/2})^{3, 5, 7}$ configuration to the $(7/2+)$ state. The anomalous spin $I = j - 1$ may be explained as a result of the surface coupling (cf. § III.iii). For a pure $g_{9/2}$ configuration, the transition would be forbidden to order $E3$ (j-forbiddenness). The transition is assumed to occur due to the admixture of a small amount of the $g_{7/2}$ orbital. The coupling to deformations of order three, which induces an $E3$ moment in the surface, may also be important for these transitions, especially in the odd-neutron nuclei. The F-factor gives the ratio of the observed transition probability to that of a $g_{7/2} \leftrightarrow p_{1/2}$ single-proton transition (cf. (7) and (10)).

depression of the $(7/2+)$ level (cf. § III.iii). The surface coupling will admix particle states of $g_{7/2}$ type and, furthermore, the coupling to the $\lambda = 3$ surface mode produces an $E3$ moment also in odd-neutron states (cf. (12)).

In Table XXVI are listed the known $E3$ transitions of $(7/2+) \leftrightarrow (1/2-)$ type. The F-factors listed in the last column of the table are derived by comparison with the transition of a single proton between $p_{1/2}$ and $g_{7/2}$ states ((7) and (10)). The comparable magnitude of the observed F-factors for odd-neutron and odd-proton nuclei is an indication that the second term in (12) is at least comparable to the first term, as suggested by the hydrodynamic estimate. There may be a tendency for the odd-neutron F-values to be somewhat smaller than those of odd-proton nuclei; this could be understood from the effect of the first term in (12) together with the A-dependence of the last term.

The appearance of smaller F-factors in this group as compared with the $M4$ transitions, as well as the somewhat larger

spread in values, may reflect the fact that the transition depends entirely on the admixture of the $g_{7/2}$ state, which again depends on the degree of deformation of the nucleus.

Examples of $E3$ transitions between other configurations have also been identified, some with very small F-factors (cf. GOLDHABER and SUNYAR, 1951). While the detailed classification of these transitions is difficult at the present time, such highly unfavoured transitions may be expected in regions of strong coupling, due to selection rules associated with the Ω_p and K quantum numbers.

iii. *$E2$ transitions; collective excitations.*

Collective excitations give rise in general to $E2$ or $M1$ radiation (cf. § VIc), and are expected to reveal themselves especially by their strongly enhanced $E2$ transition probabilities, resulting from the large electric quadrupole of the oscillating surface.

In the strongly coupled system, the low-lying collective excitations can be characterized as rotational levels. The spectrum is particularly simple in even-even nuclei where a series of states with even I decaying by pure $E2$ radiation is obtained (cf. § VIc.ii).

The first excited $(2+)$ states in even-even nuclei with measured lifetimes are listed in Table XXVII. The F-factors in column four provide a comparison of the observed transition probability with that expected for a proton transition $(j^2)_2 \rightarrow (j^2)_0$ for large j (cf. (9)).

The very large F-factors for the nuclei in regions away from closed shells confirm the interpretation of the states as rotational levels of the strongly coupled system. From the measured lifetimes one can deduce, by means of (17), the intrinsic quadrupole moments Q_0 which are listed in column five. These may be compared with the Q_0-values derived from the spectroscopically measured quadrupole moments of neighbouring isotopes, listed in column six. In the derivation of Q_0 from Q, the full strong coupling projection factor (V.9) has been assumed. The two determinations of Q_0 yield similar values. The spectroscopic values are somewhat larger than those deduced from transition probabilities, but the difference may not be significant, considering

TABLE XXVII. $E2$ transitions in even-even nuclei.

Nucleus	E (keV)	log T (sec^{-1})	F	$\|Q_0\|$ (10^{-24} cm^2) (transition)	$\|Q_0\|$ (10^{-24} cm^2) (spectroscopic)
$_{66}Dy^{160}$	85	7.91	140	9	
$_{68}Er^{166}$	80	7.91	180	10	~ 20 ($_{68}Er^{167}$)
$_{70}Yb^{170}$	84	7.94	140	9	11 ($_{70}Yb^{173}$)
$_{72}Hf^{176}$	89	8.01	120	9	14 ($_{71}Lu^{175}$)
$_{76}Os^{186}$	137	8.64	55	6	8 ($_{75}Re^{185}$)
$_{80}Hg^{198}$	411	10.1 *	6	2	2 ($_{80}Hg^{201}$)
$_{82}Pb^{204}$	374	6.34	2×10^{-3}		
$_{84}Po^{212}$	719	11.2 **	5	2	
$_{84}Po^{214}$	606	11.1 **	7	2	

* MALMFORS (1952); corrected for the statistical factor in the resonance formula (cf., e. g., STORRUSTE, 1951).

** Deduced from the branching ratio of α- and γ-decay (cf. BETHE, 1937, p. 229). The lifetime for the long range α-groups is calculated from that of the ground state by the semi-empirical formula of WAPSTRA (1953) with the inclusion of the appropriate statistical factor. The empirical energies and lifetimes are taken from the compilation of WAY et al. (1950) and HOLLANDER, PERLMAN and SEABORG (1953). The branching ratios are obtained from these references and from ELLIS and ASTON (1930) and RYTZ (1951).

The table lists the $E2$ transitions in even-even nuclei with measured lifetimes. All the transitions go from a first excited state of $(2+)$ character to the ground state $(0+)$. The F-factor in column four is the ratio of the observed transition probability to the value calculated for a proton transition $(j^2)_2 \rightarrow (j^2)_0$ for large j (cf. (9)). The intrinsic quadrupole moments Q_0 in column five are deduced from (17), assuming the levels to be of rotational character. For comparison, the last column lists the intrinsic quadrupole moment derived from available spectroscopic data on neighbouring odd nuclei (cf. Addendum to Chapters IV and V). The projection factor (V. 9) has been assumed in calculating Q_0 from Q.

the experimental uncertainties involved in both types of measurements.

The table exhibits the intimate correlations between excitation energies, reduced transition probabilities, and quadrupole moments, and also shows the expected variations of these quantities with the number of particles outside of closed shells.*

With the approach to the closed-shell configuration of Pb^{208}, the rotational description of the states becomes less appropriate, and in the immediate neighbourhood of Pb^{208} a

* Note added in proof: Recently, HUUS and ZUPANČIČ (1953) have produced the $(2+)$ first excited states in the even $_{74}W$ isotopes by means of Coulomb excitation. From the measured excitation cross section they have deduced a deformation $|Q_0| \approx 7\times10^{-24}$ cm^2 in good agreement with the trends exhibited in Table XXVII (cf. also footnote on p. 166).

TABLE XXVIII. $E2$ transitions in odd-A nuclei.

Nucleus	E (keV)	$\log T$ ($\sec^{-1}$)	states		F	$\lvert Q_0 \rvert$ (10^{-24} cm^2) (transition)
			i	f		
$_{48}Cd^{111}$	243	6.91	5/2+	1/2+	0.12	
$_{73}Ta^{181}$	481	7.74	3/2+	7/2+	0.005	
$_{80}Hg^{197}$	134	7.47	5/2—	1/2—	4.0	2
$_{80}Hg^{199}$	159	7.94	5/2—	1/2—	5.0	2

The F-factors have been calculated by comparison with a single-proton transition between states with the listed spins and parities. The Q_0-values for the Hg isotopes are obtained from (19).

weak coupling situation is expected. In this region, the collective excitations represent simple surface oscillations (cf. § VIc.i).

In the weakly coupled system, also particle excitations may be encountered among the first excited states (cf. § VIb). An example may be provided by the Pb^{204} activity with its relatively long lifetime. The fact that, for this transition, F is small compared to unity may indicate a rather pure neutron excitation, corresponding to the closed-shell structure of the protons.

The observed $E2$ transitions in odd-A nuclei are listed in Table XXVIII. The two first have the small F-factors characteristic of particle excitations. For the Hg transitions, the F-factors are larger than unity and indicate collective excitations. A first excited level of I_0+2 in these nuclei can be obtained for a rotational family with $\Omega = 1/2$ (cf. § VIc.iii); this interpretation could also account for the relatively low excitation energies as compared with that in Hg^{198}. The Q_0-values derived from (19) are just of the same magnitude as obtained for Hg^{198}, and derived from the spectroscopic data of Hg^{201} (cf. Table XXVII). The intermediate F-factors of the Hg transitions, as well as the rather large excitation energies, indicate that the strong coupling scheme is not very fully developed, and deviations from the simple rotational character of the states may be of importance.*

* Note added in proof: An example of a strongly enhanced $E2$ transition ($F \sim 100$) in an odd-A nucleus ($_{73}Ta^{181}$) has recently been found by the Coulomb excitation process (HUUS and ZUPANČIČ 1953; cf. footnote on p. 166 below).

VIII. Beta Transitions.

The analysis of β-transitions has the dual purpose of determining the intrinsic properties of the nucleon-lepton coupling, and providing information on the nuclear structure. The recent progress in experimental techniques as well as the understanding of nuclear states have led to an improved evaluation of the coupling constants in β-decay. This, in turn, now makes possible more detailed tests of nuclear wave functions.

The type of information provided by the analysis of β-transitions is in many respects similar to that derived from electromagnetic particle transitions (cf. § VIb). In particular, the classification of transitions in degrees of forbiddenness provides evidence on the spins and parities of nuclear states, while a closer study of β-decay transition probabilities gives more detailed information on the nuclear coupling scheme. In the present chapter, we consider the calculation of transition probabilities in the coupled system, and the more detailed analysis of the empirical data.*

a) Transition Operators.

The comparative half lives of allowed transitions may be written in the form

$$f_0 t = B_g \left[(1 - x) D_F(0) + x D_{GT}(0)\right]^{-1}, \qquad \text{(VIII.1)}$$

where t is the half life and f_0 the integrated Fermi function for an allowed transition (cf., e. g., KONOPINSKI, 1943), while

$$B_g = \frac{2\pi^3 \hbar^7 \ln 2}{g^2 m_e{}^5 c^4}. \qquad \text{(VIII.2)}$$

* We are indebted to Dr. O. KOFOED-HANSEN and M. Sc. A. WINTHER for valuable discussions on theoretical and experimental aspects of β-transitions.

The partial coupling constants for Fermi and Gamow-Teller interactions are $g(1-x)^{1/2}$ and $gx^{1/2}$, respectively*.

The reduced transition probabilities are given by**

$$D_F(0) = \sum_{M_f} |<i| T_\pm |f>|^2 \qquad \text{(VIII.3)}$$

and

$$D_{GT}(0) = 4 \sum_{M_f} |<i| \sum_p \vec{s}_p \tau_\pm^{(p)} |f>|^2, \qquad \text{(VIII.4)}$$

where $T_\pm = \sum \tau_\pm^{(p)}$ are components of the total isotopic spin. The operators s and τ are normalized in such a way that their proper values are $1/2$ and $-1/2$.

For the forbidden β-decays, the transition operator may consist of several terms giving rise to different spectral shapes. The analysis of such mixed transitions is of special interest for the study of the β-decay coupling, but the influence of nuclear structure is as yet more difficult to evaluate.

The forbidden transitions, which have a parity change of $(-)^{\Delta I+1}$ (with $\Delta I \neq 0$) are, however, more simple to interpret. These transitions are of pure Gamow-Teller type and exhibit a spectrum of unique shape. They are intimately related to the magnetic multipole transitions of order $\lambda = \Delta I$. The comparative half life is given by

$$f_n t = B_g [x D_{GT}(n)]^{-1}, \qquad \text{(VIII.5)}$$

where f_n is the integrated Fermi function appropriate to the considered type of transition of forbiddenness $n = \Delta I - 1$ (cf. KONOPINSKI and UHLENBECK, 1941; GREULING, 1942). The normalization employed here is such that

$$f_n = \frac{1}{[(n+1)!]^2} \int_1^{W_0} \sum_{\nu=0}^{n} (B_{n\nu} K^{2(n-\nu)} L_\nu) F_0(W, Z) p W (W_0 - W)^2 dW, \qquad \text{(VIII.6)}$$

where the symbols are defined by DAVIDSON (1951).

The reduced transition probability $D_{GT}(n)$ may be written in the form

* The influence of the so-called cross-terms (FIERZ, 1937) has been neglected. Estimates of the possible magnitude of such terms have recently been given by MAHMOUD and KONOPINSKI (1952) and by WINTHER and KOFOED-HANSEN (1953).

** The quantities $D_F(0)$ and $D_{GT}(0)$ are often denoted by $|\int 1|^2$ and $|\int \vec{\sigma}|^2$, respectively (cf., e. g., KONOPINSKI, 1943).

$$D_{GT}(n) = \sum_{\mu, M_f} |<i| \mathfrak{O}_{GT}(n, \mu) |f>|^2, \qquad \text{(VIII.7)}$$

where the transition operator is given by*, **

$$\left.\begin{aligned} \mathfrak{O}_{GT}(n, \mu) = &\left[\frac{4\pi 2^{n+3}}{(2n+3)!}\right]^{1/2} \frac{[(n+1)!]^2}{n+1} \left(\frac{mc}{\hbar}\right)^n \\ &\sum_p \vec{s}_p \cdot \vec{\nabla}_p \left[r_p^{n+1} Y_{n+1,\mu}(\vartheta_p, \varphi_p)\right] \tau_\pm^{(p)}, \end{aligned}\right\} \qquad \text{(VIII.8)}$$

which exhibits the analogy to the magnetic multipole transitions with $\lambda = n + 1$ (cf. (VII.2 and 4)). For $n = 0$, (8) reduces to

$$\mathfrak{O}_{GT}(0, \mu) = 2 \sum_p s_\mu^{(p)} \tau_\pm^{(p)}, \qquad \text{(VIII.9)}$$

where s_μ are the spherical vector components of $\vec{s}$. Equation (7) is then equivalent to (4).

b) Evaluation of Transition Probabilities.

i. *Transitions in an undeformed nucleus.*

The matrix element for allowed Fermi transitions can be simply expressed in terms of the total isotopic spin quantum numbers of the combining states if charge independence of the forces in the nucleus is assumed (cf. WIGNER and FEENBERG, 1941). From (3) one obtains the selection rule $\Delta T = 0$ and the value

$$D_F(0) = (T \mp T_z)(T \pm T_z + 1) \qquad (T_z \to T_z \pm 1) \qquad \text{(VIII.10)}$$

for the reduced transition probability.

The Gamow-Teller transition probability is more dependent on the nuclear coupling scheme. For transitions of a single particle, (4) gives

* In the notation of GREULING (1942), we have

$$D_{GT}(n) = |Q_{n+1}(\vec{\sigma}, \vec{r})|^2$$

while KONOPINSKI and UHLENBECK (1941), for $n = 1$, use the quantity B_{ij}, where

$$D_{GT}(1) = \Sigma |B_{ij}|^2.$$

** BLATT and WEISSKOPF (1952) write the transition operator in terms of

$$r^n \mathcal{Y}^\mu_{n+1,n} = 2\left[(n+1)(2n+3)\right]^{-1/2} \vec{s} \cdot \vec{\nabla}(r^{n+1} Y_{n+1,-\mu}).$$

$$D_{GT}(0) = \left\{ \begin{array}{ll} \dfrac{j+1}{j} & j = l+1/2 \\ \dfrac{j}{j+1} & j = l-1/2 \end{array} \right\} \Delta j = 0 \quad \text{(VIII.11)}$$

and

$$D_{GT}(0) = \frac{4\,l}{2\,l+1} \frac{2j_f+1}{2j_<+1} \qquad \Delta j = 1\,. \qquad \text{(VIII.12)}$$

The last formula assumes $j_> = l + 1/2$ and $j_< = l - 1/2$ ($\Delta l = 0$). For $\Delta j = 1$ and no parity change, one may also have $\Delta l = 2$, in which case the transition is second forbidden, according to the single-particle model (l-forbiddenness; cf. NORDHEIM, 1951).

For two-particle configurations, and a few three- and four-particle configurations, the matrix elements are unique for transitions between states of given J and T (cf., e. g., Table III). In more complicated configurations, the value of $D_{GT}(0)$ will depend on the particular coupling scheme.

For the forbidden transitions of pure GT type, the transition probability for a single-particle transition may be obtained from (7) and (8) by using the result (VII.8).

ii. *Transitions in the strongly coupled system.*

The value (10) for the Fermi transition probability follows directly from the assumption of a constant total isotopic spin for the nuclear states, and is not affected by the surface coupling.

The transition probabilities for Gamow-Teller transitions in the strongly coupled system can be evaluated by the same methods as used for the electromagnetic particle transitions (§ VII c.i).

The transition operators are conveniently expanded along the nuclear axis, giving (cf. VII.13)

$$\mathfrak{O}_{GT}(n,\mu) = \sum_{\nu} \mathfrak{O}'_{GT}(n,\nu)\, \mathfrak{D}^{n+1}_{\mu\nu}(\theta_i) \qquad \text{(VIII.13)}$$

in terms of the operators $\mathfrak{O}'$ expressed in the nuclear coordinate system.

For transitions with $\Delta I = n+1$ between strong coupling states with $\Omega_i = K_i = I_i$ and $\Omega_f = K_f = I_f$, one obtains

$$D_{GT}(n) = \left|\int \chi^*_{\Omega_i} \mathfrak{O}'_{GT}(n, \pm(n+1))\, \chi_{\Omega_f}\right|^2 \left|\int \varphi_i^* \varphi_f\right|^2 \frac{2I_f+1}{2I_>+1}. \quad \text{(VIII.14)}$$

If $j_i = (\Omega_p)_i = I_i$ and $j_f = (\Omega_p)_f = I_f$, for the transforming particle, the expression (14) can be written

$$D_{GT}(n) = \{D_{GT}(n)\}_{sp} \left|\int \varphi_i^* \varphi_f\right|^2 \frac{2I_<+1}{2I_>+1} \quad \text{(VIII.15)}$$

in terms of the transition probability for a single uncoupled particle (cf. § VIIIb.i). The significance of the last factors in (15) in retarding the transition has been discussed in connection with the analogous formula (VII.15).

In the discussion of the empirical data, this retardation is expressed as the unfavoured factor F, representing the ratio of D and D_{sp}. It is convenient to generalize the definition of F to include cases where $j_p \neq \Omega_p$ for the states of the transforming particle, and for which the coupling scheme has no simple analogue in the shell model. Thus, in general, for ground state transitions with $\Delta I = n + 1$,

$$F = D_{GT}(n) \left|\int \chi^*_{\Omega_i} \mathfrak{O}'_{GT}(n, \pm(n+1))\, \chi_{\Omega_f}\right|^{-2} \frac{2I_<+1}{2I_f+1}, \quad \text{(VIII.16)}$$

The above discussion includes the allowed transitions ($n = 0$) with $\Delta I = 1$. For allowed transitions with $\Delta I = 0$, one obtains directly from (4)

$$D_{GT}(0) = 4 \left|\int \chi^*_{\Omega_i} s_3 \tau_\pm \chi_{\Omega_f}\right|^2 \left|\int \varphi_i^* \varphi_f\right|^2 \frac{I}{I+1}, \quad \text{(VIII.17)}$$

where s_3 is the component of $\vec{s}$ along the nuclear axis. In this case, the F-factor is

$$F = D_{GT}(0) \frac{1}{4} \left|\int \chi^*_{\Omega_i} s_3 \tau_\pm \chi_{\Omega_f}\right|^{-2} \frac{I}{I+1}. \quad \text{(VIII.18)}$$

Additional symmetry terms may appear in (17) in the special case of $K = \Omega = 1/2$.

For the mirror transitions, the symmetry of the combining states implies an intimate relation between D_{GT} and the expect-

ation value of s_z for the states involved. For a one-particle configuration, one obtains directly from (4)

$$D_{GT}(0) = 4\frac{I+1}{I} < s_z >^2_{M=I}. \qquad \text{(VIII.19)}$$

In the strongly coupled system where the particles are coupled separately to the nuclear axis, (19) holds quite generally for mirror transitions, with s_z referring to the last odd particle. The quantity $< s_z >$ also occurs in the static magnetic moment and may be evaluated by the methods of § IVb.*

c) Discussion of Empirical Data.

Recent studies of the *ft*-values of simple nuclei have led to an improved determination of the coupling constants of β-decay (Bouchez and Nataf, 1952; Kofoed-Hansen and Winther, 1952; Trigg, 1952; Blatt, 1953). We here use the values

$$\left.\begin{aligned} B_g &= 2.6 \times 10^3 \,\text{sec} \\ x &= 0.5 \end{aligned}\right\} \qquad \text{(VIII.20)}$$

which seem to be consistent with available empirical data (cf., e. g., Winther and Kofoed-Hansen, 1953).

i. *Mirror transitions.*

The absence of an unfavoured factor arising from different surface shapes of the combining states makes possible a rather detailed analysis of the *ft*-values of mirror decays, from which information about the nuclear coupling scheme may be obtained.

Since the nuclear magnetic moment, due to the large intrinsic nucleon *g*-factor, primarily depends on $< s_z >$ (cf. IV.3), which also determines the *GT* transition probability (cf. 19), one expects rather strong correlations between magnetic moments and *ft*-values of mirror transitions. Indeed, it is found that, when the magnetic moment deviates from the shell model values, there are corresponding deviations in the mirror *ft*-values and that

* The strong coupling matrix elements for mirror transitions have been given by Davidson and Feenberg (1953) for j a constant.

TABLE XXIX. *ft*-values of mirror transitions.

Product nucleus	I	E_{max} (Me V)	$t_{1/2}$	$(ft)_{exp}$	$(ft)_p$	$(ft)_c$
$_5B^{11}$	3/2	0.958	20.39^m	3840(70)	1950	3060
$_6C^{13}$	1/2	1.200	10.1^m	4560(100)	3900	3900
$_7N^{15}$	1/2	1.683	2.1^m	3800(200)	3900	3900
$_8O^{17}$	5/2	1.745	65^s	2320(100)	2160	2160
$_9F^{19}$	1/2	2.234	19.5^s	1970(100)	1300	1800
$_{10}Ne^{21}$	3/2	2.50	22.8^s	3700(200)	—	3600
$_{11}Na^{23}$	3/2	3.073	12.0^s	4780(150)	—	3600
$_{12}Mg^{25}$	5/2	—	7.3^s	—	—	3030
$_{13}Al^{27}$	5/2	3.48	5.0^s	3350(600)	2160	3030
$_{14}Si^{29}$	1/2	3.60	4.6^s	3510(700)	1300	4350
$_{15}P^{31}$	1/2	4.06	3.1^s	4020(600)	1300	4400
$_{16}S^{33}$	3/2	4.43	2.0^s	3800(650)	3250	4850
$_{17}Cl^{35}$	3/2	4.4	1.90^s	3420(800)	3930	4850
$_{18}A^{37}$	(3/2)	4.57	1.2^s	2520(600)	3930	3750
$_{19}K^{39}$	3/2	5.13	1.06^s	3740(500)	3250	3750
$_{20}Ca^{41}$	(7/2)	4.9	0.87^s	2430(800)	2280	(2920)

The empirical data are taken from WINTHER and KOFOED-HANSEN (1953). Their estimated uncertainties for the experimental *ft*-values in column five are listed in parentheses. The second to last column gives the shell model *ft*-values, wherever they are independent of specific assumptions about nuclear forces. In the last column are listed *ft*-values for the coupled system, obtained from the wave functions discussed in the text.

the observed correlation can be understood from simple assumptions about the nuclear states (TRIGG, 1952; WINTHER, 1952; WINTHER and KOFOED-HANSEN, 1953). The existence of such a correlation strongly supports the interpretation of the observed moment shifts as reflecting a modified nuclear coupling scheme (cf. p. 52).

The calculation of mirror *ft*-values in the coupled system follows the same lines as employed in the Addendum to Chapters IV and V. Some of the details of this analysis are given below and the results are summarized in Table XXIX. In cases where the *ft*-value depends sensitively on the nuclear deformation, the coupling situation indicated by the magnetic moment has been used. For comparison, *ft*-values calculated from shell model wave functions are listed wherever the states are unique.

Calculation of mirror *ft*-values.

$A = 11$.

The magnetic moment of B^{11} indicates a rather strong surface coupling (cf. p. 48), which is further supported by the *ft*-value. The listed $(ft)_c$-value is obtained by determining the coupling situation from the magnetic moment, assuming a pure $p_{3/2}$ state ($\mu = (g_j - g_R) < j_z > + g_R I$). However, as discussed on p. 69, it seems unlikely that such a configuration can account for the whole observed moment shift. The deviation from (*jj*) coupling indicated by the magnetic moment seems also reflected in the observed *ft*-value.

$A = 13$ and 15.

The $p_{1/2}$-nuclei are influenced by the surface only through the coupling to the $p_{3/2}$ state (cf. p. 68). However, this coupling has no effect on the *ft*-value. The discrepancy between $(ft)_p$ and $(ft)_{exp}$ for $A = 13$ may again indicate a deviation from (*jj*) coupling.

$A = 17$.

Due to the stability of the O^{16} core (cf. p. 76), one expects only very little influence of the surface coupling on the *ft*-value. This is consistent with the empirical data.

$A = 19$, 29, and 31.

The magnetic moments of these $(1/2+)$ nuclei have been accounted for in terms of strong coupling states with $\Omega = 1/2$, containing $s_{1/2}$, $d_{5/2}$, and $d_{3/2}$ orbitals (cf. p. 63 ff.). The magnetic moment depends sensitively on the interference between the $d_{3/2}$ and $d_{5/2}$ orbitals, and the *ft*-value is expected to show a similar effect. Fig. 15, which is the analogue of Fig. 11, shows the characteristic asymmetry of *ft* with respect to the sign of the deformation, which accounts for the conspicuous difference between the *ft*-values for $A = 19$ and those for $A = 29$ and 31. The $(ft)_c$-values in Table XXIX have been obtained from *y*-values consistent with the observed magnetic moments. It is of interest that for F^{19} the $(ft)_c$-value differs appreciably from $(ft)_p$, although $\mu \approx \mu_{sp}$. The empirical data seem to support this expectation.

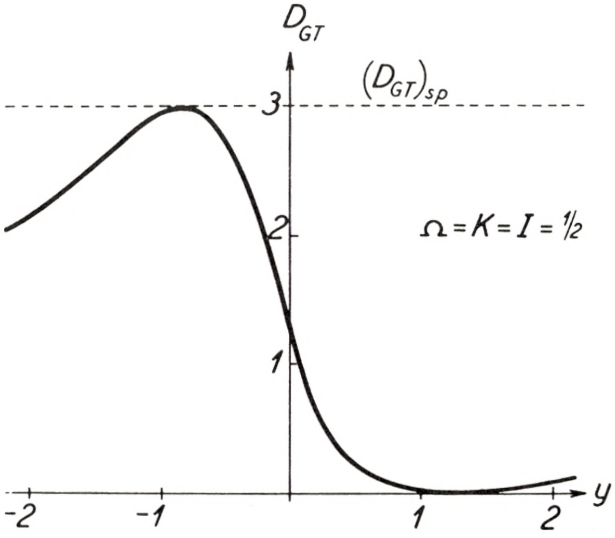

Fig. 15. *Beta decay transition probabilities arising from d-state admixture in* $I = \Omega = 1/2$ *states.* The figure gives the reduced GT-transition probability for mirror transitions between states of the type discussed in Ad. i (cf. especially caption to Fig. 11). The states are characterized by the amplitudes $a_s^2 \sim 1/3$ and $a_d^2 \sim 2/3$. The ratio of $d_{3/2}$ to $d_{5/2}$ is denoted by y. The strong asymmetry of D_{GT} with respect to the sign of y arises from the $d_{3/2}$—$d_{5/2}$ interference, and is similar to the behaviour of the magnetic moment.

$A = 21$ and 23.

In the strong coupling approximation, these nuclei are represented as $\Omega = 3/2$ states containing $d_{5/2}$ orbitals with a small admixture of $d_{3/2}$ (cf. p. 75). The $(ft)_c$-value is very sensitive to this admixture and the values given in Table XXIX correspond to a $d_{3/2}$ amplitude of $a_{3/2} = -0.2 \cdot a_{5/2}$, which is in accordance with μ (Na^{23}). In the absence of the $d_{3/2}$ interference, one would have $(ft)_c = 4300$.

$A = 25$ and 27.

The $(ft)_c$-values are calculated for strong coupling states with $j = \Omega = 5/2$ which account approximately for the magnetic moments of Mg^{25} and Al^{27} (cf. p. 76).

$A = 33$, 35, 37, and 39.

In the strong coupling approximation, these nuclei are described as $\Omega = 3/2$ states, predominantly of $d_{3/2}$ type, with a

small admixture of $d_{5/2}$. One expects the $(ft)_c$-values, just like the magnetic moments (cf. p. 72), to depend rather sensitively on the sign of the interference term, which again depends on whether the configuration is that of a single odd particle or hole. In the former case, corresponding to $A = 33$ and 35, the $(ft)_c$-values in Table XXIX are calculated for the value $a_{5/2} = -0.15\, a_{3/2}$ suggested by the magnetic moments. In the latter case ($A = 37$ and 39), the opposite sign for $a_{5/2}$ applies.

$A = 41$.

The $(ft)_c$-value listed in parenthesis corresponds to the strong coupling limit ($j = \Omega = 7/2$), but the stability of the Ca^{40} core may imply a weak coupling for Ca^{41}.

ii. *Allowed unfavoured transitions.*

The shell model has been a valuable guide in the classification of β-transitions in degrees of forbiddenness, especially through its ability to predict the parities of the combining states (MAYER, MOSZKOWSKI and NORDHEIM, 1951; NORDHEIM, 1951). At the same time, the quantitative analysis of the ft-values indicates an important influence of the dynamical aspects of the collective field. This is strikingly illustrated by the difference between the ft-values of mirror transitions and other allowed transitions. While the symmetry of the mirror states implies almost identical surface shapes, other types of transitions are in general expected to be appreciably retarded, due to surface readjustments accompanying the particle transitions.

Table XXX lists the ground state transitions in odd-A nuclei, excepting the mirror transitions, which have been classified as allowed (MAYER, MOSZKOWSKI and NORDHEIM, 1951). The F-factor in the last column provides a measure of the retardation of the observed transitions as compared with a single-particle transition between the states listed in columns four and five (cf. (16) and (18)).

It is seen that the transitions are slowed down by a factor of the order of 10—100, which is of the same order of magnitude as the reductions for $M4$ transitions (cf. Table XXV).

The allowed transitions in even-A nuclei show a behaviour

TABLE XXX. Allowed unfavoured β-transitions in odd-A nuclei.

Nucleus	E_0 (MeV)	$\log f_0 t$	particle states		F
			i	f	
$_{10}Ne^{23}$	−4.1	4.9	$d_{5/2}$	$d_{5/2}^{3/2}$	.16
$_{11}Na^{25}$	−3.7	5.2	$d_{5/2}^{3/2}$	$d_{5/2}$	.056
$_{16}S^{35}$	−0.17	5.0	$d_{3/2}$	$d_{3/2}$	.083
$_{20}Ca^{45}$	−0.22	5.6	$f_{7/2}$	$f_{7/2}$	.010
$_{21}Sc^{49}$	−1.8	5.5	$f_{7/2}$	$f_{7/2}$	.013
$_{27}Co^{61}$	−1.3	5.2	$f_{7/2}$	$f_{5/2}$	.019
$_{30}Zn^{63}$	+2.36	5.4	$p_{3/2}$	$p_{3/2}$	.012
$_{30}Zn^{69}$	−1.0	4.6	$p_{1/2}$	$p_{3/2}$	.050
$_{31}Ga^{73}$	−1.4	5.9	$p_{3/2}$	$p_{1/2}$	.0050
$_{32}Ge^{75}$	−1.1	5.0	$p_{1/2}$	$p_{3/2}$	.020
$_{33}Aa^{71}$	+0.6	5.1	$p_{3/2}$	$p_{1/2}$	.030
$_{33}As^{77}$	−0.7	5.7	$p_{3/2}$	$p_{1/2}$	.077
$_{34}Se^{73}$	+1.29	5.3	$p_{1/2}$	$p_{3/2}$	.0098
$_{34}Se^{81}$	−1.5	4.8	$p_{1/2}$	$p_{3/2}$	.031
$_{35}Br^{75}$	+1.6	5.6	$p_{3/2}$	$p_{1/2}$	.010
$_{35}Br^{77}$	+0.36	5.0	$p_{3/2}$	$p_{1/2}$	.038
$_{35}Br^{83}$	−1.05	5.3	$p_{3/2}$	$p_{1/2}$	.020
$_{35}Br^{85}$	−2.5	5.1	$p_{3/2}$	$p_{1/2}$	.030
$_{45}Rh^{105}$	−0.57	5.5	$g_{9/2}$	$g_{7/2}$	.0091
$_{50}Sn^{121}$	−0.38	5.0	$d_{3/2}$	$d_{5/2}$	.022
$_{52}Te^{127}$	−0.76	5.6	$d_{3/2}$	$d_{5/2}$	.0056
$_{60}Nd^{141}$	+0.7	5.2	$d_{3/2}$	$d_{5/2}$	.014

The empirical E_0 and $\log f_0 t$ values as well as the spin and parity of the combining states are taken from MAYER, MOSZKOWSKI and NORDHEIM (1951). The F-factors are calculated by comparison with the single-particle transitions listed in columns four and five (cf. (16) and (18)). The superscript gives the value of Ω_p in cases where it differs from j_p.

similar to that of odd-A nuclei (cf. NORDHEIM, 1951). An interesting anomaly is the decay of $_6C^{14}$ whose long lifetime may indicate an accidental cancellation in the matrix element. Additional information on the states involved in this transition could be obtained from a measurement of the γ-decay lifetime of the 2.31 MeV state in $_7N^{14}$. This state is believed to be the $T = 1$ state which is isobaric with the C^{14} ground state (cf., e. g., AJZENBERG and LAURITSEN, 1952); it decays by $M1$ radiation, and the transition matrix element is very similar to that involved in the β-decay of C^{14}.

TABLE XXXI. *l*-forbidden β-transitions in odd-A nuclei.

Nucleus	E_0 (MeV)	$\log f_0 t$	particle states		F
			i	f	
$_8O^{19}$	−4.5	5.5	$d^{3/2}_{5/2}$	$d^{1/2}_{5/2}$	.026
$_{14}Si^{31}$	−1.8	5.9	$d^{3/2}_{3/2}$	$d^{1/2}_{3/2}$	.028
$_{15}P^{33}$	−0.26	5.1	$d^{1/2}_{3/2}$	$d^{3/2}_{3/2}$	.082
$_{28}Ni^{63}$	−0.05	6.8	$f^{5/2}_{5/2}$	$f^{3/2}_{5/2}$	.0040
$_{28}Ni^{65}$	−2.10	6.6	$f^{5/2}_{5/2}$	$f^{3/2}_{5/2}$	.0067
$_{29}Cu^{61}$	+1.22	4.9	$f^{3/2}_{5/2}$	$f^{5/2}_{5/2}$	.22
$_{29}Cu^{67}$	−0.65	5.5	$f^{3/2}_{5/2}$	$f^{5/2}_{5/2}$	.053
$_{30}Zn^{65}$	+0.32	7.0	$f^{5/2}_{5/2}$	$f^{3/2}_{5/2}$	.0026
$_{32}Ge^{69}$	+1.0	6.0	$f^{5/2}_{5/2}$	$f^{3/2}_{5/2}$	.026
$_{46}Pd^{109}$	−1.0	6.2	$g^{5/2}_{7/2}$	$g^{7/2}_{9/2}$	.0018

The empirical E_0 and $\log f_0 t$ values as well as the spin and parity of the combining states are taken from MAYER, MOSZKOWSKI and NORDHEIM (1952). These transitions, which are forbidden for pure shell model configurations, occur in the coupled system due to admixtures of the states listed in columns four and five. The strong coupling notation is used and the superscript denotes the component Ω_p of angular momentum along the nuclear axis. The F-factors are obtained by comparison with a pure particle transition of the listed type (cf. (16)).

There are also other cases where it would be of interest to combine lifetime evidence on allowed GT β-transitions with that of $M1$ transitions between the corresponding isobaric states (e. g., He^6 (β-)Li^6 compared to the γ-decay of the 3.58 MeV level in Li^6. Another example is the Be^7(K)Li^{7*} (478 keV), which may be compared with the γ-decay of the excited Li^7-state.)

iii. *l-forbidden transitions.*

The special type of odd-A transitions with $\Delta I = 1$ and no parity change, which according to the shell model have $\Delta l = 2$, are listed in Table XXXI. They are classified as *l*-forbidden

transitions (MAYER, MOSZKOWSKI and NORDHEIM, 1951). Their ft-values are comparable with, although somewhat larger than those of the allowed unfavoured transitions in Table XXX, and they have spectra of allowed type.

The configuration admixtures which are a general consequence of the surface coupling can destroy the l-forbiddenness in a similar manner as for the j-forbiddenness encountered in the $E3$ transitions (§ VII d.ii). The fourth and fifth columns of Table XXXI list the l, j, and Ω values of the single-particle orbitals, which are assumed to contribute the principal part of the transition matrix element. Assuming pure states of these types, one calculates the F-factors of the last column in the same way as for the transitions in Table XXX (cf. (16)).

The appearance in Table XXXI of somewhat smaller and more erratic F-factors than in Table XXX may reflect the sensitivity of the transitions to small amplitudes of admixed states (cf. the analogous situation for the j-forbidden $E3$ transitions (Table XXVI) as compared with the $M4$ transitions (Table XXV)).

The unfavoured factors of Table XXXI are somewhat larger than those of Table XXVI, which may be associated with the greater ease with which the surface destroys the l-forbiddenness than the j-forbiddenness because of the greater energy separation between the spin-orbit partners than between neighbouring orbitals in the same shell.

iv. *Pure GT forbidden transitions.*

The forbidden transitions which are identified by their spectral shape as being of the pure GT type are listed in Table XXXII. The unfavoured factor F in the last column provides a comparison of the observed transition probability with that of a single-particle transition between the states listed in columns four and five (cf. (16)). It is seen that the F-factors, as expected, are comparable to those of the allowed unfavoured β-transitions (Table XXX) and the $M4$ isomeric transitions (Table XXV).

The two largest F-factors in Table XXXII are those of B^{10} and K^{40}. In the former case, the observed F-factor can be accounted for in terms of the projection factor alone, with no contribution from the vibrational wave functions (cf. 14 and 16). The occurrence of similar surface shapes in the two combining

TABLE XXXII. Forbidden β-transitions of pure GT type.

Nucleus	E_0 (MeV)	log $f_n t$	particle states		F
			i	f	
	odd A		$\Delta I = 2$	yes ($n = 1$)	
$_{18}A^{41}$	−2.55	8.8	$f_{7/2}$	$d_{3/2}$	.03
$_{38}Sr^{89}$	−1.46	8.3	$d_{5/2}$	$p_{1/2}$	.09
$_{38}Sr^{91}$	−3.2	8.4	$d_{5/2}$	$p_{1/2}$	.07
$_{39}Y^{91}$	−1.56	8.5	$p_{1/2}$	$d_{5/2}$	.016
$_{55}Cs^{137}$	−0.53	8.7	$g_{7/2}$	$h_{11/2}$	.011
	even A		$\Delta I = 2$	yes ($n = 1$)	
$_{17}Cl^{38}$	−4.81	8.1	$f_{7/2}^{7/2}$	$d_{3/2}^{3/2}$	.16
$_{19}K^{42}$	−3.58	8.5	$f_{7/2}^{5/2}$	$d_{3/2}^{1/2}$	.16
$_{37}Rb^{86}$	−1.82	8.5	$g_{9/2}^{9/2}$	$f_{5/2}^{5/2}$	.04
$_{38}Sr^{90}$	−0.54	8.2	$d_{5/2}^{5/2}$	$p_{1/2}^{1/2}$	.09
$_{39}Y^{90}$	−2.20	8.1	$d_{5/2}^{5/2}$	$p_{1/2}^{1/2}$	.14
$_{81}Tl^{204}$	−0.765	8.9	$p_{3/2}^{3/2}$	$s_{1/2}^{-1/2}$	.010
	even A		$\Delta I = 3$	no ($n = 2$)	
$_{5}B^{10}$	−0.56	11.3	$p_{3/2}^{-3/2}$	$p_{3/2}^{3/2}$	.23
	even A		$\Delta I = 4$	yes ($n = 3$)	
$_{19}K^{40}$	−1.36	15.1	$f_{7/2}^{7/2}$	$d_{3/2}^{-1/2}$	.24

The table lists the forbidden transitions classified by their measured spectra as of pure GT type (WU, 1950; LIDOFSKY et al., 1952; FELDMAN and WU, 1952). The log $f_n t$ values are obtained by using the formulae and curves of DAVIDSON (1951). The F-factors are obtained by comparison with a pure particle transition between the states listed in columns four and five (cf. (16)).

states is expected, since in strong coupling the occupied particle states have the same deforming power (cf. the similar situation expected for γ-transitions between the members of the ground state doublet in odd-odd nuclei (p. 113)).

In K^{40}, the F-factor as well as the magnetic moment (cf. p. 83) indicate an intermediate coupling situation. In such cases of weak or intermediate surface coupling, it is of interest to compare the observed transition probabilities with those expected for a coupling scheme arising from the influence of particle forces (cf. § IIc.iii). The unfavoured factor F_p obtained in this way is in general somewhat larger than F, in the case of many-particle configurations. Thus, for K^{40}, one finds $F_p = 0.7$.

IX. Summary.

A unified description of the nuclear structure is attempted, which takes into account individual-particle aspects as well as collective features associated with oscillations of the system as a whole (§ I). The most important of the collective types of motion, for the low energy nuclear properties, are oscillations in the nuclear shape, which resemble surface oscillations. The collective motion is associated with variations of the average nuclear field, and is therefore strongly coupled to the particle motion (§ IIa).

The particle-surface coupling implies an interweaving of the two types of motion, which depends on the particle configuration as well as on the deformability of the surface. In the immediate vicinity of major closed shells, the high stability of the spherical nuclear shape makes the coupling relatively ineffective. In such a weak coupling situation, the nucleus can be described in terms of approximately free surface oscillations and the motion of individual nucleons in a spherical potential (§ IIb.i).

With the addition of particles, the coupling becomes more effective, and the nucleus acquires a deformed equilibrium shape. For sufficiently large deformations, a simple limiting coupling scheme is realized, which bears many analogies with that of linear molecules. In the strong coupling situation, the nucleus performs small vibrations about an axially symmetric equilibrium shape. The particles moving in the deformed field are decoupled from each other and precess rapidly about the nuclear axis, following adiabatically the slow rotation of the nuclear shape (§ IIb.ii and § IIc.ii; cf. Figs. 3 and 6).

An analysis of the observed nuclear properties of the low energy region reveals many of the characteristic features of the coupled system.

For nuclei with major closed-shell configurations, or with a single extra particle, the expected weak coupling situation is especially confirmed by the high excitation energies (cf., e. g., Fig. 13) and the small quadrupole moments (§ Vc). Also magnetic moments indicate that particle motion in a closed-shell core is little influenced by the coupling (cf. O^{17}, p. 76), although the anomalous moment of Bi^{209} implies as yet unexplained features of the particle structure (cf. p. 81).

Already for configurations with a few particles, the empirical data give evidence of a major effect of the particle-surface coupling, and in regions further removed from closed shells, a rather fully developed strong coupling situation is found.

In particular, the nuclear excitation spectrum clearly indicates a structure of nuclear states governed by the strongly coupled particle and collective motions. A striking feature is the occurrence of collective excitations of rotational character, which reveal themselves by their energy trends, the regularity of their spectrum, and their short lifetimes (§ VIc.ii). The accuracy of the strong coupling description of these states in regions of large deformations is exhibited by the energy ratios within a rotational family (cf., e. g., Table XXII and also notes on pp. 93 and 166).

The particle modes of excitation can be studied especially in the long lived isomers and the β-activities. For these states, the spins and parities, which account for the order of the transitions, have confirmed the configuration assignments given by the shell model. However, the observed transition probabilities, which are appreciably smaller than would correspond to particles moving in a fixed potential, provide evidence for the readjustments of the collective field, which are a characteristic of the particle transitions in the coupled system (§§ VIb, VIId.i, VIIIc.ii and iv).

The modification of the nuclear coupling scheme arising from a strong particle-surface interaction also manifests itself in the static properties of nuclear ground states. Thus, for many-particle configurations, the ground state spin may differ from that which would result from a coupling due to particle forces (cf. Fig. 6). Especially, the occurrence of $I = j - 1$ in $(j)^3$ configurations gives evidence for a surface coupling dominating over the particle forces (§ III.iii).

The magnetic moments provide a measure of the sharing of

angular momentum between particles and surface, and support the strong coupling interpretation of nuclear states in regions removed from major closed shells (§ IVc; cf. especially Table VI). The moments are also sensitive to modifications of the particle state resulting from the non-spherical character of the potential, and thus provide rather detailed tests of nuclear wave-functions (Addendum to Chapters IV and V; cf. also Table VII). The comparison between magnetic moments and the *ft*-values of mirror β-decays further supports the interpretation of the nuclear states (§ VIIIc.i).

While many of the nuclear properties considered depend primarily on the coupling scheme, information on the collective motion of a more detailed character may be obtained from the analysis of quadrupole moments and of the energies and life-times of rotational states. It is found that the observed quadrupole moments, as well as the related $E2$ matrix elements for rotational transitions, are systematically smaller than would correspond to surface deformations of the simple hydrodynamical type (§ Vc, § VIc.ii). In this deviation, one has an interesting indication of the inadequacy of the liquid drop idealization of the nuclear collective properties, which may be associated with the non-uniformity of the nuclear density distribution (§ IIa).

The present discussion has been restricted principally to low energy phenomena, but the basic features of such a unified description retain their validity also for the higher excitations encountered in nuclear reaction processes (§ VIa). The increased level density implies a certain complexity in the nuclear states, but the fundamental nature of the individual-particle and ordered collective motions is still expected to manifest itself (§ VId; cf. also Ap. Va and b).

Thus, the recent measurements of total neutron cross-sections have revealed a structure associated with potential scattering of a single particle, as well as aspects arising from the coupling to the internal degrees of freedom of the target nucleus, which may lead to the complicated motion of the compound nucleus. It appears that the observed coupling can be understood in terms of an interaction between the incident particle and the nuclear surface oscillations of the same magnitude as implied by the low energy phenomena (Ap. Vc).

Appendix I.

Shell Structure and Deformability.

The nuclear deformability depends on the extent to which the particle structure can adjust to a deformation of the field. Thus, important deviations from the simplified surface tension description may arise for configurations with anomalously large level spacings (closed-shell nuclei) or if the deformation changes too rapidly for the particle structure to follow adiabatically (cf. GALLONE and SALVETTI, 1953; HILL and WHEELER, 1953).

For deformations preserving axial symmetry, the nucleonic states may be characterized by the quantum numbers Ω_p, denoting the components of angular momentum of the individual nucleons along the symmetry axis. For a given set of Ω_p, the deformability coefficients C_λ are proportional to the number of nucleons A, and are thus much larger than estimates based on the surface tension, which are of order $A^{2/3}$ (apart from the influence of electrostatic forces).

As the nucleus is deformed, however, states with different sets of Ω_p will cross and if, instead of following a state of constant Ω_p, one follows the state of lowest energy for any given deformation, the resultant energy dependence will on the average be of the surface tension type. (Illustrations of this effect are given in the above references).

Deviations from axial symmetry, as well as the effect of particle forces, afford a mechanism for keeping the particle structure in the state of lowest energy, provided the region of crossings is passed sufficiently slowly. If this adiabatic condition is violated, exchange of energy takes place between nucleonic and collective motion (HILL and WHEELER, 1953). One then encounters the features of the coupled system characteristic of an intermediate coupling strength (§§ IIa.iii, IIb.i and iii).

In the strong coupling situation where the nucleus performs small oscillations around a deformed equilibrium shape (§ II b.ii), this equilibrium shape may in general be estimated on the basis of a surface tension type of deformability. A finer analysis of the deformation properties in the appropriate region may be required for the detailed treatment of the vibrations around equilibrium.

The surface tension type of deformability is a statistical feature which depends on a regular level spacing. In the neighbourhood of major shell closings, the discontinuity in the level distribution implies a special stability of the spherical form corresponding to a C_λ coefficient of order A for small deformations, until the first few crossings have occurred (cf. GALLONE and SALVETTI, 1953). This results in an anomalously large phonon energy and very small quadrupole moments for such nuclei. For larger deformations, the deformability approaches the normal value with a resulting decrease in the phonon energy. The potential energy function corresponding to these features is somewhat more complicated than given by (II.5).

Appendix II.

Matrix Elements in the Perturbation Representation.

The matrix elements of H_{int} can be obtained from the matrix of $Y_\mu\ (\vartheta, \varphi)$ given by

$$<jm\,|\,Y_\mu\,|\,j'm'> = <j\,|\,h\,|\,j'><j'\,2\,m'\,\mu\,|\,j'\,2jm>, \quad \text{(Ap. II.1)}$$

where the last factor on the right hand side is the coefficient of the vector addition of the angular momenta j' and 2 to give a total j (cf. CONDON and SHORTLEY, 1935, p. 77, Table 4[3]).

The sub-matrix $<j\,|\,h\,|\,j'>$ can be expressed in terms of Racah coefficients and, for particle states of the same parity, is given by

$$<j\,|\,h\,|\,j'> = -\sqrt{\frac{5}{64\,\pi}} \begin{cases} -\sqrt{\dfrac{3\,(2j-1)\,(2j-3)}{2j\,(j-1)}} & j = j'+2 \\ +\dfrac{1}{j}\sqrt{\dfrac{3j\,(2j-1)}{(j-1)\,(j+1)}} & j = j'+1 \\ +\sqrt{\dfrac{(2j-1)\,(2j+3)}{j\,(j+1)}} & j = j' \\ -\dfrac{1}{j}\sqrt{\dfrac{3j\,(2j+3)}{(j+1)\,(j+2)}} & j = j'-1 \\ -\sqrt{\dfrac{3\,(2j+3)\,(2j+5)}{2\,(j+1)\,(j+2)}} & j = j'-2 \end{cases} \quad \text{(Ap. II.2)}$$

From (1) and the matrix elements of α_μ, which can be obtained from (A.38), one derives from (II.9) the expression (II.12) for the first order matrix elements of H_{int}.

To first order in H_{int}, the wave function (II.11) is determined by the coefficients

$$<j'; 12; IM|> = k\sqrt{\frac{\hbar\omega}{2C}}\,\frac{<j|h|j'>}{\hbar\omega + \Delta_{jj'}}, \qquad \text{(Ap. II.3)}$$

where $\Delta_{jj'}$ is the separation between the particle levels j' and j.

In terms of these coefficients, the expectation value of R_z is given by

$$<R_z> = \frac{M}{2I(I+1)}\sum_{j'}(I(I+1) - j'(j'+1) + 6)\left|<j'; 12; IM|>\right|^2 \qquad \text{(Ap. II.4)}$$

which is equivalent to (II.13) if only the diagonal term ($j' = j$) is of importance.

For a more detailed analysis of the nuclear coupling scheme, such as is needed for the evaluation of the magnetic moment, the non-diagonal matrix elements of s_z given by

$$\left.\begin{aligned} &<j = l-\tfrac{1}{2}; 12; IM|\,s_z\,|j' = l+\tfrac{1}{2}; 12; IM> \\ &= \frac{M}{2I(I+1)(2l+1)}\sqrt{\left(I+l-\frac{3}{2}\right)\left(I+l+\frac{7}{2}\right)\left(l-I+\frac{5}{2}\right)\left(I-l+\frac{5}{2}\right)}\end{aligned}\right\} \qquad \text{(Ap. II.5)}$$

are also of interest.

Appendix III.

Features of the Strong Coupling Solution.

i. *Matrix elements.*

The matrix elements of the coupling term (II.26) in the strong coupling approximation may be obtained from

$$
\begin{aligned}
&\langle j\Omega \,|\, Y_0 \,|\, j'\Omega\rangle = \\
&-\sqrt{\frac{5}{64\pi}}\left\{\begin{array}{ll}
-\frac{3}{2}\frac{1}{j(j-1)}\sqrt{(j-\Omega)(j-\Omega-1)(j+\Omega)(j+\Omega-1)} & j=j'+2 \\
\frac{3\Omega}{j(j-1)(j+1)}\sqrt{(j-\Omega)(j+\Omega)} & j=j'+1 \\
\frac{1}{j(j+1)}(3\Omega^2-j(j+1)) & j=j' \\
\frac{3\Omega}{j(j+1)(j+2)}\sqrt{(j-\Omega+1)(j+\Omega+1)} & j=j'-1 \\
-\frac{3}{2}\frac{1}{(j+1)(j+2)}\sqrt{(j-\Omega+1)(j-\Omega+2)(j+\Omega+1)(j+\Omega+2)} & =j'-2
\end{array}\right\} \qquad \text{(Ap. III.1)}
\end{aligned}
$$

which is derived from (Ap. II.1 and 2).

The expectation value $< j_z >$ is given by (II.19), while for the evaluation of $< s_z >$ one also needs the non-diagonal element

$$\left.\begin{aligned} &< j = l - \tfrac{1}{2},\ \Omega;\ IKM \,|\, s_z \,|\, j' = l + \tfrac{1}{2},\ \Omega;\ IKM > \\ &= -\frac{MK}{I(I+1)} \frac{\sqrt{\left(l+\frac{1}{2}\right)^2 - \Omega^2}}{2l+1} \left\{ 1 + (-)^{I-1/2+l} (I + 1/2)\, \delta_{\Omega,1/2}\, \delta_{K,1/2} \right\}. \end{aligned}\right\} \text{(Ap. III.2)}$$

ii. *Strong coupling for a single $j = 3/2$ particle.*

In the special case of a $j = 3/2$ particle coupled to the surface, there exists no regular strong coupling solution since, according to (II.21), the configurations ($\gamma = \pi$; $\Omega = 3/2$) and ($\gamma = 0$; $\Omega = 1/2$) are degenerate. Indeed, the proper values of H_{int} (cf. A.80) are independent of γ. In strong coupling, we may restrict ourselves to the lower of these proper values, and the wave function for the state with $I = 3/2$ may be written

$$\left.\begin{aligned} &= \left\{ |3/2;\ 3/2\ 3/2\, M > \sin\gamma/2 + |-1/2;\ 3/2\ 3/2\, M > \cos\gamma/2 \right\} \varphi_1(\beta, \gamma) \\ &+ \left\{ |1/2;\ 3/2\ 1/2\, M > \cos\gamma/2 + |-3/2;\ 3/2\ 1/2\, M > \sin\gamma/2 \right\} \varphi_2(\beta, \gamma) \end{aligned}\right\} \text{(Ap. III.3)}$$

in terms of the symmetrized basis vectors $|\ \Omega;\ IKM >$ (cf. II.15). The vibrational functions φ_1 and φ_2 represent small oscillations around a definite equilibrium β; however, the independence of the coupling energy of γ implies essential oscillations in γ, and the vibrational energies characterized by n_γ become of the order of rotational energies.

In order to determine the nuclear coupling scheme, one must solve the vibrational equation, which can be written as a matrix in the space of φ_1 and φ_2. From (II.23, 24, and 25) and (A.96 and 121-4) one obtains for the Hamiltonian of the system

$$
\left.
\begin{aligned}
H = H_0(\beta) + \frac{\hbar^2}{2B\beta^2}\frac{1}{\sin 3\gamma}\frac{\partial}{\partial\gamma}\sin 3\gamma\,\frac{\partial}{\partial\gamma} + \frac{\hbar^2}{2B\beta^2}\frac{1}{\sin^2\gamma}
\begin{pmatrix} \cos^2\frac{\gamma}{2} & 0 \\ 0 & \sin^2\frac{\gamma}{2} \end{pmatrix} \\
+ \frac{\hbar^2}{16B\beta^2}\frac{1}{\sin^2\left(\gamma-\frac{2\pi}{3}\right)}
\begin{pmatrix} 3+2\cos^2\frac{\gamma}{2}+\sqrt{3}\sin\gamma & -3\sin\gamma-2\sqrt{3}\cos^2\frac{\gamma}{2}+\sqrt{3} \\ -3\sin\gamma-2\sqrt{3}\cos^2\frac{\gamma}{2}+\sqrt{3} & 5-2\cos^2\frac{\gamma}{2}-\sqrt{3}\sin\gamma \end{pmatrix} \\
+ \frac{\hbar^2}{16B\beta^2}\frac{1}{\sin^2\left(\gamma+\frac{2\pi}{3}\right)}
\begin{pmatrix} 3+2\cos^2\frac{\gamma}{2}-\sqrt{3}\sin\gamma & -3\sin\gamma+2\sqrt{3}\cos^2\frac{\gamma}{2}-\sqrt{3} \\ -3\sin\gamma+2\sqrt{3}\cos^2\frac{\gamma}{2}+\sqrt{3} & 5-2\cos^2\frac{\gamma}{2}+\sqrt{3}\sin\gamma \end{pmatrix}
\end{aligned}
\right\} \quad \text{(Ap. III.4)}
$$

where $H_0(\beta)$ represents small vibrations in β around the equilibrium value (II.22). For sufficiently strong coupling, the vibrations in β and γ are approximately independent.

From (4) it is seen that there is a preference for the shapes $\gamma = 0$ and $\gamma = \pi$, and that there is a symmetry with respect to these two positions. An estimate of the γ-oscillations may be ob-

tained by expanding H around $\gamma = 0$ and π, and by taking into account that for $\gamma = 0$ the value of φ_1 is rather small compared to φ_2, while the opposite holds for $\gamma = \pi$. Neglecting the overlap of the vibrations centered on $\gamma = 0$ and $\gamma = \pi$, one obtains two degenerate solutions, which have the same nuclear moments.

From the wave function (3), one can determine the coupling scheme and the quadrupole moment by means of the operators

$$j_z = \frac{3}{5}\begin{pmatrix} 2\sin^2\frac{\gamma}{2} - \frac{1}{2} & \sin\gamma \\ \sin\gamma & 2\cos^2\frac{\gamma}{2} - \frac{1}{2} \end{pmatrix} \qquad \text{(Ap. III.5)}$$

and

$$Q = Q_0 \cdot \frac{1}{5}\begin{pmatrix} -\cos\gamma & \sin\gamma \\ \sin\gamma & \cos\gamma \end{pmatrix}, \qquad \text{(Ap. III.6)}$$

where Q_0 is the intrinsic quadrupole moment given by (cf. V.7)

$$Q_0 = -\frac{3}{\sqrt{5\pi}} ZR_0^2 < \beta > . \qquad \text{(Ap. III.7)}$$

From the approximate wave function, one obtains

$$< j_z > \approx 0.8 \qquad \text{(Ap. III.8)}$$

leading to (cf. IV.5)

$$\mu_c(p_{3/2}) \approx \begin{Bmatrix} 2.3 \\ -0.7 \end{Bmatrix} \quad \text{and} \quad \mu_c(d_{3/2}) \approx \begin{Bmatrix} 0.4 \\ 0.9 \end{Bmatrix}. \qquad \text{(Ap. III.9)}$$

The quadrupole moment is found to be

$$< Q > \approx 0.16\, Q_0 . \qquad \text{(Ap. III.10)}$$

Thus, the γ-oscillations somewhat reduce the values of $< j_z >$ and $< Q >$ as compared with the state $\Omega = 3/2$, $\gamma = \pi$.

The energy spectrum of the system is rather complex, since low-lying states can be obtained by excitations of the γ-vibrations without change of I, as well as by rotational excitations. A comparison between the equations for states with different I shows, however, that the ground state is an $I = 3/2$ state of the type considered above.

Appendix IV.

Solution of the Coupled Equations for Large j.

In the case of large j, a solution of the coupled system can be obtained for arbitrary strength of the coupling by starting from the corresponding classical equations and considering the quantum effects in first order.

If we assume the magnitude of the particle angular momentum to be a constant of the motion, there exists a simple classical solution for which $\vec{j}$ remains constant in a direction which may be chosen as the z-axis. The surface acquires a static deformation of the α_0 type given by

$$\bar{\alpha}_0 = -\frac{1}{2}\sqrt{\frac{5}{4\pi}}\frac{k}{C}. \qquad \text{(Ap. IV.1)}$$

The quantum effects give rise to an indeterminacy in the direction of $\vec{j}$ and of the axis of deformation. For $j \gg 1$, the angle between j and the z-axis is relatively small for the states $M = I \approx j$. To first order, we may then treat j_z as a constant, equal to j aside from corrections of order unity, and consider only the motion of the perpendicular components

$$j_{\pm} = j_x \pm i j_y. \qquad \text{(Ap. IV.2)}$$

The small inclination of the axis of deformation, with respect to the z-axis, to first order implies excitations of the α_1 and α_{-1} surface modes. In this approximation, the α_0 and $\alpha_{\pm 2}$ modes are not affected and perform independent zero-point oscillations around their equilibrium values $\bar{\alpha}_0$ and 0, respectively.

The nuclear coupling scheme is thus determined by the coupled oscillations of the α_1 and α_{-1} surface modes and the perpendicular j-components. This dynamical system possesses

three degrees of freedom, since j_+ and j_- play the role of canonical conjugates.

The equations of motion may be obtained from the Hamiltonian (II.8), where H_S is given by (II.5) and H_p may be taken as a constant. A convenient form of H_{int} for j a constant is given by (A.76). To leading order in j, one finds

$$\left.\begin{aligned} &\ddot{\alpha}_1 + \omega^2 \alpha_1 - x\omega^2 \sqrt{\frac{3\hbar\omega}{2C}} \frac{1}{\sqrt{j}} j_- = 0 \\ &i\frac{\hbar}{\sqrt{j}} \dot{j}_- + x\sqrt{\hbar\omega C}\left(3x\sqrt{\frac{\hbar\omega}{C}} \frac{1}{\sqrt{j}} j_- - \sqrt{6}\,\alpha_1\right) = 0 . \end{aligned}\right\} \quad \text{(Ap. IV.3)}$$

The dimensionless coupling constant x is given by (II.14).

This system of linear equations can be solved in terms of three independent harmonic oscillators with proper coordinates q_s. We thus write

$$\left.\begin{aligned} \alpha_1 &= \sum_{s=1}^{3} q_s e^{i\omega_s t} \\ j_- &= \sqrt{j}\,\frac{1}{x\omega^2}\sqrt{\frac{2C}{3\hbar\omega}} \sum_s (\omega^2 - \omega_s^2)\, q_s e^{i\omega_s t} . \end{aligned}\right\} \quad \text{(Ap. IV.4)}$$

The proper frequencies are found to be

$$\left.\begin{aligned} \omega_1 &= 0 \\ \left.\begin{matrix}\omega_2 \\ \omega_3\end{matrix}\right\} &= \left(\frac{3}{2}x^2 \pm \frac{1}{2}\sqrt{9x^4 + 4}\right)\omega . \end{aligned}\right\} \quad \text{(Ap. IV.5)}$$

For the uncoupled system ($x = 0$), the frequencies become 0, $\pm\,\omega$ of which the first is associated with the degeneracy of the j_z-levels, while the two latter belong to the surface oscillators. In the limit of strong coupling, the degeneracy with respect to I_z provides the zero frequency, while the rapid precession of $\vec{j}$ around the nuclear axis has the frequency

$$\omega_2 \approx 3x^2\omega , \quad \text{(Ap. IV.6)}$$

and the slow rotational motion of the system takes place with the frequency

$$\omega_3 \approx -\frac{\omega}{3x^2} . \quad \text{(Ap. IV.7)}$$

Both these limiting frequencies agree with those obtained from the strong coupling solution by considering energy level spacings associated with the quantum numbers Ω and I (cf. II.21 and 24). The three remaining degrees of freedom of the system whose frequencies remain to this order equal to ω correspond in strong coupling to the level spacings of the quantum numbers n_β, n_γ, and K.

The commutation relations of the q_s variables may be obtained from those of the α_μ and $\vec{j}$ components. One finds

$$\left.\begin{aligned} [q_1, q_1^*] &= -(\omega_2+\omega_3)\,\frac{\hbar}{C} \\ [q_2, q_2^*] &= -\frac{\omega_3^2}{\omega_2-\omega_3}\,\frac{\hbar}{C} \\ [q_3, q_3^*] &= +\frac{\omega_2^2}{\omega_2-\omega_3}\,\frac{\hbar}{C}. \end{aligned}\right\} \quad \text{(Ap. IV.8)}$$

In these coordinates, the angular momentum transferred to the surface is given by

$$< R_z > = -\frac{B}{\hbar}\sum_s \omega_s < q_s^* q_s + q_s q_s^* > \qquad \text{(Ap. IV.9)}$$

and for the ground state one obtains

$$< R_z > = \frac{I}{I+1}\,\frac{x^2}{\sqrt{x^4+\frac{4}{9}}}. \qquad \text{(Ap. IV.10)}$$

The factor $\dfrac{I}{I+1}$ which has been added equals unity to leading order, and makes the equation, in the limit of strong coupling, exact for all values of I (cf. II.20).

The transfer of angular momentum implied by (10) gives rise to a small static decrease in the magnitude of $\bar{\alpha}_0$ since the latter is proportional to $< 3 j_z^2 - j(j+1) >$ (cf. A.78). From this effect follows the projection factor (V.11).

Appendix V.

Individual-particle and Collective Features of Nuclear Reactions

The recognition of relatively undisturbed single-particle motion as an important aspect of the nuclear dynamics implies a picture of nuclear reactions, in which the incident particle interacts in the first stage with the average nuclear field. In subsequent stages, the coupling between the particle and the internal degrees of freedom of the target nucleus may lead to the formation of a compound nucleus, in which the excitation energy is shared among a large number of degrees of freedom (cf. § VI d).

In Section a) of this Appendix, a description of the reaction process is formulated, based on the assumption that the formation of the compound nucleus is initiated by the interaction of the incident particle with the surface oscillations of the target nucleus.

The formalism is applied in Section b) to the dispersion of neutrons, and the scattering cross-sections are considered for various strengths of the coupling to the compound nucleus. A sum rule for the scattering widths of the resonance levels is discussed.

The parameters of the formalism, which enter into the description of the coupling process, are considered in Section c). Recent empirical evidence, obtained from total neutron cross-sections averaged over many levels, permits an estimate of the coupling strength which may be compared with the particle-surface interaction observed in the low energy nuclear properties.

a) General Formalism.

In order to avoid inessential complexities of the mathematical formalism, we first consider the elastic scattering of an *s*-neutron on a nucleus of spin zero, and neglect the effect of inelastic pro-

cesses. The extension to a more general treatment is indicated below.

The wave function may be expanded in the form

$$\Psi = \frac{1}{r}\varphi(r)\frac{1}{\sqrt{4\pi}}\Phi_0(x) + \sum_i c_i \Psi_i(\vec{r}, x), \qquad \text{(Ap.V. 1)}$$

where Φ_0 is the ground state of the target nucleus, described by the coordinates (x) which may represent individual particles as well as collective degrees of freedom. The radial wave function of the scattered neutron is denoted by $\varphi(r)$. The Ψ_i constitute a complete orthonormal basis in the space orthogonal to Φ_0.

In the mixed representation (1), the state vector is specified by the function $\varphi(r)$ and the coefficients c_i. Assuming the coupling between the incident particle and the internal motion of the target nucleus to take place at a sharp surface ($r = R_0$), one obtains the coupled differential and algebraic equations

$$-\frac{\hbar^2}{2M}\frac{d^2}{dr^2}\varphi + V(r)\varphi = (E - E_0)\varphi \qquad r \neq R_0 \qquad \text{(Ap.V. 2)}$$

$$-\sqrt{\frac{1}{2}R_0}\,\varphi(R_0)\frac{\hbar^2}{MR_0^2}R_0\frac{\varphi'}{\varphi}\Big|_{R_0^-}^{R_0^+} + \sum_i c_i H_{0i} = 0 \qquad \text{(Ap.V. 3)}$$

$$\sqrt{\frac{1}{2}R_0}\,\varphi(R_0)H_{i0} + \sum_j c_j(H_{ij} - E\delta_{ij}) = 0, \qquad \text{(Ap.V. 4)}$$

where $(E - E_0)$ is the kinetic energy of the incident neutron (in the center of mass system) and $V(r)$ the potential to which the neutron is subjected inside the nucleus. For simplicity, we take $V(r)$ to be constant for $r < R_0$ and to rise abruptly to zero at the surface.

The matrix elements are given by

$$H_{0i} = \frac{1}{\sqrt{2\pi}}R_0^{-3/2}\int \vec{dr}\,dx\,\Phi_0^* H_{\text{int}}(\vec{r}, x)\,\Psi_i \qquad \text{(Ap.V. 5)}$$

and

$$H_{ij} = \int \vec{dr}\,dx\,\Psi_i^* H \Psi_j, \qquad \text{(Ap.V. 6)}$$

where $H_{\text{int}}(\vec{r}, x)$ is the coupling between the incident particle and the surface (cf. II.9 and 10) and H is the total Hamiltonian of the system. The most convenient choice of the basis Ψ_i de-

pends on the structure of the coupling process by which the compound nucleus is formed (cf. Ap. Vc). In some simple situations, one may take the Ψ_i to represent stationary states in the absence of the coupling to the entrance channel, i. e.

$$H_{ij} = E_i \delta_{ij}. \qquad \text{(Ap.V. 7)}$$

The equation (3) contains the discontinuity of the logarithmic derivative of φ at the surface, which may be written, by means of (2),

$$\left.\begin{aligned} R_0 \frac{\varphi'}{\varphi}\Big|_{R_0^-}^{R_0^+} &= kR_0 \cot(kR_0 + \delta) - KR_0 \cot KR_0 \\ &\equiv f(E) - f_{\mathrm{sp}}(E), \end{aligned}\right\} \qquad \text{(Ap.V. 8)}$$

where k and K are the outside and inside neutron wave numbers, and δ is the scattering phase.

The scattering cross-section is given in terms of f by (cf., e. g., Blatt and Weisskopf, 1952, Chapter VIII)

$$\sigma_{\mathrm{sc}} = \frac{\pi}{k^2}\left| 1 - \frac{f + ikR_0}{f - ikR_0} e^{-2ikR_0} \right|^2. \qquad \text{(Ap. V.9)}$$

The quantity f_{sp} in (8) is the f-function which corresponds to single-particle scattering in the fixed nuclear potential.

The equations (3) and (4) determine $\varphi(R_0)$ and the c_i; the compatibility condition provides the linear equation for f

$$\begin{vmatrix} \frac{\hbar^2}{MR_0^2}(f_{\mathrm{sp}} - f) & H_{0i} \\ H_{i0} & H_{ij} - E\delta_{ij} \end{vmatrix} = 0. \qquad \text{(Ap.V. 10)}$$

The special basis (7) gives

$$f = f_{\mathrm{sp}} + \frac{MR_0^2}{\hbar^2} \sum_i \frac{|H_{0i}|^2}{E - E_i}. \qquad \text{(Ap.V. 11)}$$

The treatment of partial waves of higher angular momentum and the effect of Coulomb forces leads to the same equation (10) for the function f, which then determines the cross-section by formulae which are generalizations of (9).

If inelastic processes are possible, one chooses an appropriate number of the Ψ_i to represent the open channels (t) other than the entrance channel. The function f is again determined by an equation of the form (10) where, however, for the open channels*

$$H_{tt} - E \to \frac{\hbar^2}{MR_0^2}[(f_{sp})_t - (\Delta_t + is_t)]. \qquad \text{(Ap. V. 12)}$$

The $(f_{sp})_t$ is the single-particle f-function appropriate to scattering in the channel, t, and Δ_t the level shift associated with long range forces. The imaginary term s_t is related to the channel width (cf. BLATT and WEISSKOPF, 1952, p. 332). Similarly, one may include radiative processes by adding a complex term to the nuclear Hamiltonian.

The effect of inelastic processes leads to complex values of f from which the elastic cross-section and the total reaction cross-section may be determined. The distribution of reaction products among the open channels is determined by the values of $\varphi_t(R_0)$.

The formulation given above, some consequences of which are considered in the following, has assumed the coupling between the incident particle and the internal structure of the target nucleus to be located at a sharp surface. The influence of a finite surface thickness as well as of other types of coupling, such as to collective volume oscillations and to particle excitations through direct particle forces, can be treated in a similar way by obtaining from the coupled equations a linear expression for f. The form of this expression may, however, in these cases be somewhat more complicated than (10).

b) Scattering Cross-sections.

In order to illustrate some of the characteristic features of nuclear reaction cross-sections, which are contained in the formalism outlined in Ap.Va, we consider in this paragraph the dispersion of neutrons in the region of sharp resonances ($kR_0 \ll 1$), and restrict ourselves to s-wave scattering.

* If the residual nucleus possesses a spin, there may be an additional constant term in (12), arising from H_{int} and representing the energy shift of the single-particle resonances in the channel t, resulting from the non-spherical nature of the potential.

i. *Weak coupling; one-level resonance.*

The coupling between the entrance channel and the compound nucleus may be termed weak if the second term in (11) is small compared to the first, except in the immediate neighbourhood of the energies E_i, i. e. for

$$\frac{MR_0^2}{\hbar^2}\frac{|H_{0i}|^2}{|f_{sp}|} \ll D, \qquad \text{(Ap.V. 14)}$$

where D is the level distance in the spectrum of E_i.

When the condition (14) is fulfilled, the impinging particle interacts mainly with the average potential of the target nucleus for most incident energies. This potential scattering depends on the distance from the nearest single-particle level and may take on all values from 0 to $4\pi\lambda\!\!\!^{-2}$. If $K R_0 \gg 1$, the potential scattering for most energies is close to that of an impenetrable sphere ($f = \infty$), but characteristic differences from this limit are expected, and experimental evidence on cross-sections far away from resonances may give information on the motion in the average potential*.

In the immediate neighbourhood of an energy E_i, the cross-section varies rapidly. If the potential scattering is small compared to $4\pi\lambda\!\!\!^{-2}$ ($f_{sp} \gg kR$; cf. (9)), one obtains a resonance of the usual type

$$\sigma = \frac{\pi}{k^2}\frac{\Gamma^2}{(E-E_r)^2+\frac{1}{4}\Gamma^2}, \qquad \text{(Ap.V. 15)}$$

where the resonance energy E_r is given by

$$f(E_r) = 0, \qquad \text{(Ap.V. 16)}$$

leading to

$$E_r = E_i - \frac{MR_0^2}{\hbar^2}\frac{|H_{0i}|^2}{f_{sp}} \qquad \text{(Ap.V. 17)}$$

which, in view of (14), is much closer to E_i than the neighbouring levels. The scattering width Γ and the reduced width γ are given by

* The term "potential scattering" is sometimes used to denote the scattering from an impenetrable sphere (cf., e. g., BLATT and WEISSKOPF, 1952). The recognition of the significance of single-particle nuclear motion for the course of nuclear reactions would seem, however, to make it more natural to reserve the term for the scattering in the actual nuclear potential. We here follow this latter terminology.

$$\Gamma = 2\,kR_0\gamma = -\frac{2\,kR_0}{f'(E_r)} \qquad \text{(Ap.V. 18)}$$

which, according to (11) and (17), gives

$$\Gamma = 2\,kR_0\frac{MR_0^2}{\hbar^2}\frac{|H_{0i}|^2}{f_{\mathrm{sp}}^2} \qquad \text{(Ap.V. 19)}$$

This value for the width is small compared to D by (14) and the assumption $f_{\mathrm{sp}} \gg kR_0$.

The potential scattering becomes comparable with the resonance maximum in the neighbourhood of the resonance energies E_n for single-particle scattering, given by

$$f_{\mathrm{sp}}(E_n) = 0\,. \qquad \text{(Ap.V. 20)}$$

The energy regions in which $\sigma_{\mathrm{pot}} \sim 4\pi\lambda^2$ are given by

$$|E - E_n| \lesssim \Gamma_{\mathrm{sp}}\,, \qquad \text{(Ap.V. 21)}$$

where

$$\Gamma_{\mathrm{sp}} = 2\,kR_0\gamma_{\mathrm{sp}} = 2\,kR_0\frac{\hbar^2}{MR_0^2} \qquad \text{(Ap.V. 22)}$$

represents the single-particle scattering width. In the regions (21), the form of the compound resonances is essentially modified by the potential scattering and, for $|E - E_n| \ll \Gamma_{\mathrm{sp}}$, the influence of the compound state appears as a narrow dip in the cross-section.

A simple interpretation of (14) may be obtained by using the approximation

$$f_{\mathrm{sp}}\frac{\hbar^2}{MR_0^2} \approx E_n - E \qquad \text{(Ap.V. 24)}$$

valid for $|E - E_n| \ll \Delta$, where Δ is the single-particle level distance (cf. (VI.7)). By means of (24) the condition (14) may be written

$$\frac{|H_{0i}|^2}{|E - E_n|\,D} \ll 1 \qquad \text{(Ap.V. 25)}$$

which is just the condition that the coupling H_{0i} to the entrance channel does not appreciably modify the compound states. Therefore, the states Ψ_i act individually and influence the scattering only in small energy intervals around the E_i-values.

In the region $|E-E_n| < \Gamma_{sp}$, the condition for weak coupling is modified, corresponding to the fact that the single-particle levels are only defined to within an energy Γ_{sp}. The analysis of (11) shows that in this region the less stringent condition

$$\frac{|H_{0i}|^2}{\Gamma_{sp} D} \ll 1 \qquad \text{(Ap.V. 26)}$$

is sufficient to ensure that the Ψ_i states act individually. The fact that (26) implies a scattering which, to first approximation, is of potential character, may be understood by observing that $2\pi(\hbar D)^{-1}|H_{0i}|^2$ represents the probability per unit time for coupling of the incident particle to the compound states. If this probability is small compared to $\hbar^{-1}\Gamma_{sp}$, which is the probability per unit time for escape from the single-particle state, the coupling is of only minor importance.

For $|E-E_n| \sim \Delta$, several single-particle levels are simultaneously effective, and the condition (14) can be interpreted in the same way as (25) by considering the total perturbation caused by all the single-particle levels.

ii. *Strong coupling; many-level resonances.*

When the conditions (14) or (26) are not fulfilled, the coupling between the states Ψ_i and the entrance channel leads to quasi-stationary states of the compound nucleus, essentially different from the Ψ_i. The coupling strongly mixes the states Ψ_i over an energy region given by the left hand side of (14).

Some of the properties of the scattering in the strong coupling region can be illustrated by assuming that, over the region of strong mixing, the Ψ_i can be approximated by a spectrum of uniform spacing D with a constant coupling matrix element $|H_{0i}| = H_c$. In this case, (11) can be written

$$f = f_{sp} + \frac{MR_0^2}{\hbar^2}\frac{\pi H_c^2}{D}\cot\frac{\pi}{D}(E-E_i). \qquad \text{(Ap.V. 27)}$$

It is seen that the resonances E_r of the compound nucleus ($f(E_r)=0$), which are close to E_i for weak coupling, move halfway in between the energies E_i when the coefficient of the contangent in (27) becomes large compared to f_{sp}.

The resonance scattering widths can be obtained from (18) and are found to be

$$\Gamma = \frac{2k}{K}\frac{D}{\pi}\left[\frac{\pi^2 H_c^2}{D\Delta} + \frac{D\Delta}{\pi^2 H_c^2}\cot^2 KR_0\right]^{-1}, \qquad \text{(Ap.V. 28)}$$

which is a generalization of (19), to which (28) reduces when the last term in the parenthesis dominates (weak coupling).

In the strong coupling region, the behaviour of the cross-section in between resonances is determined by the contribution of many far-off compound states, which dominates over the potential scattering. The variation of this background scattering depends on the coefficient of the cotangent in (27). Only when this coefficient is large compared to unity does the cross-section away from resonance approach a constant value, which then equals that of hard sphere scattering.

The foregoing analysis leads to the following picture of the scattering process in the various coupling regions (cf. Fig. 16).

For very small coupling

$$\frac{H_c^2}{D} \ll \Gamma_{\mathrm{sp}}, \qquad \text{(Ap.V. 29)}$$

the weak coupling situation applies for all incident energies and the principal part of the cross-section is determined by the potential scattering.

When (29) no longer holds, a strong coupling situation exists in the neighbourhood of the single-particle levels. Inside the region of strong coupling, the reduced scattering widths are of order (cf. (28))

$$\gamma = \left(\frac{D}{\pi H_c}\right)^2 \frac{\hbar^2}{MR_0^2} \qquad \text{(Ap.V. 30)}$$

while, at larger distances from the single-particle level, where the coupling is weak, the widths become very much smaller. A measure of the extent of the strong coupling region can be obtained as the energy interval W over which the reduced widths exceed half the maximum value (30). From (28) one finds

$$W = 2\pi\frac{H_c^2}{D}. \qquad \text{(Ap.V. 31)}$$

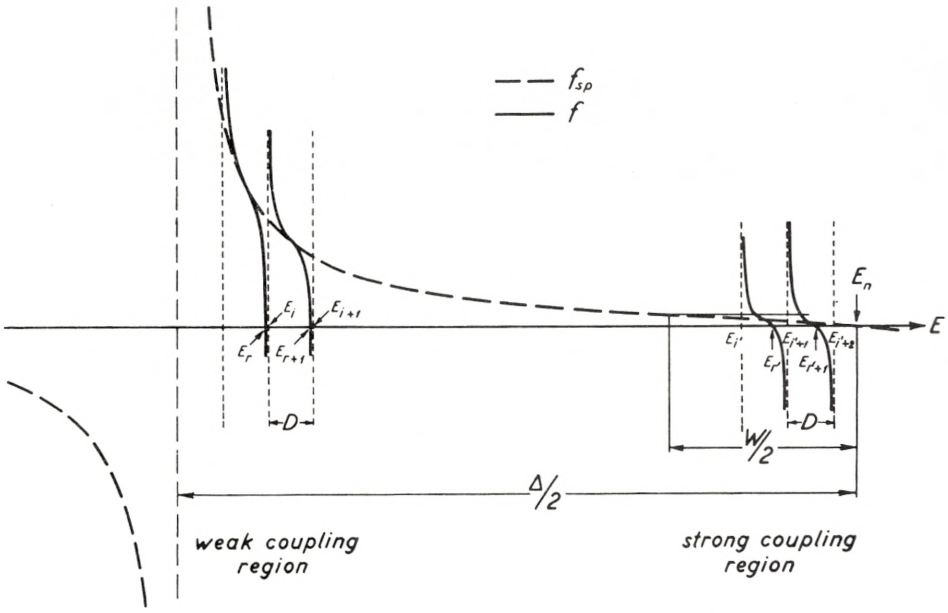

Fig. 16. *Scattering f-function in coupled model.* The scattering cross-sections can be simply expressed in terms of the logarithmic derivative f of the wave function at the nuclear surface (cf., e. g., (9)). The broken curve gives the f-function for pure single-particle scattering in the average nuclear potential. At the energies E_n, corresponding to the virtual single-particle states, with the spacing Δ, f_{sp} vanishes, while half way between these energies f_{sp} has poles. The coupling to the internal motion of the target nucleus, which is assumed to take place at the nuclear surface, adds a rapidly varying part to the total f-function (cf. (11)). The compound nucleus is described in terms of the states Ψ_i which would represent stationary states in the absence of the coupling to the entrance channel. At the energies E_i, which have on the average a spacing D, the f-function has a pole, while a resonance energy E_r of the compound nucleus (for which $f = 0$) occurs in each interval $E_i < E < E_{i+1}$.

The relative magnitude of the two contributions to f depends on the distance from the nearest single-particle level E_n. At large distances from E_n, the value of f_{sp} dominates and, to a first approximation, the cross-section is that of potential scattering. The coupling gives rise to resonances lying very close to the E_i and the scattering widths, which depend inversely on the energy derivative of f at resonance, are small (weak coupling region). Near to the E_n-values, the f-function is determined principally by the coupling term (strong coupling region). In this region, which extends over an energy interval W (cf. (31)), the resonance states result from the coupling of many Ψ_i-states, and the resonance energies lie essentially midway between the E_i. The scattering widths are relatively large in the strong coupling region, being of the order of Δ/W times the average resonance scattering width (cf. the sum rule (33 a)); the off-resonance scattering results mainly from the influence of many far-off resonances.

This energy is related to the probability per unit time for the formation of the compound nucleus, and can also be written in the form (VI.6), in terms of the mean free path of the particle for energy exchanges in the target nucleus.

For a coupling strength so great that W becomes comparable with or exceeds Δ, the region of strong coupling extends over the entire energy interval, and no structure associated with single-particle motion remains. In this situation, the entering particle shares its energy with many degrees of freedom of the compound nucleus before completing a single traversal of the nuclear field.

iii. *Sum rule for scattering widths.*

As long as the region of strong coupling W is small compared with the single-particle level spacing Δ, there exists a simple sum rule for the reduced scattering widths. This may be obtained, in its most general form, directly from (10). Since the scattering widths are appreciable only in regions around the single-particle levels E_n, one may use the form (24) for f_{sp}. The equation (10) is then equivalent to the secular equation for a bound state problem. The proper values and proper function for $f = 0$ give the resonance energies E_r of the compound nucleus and the state vectors of the scattering system at these resonances.

The reduced widths depend on $f'(E_r)$ and can be expressed in terms of the minors of (10) which, in turn, are simply related to the state vector at resonance. Thus, one obtains

$$\gamma_r = \left(\frac{\frac{1}{2} R_0 \varphi^2(R_0)}{\frac{1}{2} R_0 \varphi^2(R_0) + \sum_i c_i^2} \right)_r \frac{\hbar^2}{M R_0^2} \qquad \text{(Ap.V. 32)}$$

which expresses γ_r in terms of the reduced width of the single-particle level times the probability of finding the single-particle motion in the compound state (r). From the completeness of the states (r) one gets immediately

$$\sum_r \gamma_r = \frac{\hbar^2}{M R_0^2} \qquad \text{(Ap.V. 33)}$$

$$= \gamma_{\mathrm{sp}}, \qquad \text{(Ap.V. 33 a)}$$

where the sum is to be extended over the scattering resonances in the region $-\Delta/2 < E - E_n < \Delta/2$.*

As W approaches Δ, the single-particle level strength becomes approximately uniformly distributed over all the compound levels, corresponding to the relation (cf., e. g., WEISSKOPF, 1950)

$$\Gamma \approx \frac{D}{\Delta} \Gamma_{\mathrm{sp}} = \frac{2k}{K} \frac{D}{\pi}. \qquad \text{(Ap.V. 34)}$$

It may be noted that the sum rule (33a) is independent of the shape of the nuclear potential and of the particle angular momentum as well as of the types of couplings considered.

Similar sum rules hold for other properties of the compound levels, which depend on the content of a particular single-particle state. Thus, for a radiative transition to the ground state, the single-particle width may be considered as distributed over the compound levels, whose average radiative width, for the corresponding transition, may be represented by an expression equivalent to the first part of (34)**. However, for $W < \Delta$, the distribution will not be uniform, and the single-particle radiative width will be mainly concentrated on the compound levels in an energy region W around the unperturbed single-particle state.

c. Discussion.

In the application of the general formalism outlined in the preceding sections, the significant features of the nuclear structure are contained in the states Ψ_i in terms of which the properties of the compound nucleus are characterized.

The choice of a basis which diagonalizes all couplings except those to the entrance channel (cf. 7) is particularly appropriate

* Sum rules for reduced widths have been considered by TEICHMANN and WIGNER (1952) who have especially discussed the sums over channels leading from a particular compound state. Arguments for a relation similar to (33) are contained in the discussion following Eq. (31 b) of this reference. The factor 3/2 appearing in the estimate obtained by these authors arises from the assumption of a constant neutron wave function inside the nucleus.

** An expression for the partial radiative width of a compound state, similar to the first part of (34), has been given by BLATT and WEISSKOPF (1952; p. 646). However, as an estimate of the single-particle level spacing which enters in this expression, these authors have suggested a value of about 0.5 MeV for a medium heavy nucleus. The present estimate for Δ ($\sim$ 20 MeV) thus leads to a considerable decrease in the radiative widths.

if one can assume that, already after the first energy exchange between the incident particle and the target nucleus has taken place, the subsequent couplings proceed so rapidly that no structure associated with individual configurations remains.

In this situation, the states Ψ_i, though highly complex, have a certain uniformity of statistical nature. As a first approximation, one may assume the $|H_{0i}|$ to have a constant value H_c, and the level energies E_i to be approximately evenly spaced with a separation D. The gross features of the nuclear level structure may then be characterized by the coupling parameter W, representing the energy region around the single-particle resonances, where the compound nucleus is formed with appreciable probability (cf. Ap.V b.ii and also § VI d).

In general, one expects simple types of motion to manifest themselves also in intermediate stages of the reaction. The choice of the basis (7) is then less appropriate, since the assumption of a constant H_{0i} is no longer valid. The resulting features of the reaction process may be taken into account by including among the Ψ_i a number of states representing the structure of the intermediate stages.

Such effects may, for instance, be significant for very deformed target nuclei, where the entering particle has a large probability of setting the nucleus in rotation (cf. § VI c.ii). The rotational excitation energy is not easily transmitted to the other degrees of freedom of the nucleus, and may with appreciable probability be returned to the entrance channel, or may give rise to an inelastic process without the formation of a compound nucleus. To describe these features, one may consider as a first approximation only the potential scattering and the specific couplings to the rotational motion. It may be possible to include the additional couplings leading to the compound nucleus formation, by means of a uniform set of states, whose coupling to the simple motion may be characterized by parameters similar to W.

Recently, important evidence on the formation of the compound nucleus has been obtained from the analysis of total neutron cross-sections, averaged over many resonances (Barschall, 1952; Feshbach, Porter, and Weisskopf, 1953). The effect of the compound nucleus formation on such average cross-sections can be described as an absorption, since one may con-

sider the problem in terms of the scattering of neutron wave-packets with a time extension short compared with the periods of the compound states. A particle entering the complex motion is, therefore, effectively lost from the wave-packet. Such an absorption can be represented by an imaginary potential (cf., e. g., BETHE, 1940).

In the simplified situation discussed above, where specific structures of the intermediate stages of the coupling process can be neglected, the averaged total cross-sections can thus be obtained by considering single-particle scattering in a constant complex potential. The coupling energy W is related to the imaginary part of the potential V by

$$W = -2\,Im(V). \qquad \text{(Ap.V. 35)}$$

The analysis of the empirical data has shown that many features of the averaged total cross-sections can be accounted for in terms of such a complex potential with $Im(V) \approx -1$ MeV, corresponding to $W \approx 2$ MeV (FESHBACH, PORTER, and WEISSKOPF, 1953). Thus, the observed cross-sections resemble those of single-particle scattering, in which the individual resonances are broadened by about two MeV.*

The coupling which leads to the compound nucleus formation may result from the interaction of the incident particle with the surface oscillations or other collective modes of the target nucleus, or from direct collisions with individual nucleons. The contribution of the surface coupling to W may be estimated from the matrix elements in Chapter II. For the average coupling matrix element H_c, one has

$$H_c^2 \approx \frac{D}{\Delta} \sum_i |H_{0i}|^2, \qquad \text{(Ap.V. 36)}$$

where the sum is extended over all states within the single-particle level spacing Δ. This sum represents a closure over all variables

* In fitting the experimental cross-sections, FESHBACH, PORTER, and WEISSKOPF (1953) have used the parameters $V_0 = 19$ MeV, for the real part of the potential, and $R_0 = 1.45 \times A^{1/3} \times 10^{-13}$ cm for the nuclear radius. While the agreement between the calculated and measured cross-sections is striking, these parameters do not seem compatible with the positions of the single-particle levels, assumed by the shell model, which for the above radius requires a potential of about 30 MeV. Thus, for example, the observed large cross-sections below 1 MeV for elements with $A \approx 90$ result, for $V_0 = 19$ MeV, from a virtual $2p$ level, while already for lighter nuclei, $2p$ states, bound by about 8 MeV, have been identified (cf., e. g., Tables XII and XXV).

except the radial quantum number of the particle, and one obtains (cf. (II.9) and (A.38))

$$\sum_i |H_{0i}|^2 = <0|H_{\text{int}}^2|0> = \frac{5}{8\pi} k^2 \frac{\hbar\omega}{C} \qquad \text{(Ap.V. 37)}$$

for a particle incident on an undeformed nucleus. From (31), (36), and (37) one then finds

$$W = \frac{5}{4} \frac{k^2}{\Delta} \cdot \frac{\hbar\omega}{C}. \qquad \text{(Ap.V. 38)}$$

The hydrodynamical surface parameters (Figs. 1 and 2) and the expression (VI.7) for Δ lead to values for W of about 2 and 3 MeV for a heavy and medium heavy nucleus, respectively. It thus appears that the surface coupling is adequate to account for the observed probabilities for compound nucleus formation.

In the case of strongly deformed target nuclei, one obtains

$$<0|H_{\text{int}}^2|0> = \frac{1}{4\pi} k^2 \beta^2 \qquad \text{(Ap.V. 39)}$$

which represents an increase over (37) by a factor of the order of the number of phonons present in the deformed state. However, the major part of this very strong coupling leads to rotational excitations and thus gives rise to features in the reaction process that cannot be represented by the scattering in a fixed complex potential (see above). A detailed study of elastic as well as inelastic neutron cross-sections for very deformed nuclei (especially in the regions $155 < A < 185$ and $A > 225$) would thus be of interest. In addition to rotational interactions, the surface coupling gives rise to the excitation of vibrational modes, which may rather rapidly transmit their energy to additional degrees of freedom and result in the formation of a compound nucleus. An estimate of these couplings can be obtained from (39) by subtracting the rotational interactions, and one finds a value for the absorption parameter W of about 3/5 of the estimate (38).

With increasing energy of the impinging particle, couplings to collective modes of higher frequencies are expected to be of increasing importance, and also the direct particle forces can excite an increasing number of degrees of freedom of the target

nucleus. A compensating effect sets in when the particle energy becomes comparable with the kinetic energies of the target nucleons. The short time spent by the particle in the nucleus, together with the decreasing nucleon scattering cross-sections, then implies a decrease in the probability for formation of the compound nucleus. For bombarding energies in the region of 100 MeV, an appreciable transparency of the nucleus has been observed and has been interpreted in terms of the single-particle features embodied in the optical model of the nucleus (SERBER, 1947; FERNBACH, SERBER, and TAYLOR, 1949).

Appendix VI.

Nuclear Excitation by the Electric Field of Impinging Particles.

Important information may be obtained from the excitation of nuclei by bombardment with heavy charged particles whose energies are sufficiently below the Coulomb barrier to exclude the influence of nuclear forces. Since only electrostatic forces are then operative, the experiments can be analyzed in terms of relatively simple properties of the nuclear structure. Recently, TER-MARTIROSYAN (1952) has given a rather detailed treatment of such processes*. We here summarize some of the results of this analysis, attempting in particular to indicate the relations to the electromagnetic radiative transitions (cf. Chapter VII).

A great simplicity in the analysis arises from the fact that one can describe the projectile as following a classical trajectory. The condition for such a classical treatment is (cf. N. BOHR, 1948, § 1.3).

$$\varkappa = 2\frac{Z_1 Z_2 e^2}{\hbar v} \gg 1, \qquad \text{(Ap.VI. 1)}$$

where Z_1 and Z_2 are the charge numbers of the projectile and the target nucleus, respectively, and where v is the velocity of the incident particle.

This condition is always fulfilled when the bombarding energy is sufficiently low that penetration through the Coulomb barrier, and thus the influence of nuclear forces, is negligible.

One can then describe the influence of the particle on the nucleus in terms of a time-dependent potential

* Various aspects of these reactions have also been previously considered (WEISSKOPF, 1938; RAMSEY, 1951; MULLIN and GUTH, 1951; HUBY and NEWNS, 1951; BREIT, HULL, and GLUCKSTERN, 1952).

$$V(t) = \sum_{p=1}^{Z_2} \frac{Z_1 e^2}{|\vec{r}(t) - \vec{r}_p|}, \qquad \text{(Ap.VI. 2)}$$

where $\vec{r}_p$ are the coordinates of the target protons and where $\vec{r}(t)$ gives the trajectory of the incident particle, considered as a point charge. This potential gives rise to nuclear transitions of electric multipole character. Of special interest are the collective transitions, for which the excitation cross-sections are particularly large. The low energy collective transitions are induced by the quadrupole component of (2), given by

$$V_2(t) = \frac{4\pi}{5} Z_1 e^2 \sum_{\mu} \sum_{p} r_p^2 \, Y^*_{2\mu}(\vartheta_p, \varphi_p) \, Y_{2\mu}(\vartheta(t), \varphi(t)) \left[r(t)\right]^{-3}. \qquad \text{(Ap.VI. 3)}$$

The method of Coulomb excitation may also find application to other multipole transitions*, but these are in general expected to have appreciably smaller cross-sections. Magnetic transitions are weak due to the small velocity of the projectile.

Since the field of the particle produces only a small perturbation in the internal nuclear wave function, the probability for excitation of a given level may be written

$$P = \sum_{M_f} |b(M_f)|^2, \qquad \text{(Ap.VI. 4)}$$

where M_f is the magnetic quantum number of the final state and

$$b(M_f) = \frac{1}{i\hbar} \int_{-\infty}^{+\infty} \langle f | V(t) | i \rangle e^{i\omega t} dt \qquad \text{(Ap.VI. 5)}$$

with

$$\hbar\omega = E_f - E_i = \Delta E. \qquad \text{(Ap.VI. 6)}$$

For a quadrupole transition, one obtains

$$b(M_f) = \frac{4\pi}{5} \frac{Z_1 e}{i\hbar} \sum_{\mu} \langle i | \mathfrak{M}_e(2, \mu) | f \rangle \int_{-\infty}^{+\infty} \frac{1}{r^3} Y_{2\mu}(\vartheta, \varphi) \, e^{i\omega t} dt \qquad \text{(Ap.VI. 7)}$$

in terms of the nuclear matrix elements of the quadrupole operator $\mathfrak{M}_e(2, \mu)$ given by (VII.5).

* The electric dipole transitions have been considered in detail, for all values of $\varkappa$, by MULLIN and GUTH (1951), HUBY and NEWNS (1951), and TER-MARTIROSYAN (1952). MULLIN and GUTH (1951) have also considered the quantum mechanical treatment of $E2$ transitions, but their cross-sections seem to be too small, as a result of the assumption of a scalar property of the quantity $M_{2\,\mathrm{Born}}(\vec{k}, \vec{k}')$ implied in the equation following (29) of their paper.

The classical orbit of the projectile is a hyperbola and it is convenient to choose a coordinate system whose xy plane is that of the orbit and whose x-axis is the focal line. The orbit may be given in the following parametric representation

$$\left.\begin{aligned} x &= a\,(\cosh\omega + \varepsilon) \\ y &= a\sqrt{\varepsilon^2 - 1}\,\sinh w \\ r &= a\,(\varepsilon\cosh w + 1) \\ t &= \frac{a}{v}\,(\varepsilon\sinh w + w), \end{aligned}\right\} \qquad \text{(Ap.VI. 8)}$$

where

$$a = \frac{Z_1 Z_2 e^2}{m v^2} \qquad \text{(Ap.VI. 9)}$$

is half the distance of closest approach in a head-on collision. The reduced mass is denoted by m. The orbital eccentricity ε is

$$\varepsilon = \left[1 + \left(\frac{p}{a}\right)^2\right]^{1/2}, \qquad \text{(Ap.VI. 10)}$$

in terms of the impact parameter p. The angle of deflection ϑ in the center of mass system is given by

$$\tan\frac{\vartheta}{2} = \frac{a}{p}. \qquad \text{(Ap.VI. 11)}$$

The transition amplitude can now be written

$$) = i\sqrt{\frac{\pi}{5}}\,\frac{Z_1 e}{\hbar v}\,\frac{1}{a^2}\left\{B_e(2)\right\}^{1/2} < I_f\,2\,M_f M_i - M_f \,|\, I_f\,2\,I_i M_i > S^{(2)}_{M_f - M_i} \qquad \text{(Ap.VI. 12)}$$

where $B_e(2)$ is given by (VII.2). The non-vanishing components of $S^{(2)}_\mu$ are given by

$$S^{(2)}_0 = \int_{-\infty}^{+\infty} e^{i\xi(\varepsilon\sinh w + w)}\,\frac{1}{(\varepsilon\cosh w + 1)^2}\,dw \qquad \text{(Ap.VI. 13)}$$

$$= -\sqrt{\frac{3}{2}}\int_{-\infty}^{\infty} e^{i\xi(\varepsilon\sinh w + w)}\,\frac{(\cosh w + \varepsilon \mp i\sqrt{\varepsilon^2 - 1}\,\sinh w)^2}{(\varepsilon\cosh w + 1)^4}\,dw, \qquad \text{(Ap.VI. 14)}$$

where

$$\xi = \frac{\Delta E}{2E}\,\frac{Z_1 Z_2 e^2}{\hbar v}. \qquad \text{(Ap.VI. 15)}$$

The quantity $\varepsilon\xi$ represents the ratio of the collision time to the nuclear period $\tau = \omega^{-1}$. For values of $\varepsilon\xi$ of the order of or larger than unity, the collision becomes approximately adiabatic with a resulting small excitation probability, decreasing exponentially with $\varepsilon\xi$.

The differential cross-section for excitation associated with a scattering into the solid angle $d\Omega$ is

$$d\sigma_{\text{exc}}(\vartheta) = \frac{1}{4} a^2 \sin^{-4}\frac{\vartheta}{2} P d\Omega, \qquad \text{(Ap.VI. 16)}$$

while the total cross-section for excitation of the state in question becomes

$$\sigma_{\text{exc}} = \frac{2\pi^2}{25}\frac{1}{Z_2^2 e^2}\left(\frac{mv}{\hbar}\right)^2 B_e(2)\, g_2(\xi), \qquad \text{(Ap.VI. 17)}$$

with

$$g_2(\xi) = \sum_{\mu}\int_1^{\infty} \varepsilon\, d\varepsilon \left| S_{\mu}^{(2)}\right|^2. \qquad \text{(Ap.VI. 18)}$$

The function $g_2(\xi)$ is plotted in Fig. 17.

From the relative values of the transition amplitudes $b(M_f)$ the angular distribution of the γ-radiation following the excitation can be determined*.

While the angular distribution may give information about the spins of the states involved and about the multipole order of the emitted γ-rays, the measurement of σ_{exc} for the excitation from level c to level d leads to a determination of the quantity $\{B_e(2)\}_{c\to d}$. This information is thus similar to that obtained from a lifetime measurement for the inverse transition, for which the $E2$ radiative probability is given by (cf. (VII.1))

$$T = \frac{4\pi}{75}\frac{1}{\hbar}\left(\frac{\omega}{c}\right)^5 \{B_e(2)\}_{d\to c}. \qquad \text{(Ap.VI. 19)}$$

The nuclear matrix elements for the excitation and decay are related by

$$B_{c\to d} = B_{d\to c}\cdot\frac{2I_d+1}{2I_c+1}. \qquad \text{(Ap.VI. 20)}$$

* Recently, explicit expressions for the angular distribution of the γ-radiation following Coulomb excitation have been given by ALDER and WINTHER (1953).

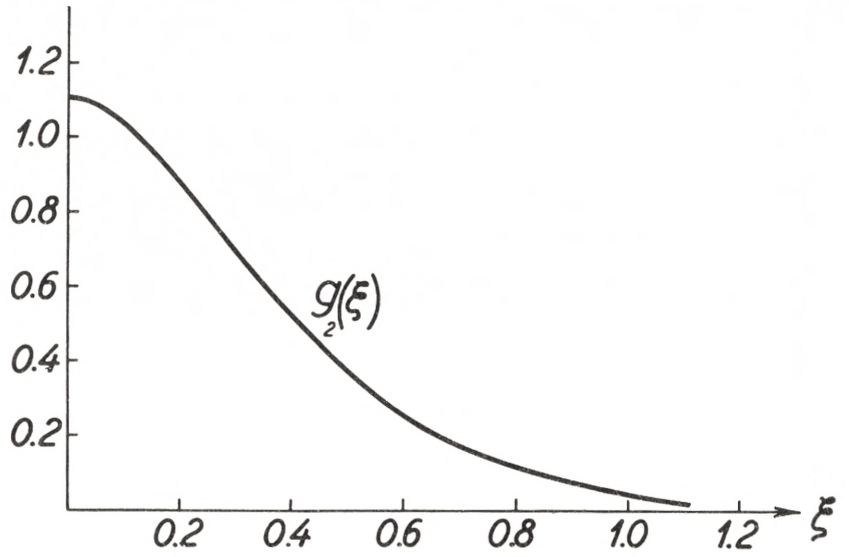

Fig. 17. *Function $g_2(\xi)$ appearing in cross-sections for Coulomb excitation.* The cross-section for Coulomb excitation produced by the electric quadrupole field of the impinging particles is given by (17), which contains the function $g_2(\xi)$, where ξ, given by (15), is a measure of the ratio between the collision time and the nuclear period. The function $g_2(\xi)$ is expressed by means of (13), (14), and (18) in terms of integrals over the trajectories of the particles. The integrals have been numerically evaluated by ALDER and WINTHER (1953), whose results we reproduce in this figure.

The evaluation of the reduced transition probabilities B for various types of transitions in the coupled system has been given in Chapter VII.

The large values of $B_e(2)$ for nuclear collective transitions make the method of Coulomb excitation especially suited for the study of rotational and vibrational states (§ VI c).

Note added in proof: Recently, the feasibility of Coulomb excitation has been exhibited by the observation of the γ-radiation following the nuclear excitation (MCCLELLAND and GOODMAN, 1953; HUUS and ZUPANČIČ, 1953). By this method important evidence has been obtained on the rotational spectrum of the odd-A nucleus, $_{73}Ta^{181}$ (cf. HUUS and ZUPANČIČ (1953), whose results we here summarize).

The first strongly excited level has been found at 137 keV. Since the ground state of Ta^{181} has $I_0 = 7/2$, the first rotational state is expected to have $I = 9/2$ and an energy of $9\hbar^2/2\Im$ (cf. VI. 4). Thus, assuming a similar moment of inertia as in the neighbouring even-even nucleus $_{72}Hf^{180}$, whose first excited (2+) state has an energy of 93 keV (cf. SCHARFF-GOLDHABER, 1953), the first rotational state in Ta^{181} should have an energy of about 140 keV, in good agreement with the observed value.

The second rotational state in Ta^{181}, with $I = 11/2$, should have an energy

of 20/9 times that of the first (9/2) state, and should also be strongly excited. This was confirmed by the observation of a γ-ray of 300 keV resulting from the Coulomb excitation.

The energy dependence of the excitation cross-sections for the two states was found to be in good agreement with (Ap. VI. 17), using the numerical results for $g_2(\xi)$ of ALDER and WINTHER (1953), thus supporting the $E2$ interpretation of the excitation process.

From the magnitude of the observed cross-section for the excitation of the 137 keV line, the reduced transition probability $B_e(2)$ can be obtained from (Ap. VI. 17). By means of (VII. 18) and (Ap. VI. 20), one derives an intrinsic quadrupole moment of $|Q_0| \sim 7 \times 10^{-24}$ cm^2, which is in good agreement with the trend of the deformations deduced from lifetime measurements of first excited states in even-even nuclei (cf. Table XXVII). The value of Q_0 may also be compared with the spectroscopic quadrupole moment (cf. Table XVIII) which yields, by means of the projection factor (V. 9), a deformation of $Q_0 \sim 14 \times 10^{-24}$ cm^2, which is again of the same order of magnitude; the difference may not be significant in view of the experimental uncertainties.

The cross-section for the production of the 300 keV γ-ray depends also on the branching ratio between the direct ground state transition ($11/2 \rightarrow 7/2$) and the cascading ($11/2 \rightarrow 9/2 \rightarrow 7/2$) via the first excited state. From a comparison of the cross-sections for the 300 keV and 137 keV γ-rays, a branching ratio of about 1:4 has been deduced. While the cross-over transition is of pure $E2$ type, the cascade may proceed by $M1$ as well as by $E2$ transitions. The $E2$ transition probabilities can be determined from the value of Q_0 (VII. 18 and 19), and the $M1$ transition probability can be related to the magnetic moment of the ground state (VII. 20 and IV. 9). From the observed magnetic moment (Table XVIII) and the value $Q_0 = 7 \times 10^{-24}$ cm^2, and using the internal conversion coefficients of ROSE et al. (1951) and of GOLDHABER and SUNYAR (1951), one calculates a branching ratio of about 1:1. While the observed branching ratio confirms the relatively strong competition of $E2$ with $M1$ radiation in rotational transitions, it is still somewhat smaller than the calculated ratio; however, the theoretical estimate is very sensitive to the value of the ground state magnetic moment, and a precision determination of μ (Ta^{181}) would thus be of interest.

References.

H. Aeppli, H. Albers-Schönberg, H. Frauenfelder, and P. Scherrer (1952), Helv. Phys. Acta **25,** 339 (Ad. v).

F. Ajzenberg and T. Lauritsen (1952), Rev. Mod. Phys. **24,** 321. (Ad. v; VIb; VIc.i; VIIIc.ii).

F. Alder and K. Halbach (1953), Helv. Phys. Acta **26,** 426. (Ad.iii).

K. Alder and A. Winther (1953), submitted to the Physical Review. (Ap. VI).

W. Arber and P. Stähelin (1953), Helv. Phys. Acta **26,** 433. (III. iv).

J. R. Arnold and T. Sugihara (1953), Phys. Rev. **90,** 332. (VI c.ii).

F. Asaro and I. Perlman (1952), Phys. Rev. **87,** 393. (VIc.ii).

F. Asaro and I. Perlman (1953), submitted to the Physical Review. (VI c.ii).

J. M. Baker, B. Bleaney, K. D. Bowers, P. F. D. Shaw, and R. S. Trenam (1953), Proc. Phys. Soc. A **66,** 305. (Ad. vii).

H. H. Barschall (1952), Phys. Rev. **86,** 431 (VId; Ap.Vc).

E. H. Bellamy and K. F. Smith (1953), Phil. Mag. **44,** 33. (Ad. v and xi).

A. Berthelot (1944), Ann. Phys. (11) **19,** 117. (VIIb.ii).

H. A. Bethe (1937), Rev. Mod. Phys. **9,** 69. (VIId.iii).

H. A. Bethe (1940), Phys. Rev. **57,** 1125. (Ap.Vc).

F. Bitter (1949), Phys. Rev. **76,** 150. (Ad. vi).

D. H. Black (1924), Proc. Roy. Soc. A **106,** 632. (VIc.ii).

J. M. Blatt (1953), Phys. Rev. **89,** 83. (VIIIc).

J. M. Blatt and V. F. Weisskopf (1952), Theoretical Nuclear Physics. J. Wiley and Sons, New York. (VII a; VII b.i; VII b.ii; VIII a; Ap. V a; Ap. V b.i and iii).

F. Bloch (1951); Phys. Rev. **83,** 839. (IV c).

G. S. Bogle, H. J. Duffus, and H. E. D. Scovil (1952), Proc. Phys. Soc. A **65,** 760. (Ad. vii).

A. Bohr (1951), Phys. Rev. **81,** 134. (I; II b.ii; IV; IVb; Vb).

A. Bohr (1951 a), Phys. Rev. **81,** 331. (Ad. iv and vi).

A. Bohr (1952), Dan. Mat. Fys. Medd. **26,** no. 14. (Quoted in the text as A).

A. Bohr, J. Koch, and E. Rasmussen (1952), Arkiv f. Fysik **4,** 455. (Ad. iv).

A. Bohr and B. R. Mottelson (1952), Physica **18,** 1066. (VIb; VIc.ii; VII d.i).

A. Bohr and B. R. Mottelson (1953), Phys. Rev. **89,** 316. (I; VI c.ii).

A. Bohr and B. R. Mottelson (1953 a), Phys. Rev. **90**, 717. (VI c.ii).
A. Bohr and V. F. Weisskopf (1950), Phys. Rev. **77**, 94. (Ad. iv and vi).
N. Bohr (1936), Nature **137**, 344. (I; VI d).
N. Bohr and F. Kalckar (1937), Dan. Mat. Fys. Medd. **14**, no. 10. (I).
N. Bohr and J. A. Wheeler (1939), Phys. Rev. **56**, 426. (I).
N. Bohr (1948), Dan. Mat. Fys. Medd. **18**, no. 8. (Ap. VI).
M. Born and W. Heisenberg (1924), Zs. f. Physik **23**, 388. (II a.iii).
R. Bouchez and R. Nataf (1952), C. R. **234**, 86; Phys. Rev. **87**, 155. (VIII c).
G. Bouissières, P. Falk-Vairant, M. Riou, J. Teillac, and C. Victor (1953), C. R. **236**, 1874. (VI c.ii).
G. Breit, M. H. Hull Jr., and R. L. Gluckstern (1952), Phys. Rev. **87**, 74. (Ap. VI).
P. Brix (1953), Phys. Rev. **89**, 1245. (Ad. v).
P. Brix and H. Kopfermann (1949), Zs. f. Physik **126**, 344. (V d; Ad. v).
P. Brix and H. Kopfermann (1952), Phys. Rev. **85**, 1050. (V d; Ad. v).
B. M. Brown and D. H. Tomboulian (1952), Phys. Rev. **88**, 1158. (Ad. viii).
H. B. G. Casimir (1936), On the Interaction between Atomic Nuclei and Electrons. Teyler's Tweede Genootschap, Haarlem. (I; V).
E. U. Condon and G. H. Shortley (1935), The Theory of Atomic Spectra. The University Press, Cambridge. (Ap. II).
S. M. Dancoff (1950), Phys. Rev. **78**, 382. (II b.iii).
J. M. Daniels, M. A. Grace, H. Halban, N. Kurti, and F. N. H. Robinson (1952), Phil. Mag. **43**, 1297. (Ad. xi).
J. P. Davidson Jr. (1951), Phys. Rev. **82**, 48. (VIII a; VIII c.iv).
J. P. Davidson and E. Feenberg (1953), Phys. Rev. **89**, 856. (II a.iii; II b.ii; II b.iii; IV; Ad. i; VIII b.ii).
H. G. Dehmelt (1952), Zs. f. Physik **133**, 528. (Ad. iii and xi).
H. G. Dehmelt and H. Krüger (1951), Zs. f. Physik **129**, 401. (Ad. iii).
H. G. Dehmelt and H. Krüger (1951 a), Zs. f. Physik **130**, 385. (Ad. v).
D. M. Dennison (1940), Phys. Rev. **57**, 454. (VI c.i).
A. de-Shalit (1951), Helv. Phys. Acta **24**, 296. (IV c).
S. S. Dharmatti and H. E. Weaver Jr. (1952), Phys. Rev. **85**, 927. (Ad. vi).
S. S. Dharmatti and H. E. Weaver Jr. (1952 a), Phys. Rev. **86**, 259. (Ad. ii).
W. C. Dickinson (1950), Phys. Rev. **80**, 563. (Ad.).
P. A. M. Dirac (1947), The Principles of Quantum Mechanics. (3rd Ed.). Oxford University Press. (II b.i).
A. S. Douglas (1953), Nature **171**, 868 (II a.iii).
A. R. Edmonds and B. T. Flowers (1952), Proc. Roy. Soc. A **214**, 515. (II c.iii).
A. R. Edmonds and B. T. Flowers (1952 a), Proc. Ryo. Soc. A **215**, 120. (II c.iii; III.ii, iii, and iv).
J. T. Eisinger, B. Bederson, and B. T. Feld (1952), Phys. Rev. **86**, 73. (Ad. iv; Ad. vi; Ad. xi).

R. J. Elliot and K. W. H. Stevens (1952), Proc. Phys. Soc. A **65**, 370. (Ad. vii).
C. D. Ellis and G. H. Aston (1930), Proc. Roy. Soc. A **129**, 180. (VII d.iii).
E. Feenberg (1947), Rev. Mod. Phys. **19**, 239. (II a.i).
E. Feenberg and K. C. Hammack (1949), Phys. Rev. **75**, 1877. (IV).
E. Feenberg and K. C. Hammack (1951), Phys. Rev. **81**, 285. (II a.iii; V b).
L. Feldman and C. S. Wu (1952), Phys. Rev. **87**, 1091. (VIII c.iv).
S. Fernbach, R. Serber, and T. B. Taylor (1949), Phys. Rev. **75**, 1352. (Ap. V c).
H. Feshbach and V. F. Weisskopf (1949), Phys. Rev. **76**, 1550. (VI d).
H. Feshbach, C. E. Porter, and V. F. Weisskopf (1953), Phys. Rev. **90**, 166. (VI d; Ap. V c).
M. Fierz (1937), Zs. f. Physik **104**, 553. (VIII a).
M. Fierz (1943), Helv. Phys. Acta **16**, 365. (VII b.ii).
B. H. Flowers (1952), Proc. Roy. Soc. A **212**, 248. (II c.iii).
B. H. Flowers (1952 a), Proc. Roy. Soc. A **215**, 398. (II c.iii; III.iii).
B. H. Flowers (1952 b), Phys. Rev. **86**, 254. (II c.iii; III.ii; VI c.ii).
B. H. Flowers (1952 c), Phil. Mag. (7), **43**, 1330. (IV a; Ad. iv).
S. Flügge (1941), Ann. d. Phys. (5), **39**, 373. (VII b.ii).
S. Flügge and K. Woeste (1952), Zs. f. Physik **132**, 384. (II a.i).
L. L. Foldy and F. J. Milford (1950), Phys. Rev. **80**, 751. (II b.i; IV).
K. W. Ford (1953), Phys. Rev. **90**, 29. (II b.ii; II b.iii; II c.ii; V d; VI c.ii).
S. Gallone and C. Salvetti (1951), Phys. Rev. **84**, 1064. (V b).
S. Gallone and C. Salvetti (1951 a), Il Nuovo Cimento (9) **8**, 970. (V b).
S. Gallone and C. Salvetti (1953), Il Nuovo Cimento (9) **10**, 145. (II a.ii; Ap. I).
S. Geschwind, G. R. Gunther-Mohr, and G. Silvey (1952), Phys. Rev. **85**, 474. (Ad. v).
M. Goldhaber and R. D. Hill (1952), Rev. Mod. Phys. **24**, 179. (III.iii; VI b; VI c.ii; VII d; VII d.i).
M. Goldhaber and A. W. Sunyar (1951), Phys. Rev. **83**, 906. (I; VI b; VI c.ii; VII d; VII d.i; VII d.ii; Ap.VI).
M. Goldhaber and E. Teller (1948), Phys. Rev. **74**, 1046. (II a.i).
W. Gordy (1949), Phys. Rev. **76**, 139. (V; V a).
C. J. Gorter, H. A. Tolhoek, O. J. Poppema, M. J. Steenland, and J. A. Beun (1952), Physica **18**, 135. (Ad. xi).
R. L. Graham and R. E. Bell (1953), Canadian J. of Physics **31**, 377. (VII d.i).
E. Greuling (1942), Phys. Rev. **61**, 568. (VIII a).
W. A. Hardy, G. Silvey, and C. H. Townes (1952), Phys. Rev. **85**, 494. (Ad. viii).
J. A. Harvey (1951), Phys. Rev. **81**, 353. (VI b).
J. A. Harvey (1953), Canadian J. of Physics **31**, 278. (VI b).
O. Haxel, J. H. D. Jensen, and H. E. Suess (1950), Zs. f. Physik **128**, 295. (I; III.i; III.ii; IV).

O. Haxel, J. H. D. Jensen, and H. E. Suess (1952), Ergebn. d. Exakten Wiss. **26**, 244. (I).
G. Herzberg (1950), Molecular Spectra and Molecular Structure I. D. van Nostrand, New York. (II b.ii; VI c.ii; VII c.i).
D. L. Hill and J. A. Wheeler (1953), Phys. Rev. **89**, 1102. (I; II a.ii; VI d; VII c.i; Ap. I).
R. D. Hill (1949), Phys. Rev. **76**, 998. (V).
R. D. Hill (1950), Phys. Rev. **79**, 1021. (VI b).
A. J. M. Hitchcock (1952), Phys. Rev. **87**, 664. (II c.iii; III.iv; IV a; Ad. xi).
A. J. M. Hitchcock (1952 a), Dissertation, Cambridge. (II c.iii; III.iv).
J. M. Hollander, I. Perlman, and G. T. Seaborg (1953), Rev. Mod. Phys. **25**, 469. (VI c.ii; VII d.iii).
N. J. Hopkins (1952), Phys. Rev. **88**, 680. (VII d.i).
H. Horie, M. Umezawa, Y. Yamaguchi, and S. Yoshida (1951), Progress Theor. Phys. **6**, 254. (VI c.ii).
H. Horie and S. Yoshida (1951), Progress Theor. Phys. **6**, 829. (IV a).
R. Huby and H. C. Newns (1951), Proc. Phys. Soc. A **64**, 619. (Ap. VI).
T. Huus and Č. Zupančič (1953), Dan. Mat. Fys. Medd. **28**, no. 1. (VI c.iii; VII d.iii; Ap. VI).
D. R. Inglis (1952), Phys. Rev. **87**, 915. (III.iv; Ad. iii; VI b).
V. Jaccarino, B. Bederson, and H. H. Stroke (1952), Phys. Rev. **87**, 676. (Ad. xi).
C. D. Jeffries (1953), Phys. Rev. **90**, 1130. (III.iii; Ad. vii).
C. D. Jeffries, H. Loeliger, and H. H. Staub (1952), Phys. Rev. **85**, 478. (Ad. vii).
W. Jekeli (1952), Zs. f. Physik **131**, 481. (II b.i; VII b.ii).
J. H. D. Jensen and M. G. Mayer (1952), Phys. Rev. **85**, 1040. (IV c).
F. M. Kelly (1952), Proc. Phys. Soc. A **65**, 250. (Ad. iv).
K. G. Kessler (1950), Phys. Rev. **79**, 167 (Ad. iii).
C. Kikutchi, M. H. Sirvetz, and V. W. Cohen (1952), Phys. Rev. **88**, 142. (Ad. xi).
J. G. King and V. Jaccarino (1953), Bul. Am. Phys. Soc. **28**, nr. 2, p. 11. (Ad. iii).
P. F. A. Klinkenberg (1952), Rev. Mod. Phys. **24**, 63. (Ad.).
L. J. Koester, H. L. Jackson, and R. K. Adair (1951), Phys. Rev. **83**, 1250. (Ad.i; VI b).
O. Kofoed-Hansen and A. Winther (1952), Phys. Rev. **86**, 428. (IV a; VIII c).
E. J. Konopinski (1943), Rev. Mod. Phys. **15**, 209. (VIII a).
E. J. Konopinski and G. E. Uhlenbeck (1941), Phys. Rev. **60**, 308. (VIII a).
H. Kopfermann (1951), Naturwiss. **38**, 29. (V d; Ad. iii).
H. Krüger and U. Meyer-Berkhout (1952), Zs. f. Phys. **132**, 171. (Ad. iii).
H. Kuhn and G. K. Woodgate (1951), Proc. Phys. Soc. A **64**, 1090. (Ad. ii).

D. KURATH (1950), Phys. Rev. **80,** 98. (II c.iii; III.iii).
D. KURATH (1952), Phys. Rev. **87,** 218 (A). (II c.iii; III.iv).
D. KURATH (1952 a), Phys. Rev. **88,** 804. (Ad. iii).
D. KURATH (1953), submitted to the Physical Review. (II c.iii; III.iv).
H. LEW (1953), Phys. Rev. **89,** 530. (Ad. v).
L. LIDOFSKY, P. MACKLIN, and C. S. WU (1952) Phys. Rev. **87,** 391. (VIII c.iv).
I. S. LOWEN (1941) Phys. Rev. **59,** 835. (VII b.ii).
J. E. MACK (1950), Rev. Mod. Phys. **22,** 64. (III.iii; Ad.).
H. M. MAHMOUD and E. J. KONOPINSKI (1952), Phys. Rev. **88,** 1266. (VIII a).
K. G. MALMFORS (1953), Arkiv f. Fysik **6,** 49. (VII d.iii).
M. G. MAYER (1950), Phys. Rev. **78,** 16. (I; III i; III ii; IV).
M. G. MAYER (1950 a), Phys. Rev. **78,** 22. (II c.iii; III.ii; III.iii).
M. G. MAYER, S. A. MOSZKOWSKI, and L. W. NORDHEIM (1951), Rev. Mod. Phys. **23,** 315. (IV a; VI b; VIII c.ii and iii).
C. L. MCCLELLAND and C. GOODMAN (1953), submitted to the Physical Review. (Ap. VI).
L. MEITNER and O. R. FRISCH (1939), Nature **143,** 239. (I).
D. W. MILLER, R. K. ADAIR, C. K. BOCKELMAN, and S. E. DARDEN (1952), Phys. Rev. **88,** 83. (VI d).
A. C. G. MITCHELL (1951), Phys. Rev. **83,** 183. (VI b).
H. MIYAZAWA (1951), Progress Theor. Phys. **6,** 263. (IV c).
H. MIYAZAWA (1951 a), Progress Theor. Phys. **6,** 801. (IV, IV c; V d; Ad. iii).
M. MIZUSHIMA and M. UMEZAWA (1952), Phys. Rev. **85,** 37; **86,** 1055. (IV a).
S. A. MOSZKOWSKI (1951), Phys. Rev. **83,** 1071. (VI b; VII a; VII d.i; VII d.ii).
S. A. MOSZKOWSKI (1953), Phys. Rev. **89,** 474. (VII a; VII b.i; VII d.i).
C. J. MULLIN and E. GUTH (1951), Phys. Rev. **82,** 141. (Ap. VI).
K. MURAKAWA and S. SUWA (1952), Reports of the Institute of Science and Technology, University of Tokyo **6,** no. 4. (Ad. iii).
K. MURAKAWA and S. SUWA (1952 a), Phys. Rev. **87,** 1048. (Ad. iii; Ad. iv).
N. NERESON and S. DARDEN (1953), Phys. Rev. **89,** 775. (VI d).
H. H. NIELSEN (1951), Rev. Mod. Phys. **23,** 90. (VI c.ii).
M. NOGAMI (1948), Progress Theor. Phys. **3,** 362. (II b.i).
L. W. NORDHEIM (1949), Phys. Rev. **75,** 1894. (IV).
L. W. NORDHEIM (1951), Rev. Mod. Phys. **23,** 322. (VI b; VIII b.i; VIII c.ii).
S. A. OCHS and P. KUSCH (1952), Phys. Rev. **85,** 145. (Ad. vi).
S. A. OCHS, R. A. LOGAN, and P. KUSCH (1950), Phys. Rev. **78,** 184. (Ad. iv).
R. K. OSBORN and L. L. FOLDY (1950), Phys. Rev. **79,** 795. (IV c).
D. PFIRSCH (1952), Zs. f. Physik **132,** 409. (II a.iii; V c).
P. PREISWERK and P. STÄHELIN (1952), Physica **18,** 1118. (VI c.ii).

M. H. L. Pryce (1952), Proc. Phys. Soc. A **65**, 773. (VI b; VI c.i).
G. Racah and I. Talmi (1952), Physica **18**, 1097. Cf. also recent work by G. Racah quoted in this reference. (II c.iii; III. ii and iii).
J. Rainwater (1950), Phys. Rev. **79**, 432. (I; II a.iii; V; V c).
N. F. Ramsey (1951), Phys. Rev. **83**, 659. (Ap. VI).
M. E. Rose, G. H. Goertzel, B. I. Spinrad, J. Harr, and P. Strong (1951), Phys. Rev. **83**, 79. (Ap.VI).
S. Rosenblum and M. Valadares (1952), C. R. **235**, 711. (VI c.ii).
L. Rosenfeld (1948). Nuclear Forces. North-Holland Publishing Company, Amsterdam. (II a.ii).
L. Rosenfeld (1951), Physica **17**, 461. (V).
M. Ross (1952), Phys. Rev. **88**, 935. (IV c).
A. Russek and L. Spruch (1952), Phys. Rev. **87**, 1111. (IV c).
A. Rytz (1951), C. R. **233**, 790. (VII d.iii).
R. G. Sachs (1948), Phys. Rev. **74**, 433; Phys. Rev. **75**, 1605. (IV; IV c).
G. Scharff-Goldhaber (1952), Physica **18**, 1105. (VI c.ii).
G. Scharff-Goldhaber (1953), Phys. Rev. **90**, 587. (VI c.ii; Ap.VI).
L. I. Schiff (1951), Phys. Rev. **84**, 1. (IV c).
T. Schmidt (1937), Zs. f. Physik **106**, 358. (IV; IV a).
R. Serber (1947), Phys. Rev. **72**, 1114. (Ap. V c).
W. von Siemens (1951), Naturwiss. **38**, 455. (Ad. iv).
A. B. Smith, R. S. Caird, and A. C. G. Mitchell (1952), Phys. Rev. **88**, 150. (III.iii).
L. Spruch (1950), Phys. Rev. **80**, 372. (IV c).
P. Stähelin and P. Preiswerk (1951), Helv. Phys. Acta **24**, 623 (VI c.ii).
B. Stech (1952), Zs. f. Naturforsch **7 a**, 401. (VII a; VII b.i).
H. Steinwedel and J. H. D. Jensen (1950), Zs. f. Naturforsch. **5 a**, 413. (II a.i).
R. Sternheimer (1951), Phys. Rev. **84**, 244. (Ad.).
R. Sternheimer (1952), Phys. Rev. **86**, 316. (Ad.).
A. Steudel (1952), Zs. f. Phys. **132**, 429. (Ad. v).
A. Storruste (1951), Investigation of Gamma-Rays by the Scintillation Method. Dissertation, Oslo. (VII d.iii).
H. E. Suess and J. H. D. Jensen (1952), Arkiv f. Fysik **3**, 577. (VI b).
S. Suwa (1952), Phys. Rev. **86**, 247. (Ad. v).
W. J. Swiatecki (1951). Proc. Phys. Soc. A**64**, 226. (II a.i).
I. Talmi (1951), Phys. Rev. **83**, 1248. (Ad. xi).
I. Talmi (1952), Helv. Phys. Acta **25**, 185. (II c.iii; III.iii).
I. Tamm (1945), J. Phys. (USSR) **9**, 449. (II b.iii).
T. Teichmann and E. P. Wigner (1952), Phys. Rev. **87**, 123. (Ap. V b.iii).
E. Teller and J. A. Wheeler (1938), Phys. Rev. **53**, 778. (II a.i).
K. A. Ter-Martirosyan (1952), Zh. Eksper. Teor. Fiz. **22**, 284. (VII a; Ap. VI).
S. Tomonaga (1946), Progress Theor. Phys. **1**, 83, 109. (II b.ii).

C. H. Townes, H. M. Foley, and W. Low (1949), Phys. Rev. **76,** 1415. (I; V; V a).
G. L. Trigg (1952), Phys. Rev. **86,** 506. (VIII c; VIII c.i).
F. Villars (1947), Helv. Phys. Acta **20,** 476. (IV; IV c).
R. van Wageningen and J. de Boer (1952), Physica **18,** 369. (V c).
H. Walchli, R. Livingston, and W. J. Martin (1952), Phys. Rev. **85,** 479. (Ad. ix).
H. E. Walchli, W. E. Leyshon, and F. M. Scheitlin (1952 a), Phys. Rev. **85,** 922. (Ad. xi).
M. Walt, R. L. Becker, A. Okazaki, and R. E. Fields (1953), Phys. Rev. **89,** 1271. (VI d).
A. H. Wapstra (1952), Physica **18,** 799. (VI c.ii).
A. H. Wapstra (1953), The Decay Scheme of Pb^{209}, Bi^{207} and Bi^{214} and the Binding Energies of the Heavy Nuclei. Dissertation, Amsterdam. (VI c.ii; VII d.iii).
K. Way, L. Fano, M. R. Scott, and K. Thew (1950). Nuclear Data. National Bureau of Standards, Circular 499. (VII d.iii).
V. F. Weisskopf (1938), Phys. Rev. **53,** 1018. (Ap. VI).
V. F. Weisskopf (1950), Helv. Phys. Acta **23,** 187. (Ap. V b.iii).
V. F. Weisskopf (1951), Phys. Rev. **83,** 1073. (VII a).
V. F. Weisskopf (1952), Physica **18,** 1083. (II c.iii; VI d).
E. P. Wigner (1931), Gruppentheorie und ihre Anwendung auf die Quantenmechanik der Atomspektren. F. Vieweg, Berlin. (II b.ii).
E. P. Wigner and E. Feenberg (1941), Reports on Progress in Physics, **8,** 274. (VIII b.i).
A. Winther (1952), Physica **18,** 1079. (VIII c.i).
A. Winther and O. Kofoed-Hansen (1953), Dan. Mat. Fys. Medd. **27,** no. 14. (VIII a; VIII c; VIII c.i).
K. Woeste (1952), Zs. f. Physik **133,** 370. (II a.i).
C. S. Wu (1950), Rev. Mod. Phys. **22,** 386. (VIII c.iv).

Det Kongelige Danske Videnskabernes Selskab
Matematisk-fysiske Meddelelser, bind **27**, no. 16.

Mat. Fys. Medd. Dan. Vid. Selsk. **27**, no. 16 (1953)(ed. 2, 1957)

COLLECTIVE AND INDIVIDUAL-PARTICLE ASPECTS OF NUCLEAR STRUCTURE

BY

AAGE BOHR AND BEN R. MOTTELSON

SECOND EDITION

København 1957
i kommission hos Ejnar Munksgaard

Fotografisk optryk

STATENS TRYKNINGSKONTOR

Un 27-2

Preface to the Second Edition

The general approach to the analysis of nuclear structure which was followed in this paper has been considerably developed during the past four years and has been applied in the interpretation of a large body of experimental data. The 1953 paper is being reproduced without changes, but we take the present opportunity to indicate some of the main lines along which the development has proceeded and to give a number of references to later work.

The description of nuclear dynamics in terms of individual particle motion and collective oscillations is based on a set of equations representing the coupled motion of the particle and collective degrees of freedom. The form of these equations follows largely from considerations of the symmetry properties of the system, and is thus expected to have a rather general validity. Some of the parameters involved, however, such as the stability of the nuclear shape against distortion or the mass associated with the collective flow, depend on more specific features of the nuclear collective motion.

As a first orientation, one attempted to employ values for these parameters obtained from a liquid drop model, but already the early analysis of various nuclear properties showed the limitations of this comparison. The inadequacy of the liquid drop estimates was especially clearly brought out by the comparison of the nuclear moments of inertia with the deformations deduced from the rate of the electric quadrupole rotational transitions (§ VIc. ii; Ford, 1954; Sunyar, 1955).

An improved understanding of the collective nuclear properties has come from the efforts to derive these directly from the motion of the nucleons; this analysis has revealed the important influence of the nuclear shell structure on the collective motion. The effect on the moment of inertia is at present the best understood (Inglis, 1954; Bohr and Mottelson, 1955; Moszkowski,

1956), but also tentative beginnings have been made with respect to the analysis of other collective parameters (cf. Ap. I; INGLIS, 1955; MOSZKOWSKI, 1956; ARAÚJO, 1956; ALDER et al., 1956). The inadequacy of the liquid drop model with irrotational flow implies that the collective coordinates considered as functions of the nucleonic variables are of more general form than (II.2), and depend on the nucleonic velocities as well as positions (BOHR and MOTTELSON, 1955). The problem of deriving the collective nuclear properties from the equations for a system of interacting particles has been considered by a number of different methods; in addition to the references quoted in ALDER et al. (1956, p. 528), the following papers on the subject have recently appeared: COESTER (1956), DAVIDOV and FILLIPOV (1956), LIPKIN, DESHALIT, and TALMI (1956), LÜDERS (1956), NATAF (1957), SKYRME (1957), TOMONAGA (1956), PEIERLS and YOCCOZ (1957), YOCCOZ (1957); cf. also the review article by TAMURA (1957).

In 1953, it was not always clear which coupling scheme would be most appropriate to a particular nucleus. As a result of the extensive experimental study of nuclear rotational and vibrational spectra, it seems now established that the strong coupling scheme, characterized by a relatively large equilibrium deformation and a rotational band structure of the energy levels, provides a good starting point for nuclei in the regions $A \sim 25$, $150 < A < 190$, and $A > 222$ (cf. the data summarized in ALDER et al., 1956). Outside these regions, and excluding the nuclei immediately adjacent to closed shells, it has been possible to interpret many features of the observed lowest states of even-even nuclei in terms of quadrupole vibrations about a spherical equilibrium (SCHARFF-GOLDHABER and WENESER, 1955; JEAN and WILETS, 1955; ALDER et al., 1956). In these latter regions, the odd-A nuclei present a more complicated picture, which is not yet well understood, but which may possibly be related to intermediate coupling schemes (§ IIb. iii; FORD, 1953; CHOUDHURY, 1954; J. RAZ, 1955).

In the region where the strong coupling scheme applies, the great simplicity of the nuclear structure has made possible a rather detailed description of the low energy excitation spectrum as well as of the different types of transitions between the nuclear states. The simple relationships between the states within a rotational band have been further exploited (ALAGA, ALDER, BOHR, and

MOTTELSON, 1955; BOHR, FRÖMAN, and MOTTELSON, 1955; SATCHLER, 1955; KERMAN, 1955) and, in addition, the analysis of independent particle motion in non-spherical fields has made possible the interpretation of intrinsic excitations and the calculation of equilibrium shapes (NILSSON, 1955; MOSZKOWSKI, 1955; MOTTELSON and NILSSON, 1955, 1957; GOTTFRIED, 1956). In the α-decay of the heavy elements, the influence of the nuclear shape on the intensities of the fine structure components has been analyzed (RASMUSSEN and SEGALL, 1956; STRUTINSKY, 1956; FRÖMAN, 1957). In the β- or γ-transitions between different intrinsic states, there are important selection rules associated with quantum numbers appropriate to the motion in a deformed field (ALAGA et al., 1955; ALAGA, 1955; MOTTELSON and NILSSON, 1957). More detailed estimates have shown that the readjustment of the collective field (cf. p. 107) has in most cases only a small effect on the transition rate (SUEKANE, 1953; REDLICH and WIGNER, 1954).

While a great amount of evidence has been accumulated on the rotational and single particle excitation spectra of the deformed nuclei, relatively little information has been obtained regarding collective vibrations in these nuclei. Quite recently, however, there has appeared some evidence for the occurrence of levels with the expected properties of β- and γ-vibrations; also odd parity states resembling octupole vibrations have been observed in certain regions of elements (cf. the data summarized by ALDER et al., 1956, and by PERLMAN and RASMUSSEN, 1957).

The important influence of the residual two body interactions on various features of the low energy nuclear properties has been emphasized by recent work. One may especially mention the analysis of nuclear spectra for configurations with a few particles outside of closed shells (cf., e. g., the review by ELLIOTT and LANE, 1957) and the interpretation of magnetic moments which provides an especially sensitive test of configuration mixing (BLIN-STOYLE and PERKS, 1954; ARIMA and HORIE, 1954; and the review by BLIN-STOYLE, 1956). Moreover, the role of the pairing energy is reflected in the intrinsic excitation spectra of even-even nuclei as well as by the analysis of the kinetic and potential energy of the collective motion(cf., e. g., ALDER et al., 1956). It is not yet clear to what extent these forces simply represent the direct interactions between the particles outside of closed shells, and to

what extent they are to be ascribed to the effective forces resulting from the polarization of the nucleus (cf. § IIc. i).

A description of nuclear reaction processes, similar to that developed in § VId and Ap. V, has been considered by a number of authors (SCOTT, 1954; LANE, THOMAS, and WIGNER, 1955; FRIEDMAN and WEISSKOPF, 1956). An instructive example which exhibits some of the conditions for the applicability of the optical model is provided by the direct coupling between the incident particle and the nuclear rotational motion (cf. the discussion in Ap. Vc). A number of consequences of an extended optical model which includes the effect of such direct couplings have been derived (cf., e. g., BRINK, 1955; HAYAKAWA and YOSHIDA, 1955; DROZDOV, 1956; MOSHINSKY, 1956; MARGOLIS and TROUBETZKOY, 1957; GRIBOV, 1957). In the nuclear fission reaction, the strong coupling scheme should provide a good description of the spectrum of fission channels at the saddle point, and some of the consequences of such a model have been discussed (BOHR, 1955).

In this brief summary, it has not been possible to mention explicitly the many experimental studies which have guided the theoretical developments. For the understanding of the low energy nuclear structure, the decay scheme studies and the Coulomb excitation experiments have in recent years played an especially important part. The first definite results of Coulomb excitation experiments were reported in 1953, shortly after this article was sent to the printer. For a review of the developments in this field, cf. HEYDENBURG and TEMMER (1956) and ALDER, BOHR, HUUS, MOTTELSON, and WINTHER (1956).

Aage Bohr and Ben R. Mottelson.

March 1, 1957.
Institute for Theoretical Physics
University of Copenhagen,
and
CERN, Theoretical Study Division,
Copenhagen, Denmark.

References.

G. Alaga (1955), Phys. Rev. **100,** 432.

G. Alaga, K. Alder, A. Bohr, and B. R. Mottelson (1955), Mat. Fys. Medd. Dan. Vid. Selsk. **29,** no. 9.

K. Alder, A. Bohr, T. Huus, B. R. Mottelson, and A. Winther (1956), Revs. Mod. Phys. **28,** 432.

J. M. Araújo (1956), Nuclear Physics **1,** 259.

A. Arima and H. Horie (1954), Prog. Theor. Phys. **11,** 509.

R. J. Blin-Stoyle (1956), Revs. Mod. Phys. **28,** 75.

R. J. Blin-Stoyle and M. A. Perks (1954), Proc. Phys. Soc. (London) A **67,** 885.

A. Bohr, (1955), Proc. Intern. Conf. Geneva, **2,** 151. U. N., New York 1956.

A. Bohr, P. O. Fröman, and B. R. Mottelson (1955), Mat. Fys. Medd. Dan. Vid. Selsk. **29,** no. 10.

A. Bohr and B. R. Mottelson (1955), Mat. Fys. Medd. Dan. Vid. Selsk. **30,** no. 1.

D. M. Brink (1955), Proc. Phys. Soc. (London), A **68,** 994.

D. C. Choudhury (1954), Mat. Fys. Medd. Dan. Vid. Selsk. **28,** no. 4.

F. Coester (1956), Nuovo Cimento **4,** Ser. 10, 1307.

A. S. Davydov and G. F. Filipov (1956), Physica **XXII,** 1167.

S. I. Drozdov (1955, 1956), Journ. Exp. Theor. Physics USSR **28,** 734, 736; **30,** 786.

J. P. Elliott and A. M. Lane (1957), to appear in Handbuch der Physik (Springer Verlag, Berlin).

K. W. Ford (1953), Phys. Rev. **90,** 29.

K. W. Ford (1954), Phys. Rev. **95,** 1250.

F. L. Friedman and V. F. Weisskopf (1955), Niels Bohr and the Development of Physics, Pergamon Press, London, W. Pauli ed.

P. O. Fröman (1957), Mat. Fys. Skr. Dan. Vid. Selsk. **1,** no. 3.

K. Gottfried (1956), Phys. Rev. **103,** 1017.

S. Hayakawa and S. Yoshida (1955), Prog. Theor. Phys. **14, 1.**

N. P. Heydenburg and G. M. Temmer (1956), Ann. Rev. of Nuclear Science, vol. 6, J. G. Becheley ed.

D. R. Inglis (1954), Phys. Rev. **96,** 1059.

D. R. Inglis (1955), Phys. Rev. **97,** 701.

M. Jean and L. Wilets (1955), C. R. **241,** 1108; Phys. Rev. **102,** 788 (1956).

A. K. Kerman (1956), Mat. Fys. Medd. Dan. Vid. Selsk. **30,** no. 15.

A. M. Lane, R. G. Thomas, and E. P. Wigner (1955), Phys. Rev. **98,** 693.
H. J. Lipkin, A. de-Shalit, and I. Talmi (1956), Phys. Rev. **103,** 1773.
G. Lüders (1956), Z. f. Naturforsch. **11a,** 617 and in press.
B. Margolis and E. Troubetzkoy (1957), Phys. Rev. **106,** 105.
M. Moshinsky (1956), Revista Mexicana de Fisica **5,** 1.
S. A. Moszkowski (1955), Phys. Rev. **99,** 803.
S. A. Moszkowski (1956), Phys. Rev. **103,** 1328.
B. R. Mottelson and S. G. Nilsson (1955), Phys. Rev. **99,** 1615.
B. R. Mottelson and S. G. Nilsson (1957), to appear in Mat. Fys. Medd. Dan. Vid. Selsk.
R. S. Nataf (1957), Nuclear Physics **2,** 497.
R. E. Peierls and J. Yoccoz (1957), Proc. Phys. Soc. (London) **A 70,** 381.
S. G. Nilsson (1955), Mat. Fys. Medd. Dan. Vid. Selsk. **29,** no. 16.
I. Perlman and J. O. Rasmussen (1957), to appear in Handbuch der Physik (Springer Verlag, Berlin).
J. O. Rasmussen and B. Segall (1956), Phys. Rev. **103,** 1298.
B. J. Raz (1955), Dissertation, Rochester University.
M. G. Redlich and E. P. Wigner (1954), Phys. Rev. **95,** 122.
G. R. Satchler (1955), Phys. Rev. **97,** 1416.
G. Scharff-Goldhaber and J. Weneser (1955), Phys. Rev. **98,** 212.
J. M. C. Scott (1954), Phil. Mag. **45,** 441.
T. H. R. Skyrme (1957), Proc. Roy. Soc. A (London), to be published.
S. Suekane (1953), Prog. Theor. Phys. **10,** 480.
A. W. Sunyar (1955), Phys. Rev. **98,** 653.
V. M. Strutinsky (1956), J.E.T.P., USSR, **30,** 411.
T. Tamura (1957), to appear in Fortschritte der Physik.
S. Tomonaga (1956), Report at the Intern. Congress of Theor. Phys., Seattle.
F. Villars (1957), Nuclear Physics **3,** 240.
J. Yoccoz (1957), Proc. Phys. Soc. (London) **A 70,** 388.